UNIVERSITE BRETAGNE LOIRE

UNIVERSITÉ DE NANTES

Thèse de Doctorat

Thibault COLOMBANI

Mémoire présenté en vue de l'obtention du
grade de Docteur de l'Université de Nantes
sous le sceau de l'Université Bretagne Loire

École doctorale : Biologie-Santé

Discipline : Biologie, médecine et santé
Spécialité : Immunologie
Unité de recherche : Centre de Recherche en Cancérologie et Immunologie Nantes-Angers (INSERM UMR1232)

Soutenue le vendredi 3 Mars 2017

Compréhension immunologique de la stimulation de la réponse immunitaire par des molécules synthétiques : Applications thérapeutiques

Jury

Rapporteurs :	**Patrick MIDOUX**, Directeur de recherche, Université d'Orléans **Georges VASSAUX**, Directeur de recherche, Université de Nice-Sophia Antipolis
Examinateurs :	**Olivier LAMBERT,** Directeur de recherche, Université de Bordeaux I **Frédéric ALTARE**, Directeur de recherche, Université de Nantes
Directeur de Thèse :	**Bruno PITARD**, Directeur de recherche, Université de Nantes

REMERCIEMENTS

En premier lieu, je tenais à vous remercier sincèrement Bruno, pour ces quatre années et demie passées au sein de votre équipe. Vous m'avez tout d'abord donné ma chance durant mon M2 au cours duquel j'ai pu découvrir le monde merveilleux des vecteurs non-viraux, puis vous m'avez accordé votre confiance en me confiant ce travail de thèse. Merci pour ces échanges constructifs, pour votre sens critique, et pour votre démarche scientifique aboutie m'ayant apprise à ne jamais perdre de vue les applications de nos recherches. Bruno, merci de m'avoir donné les moyens de mener au bout tous ces projets, ainsi que de m'avoir accordé une grande liberté dans leurs cheminements. Même si votre mise en disponibilité n'a pas toujours été facile à gérer, cela m'a permis d'aborder des sujets divers et variés et surtout d'acquérir toute l'autonomie nécessaire à la poursuite de ma carrière scientifique, ici ou ailleurs.

Hervé Le Marec, merci de m'avoir accueilli au sein de l'institut du thorax pendant la plus grande partie de ma thèse, et d'avoir accepté d'assurer l'intérim de sa direction pendant 2 ans. Je n'aurais malheureusement pas utilisé de puce à ADN afin d'approfondir l'étude de certaines de nos molécules. Merci Marc Grégoire de m'avoir accueilli au sein du Centre de Recherche en Cancérologie et Immunologie Nantes Angers pour finir mon travail de thèse.

Je voudrais remercier Patrick Midoux, George Vassaux, Olivier Lambert et Frédéric Altare pour avoir accepté de juger et de critiquer mon travail de thèse en endossant le rôle membre de mon jury. Merci également à Gilles Besin pour l'aide apporté au cours des comités de suivi de thèse.

Thomas, collègue et compagnon durant toutes ces années, je n'ai pas vraiment de mots assez forts pour te remercier et un simple « Merci » serait loin d'être suffisant. Je ne pourrais dire ce qui me manquera le plus : nos discussions scientifiques sur tous les projets que nous avons mené (ou sur tous ceux auxquels nous avons réfléchi), nos longs échanges animés sur la vie, sur le monde, sur tout et à la fois sur rien, ou bien serait-ce cette solidarité sans faille dont nous avons fait preuve durant toutes ces années, parfois contre vents et marées ? Une chose est sûre, tu m'auras transmis le virus de la course à pied (et qui l'aurait cru ?), et je m'efforcerai de continuer à l'incuber bien au chaud, là où m'emmènera la vie, afin qu'à mon tour je puisse contaminer de nouvelles personnes. Dois-je vraiment m'éterniser sur tes qualités en tant que chercheur ? Sur tous les « trucs et astuces » indispensables que tu m'as appris au cours des mois ? Ou dois-je parler de ta bonne humeur et de cette chaleur humaine dont tu débordes, et qui ont fait de ces 4 années des moments inoubliables ? Thomas, je te souhaite sincèrement et du fond du cœur le meilleur pour la suite, tant sur le plan personnel que sur le plan professionnel. Si l'aventure de cette thèse a été si belle et enrichissante, c'est en grande partie grâce à toi. Thomas, Merci.

J'aimerai également remercier toutes les personnes avec qui j'ai pu travailler au cours de ces dernières années, tant pour leur aide inestimable et leurs précieux conseils, que pour tous ces échanges en salle de manip' ou bien au détour d'un couloir (ou d'un café). Benoît, merci de m'avoir formé à la RT-qPCR à mon arrivée. Finalement tu vois, on en aura fait quelque chose de tes miRNA ! Emilie, merci pour ta gentillesse et pour m'avoir montré les joies de la biologie moléculaire. Grâce à toi les ELISA n'ont plus de

secrets pour moi. Merci à toi Mathieu de la patience dont tu as fait part pour m'expliquer tous ces trucs chimiques au début de ma thèse et pour m'avoir appris à former des liposomes (même si l'élève n'a jamais réussi à dépasser le maître). Et dans la même lignée : merci à toi Damien, mon « dealer de poudre blanche » m'ayant fourni sans faillir jusqu'à la fin en lipides, mais également pour ton professionnalisme et ton aide sur les publications jusqu'à la fin (et même après). Mallory, je ne t'oublie pas, merci à toi pour ta pédagogie dans l'apprentissage du western blot et pour m'avoir aidé à résoudre bien des problèmes d'optimisation. Même sous tes nouveaux horizons, mon petit doigt me dit que nous continuerons à collaborer mais au travers d'autres responsabilités. Nathalie, merci d'avoir égayé tous ces lundis et vendredis matins en culture cellulaire : notre duo vocal inimitable va me manquer. Gilliane, merci pour ces discussions scientifiques et pour m'avoir montré le monde intriguant de Crispr-Cas9. Stéphanie, merci pour ta patience et tes explications sur l'art de la PCR et du séquençage de plasmide. Françoise, merci pour ta bienveillance à mon égard et ton soutien sans faille. Alors comme ça : le DOSRI, c'est magique ? Christian, ce petit coin de corse dans un monde de bretons. Merci pour ces nombreux moments de détente au détour d'un café et même si nous sommes des incompris : Forza Bastia !

J'ai une pensée particulière envers le club de course de l'institut du thorax. Coach Jade, Pauline, Flavien, Agnès, Julien… Merci pour tous ces moments en extérieur où j'ai pu longuement me changer les idées, relativiser, et me prendre une bonne bouffée d'oxygène surtout dans les moments difficiles.

Ayant eu l'opportunité de me lancer dans une aventure toute particulière en parallèle de ma thèse, je tiens bien évidemment à remercier très chaleureusement mes Cysmyk-girls : Nadjet, Nejma, Sophie et Lindzy. Votre aide aura été précieuse dans ce projet, et je n'oublierai pas toutes ces attentions et longues discussions entrepreneuriales autour de ce projet qui a rythmé ma vie en dehors du labo (« KissKissBankBank » !). Maxime et Carole, j'ai forcément une pensée émue envers vous deux : je suis heureux d'avoir pu transmettre un peu de ma passion pour la création d'entreprise et de voir que cela vous réussit ! Valentine, merci pour nos longs débats et échanges sur la Recherche et le lien public-privé (indispensable !). Grâce à toi, je me sentais un peu moins seul dans mes ambitions de changer la Science, à ma manière.

J'ai sûrement oublié beaucoup de monde, et je m'en excuse. Mais encore une fois : merci à tous d'avoir fait de ces 4 ans et quelques des années inoubliables de ma vie ayant forgé le scientifique et la personne que je serai demain.

Merci à mes amis qui m'ont supporté pendant ces longues et éprouvantes années, et pour avoir compris mon manque de disponibilité. Même si à votre grand regret ma culture cinématographique est encore loin d'être « au top », tous ces moments en votre compagnie ont été précieux et inoubliables.

Enfin, Papa, Maman, Hugues et Vincent, merci à vous pour votre soutien inconditionnel durant toutes ces années. Le monde dans lequel j'ai évolué vous était étranger et bien souvent incompréhensible. Pourtant, vous étiez toujours là, à me proposer votre aide, et cela a énormément compté pour moi. J'ai de la chance de vous avoir. Une des valeurs les plus importantes que vous m'avez inculqué est qu' « Il ne faut jamais oublier de là où l'on vient et qui l'on est, pour savoir là où l'on va ». Dès

lors, je vais finir mes remerciements avec une pensée forte et très émue envers vous qui êtes partis bien trop tôt et qui auraient souhaité assister à cette soutenance : je vous dédis ce manuscrit. Papy, Mamy (-ya), Merci.

SOMMAIRE

REMERCIEMENTS 2
SOMMAIRE 5
LISTE DES FIGURES 8
LISTE DES TABLEAUX 9
ABBREVIATIONS 10
AVANT-PROPOS 14
GENERALITES 15
Partie 1 : La réponse immunitaire innée 16
1. Le système immunitaire inné et la vaccination 16
2. Les récepteurs de l'immunité innée ou PRRs 20
2.1. Les récepteurs membranaires 21
2.1.1 Les récepteurs *Toll-like* (TLRs) 21
2.1.1.1 Structure 21
2.1.1.2. Signalisation 22
2.1.2. Les récepteurs des lectines de type C (CLRs) 24
2.1.2.1. Structure 24
2.1.2.1. Signalisation induite par la dectine-1 24
2.2. Les récepteurs cytoplasmiques 25
2.2.1. Les récepteurs NOD-Like (NLR) 25
2.2.1.1. NOD1 et NOD2 26
2.2.1.2. L'inflammasome 27
2.2.2. Les récepteurs *RIG-Like* (RLR) 28
2.2.3. Les récepteurs cytosoliques d'ADN (CDS) 29
3. Les PAMPS ou ligands de la réponse immunitaire innée 30
3.1. Le lipopolysaccharide (LPS) 31
3.2. Le peptidoglycane (PGN) 32
3.3. L'acide lipotéichoïque (LTA) 33
3.4. La flagelline 34
3.5. Les lipoprotéines (LP) 35
3.6. Les Glycoprotéines (GP) 35
3.7. Les acides nucléiques 36
3.7.1. L'acide ribonucléique simple brin (ARNsb) ou double brin (ARNdb) 36
3.7.2. Les acides désoxyribonucléiques (ADN) 37
3.8. Le zymosane 38
3.9. Les glycosylphosphatidylinositols ou GPIs 38

Partie 2 : Stimulation de la réponse immunitaire innée par les acides nucléiques. 40
1. Introduction ... 40
2. Les récepteurs des acides nucléiques ... 41
2.1. Les récepteurs endosomaux ou TLRs ... 41
2.1.1. Le TLR3 ... 42
2.1.2. Le TLR7 et 8 ... 43
2.1.3. Le TLR9 ... 44
2.2. Les récepteurs intracytoplasmiques ... 46
2.2.1. Les RLRs ... 46
2.2.2. Les CDS ... 49
2.2.2.1. DHX9 et DHX36 ... 49
2.2.2.2. DAI ... 50
2.2.2.3. IFI16 (ou IFI204 chez la souris) ... 52
2.2.2.4. cGAS ... 53
2.2.2.5. AIM2 ... 54
2.3. Conclusion ... 55
3. Les agonistes des récepteurs d'acides nucléiques ... 56
3.1. Les agonistes des récepteurs d'ARN ... 58
3.2. Les agonistes des récepteurs d'ADN ... 58
4. Application à la vaccination ... 59
Partie 3 : Lipides cationiques et immunomodulation ... 62
1. Généralités ... 62
2. Transfert de gènes et lipoplexes ... 64
2.1. Les lipoplexes ... 65
2.1.1. Propriétés physicochimiques et complexation ... 66
2.1.2. Internalisation des lipoplexes ... 68
2.1.3. Echappement de l'endosome ... 70
2.1.4. Dissociation du complexe ADN/Lipide cationique ... 72
2.1.5. Traffic intracellulaire du plasmide et importation nucléaire ... 72
3. Stimulation de la réponse immunitaire par les lipides cationiques ... 75
3.1. Voies de signalisation cellulaires activées par les lipides cationiques ... 76
3.1.1. La voie NFκB-dépendante ... 76
3.1.2. Les voies NFκB-indépendantes ... 77
3.1.3. La voie de l'apoptose ... 79
3.1.4. La voie de l'inflammasome ... 80
3.2 Influence de composition des lipides cationiques ... 82
4. Les dérivés lipidiques d'aminoglycosides ... 83

RESULTATS 85
Article 1 : Mécanisme de la vaccination à ADN médiée par le 704 86
Article 1 : Mechanism of 704-mediated DNA vaccine 88
Article 2 : Développement de nouveaux adjuvants lipidiques pour l'immunothérapie anticancéreuse 121
Article 2 : Aminoglycoside lipidic derivatives induce innate immunity and suppress tumor growth through phosphatidylinositol phospholipase C pathway and caveolae-dependent endocytosis 123
Article 3 : Influence de l'assemblage supramoléculaire des liposomes sur l'efficacité de transfection. 163
Article 3 : Self-assembling complexes between binary mixtures of lipids with different linkers and nucleic acids promote universal mRNA, DNA and siRNA delivery 164
CONCLUSION ET PERSPECIVES 177
Compréhension des mécanismes immunologiques du 704 en vue d'un développement préclinique chez l'homme 178
Stimulation de la réponse immuntaire par les lipides cationiques dérivés d'aminoglycosides 179
Développement d'une approche originale basée sur l'assemblage supramoléculaire des lipoplexes pour le développement de vecteurs de transfections universels 181
Conclusion générale 182
ANNEXES 183
Article 4 : Design of ionizable lipids to overcome the limiting step of endosomal escape - Application in the intracellular delivery of mRNA, DNA and siRNA. 185
Article 5 : Important role of phosphoramido linkage in imidazole-based dioleyl helper lipids for liposome stability and primary cell transfection. 203
Article 6 : Liposome-based Formulation for Intracellular Delivery of Functional Proteins 217
Article 7 : Evaluation of tetrafunctional block copolymers as synthetic vectors for lung gene transfer. 227
BIBLIOGRAPHIE 237

LISTE DES FIGURES

FIGURE 1 ; INITIATION DE LA REPONSE IMMUNITAIRE 17
FIGURE 2 : INITIATION DE LA REPONSE IMMUNITAIRE ADAPTATIVE PAR LES CPAS 18
FIGURE 3 : STRUCTURE DES TLRS 21
FIGURE 4 : VOIES DE SIGNALISATION ET LIGANDS DES DIFFERENTS TLRS 22
FIGURE 5 : VOIE DE SIGNALISATION DE LA DECTINE-1 25
FIGURE 6 : VOIES DE SIGNALISATION DE NOD1 ET NOD2 26
FIGURE 7 : STRUCTURE ET VOIE DE SIGNALISATION DES DIFFERENTS INFLAMMASOMES 27
FIGURE 8 : VOIES DE SIGNALISATION ET LIGANDS DES RLRS 28
FIGURE 9 : VOIES DE SIGNALISATION ET LIGANDS DES CDS 29
FIGURE 10 : RECONNAISSANCE DES PAMPS APPARTENANT A DIFFERENTES CLASSES DE PATHOGENES 30
FIGURE 11 : REPONSE IMMUNITAIRE DE L'HOTE AU LPS, VIA LA VOIE DE SIGNALISATION TLR4-MD2 31
FIGURE 12 : REPONSE IMMUNITAIRE DE L'HOTE AUX PEPTIDOGLYCANES VIA LES VOIES DE SIGNALISATION TLR2 ET NOD2 32
FIGURE 13 : ACIDE LIPOTEICHOÏQUE ET RECONNAISSANCE PAR LE COMPLEXE TLR2/TLR6 33
FIGURE 14 : STRUCTURE ET RECONNAISSANCE DE LA FLAGELLINE PAR LE TLR5 34
FIGURE 15 : RECONNAISSANCE DES LIPOPROTEINES PAR LE TLR2 35
FIGURE 16 : RECONNAISSANCE DE L'ARN ET VOIES DE SIGNALISATION 36
FIGURE 17 : RECONNAISSANCE DE L'ADN ET VOIES DE SIGNALISATION 37
FIGURE 18 : RECONNAISSANCE DU ZYMOSANE A LA SURFACE DES LEVURES ET VOIES DE SIGNALISATION 38
FIGURE 19 : STRUCTURE DES GLYCOSYLPHOSPHATIDYLINOSITOLS (GPIS) ET VOIES DE SIGNALISATION 39
FIGURE 20 : RECONNAISSANCE DES ACIDES NUCLEIQUES AU NIVEAU DES ENDOSOMES 41
FIGURE 21 : VOIE DE SIGNALISATION TLR3-TRIF DEPENDANTE 42
FIGURE 22 : VOIE DE SIGNALISATION DES TLR7 ET 8 44
FIGURE 23 : VOIE DE SIGNALISATION DU TLR9 45
FIGURE 24 : STRUCTURE ET VOIES DE SIGNALISATIONS DES RLRS 48
FIGURE 25 : VOIE DE SIGNALISATION DES DHX9 ET 36 49
FIGURE 26 : VOIE DE SIGNALISATION DE DAI 50
FIGURE 27 : VOIE DE SIGNALISATION D'IFI16 52
FIGURE 28 : VOIS DE SIGNALISATION DE CGAS 53
FIGURE 29 : VOIE DE AIM2 ET DE L'INFLAMMASOME 55
FIGURE 30 : STRUCTURE SCHEMATIQUE DES LIPIDES CATIONIQUES ET ORGANISATION EN SOLUTION 62
FIGURE 31 : REPRESENTATION SCHEMATIQUE DE LA DELIVRANCE D'ADN AU SEIN DES CELLULES PAR DES LIPOPLEXES 65
FIGURE 32 : LIPOPLEXES EN FONCTION DES 3 ZONES DE STABILITE COLLOÏDALE 67
FIGURE 33 : REPRESENTATION SCHEMATIQUE DES DEUX PHASES LAMELLAIRES 68
FIGURE 34 : VOIES D'ENTREES AU SEIN DES CELLULES MAMMIFERES 69
FIGURE 35 : MECANISMES D'ECHAPPEMENT ENDOSOMAL 71
FIGURE 36 : MODELE D'IMPORT NUCLEAIRE SPECIFIQUE D'UN PLASMIDE 74
FIGURE 37 : LE LIPIDE CATIONIQUE DIC14-AMIDINE STIMULE LES CELLULES DENDRITIQUES PAR L'INTERMEDIAIRE DU TLR4 76
FIGURE 38 : PROPOSITION DU MECANISME D'ACTIVATION DE LA REPONSE IMMUNITAIRE PAR LES LIPIDES CATIONIQUES VIA UNE VOIE DE STIMULATION NFKB- ET MYD88-INDEPENDANTE 78
FIGURE 39 : MECANISME POSSIBLE DE L'ACTIVATION DE LA VOIE DE SIGNALISATION PRO-APOPTOTIQUE PAR LES LIPIDES CATIONIQUES 80
FIGURE 40 : ACTIVATION DE LA VOIE DE L'INFLAMMASOME PAR LES LIPIDES CATIONIQUES 81
FIGURE 41 : STRUCTURE DES LIPOAMINOGLYCOSIDES ET CO-LIPIDES UTILISES AU COURS DE CE TRAVAIL DE THESE 84

LISTE DES TABLEAUX

TABLEAU 1 : AGONISTES DES RECEPTEURS AUX ACIDES NUCLEOIQUES AU STADE DE DEVELOPPEMENT PRE-CLINIQUE OU CLINIQUE . 57
TABLEAU 2 : VACCINS A ADN COMMERCIALISES A USAGE VETERINAIRE 59

ABBREVIATIONS

AD	acidic transactivating domain
ADN	acide désoxyribonucléique, soit simple brin (ADNsb) soit double brin (ADNdb)
Ag	antigène
AFP	alpha-fœtoprotéine
AIM2	absent in melanoma 2
ARN	acide ribonucléique, soit simple brin (ARNsb), soit double brin (ARNdb)
ASC	apoptosis-associated speck-like protein containing a CARD
BET	bromure d'éthidium
BID	Bcl2 interacting protein
BIR	baculovirus inhibitor repeats
BMDC	bone marrow-derived dendritic cell
CARD	caspase recruitment domain
CD	cluster de différenciation
c-di-GMP	cyclic diguanylate monophosphate
CDS	cytosolic DNA sensors
cGAMP	cyclic guanosine monophosphate - adénosine monophosphate
cGAS	cyclic GMP-AMP synthase
CLR	C-type lectin receptors
CPA	cellule présentatrice de l'antigène « professionnelles »
CTLD	C-type lectin-like domain
DAG	diacylglycerol
DAI	DNA-dependent activator of IFN-regulatory factors
DAMP	motifs moléculaires associés aux dégâts
DOPE	dioléoylphosphatidyléthanolamine
DOTAP	chlorure de 1,2-dioleoyloxy-3-trimethylammoniumpropane
DTS	DNA nuclear targeting sequence
ERK	extracellular signal-regulated kinases
FDA	Food and Drug Administration

GP	glycoprotéine
GPI	glycosylphosphatidylinositol
IFI16/204	interferon inductible protein 16 / 204
Ig	immunoglobulins
IKKs	IκB kinases
IL	interleukine
IP3	inositol 1,4,5-trisphosphate
IPS-1	interferon-beta promoter stimulator 1
ITAM	immunoreceptor tyrosine-based activation motif
IRAK	interleukin-1 receptor-associated kinase
IRF	interferon regulatory factors
KC	kanamycine-cholesterol
LBP	LPS binding protein
LGP2	laboratory of genetics and physiology 2
LP	lipoprotéine
LPS	lipopolysaccharide
LRR	leucine-rich repeat
LTA	acide lipotéichoïque
LTc	lymphocytes T cytotoxique
LTh	lymphocytes T helper
MAPK	mithogen-activated protein kinases
MAVS	mitochondrial antiviral-signaling protein
MD-2	myeloid differentiation factor 2
MDA-5	melanoma-differentiation-associated gene 5
MDP	muramyl dipeptide
MLV	large multilamellar vesicles
MyD88	myeloid differentiation primary response gene 88
NACHT / NOD / NBD	nucleotide-binding domain
NFAT	nuclear factor of activated T-cells
NFκB	nuclear factor kappa-light-chain-enhancer of activated B cell
NLR	NOD-Like receptors
NLS	signal de localisation nucléaire
NPC	nuclear pore complex

NTase	nucléotidyltransférases
ODN	oligodéoxynucléotides
PAMP	motifs moléculaires associés aux pathogènes
pb	paire de bases
PEG	polyethylene glycol
PGN	peptidoglyane
PI3K	phosphoinositide (PI)-3 kinase
PIP2	phosphatidylinositol-4,5-bisphosphate
PKC	protéine kinase C
PLC	phospholipase C
PNase 1	polynucléotide phosphorylase 1
Poly(I :C)	polyinosinic:polycytidilic
PRR	récepteurs de reconnaissance de motifs moléculaires
PYD	pyrin domain
RC	rapport de charge
RICK	receptor-interacting serine/threonine kinase
RIG-1	retinoic-acid-inducible protein 1
RIP1 et 2	receptor-interacting protein 1 et 2
RLR	RIG-I-Like receptors
ROS	reactive oxygen species
siRNA	short interfering RNA
SRK	SRC family kinases
STING	stimulator of interferon gene
SUV	small unilamellar vesicles
SyK	spleen tyrosine kinase
TAK1	transforming growth factor beta-activated kinase 1
TBK1	TANK-binding kinase 1
TGKC	tri-guanidium-kanamycine-cholestétol
TIR	toll/IL-1 receptor
TIRAP	toll-interleukin 1 receptor domain-containing adapter protein
TLR	toll-like receptors
TNF	tumor necrosis factor
TRADD	TNFR-1-associated death domain

TRAF	TNF receptor associated factor
TRAM	TRIF-related adaptor molecule
TRIF	TIR-domain-containing adapter-inducing interferon-β
VIH	virus de l'immunodéficience humaine
WTA	wall teichoic acids
ZBP1	Z-DNA binding protein 1

AVANT-PROPOS

Les 20 dernières années ont été le théâtre d'une révolution de nos connaissances dans le domaine de l'immunologie, notamment dans la compréhension des cellules, récepteurs, et molécules qui contribuent à la réponse immunitaire innée. Elles ont également changé notre vision sur l'action du système immunitaire inné dans l'induction d'une réponse immunitaire adaptative protectrice. De plus avec l'achèvement en 2003 du Projet Génome Humain, le plus grand projet collaboratif international dans le domaine de la biologie, le développement des biothérapies a connu un essor sans précédent afin d'apporter des solutions à de nombreux défis en santé humaine et animale dans le but de lutter contre des maladies héréditaires ou acquises.

Basées sur l'utilisation de macromolécules issues du vivant, les biothérapies regroupent un champ vaste d'applications thérapeutiques comme la thérapie génique, les thérapies cellulaires et tissulaires, et l'immunothérapie. Parmi les différentes approches développées, la délivrance de molécules thérapeutiques sous forme d'acides nucléiques revêt un intérêt tout particulier. En effet, la technologie du transfert de gènes permet soit de réparer des cellules défectueuses en leur apportant une copie du gène sain, soit d'activer le système immunitaire par l'expression d'un antigène d'intérêt thérapeutique. Néanmoins, malgré le développement de nombreux outils de thérapie génique ou d'immunothérapie, peu d'applications thérapeutiques ont actuellement vu le jour à cause de nombreuses limitations, mettant ainsi en évidence la nécessité d'optimiser les stratégies actuelles et de développer de nouvelles alternatives.

L'équipe dirigée par Bruno PITARD, au sein de laquelle j'ai effectué ces trois années de thèse, travaille sur le développement de nouveaux vecteurs synthétiques pour le transport d'acides nucléiques afin d'améliorer leurs délivrances et leurs expressions au sein des cellules (pour la thérapie génique), mais également afin de stimuler efficacement le système immunitaire dans le cadre de la vaccination à ADN. Dès lors, mon travail de thèse a tout d'abord consisté à comprendre les mécanismes immunologiques engagés par une formulation vaccinale composée d'un copolymère à blocs amphiphile formulé avec de l'ADN, lui conférant la capacité d'induire une forte et protectrice réponse immunitaire dans différents protocoles d'immunothérapie. La seconde partie de ma thèse a été consacrée à l'étude de l'influence de la structure des lipides cationiques sur la stimulation de la réponse immunitaire et les voies de signalisation engagées afin de développer de nouveaux adjuvants prometteurs pour l'immunothérapie. Enfin, la dernière partie de mon travail a consisté à l'étude de l'influence de l'assemblage supramoléculaire des lipoplexes sur l'efficacité de transfection, afin de développer un vecteur universel pour la délivrance de différentes classes d'acides nucléiques au sein de différents types cellulaires.

GENERALITES

GENERALITES

Partie 1 : La réponse immunitaire innée

1. Le système immunitaire inné et la vaccination

Le système immunitaire inné constitue la première ligne de défense d'un organisme contre les agents pathogènes et les éléments étrangers ayant réussis à passer les barrières physiques et physiologiques. Il se caractérise par 2 fonctions majeures :

- La reconnaissance des agents infectieux de manière non-spécifique, discriminant les éléments du soi et du non-soi.
- La destruction des envahisseurs par la mise en place d'un large éventail de réponses immunitaires.

La détection des agents pathogènes passe par l'intermédiaire de récepteurs de reconnaissance de motifs moléculaires ou PRRs (Janeway, 1989) qui sont exprimés de manière constitutive par les cellules immunitaires de notre organisme comme les cellules dendritiques, les macrophages ou les neutrophiles (Kawai and Akira, 2010). Ces PRRs vont reconnaître des motifs moléculaires associés aux pathogènes (PAMPs), qui sont très conservés entre les groupes de pathogènes et essentiels à leur cycle de vie, ou bien des motifs moléculaires associés aux dégâts (DAMPs) qui sont libérés lors de dommages cellulaires ou tissulaires suite à une infection ou à une inflammation. La reconnaissance des PAMPs et DAMPs par les PRRs va permettre une induction rapide de la réponse immunitaire innée par l'organisme grâce à l'activation de nombreuses voies de signalisation complexes aboutissant à la mise en place d'une réponse pro-inflammatoire protectrice médiée par de nombreuses cytokines et chémokines facilitant l'élimination du pathogène.

Caractérisée par sa vitesse de mise en place permettant le développement d'une protection rapide (dès les premières minutes après l'infection par un pathogène), la réponse immunitaire innée décline néanmoins rapidement via de nombreux mécanismes de rétrocontrôles négatifs. Cela permet notamment de limiter les dommages tissulaires qui pourraient être engendrés à cause de ses mécanismes effecteurs non-spécifiques. De plus, la réponse immunitaire innée n'est pas douée d'une mémoire immunologique, l'empêchant donc d'être plus rapide ou plus efficace lors d'un second contacte avec un même agent pathogène. Ainsi, afin d'engendrer une réponse protectrice sur le long terme contre les pathogènes, la réponse immunitaire innée va permettre l'activation de la deuxième ligne de défense : le système immunitaire adaptatif. Bien souvent décrit comme 2 systèmes distincts, il faut plutôt les considérer comme 2 entités collaborant étroitement et se superposant. En effet, Il est à présent avéré que la bonne stimulation du système immunitaire inné est un facteur indispensable à la génération d'une réponse immunitaire adaptative protectrice et durable dans le cadre de la vaccination. Ce sont notamment les cellules présentatrices de l'antigène « professionnelles » (CPAs) appartenant à la réponse immunitaire innée qui vont permettre l'activation de la réponse immunitaire adaptative

via la présentation d'antigènes. De même, le système immunitaire adaptatif possède de nombreuses cellules exprimant des récepteurs de reconnaissance de la réponse immunitaire innée, et utilise en tant qu'effecteurs finaux de nombreuses cellules et molécules appartenant à la réponse immunitaire innée (**Figure 1**).

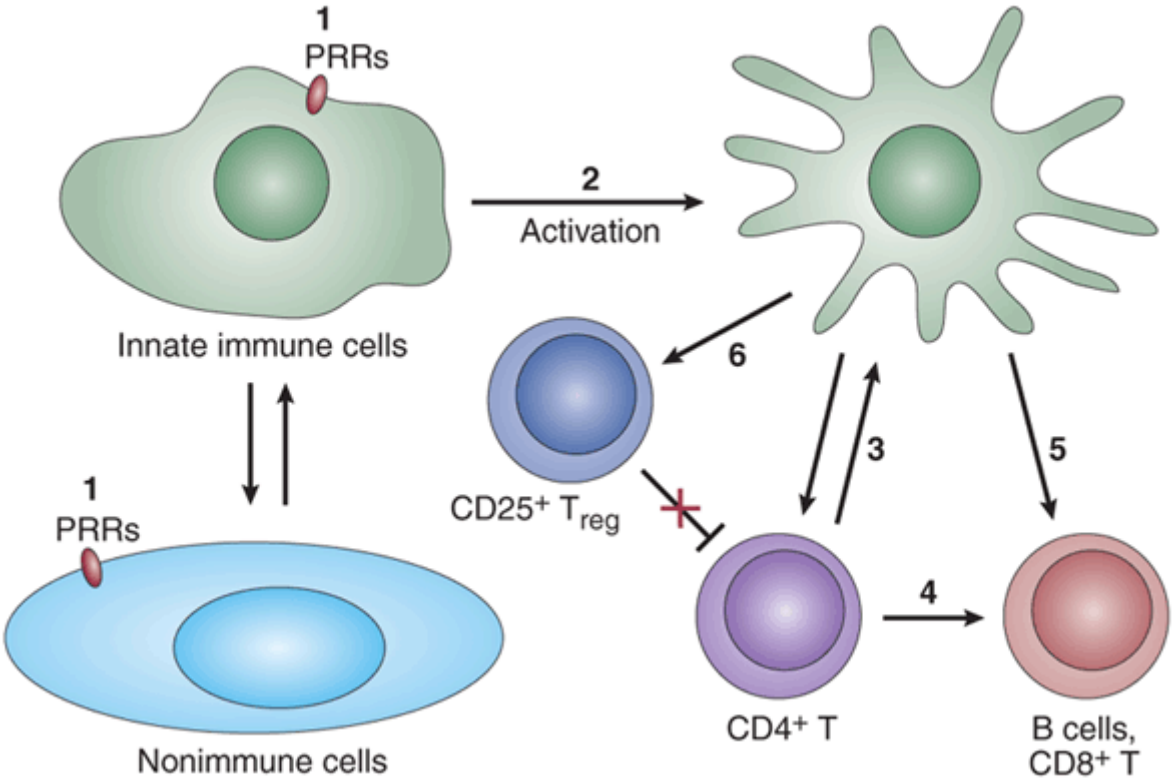


Figure 1 ; Initiation de la réponse immunitaire. Au cours de la vaccination, (1) les PAMPs des agents pathogènes ou les Ag vaccinaux vont pouvoir être reconnus par les cellules immunitaires résidentes ou certaines cellules non-immunitaires, ce qui va engendrer la production de cytokines et de chémokines. (2) Certaines cellules immunitaires, les cellules présentatrices de l'antigène (CPAs) vont pouvoir suite à la reconnaissance de leur Ag, s'activer, migrer dans les ganglions lymphatiques, et aller stimuler les cellules de la réponse immunitaire adaptative. (3) Lors de la reconnaissance de l'Ag, les cellules immunitaires adaptatives vont alors pouvoir s'activer et commencer leur expansion clonale. (4) L'interaction entre les Lymphocytes T helpers et les lymphocytes B permet l'activation des lymphocytes B, leur expansion et leur conversion en plasmocytes afin de pouvoir sécréter des anticorps spécifiques. (5) Les cellules dendritiques peuvent également activer directement les lymphocytes T CD8 pour les éduquer et leur permettre de devenir des lymphocytes T cytotoxiques (LTc), ou bien (6) sécréter des facteurs solubles qui vont supprimer l'effet immunosuppresseur des lymphocytes T régulateur CD25+. Une partie des cellules de la réponse immunitaire adaptative vont également se transformer en cellules mémoires, et permettre lors d'une seconde rencontre d'induire une réponse immunitaire plus rapide et plus efficace (d'après Pashine et al., 2005).

Le rôle des CPA apparaît ainsi crucial afin d'induire une réponse immunitaire efficace dans le cadre de protocoles vaccinaux. En effet, même si toutes les cellules nucléées de l'organisme sont capables de présenter des antigènes intracellulaires grâce aux molécules de CMH de type I (« complexe majeure d'histocompatibilité de type I ») qu'elles expriment à leur surface, seulement les CPAs peuvent reconnaître les antigènes extracellulaires, mais également migrer au sein des ganglions lymphatiques afin d'activer les cellules de l'immunité adaptative. Parmi elles, deux populations cellulaires sont d'une importance toute particulière :

- Les cellules dendritiques qui sont reconnues comme étant les cellules clefs dans la réponse immunitaire innée mais également dans l'initiation de la réponse immunitaire adaptative. Elles sont Issues de la famille des monocytes et sont présentes dans un état immature au sein des tissus périphériques exposés à l'environnement extérieur (tels que la peau, les poumons ou l'intestin). Lors de la reconnaissance d'antigènes et de pathogènes par l'intermédiaire d'un large panel de PRRs (Cerboni et al., 2013), elles vont être capables de les capturer par phagocytose ou endocytose, et de les présenter à leur surface sous formes de peptides associés aux molécules de CMH de classe I ou II. Cela va induire leur maturation, leur migration en direction des organes lymphoïdes secondaires, l'augmentation de l'expression de leurs molécules de CMH, ainsi que la surexpression de leurs molécules de co-stimulation (B7-1 et B7-2) afin de permettre l'activation des lymphocytes T en cellules effectrices ou mémoires dans le but de lutter efficacement contre les infections en cours ou à venir (**Figure 2**) (van den Boorn et al., 2012).

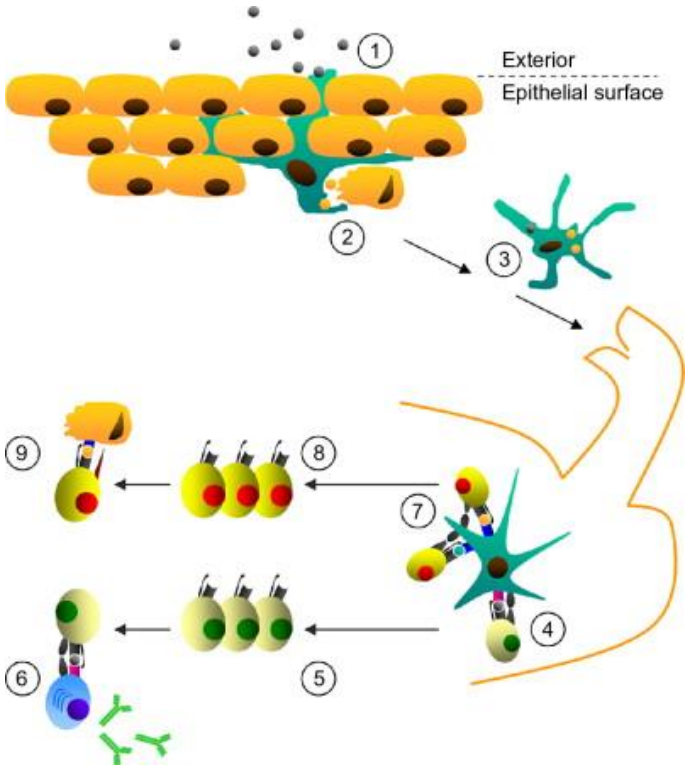


Figure 2 : Initiation de la réponse immunitaire adaptative par les CPAs. Les cellules présentatrices de l'antigène (comme les cellules dendritiques) résident au niveau des tissus périphériques exposés à l'environnement extérieur afin de détecter la présence de constituants issus de pathogènes ou bien d'agents vaccinaux (1), ainsi que des débris de cellules stressées ou mourantes (2). Lors de leur activation, les cellules dendritiques vont pouvoir migrer dans les nœuds lymphatiques (3) où elles vont acquérir un phénotype fortement immunoimmunostimulateur et procéder à la dégradation des antigènes en peptides afin de les présenter sur leur CMH de classe I ou II. (4) Les cellules dendritiques vont pouvoir activer les LTh (Lymphocytes T helper) en leur présentant les antigènes via leur CMH de classe II. (5) Les LTh activés vont pouvoir proliférer et aider à la maturation des lymphocytes B en plasmocytes afin qu'ils puissent sécréter des anticorps spécifiques (6). (7) De manière simultané, ses cellules dendritiques peuvent également activer les lymphocytes T CD8+ en leur présentant les antigènes via le CMH de classe I, ce qui va permettre leur prolifération (8), leur migration vers le site infecté, et leur différenciation en LTc (van den Boorn et al., 2012).

- Les macrophages, également des cellules appartenant à la famille des monocytes. Ils peuvent être issus de la différenciation de monocytes recrutés sur le site de l'infection, ou de monocyte « résidents » car présents à des endroits spécifiques de l'organisme susceptibles aux infections (foie, poumon…) ou stratégiques (rate…) pour pouvoir se déployer rapidement en cas d'infections par des agents pathogènes (Ginhoux and Jung, 2014). Les macrophages vont pouvoir reconnaître les PAMPs, DAMPs et les antigènes via leurs PRRs afin d'aider à la suppression des agents infectieux et des cellules endommagées ou mortes. Cela va s'effectuer grâce au phénomène de phagocytoses ainsi que la sécrétion de cytokines et chémokines permettant le recrutement de nouvelles cellules immunitaires. Contrairement aux cellules dendritiques, les macrophages vont devoir être préalablement activés par la présence de produits bactériens (comme le LPS) ou la sécrétion d'IFNγ (par les lymphocytes T) pour exprimer à la fois le CMH de classe II leur permettant de présenter les antigènes aux cellules du système immunitaire adaptatif, mais également leurs molécules de co-stimulation B7. Cela fait, ils vont pouvoir à leur tour stimuler les lymphocytes T effecteurs et mémoires.

2. Les récepteurs de l'immunité innée ou PRRs

La plupart des récepteurs de l'immunité innée découverts et caractérisés peuvent être classés en 5 grandes familles en fonction des homologies entre leurs domaines protéiques. On distingue généralement les TLRs *(« Toll-like receptors »*), les CLRs (« *C-type lectin receptors* »), les NLRs (« *NOD-Like receptors »*), les RLRs (« *RIG-Like receptors »*) et les CDS (« *cytosolic DNA sensors* »).

De plus, en fonction de leur localisation cellulaire, ces familles peuvent elles-mêmes être regroupées en deux catégories :

- Les récepteurs membranaires (TLRs et CLRs) localisés au niveau de la membrane plasmique des cellules ou bien dans la membrane des endosomes. Ils vont reconnaître respectivement la présence de ligands microbiens dans l'espace extracellulaire ou dans le compartiment endosomal.
- Les récepteurs intracytoplasmiques (NLRs, RLRs et CDS) qui vont reconnaître la présence de pathogènes intracellulaires.

Cette compartimentation des récepteurs joue un rôle majeur dans le développement de la réponse immunitaire. Tout d'abord, elle évite une activation des PRRs par des molécules du soi partagées avec les agents pathogènes (comme les acides nucléiques) et ainsi prévient une réponse auto-immune. De plus, en fonction de la localisation du récepteur (Cytoplasmique ou membranaire), des voies de signalisation différentes vont être mises en place.

Un des composants majeurs de la réponse immunitaire induite par les PRRs est l'activation de facteurs de transcription, qui vont induire la production de messagers chimiques essentiels à l'initiation d'une immunité innée et adaptative : Les cytokines pro-inflammatoires et les interférons (IFNs) de type 1. De plus, les PRRs vont également initier des mécanismes non-transcriptionnels tels que l'induction de la phagocytose, de l'autophagie, de la mort cellulaire et la maturation de certaines cytokines par l'intermédiaire de voies de transduction étroitement contrôlées.

2.1. Les récepteurs membranaires

2.1.1 Les récepteurs *Toll-like* (TLRs)

2.1.1.1 Structure

Les TLRs sont actuellement les récepteurs les plus étudiés, les mieux caractérisés, et sont considérés comme étant les premiers détecteurs des agents pathogènes au cours d'une infection. Ce sont des récepteurs de signalisation membranaires, présents au sein des cellules de l'immunité innée, de l'immunité adaptative, mais également chez les cellules non-immunitaires. Cette famille de récepteur comporte 13 membres, 10 chez l'Homme (TLR1-TLR10) et 12 chez la souris (TLR1-TLR9 et TLR11-13), qui sont localisés :

- Soit au niveau de la membrane plasmique des cellules pour les TLR1, 2, 4, 5, 6 et 10, afin de reconnaître des PAMPs dérivés de bactéries, champignons, ou protozoaires.
- Soit au niveau de la membrane endosomale pour les TLR3, 7, 8, 9, 11 et 13, afin de détecter des PAMPs dérivés de nombreux virus et bactéries sous forme d'acides nucléiques (Kawai and Akira, 2010).

D'un point de vue structural, les TLRs sont des glycoprotéines de type 1 membranaires constituées : d'un domaine extracellulaire LRR (« *Leucine-Rich Repeat* ») comportant 19 à 25 copies en tandem de motifs riches en leucine permettant la reconnaissance des PAMPs, d'un domaine transmembranaire, et d'un domaine cytoplasmique TIR (« *Toll/IL-1 Receptor* ») très conservé, composé d'environ 200 acides aminés et comprenant 3 boîtes essentielles pour la mise en place de la signalisation intra-cytoplasmique (**Figure 3**).

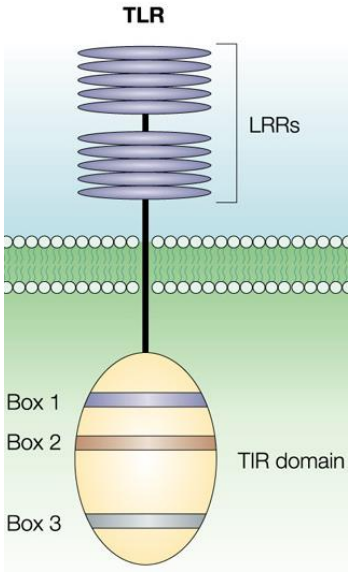


Figure 3 : Structure des TLRs. Le domaine extracellulaire LRR comporte 19 à 25 copies en tandem de motifs riches en leucine, composés chacun de 24 à 29 acides aminés. Le domaine intracellulaire TIR est caractérisé par la présence de 3 régions extrêmement conservées (aussi appelé les boîtes 1, 2 et 3) essentielles pour la signalisation (modifiée d'après Akira and Takeda, 2004).

2.1.1.2. Signalisation

Lors de l'interaction avec leurs ligands via leurs domaines LRRs extracellulaires, les TLRs vont s'associer en homo- ou en hétérodimères, permettant le recrutement de différentes molécules adaptatrices contenant un domaine TIR :

- MyD88 (« *Myeloid differentiation primary response gene 88* »)
- TRIF (« *TIR-domain-containing adapter-inducing interferon-β* »)
- TIRAP (« *Toll-interleukin 1 receptor domain-containing adapter protein* »)
- TRAM (« *TRIF-related adaptor molecule* »).

Le recrutement de ces différentes protéines va permettre l'activation de nombreux facteurs de transcription comme NFκB (« *nuclear factor kappa-light-chain-enhancer of activated B cell* ») et les IRFs (« *Interferon regulatory factors* »), l'activation de la voie des MAPKs (« *mithogen-activated protein kinases* »), et ainsi permettre la production de cytokines pro-inflammatoires, de chémokines, d'interférons de type 1 et de molécules de co-stimulation (Akira et al., 2006). L'ensemble des voies de signalisation est présenté sur la **Figure 4**.

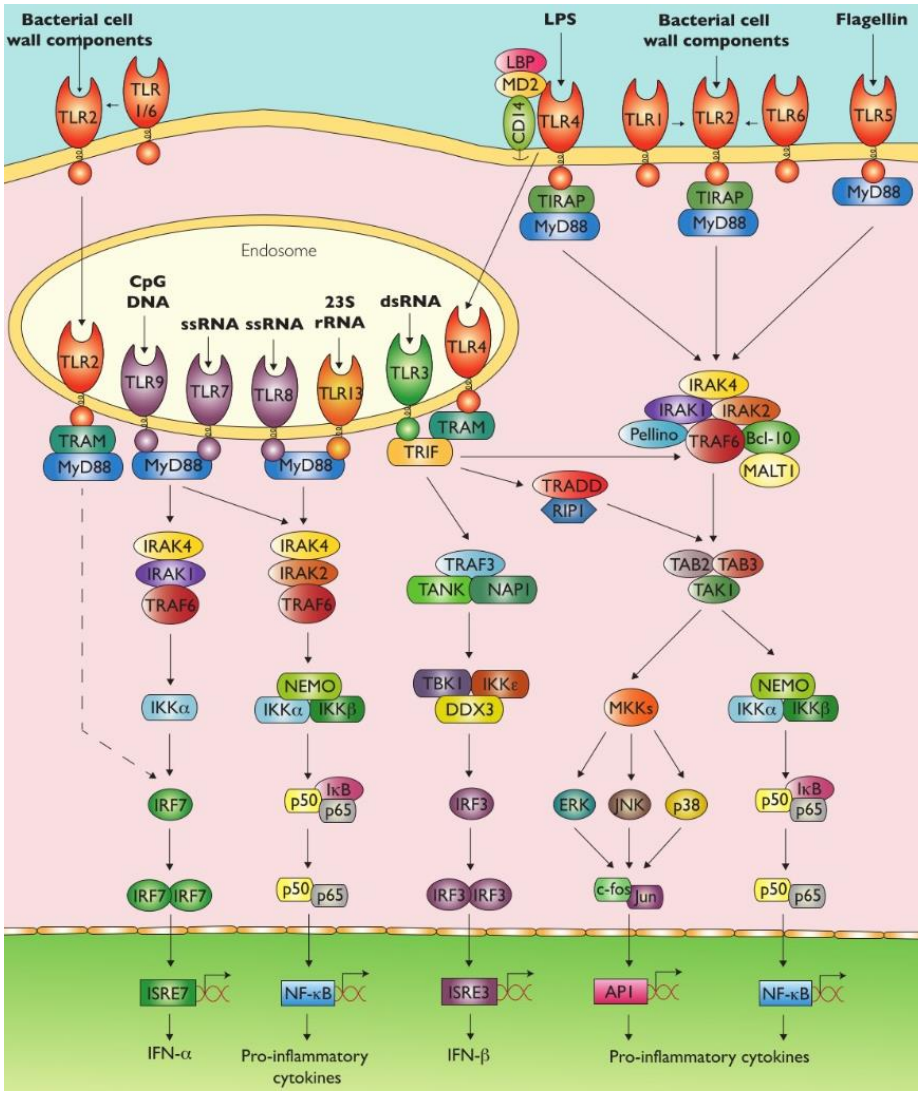


Figure 4 : Voies de signalisation et ligands des différents TLRs. Les TLR10, 11 et 12 ne sont pas mentionnés (source : www.invivogen.com).

Suite à la reconnaissance de leurs ligands respectifs, tous les TLRs (à l'exception du TLR3) vont pouvoir recruter la protéine adaptatrice MyD88 et mettre en place une voie de signalisation MyD88-dépendante de manière séquentielle :

- Tout d'abord, MyD88 va pouvoir soit interagir directement avec les TLRs via son domaine C-terminal TIR, soit indirectement par l'intermédiaire de la protéine adaptatrice TIRAP (pour les TLR 1, 2, 4 et 6).
- Puis, MyD88 va ensuite s'oligomériser pour former un complexe protéique du nom de myddosome, composé de 6 à 8 molécules de MyD88, de TIRAP, et de protéines de signalisation de la famille des IRAKs (« *Interleukin-1 receptor-associated kinase* »). IRAK4 va être le premier membre de cette famille recruté au niveau du myddosome, afin de permettre la phosphorylation et l'activation de IRAK1 et IRAK2 pour qu'ils puissent interagir avec MyD88, mais également avec la protéine TRAF6 (« *TNF receptor associated factor* 6»).
- Enfin, TRAF6 va permettre le recrutement d'un complexe protéique contenant TAK1 («*Transforming growth factor beta-activated kinase 1* »), qui à son tour va pouvoir activer le facteur de transcription NFκB et les MAPKs afin d'initier la transcription et la traduction de nombreuses cytokines pro-inflammatoires, chémokines, IFNs et autres gènes TLRs-inductibles.

Pour le TLR3, mais également pour le TLR4, c'est la protéine adaptatrice TRIF qui va être recrutée lors de la reconnaissance de leurs ligands, induisant ainsi une voie de signalisation TRIF-dépendante. Pour cela, TRIF va interagir directement avec le TLR3, ou bien avoir besoin de la molécule adaptatrice TRAM pour le TLR4, et permettre :

- Le recrutement de TRAF6 et la mise en place de cascades de signalisation similaires à la voie MyD88.
- Le recrutement de la protéine TRADD (« *TNFR-1-associated death domain* ») et ainsi former un complexe multi-protéique permettant l'activation du facteur de transcription NFκB.
- Ou bien l'interaction avec TRAF3 afin de recruter des protéines non-canoniques de la famille des IKKs (« *IκB kinases* »), comme TBK1 (« *TANK-binding kinase* 1 ») et IKKε, et induire l'activation des IRF3, leur translocation dans le noyau et la transcription des gènes des interférons de types 1.

2.1.2. Les récepteurs des lectines de type C (CLRs)

2.1.2.1. Structure

Il existe des centaines de CLRs regroupés en 17 groupes différents et extrêmement hétérogènes (Zelensky and Gready, 2005), reconnaissant une large variété de PAMPs issus d'agents pathogènes. Ces récepteurs peuvent être solubles ou liés à des membranes cellulaires, et possèdent tous un domaine CTLD (« *C-type lectin-like domain* ») pouvant lier le calcium, les carbohydrates, mais également de nombreux autres ligands.

La plupart des CLRs agissent comme des opsonines, en se liant à des antigènes afin de faciliter leur phagocytose par les cellules immunitaires (et n'activent donc pas directement de voies de signalisation). Cependant, certains d'entre eux sont capables d'initier des cascades de signalisation intracellulaires aboutissant à la production d'une réponse immunitaire pro-inflammatoire. C'est notamment le cas de la dectine-1, un récepteur exprimé spécifiquement dans certaines cellules immunitaires (cellules dendritiques, macrophages, leneutrophiles et monocytes), qui est une protéine transmembranaire de type 2 constituée :

- D'un domaine extracellulaire CTLD atypique, qui ne nécessite pas la liaison préalable de calcium pour reconnaître son ligand.
- D'une queue intracellulaire possédant un motif ITAM (« *Immunoreceptor Tyrosine-based Activation Motif* ») modifié, appelé hemITAM.

2.1.2.1. Signalisation induite par la dectine-1

Lors de la reconnaissance de molécules de la famille des β-glucanes ou les immunoglobulines A (IgA), la dectine-1 va initier son internalisation par phagocytose et induire une cascade de signalisation intracellulaire régulant l'expression et la production de cytokines (Hoving et al., 2014). Cette signalisation est engendrée par deux voies différentes : la voie SyK (« *spleen tyrosine kinase* ») dépendante ou indépendante.

Pour la voie SyK-dépéndante, la dimérisation de la dectine-1 après la reconnaissance de son ligand va permettre le recrutement de SyK via les domaines hemITAM intracellulaires, et engendrer sa phosphorylation par les kinases SRKs (« *Src family kinases* »). Une fois phosphorylée, SyK va pouvoir activer la PLCγ2 (« phospholipase C gamma-2 ») qui va alors hydrolyser du PIP2 (« phosphatidylinositol-4,5-bisphosphate ») en IP3 (« inositol 1,4,5-trisphosphate ») et en DAG (« diacylglycerol »). L'IP3 va alors soit initier la libération du calcium du réticulum endoplasmique vers le cytoplasme afin de permettre l'activation du facteur de transcription NFAT (« *Nuclear factor of activated T-cells* ») (Goodridge et al., 2007), soit agir en coopération avec le DAG et jouer le rôle de messager secondaire régulant l'activation de la voie canonique du NFκB (**Figure 5**).

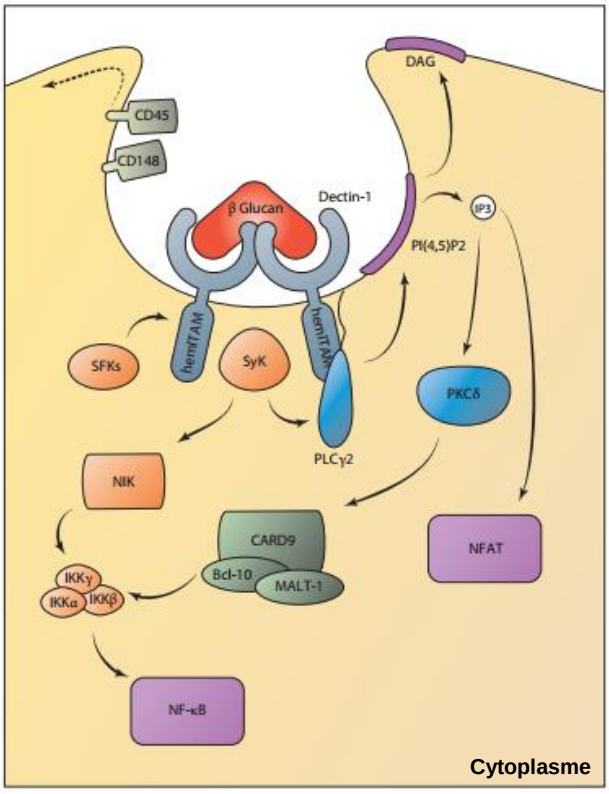


Figure 5 : Voie de signalisation de la Dectine-1. La reconnaissance des β-glucanes par la Dectine-1 permet l'activation des voies de signalisation NFκB et NFAT (d'après Brubaker et al., 2015).

La voie SyK-indépendante quant à elle, permet la répression de l'activation de la voie non-canonique du NFκB, en induisant la phosphorylation de la sous-unité p65 du NFκB par l'intermédiaire de la protéine Raf-1. Cela va inhiber la formation du complexe de signalisation et permettre une régulation fine de la libération de cytokines pro-inflammatoires (Gringhuis et al., 2009).

2.2. Les récepteurs cytoplasmiques

2.2.1. Les récepteurs NOD-Like (NLR)

Les NLRs sont des récepteurs intracellulaires au nombre de 22 chez l'Homme et de 34 chez la souris. Ils reconnaissent les PAMPs entrés dans la cellule via des pores ou phagocytoses, ainsi que différents DAMPs. Ils sont composés de 3 éléments :

- Un domaine LRR, qui permet la reconnaissance du ligand.
- Un domaine central NACHT/NOD (« *nucleotide-binding domain* »), qui permet l'oligomérisation des récepteurs et la création d'un complexe de signalisation actif.
- Un domaine variable CARD (« *caspase recruitment domain* »), ou PYD (« *pyrin domain* »), ou BIR (« *baculovirus inhibitor repeats* »), ou AD (« *acidic transactivating domain* »), qui permet d'activer différentes voies de signalisation cellulaires.

Classiquement, ces récepteurs peuvent engendrer 4 grandes catégories fonctionnelles : L'activation de la transduction du signal par la voie NFκB et des MAPKs, l'induction de l'autophagie, l'activation de la transcription, et l'assemblage de l'inflammasome (Motta et al., 2015).

2.2.1.1. NOD1 et NOD2

NOD1 et NOD2 (aussi connus sous les noms de CARD4 et CARD5) sont les NLRs les mieux caractérisés et décris. Ils sont composés d'un domaine LRR c-terminal, d'un domaine d'oligomérisation, et d'une partie n-terminale comprenant 1 (NOD1) ou 2 (NOD2) domaines CARDs. Localisés dans le cytoplasme d'une grande variété de cellules mais également au sein de certaines membranes plasmiques, ils vont reconnaitre les peptidoglycanes qui constituent majoritairement les parois bactériennes.

Lors de la reconnaissance de leurs ligands, ces récepteurs vont s'oligomériser et permettre le recrutement de la protéine adaptatrice RIP2 (« receptor-interacting protein 2 ») grâce à leurs domaines CARDs. RIP2 va alors pouvoir activer la voie NFκB et des MAPKs, permettant l'expression et la production de cytokines (**Figure 6**) (Saxena and Yeretssian, 2014).

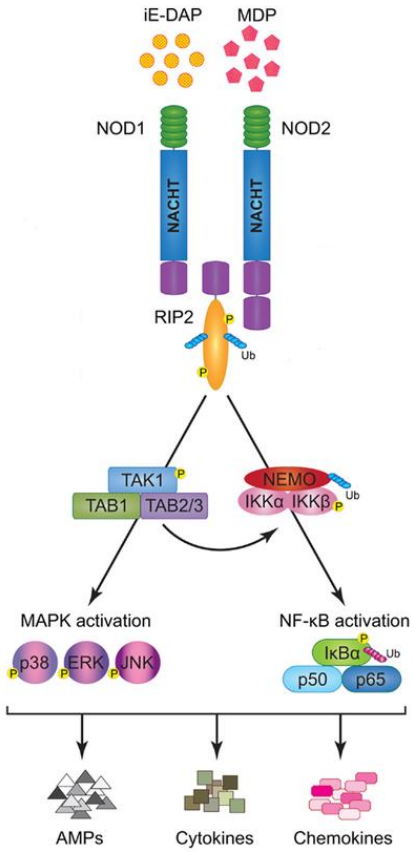


Figure 6 : Voies de signalisation de NOD1 et NOD2. Après la reconnaissance de leurs ligands, les NODs vont recruter la protéine adaptatrice RIP2 via leur domaine CARD, et permettre l'activation de la voie NFκB et de la voie des MAPKs (modifiée d'après Saxena and Yeretssian, 2014).

2.2.1.2. L'inflammasome

La stimulation de cellules immunitaires (comme les macrophages ou les cellules dendritiques) par des PAMPs peut aboutir à la formation d'un complexe protéique appelé inflammasome, composé de protéines de la famille des NLRs (NLRP3, NLRC4, NLRP1), ou de la protéine AIM2 (« *absent in melanoma 2* ») ou bien de la protéine ASC (« *apoptosis-associated speck-like protein containing a CARD* »). Cet assemblage protéique va s'associer avec une caspase inactive, la procaspase-1 et l'activer par clivage en caspase-1 (**Figure 7 A**). Puis à son tour, cette caspase va permettre le clivage et la maturation des interleukines 1β (IL-1β) et 18, aboutissant à leurs sécrétions dans le milieu extracellulaire (**Figure 7 B**) (Schroder and Tschopp, 2010).

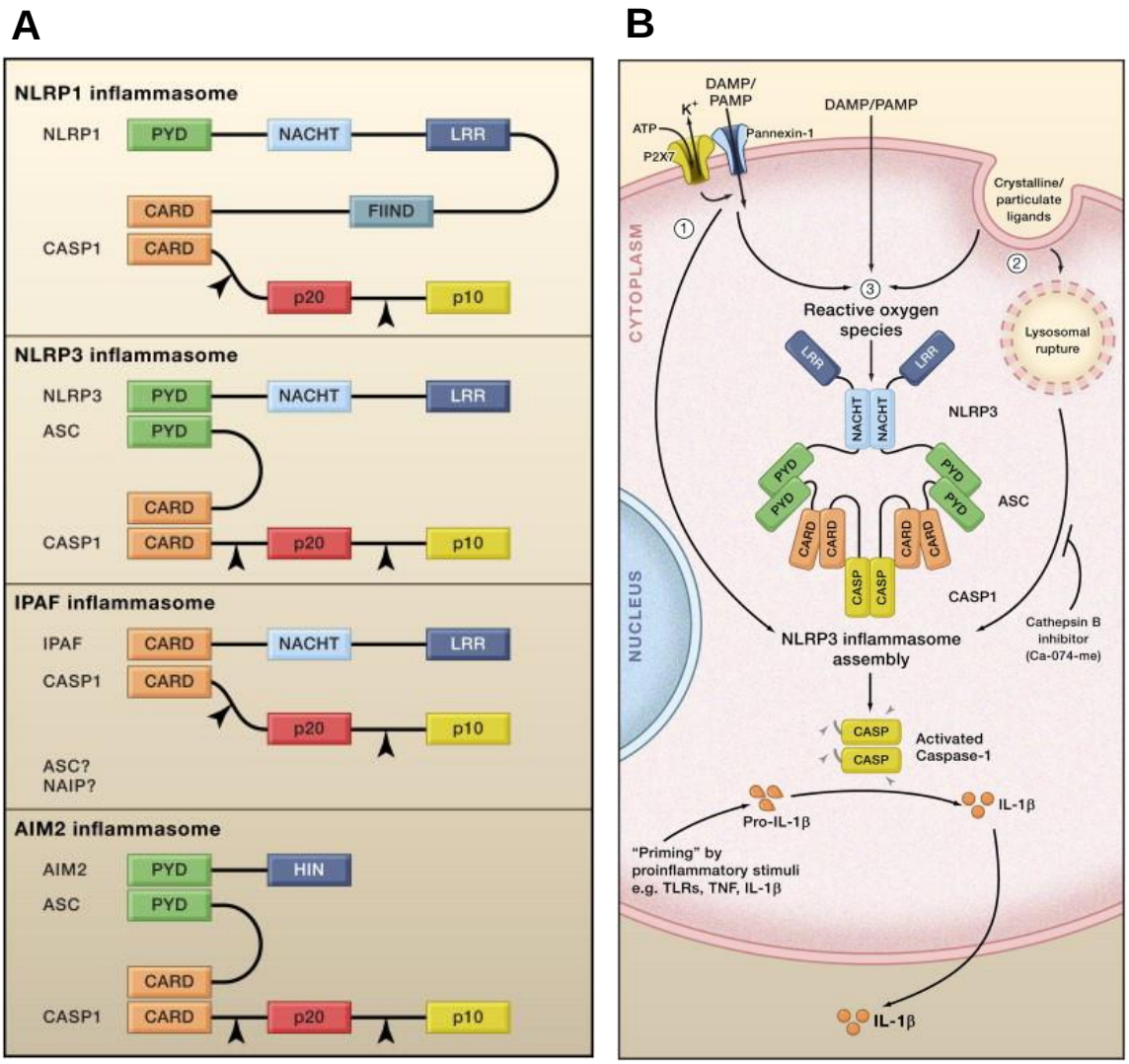


Figure 7 : Structure et voie de signalisation des différents inflammasomes. (A) Structure de l'inflammasome NLRP1, NLRP3, NLRC4 (ou IPAF), et AIM2. (B) Voie de signalisation de l'inflammasome NLRP3. Tous les DAMPS et les PAMPs vont permettre la génération de ROS (« *reactive oxygen species* ») qui vont être reconnus et engendrer la formation de l'inflammasome NLRP3. Cela va aboutir à l'activation de la Caspase-1, qui va à son tour induire la maturation et la sécrétion de cytokines pro-inflammatoires comme l'interleukine-1β et 18 (modifiée d'après Schroder and Tschopp, 2010).

2.2.2. Les récepteurs *RIG-Like* (RLR)

Les RLRs constituent une famille de récepteurs cytoplasmiques, reconnaissant les acides ribonucléiques viraux doubles brins (ARNdb) ou simples brins (ARNsb), composée de 3 membres : RIG-1(« *retinoic-acid-inducible protein 1* »), MDA-5 (« *melanoma-differentiation-associated gene 5* ») et LGP2 (« *laboratory of genetics and physiology 2* »).

RIG-I et MDA-5 possèdent une voie de signalisation commune. En effet, lors de la détection d'ARN, ils recrutent la molécule adaptatrice IPS-1 (« *interferon-beta promoter stimulator 1* ») qui va induire la transduction du signal par l'intermédiaire de la voie NFκB, des IRF3 et des IRF7 (Kawai et al., 2005). Cela va engendrer la production d'une réponse pro-inflammatoire ainsi que la sécrétion d'interférons de type 1. Quant à LGP2, il ne possède pas de domaine de transduction du signal. Il va donc agir comme un rétrocontrôle négatif de la voie de signalisation, soit en se liant de manière compétitive à l'ARN et en formant un complexe protéique avec IPS-1, soit en se liant directement à RIG-1 par l'intermédiaire d'un domaine de répression (Saito et al., 2007). La voie de signalisation des RLRs est synthétisée dans la **Figure 8** et ces récepteurs seront davantage développés dans la **Partie 2** (**2.2**.1. Les RLRs) de ce manuscrit.

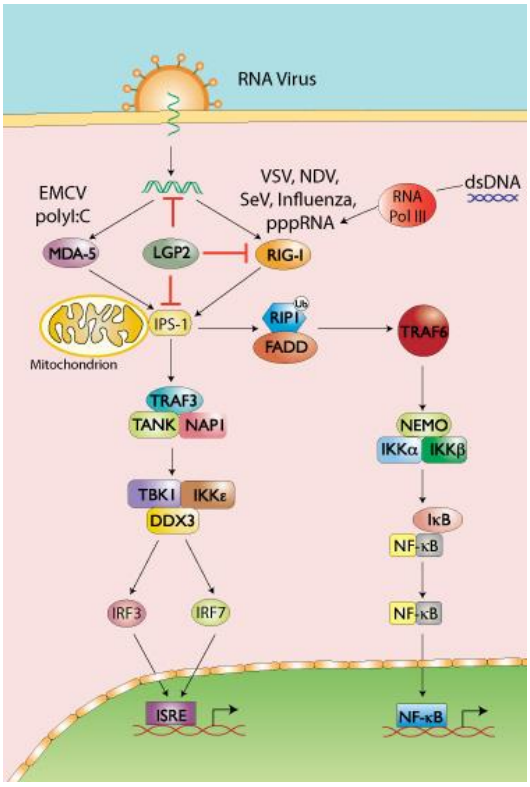


Figure 8 : Voies de signalisation et ligands des RLRs (Modifiée depuis www.invivogen.com).

2.2.3. Les récepteurs cytosoliques d'ADN (CDS)

Les CDS sont des récepteurs intracellulaires qui permettent la reconnaissance des acides désoxyribonucléiques doubles brins (ADNdb) du soi ou du non-soi, présents de manière aberrante dans le cytoplasme des cellules eucaryotes. La grande diversité de ces récepteurs n'en fait pas moins un système de reconnaissance de l'ADNdb très redondant, permettant l'activation de nombreuses voies de signalisation notamment via :

- Le recrutement de différentes protéines adaptatrices telles que STING *(« stimulator of interferon gene »*) (Ishikawa and Barber, 2008), la β-caténine (Yang et al., 2010), et MyD88 (Kim et al., 2010), afin d'initier la transduction de signaux au travers de la voie NFκB et des IRFs, aboutissant à la production de cytokines pro-inflammatoires, de chémokines et d'interférons de type 1 et 3 (Zhang et al., 2011a)
- La formation de l'inflammasome (Jones et al., 2010).

L'ensemble de ces récepteurs et voies de signalisation sont résumés dans la **Figure 9** et seront détaillés dans la **Partie 2** (**2.2**.2. Les CDS) de ce manuscrit.

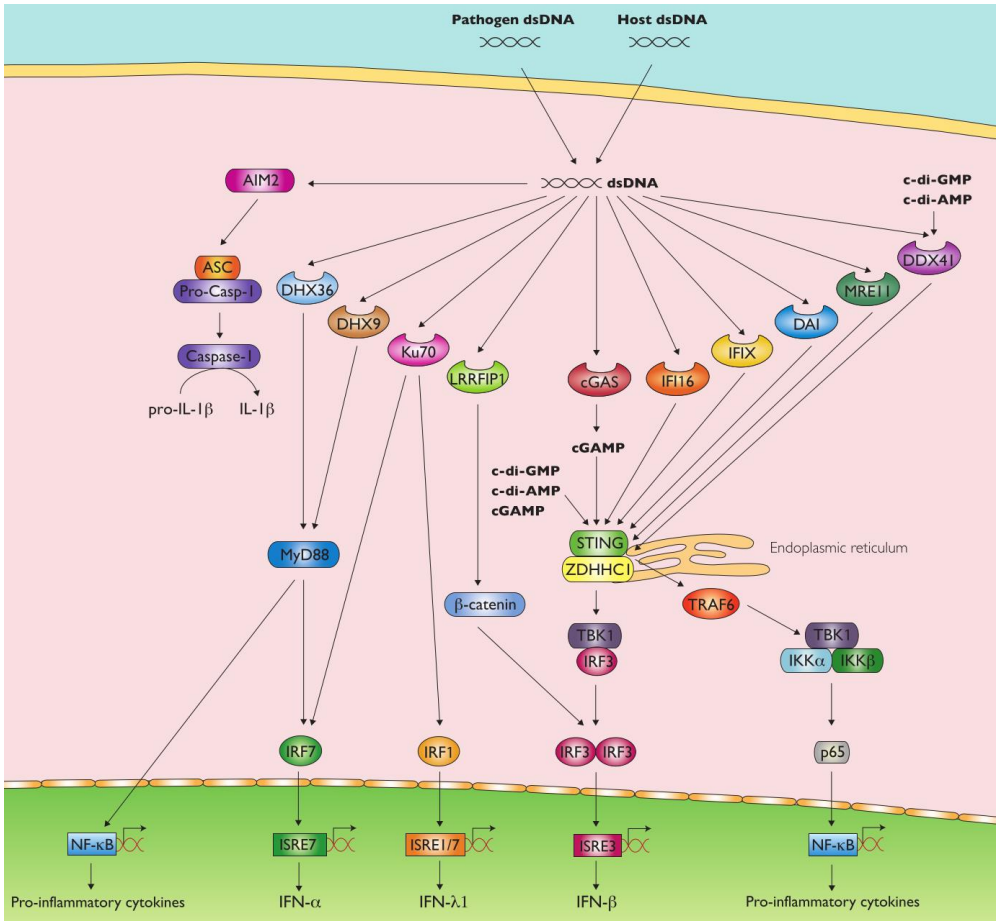


Figure 9 : Voies de signalisation et ligands des CDS (Modifiée depuis www.invivogen.com).

3. Les PAMPS ou ligands de la réponse immunitaire innée

Le répertoire des différents PRRs exprimés par les organismes est extrêmement varié, à l'image de la diversité des pathogènes qu'il peut détecter. Cette reconnaissance est par ailleurs basée sur la composition biochimique légèrement différente de ces agents pathogènes, ainsi que sur leur cycle de vie très éloigné de celui de l'hôte. De plus, pour une même classe de pathogènes, sa détection par le système immunitaire inné va s'effectuer par une multitude de PRRs qui vont détecter de nombreux PAMPs, et ainsi activer différentes voies de signalisation afin d'engendrer à une réponse inflammatoire protectrice comme résumé dans la

Figure 10 (Akira et al., 2006).

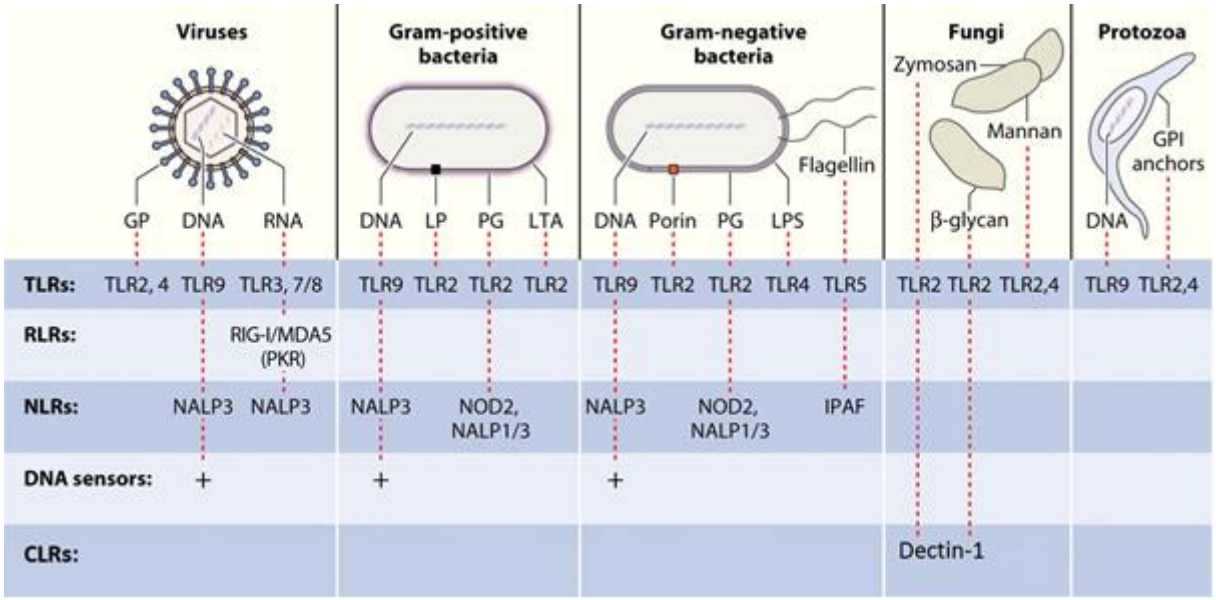


Figure 10 : Reconnaissance des PAMPs appartenant à différentes classes de pathogènes. Les virus, bactéries, champignons et protozoaires possèdent de nombreux PAMPs parfois partagés entre ces différentes classes de pathogènes. Les PAMPs majeures sont les acides nucléiques (ADNdb, ARNsb, l'ARNdb, et ARN 5'-triphosphate), les glycoprotéines de surface (GP), les lipoprotéines (LP) et les composants des membranes des pathogènes comme les peptidoglycanes (PG), l'acide lipotéichoïque (LTA), les lipopolysaccharides (LPS) et les Glycosylphosphatidylinositol (GPI anchors) (Modifiée d'après Mogensen, 2009).

3.1. Le lipopolysaccharide (LPS)

Le LPS est le composant majeur de la paroi des bactéries Gram négative, les protégeant de leur environnement extérieur. Il est composé de 3 domaines : Le lipide A ancré dans la membrane, une partie centrale oligosaccharidique, et l'antigène O extracellulaire (**Figure 11 A**).

Le lipide A est le PAMP majeur du LPS. Il est composé d'un squelette possédant des motifs disaccharidiques mono- ou di-phosphorylés et de chaînes d'acides gras acétylées. De plus, c'est le niveau de phosphorylation et d'acétylation de ces structures qui détermine les propriétés immunostimulantes du LPS (Albiger et al., 2007).
Afin d'induire la réponse immunitaire, le LPS va interagir avec de nombreuses protéines à la surface de la cellule. Tout d'abord la LBP (« LPS binding protein »), une protéine soluble, va directement se lier avec le LPS dans le milieu extracellulaire et favoriser son association avec la protéine CD14 (« cluster de différenciation 14 »). Puis, le CD14 va permettre le transfert de manière efficace du LPS vers le complexe TLR4/MD-2 (« *myeloid differentiation factor 2* ») et ainsi activer les voies de signalisation MyD88- et TRIF-dépendante aboutissant à la production de cytokines pro-inflammatoires, de chémokines, et d'interférons de type 1 (Lu et al., 2008) (**Figure 11 B**).

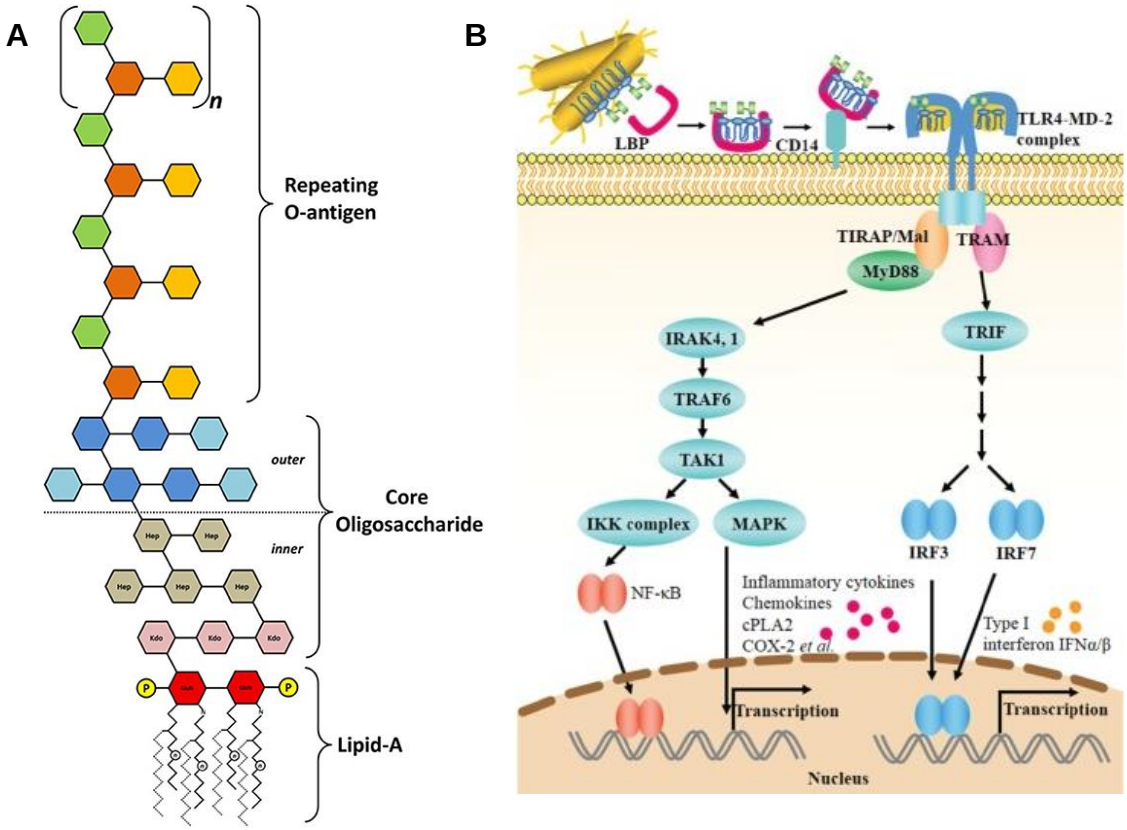


Figure 11 : Réponse immunitaire de l'hôte au LPS, via la voie de signalisation TLR4-MD2. (A) Structure du LPS. (B) Le LPS de la membrane extérieure des bactéries Gram négative est reconnu par la LBP. Le complexe LBP-LPS va ensuite interagir avec la protéine CD14 permettant le transfert du LPS vers le complexe TLR4-MD2, et ainsi induire l'initiation de la signalisation intracellulaire MyD88- et TRIF-dépendante (Serrato, 2014; Wang et al., 2015).

3.2. Le peptidoglycane (PGN)

Le peptidoglycane (PGN) est un composé de la paroi des bactéries assurant le maintien de sa forme, et lui conférant une protection contre les changements de pression osmotique. Il est présent sous deux formes :

- Une fine couche entre les membranes des bactéries Gram négative.
- Une couche épaisse entourant la membrane des bactéries Gram positive.

Le PGN est constitué de chaines linéaires de sucres (N-acetylglucosamines et acides N-acetylmuramiques), reliées entre elles par des ponts peptidiques afin de former de larges macromolécules entourant la membrane cytoplasmique (**Figure 12 A**). La reconnaissance des PGNs va s'effectuer au niveau de la membrane extracellulaire des cellules par le TLR2, uniquement après avoir été libérés suite à un remodelage de la paroi bactérienne, son autolyse ou bien l'action de lysozymes intestinaux. Elle va engendrer l'activation de la voie MyD88-dépendante et aboutir à la production de cytokines pro-inflammatoires.
En parallèle, un des dérivés des peptidoglycanes, le MDP (« *muramyl dipeptide* »), peut être produit au sein du cytoplasme des cellules et être reconnu par les récepteurs NOD2. Cette reconnaissance va dès lors induire l'activation de la protéine RICK (« receptor-interacting serine/threonine kinase ») qui va moduler l'activation de la voie NFκB et ainsi réguler la réponse immunitaire induite par les PGNs (**Figure 12 B**) (Strober et al., 2006).

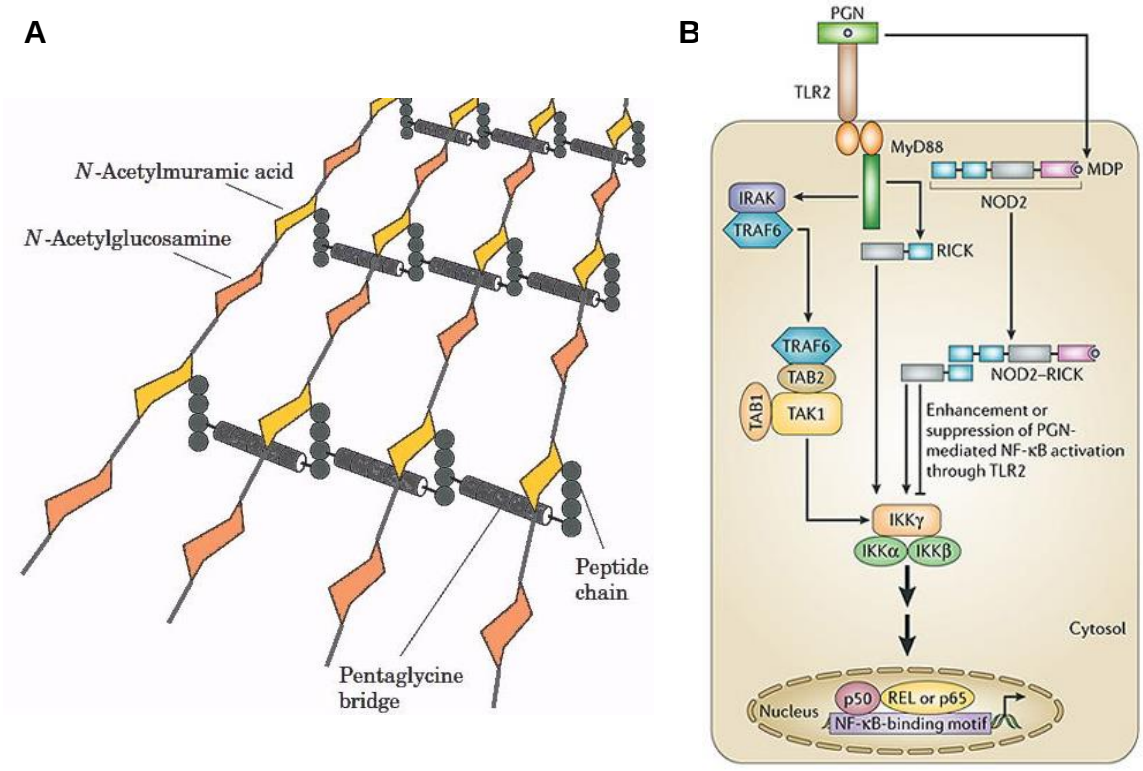


Figure 12 : Réponse immunitaire de l'hôte aux peptidoglycanes via les voies de signalisation TLR2 et NOD2. (A) Structure des peptidoglycanes. (B) Leur détection par le TLR2 engendre une signalisation MyD88-dépendante aboutissant à l'activation de la voie NFκB, tandis que la détection d'un de leur dérivé, le MDP (Muramyl dipeptide), engendre sa modulation (Modifiée d'après www3.nd.edu et Strober et al., 2006).

3.3. L'acide lipotéichoïque (LTA)

Les acides téichoïques sont les deuxièmes composants majeurs des parois des bactéries Gram positive. Ce sont des polymères anioniques, généralement composés de répétitions d'unités de polyglycérol phosphate ou de polyribitol phosphate ancrées : soit (i) de manière covalente aux PGNs formant les WTA (« *wall teichoic acids* »), soit (ii) via une partie glycolipidique aux membranes cytoplasmiques formant les LTA (**Figure 13 A**) (Neuhaus and Baddiley, 2003).

Le LTA est un PAMP qui va être reconnu à la surface cellulaire par un hétérodimère composé du TLR2 et du TLR6, associé à deux co-récepteurs : le CD14 et le CD36. En effet, ses chaînes lipidiques vont pouvoir interagir avec deux poches spécifiques au niveau du domaine extracellulaire du TLR2, et ainsi permettre l'initiation d'une réponse MyD88-dépendante passant par l'activation de la voie NFκB et des MAPKs, et la production de cytokines pro-inflammatoires et de molécules de co-stimulations (**Figure 13 B**) (Lebeer et al., 2010).

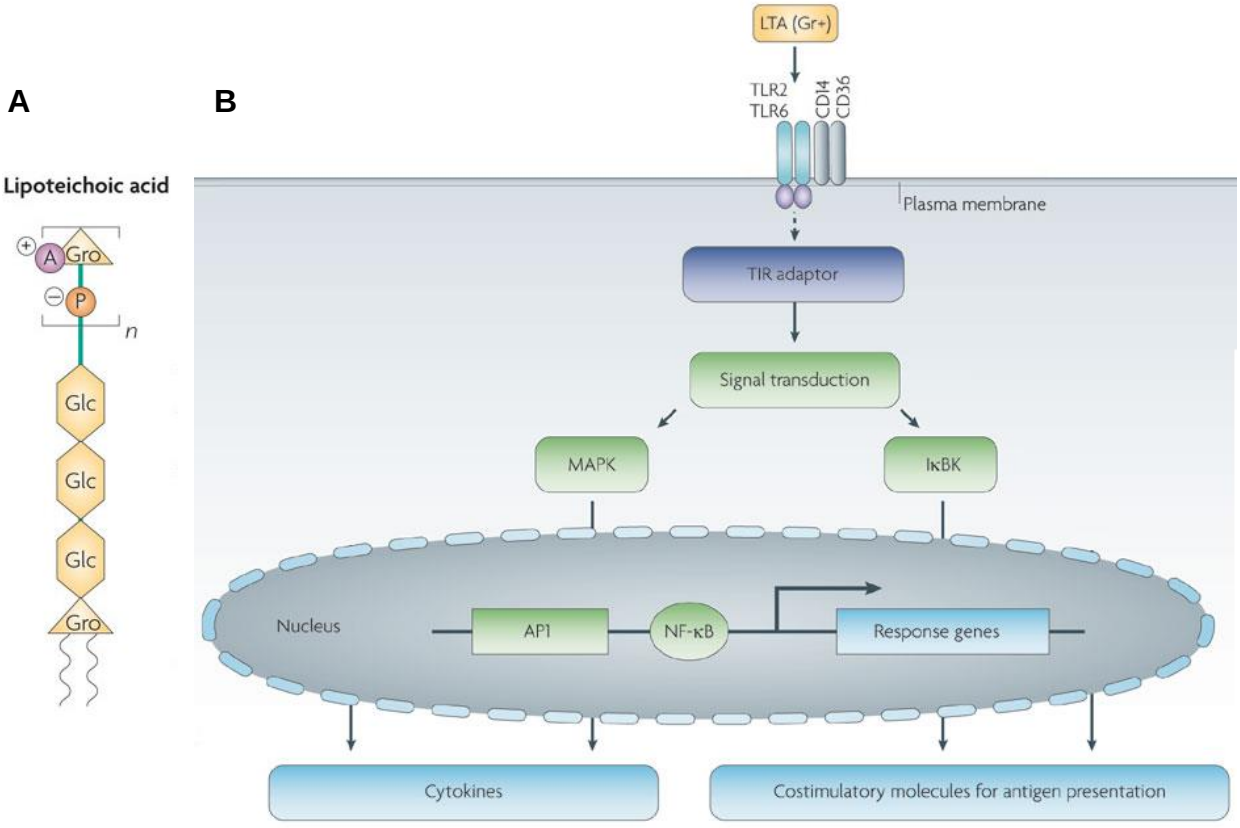


Figure 13 : Acide lipotéichoïque et reconnaissance par le complexe TLR2/TLR6. (A) Structure de l'acide lipotéichoïque (LTA). Le LTA est composé d'une partie glycolipidique ancrée dans la membrane des bactéries, et d'une longue chaine d'unité de polyglycérol phosphate ou de polyribitol phosphate. (B) La reconnaissance du LTA par un hétérodimère de TLR2-TLR6 engendre une voie de signalisation MyD88-dépendante, activant NFκB et les MAPKs. Gro : Glycérol, Glc : polyglycérol phosphate, P : Phosphate, A : D-alanine ester ou substitutions glycosyl (modifiée d'après Lebeer et al., 2010)**.**

3.4. La flagelline

Afin de posséder une mobilité favorisant leur capacité infectieuse, de nombreuses bactéries disposent de flagelles constitués : (i) d'une partie motrice intracellulaire qui anime (ii) un filament extracellulaire formé de (iii) protofilaments dont le constituant principale est la flagelline, une molécule composée de 4 domaines globulaires (D0, D1, D2 et D3) reconnue au niveau de son domaine D1 par le TLR5 (**Figure 14 A**). Cette reconnaissance va engendrer la dimérisation du TLR5, et l'initiation d'une voie MyD88-dépendante permettant la production de cytokines pro-inflammatoires via l'activation de NFκB et des MAPKs (**Figure 14 B**).

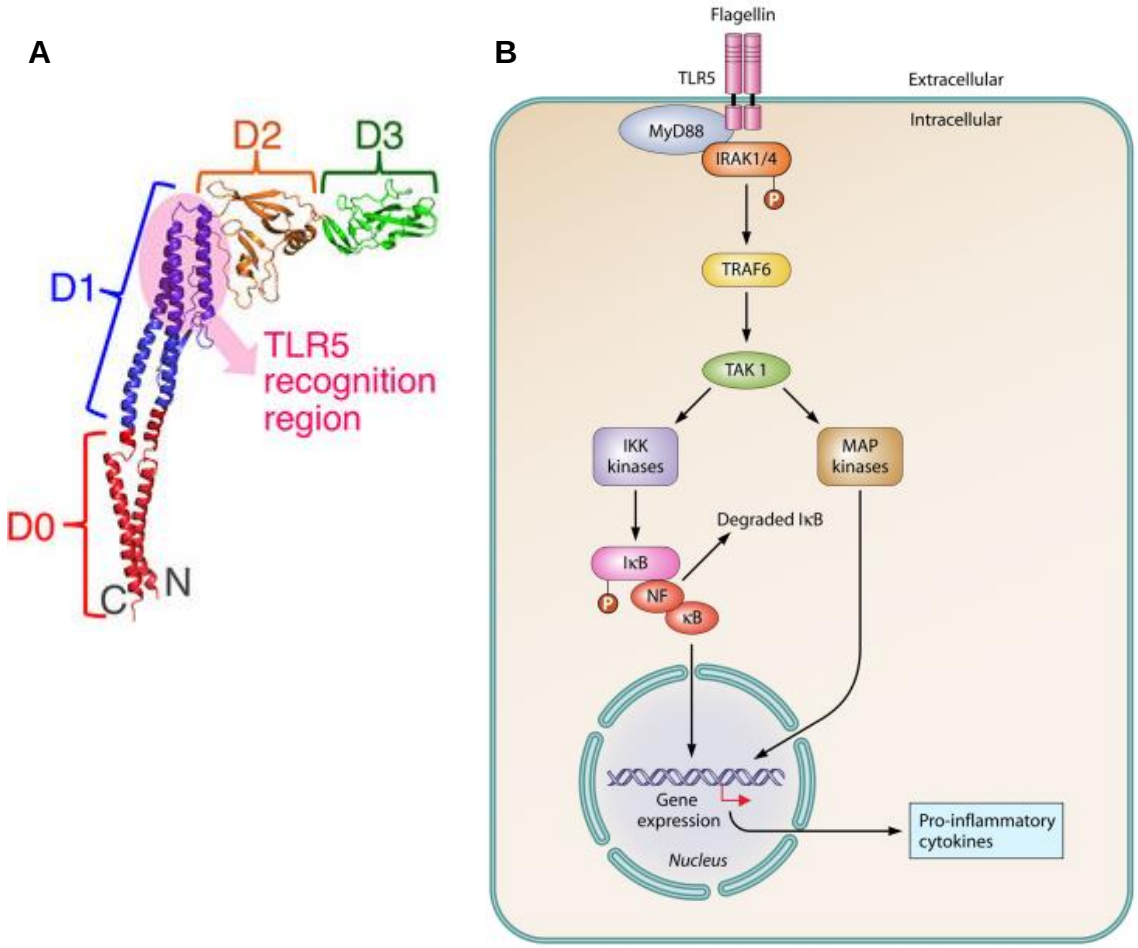


Figure 14 : Structure et reconnaissance de la flagelline par le TLR5. (A) La flagelline est une protéine qui consiste en 4 domaines globulaires D0, D1, D2 et D3. C'est le domaine conservé D1 qui va être reconnu par le TLR5. (B) La flagelline va se lier au TLR5 induisant sa dimérisation, le recrutement de la protéine adaptatrice MyD88, l'activation de IRAK1/4 et de TRAF6, et ainsi engendrer la voie NFκB et des MAPKS. Cela va permettre l'expression et la production de cytokines pro-inflammatoires (d'après Gupta et al., 2014; Lu and Swartz, 2016).

3.5. Les lipoprotéines (LP)

Afin de permettre le transport et l'ancrage de protéines au niveau de leur membrane ou de leur paroi extracellulaire, les bactéries utilisent un mécanisme de modifications post-traductionnelles résultant en la formation de lipoprotéines di- ou tri-acétylées. Ces lipoprotéines vont avoir de nombreuses fonctions essentielles comme l'internalisation des nutriments, la transduction de signaux et l'adhésion, ou bien contribuer aux fonctions de virulence dans le cas de bactéries pathogènes (la colonisation, l'invasion et l'échappement au système immunitaire).

Les lipoprotéines vont être reconnues par le TLR2 suivant des mécanismes différents (**Figure 15**):

- Pour les LPs di-acétylées, leurs chaînes lipidiques vont pouvoir se lier au niveau des poches hydrophobes extracellulaires du TLR2, tandis que leurs têtes peptidiques vont pouvoir interagir avec le TLR6.
- Pour les LPs tri-acétylées, leurs chaînes lipidiques vont pouvoir interagir avec les parties hydrophobes du TLR2 et du TLR1.

Cela va engendrer la formation d'hétérodimères qui vont promouvoir la mise en place d'une signalisation MyD88-dépendante, aboutissant à l'expression et la production de cytokines pro-inflammatoires.

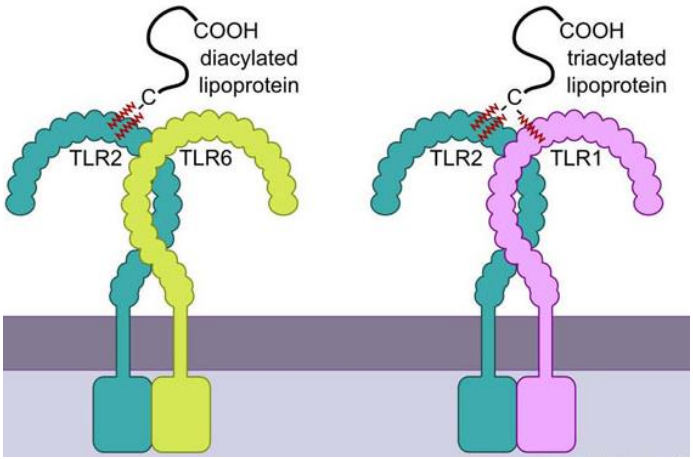


Figure 15 : Reconnaissance des lipoprotéines par le TLR2 (D'après Wells, 2011).

3.6. Les Glycoprotéines (GP)

Certains virus possèdent une enveloppe virale protégeant leur capside, composée classiquement de portions de membranes cellulaires (des phospholipides et des protéines), mais également de glycoprotéines virales servant à la liaison avec les récepteurs membranaires de l'hôte. Ces glycoprotéines sont des protéines glycosylées, qui contiennent des chaînes olygosaccharidiques (ou des glycanes) attachées à des chaînes secondaires polypeptidiques. Elles vont être reconnues soit par le TLR2 (comme la glycoprotéine B du cytomégalovirus), soit par le TLR4 (comme la protéine de fusion F du RSV (« *Respiratory syncytial virus* »)) et induire la production de cytokines pro-inflammatoires et d'IFNs de type I (Boehme and Compton, 2004).

3.7. Les acides nucléiques

3.7.1. L'acide ribonucléique simple brin (ARNsb) ou double brin (ARNdb)

L'ARN est une molécule biologique présente chez pratiquement tous les êtres vivants, les virus et les bactéries. C'est un enchaînement de nucléotides linéaires composés de groupements phosphates, de riboses et de bases nucléiques liées entre elles par des liaisons phosphodiesters. L'ARN peut être présent sous forme monocaténaire (simple brin), ou bien sous forme double brin (avec des brins complémentaires).

Cet acide ribonucléique va pouvoir être reconnu dans 2 compartiments différents :

- Au niveau des endosomes par le TLR7 8 (ARNsb) ou le TLR3 (ARNdb), et aboutir à l'activation de la voie MyD88-dependante ou TRIF-dépendante, induisant la production de cytokines pro-inflammatoires et d'IFNs de type 1.
- Au niveau du cytoplasme par les RLRs, où il va permettre la mise en place d'une voie MAVS-dépendante se finalisant également par la production de cytokines pro-inflammatoires et d'IFNs de type 1.

L'ensemble des récepteurs et voies de signalisation de l'ARN sont synthétisés dans la **Figure 16** et seront détaillés davantage dans la **Partie 2** (**2.** Les récepteurs des acides nucléiques) de ce manuscrit.

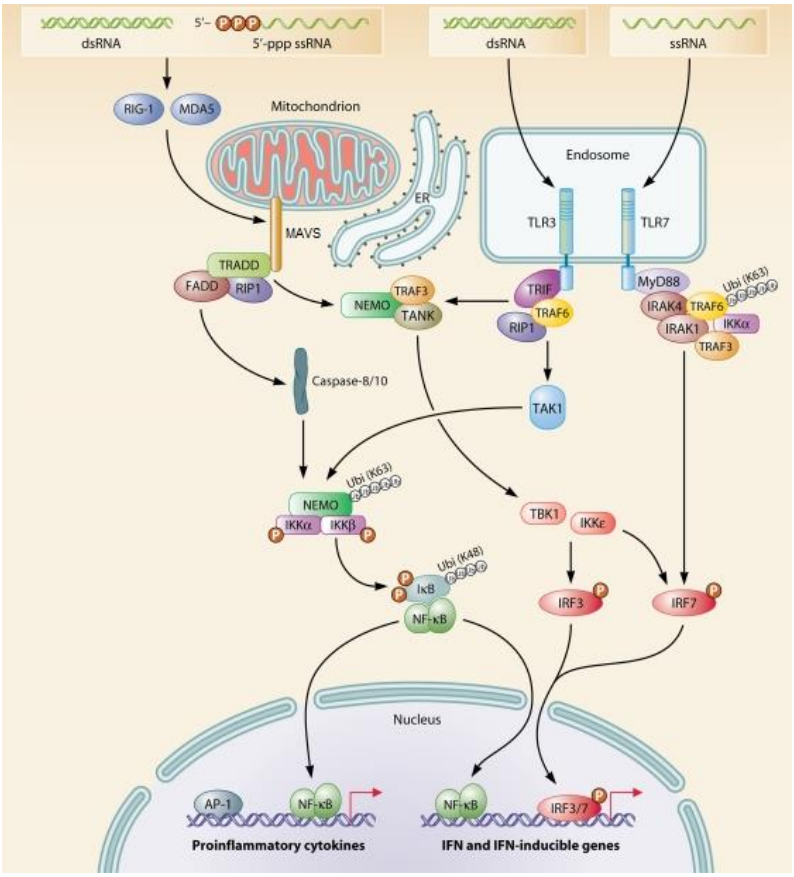


Figure 16 : Reconnaissance de l'ARN et voies de signalisation (modifiée d'après Mogensen, 2009).

3.7.2. Les acides désoxyribonucléiques (ADN)

L'ADN est une macromolécule biologique contenant toute l'information génétique permettant le développement et le fonctionnement des êtres vivants, virus et bactéries. Au même titre que l'ARN, l'ADN fait partie des acides nucléiques, à l'exception qu'il est composé de désoxyriboses (en place du ribose). Sa composition chimique ne varie pas en fonction de son origine (cellules de mammifères ou micro-organismes), rendant sa reconnaissance basée essentiellement sur sa localisation au sein de la cellule. En effet l'ADN est normalement situé au sein du noyau des cellules mammifères, ainsi les différents senseurs à ADN vont être localisés dans les autres compartiments (endosome ou cytoplasme).

Il existe des dizaines de senseurs d'ADN, qui sont résumés dans la **Figure 17** et qui seront davantage détaillés dans la **Partie 2** (**2.** Les récepteurs des acides nucléiques) de ce manuscrit.

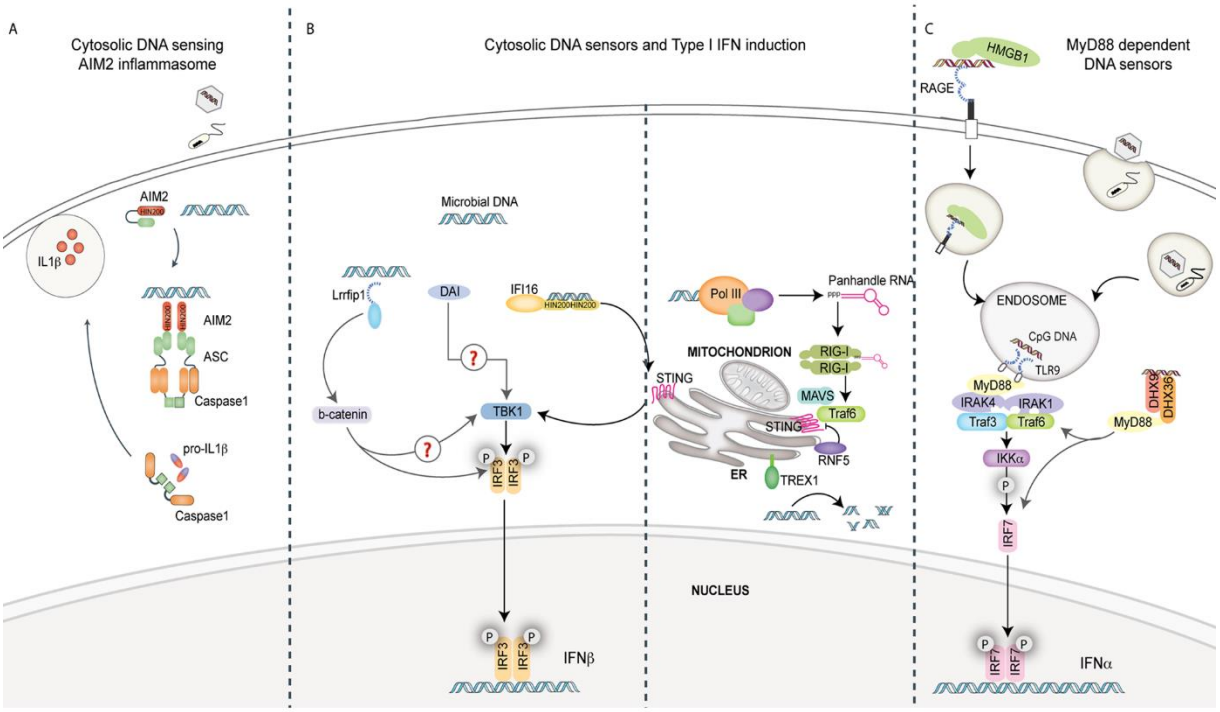


Figure 17 : Reconnaissance de l'ADN et voies de signalisation. (A) Reconnaissance de l'ADN cytoplasmique par l'inflammasome AIM2. (B) Représentations de 4 CDS connus et caractérisés. (C) Reconnaissance de l'ADN endosomal par le TLR9 (Sharma and Fitzgerald, 2011).

3.8. Le zymosane

De nombreux PAMPs ont été identifiés chez les champignons, et se localisent au niveau de la paroi ou de la surface cellulaire de ces pathogènes. L'un d'entre eux, le zymosane, est un complexe de protéines et de glucides formé principalement (Gantner et al., 2003):

- De β-glucanes, composés de chaînes polysaccharidiques de β-D-glucose liées entre elles.
- De mannanes, formés de chaines polysaccharidiques composées de centaines de mannoses.
- De chitines, composées de chaînes polysaccharidiques de N-acetylglucosamine.

Le zymosane peut être reconnu par des hétérodimères de TLR2/6 ainsi que par la Dectine-1, permettant la mise en place d'une réponse immunitaire pro-inflammatoire par l'intermédiaire de la voie MyD-88-dépendante et SyK-dépendante (Brubaker et al., 2015) (**Figure 18**).

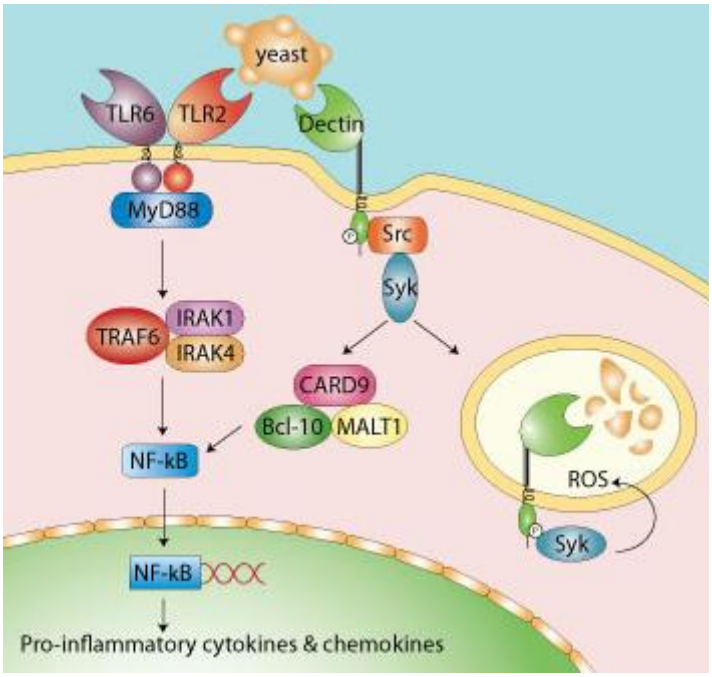


Figure 18 : Reconnaissance du zymosane à la surface des levures et voies de signalisation (http://www.invivogen.com).

3.9. Les glycosylphosphatidylinositols ou GPIs

Outre l'ADN, les ligands majeurs des protozoaires responsables de leur caractère pathogène sont les GPIs (« glycosylphosphatidylinositols ») : des glycolipides permettant l'ancrage de nombreux antigènes ou protéines à leur surface. Ils possèdent une structure commune représentée dans la **Figure 19 A**, qui est attachée à la partie C-terminale des protéines par une liaison peptidique. Le GPI va être détecté au niveau des membranes de l'hôte par le TLR2 et 4, ce qui va induire l'expression et la production de cytokines pro-inflammatoires via l'activation de la voie NFκB (**Figure 19 B**) et des MAPKs (Debierre-Grockiego, 2010).

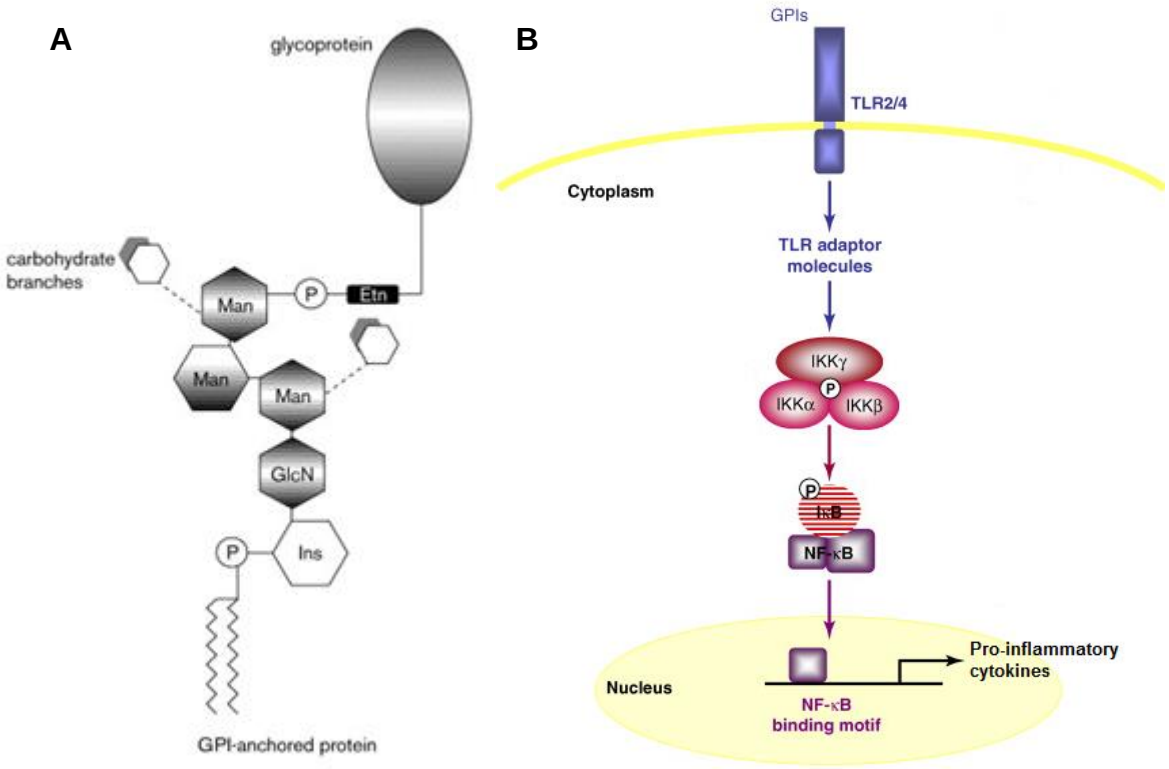


Figure 19 : Structure des glycosylphosphatidylinositols (GPIs) et voies de signalisation. (A) Structure schématique des GPIs. Etn, ethanolamine; Man, mannose; Gal, galactose; GlcN, glucosamine non-acétylé; Ins, inositol et P, phosphate. (B) La détection des GPIs par le TLR2 et 4 va permettre l'activation de la voie NFκB et des MAPKs (absent de cette figure) permettant la sécrétion de cytokines pro-inflammatoires (Modifiée d'après Ropert and Gazzinelli, 2000; Debierre-Grockiego, 2010).

Partie 2 : Stimulation de la réponse immunitaire innée par les acides nucléiques.

1. Introduction

L'ensemble des organismes vivants, incluant les virus, les bactéries ou mêmes les pathogènes eucaryotes, possèdent des acides nucléiques contenant l'ensemble de leur information génétique. Leur reconnaissance par le système immunitaire innée via les PRRs représente un enjeu majeur dans la lutte contre les infections, permettant la mise en place de cascades de signalisation aboutissant à la production d'IFNs de type I (IFN-α et IFN-β) ainsi que de cytokines pro-inflammatoires telles que l'IL-6 (« interleukine-6 »), l'IL-1β, ou bien le TNF-α (« *tumor necrosis factor-α* »).

D'un point de vue chimique, la composition principale des acides nucléiques issus des cellules mammifères et des micro-organismes pathogènes est identique. Cela nécessite dès lors la mise en place de stratégies de reconnaissance particulière afin d'éviter d'engendrer des réactions auto-immunes suite à la détection inappropriée des acides nucléiques du soi. Ces stratégies sont essentiellement basées sur (i) la localisation cellulaire des acides nucléiques (en reconnaissant notamment la présence anormale d'ADN au sein du cytoplasme ou des endosomes des cellules), ou sur (ii) la reconnaissance de motifs particuliers absents au niveau des acides nucléiques des cellules mammifères (comme des îlots CpG hypométhylés de l'ADN ou des motifs 5'-triphosphate de l'ARN).

Pour une description claire dans la suite de cette partie, les PRRs reconnaissant les acides nucléiques seront divisés en 2 groupes en fonction de leurs localisations cellulaires et de leurs structures :

- Le premier est constitué de différents membres de la famille des TLRs. Ils sont présents majoritairement au sein des cellules immunitaires (comme les cellules dendritiques, les macrophages ou les lymphocytes B) et sont localisés au niveau des membranes endosomales afin de surveiller la présence d'acides nucléiques d'origine bactérienne ou virale dans la lumière des endosomes et des lysosomes.
- Le second groupe de récepteurs est quant à lui bien moins caractérisé. Il est composé de l'ensemble des RLRs et CDS qui vont permettre la reconnaissance des acides nucléiques dans le cytoplasme de presque toutes les cellules de l'organisme (Wu and Chen, 2014).

2. Les récepteurs des acides nucléiques

2.1. Les récepteurs endosomaux ou TLRs

La reconnaissance des acides nucléiques présents au sein du compartiment endosomal se fait par l'intermédiaire des TLRs, récepteurs de l'immunité innée les mieux caractérisés dont la structure a été présentée dans la **Partie 1** (**2.1**.1.1 Structure) de ce manuscrit. Au total, 4 TLRs vont reconnaître de manière spécifique les acides nucléiques, via deux voies de signalisation distinctes (**Figure 20**) :

- La voie TRIF-dépendante activée lors de la reconnaissance d'ARNdb par le TLR3.
- La voie MyD88-dépendante activée suit à l'interaction entre l'ARNsb et les TLR7 et 8, ou entre l'ADN et le TLR9.

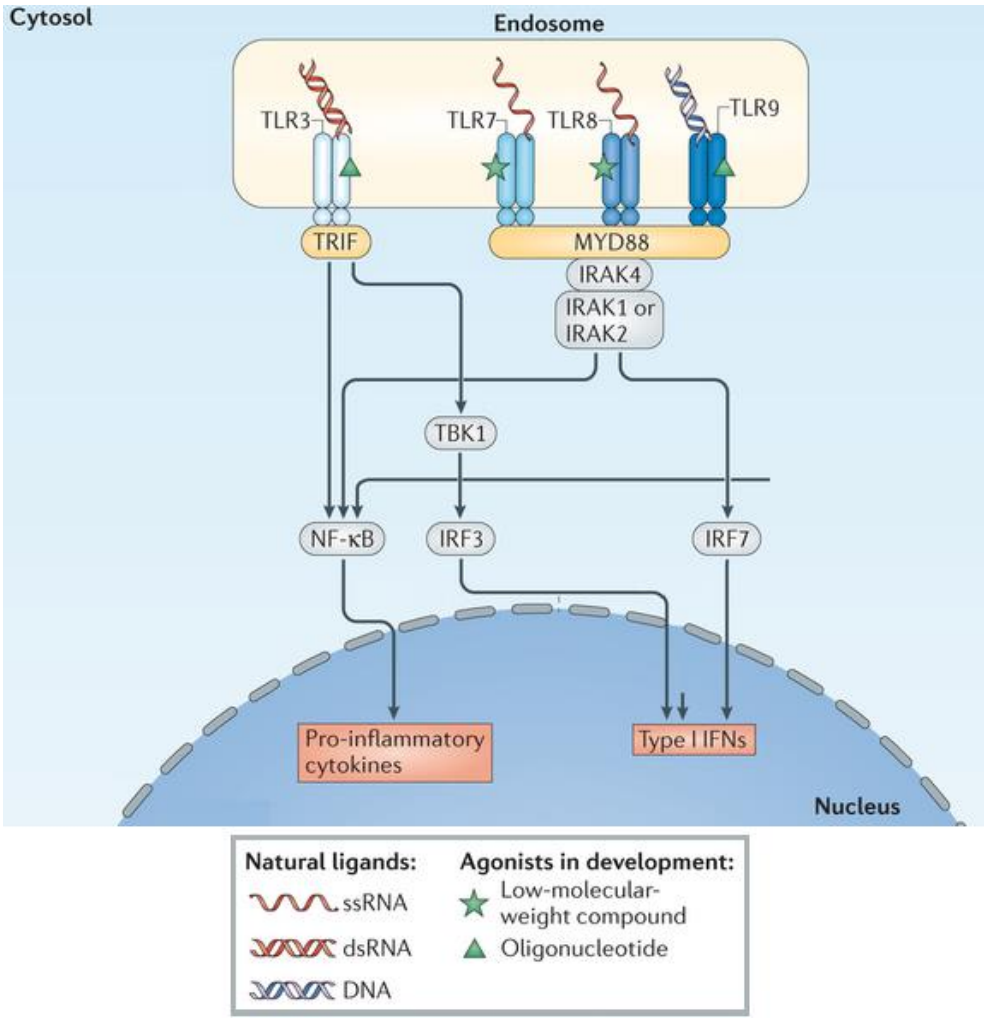


Figure 20 : Reconnaissance des acides nucléiques au niveau des endosomes. Sur cette figure, les récepteurs sont indiqués en bleu, les protéines adaptatrices en jaune, et les voies de signalisation en gris. L'activation de ces cascades de signalisation permet la production d'IFNs de type 1 et de cytokines pro-inflammatoires (encadrés rouges) (modifiée d'après Junt and Barchet, 2015).

2.1.1. Le TLR3

Le TLR3 est un récepteur localisé au niveau des compartiments intracellulaires des cellules immunitaires (macrophages, lymphocytes B et cellules dendritiques), mais peut également être localisé à la surface de certaines cellules comme les cellules NK, les cellules épithéliales et les fibroblastes (Hornung et al., 2002; Paludan et al., 2011).

D'un point de vue fonctionnel, il est proposé que le TLR3 reconnaisse au niveau de son ectodomaine des ARNdb de 40 à 50 pb minimum. Cette reconnaissance va engendrer sa dimérisation (Liu et al., 2008) et le recrutement au niveau des endosomes de la protéine adaptatrice TRIF par l'intermédiaire du domaine intracellulaire TIR (Funami et al., 2007). Via sa région N-terminale, TRIF va quant à elle lier les molécules TRAF3, TRAF6 et TBK1 qui sont cruciales pour l'activation des l'IRFs et la production d'interférons de type I (Sasai et al., 2010a; Tatematsu et al., 2010). De plus, TRIF va également pouvoir s'associer avec la molécule RIP1 (« *receptor-interacting protein 1* ») via son domaine C-terminal RHIM et permettre, en synergie avec TRAF6, d'engendrer l'activation de NFκB et la production de cytokines pro-inflammatoires (Meylan et al., 2004; Sato et al., 2003) (**Figure 21**).

La reconnaissance de l'ARNdb se faisant au niveau du compartiment endosomal, son internalisation et sa délivrance dans les endosomes sont des étapes essentielles à l'activation du TLR3. Ainsi, les poly(I:C) (des ARN double brin synthétiques) peuvent être internalisés par une endocytose dépendante de la clathrine (Itoh et al., 2008) ou bien dépendante de l'interaction avec le récepteur CD14 (dans certains types cellulaires comme les macrophages murins ou les cellules épithéliales bronchiales humaines) afin d'être reconnus par le TLR3 et de stimuler la réponse immunitaire innée.

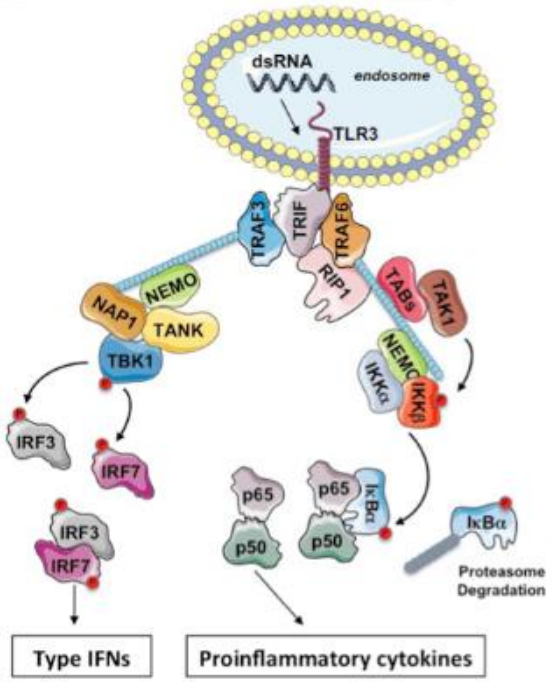


Figure 21 : Voie de signalisation TLR3-TRIF dépendante. Une fois internalisé, l'ARNdb va être reconnu par le TLR3, engendrer sa dimérisation, ce qui va permettre le recrutement de la molécule adaptatrice TRIF, permettant la mise en place de cascades de signalisation aboutissant à la production d'IFNs de type I via les IRFs ou de cytokines pro-inflammatoires via NFκB (d'après Xie, 2013 et institut-lwoff.fr/en/apoptosis-mitochondria-and-cell-survival#projet-2).

2.1.2. Le TLR7 et 8

Le TLR7 est un récepteur qui se situe initialement au niveau du réticulum endoplasmique des cellules dendritiques plasmacytoïdes et des lymphocytes B inactifs. Lors de l'activation de ces cellules, il va être rapidement exporté au niveau des endosomes grâce à l'action des molécules UNC93B1et gp96 (Kim et al., 2008), afin d'entrer en contact avec ses ligands :

- Des ARNsb (souvent d'origine virale) contenant des séquences nucléotidiques riches en guanosine ou en uridine (Akira et al., 2006).
- Des petits ARN interférences ou siRNA (« *short interfering RNA* ») (Hornung et al., 2005).

Le TLR8 quant à lui, est phylogénétiquement et fonctionnellement très proche du TLR7. Il reconnaît également les ARNsb et est situé préférentiellement au sein des endosomes des cellules dendritiques myéloïdes et des monocytes (Heil et al., 2004).

Afin d'activer la réponse immunitaire innée médiée par les TLR7 et 8, l'endocytose des particules virales extracellulaires ainsi que le phénomène d'autophagie des intermédiaires de réplications virales présents dans le cytoplasme constituent des étapes essentielles à la délivrance d'ARNsb dans le compartiment endosomal (Lee et al., 2007).

Que ce soit le TLR7 ou le TLR8, ces deux récepteurs vont activer 3 voies de signalisation intracellulaires majeures dépendantes de la protéine adaptatrice MyD88 : la voie NFκB, des MAPKs et des IRFs. En effet lors de la reconnaissance d'ARNsb, les TLR7 et 8 vont former des homodimères conduisant au recrutement de MyD88 (grâce à leur domaine TIR intracytoplasmique) ce qui va aboutir à la formation d'un complexe multiprotéique comportant les kinases IRAK1 et 4. Ce complexe va pouvoir recruter la protéine TRAF6, aboutissant à l'activation de l'IRF7 qui va alors migrer au sein du noyau des cellules et permettre l'expression des gènes codant pour les interférons de type I. Le complexe IRAK1/TRAF6 peut également se dissocier du TLR, aller activer la protéine TBK1 par polyubiquitination, et ainsi engendrer l'activation de NFκB et des MAPKs aboutissant à la production de cytokines pro-inflammatoires (Akira and Takeda, 2004) (**Figure 22**).

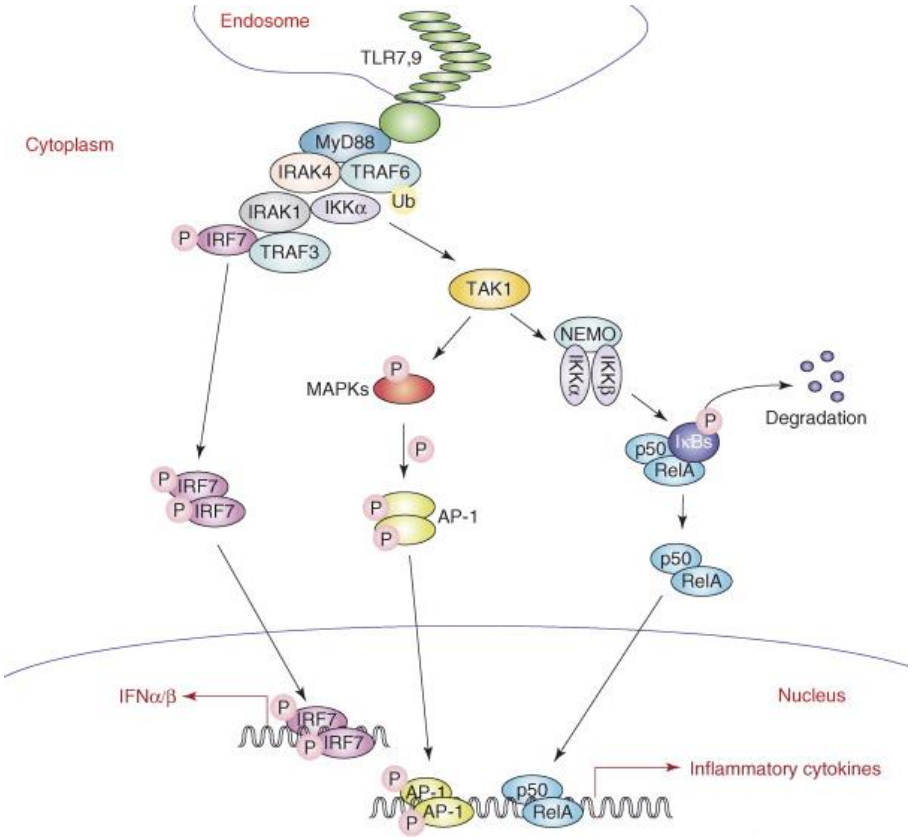


Figure 22 : Voie de signalisation des TLR7 et 8. Le TLR7 et 8 sont exprimés dans le compartiment endosomal. Ces TLRs mettent en place une voie de signalisation MyD88-dépendante afin d'engendrer la production de cytokines pro-inflammatoires par l'intermédiaire l'activation de NFκB et des MAPKs, ou la production d'IFNs de type 1 par le biais des IRF7 (modifiée d'après Kawai and Akira, 2007).

2.1.3. Le TLR9

Le TLR9 est le premier PRR identifié comme pouvant reconnaître de l'ADN étranger au sein de cellules de l'organisme (Hemmi et al., 2000). Il est initialement présent au niveau du réticulum endoplasmique des cellules sous forme inactive (principalement des cellules dendritiques plasmacytoïdes), est transloqué au niveau des endosomes lors de l'internalisation d'ADN (Latz et al., 2004), et va être activé par l'acidification de ce compartiment ainsi que l'activation de protéases acides lysosomales permettant son clivage.

Au niveau de la membrane des endosomes, le TLR9 va reconnaître spécifiquement de l'ADNdb bactérien ayant la particularité de posséder des îlots CpG hypométhylés au sein de sa structure (contrairement à l'ADNdb eucaryote). Cet ADNdb batérien va être introduit dans le compartiment endosomal de la cellule soit au cours du mécanisme d'endocytose, soit via le phénomène d'autophagie permettant le passage d'ADNdb cytoplasmiques vers l'endosome (Hemmi et al., 2000; Ahmad-Nejad et al., 2002; Lee et al., 2007).

La reconnaissance de l'ADN par le TLR9 va permettre son activation et l'induction d'une voie de signalisation MyD88-dépendante similaire aux TLR7 et TLR8. Cela va permettre la production de cytokines pro-inflammatoires via l'activation de NFκB de des MAPKs (par l'intermédiaire de TBK1), ou la production d'IFNs de type 1 par l'activation des IRF7 (**Figure 23**) (Akira and Takeda, 2004). L'activation de ces différentes cascades de signalisation intracellulaires est dépendante du compartiment dans lequel le TLR9 reconnait son ligand : Si cela s'effectue dans les endosomes précoces alors la voie NFκB sera priorisée, tandis que ce sera la voie des IRF7 dans les endolysosomes (Sasai et al., 2010b).

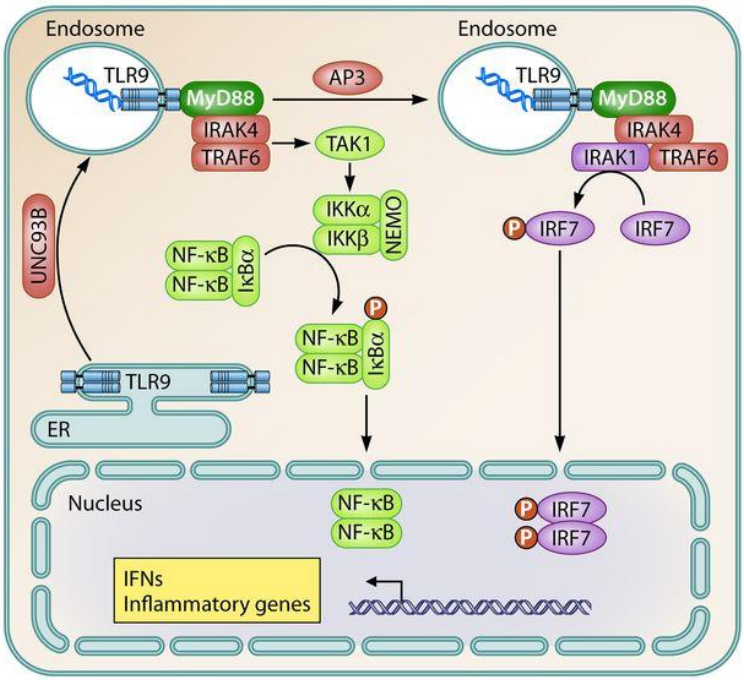


Figure 23 : Voie de signalisation du TLR9. Le TLR9 initialement situé dans le réticulum endoplasmique, va être transloqué dans les endosomes contenant de l'ADN afin de détecter et d'initier différentes cascades de signalisation. Cette translocation nécessite la présence des protéines UNC93B. Après l'acidification des endosomes, le TLR9 va reconnaître l'ADN, s'activer, et recruter la protéine adaptatrice MyD88, ainsi que IRAK1 et IRAK4 qui sont essentielles à l'activation de la voie de l'IRF7 et NFκB respectivement (modifiée d'après Paludan, 2015).

2.2. Les récepteurs intracytoplasmiques

Le domaine de reconnaissance des acides nucléiques par les TLRs est tourné vers l'intérieur des endosomes, rendant ces récepteurs aveugles aux micro-organismes qui ont réussi à envahir le cytoplasme de la cellule hôte et qui se sont répliqués avec succès. De plus, la plupart des cellules non-immunitaires susceptibles aux infections (comme les cellules épithéliales ou les fibroblastes présents au niveau des muqueuses) n'expriment pas les TLRs responsables de la détection des acides nucléiques mais sont néanmoins capables d'engendrer une réponse immunitaire innée efficace contre les infections par des agents pathogènes.

Pour cela, un système de surveillance intrinsèque existe au niveau du cytoplasme afin de lutter contre les microbes qui envahissent à la fois les cellules immunitaires et non-immunitaires. Cette surveillance passe par le biais de récepteurs qui sont répartis en deux catégories en fonctions de l'acide nucléique qu'ils vont reconnaître : les RLRs pour l'ARN, et les CDS pour l'ADN.

2.2.1. Les RLRs

Les RLRs sont des récepteurs cytoplasmiques qui vont induire la production d'IFNs de type I et de cytokines pro-inflammatoires suite à la reconnaissance d'ARNdb viraux ou d'ARNsb. Cette famille de récepteurs comporte 3 membres : RIG-1, MDA-5 et LGP2. Ils possèdent tous les 3 une structure proche composée (**Figure 24 A**) :

- D'un domaine central « DExH-box RNA helicases » qui permet la reconnaissance des ARN.
- D'un domaine C-terminal (CTD) qui confère une partie de leur spécificité pour leurs ligands.
- De deux domaines de signalisation CARD intracytoplasmiques qui permettent la transduction du signal (uniquement pour RIG-1 et MDA-5) (Saito et al., 2007).

RIG-1 et MDA-5 possèdent une voie de signalisation commune, mais vont reconnaître de manière préférentielle différents types d'ARN. Ils vont notamment pouvoir tous les deux reconnaître le poly(I:C), mais de manière dépendante de sa taille. En effet, les longs fragments (>4000pb) sont préférentiellement reconnus par MDA-5, tandis que ceux plus courts générés au cours de digestions enzymatiques (~300pb) sont reconnus par RIG-1 (Kato et al., 2008).
Pour RIG-1, ses ligands spécifiques peuvent être classés en deux catégories. Tout d'abord, les ARN possédant un groupement 5'-triphosphate normalement absent sur les ARNm de la cellule hôte, discriminant ainsi les ARN du soi et du non-soi (Hornung et al., 2006; Pichlmair et al., 2006). Puis, les courts ARNdb, possédant des groupements 5'-Hydroxyl (5'-OH) et 3'-monophosphoryl, issus de la dégradation de l'ARN par la RNase L.
Pour MDA-5, ses ligands spécifiques sont bien moins caractérisés. Sa fonction principale semble être la reconnaissance des longs ARNdb, comme certains poly(I:C)

ou la forme réplicative de l'ARNdb du picornavirus (Feng et al., 2012). Il en est de même pour LGP2 où la nature de ses ligands ARNs est encore méconnue.

La reconnaissance de l'ARN par les RLRs va induire le recrutement de la molécule adaptatrice MAVS (« *Mitochondrial antiviral-signaling protein*») au niveau de la membrane des mitochondries. MAVS va ensuite permettre le recrutement de multiples protéines de la famille TRAF (comme TRAF2 et TRAF5) qui vont agir de manière redondante avec TRAF6 pour permettre (**Figure 24 B**):

- Soit l'activation de TBK1 induisant la voie NFκB et la production de cytokines pro-inflammatoires.
- Soit l'activation de l'IRF3 permettant la production d'IFNs de type 1 (Liu et al., 2013).

LGP2 n'ayant pas de domaine de transduction du signal, il va quant à lui agir comme un rétrocontrôle négatif de la voie de signalisation en se liant :

- De manière compétitive à l'ARN et en formant un complexe protéique avec MAVS.
- Directement à RIG-1 par l'intermédiaire d'un domaine de répression (Saito et al., 2007).

Bien qu'étant un senseur à ARN, RIG-1 permet également indirectement de détecter la présence d'ADN intracytoplasmique. En effet, certains ADN cytoplasmiques de forme B (comme les poly(dA:dT)) peuvent être transcrits en ARNdb par l'intermédiaire par l'ARN polymérase III. Cet ARNdb contient des motifs 5'-triphosphate, pouvant alors être reconnus par RIG-I (Ablasser et al., 2009; Chiu et al., 2009) et engendrer la mise en place de la voie de signalisation MAVS-dépendante. Bien que redondant avec le système de reconnaissance de l'ADN double brin, cette voie de signalisation reste le seul mécanisme de détection d'ADN intracytoplasmique pour certaines cellules n'appartenant pas au système immunitaire qui sont dépourvues de senseurs à ADN.

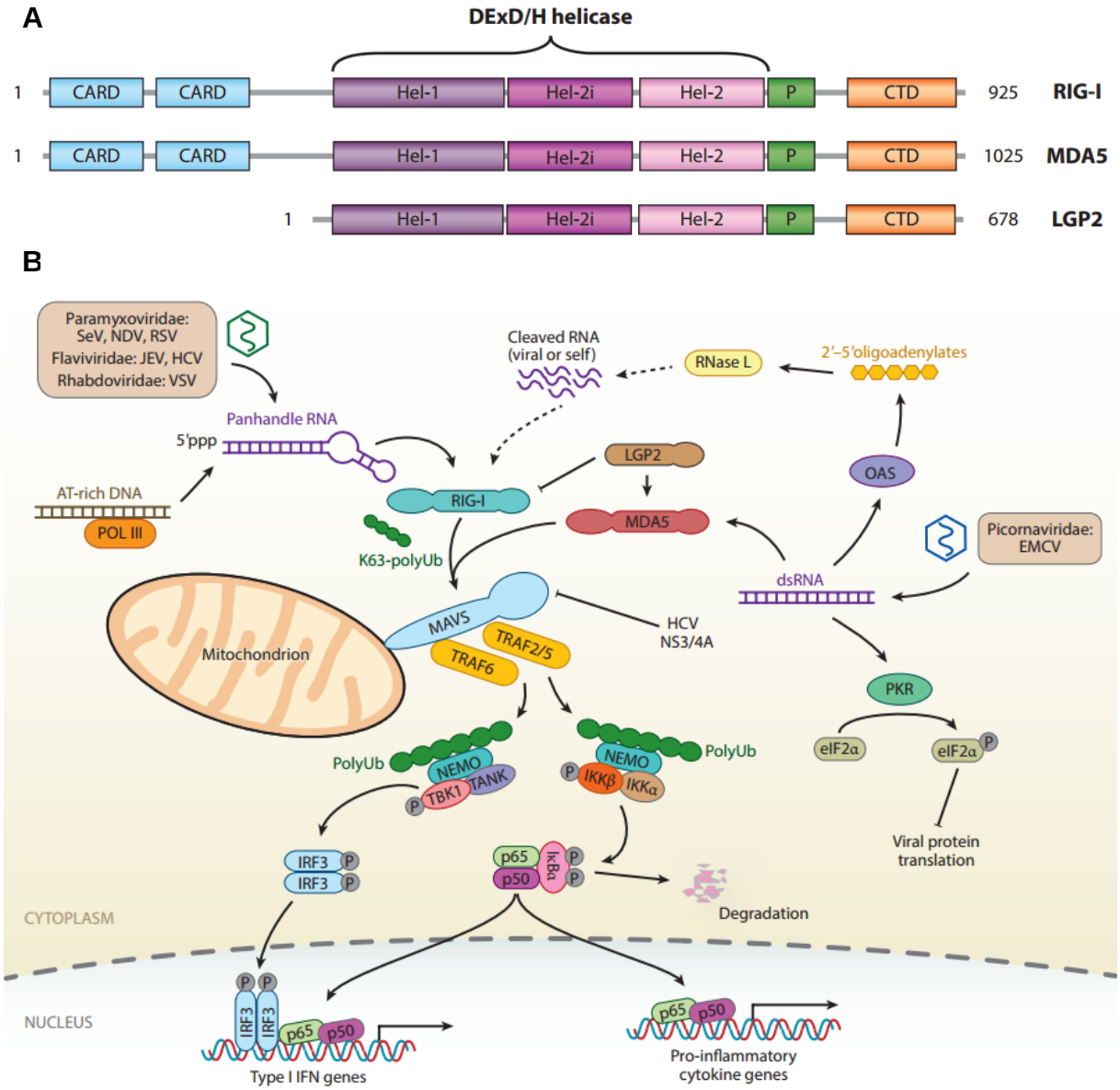


Figure 24 : Structure et voies de signalisations des RLRs. (A) Structure des récepteurs RIG-1, MDA-5 et LGP2. (B) Reconnaissance cytosolique de l'ARN. Lors de la liaison de leurs ligands, RIG-1 et MDA-5 vont recruter la protéine adaptatrice MAVS au niveau des mitochondries, permettant à son tour de recruter et d'activer les E3 ligases TRAF2, TRAF5 et TRAF6. Ce complexe va alors induire l'activation de la voie NFκB et des IRF3, et permettre la production de cytokines pro-inflammatoires et d'IFNs de type 1 respectivement . LGP2 quant à lui, va jouer un rôle de rétrocontrôle négatif en se liant de manière compétitive à l'ARN ou en se liant à RIG-1 via son domaine de répression (d'après Wu and Chen, 2014).

2.2.2. Les CDS

2.2.2.1. DHX9 et DHX36

Dans le cadre de la reconnaissance de l'ADN, les îlots CpG ont été longuement identifiés comme étant reconnus exclusivement par le TLR9. Néanmoins, des études récentes sur des cellules dendritiques plasmacytoïdes ont mis en évidence la possibilité d'activer l'expression d'IFNs de type 1 de manière indépendante du TLR9, mais dépendante de MyD88. C'est en 2010 que Kim et al. ont identifié deux protéines intracytoplasmiques de la famille des DExD/H box hélicase, DHX9 et DHX36, comme responsable de cette reconnaissance des motifs CpG et capable stimuler la voie MyD88.

En effet, DHX36 va reconnaître spécifiquement les CpG de type A formés d'un squelette phosphodiester-phosphorothioate contenant : un unique motif CpG à l'intérieur d'une séquence palindromique, ainsi qu'une queue polyG en position 3'. Cette détection va s'effectuer par l'intermédiaire de son domaine hélicase et permettre le recrutement de MyD88, aboutissant à la stimulation de la voie des IRF7 et la production d'IFNs de type 1. Pour DHX9, il va quant à lui pouvoir reconnaître les CpG de type B formés d'un squelette phosphorothioate avec de multiples motifs CpG. Cette détection par l'intermédiaire de sa région C-terminale va permettre également le recrutement de MyD88, qui va aboutir à l'activation de la voie NFκB et la production de TNF et d'IL-6 (**Figure 25**)

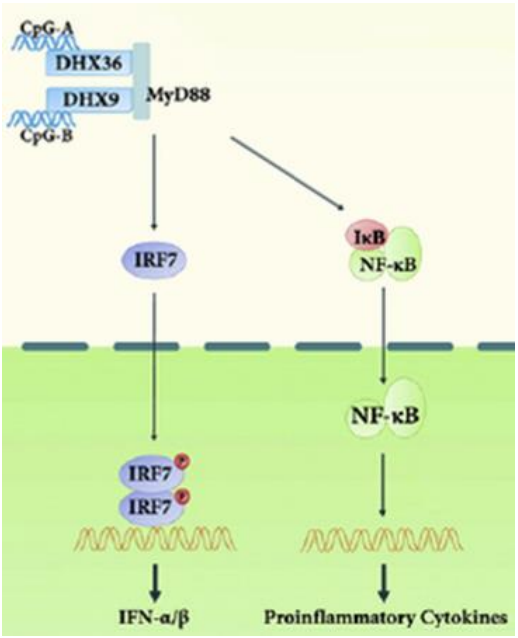


Figure 25 : Voie de signalisation des DHX9 et 36 (modifié d'après Ma and He, 2014).

De manière intéressante, DHX9 peut également se lier aux ARNdb via sa région N-terminale contenant deux sites de liaisons à l'ARN. Sa région C-terminale va alors servir à interagir avec la protéine MAVS, permettant l'activation de la même voie de signalisation que les RLRs (Zhang et al., 2011b).

2.2.2.2. DAI

DAI (« *DNA-dependent activator of IFN-regulatory factors* »), aussi appelé DML-1/ZBP1 (« *Z-DNA Binding Protein* 1 ») a été la première molécule suggérée comme pouvant reconnaître de l'ADN double brin au sein du cytoplasme des cellules (Takaoka et al., 2007). Initialement décrit comme pouvant lier la forme Z de l'ADN (grâce à ses domaines de liaisons Zα, Zβ et D3), il s'est rapidement avéré que DAI pouvait également interagir avec la forme B de l'ADN majoritaire dans les milieux physiologiques. La liaison de DAI avec ses ligands va engendrer le recrutement de la molécule adaptatrice STING (« *stimulator of interferon* gene ») et induire deux voies de signalisation différentes : d'une part, STING va permettre l'activation de la voie NFκB via le recrutement des protéines RIP1 et RIP3, ce qui va aboutir à la production de cytokines pro-inflammatoires. D'autre part, STING va activer la voie des IRF3 via la kinase TBK1 et permettre la transcription des gènes des IFNs de type 1 (**Figure 26**). L'expression de DAI étant par ailleurs activée par les interférons de type I, une boucle d'amplification va donc se mettre en place lors de la reconnaissance d'ADN exogène, permettant une augmentation de sa détection ainsi que la mise en place d'une réponse efficace.

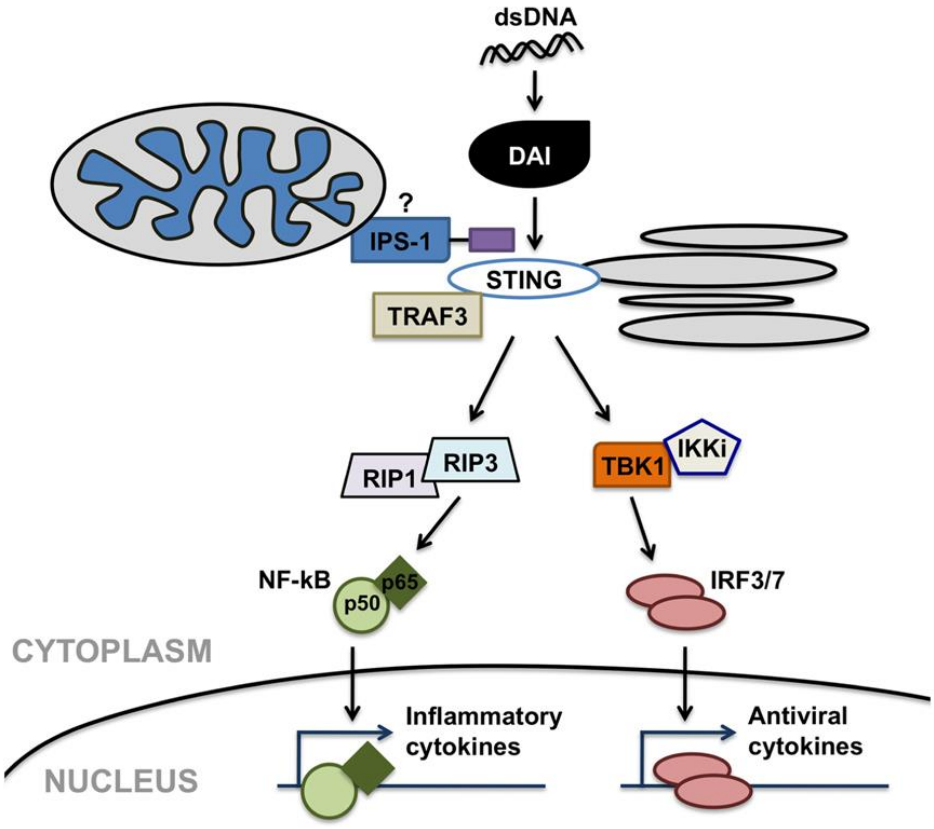


Figure 26 : Voie de signalisation de DAI. Dans le cytoplasme, DAI va pouvoir reconnaître l'ADN double brin par l'intermédiaire de ses domaines Zα, Zβ et D3 aboutissant à la mise en place de deux voies de signalisation : La voie des IRFs par l'intermédiaire de la protéine TBK1 aboutissant à la production d'IFNs de type 1, et la voie NFκB par l'intermédiaire des protéines RIP3-RIP1 aboutissant à la production de cytokines pro-inflammatoires (Marriott, 2012).

Le recrutement et l'engagement de la voie de signalisation STING-dépendante ne sont pas spécifique à DAI et peuvent être effectués par de nombreux autres CDS. En effet, STING est une protéine adaptatrice importante située au niveau de la membrane externe des mitochondries et du réticulum endoplasmique. Lors de la reconnaissance d'ADN intracytoplasmique, elle va pouvoir induire la voie des IRF3/7 et NFκB après son recrutement, aboutissant respectivement à la production d'IFN de type I (Ishikawa and Barber, 2008; Zhong et al., 2008) et de cytokines pro-inflammatoires (Abe and Barber, 2014).
STING peut également être directement par le c-di-GMP (« cyclic diguanylate monophosphate ») (Burdette et al., 2011), ou le cGAMP (« cyclic guanosine monophosphate - adénosine monophosphate ») (Wu et al., 2013) produits par le senseur à ADN intracytoplasmique cGAS (« *cyclic GMP-AMP* synthase »). Là où MyD88 joue un rôle important dans la reconnaissance des motifs CpG, STING est la clé de voûte de la reconnaissance et de la signalisation associées aux ADN simple ou double brin intracellulaires (qu'ils soient de forme A, B ou Z).

2.2.2.3. IFI16 (ou IFI204 chez la souris)

IFI16 ou 204 (« *Interferon inductible protein 16 ou 204* ») est un senseur à ADN de la famille des protéines PYHIN, contenant un domaine pyrine et deux domaines HIN-200 permettant la liaison d'ADN. Initialement décrit comme étant une protéine nucléaire due à la présence d'un signal de localisation nucléaire (NLS), il a été démontré qu'en fonction du type cellulaire, IFI16 pouvait être également localisé dans le cytoplasme, ou bien dans les deux compartiments à la fois (Veeranki and Choubey, 2012).

IFI16 est un récepteur un peu particulier, pouvant reconnaître à la fois l'ADN simple ou double brin grâce à ses domaines HIN-200. Cette liaison va permettre le recrutement de la molécule adaptatrice STING, qui va soit activer la voie NFκB afin d'engendrer la production de cytokines pro-inflammatoires, soit induire la voie des IRF3 par l'intermédiaire de TBK1 et permettre la transcription des gènes des interférons de type 1 (Unterholzner et al., 2010) (**Figure 27**).

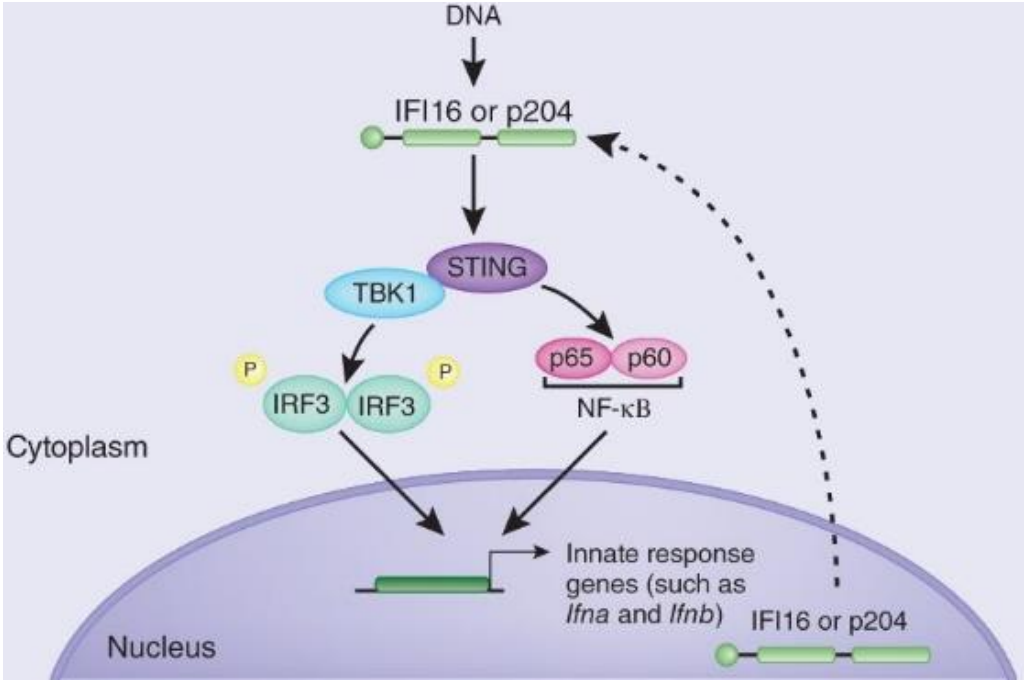


Figure 27 : Voie de signalisation d'IFI16. IFI16 peut reconnaître l'ADN par l'intermédiaire de ses deux domaines HIN. Une fois activé, IFI16 va interagir avec la protéine adaptatrice STING qui va activer la phosphorylation des IRF3 par l'intermédiaire de TBK1, ou l'activation de NFκB, aboutissant à la production d'IFN de type I et de cytokines pro-inflammatoires (modifiée d'après Goubau et al., 2010).

2.2.2.4. cGAS

En 2013, une nouvelle voie de signalisation utilisant la cGAS a été découverte en amont de STING, permettant une avancée dans la compréhension des mécanismes de reconnaissance de l'ADN (Wu et al., 2013). Appartenant à la famille des nucléotidyltransférases (« NTases »), cGAS va pouvoir reconnaître l'ADN double brin cytoplasmique grâce à son domaine de liaison, ce qui va engendrer son changement de conformation et ainsi rendre son site actif accessible. Dès lors, les substrats de cette enzyme (ATP et GTP) vont pouvoir y accéder et y être transformés en cGAMP (Cai et al., 2014). Le cGAMP va ensuite pouvoir diffuser dans le cytoplasme des cellules jusqu'au contact de STING, l'activer directement, et ainsi induire la mise en place de la cascade de signalisation STING-dépendante aboutissant à l'activation des voies des IRF3 et de NFκB (**Figure 28**).

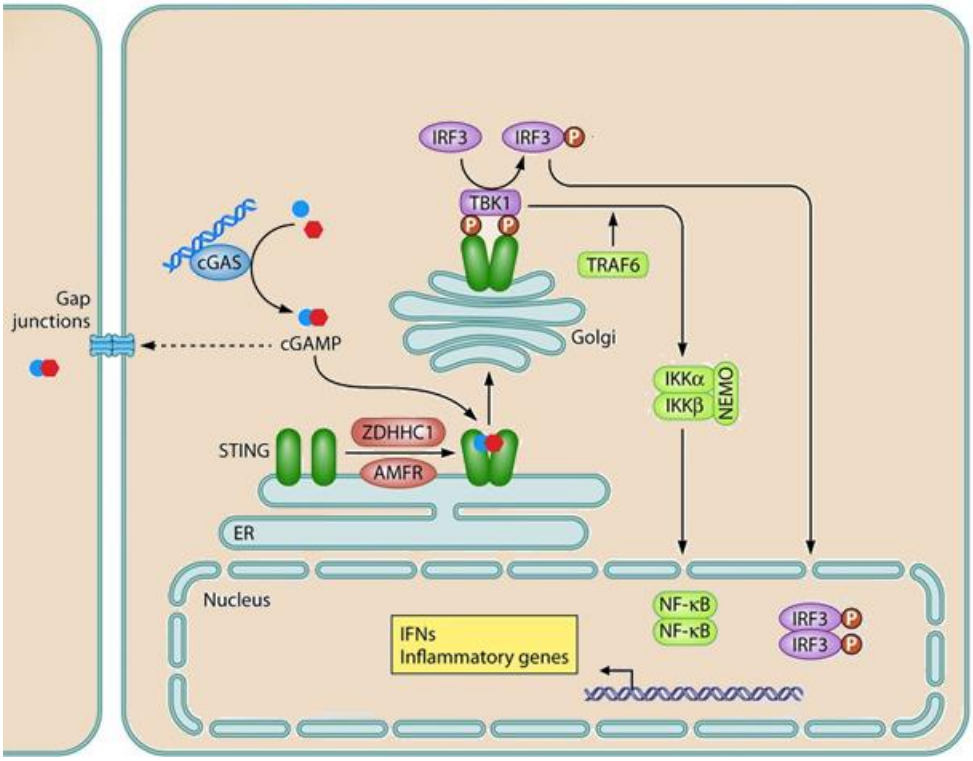


Figure 28 : Vois de signalisation de cGAS. Lors de la reconnaissance d'ADN double brin, cGAS va permettre la transformation d'ATP et de GTP en cGAMP qui est un médiateur activant la protéine STING. Lors de son activation, STING va induire la stimulation des voies NFκB et IRF3, permettant la production de cytokines pro-inflammatoires et d'IFNs de type I (modifiée d'après Paludan, 2015).

2.2.2.5. AIM2

La plupart des voies de reconnaissance de l'ADN intracytoplasmique impliquent l'activation de la voie NFκB ou des IRFs, aboutissant à la production de cytokines pro-inflammatoires et d'interférons de type 1. Néanmoins, des études ont démontré que l'introduction au sein de cellules d'ADN double brin permet également la production d'IL-1β et d'IL18, suggérant l'implication d'autres voies de signalisation comme celle de l'inflammasome.

C'est le senseur d'ADN AIM2 qui a été identifié comme responsable de l'activation de cette voie atypique. Il appartient à la famille des PYHIN tout comme IFI16, et est composée :

- D'un domaine PYD responsable de la liaison avec ses protéines effectrices en partie N-terminale
- De domaines HIN-200 capables de reconnaître l'ADN double brin au niveau C-terminal.

Lors de la détection d'ADN dans le cytoplasme, AIM2 va recruter la protéine adaptatrice ASC par l'intermédiaire de son domaine PYD. ASC va alors interagir avec la pro-caspase 1 via leurs domaines CARD respectifs et former un complexe multiprotéique du nom d'inflammasome. Au sein de ce complexe, la pro-caspase 1 va être activée par clivage, en caspase 1, puis va à son tour engendrer le clivage et la maturation des interleukines 1β et 18 afin de permettre leurs sécrétions (Muruve et al., 2008; Pétrilli et al., 2007) (**Figure 29**).

L'expression d'AIM2 étant régulée par les IFNs, cela suggère que cette protéine va être impliquée au sein d'une boucle d'amplification de la réponse immunitaire. En effet, l'entrée d'ADN dans les cellules va dans un premier temps engendrer l'activation de la voie MyD88 ou STING, ce qui va aboutir à la production d'interférons de type 1. Cela va permettre la surexpression d'AIM2, la sur-activation de l'inflammasome, et ainsi produire une réponse immunitaire plus efficace (Landolfo et al., 1998).
L'assemblage de l'inflammasome AIM2 peut également conduire à un mécanisme de mort cellulaire appelé pyroptose, impliquant la perte de l'intégrité membranaire de la cellule (Bergsbaken et al., 2009).

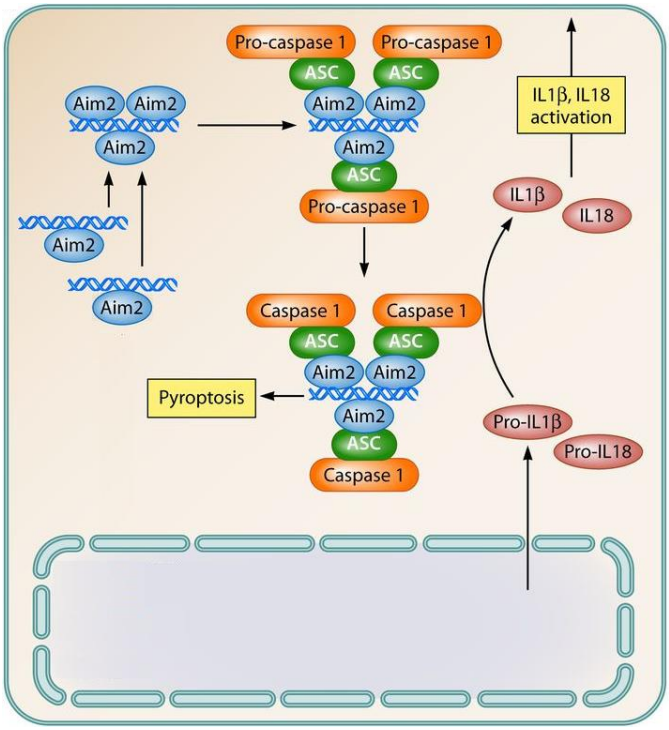


Figure 29 : Voie de AIM2 et de l'inflammasome. AIM2 est un membre de la famille des PYHIN liant l'ADN par son domaine HIN-200. Lors de sa complexation avec la protéine adaptatrice ASC, AIM2 va recruter la pro-caspase 1 via son domaine CARD pour former l'inflammasome. Cela va induire l'activation de la caspase 1 permettant la maturation puis la sécrétion des interleukines 1β et 18, ainsi que le mécanisme de pyroptose (modifiée d'après Paludan, 2015).

2.3. Conclusion

La grande diversité ainsi que la redondance des différents systèmes de reconnaissance de l'ADN et de l'ARN dans les cellules mammifères (que ce soit au niveau endosomal ou cytoplasmique) illustrent bien à la fois l'importance de la détection des acides nucléiques par les cellules mais également leur fort caractère stimulateur du système immunitaire.

Dans le cadre de la vaccination ou de l'immunothérapie, cela peut être exploité afin d'augmenter l'immunogénicité des formulations et ainsi engendrer une réponse immunitaire plus efficace. Néanmoins dans le cadre de la thérapie génique, cette propriété peut s'avérer délétère. En effet, que ce soit l'ADN comme le vecteur, rester inerte afin d'éviter d'activer le système immunitaire innée comme adaptatif représente une condition importante pour la réussite du traitement. Ainsi, des stratégies de modifications de ces deux composants sont envisageables afin de diminuer leurs caractères immunostimulateurs.

3. Les agonistes des récepteurs d'acides nucléiques.

Déjà utilisés au cours d'essais cliniques afin améliorer la réponse immunitaire contre certains cancers peu immunogènes ou bien en tant qu'adjuvants au sein de formulations vaccinales thérapeutiques ou prophylactiques (**Tableau 1**), l'utilisation d'agonistes des récepteurs des acides nucléiques s'avère être une stratégie intéressante afin de stimuler efficacement le système immunitaire innée de multiples façons. D'une part, ces agonistes (comme les oligonucléotides) vont permettre d'induire des mécanismes cellulaires intrinsèques et des effecteurs antiviraux médiés par les IFNs. De plus, ils vont permettre également d'activer les cellules dendritiques qui vont alors sécréter des cytokines pro-inflammatoires, maturer, ainsi que présenter des antigènes aux cellules de la réponse immunitaire adaptative.

Afin d'éviter les effets indésirables de ces agonistes (une réponse systémique inflammatoire et des symptômes proches de la grippe ou de l'arthralgie), ils sont souvent utilisés de manière locale (Huen and Rook, 2014), ou bien en ciblant les cellules présentatrices de l'antigène professionnelles en étant liés de manière covalente à des antigènes ou en étant empaquetés dans des nanoparticules (Kastenmüller et al., 2011; Ilyinskii et al., 2014).

Les récentes découvertes sur la structure et la fonction des différents TLRs, RLRs et CDS reconnaissant les acides nucléiques permettent de nombreux espoirs quant au développement rationnel de nouveau agonistes de ces récepteurs, même si la plupart des molécules actuellement en essais cliniques ont été découvertes comme immunostimulantes bien avant la compréhension de leurs mécanismes d'actions.

Compound (Company)	Chemical composition	Clinical Phase	Comments	Refs and ClinicalTrials.gov identifiers
TLR3 agonists				
Poly-ICLC/ Hiltonol (Oncovir)	Nucleotide-based agonist	I–II	Enhancement of multi-peptide vaccine efficacy in glioblastoma	NCT01920191
		II	Solid tumours	NCT01984892
Poly(I:C_{12}U)/ Rintatolimod. Trade name: Ampligen (HemispheRx Biopharma)	Nucleotide-based agonist	III	Chronic fatigue syndrome	NCT00215813
		I–II	Adjuvant for influenza vaccine	NCT01591473
TLR7 agonists				
Imiquimod (originator 3M Pharmaceuticals; owners: Valeant Pharmaceuticals International and MEDA; licensee for Japan: iNova Pharmaceuticals; sub-licensee for Japan: Mochida Pharmaceutical; generic versions: Taro Pharmaceutical Industries, Glenmark Generic). Trade names: Aldara, Zyclara (both MEDA, Valeant Pharmaceuticals), Vyloma (Valeant Pharmaceuticals), Beselna (Mochida Pharmaceuticals).	Low-molecular-weight compound	Approved	• Approved for genital warts and skin cancers (including actinic keratosis and basal cell carcinoma) • Additional clinical trials are ongoing	33
AZD8848 (AstraZeneca and Dainippon Sumitomo)	Low-molecular-weight compound	II	Intranasal administration for allergic rhinitis	NCT01788813
GSK-2245035 (GlaxoSmithKline)	Low-molecular-weight compound	II	Respiratory allergies including asthma	NCT01607372
GS-9620 (Gilead)	Low-molecular-weight compound	II	HBV infection	NCT02166047
			HCV infection	NCT01591668
TMX-101/ Vesimune (Telormedix)	Low-molecular-weight compound	II	Liquid formulation of imiquimod (intravesical administration) for the treatment of non-invasive bladder cancer	NCT01731652
TLR7 and TLR8 agonists				
Resiquimod (MEDA)	Low-molecular-weight compound	II	Adjuvant in protein or peptide vaccines for tumours	NCT00960752, NCT01204684 and others
Resiquimod topical (Spirig)	Low-molecular-weight compound	II	Actinic keratosis	NCT01583816
TLR8 agonists				
VTX-2337 (VentiRx)	Low-molecular-weight compound	II	VTX2337 used alongside chemotherapy and cetuximab (EGFR-specific antibody) for the treatment of squamous cell carcinoma of the head and neck	NCT01836029
TLR9 agonists				
Kappaproct (InDex Pharmaceuticals)	Nucleotide-based agonist	III	Used to increase steroid sensitivity in patients with ulcerative colitis	NCT01493960
MGN-1703/dSLIM (Mologen)	Nucleotide-based agonist	II–III	Colorectal cancer	NCT01208194
			SCLC	NCT02200081
MGN-1601 (Mologen)	Nucleotide-based agonist	PoC study	MGN-1601 is a combination of MGN-1703 plus allogeneic cancer cells for the treatment of renal cell cancer	NCT01265368
SD101 (Dynavax)	Nucleotide-based agonist	I–II	Used in combination with low-dose radiation for lymphomas	NCT02266147 and NCT01745354
Heplisav-B (Dynavax)	Nucleotide-based agonist	III	Hepatitis B virus (HBV) vaccine comprising a TLR9 agonist (1018 ISS) and HBV surface antigen	NCT02117934
AV7909 (Emergent Biosolutions)	Nucleotide-based agonist	II	New anthrax vaccine comprising a TLR9 agonist (CpG7909) and the existing anthrax vaccine BioThrax	NCT01263691
Cytosolic nucleic acid sensor agonists (in preclinical Phases)				
ADU-S100 (Aduro and Novartis)	Nucleotide-based agonist	STING	Cyclical dinucleotides for the treatment of cancer	NA
ImOl-100 (Rigontec)	Nucleotide-based agonist	RIG-I	Minimal RNA mimic of PPP-RNA for the treatment of cancer and infection	NA
MCT-465 (Multicell Technologies)	Nucleotide-based agonist	RIG-I, MDA5 and TLR3	High-molecular-weight dsRNA for the treatment of cancer, and HBV and HCV infections	NA
Isoflavones e.g. KIN-100 (Kineta)	Low-molecular-weight compound	IRF3 or an upstream target	Low-molecular-weight compounds for the treatment of viral infections	NA
SB-9200 (Spring Bank Pharmaceuticals)	Low-molecular-weight compound	RIG-I and NOD2	Small-molecule nucleic acid hybrid for the treatment of viral Infections	NA

Tableau 1 : Agonistes des récepteurs aux acides nucléiques au stade de développement pré-clinique ou clinique. Les données sont collectées jusqu'à Mars 2015. dsRNA = ARNdb ; EGFR = *epidermal growth factor receptor* ; HBV = virus de l'hépatite B ; NA = no applicable ; PoC study = étude de preuve de concept ; SCLC = cancer du poumon à petites cellules (Junt and Barchet, 2015).

3.1. Les agonistes des récepteurs d'ARN

Découverts de manière empirique, les produits polynucléotidiques issus de l'action de l'enzyme PNase 1 (« polynucléotide phosphorylase 1 ») ont été les premiers agonistes étudiés intensivement pour leur capacité à induire une réponse immunitaire médiée par les IFNs (Field et al., 1967). L'un d'entre eux le poly(I:C), un ARN mimétique double brin composé d'acide polyinosinic:polycytidilic, est capable d'être reconnu par le TLR3 et MDA-5 (Alexopoulou et al., 2001; Gitlin et al., 2006) et d'induire une stimulation efficace de la réponse immunitaire innée.
Actuellement, des essais cliniques utilisent des analogues de cet acide nucléique, les poly-ICLC, formulés avec des poly-L-Lysines afin d'améliorer leur résistance aux RNases. Ces poly-ICLC possèdent des propriétés immunostimulantes proche de celles des virus, et sont actuellement évalués en tant qu'adjuvants prometteurs pour le développement de vaccins anticancéreux (Ammi et al., 2015).

Une autre famille de molécules, les dérivés des imidazoquinolines, est également capable de jouer le rôle d'agoniste des récepteurs d'ARN. Parmi elle, l'imiquimod peut se lier au TLR7 (Hemmi et al., 2002) et est à ce jour le seul agoniste des récepteurs aux acides nucléiques approuvé aux Etats Unis par la FDA (« *Food and Drug Administration* »). Son utilisation permet l'induction d'une production locale de cytokines pro-inflammatoires, le recrutement sur place de cellules immunitaires, ainsi que l'amélioration de la présentation des antigènes aux lymphocytes T, en faisant une molécule révolutionnaire pour le traitement de nombreuses tumeurs malignes dermatologiques (Huen and Rook, 2014). Le resiquimod, un autre membre de cette famille, est quant à lui un stimulateur à la fois du TLR7 et du TLR8, permettant d'activer de nombreux types cellulaires et d'engendrer la sécrétion d'un large panel de cytokines (Huen and Rook, 2014).

3.2. Les agonistes des récepteurs d'ADN

Synthétisés de manière rationnelle, les CpG-ODN (« oligodéoxynucléotides ») sont des molécules agonistes du TLR9 inspirées des propriétés immunostimulantes des ADN bactériens riches en motifs CpG hypométhylés (Krieg et al., 1995). Leur structure a été optimisée afin d'activer de manière préférentielle les lymphocytes B ou les cellules dendritiques plasmacytoïdes. Ces agonistes ont subi une perte d'intérêt à leur égard dû à de nombreux essais cliniques non concluant vis-à-vis du bénéfice de leur utilisation au sein de formulations vaccinales thérapeutiques anti-cancéreuses. Néanmoins depuis quelques années, leur utilisation en tant qu'adjuvants au sein de formulations vaccinales contre des agents infectieux présente un regain d'intérêt avec notamment des résultats prometteurs dans la lutte contre le virus de l'hépatite B et l'Anthrax, même chez des patients immunodéprimés par le VIH (« virus de l'immunodéficience humaine ») (Scheiermann and Klinman, 2014).

4. Application à la vaccination

La vaccination à base d'acides nucléiques est une approche thérapeutique prometteuse dont les bases ont été posées dans les années 90. En effet, des travaux pionniers ont montré que l'injection intramusculaire d'ADN plasmidique ou d'ARNm nus codant pour des gènes eucaryotes conduisait à l'expression endogène de protéines et permettait d'engendrer une réponse immunitaire spécifique contre elles (Wolff et al., 1990; Jiao et al., 1992; Ulmer et al., 1993). Par la suite, de nombreux travaux d'immunisations à base d'acides nucléiques ont été développés et ont permis d'obtenir un outil prometteur pour la lutte contre de nombreux défis en santé humaine et animale, comme les maladies infectieuses, le cancer, ou les allergies.

Les vaccins à ARN, ils arrivent aujourd'hui à une étape clé de leur développement avec de nombreux essais précliniques et cliniques en cours. Néanmoins actuellement, aucunes données sur leur efficacité n'a pu permettre leur approbation et commercialisation (Kreiter et al., 2016). A l'inverse depuis 2005, 4 vaccins à ADN à usage vétérinaire ont été commercialisés en faisant une approche thérapeutique plus aboutie: (i) contre le virus West Nile chez le cheval, (ii) contre le virus de l'anémie nécrotique infectieuse chez le saumon d'élevage, (iii) pour l'expression d'une hormone de libération de l'hormone de croissance chez le porc et (iv) contre le mélanome canin (**Tableau 2**). Ainsi dans la suite de cette partie, je ne traiterais que des tenants et aboutissants de la vaccination à ADN.

Nom	Cible du vaccin	Société	Année	Espèce	Réponse immunitaire
West Nile Innovator	Virus West Nile	Centers for Disease Control and Prevention and Fort Dodge Laboratories	2005	Cheval	Anticorps neutralisant
Apex-IHN	Virus de l'anémie nécrotique	Novartis	2005	Saumon d'élevage	Innée et adaptative
LifeTide-SW5	Hormone de libération de l'hormone de croissance	VGX Animal Health	2008	Porc	Sans objet
Oncept	Mélanome	Merial	2010	Chien	Anticorps

Tableau 2 : Vaccins à ADN commercialisés à usage vétérinaire. (D'après (Liu, 2011)

La vaccination à ADN comporte de nombreux avantages par rapport aux vaccins d'autres générations. Cela comprend notamment :

- La sécurité d'utilisation, car les plasmides utilisés sont non-réplicatifs au sein des cellules eucaryotes.
- Une rapide adaptation aux variations antigéniques, par de simples techniques de clonage.
- Des systèmes de productions simples et peu coûteux, via une amplification et une purification au sein de bactéries Escherichia coli.
- La possibilité de combiner des vaccins à ADN entre eux.
- Le potentiel d'être utilisé dans des environnements dépourvus d'une chaîne du froid, en raison de la grande stabilité de l'ADN.

De plus, contrairement aux vaccins classiques qui ne permettent souvent que l'induction de réponses immunitaire à médiation humorale contre un antigène cible, les vaccins à ADN sont également capables d'induire la mise en place des réactions immunitaires à médiation cellulaire en générant des lymphocytes Th1 et des lymphocytes T CD8+ (Liu, 2011), grâce à la présentation de l'antigène par le CMH de type 1 des cellules transfectées.

Malgré les applications vétérinaires homologuées, la vaccination à ADN est toujours confrontée à des limitations d'immunogénicité qui ont jusqu'à aujourd'hui empêché son utilisation à l'échelle mondiale, surtout chez l'Homme. En effet, les résultats prometteurs obtenus dans les modèles animaux de petits rongeurs sont difficilement observables chez les grandes espèces (y compris les primates non-humains ou humains). Cependant, de nombreuses stratégies visant à surmonter ces limites sont actuellement étudiées au cours d'essais cliniques, comme l'amélioration de la délivrance de l'ADN dans les cellules cibles, ou l'utilisation d'adjuvants au sein des formulations vaccinales.

En ce sens, notre équipe a participé à un travail collaboratif visant à améliorer un protocole de vaccination à ADN chez la souris contre un antigène modèle (la β-galactosidase), grâce à l'utilisation d'un copolymère à blocs tétrabranché, le 704 (McIlroy et al., 2009). En effet, le recours à ce polymère a permis de réduire drastiquement la dose d'ADN codant nécessaire à l'établissement d'une réponse immunitaire à médiation humorale et cellulaire, et cela d'un facteur 50 par rapport à de l'ADN nu. Néanmoins, le 704 ne possédant pas de propriétés immunostimulantes, la mise en place de cette réponse efficace a nécessité l'ajout d'un ADN non-codant possédant des motifs CpG agissant comme un adjuvant, soulignant l'importance de la stimulation des récepteurs cellulaires responsables de la reconnaissance des acides nucléiques. De plus, cette formulation vaccinale a également démontré son efficacité dans un modèle murin de tumeurs hépatiques exprimant la β-galactosidase, permettant l'inhibition de la croissance tumorale et illustrant ainsi la mise en place d'une immunité anti-cancéreuse.
A la suite de ces travaux, notre équipe a confirmé la capacité des copolymères à blocs amphiphiles à induire une forte réponse immunitaire couplée à l'utilisation d'une faible dose d'ADN. Tout d'abord, dans le cadre d'un protocole vaccinal contre le carcinome hépatocellulaire chez la souris, nous avons montré que l'injection intramusculaire de 10µg de plasmide codant pour l'AFP formulé au 704 (4 à 5 mois après l'induction des tumeurs hépatiques) a permis de développer une réponse immunitaire à médiation cellulaire robuste conduisant à la diminution du nombre et du volume des nodules tumoraux hépatiques (Cany et al., 2011). De plus, dans le contexte d'un protocole d'immunothérapie dans un modèle murin d'asthme allergique, nous avons pu démontrer que la vaccination de souris, via une formulation composée de 704 et d'un plasmide codant pour l'antigène Derf1, permettait la mise en place d'une réponse immunitaire efficace et spécifique, à la fois à médiation humorale et cellulaire, de type Th1 et Tc1 (Beilvert et al., 2012).

Dès lors, l'utilisation du copolymère à blocs 704 a permis de dépasser certaines limitations relatives à la vaccination à ADN, notamment en diminuant drastiquement la quantité d'ADN nécessaire tout en induisant une forte et protective réponse immunitaire à médiation humorale et cellulaire. Néanmoins, son mode d'action reste mal connu, et sa compréhension permettrait d'améliorer encore les formulations

vaccinales afin d'augmenter les réactions immunitaires contre des antigènes d'intérêts. Dans ce but, notre équipe a effectué une étude afin d'élucider les mécanismes impliqués dans la vaccination à ADN médiée par le 704, afin de déterminer les cellules, les récepteurs, ainsi que les motifs présents au sein des plasmides qui sont nécessaires à l'induction d'une réponse immunitaire protectrice. L'ensemble de ces travaux sont présentés dans l'**Article 1** : Mécanisme de la vaccination à ADN médiée par le 704.

Partie 3 : Lipides cationiques et immunomodulation

1. Généralités

Les lipides cationiques sont des molécules amphiphiles, positivement chargées, composées de 3 parties fonctionnelles (**Figure 30 A**) :

- Une tête polaire hydrophile positivement chargée, constituée généralement d'un groupement amine protonable qui va pouvoir interagir avec les charges négatives portées par les phosphates des acides nucléiques.
- Un segment hydrophobe responsable de l'auto-assemblage des molécules en solution et de l'interaction avec les membranes cellulaires.
- Un espaceur, reliant les deux parties précédentes et assurant l'intégrité ainsi que la biodégradabilité du lipide cationique.

Ces lipides peuvent être classés en plusieurs catégories, soit en fonction de leur tête polaire (monocationiques ou polycationiques), soit en fonction de leur segment hydrophobe (dérivé du cholestérol ou possédant des chaînes alkyles).

Présents sous forme de micelles en solution, l'assemblage des lipides cationiques en liposomes peut nécessiter l'ajout d'un lipide neutre (ou co-lipide) comme la DOPE (« dioléoylphosphatidyléthanolamine ») ou le cholestérol, même si la plus part d'entre eux forment des liposomes chargés positivement de manière spontanée (**Figure 30 B**) (Martin et al., 2005; Montier et al., 2008).

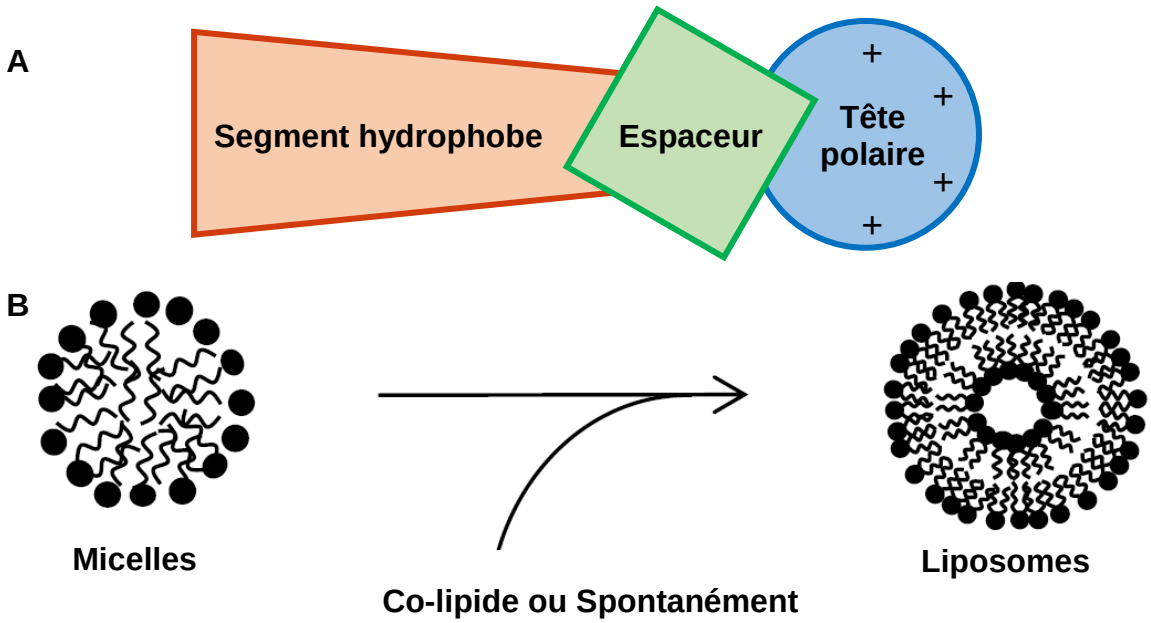


Figure 30 : Structure schématique des lipides cationiques et organisation en solution. (A) Les lipides cationiques sont composés de 3 parties : une tête polaire chargée positivement généralement formée d'un groupement amine, un segment hydrophobe souvent composé de chaînes alkyls ou d'un groupement cholestérol, et d'un espaceur reliant les deux afin d'assurer l'intégrité de la molécule ainsi que de permettre l'intégration de fonctions biodégradables. (B) Organisation des lipides cationiques en solution aqueuse sous forme de micelles (monocouches lipidiques) ou de liposomes (bicouches lipidiques).

Les travaux fondateurs de Felgner et al. en 1987 ont ouvert la voie à l'utilisation des lipides cationiques pour la délivrance de molécules hydrophobes au sein des cellules, comme les acides nucléiques, les peptides et les protéines (Xiong et al., 2011; Christensen et al., 2011; Zhang et al., 2012), en faisant l'une des catégories de vecteurs les plus prometteuses pour la délivrance de molécules de manière systémique (Mishra et al., 2013; Pezzoli et al., 2013; Cortesi et al., 2014). Néanmoins certains travaux ont démontré que les lipides cationiques, précédemment considérés comme une alternative sûre aux vecteurs viraux, ne sont pas des molécules inertes mais peuvent activer de nombreuses cascades de signalisation et activités cellulaires impliquées dans la réponse immunitaire (Vangasseri et al., 2006; Yan et al., 2007; Tanaka et al., 2008; Wilmar et al., 2012; Lonez et al., 2014). L'effet des lipides cationiques sur ces voies de signalisation est par ailleurs redondant avec ce qui a déjà été observé pour d'autres lipides comme les phospholipides (O'Donnell and Murphy, 2012), les acides gras (Calder, 2006), et les lipides microbiens (van der Kleij and Yazdanbakhsh, 2003). Dans le cadre de certaines stratégies thérapeutiques, comme l'immunothérapie ou bien la vaccination, de telles propriétés peuvent s'avérer intéressante afin d'utiliser les lipides cationiques en tant que potentielles molécules adjuvantes (Chen et al., 2007; Korsholm et al., 2012; Meraz et al., 2014; Tada et al., 2015). Cependant dans le contexte de la thérapie génique, cela peut s'avérer délétère dès lors que l'on souhaite s'affranchir de toutes stimulations du système immunitaire.

2. Transfert de gènes et lipoplexes

Un des enjeux du développement d'une large variété d'applications thérapeutiques réside dans l'amélioration de la délivrance d'acides nucléiques au sein des cellules afin qu'ils soient mieux exprimés et qu'ils permettent une production optimale de la protéine d'intérêt. Pour cela, de nombreuses barrières sont à franchir. Tout d'abord, les acides nucléiques peuvent être dégradés avant même d'atteindre la cellule à cause de nombreuses nucléases présentent dans l'espace extracellulaire (Wolff and Budker, 2005). Puis, seuls, ils ne peuvent franchir que très difficilement les membranes cellulaires, car ils possèdent de nombreuses charges négatives au niveau de leurs groupements phosphates empêchant l'interaction avec les protéines anioniques membranaires (Felgner et al., 1987; Farhood et al., 1992). De plus, la transfection *in vitro d'*un acide nucléique seul va aboutir à sa séquestration au sein des endosomes et ne permettre qu'une très faible expression, et sa transfection *in vivo* dans le muscle squelettique ne va permettre une expression que dans 1 à 2 % des fibres musculaires (Levy et al., 1996). Enfin pour l'ADN, même s'il arrive à entrer au sein des cellules, sa migration jusqu'au noyau va constituer un obstacle supplémentaire afin qu'il puisse être exprimé.

De nombreuses techniques ont alors été envisagé afin d'aider ces acides nucléiques à passer au travers de ces barrières biologiques de façon efficace, non-toxique, tout en ciblant un type cellulaire particulier. Parmi elles, une attention toute particulière a été attribuée au développement des vecteurs synthétiques de par leur facilité de production (basés sur des molécules simples), de caractérisation et de purification, en faisant des vecteurs peu coûteux à produire et sans limites théoriques dans la taille du gène qu'ils peuvent véhiculer (Kreiss et al., 1999).

2.1. Les lipoplexes

En tant que vecteurs synthétiques, les lipides cationiques constituent de puissants outils pour le transfert d'acides nucléiques au sein de nombreuses populations cellulaires *in vitro*, mais leur efficacité *in vivo* s'avère encore limitée et à améliorer. Leur association sous forme de micelles ou de liposomes avec les acides nucléiques va permettre la formation d'assemblages supramoléculaires du nom de lipoplexes, dont les caractéristiques physicochimiques vont :

- Être grandement modifiées par le rapport de charge (RC), qui est défini comme le rapport entre le nombre de charges positives apportées par les lipides cationiques sur le nombre de charges négatives apportées par les acides nucléiques.

$$RC = \frac{Nombre\ de\ charges\ (+)\ des\ lipides\ cationiques}{Nombre\ de\ charges\ (-)\ des\ acides\ nucléiques}$$

- Influencer de nombreux mécanismes comme les voies d'entrée dans la cellule, l'efficacité de l'échappement endosomal, mais également le comportement *in vivo* dans les fluides biologiques. La **Figure 31** présente un résumé des différentes étapes du transfert d'acides nucléiques par les lipides cationiques qui vont être détaillées par la suite.

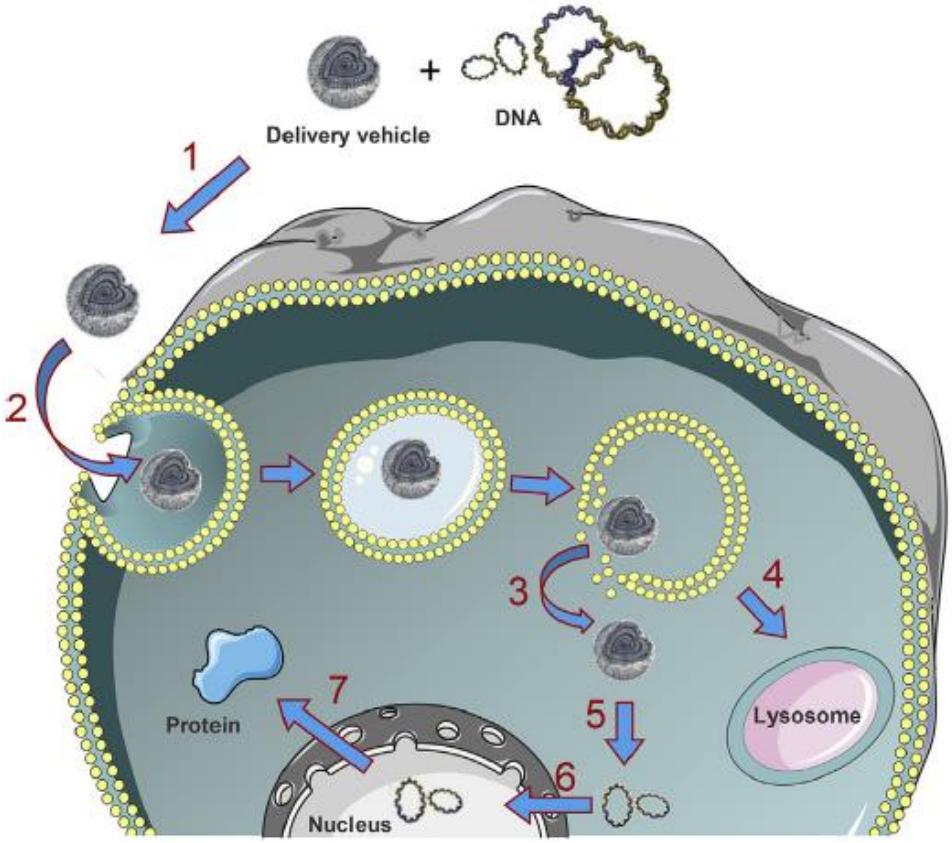


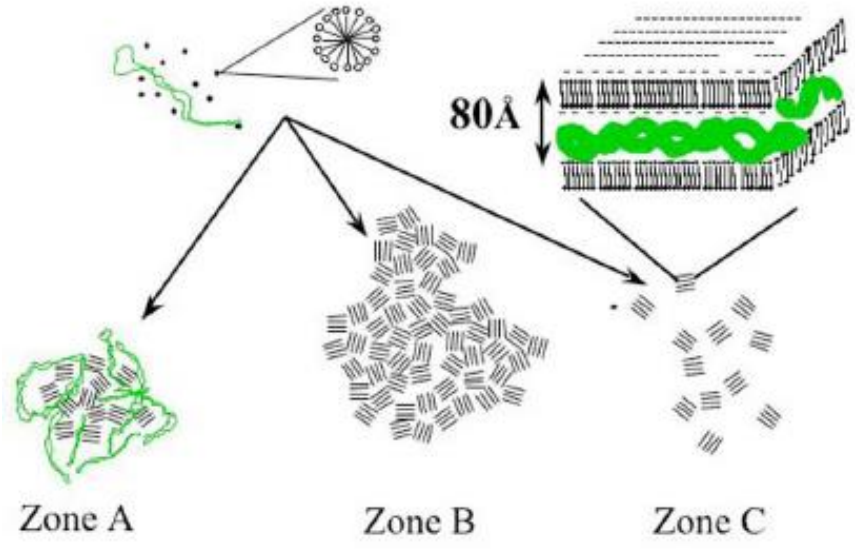
Figure 31 : Représentation schématique de la délivrance d'ADN au sein des cellules par des lipoplexes (complexes lipide cationique/ADN). 1) Complexation du vecteur et de l'ADN. 2) Entrée dans la cellule par endocytose. Un phénomène de fusion membranaire peut également se produire au niveau de la membrane plasmique aboutissant à la délivrance directe de l'ADN dans le cytoplasme. 3) Echappement endosomal vers le cytoplasme. 4) Dégradation lysosomale. 5) Décomplexation de l'ADN du lipoplexe. 6) Entrée dans le noyau. 7) Transcription puis traduction en protéine (Pitard and Habrant, 2016).

2.1.1. Propriétés physicochimiques et complexation

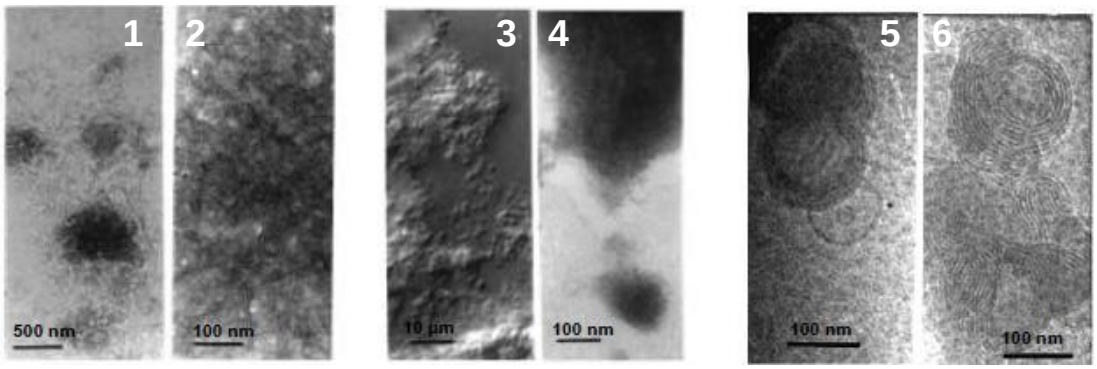
Afin de caractériser les lipoplexes, de nombreuses techniques sont utilisées comme (i) la mesure de leur taille par diffusion quasi-élastique de la lumière ainsi que par microscopie électronique, (ii) l'évaluation de la complexation de l'ADN par électrophorèse sur gel d'agarose ou via un spectrofluoromètre (afin de suivre l'extinction de la fluorescence du bromure d'éthidium (BET) en solution) et (iii) la mesure du potentiel zeta des lipoplexes pour définir leur charge de surface (Barteau et al., 2008). Ces méthodes permettent en général, de définir trois zones distinctes qui sont résumées dans la **Figure 32** :

- La zone A, qui est composée de lipoplexes qui sont chargés négativement, de petite taille et colloïdalement stables, où les acides nucléiques ne sont pas entièrement complexés et coexistent sous forme peu condensée ou libre dans la solution (en excès). Ces lipoplexes ont une efficacité de transfection qui est quasi-nulle.
- La zone B, qui est formée de lipoplexes qui sont proche de l'electroneutralité, ce qui engendre l'absence de répulsion électrostatique entre les lipoplexes et conduit à leur agrégation par interaction hydrophobe. Cela aboutit à la formation de précipités visibles à l'œil nu et colloïdalement instables. Néanmoins, l'intégralité des acides nucléiques est complexée au sein des lipoplexes. Leur activité de transfection est faible, probablement à cause de leur taille importante limitant l'internalisation par les cellules.
- La zone C, qui est faite de lipoplexes qui sont chargés positivement, de petite taille et colloïdalement stables, où les acides nucléiques y sont fortement condensés. Ces lipoplexes peuvent s'associer aux membranes cellulaires par interactions électrostatiques, et transfectent très efficacement des cellules *in vitro*.

A



B



C

Zone	A	B	C
Rapport de charge	Faible	Intermédiaire	Élevé
Stabilité colloïdale	Stable	Instable	Stable
Taille	Petite	Grande	Petite
Potentiel zeta	Négatif	Autour de la neutralité	Positif
Complexation des acides nucléiques	Incomplète	Complète	Complète

Figure 32 : Lipoplexes en fonction des 3 zones de stabilité colloïdale. A) Représentation schématique des lipoplexes obtenus par l'association de lipides cationiques et d'ADN. B) Observation en Cryo-TEM des lipoplexes issus des trois zones de stabilité colloïdale. C) Propriété des lipoplexes en fonction du rapport de charge (Pitard et al., 1997; Pitard, 2002; Barteau et al., 2008).

On peut également classer les lipoplexes selon deux types d'organisations supramoléculaires des bicouche lipidiques : (i) Une phase lamellaire L_α qui représente une structure concentrique multilamellaire dite « en oignon » où l'ADN va pouvoir être pris en sandwich entre deux couches de lipides (**Figure 33 A**), ou (ii) une phase hexagonale inversée H_{II} (**Figure 33 B**) (Koltover et al., 1998; Pitard et al., 1999). L'existence de ces deux types d'organisations dépend à la fois du lipide cationique, mais également de l'association ou non avec un co-lipide : par exemple la DOPE favoriserait l'adoption de la phase H_{II}. Cette organisation des lipoplexes va avoir une incidence directe sur leur capacité à fusionner avec les membranes cellulaires, notamment au niveau des endosomes, impactant ainsi l'efficacité de transfection (Barteau et al., 2008).

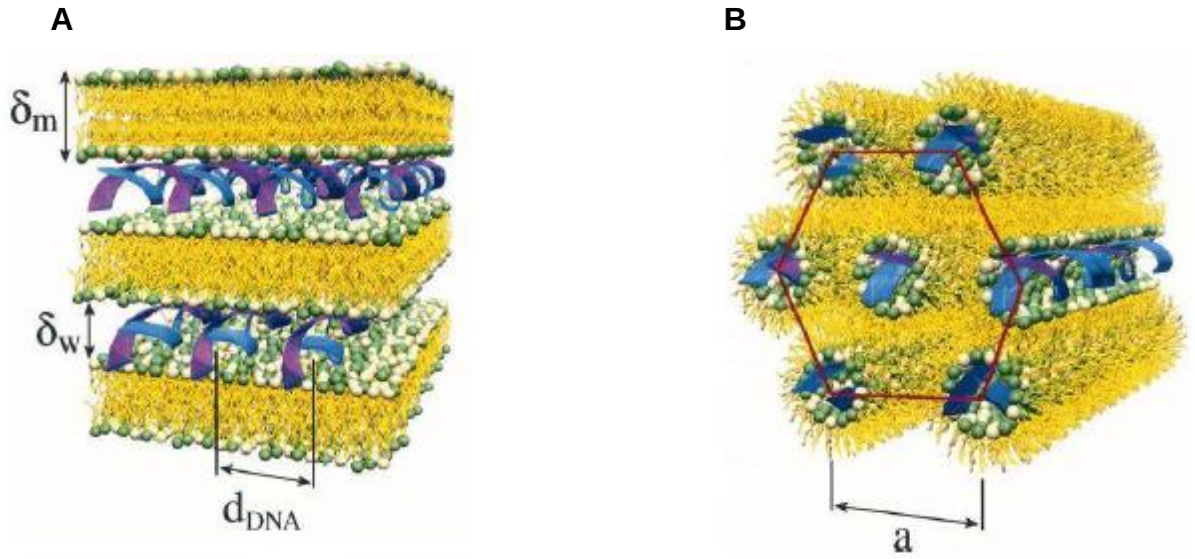


Figure 33 : Représentation schématique des deux phases lamellaires. A) Phase lamellaire L_α. B) phase hexagonale inversée H_{II}. En vert/blanc : tête hydrophile, en jaune : queue hydrophobe, en bleu/violet : ADN (Koltover et al., 1998).

2.1.2. Internalisation des lipoplexes

En absence de ligands spécifiques présents à leur surface, les lipoplexes interagissent avec les membranes cellulaires par le biais d'interactions électrostatiques non spécifiques (entre leur charge globale positive et la charge globale négative des membranes). En effet, les molécules anioniques présentent à la surface des membranes cellulaires (comme les protéoglycanes et les intégrines) jouent un rôle déterminant dans la fixation des lipoplexes, mais également des polyplexes et des peptides cationiques (Behr et al., 1989; Labat-Moleur et al., 1996; Tyagi et al., 2001; Richard et al., 2005).

Suite à ce contact, les lipoplexes vont ensuite pouvoir être internalisés par les cellules, néanmoins les mécanismes impliqués ne sont pas encore très bien établis. Même s'il n'est pas exclu qu'une partie des lipoplexes puissent directement fusionner avec les membranes cellulaires afin de délivrer directement les acides nucléiques (Felgner et al., 1987, 1995), la plupart de travaux actuels mettent en évidence l'importance et l'implication du phénomène d'endocytose dans l'internalisation des lipoplexes

(Elouahabi and Ruysschaert, 2005; Khalil et al., 2006). L'endocytose peut se produire par de nombreux mécanismes qui peuvent être classés en deux grandes catégories (**Figure 34**) (Conner and Schmid, 2003) :

- La phagocytose, qui consiste principalement à internaliser des particules de grande taille après leur reconnaissance par des récepteurs spécifiques présent à la surface de certaines cellules spécialisées (comme les cellules immunitaires).
- La pinocytose, qui permet l'entrée de fluides et de solutés au sein de toutes les cellules, et qui fait intervenir au moins 4 mécanismes différents : (i) La macropinocytose, qui permet la formation de grandes vésicules (>1µm de diamètre) afin d'internaliser un grand volume de milieu extracellulaire ; (ii) l'endocytose cavéole-dépendante qui induit la formation de vésicules de moyenne taille (~120nm de diamètre) au niveau de régions membranaires riches en cholestérol et sphingolipides ; (iii) l'endocytose clathrine-dépendante qui engendre la formation de vésicules de petite taille (~60nm de diamètre) afin d'internaliser de petites molécules comme des lipoprotéines de basse densité (LDL-cholestérol), la transferrine, ou bien le recyclage des protéines membranaires ; et (iv) l'endocytose cavéole- et clathrine-indépendante qui permet la formation de vésicules de taille intermédiaire (~90nm) mais dont les mécanismes sont très peu connus.

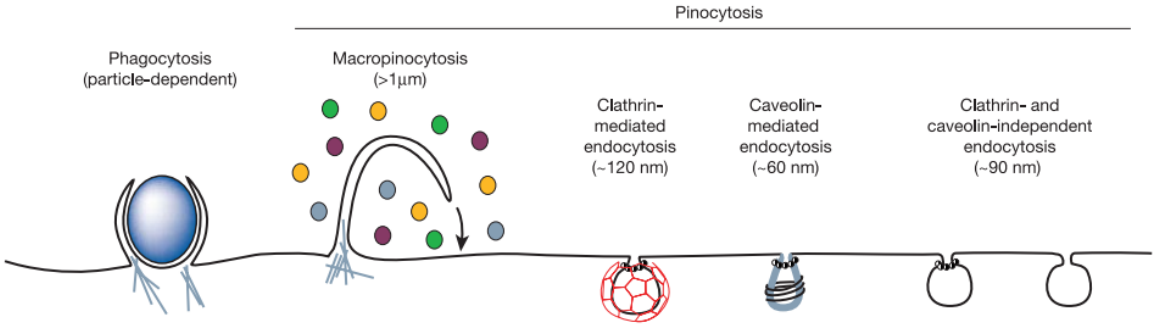


Figure 34 : Voies d'entrées au sein des cellules mammifères. Les mécanismes d'endocytose utilisés par les cellules dépendent de la taille des particules internalisées, des récepteurs éventuellement mis en jeu, et des molécules impliquées dans la formation des vésicules (Conner and Schmid, 2003).

Les récents travaux effectués sur les mécanismes d'entrée des lipoplexes ont permis de mettre en avant que l'endocytose clathrine-dépendante serait la voie majeure d'internalisation de ces complexes (80%), tandis que la voie cavéole-dépendante ne conduirait à l'entrée que de 10 à 20% des lipoplexes (Zuhorn et al., 2002; Rejman et al., 2004; Wasungu and Hoekstra, 2006). De plus au cours d'un travail collaboratif, notre équipe a également pu confirmer que la voie d'entrée des lipides cationiques les plus efficaces développés au sein de notre laboratoire passait par une endocytose clathrine-dépendante, tandis que les moins efficaces entraient par endocytose cavéole-dépendante (Billiet et al., 2012). Néanmoins, ces résultats sont à nuancer car les mécanismes d'entrée des lipoplexes dans les cellules sont dépendants de leur taille, de leur nature, mais également du type cellulaire transfecté.

2.1.3. Echappement de l'endosome

Après leur internalisation par endocytose, les lipoplexes restent piégés au sein des endosomes sans accès direct au cytoplasme ou bien au noyau. De plus, ces endosomes vont fusionner avec des lysosomes conduisant à la dégradation de leur contenu via acidification du pH (4,5-5) et l'action d'hydrolases acides (comme la DNAse II qui va être susceptible de dégrader les acides nucléiques internalisés). Ainsi l'échappement des lipoplexes de l'endosome représente une étape cruciale pour la délivrance des acides nucléiques au sein de la cellule (Varkouhi et al., 2011), et peut s'effectuer : (i) soit par fusion des membranes des endosomes et des lipoplexes (**Figure 35 A**), (ii) soit par l'éclatement des endosomes par l'intermédiaire d'un choc osmotique (**Figure 35 B**).

Le mécanisme le plus souvent proposé repose sur la fusion membranaire. En effet, il a été observé dès les prémices de l'utilisation des lipides cationiques que l'ajout de la DOPE (un co-lipide fusogénique pH-sensible) permettait une meilleure libération des acides nucléiques dans le cytoplasme et augmentait ainsi l'efficacité de transfection (Farhood et al., 1992). Ce co-lipide permet la formation d'une bicouche lipidique stable à pH 7, mais va induire un changement dans l'organisation des lipoplexes à pH acide (5-6). Cela va engendrer la fusion des lipoplexes avec les membranes des endosomes, leur déstabilisation, et la libération de leur contenu dans le cytoplasme (Cullis et al., 1986; Wrobel and Collins, 1995; Almofti et al., 2003).

L'autre hypothèse de mécanisme repose sur le phénomène d'éponge à proton, basé sur la présence au sein de certains lipides, peptides ou polymères, de groupements dits « protonables » offrant un pouvoir tampon important. En effet, lors de l'acidification des endosomes précoces par les ATPases à protons (suite à l'internalisation des lipoplexes/polyplexes), ces groupements vont être capables d'absorber les protons et ainsi empêcher l'acidification de l'endosome, amenant les pompes à protons à fonctionner de manière disproportionnée. L'entrée d'anions et d'eau va ainsi conduire au gonflement de l'endosome jusqu'à sa rupture et la libération de son contenu dans le cytoplasme (Sonawane et al., 2003). Ce mécanisme est notamment utilisé par les co-lipides contenant des groupements imidazoles (Midoux et al., 2002; Kumar et al., 2003; Mével et al., 2008; Midoux et al., 2009; Billiet et al., 2012; Gonçalves et al., 2014; Mével et al., 2015) qui sont protonables dans les endosomes au cours de l'acidification et qui vont ainsi favoriser l'échappement endosomal par leur propriété d'éponge à proton, mais également par leur propriété à fusionner avec la membrane de l'endosome suite à leur protonation, en faisant une classe de molécule particulièrement intéressante utilisant les deux mécanismes d'échappement de l'endosome.

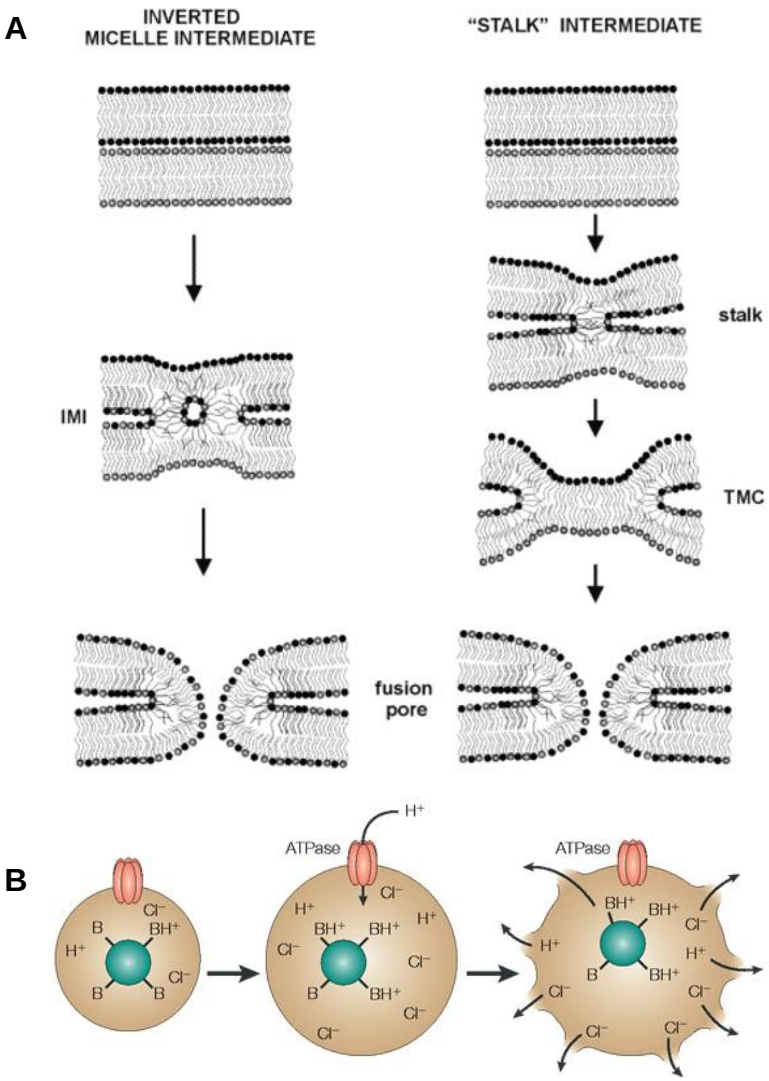


Figure 35 : Mécanismes d'échappement endosomal. A) Mécanisme de fusion membranaire. Gauche : Fusion membranaire avec la formation d'un pore via un intermédiaire en micelle inversée (IMI). Droite : Formation d'un pore par accolement direct des membranes (TMC) et la formation d'un pédicule (Stalk) ((Hafez and Cullis, 2001). B) Mécanisme d'éponge à proton. Le cargo contenu dans l'endosome (vert) contient des fonctions protonables (B) qui vont se protoner lors de l'acidification de l'endosome (BH) ce qui va avoir un effet tampon, engendrer une trop grande entrée d'eau et de contre-ions, et ainsi conduire à la rupture de l'endosome par pression osmotique (Pack et al., 2005).

La sortie des endosomes constituant une étape clef dans l'amélioration des systèmes de délivrance des acides nucléiques (Gilleron et al., 2013), notre équipe a collaboré à une étude sur l'optimisation de vecteurs simples et monocomposants (des lipides ionisables) afin de dépasser les limites de l'échappement endosomal (Habrant et al., 2016). Par le biais d'une étude structure-activité, nous avons pu mettre en évidence que la présence de segments hydrophobes saturés et/ou plus courts que des chaines oleyls (C18) diminue l'efficacité de transfection en étant moins favorable à l'échappement endosomal (Zhi et al., 2010). Par contre, l'ajout de fonctions esters endogènes au niveau du linker permettait d'améliorer l'efficacité de transfection des acides nucléiques au sein de différents types cellulaires, en favorisant le mécanisme de « mélange lipidique » entre les lipoplexes et la membrane endosomale et donc l'échappement et la libération des acides nucléiques des endosomes.

2.1.4. Dissociation du complexe ADN/Lipide cationique

Après l'échappement endosomal, la dissociation des complexes acide nucléique/ lipide cationique constitue une étape déterminante afin qu'ils puissent être importés dans le noyau pour permettre leur transcription (ADN) ou bien être accessible dans le cytoplasme afin de pouvoir être traduit (ARNm) ou exercer leur effet inhibiteur (siRNA). En effet, il a été démontré notamment que la présence de lipides cationiques liés à l'ADN inhibait fortement son expression dans le noyau d'ovocytes de xénope comparé à de l'ADN nu (Zabner et al., 1995).

Communément, le modèle de dissociation accepté est celui proposé par Xu et Szoka (1996). Il repose sur la libération des acides nucléiques des lipoplexes durant l'échappement endosomal, délivrant ainsi les acides nucléiques seuls dans le cytoplasme. En effet au cours de l'échappement, l'interaction lipides cationiques/lipides anioniques des membranes endosomales va s'avérer nettement plus forte que l'interaction lipides cationiques/acides nucléiques (du fait de l'ajout d'interactions hydrophobes), libérant ainsi les acides nucléiques des lipoplexes pour qu'ils puissent rejoindre le cytoplasme. De plus, une fois dans le compartiment intracytoplasmique, les lipoplexes peuvent également se lier à d'autres composants anioniques (ARN, Protéines) entrant en compétition avec les acides nucléiques transportés et permettant ainsi leur libération (Scherman et al., 1998).

2.1.5. Traffic intracellulaire du plasmide et importation nucléaire

Suite à l'échappement endosomal, les molécules d'ARN peuvent directement être traduites en protéine (ARNm) ou bien effectuer leur effet inhibiteur (siRNA). En revanche, l'ADN doit encore rejoindre le noyau pour y être transcrit en ARNm par l'ARN polymérase II. Cette dernière étape représente une des principales limites à l'efficacité de transfection, et son amélioration est encore particulièrement difficile à l'heure actuelle (Sacramento et al., 2010). En effet, il a été démontré que l'injection cytosolique de plasmides ne conduisait qu'à 3% l'expression attendue (par rapport à son injection intranucléaire)(Graessmann et al., 1989), et que seulement 0,1 à 5% des plasmides délivrés par des lipides cationiques arrivaient à atteindre le noyau (Pollard et al., 1998; Cohen et al., 2009).

De nombreux obstacles ont été identifiés comme limitant le trafic et l'internalisation nucléaire de l'ADN au sein des cellules eucaryotes. Le premier est la présence de nombreuses nucléases intracytoplasmiques. Ces enzymes vont pouvoir rapidement dégrader l'ADN libre présent au sein du cytoplasme (environ 1 heure) (Vaughan et al., 2006; Ha et al., 2011), ne lui laissant que peu de temps pour rejoindre le noyau. De plus, la mobilité de l'ADN au sein du cytoplasme est extrêmement limitée d'autant plus que le plasmide est de grande taille. En effet, le cytosol est composé d'un maillage fin qui constitue le cytosquelette (Dauty and Verkman, 2005; Geiger et al., 2006) ainsi que de nombreuses biomolécules qui vont limiter la diffusion des macromolécules (Luby-Phelps, 2000). Enfin, le dernier obstacle est constitué de la membrane nucléaire elle-même, qui comporte des pores nucléaires ou NPC (« nuclear pore complex ») permettant le transport passif de molécules d'un poids moléculaire inférieur à 70kDa

et d'un diamètre de 10nm (Melchior and Gerace, 1995), trop petits pour laisser le passage d'ADN plasmidique (même condensé au sein de lipoplexes).

Dès lors, 3 possibilités existent afin permettre le passage d'ADN du cytoplasme vers le noyau :

- Certaines études ont mis en évidence que des lipoplexes avaient la capacité de fusionner avec la membrane nucléaire afin de relarguer directement l'ADN au sein du noyau (Kamiya et al., 2002).
- Durant la division cellulaire, la membrane nucléaire va se rompre de façon transitoire permettant ainsi l'entrée du transgène dans le noyau. Néanmoins, étant donné qu'il est possible de transfecter des cellules post-mitotiques *in vitro* mais également *in vivo,* cette rupture de la paroi nucléaire ne semble être qu'un facilitateur, et non une condition *sine qua non* à l'import nucléaire d'ADN.
- Le plasmide peut également entrer au sein du noyau via les NPC par l'intermédiaire d'un transport actif basé sur les importines (Brisson and Huang, 1999). En effet, ces protéines vont faire des allers-retours entre le cytoplasme et le noyau afin d'y faire entrer des protéines contenant des séquences NLS (par les NPC qui vont alors augmenter de taille jusqu'à 30nm de diamètre). Ainsi une des stratégies prometteuses repose notamment sur l'utilisation des facteurs de transcription pour importer l'ADN au sein du noyau. Ce sont des protéines capables d'interagir de façon spécifique avec les plasmides et contenant des séquences NLS afin d'être pris en charge par les importines (Dean, 1997; Dean et al., 1999, 2005) (**Figure 36**). Il a notamment été démontré que l'ajout de 5 motifs de fixation du facteur de transcription NFκB au niveau du plasmide permet de multiplier par 10 l'efficacité de transfection (Mesika et al., 2005), et que la stimulation de la translocation du facteur NFκB par l'ajout de TNFα permet également de faciliter la transfection de plasmides comprenant les dits motifs de fixation.

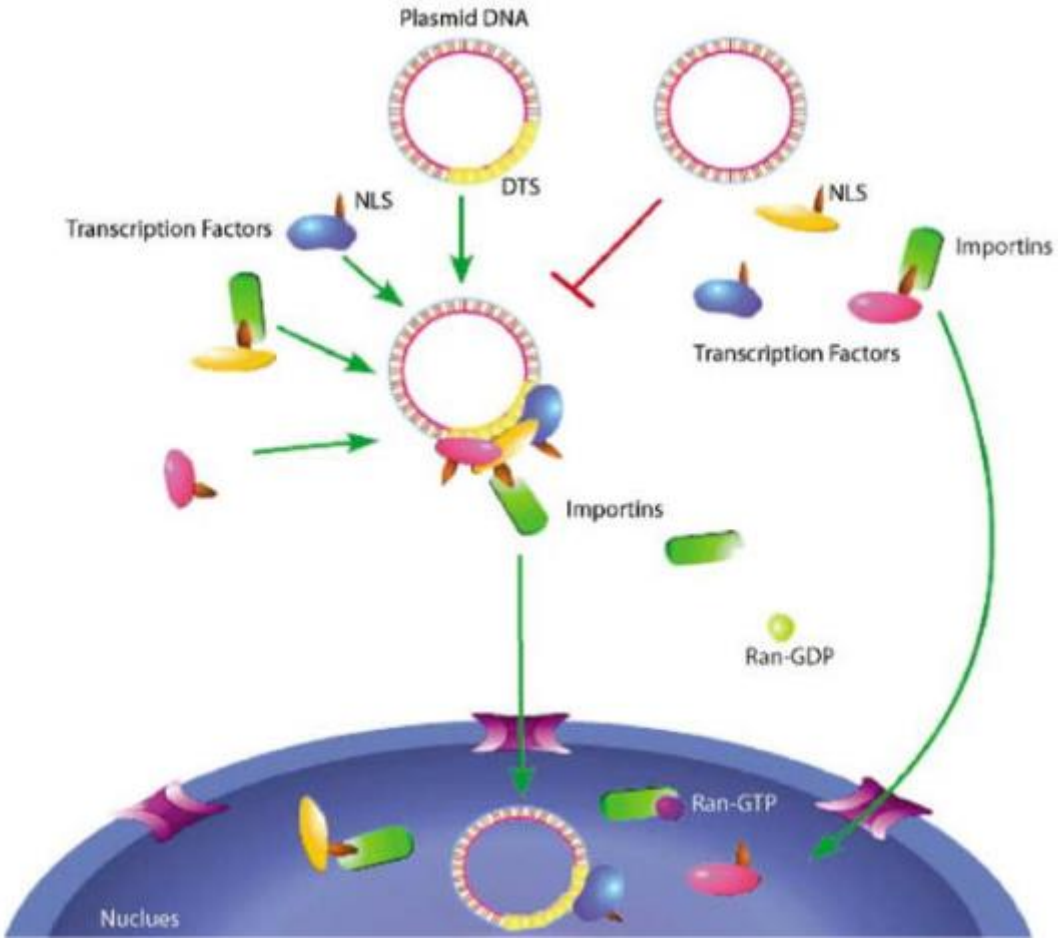


Figure 36 : Modèle d'import nucléaire spécifique d'un plasmide. Les plasmides présentent des DTS (« DNA nuclear targeting sequence ») interagissant avec les facteurs de transcription cytoplasmiques pour former des complexes ADN-protéine. Les facteurs de transcription comportant des séquences NLS, ils vont ensuite être pris en charge par les importines, ce qui va engendrer l'acheminement des complexes au sein du noyau via les pores nucléaires (Dean et al., 2005).

3. Stimulation de la réponse immunitaire par les lipides cationiques

La stimulation du système immunitaire par la plupart des dérivés lipidiques, notamment ceux d'origine bactérienne (comme le LPS et les lipoprotéines), s'effectue par l'intermédiaire du TLR2, du TLR4, et de leurs co-récepteurs respectifs (MD2/CD14/LBP) (Ostuni et al., 2010). Comme décrit précédemment dans **la Partie 1** (2.1.1.2. Signalisation), l'activation de ces TLRs va permettre l'activation de 2 voies de signalisation majeures :

- Soit MyD88-dépendante, aboutissant à l'activation de NFκB et des MAPKs.
- Soit TRIF-dépendante, engendrant l'activation des IRFs.

Ces voies vont permettre l'expression de nombreux facteurs pro-inflammatoires comme des cytokines, des chémokines, ainsi que des molécules de co-stimulations.

De nombreuses hypothèses sur l'action des lipides cationiques sur la signalisation cellulaire ont été émises. En effet, une forte densité de charges positives à la surface cellulaire peut être reconnue comme un signal de danger pour les cellules, induisant une réaction pro-apoptotique, pro-inflammatoire, ou contribuant à l'activation de cascades de signalisation classiquement activées par des composants cationiques endogènes (comme la spermine ou la lysine) (Ray et al., 2012; Verzola et al., 2012). De plus, il semblerait que l'insertion de lipides chargés positivement au sein des membranes cellulaires et leurs interactions avec des lipides neutres ou chargés négativement pourraient également altérer de manière forte les propriétés physicochimiques de ces membranes (Carmona-Ribeiro et al., 1997; Dymond and Attard, 2008) et affecter l'activité des protéines membranaires (Lonez et al., 2012). Dès lors, une meilleure connaissance de la relation entre la structure et l'effet des lipides cationiques sur la réponse immunitaire est nécessaire afin de construire des molécules spécifiques à chaque application avec (i) des propriétés adjuvantes pour l'immunothérapie ou la vaccination, ou bien (ii) inerte pour la thérapie génique.

Au cours de cette section, j'illustrerai mes propos avec 3 lipides cationiques très largement décrits pour leurs propriétés immuno-adjuvantes :

- Le diC14 amidine et RPR206252 développés par l'équipe de J.M. Ruysschaert (Ruysschaert et al., 1994b; Lonez et al., 2014), composés de 2 chaînes alkyles saturées de 14 carbones et de têtes polaires comportant des fonctions amines.
- Le DOTAP (« Chlorure de 1,2-dioleoyloxy-3-trimethylammoniumpropane ») développé par l'équipe de J.R. Silvius (Stamatatos et al., 1988), composé de 2 chaînes alkyles insaturées de 18 carbones et d'une tête polaire ammonium.

3.1. Voies de signalisation cellulaires activées par les lipides cationiques

3.1.1. La voie NFκB-dépendante

Parmi les lipides cationiques, les liposomes de DiC14 amidine sont capables d'induire la sécrétion de cytokines similaires à celles produites lors de l'activation du TLR4 par le LPS. En effet, le traitement de cellules dendritiques humaines et murines par ces lipides permet la sécrétion d'une large variété de cytokines pro-inflammatoires (Tanaka et al., 2008) via l'induction de la voie de signalisation MyD88-dépendante permettant l'activation de NFκB (Lonez et al., 2012).
Cette stimulation de la réponse immunitaire par le DiC14-amidine est strictement TLR4-dépendante, car le traitement de BMDC (« *Bone Marrow-derived Dendritic Cell* ») issus de souris TLR4-/-, MD2-/- ou MyD88-/- par ce lipide cationique ne permet pas la production de ces cytokines. Il est également à noter que les liposomes de DiC14 amidine permettent également d'engager d'autres cascades de signalisation NFκB-indépendantes activées classiquement par le TLR4. Cela passe notamment par l'expression de molécules de co-stimulation par l'intermédiaire de la protéine adaptatrice MyD88 et de la voie des MAPKs, mais également par la production d'IFNs via la protéine adaptatrice TRIF et la voie des IRFs (**Figure 37**).

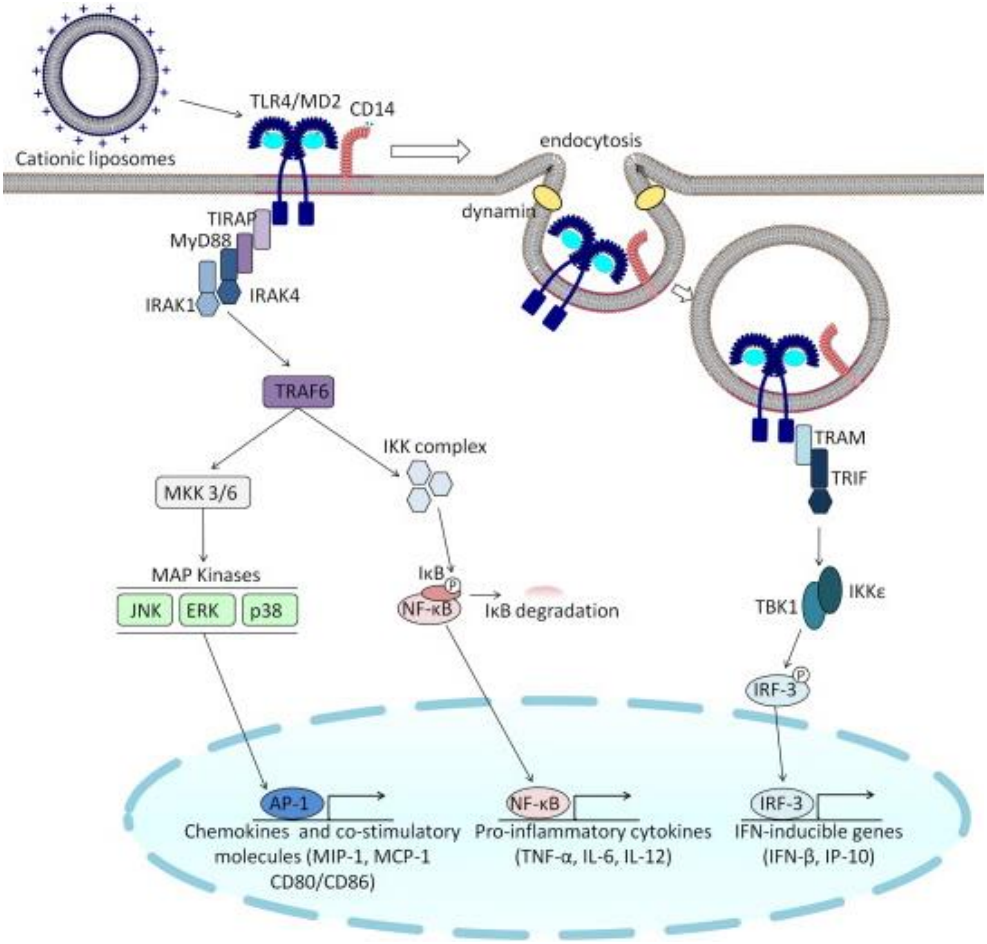


Figure 37 : Le lipide cationique DiC14-amidine stimule les cellules dendritiques par l'intermédiaire du TLR4. Cette stimulation va (i) permettre l'induction de la voie de signalisation MyD88-dépendante permettant l'activation de NFκB et des MAPKs aboutissant à la sécrétion de cytokines pro-inflammatoires et de chémokines, ainsi que l'expression de molécules de co-stimulation ; et (ii) permettre l'induction de la voie de signalisation TRIF-dépendante activant l'IRF3 et conduisant à l'expression des gènes inductibles par les interférons (Lonez et al., 2012).

Un autre lipide cationique peut également stimuler la voie NFκB : le RPR206252. Ce dérivé lipidique possède quelques similarités avec les lipoprotéines (ligands naturels du TLR2), comme la présence de groupements amines le long de son segment hydrophile et de chaînes alkyles saturées. L'utilisation de ce composé sur des lignées cellulaires de macrophages humains ou murins permet d'induire l'activation de la voie NFκB aboutissant à la production de cytokines pro-inflammatoires, de manière TLR2- et CD14-dépendante (peu importe l'hétérodimère TLR2/TLR1 ou TLR2/TLR6 formé)(Lonez et al., 2014).

3.1.2. Les voies NFκB-indépendantes

La plupart des lipides cationiques ne sont pas capable d'activer la voie de signalisation NFκB-dépendante, ni la sécrétion de certaines cytokines pro-inflammatoires comme le TNF-α (Vangasseri et al., 2006; Yan et al., 2007). Pourtant, ils ne sont pas pour autant inertes pour les cellules, et peuvent stimuler d'autres voies de signalisation associées à la réponse immunitaire innée. C'est notamment le cas du DOTAP qui va permettre la sécrétion par les BMDC de cytokines et chémokines dépendantes de la voir des MAPKs par l'intermédiaire de la PI3K (« phosphoinositide (PI)-3 kinase ») (**Figure 38 A**) (Yan et al., 2007, 2008).

Certains agonistes faibles du TLR4 activent exclusivement la voie TRIF-dépendante (Mata-Haro et al., 2007) par l'intermédiaire du co-récepteur CD14 qui va permettre la reconnaissance de ces agonistes ainsi que le regroupement des TLR4 en microdomaines lipidiques. Cela va induire l'endocytose des complexes agonistes/TLR4/CD14 et permettre l'activation des IRF3 (Regen et al., 2011; Zanoni et al., 2011). Ainsi, Les lipides cationiques étant des dérivés lipidiques, l'hypothèse la plus probable de leur mode d'action repose sur leur reconnaissance en tant qu'agonistes faibles par le TLR4. Cela permet par exemple, d'expliquer le fait que les liposomes à base de DOTAP (DOTAP/Cholestérol/ Phosphatidylcholine) peuvent engendrer l'expression d'une large variété de cytokines de manière dépendante du TLR4 mais indépendante de NFκB (Kedmi et al., 2010), et que cette activité agoniste peut être modulée en faisant varier la composition des liposomes (**Figure 38 B**).

La protéine clef dans l'activation des voies NFκB-indépendantes par les lipides cationiques pourrait dès lors être le CD14. C'est une glycoprotéine possédant au sein de sa structure une large poche hydrophobe, recouverte par un regroupement de résidus chargés positivement, capable d'interagir avec les régions hydrophiles (Kim et al., 2005) d'une grande variété de ligands lipidiques (comme le LPS, les lipopeptides, les phospholipides…) (Asai et al., 2007; Erridge et al., 2008). En effet, des évidences de l'interaction entre les lipides cationiques immunostimulateurs et le CD14 ont été démontrées, majoritairement grâce à l'insertion des chaînes alkyles présentes au niveau de leurs segments hydrophobes au sein de la poche hydrophobe du CD14 (Piazza et al., 2009). Cela expliquerait par ailleurs l'effet inhibiteur de certains lipides cationiques sur la stimulation induite par le LPS (Leon-Ponte et al., 2005) ou les lipooligosaccharides (Piazza et al., 2010) entrant ainsi en competition pour la liaison du CD14.

De plus, le CD14 peut jouer le rôle de co-récepteur pour de nombreux TLRs, que ce soit le TLR4 afin de faciliter la reconnaissance du LPS mais également le TLR1, 2, 3 et 6. Il peut être exprimé à la surface des cellules myélomonocytaires comme un récepteurs aux GPIs ou alors être sécrété dans le sérum sous forme soluble. S'il est membranaire, le CD14 va pouvoir interagir avec les intégrines β2 (CD11b ou CD11c dans les CPAs) au sein de microdomaines membranaires et engendrer 2 voies de signalisation différentes :

- Soit TLR4-indépendante par l'intermédiaire de la PLCγ2, de la SFK et/ou de la PI3K. Cela va aboutir à la libération dans le cytoplasme d'IP3, de calcium, et de ROS (« *reactive oxygen species* »), à l'activation de NFAT et des MAPKs, et enfin à l'expression de molécules de co-stimulations, de cytokines et de chémokines (Zanoni et al., 2009) (**Figure 38 A**).
- Soit TLR4-dépendante via l'internalisation du complexe TLR4/CD14/agoniste, et induire la stimulation de la voie TRIF, l'activation des MAPKs et des IFR3, et l'expression de molécules de co-stimulation ainsi que la production d'IFNs de type 1(Ostuni et al., 2010) (**Figure 38 B**).

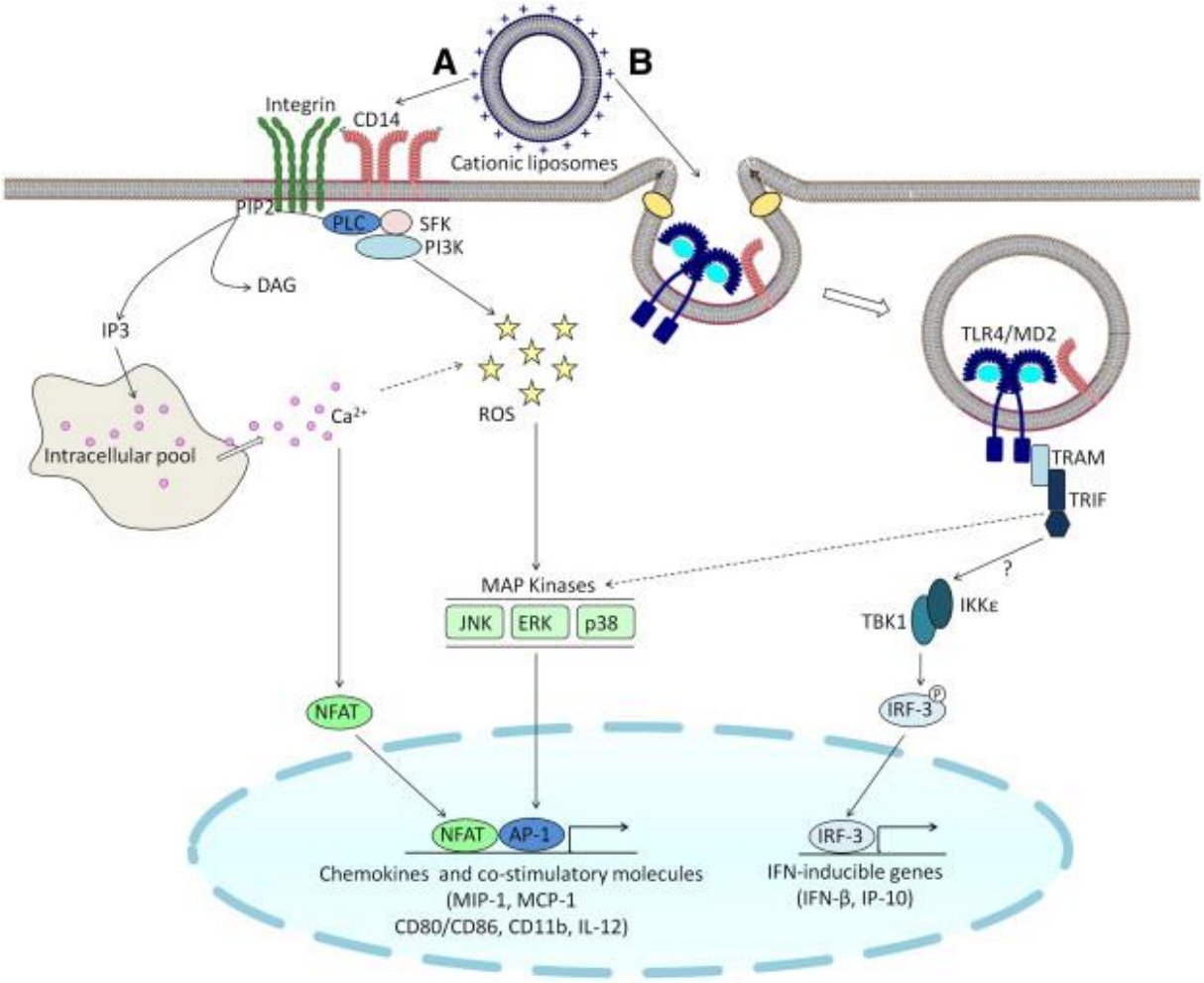


Figure 38 : Proposition du mécanisme d'activation de la réponse immunitaire par les lipides cationiques via une voie de stimulation NFκB- et MyD88-indépendante. (A) Les lipides cationiques induisent le regroupement des intégrines (CD11b ou CD11c) engendrant leur reconnaissance par le CD14, et provoquant l'activation de la PLC, de SRK et/ou de PI3k, ainsi que la libération de calcium intracellulaire et d'IP3. Cela permet ensuite l'activation de NFAT de manière TLR4-indépendante, l'activation des MAPKs via les ROS, et enfin l'expression de molécules de co-stimulation et la sécrétion de cytokines et de chémokines. (B) Une activation des IRF3 et des MAPKs peut également être médiée par les lipides cationiques, par l'intermédiaire d'une voie de signalisation TLR4- et TRIF-dépendante (Lonez et al., 2012).

3.1.3. La voie de l'apoptose

Le phénomène d'apoptose induit par les lipides cationiques est essentiellement observé au sein des cellules phagocytaires (Aramaki et al., 1999, 2000), suggérant ainsi l'implication de la phagocytose dans l'induction de cette voie. Ce phénomène serait dû à leur effet cytotoxique, qui est fortement dépendant de plusieurs facteurs comme la nature du lipide cationique, la taille des liposomes, et la concentration utilisée (Filion and Phillips, 1997; Carmona-Ribeiro, 2000).

L'induction de l'apoptose par les lipides cationiques implique de nombreux événements cellulaires, comme la libération de ROS dans le cytoplasme, l'activation de plusieurs kinases (protéine kinase C (PKC) et MAPKs), la dépolarisation de la membrane mitochondriale, la libération du cytochrome C et l'activation de caspases. C'est notamment le cas des liposomes composés de stéarylamine (SA-liposomes) (Iwaoka et al., 2006; Arisaka et al., 2010), qui vont induire l'apoptose via l'activation de :

- La p38 MAPK aboutissant à la production de ROS.
- La caspase 8 induisant le clivage de la protéine BID (« Bcl2 interacting protein ») en t-BID, sa translocation dans les mitochondries et la libération du cytochrome C dans le cytoplasme.
- La translocation de la PKCγ dans le noyau.

Au vue des voies de signalisation impliquées, l'interaction entre les lipides cationiques et le CD14 est aussi probablement responsable de l'initiation de l'apoptose en parallèle de l'induction d'une réponse pro-inflammatoire. En effet, le CD14 est capable d'engendrer le regroupement des intégrines β2 au sein de microdomaines lipidiques et de moduler l'activité de la PKCγ. Cela va induire la libération de calcium dans le cytoplasme, la génération de ROS, et l'activation de la voie des MAPKs et des caspases pro-apoptotiques (**Figure 39 A**). La voie TLR4-dépendante peut aussi être impliquée via le recrutement de la protéine RIP-1 par l'intermédiaire de la molécule adaptatrice TRIF, permettant l'activation des mêmes voies de signalisation (Kaiser and Offermann, 2005) (**Figure 39 B**).

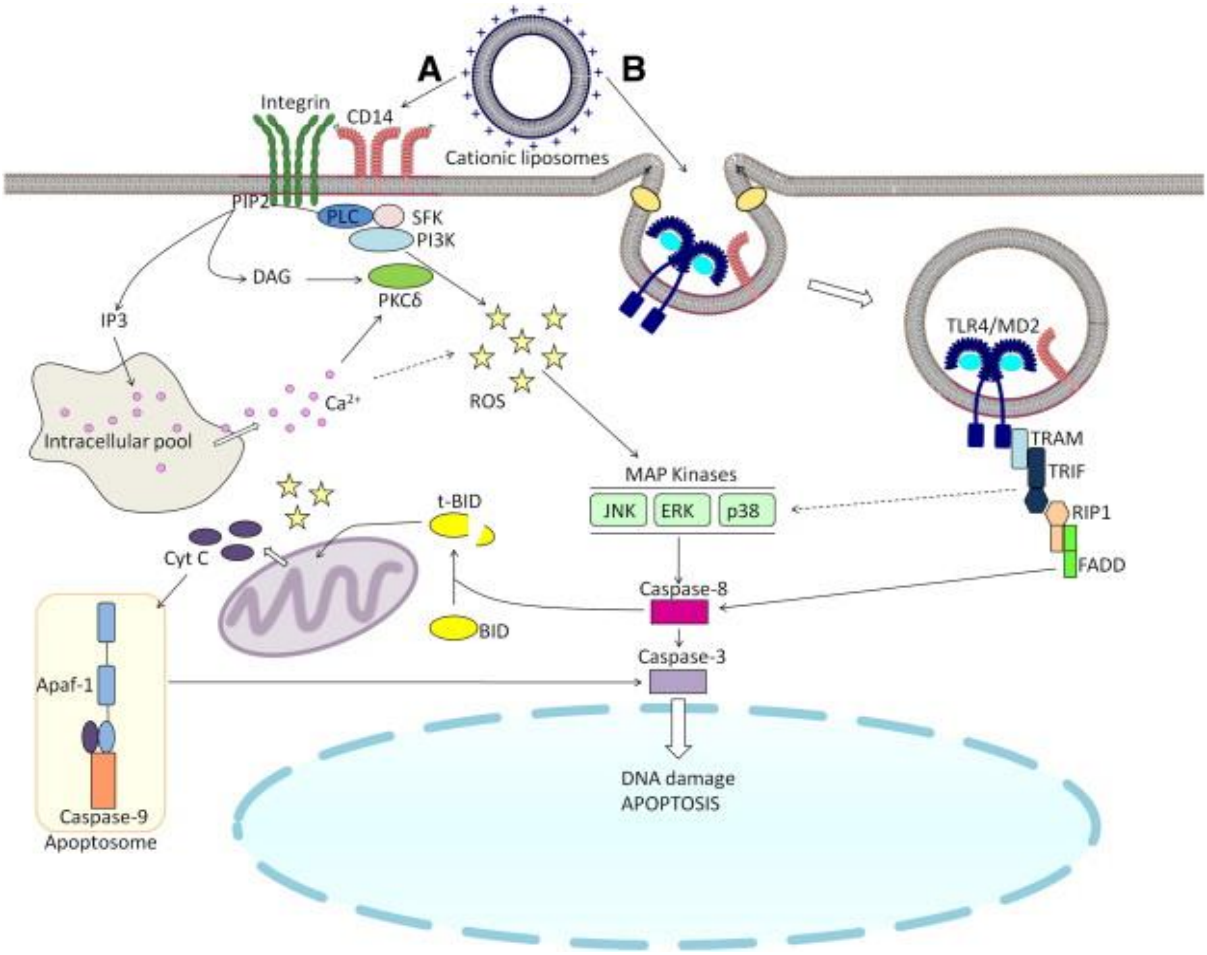


Figure 39 : Mécanisme possible de l'activation de la voie de signalisation pro-apoptotique par les lipides cationiques. (A) Les lipides cationiques peuvent engendrer le regroupement des intégrines β2 (CD11b ou CD11c) via leur reconnaissance par le CD14, ce qui va induire l'activation de la PKC, de SFK, de PI3K et/ou de la PKC-γ et aboutir à la libération de calcium intracellulaire, la production d'IP3 et la libération de ROS. Les ROS vont alors pouvoir activer les MAPKs aboutissant à l'activation de la caspase-8 et de la caspase 3, induire le clivage de BID en t-BID et sa translocation dans les mitochondries, et la libération de cytochrome C dans le cytoplasme. (B) Les lipides cationiques peuvent également être reconnus par le complexe TLR4/MD2/CD14, induire le recrutement de RIP-1 par l'intermédiaire de la protéine adaptatrice TRIF et ainsi activer les MAPKs qui vont engendrer la voie de signalisation pro-apoptotique (Lonez et al., 2012).

3.1.4. La voie de l'inflammasome

Les lipides cationiques sont également capables d'induire la sécrétion d'IL-1b par l'intermédiaire de la voie de l'inflammasome, qui est une cascade de signalisation à considérer séparément et qui nécessite un processus d'activation en 2 étapes (Gross et al., 2011) :

- Tout d'abord, la stimulation du système immunitaire (généralement par un ligand des TLRs) aboutissant à l'expression et la production du précurseur de cette cytokine (pro-IL-1β) dans le cytoplasme afin d'activer la voie NFκB-dépendante. Ainsi, comme d'autres ligands des TLRs, les liposomes de diC14-amidine en sont capables au sein des macrophages humains dérivés de monocytes, et de manière dépendante du TLR4 (Wilmar et al., 2012).

- Puis, l'activation de la voie de l'inflammasome, engendrant le clivage du précurseur en IL-1β et sa sécrétion dans le milieu extracellulaire. Même si le mécanisme d'activation de l'inflammasome reste encore méconnu, l'implication de la reconnaissance de facteurs mitochondriales libérés dans le cytoplasme (comme les ROS) est largement acceptée (Vanaja et al., 2015). De plus, la voie de l'apoptose et de l'inflammasome étant très proche, il est probable que certains lipides cationiques (si ce n'est tous) puissent activer la voie de l'inflammasome en permettant la libération de ROS dans le cytoplasme et l'activation des caspases-3 et -8 via la voie des MAPKs. Cela va aboutir au clivage de la pro-IL-1β en IL-1β et sa sécrétion dans le milieu extracellulaire (**Figure 40**). C'est notamment le cas du diC14-amidine qui est capable d'initier le clivage de la pro-IL-1β en IL-1β et de promouvoir sa sécrétion dans le milieu extracellulaire (Wilmar et al., 2012) ou du RP206252 qui peut engendrer l'activation de l'inflammasome NLRP3 (Lonez et al., 2014).

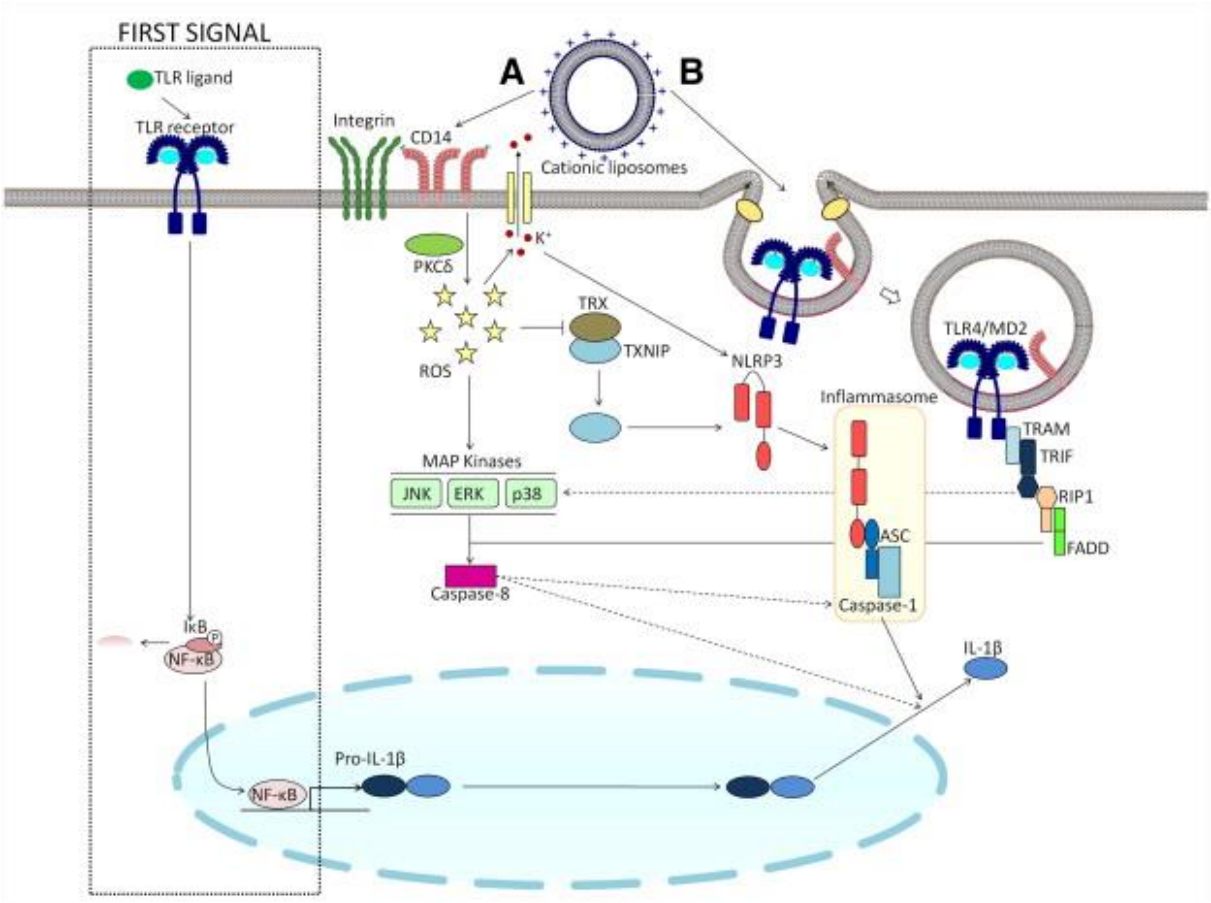


Figure 40 : Activation de la voie de l'inflammasome par les lipides cationiques. Cette activation nécessite un processus en 2 étapes. Tout d'abord, le premier signal passe par l'activation de la voie NFκB soit par les lipides cationiques, soit via des ligands des TLRs. Cela va permettre l'expression et la production de pro-IL-1β. Puis, (A) les lipides cationiques vont permettre le regroupement des intégrines β2 via le CD14, ce qui va engendrer la libération de ROS dans le cytoplasme, l'activation de la caspase 8 par l'intermédiaire des MAPKs et l'induction de l'inflammasome NLRP3. Cela va aboutir au clivage de la pro-IL-1β en IL-1β fonctionnelle qui va pouvoir être sécrété. (B) Les lipides cationiques peuvent également activer la voie de signalisation TRIF-dépendante via leur détection par le TLR4, aboutissant également à la stimulation de la voie des MAPKs, de la caspase 8, et permettent le clivage et la sécrétion d'IL-1β (Lonez et al., 2012).

3.2 Influence de composition des lipides cationiques

Bien que les lipides cationiques soient capables de stimuler de nombreuses voies de signalisation cellulaires, cela est dépendant de nombreux facteurs tels que leurs natures, leurs formulations, ou bien la taille des liposomes formés.

En effet, si l'on regarde les propriétés immunostimulantes de ces molécules, la nature de leur structure influence fortement leur caractère adjuvant. Pour la tête polaire, de nombreuses études ont mis en évidence que les fonctions amidines et amines quaternaires sont plus immunostimulantes que les amines tertiaires (Vangasseri et al., 2006; Yan et al., 2007; Tanaka et al., 2008). Pour ce qui est du segment hydrophobe, les lipides composés de chaînes alkyles insaturées ou de courtes chaînes alkyles saturées sont bien plus efficaces pour induire la libération de cytokines et de médiateurs pro-inflammatoires que ceux possédants de longues chaînes alkyles saturées (Vangasseri et al., 2006).

En ce qui concerne la formulation des lipides cationiques, il est clairement établi que les formuler avec des lipides neutres permet d'augmenter fortement leur effet pro-apoptotique, de manière dépendante du ratio entre les 2 (Takano et al., 2003; Kusumoto and Ishikawa, 2010). De même, l'action pro-apoptotique des lipides cationiques peut également être modulée en modifiant la fluidité des liposomes, notamment avec l'ajout de cholestérol ou d'un revêtement composé de PEGs (*« polyethylene glycol »*), afin de réduire leur internalisation et donc l'induction de l'apoptose par les cellules. Néanmoins, même si l'association en liposomes est importante pour leur internalisation, il semblerait que la reconnaissance des lipides cationiques se fasse à l'échelle du monomère. En effet, le DOEPC (« 1,2-dioleoyl-*sn-glycero*-3-ethylphosphocholine ») dilué dans le DMSO est toujours capable de stimuler l'expression des molécules de co-stimulation dans les cellules dendritiques, suggérant que la concentration micellaire critique des lipides cationiques est un facteur important à prendre en considération (Vangasseri et al., 2006).

Enfin, il est également rapporté que l'induction de l'apoptose par les lipides cationiques est grandement influencée par la taille des liposomes. Par exemple, les liposomes de grandes tailles comme les MLV (« *large multilamellar vesicles* ») engendrent une activité pro-apoptotique bien plus forte que ceux de petites tailles comme les SUV (« *small unilamellar vesicles* »), et cela pour une même composition (Aramaki et al., 1999; Takano et al., 2003).

4. Les dérivés lipidiques d'aminoglycosides

Les aminoglycosides constituent une grande famille de molécules possédant une activité antibiotique, basés sur des sucres modifiés naturellement synthétisés par des bactéries de l'ordre des actinomycètes. Ils sont composés d'un noyau 2-deoxystrepamine, substitué par des aminosucres soit en position 4 et 5 (4,5-DDS, comme pour la paromomycine et la néomycine), soit en position 4 et 6 (4,6-DDS, comme pour la kanamycine et la tobramycine). Grâce à de nombreuses fonctions amines portées par leurs sucres (jusqu'à 6 pour la néomycine), un couplage chimique sélectif est possible afin de leur ajouter un groupement hydrophobe (chaînes d'acides gras ou cholestérol) et ainsi obtenir un grand nombre de composés amphiphiles positivement chargés : les Lipoaminoglycosides.

Le premier composé de cette famille fut synthétisé par l'équipe de J.M. Lehn à partir d'une tête polaire kanamycine et d'un segment hydrophobe cholestérol, aboutissant à la création de la Kanamycine-Cholesterol (KC) et de son dérivé tri-guanidylé, la tri-guanidium-kanamycine-cholestétol (TGKC) (Belmont et al., 2002). Utillisant la capacité naturelle des aminoglycosides à fixer les acides nucléiques, comme l'ARN de la sous-unité 30s des ribosomes bactériens, ces vecteurs ce sont avérés efficaces afin de délivrer des plasmides aussi bien *in vitro* que *in vivo* chez la souris. Suite à ces résultats prometteurs, de nombreux autres lipoaminoglycosides ont par la suite été développés (Sainlos et al., 2005; Desigaux et al., 2007; Mével et al., 2012; Habrant et al., 2016) en se basant sur l'utilisation :

- D'une grande variété structurale de têtes polaires issues de composants naturels.
- De différents segments hydrophobes dérivés du cholestérol ou de chaînes aliphatiques.
- De différents espaceurs conférant certaines propriétés de biodégradation aux lipoaminoglycosides.

Au cours de ce travail de thèse, nous avons utilisés de nombreux lipides cationiques dérivés d'aminoglycosides qui sont résumés dans la **Figure 41 A-E**. Ces lipoaminoglycosides comportent de nombreuses variations structurales :

- 4 têtes polaires aminoglycosides différentes (néomycine, paromomycine, tobramycine et kanamycine).
- 5 espaceurs différents (succinyl, adipyl, dithioglycolyl, succinyl-serinyl et phosphoramine)
- 5 segments hydrophobes différents (di-oleyl, di-stearyl, di-palmityl, di-myristyl et cholesterol).

Nous avons étudié ces dérivés lipidiques soit seuls, afin de déterminer la relation entre leur structure et leur propriété immunostimulante ainsi que les mécanismes et voies de signalisation associés (présenté dans l'**Article 2** : Développement de nouveaux adjuvants lipidiques pour l'immunothérapie anticancéreuse.) ; soit formuler avec des co-lipides (**Figure 41 F**) afin d'étudier l'influence de la structure de l'espaceur sur l'organisation de la bicouche lipidique des liposomes et l'efficacité de transfection (présenté dans l'**Article 3** : Influence de l'assemblage supramoléculaire des liposomes sur l'efficacité de transfection.).

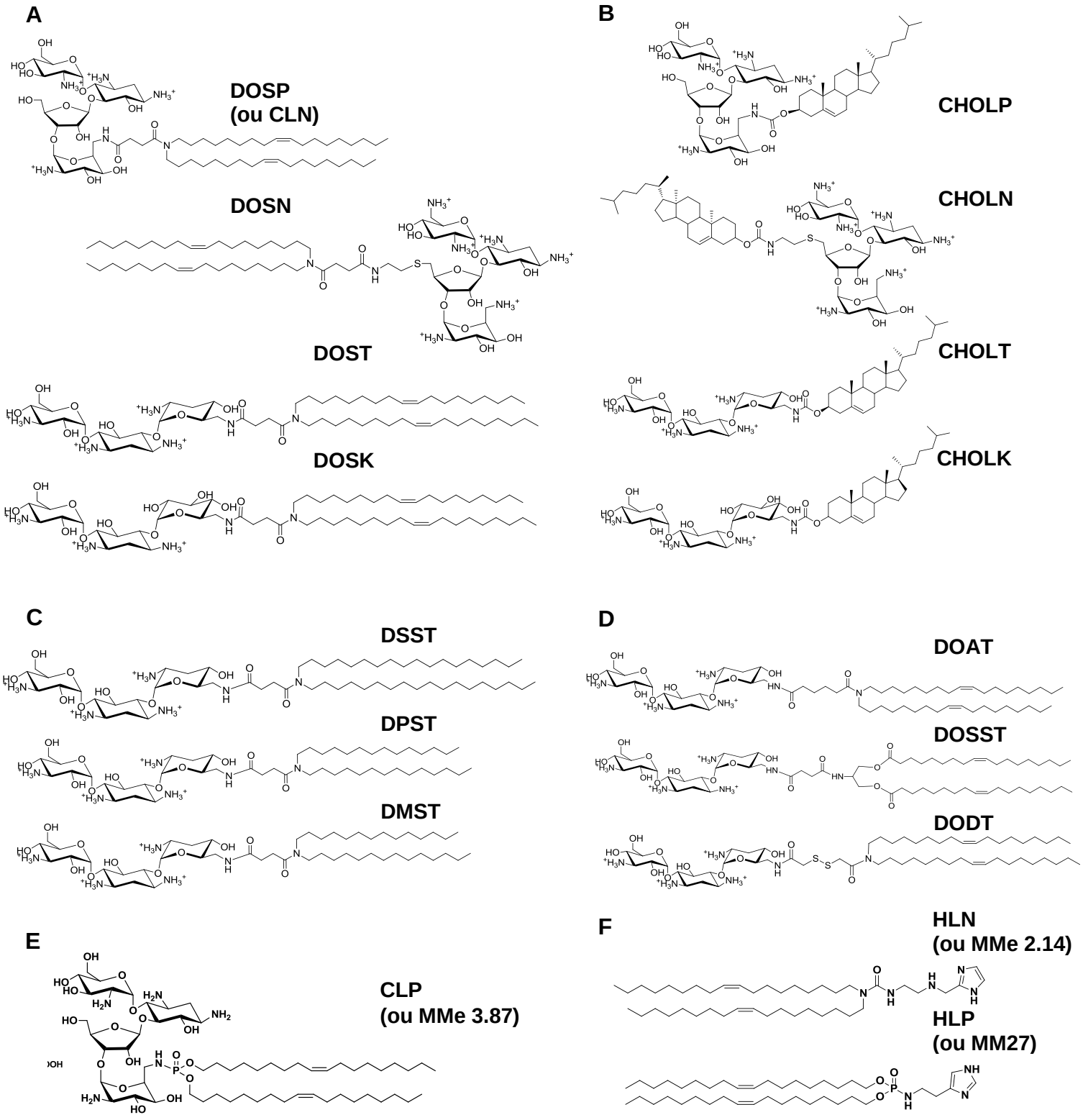


Figure 41 : Structure des Lipoaminoglycosides et co-lipides utilisés au cours de ce travail de thèse. A) Lipoaminoglycosides avec une variation de la tête polaire (DOSP ou CLN : Di-Oleyl-Succinyl Paromomycin, DOSN : Di-Oleyl-Succinyl-Neomycin , DOST : Di-Oleyl-Succinyl-Tobramycin et DOSK : Di-Oleyl-Succinyl-Kanamycin). B-C) Lipoaminoglycosides avec une variation du segment hydrophobe. B) Dérivés du cholestérol (CHOLP : Cholesterol-Paromomycin, CHOLN : Cholesterol-Neomycin, CHOLT : Cholesterol-Tobramycin et CHOLK : Cholesterol-Kanamycin). C) Dérivés de chaînes d'acides gras (DSST : Di-Stearyl-Succinyl-Tobramycin, DPST : Di-Palmityl-Succinyl-Tobramycin, DMST : Di-Myristyl-Succinyl-Tobramycin). D) Lipoaminoglycosides avec une variation de l'espaceur (DOAT : Di-Oleyl-Adipyl-Tobramycin, DOSST : Di-Oleyl-Succinyl-Serinyl-Tobramycin, et DODT : Di-Oleyl-Dithioglycolyl-Tobramycin). E) Lipoaminoglycoside avec un espaceur phosphoramide (MMe 3.87 ou CLP). F) Co-lipides (MMe 2.14 ou HLN, MM27 ou HLP).

RESULTATS

Article 1 : Mécanisme de la vaccination à ADN médiée par le 704

Au cours des 25 dernières années, des progrès considérables ont été faits dans le domaine de la thérapie génique, aboutissant à la mise en place de nombreux essais cliniques chez l'homme dans le cadre de maladies génétiques ou acquises. Parmi ces applications, la vaccination à ADN a suscité un grand intérêt au cours d'essais précliniques avec des résultats intéressants contre l'influenza, le VIH et de de nombreux cancers, laissant la porte ouverte au développement de stratégies vaccinales innovantes (Kay, 2011; Collins and Thrasher, 2015). Néanmoins, les essais cliniques chez l'homme se sont avérés décevant à cause de l'induction d'une réponse immunitaire insuffisante à l'obtention d'un effet protecteur. Les principales causes de ces échecs sont attribuées à la difficulté de délivrer efficacement de l'ADN codant pour un antigène d'intérêt au sein des cellules *in vivo* (Fu et al., 1999). De plus, pour des raisons de tolérance et de sécurité, la dose d'ADN administrable chez l'homme est fortement limitée (0,01 à 0,07 mg/kg contre 1 à 4 mg/kg chez la souris). Dès lors, le développement de vaccins à ADN utilisables nécessite la mise au point de formulations dont l'efficacité sera amélioré d'un facteur 100 par rapport aux outils actuels.

En ce sens, le développement de nouveaux vecteurs plus efficaces pour la délivrance d'ADN représente un axe de recherche majeur dans l'amélioration des formulations vaccinales. En effet le vecteur idéal en plus d'être utilisable *in vivo*, se doit tout d'abord de pouvoir être administré de nombreuses fois au cours d'un protocole de vaccination et ainsi ne pas induire de réponse immunitaire contre lui-même. De plus, il doit pouvoir permettre la délivrance directe du plasmide au sein du cytoplasme afin d'éviter sa dégradation dans le compartiment endosomal, mais également afin qu'il puisse être capable de stimuler efficacement les différents senseurs à ADN intracytoplasmiques (CDS) dans le but d'induire la sécrétion de divers cytokines, chémokines, et molécules de co-stimulation capables de stimuler la réponse immunitaire innée. Enfin, le vecteur idéal doit également permettre la mise en place d'une réponse immunitaire à médiation cellulaire de type Th1 afin de détruire les cellules infectées (ou bien les cellules tumorales), ainsi qu'à médiation humorale de type Th2 afin de permettre la sécrétion d'anticorps dans le but de bloquer l'infection.

Dès lors, les copolymères à blocs apparaissent comme des candidats idéaux en tant que vecteurs pour la vaccination à ADN. En effet ils permettent tout d'abord une amélioration significative de l'efficacité de transfection, notamment en permettant une délivrance direct des acides nucléiques au sein du cytoplasme des cellules (Chèvre et al., 2011), et non par endocytose comme observé classiquement. L''un d'entre eux, le 704 (un copolymère à bloc tétrabranché, composé de motifs d'oxyde d'éthylène et d'oxyde de propylène branchés par leurs extrémités hydrophobes à une éthylène diamine centrale), a notamment permis de réduire d'un facteur 50 la dose d'ADN codant nécessaire à l'établissement d'une réponse immunitaire à médiation humorale et cellulaire robuste par rapport à l'ADN nu (McIlroy et al., 2009). Néanmoins, cela ne fut possible qu'en ajoutant un ADN non-codant possédant des motifs CpG, jouant ainsi le rôle d'adjuvant en stimulant directement CDS. L'efficacité de la vaccination à ADN médié par le 704 a par ailleurs été démontrée dans un modèle de carcinome hépatique murin induit (en engendrant une régression du nombre et du volume des nodules tumoraux), et est à présent en cours de développement préclinique et clinique.

Bien que ces différentes études aient prouvé l'efficacité de l'utilisation de formulations vaccinales composées d'ADN et de 704, ses mécanismes immunologiques restent encore à définir. En effet, connaître les cellules, les récepteurs, ainsi que les motifs présents au sein des plasmides responsables de l'induction d'une réponse immunitaire protectrice est crucial afin d'améliorer encore les vaccins à ADN dans l'optique d'accroître les réactions immunitaires contre des antigènes d'intérêt. L'ensemble des résultats obtenus au cours de cette étude ont fait l'objet de l'écriture d'un article scientifique en cours de soumission.

Article 1 : Mechanism of 704-mediated DNA vaccine

Mechanism of 704-mediated DNA vaccine

Thibault Colombani,[1,§] Thomas Haudebourg,[1,§] Benoit Chatin,[2] Barton Ford Haynes,[3] Damien Habrant,[4] and Bruno Pitard*,[1,4]

[1] CRCINA, INSERM, Université d'Angers, Université de Nantes, Nantes, France.

[2] L'institut du thorax, INSERM, CNRS, UNIV Nantes, Nantes, France.

[3] Duke Human Vaccine Institute, Duke University School of Medicine, Durham, NC 27710

[4] In-Cell-Art, 21 rue de la Noue Bras de Fer, 44200 Nantes, France.

[§] These authors contributed equally to this work

*Corresponding author : Bruno PITARD, Inserm UMR1232, CNRS ERL, Université de Nantes, 22 boulevard Bénoni Goullin, 44000 Nantes, France. Tel: +33(0)228080350; E-mail: bruno.pitard@univ-nantes.fr.

ABSTRACT

Genetic immunization is an attractive approach for prophylactic and therapeutic vaccination. Gene delivery systems could be of viral or non-viral origins, and research in this area relies on improving these systems both in terms of efficacy and safety. We recently reported that amphiphilic block copolymer 704 holds promises as a non-viral vector for DNA vaccination, by dramatically decreasing the dose of antigen encoding plasmid DNA required to trigger an immune response, compared to non-formulated DNA. In the current study, we report that 704-mediated DNA vaccine induces the production of specific antibodies against gp120 HIV envelop proteins while using DNA at the nanogram scale. We then showed that dendritic cells antigens expression is not necessary contrary to muscle cells transfection to induce dramatic enhancement of plasmid DNA immunity. To elucidate mechanism of 704-mediated DNA vaccination and the implication of the innate immune system, we evaluated pathways involved in DNA sensing by using STING-/-, MyD88-/- and Tmem176b-/- mice. We also studied the influence of formulations containing plasmid DNA enriched with unmethylated CpG motifs, various TLR ligands, or mRNA coding for DHX9 and 36 DNA sensors. Results showed that intracytoplasmic DNA sensing leading to both interferons and NFκB cascade stimulation is strongly involved in the induction of humoral immune response obtained with 704, confirming its ability to directly deliver DNA into the cytosol.

Considering that naked DNA vaccination failed to induce protection in human clinical trials and that 704-mediated vaccination increases both unique antigen expression and strongly stimulate the innate immunity, 704 represents a highly promising vector towards human DNA vaccination.

INTRODUCTION

DNA vaccination is a particularly attractive method to treat various diseases. This approach has seen renewed global interest over the last couple of years following advances in understanding the human immune system.

At its most basic level, a DNA vaccine is a simple molecule of closed circular DNA that contains a gene encoding an antigen of interest, driven by a strong promoter.[1] It is inexpensive, robust, easy to produce and to transport, amenable to facile modification and is essentially "off the shelf".[2] Discovered by Jon Wolff 25 years ago, this mode of in vivo immunogenic gene transfer has been extensively studied in initial preclinical testing against various targets such as influenza, HIV and several different types of cancers, resulting in exciting results that led to the initiation of human clinical trials with much enthusiasm. However, the promising preliminary results observed in small animals were not replicated in human subjects. This was attributed to insufficient expression of the antigen in protein form the DNA vector in the human host, and very high DNA doses (in the milligram range per injection) were required to trigger a comparable biological response.[3] In this context, several research groups focused their efforts on enhancing expression of the antigen, which led to incrementally increase the immunity of such systems. Apart from modifying the backbone of the DNA, technologies such as electroporation (injecting the DNA vaccine followed by applying an electric pulse around the area)[4–8] and gene gun (bombarding the skin with nano-particles coated with DNA)[9,10] have been forerunners in this area. However, these technologies did not achieve stellar immunity in human patients. Recently, it was discovered that getting large amount of antigen expression from the vaccine might only be part of the solution. Indeed, it is now accepted that a prerequisite for a strong immune response is the "innate" effect of a vaccine. In other

words, the vaccine needs to activate sensors in the body that set off an alarm signal and trigger an immediate “danger response”, much like what happens during the course of an actual bacterial or viral infection.[11] The activation of such a “danger response” is an essential step for creating a local environment favorable for a proper deployment of immune cells against an invading pathogen, or a tumor. As such, an ideal vaccine formulation should not only deliver the target protein antigen, but also sufficiently activate the danger sensors in the body. Such a breakthrough methodology could be obtained from the synthetic formulation consisting of a plasmid DNA associated with a tetrafunctional amphiphilic block copolymer, made up of four poly ethylene oxide - poly propylene oxide (PEO-PPO) blocks centered on an ethylenediamine moiety. In preclinical models, this formulation has demonstrated a dramatic enhancement of target protein production,[12,13] and was shown to proceed via an intracellular delivery mechanism that maximizes access of the vaccine to danger sensors in the body.[14] We have already demonstrated its ability to improve DNA vaccine performance in a highly relevant animal model of hepatocellular carcinoma observing elimination of tumors expressing the target protein (currently under preclinical and clinical development),[15] and also in a relevant mouse model of allergic asthma by using plasmid DNA encoding Derf1.[16,17]

The potential of this tetrafunctional block copolymer / DNA vaccine prompted us to explore the immunogenicity and functionality of antibodies against HIV envelop proteins. Our objective was to decrease the necessary DNA amount to the nanogram dose and to elucidate the mechanism by which this tetrafunctional block copolymer dramatically improves the efficiency of DNA vaccines.

MATERIALS AND METHODS

Animal procedures

Myd88-/-, Sting-/-, TLR3-/-, MAVS-/-, Tmem176b-/- and C57BL/6 mice 8 weeks old (Elevage Janvier, Le Genest, France) were housed in conventional conditions according to INSERM (Institut National de la Santé et de la Recherche Médicale) guidelines. All animal experiments were performed in accordance with the recommendations of French Ministry of Higher Education and Research, and approved by an ethics committee in animal experimentation under reference APAFIS#7897.

For *i.m*. DNA/RNA vaccination, mice were anesthetized with isoflurane (1-3% for maintenance, up to 5 for induction) in oxygen from a precision vaporizer (Tem Sega, Pessac, France), then different DNA/RNA-polymer formulations were injected into both *tibialis anterior* muscles using an Insumed Pic Indolore 30G syringe (Artsana, Grandate ,Italy). Two sites were injected per animal, so DNA doses are given per *tibialis anterior*. In all cases, the injection volume was 50 µl per injection site. After vaccination, sera were recovered for analysis of the humoral immune response at the end of each experiment.

Nucleic acids preparation and formulation

The pCMV-LacZ plasmid (Clontech, St Germain en Laye, France) is a plasmid encoding coding the β-Galactosidase (β-Gal) under the control of the human cytomegalovirus (CMV) immediate-early gene promoter was used as antigen. The pCMV-LacZ-miR133a-3p or pCMV-LacZ-miR142a-3p were constructed by cloning 4 miRNA 133a-3p targeting sequences (Forward : cagctggttgaggggaccaaa, Reverse : tttggtcccctcaaccagctg) or 4 miRNA 142a-3p targeting sequences (Forward :

tccataaagtaggaaacactaca, Reverse : tgtagtgtttcctactttatgga) into the 3'UTR of LacZ gene which inhibit respectively the expression on muscular fibers or dendritic cells.

The pCpGrich-LacZ was constructed by cloning the LacZ gene from the pCpGfree-LacZ into the pCpGrich-mcs backbone (InvivoGen, San Diego – USA). pCpGrich-LacZ contains 88 CpG dinucleotides motifs whereas pCpGfree-LacZ have none. Both plasmids encoding for β-Gal under the control of CMV enhancer and the human elongation factor 1 alpha core promoter.

The CH505 TF gp120 plasmid encoding for the gp120 HIV envelop protein was kindly supplied by Barton Ford Haynes (Duke University, USA).

All plasmids prepared were purified using EndoFree plasmid purification columns (Qiagen, Courtaboeuf, France) and were confirmed to be free of endotoxin contamination (endotoxin <0.1 EU/µg plasmid DNA) by the Limulus amoebocyte lysate assay (Lonza, Clermont-Ferrand, France). The non-coding pVAX DNA was purchased to Life technologies (Saint Aubin, France) and non-coding pQE30 to Clontech.

The non-coding unmodified mRNA was purchase to TriLink BioTechnologies (San Diego, USA). The mRNA-LacZ, mRNA-DHX9 and mRNA–DHX36 (TriLink BioTechnologies) are unmodified ARCA capped messenger RNA, coding respectively for β-Galactosidase protein, DHX9 and DHX36 DNA sensors.

The TLR9 agonist ODN1826 and antagonist ODN 2088 were purchased to InvivoGen.

The tetrafunctional block copolymers 704, was kindly supplied by In-Cell-Art (Nantes, France).

Plasmid DNA, mRNA and ODNs were formulated immediately prior to *i.m.* injection as previously described.[13]

Cell culture condition and transfection.

Immature dendritic cell (JAWSII; CRL-11904, ATCC, RockvilleMD, USA) were grown in RPMI1640 supplemented with 10% heat-inactivated Fetal Calf Serum (FCS, Eurobio, Courtaboeuf, France), 100U/mL penicillin (Life technologies, Villebon sur Yvette, France), 10µg/mL streptomycin (Life technologies) and 5ng/mL murine GM-CSF (Life technologies).

Twenty-four hours prior to transfection, cells were seeded in 24-well culture plates at a density of 60 000 cells in 1 mL of complete medium and incubated at 37°C in a humidified 5% CO_2 /95% air containing atmosphere. Thirty minutes before transfection, medium was removed and replaced by 400µL of complete medium. One hundred microliters of lipoplexes was prepared by mixing two equal solutions containing 0,5µL pCMV-LacZ-miR142a-3p and the ionizable lipid DOSK (Di-Oleyl-Succynyl-Kanamycin) at a charge ratio (±) of 5, then deposed in each well.

B-Galactosidase expression.

For *in vitro* β-Galactosidase expression experiments, cells were washed after 24h of incubation at 37°C 5% humidified CO_2 with PBS and lysed in Reporter Lysis Buffer 1x (Promega, Charbonnieres, France) supplemented with 1 tablet per 50 mL of complete Mini Protease Inhibitor Cocktail (Roche, Meylan, France) according to manufacturer's recommendations. After overnight freezing cycle, cell lysates were centrifuged at 10 000 rpm during 5 min.

For *in vivo* β-Galactosidase expression experiments, *tibialis anterior* muscles were dissected 7 days after *i.m.* injection and immediately frozen in liquid nitrogen. Then

muscles were sheared by Ultra-Turrax ® T25 basic (IKA, Lille, France) in Reporter lysis buffer (Promega) supplemented with protease inhibitor cocktail (Roche).
The expression was then quantified in cells lysates and muscle extracts using the Beta-Glo Assay System (Promega) according to the manufacturer's protocol.

Measurement of immune response.

Cytokines expression were determined by RT-qPCR analysis. Briefly, muscles were sampled as described above. Total RNA was extracted from muscles with TRIzol® (Life technologies) according to the manufacturer's protocol. RT-qPCR were then realized in 2 phases: first, reverse transcriptions of RNA in cDNA were conducted using High Capacity cDNAReverse Transcription Kits (Life technologies) on GeneAmp® PCR System 9700 Thermal Cycler (Life technologies). Then, Real-time PCR were effectuated using Taqman® Gene expression assays on StepOnePlus™ Real-Time PCR System (Life technologies). Probes used to amplify specific gene products from murin cDNA (Life technologies) were : for IL-1β : Mm00434228_m1 ; for IL-6 : Mm00446190_m1 ; for IL-10 : Mm00439614_m1 ; for ZBP1 : Mm00457979_m1 ; for IFI204 : Mm00492602_m1 ; for DHX9 : Mm00456021_m1 ; for DHX36 : Mm00661002_m1 ; for TNFα : Mm00443260_g1; for IFNγ : Mm01168134_m1; for HPRT (Housekeeping gene) : Mm00446966_m1.

Cytokines secretion were measured on muscle extracts by FlowCytomix™ Multiplex Technology (Ebioscience, Paris, France). Muscles were dissected, frozen in liquid nitrogen, placed on eppendorfs with PBS supplemented with protease inhibitor cocktail (Roche), crushed using TissueLyser II (Qiagen) with 2 cycles of 3 min frequency 30 and ten 5 freeze/thaw cycles were performed on muscle lysates.

Cytokines were measures on lysates using Mouse Th1/Th2 FlowCytomix™ 10-plex RTU kit (Ebioscience, Paris, France) on BD FACSVerse™ (BD Biosciences, Rungis, France).

Humoral immune responses were measured by enzyme-linked immunosorbent assay (ELISA). 96-well plates (Nunc Maxisorp, Roskilde, Denmark) were coated overnight at 4 °C with 5 µg/ml of recombinant βGal or 2µg/mL of gp120 protein in 50 mmol/l NaHCO3 pH 9.5, and then blocked for 1 hour at room temperature with PBS 0.05% Tween-20 1% bovine serum albumin before distributing diluted sera in triplicate. Plates were incubated at 37 °C for 90 minutes, then βGal-specific IgG was detected using peroxidase-conjugated goat anti-mouse IgG (Jackson ImmunoResearch, Newmarket, UK) diluted 1/5,000 in PBS 0.05% Tween-20 1% bovine serum albumin. Plates were washed three times in PBS 0.05% Tween-20 between steps, and peroxidase activity was revealed with 1 mg/ml ortho-phenylene diamine in pH5 citrate buffer. Reactions were stopped by addition of 1 mol/l H2SO4, then absorbance (A) was measured at 492 nm. Anti-gp120 titers were determined by measuring the absorbance at 490nm of sera diluted at 1/2000. Anti-βGal titers were determined using cascading dilution from 1/800 to 1/1638400 for each samples, then by tracing a linear trend curve in the linear portion of the curve between 0 and 1 of absorbance to determine the theoretical dilution value for absorbance=1 (ThDiA1), and calculated by 1/ThDiA1. A standard β-Gal-specific mouse serum was included in each ELISA plate to normalized results.

Statistical analysis

Statistical analyses were performed using GraphPad Prism software (La Jolla, CA, USA). Values are expressed as the mean ± SEM. Significant differences between groups are indicated * $P<0.05$ ** $p<0.01$ *** $p<0.01$ by Mann-Whitney test.

Results

704-mediated DNA vaccination dramatically reduces the amount of DNA required while triggering an effective production of antibodies against gp120 HIV envelope protein.

In order to improve therapeutic strategies currently used to fight HIV infections, the development of novel vaccine formulations is of particular interest, especially in order to allow the production of specific neutralizing antibodies against HIV envelop proteins such as gp120[18] to prevent virus binding to the CD4 receptor as well as its entry into cells.[19] To this end, we investigated whether a DNA vaccine composed of a plasmid encoding the gp120 (CH505 TF gp120 plasmid) alone or formulated with 704 could induce an effective antibodies production at low amount of injected DNA. After 4 intramuscular injections at day 0, 21, 42 and 63 with various amounts of plasmid DNA ranging from 0.2 to 50 μg, we measured at day 84 the anti-gp120 antibody titer by ELISA assay. As shown in Figure 1, 704-mediated DNA vaccination induced a significant anti-gp120 antibody titer at 0,2 μg of DNA and a maximal humoral immune response starting from 1 μg of DNA. Interestingly, 50 μg of unformulated DNA failed to generate the maximum of antibodies production, reaching only humoral response comparable to that obtained with 0.2 μg of 704-formulated plasmid. These results clearly demonstrate that 704-mediated DNA encoding gp120 vaccination leads to a strong specific antibodies production, reducing the amount of DNA required by 250 fold compared to unformulated plasmid.

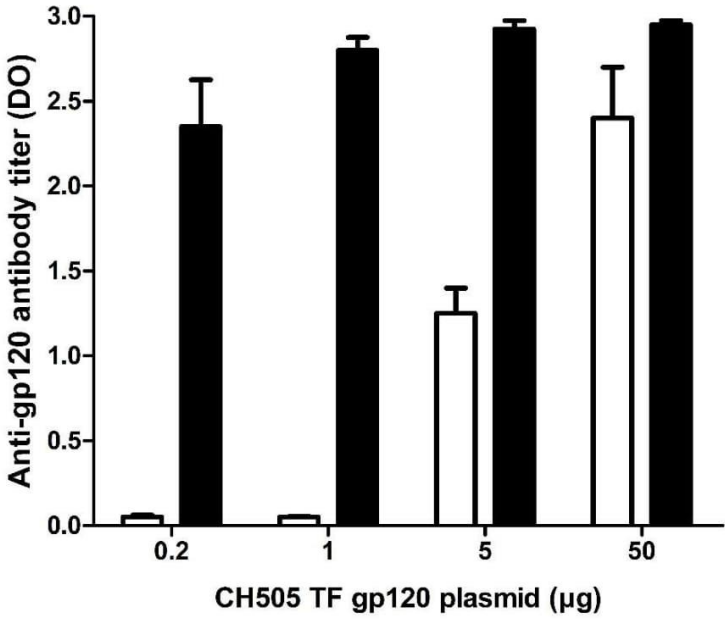


Figure 1: 704-mediated DNA vaccination against gp120 HIV envelope protein. Mice were injected i.m at day 0, 21, 42 and 63 with 50, 5, 1 or 0.2 µg of CH505 TF gp120 plasmid DNA unformulated (white) or formulated with 704 block copolymer (black). Humoral immune response was determined at day 84 by ELISA for anti-gp120 total IgG. Dose are given per *tibialis anterior.*

Formulating DNA with 704 led to high cytokine and interferon productions

Recent studies have shown that immunogenicity of DNA vaccines are regulated by DNA innate immune recognition via several cellular danger sensors[20] that lead to induce interferons (IFNs) and pro-inflammatory cytokines production.[21] In order to assess if 704 block copolymer contributes to increase danger sensors activation, we first evaluated the ability of plasmid DNA alone or formulated with 704 to trigger the production of key molecules implicated in the induction of an effective immune response. After intramuscular injection of 2 µg of pCMV-LacZ alone or formulated, we measured the kinetics of production of cytokines and interferons including interleukine 2 (IL-2), IL-5, IL-6, IL-10, IFNγ and tumor necrosis factor α (TNFα) into the injected *tibialis anterior* (Figure 2). Despite the fact that 704 alone does not allow any stimulation of the immune response (data not shown), results show that 2 hours after injection of DNA formulated with 704, a higher production of IL-6 and TNFα was observed, compared to DNA alone. This effect persists 6 h and 24 h after injection for TNFα but disappears at 24h for IL-6. Regarding IFNγ and IL-10, statistically significant increase compared to non-formulated DNA was observed mainly 24 h after intramuscular injection. No differences between DNA alone or formulated with 704 were observed for IL-2 and IL-5 production. These results strongly suggest that 704 helps to increase the recognition of plasmid DNA by danger sensors in order to generate a better stimulation of the immune response compared to that obtained with naked DNA.

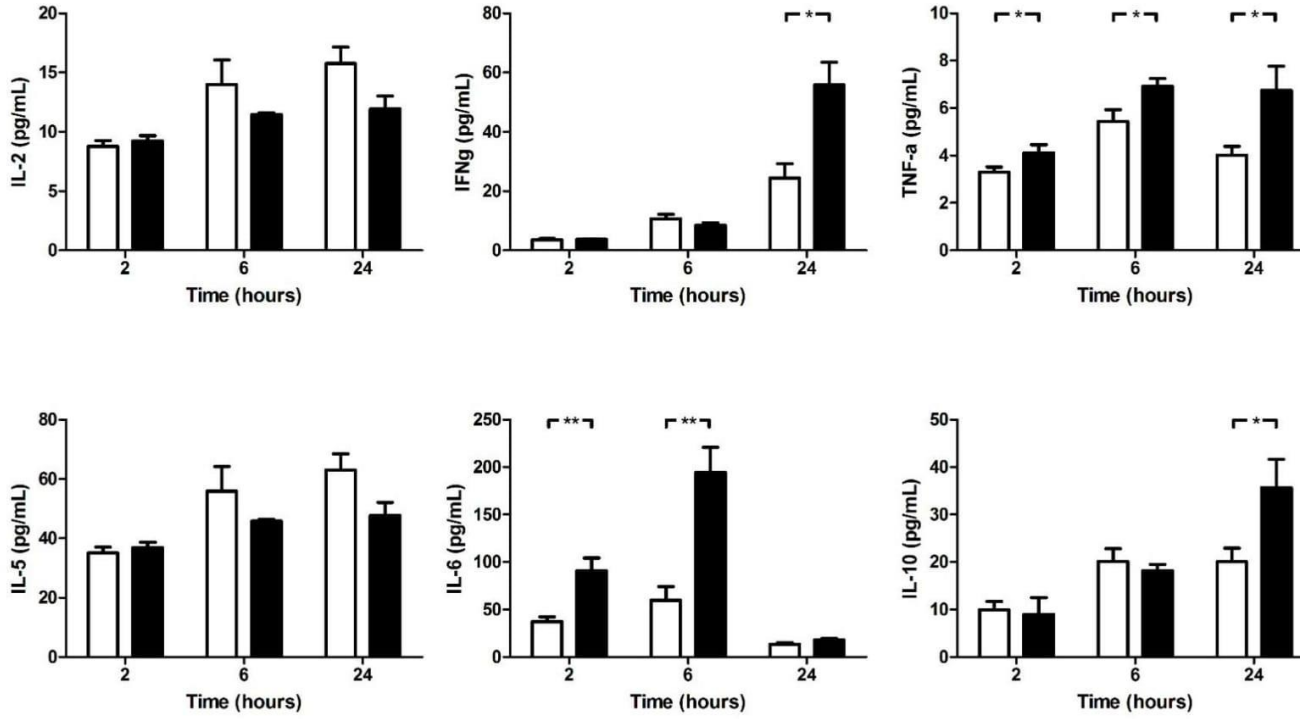


Figure 2: Vaccination with 704 allowed to trigger a danger signal that results in cytokines and interferons productions. Groups of mice (n=6) were injected i.m with 2 µg of pCMV-LacZ alone (white) or formulated with 704 (black). Cytokine secretions level into *tibialis anterior* were quantified at 2, 6 or 24 hours by FlowCytomix assay. Data are shown as mean ± SEM. Significant differences between groups are indicated. *P<0,05 **P<0.01 by Mann-Whitney test. Dose are given per *tibialis anterior.*

Induction of humoral-mediated immune response by 704 DNA vaccine is dependent of muscle fibers antigen expression

It is commonly accepted in the literature that one of the most crucial steps of DNA vaccination is the ability to efficiently deliver DNA into muscle cells or antigen-presenting cells (APCs) like dendritic cells (DCs), in order to express the antigen of interest.[22,23] We therefore investigated the importance of plasmid DNA expression in muscular or dendritic cells on the ability of 704-mediated DNA vaccination to trigger an effective antibodies production. For this study, mice were injected on day 0 and day 21 with 2 µg of pCMV-lacZ plasmid DNA formulated with 704, containing either muscle specific miRNA133a-3p targeting sites[24] (pCMV-LacZ-miR133a-3p) or APCs specific miRNA 142a-3p targeting sites[25] (pCMV-LacZ-miR142a-3p) which inhibit βGal expression in muscle fibers or DCs, respectively. Six muscles per group were excised at days 7 after the first 704/DNA injection to compare levels of β-galactosidase expression in different groups, whereas the humoral immune response was measured in the remaining mice at day 42. As shown in Figure 3a, βGal expression in muscles was decreased by 10 fold with miR133a-3p compared to miR142a-3p, leading to a dramatic reduction of anti-βGal antibody titer. In parallel, we also confirmed the efficacy of miR142a-3p inhibition in immortalized immature dendritic cells (JAWSII) compared to miR133a-3p (Figure 3b). These results strongly suggest that the expression of the plasmid within muscles cells is of crucial importance (compared to that in DCs) to generate an efficient 704-mediated DNA vaccination.

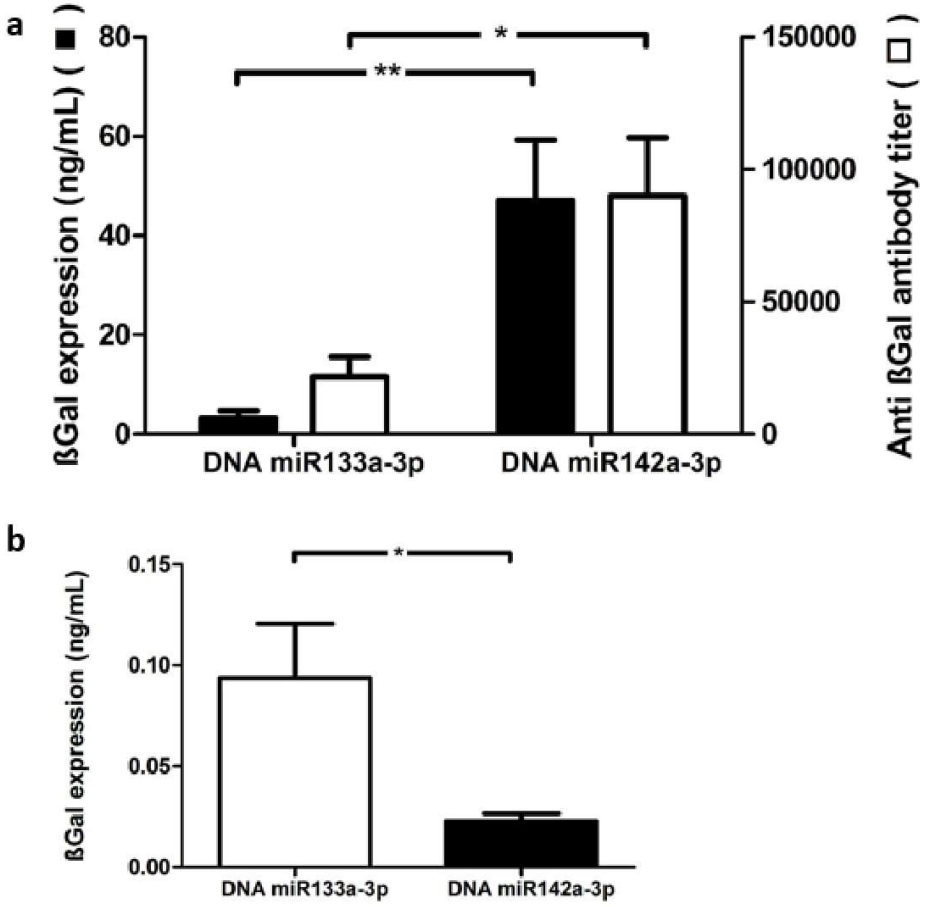


Figure 3 : Expression in muscle fibers but not in APCs is crucial for 704-mediated DNA vaccine (a) Groups of mice (n=8) were injected i.m with 2 µg of pCMV-LacZ miR133a-3p or 2 µg of pCMV-LacZ miR142-3p formulated with 704. Expression level of β-galactosidase (black) in *tibialis anterior* (n=6 muscles) was determined at day 7 and humoral immune response (n=5) (white) was determined at day 42. (b) JAWSII cells were transfected with 500 ng of pCMV-LacZ miR133a-3p (white) or 500 ng of pCMV-LacZ miR142-3p (black) complexed with DOST at CR=5. Expression level of β-galactosidase was determined 24 hours later. Data are shown as mean ± SEM. Significant differences between groups are indicated. *P<0,05 **P<0.01 by Mann-Whitney test. Dose are given per *tibialis anterior.*

DNA but not RNA acts like an adjuvant when formulated with 704

Both DNA and RNA have demonstrated an effective vaccine adjuvant effect by inducing immunity through the stimulation of nucleic acids sensors localized in endosomal or cytoplasmic compartment. Indeed, DNA is widely described as a ligand of DNA sensors through unmethylated CpG motifs or the recognition of its double-stranded form,[26] while RNA is recognized by RNA sensors via GU-rich sequences,[27] 5'-triphosphate,[28] or its double-stranded RNA form.[29]

We therefore decided to investigate whether or not DNA and RNA led to the same innate immune stimulation after 704-mediated delivery. To this end, mice were injected intramuscularly on day 0 with 10 µg of either non-coding pVAX plasmid or non-coding unmodified mRNA formulated with 704. Cytokine genes expression into injected *tibialis anterior* were determined 6 or 24 h after the initial injection. Results show that 6 hours after the delivery into muscles, DNA formulated with 704 induced a dramatic overexpression of IL-6, IL-10, IFNγ and TNFα compared to RNA as well as an IL-2 sur-expression after 24h (Figure 4a). However, we noticed that 704/RNA formulation induces a weak over-expression of IL-5 6 h post-injection.

To go further in the analysis, we evaluated the impact of nucleic acids composition on humoral immune response. For this study, mice were injected i.m at day 0 and 21 with 10 µg of plasmid (pCMV-LacZ) or mRNA (mRNA-LacZ) encoding the same βGal, formulated with 704. Humoral immune response was monitored at day 42. As shown in Figure 4b, we observed that 704-mediated RNA vaccination failed to induce the production of specific antibodies against βGal compared to DNA vaccination (Figure 4b) despite a similar βGal expression level in muscles (data not shown). Altogether, these results demonstrate that 704-mediated vaccination requires DNA but not RNA to induce an effective immune response, but also suggest

that stimulatory unmodified mRNA molecules were probably deliver directly into the cytosol preventing their recognition by endosomal TLR7/8.

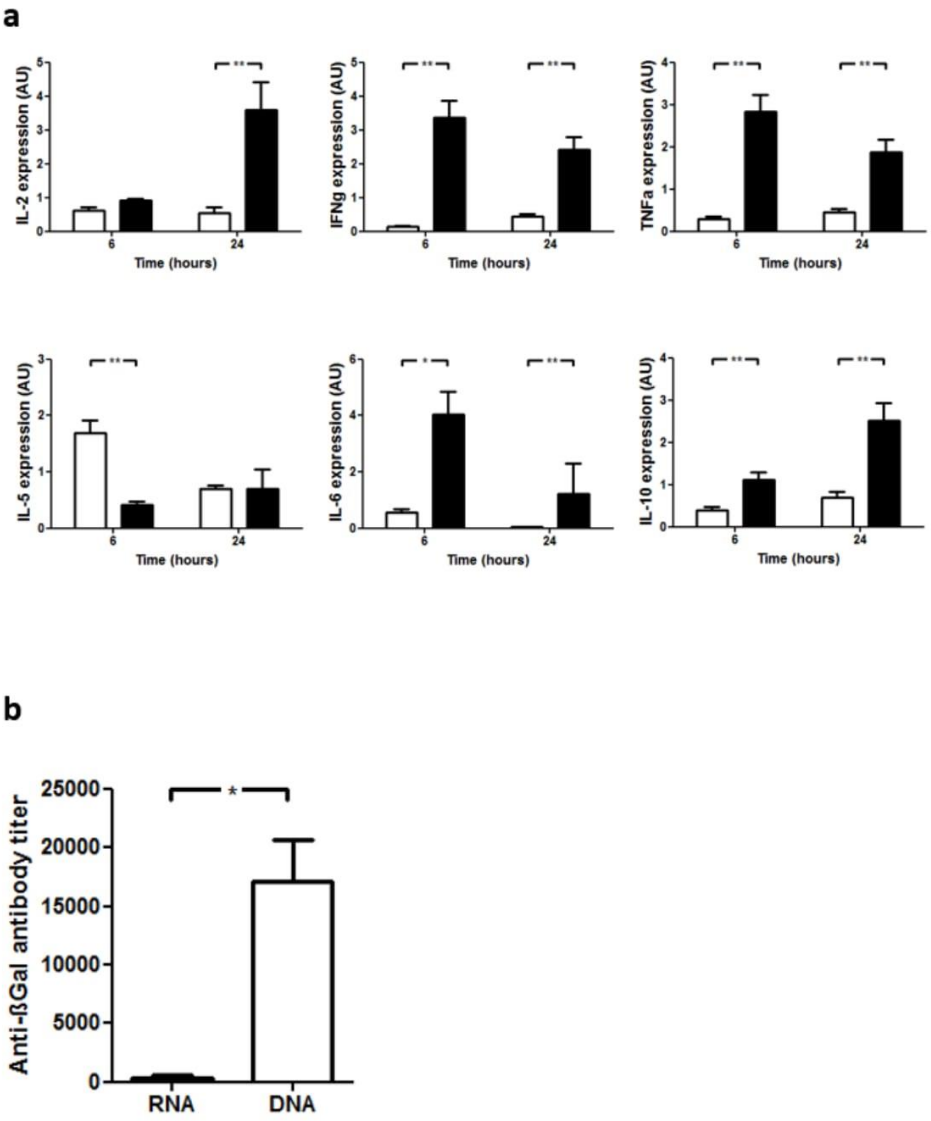


Figure 4 : DNA but not RNA is able to produce an innate and adaptative immune responses when formulated with 704. (a) Groups of mice (n=6) C57BL/6 were injected i.m with 25 µg of non-coding mRNA (white) or non-coding pVax DNA (white) formulated with 704. Cytokine expression levels into *tibialis anterior* (n=6 muscles) were determined 6 or 24 hours after injection by RT-qPCR analysis and normalized against the expression levels of HPRT (housekeeping gene). Data are expressed as the $2^{-\Delta\Delta}CT$ formula. (b) Groups of mice (n=5) C57BL/6 were injected i.m with 10 µg of mRNA LacZ or pCMV-LacZ formulated with 704. Humoral immune response was determined at day 42. Data are shown as mean ± SEM. Significant differences between groups are indicated. *P<0,05 **P<0.01 by Mann-Whitney test. Dose are given per *tibialis anterior.*

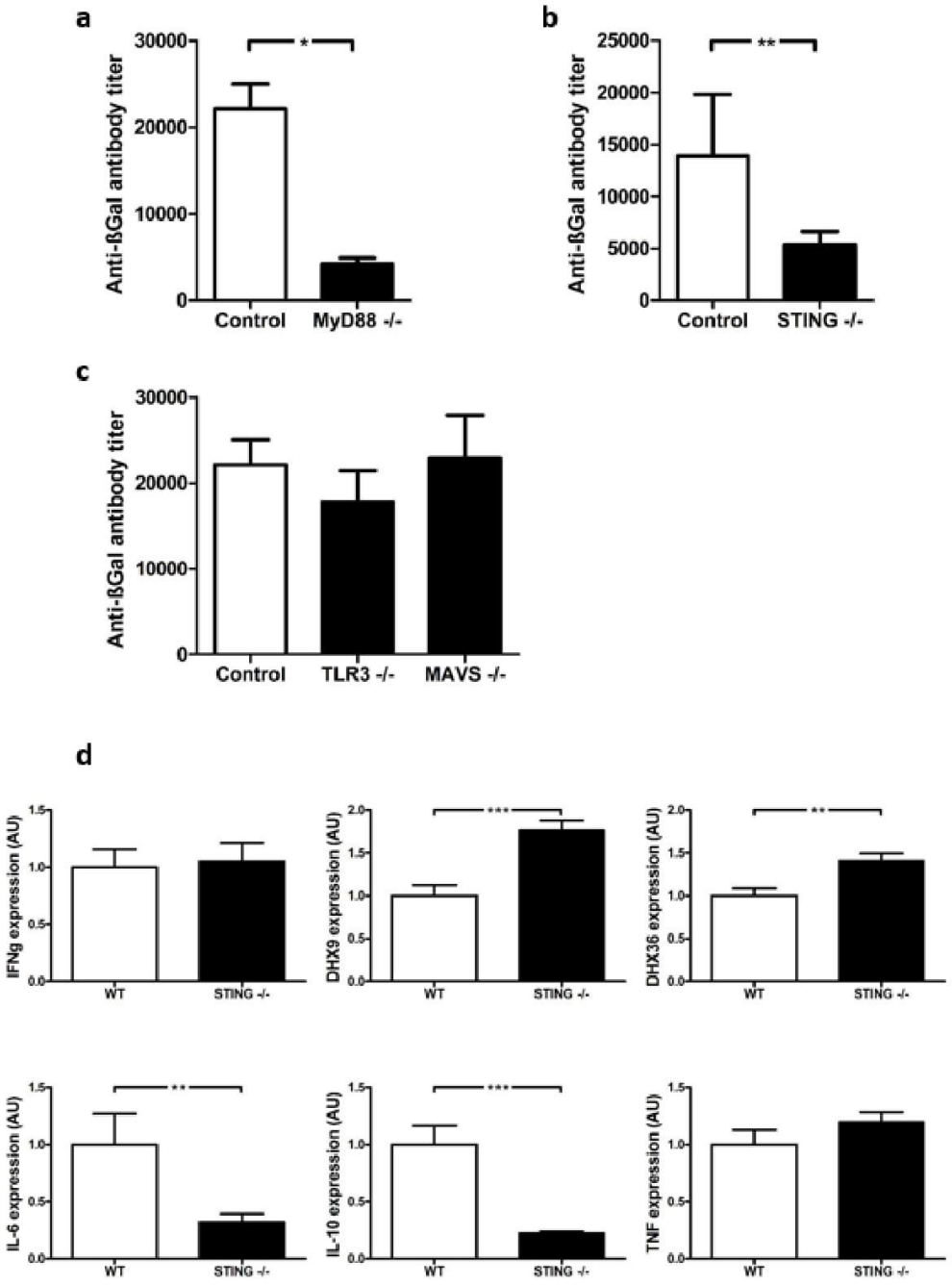
704/DNA vaccine mechanism is dependent of MyD88 and STING pathways

Although DNA has been described for many years as an immunostimulant (mainly in cytoplasm), it is only in the past 10 years that molecular bases as well as signaling cascades involved in its recognition have been revealed. It is now well established that unmethylated CpG DNA motifs as well as classical B-form double-stranded DNA are potent immune stimulators that induce respectively the recruitment of adaptator molecules MyD88 (myeloid differentiation primary response gene 88) and STING (stimulator of IFN genes).[30,31] Thus, we investigated the contribution of DNA sensing pathways on the efficacy of 704/DNA vaccine. To this purpose, MyD88-/-, STING-/-, TLR3-/- (double-stranded RNA sensor) and MAVS-/- (adaptator molecules of RIG-1 RNA sensor) mice were vaccinated with βGal-encoding plasmid formulated with 704, then humoral immune response were analyzed and compared to those obtained with wild type mice. Results shown that impairment of MyD88 expression (Figure 5a) as well as STING expression (Figure 5b) dramatically reduced the production of specific antibodies by 3 to 5 fold compared to control mice. As expected, TLR3-/- and MAVS-/- vaccinated mice displayed the same anti-βGal antibody titer compared to control mice (Figure 5c).

To go further, we also observed in STING-/- mice the expression profile of cytokines into *tibialis anterior* 6 h after the first injection as well as the expression of aspartate-glutamate-any amino acid-aspartate/histidine (DExD/H)-box helicase 36 (DHX36) or 9 (DHX9), 2 DNA sensors dependent of MyD88 pathway responsible for CpG recognition.[32] As shown in Figure 5d, the lack of STING expression induced a dramatic diminution of both IL-6 and IL-10 expression compared to control mice. Surprisingly, this STING impairment lead to an overexpression of both DHX9 and DHX36, while no effect was observed on IFNγ and TNFα. These results strongly

suggest that both MyD88 and STING pathways equally contribute to the sensing of DNA delivered by 704 and may be able to compensate each other.

Based on this set of data, we decided to evaluate the influence of plasmid backbone CpG enrichment on 704/DNA vaccine efficacy. Using mice injected with a plasmid DNA encoding for βGalactosidase rich in unmethylated CpG motifs (88 CpG dinucleoties ; CpGHigh) or without unmethylated CpG motifs (CpGLow), we observed that the presence of CpG motifs within the DNA delivered by 704 led to a better production of IL-5, IL-6, IL-10 and TNFα into muscles 2 hours after administration (Figure 5e). In addition, IL-5 and TNFα increase persisted after 6 hours, whereas no effect on IL-2 and IFNγ production could be observed. ELISA analysis of anti-βGal antibody-titer confirmed the cytokines production results, where CpGHigh plasmid induced 3 fold better humoral immune response than CpGLow plasmid (Figure 5f). These results clearly demonstrate the implication of receptor responsible for CpG motifs recognition on immune mechanism stimulated by 704-mediated DNA vaccination.


a
Anti-ßGal antibody titer
30000
20000
10000
0
*
Control
MyD88 -/-
b
Anti-ßGal antibody titer
25000
20000
15000
10000
5000
0
**
Control
STING -/-
c
Anti-ßGal antibody titer
30000
20000
10000
0
Control
TLR3 -/-
MAVS -/-
d
IFNg expression (AU)
DHX9 expression (AU)
DHX36 expression (AU)
IL-6 expression (AU)
IL-10 expression (AU)
TNF expression (AU)
WT
STING -/-

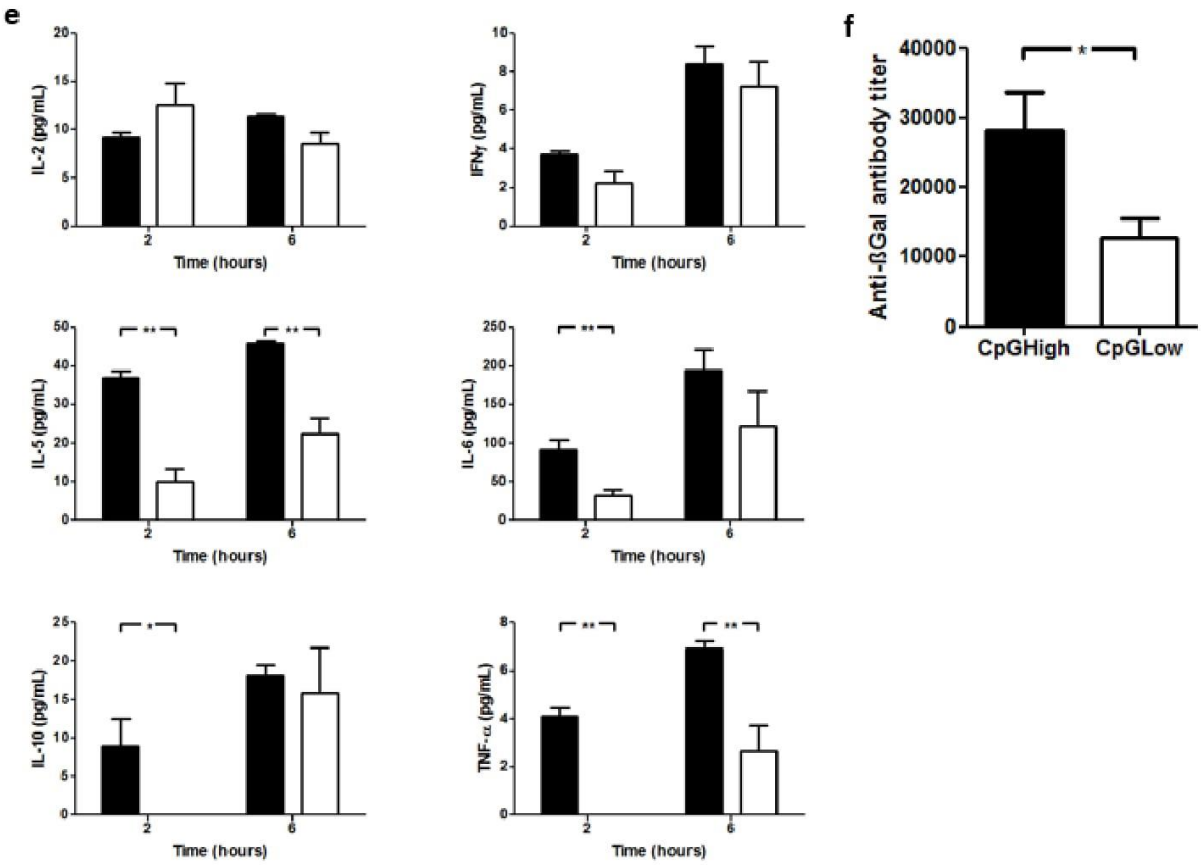


Figure 5 : DNA sensing pathways are involved in 704-DNA vaccine. (a) Groups of mice (n=6) C57BL/6 (Control) or C57BL/6 Myd88-/- were injected i.m with 50 µg of pCMV-LacZ formulated with 704. Humoral immune response was determined at day 42. (b) Groups of mice (n=5) C57BL/6 (Control) or C57BL/6J-Tmem173gt/J mice (Sting -/-) were injected i.m with 1.5 µg of pCMV-LacZ formulated with 704. Humoral immune response was determined at day 42. (c) Groups of mice (n=6) C57BL/6 (Control), C57BL/6 TLR3 -/- or C57BL/6 MAVS -/- were injected i.m with 50 µg of pCMV-LacZ formulated with 704. Humoral immune response was determined at day 42 by ELISA assay.(d) Groups of mice (n=5) C57BL/6 (Control) or C57BL/6J-Tmem173gt/J mice (Sting -/-) were injected i.m with 1.5 µg of pCMV-LacZ formulated with 704. Cytokine expression levels into *tibialis anterior* (n=10 muscles) were determined 6 h after injection by RT-qPCR analysis and normalized against the expression levels of HPRT (housekeeping gene). Data are expressed as the $2^{-\Delta\Delta}$CT formula. (e-f) Groups of mice (n=12) were injected i.m with 2 µg of pCpGHigh-LacZ (black) or 2 µg of pCpGLow-LacZ (white) formulated with 704. (e) Cytokine secretions level into *tibialis anterior* (n=6 muscles) were quantified at 2 or 6 hours by FlowCytomix assay. (f) Humoral immune response (n=5) were determined at day 42. Data are shown as mean ± SEM. Significant differences between groups are indicated. *P<0,05 **P<0.01 by Mann-Whitney test. Dose are given per *tibialis anterior.*

Direct delivery into cytosol of DNA by 704-mediated vaccination

We then investigated if the observed effect on cytokines and antibodies production triggered by the presence CpG motifs into the plasmid backbone could originate from an endosomal TLR9 stimulation.[33] To this end, we evaluated if specific anti-βGal antibodies production triggered by 704-mediated CpGHigh plasmid DNA delivery could be modulated by addition in the formulation of an agonist (ODN1826) or an antagonist (ODN2088) of TLR9. As shown in Figure 6a, neither agonist nor antagonist of the endosomal DNA sensor were able to modulate the humoral immune response induced by the formulation.

To go further, we investigated the importance of endocytosis on the efficacy of 704/DNA vaccine to efficiently transfect muscle fibers and induce humoral immune response. For this study, we used a relevant mouse model deficient for Tmem176b (C57BL/6 Tmem176b-/-), a non-selective cation channel that finely regulated the phagosomal pH which is crucial for endocytosis.[34] These mice and control C57BL/6 mice were injected once with pGWIZ-Luc in order to measure luciferase expression 7 days later, or twice with pCMV-LacZ on day 0 and 21 then humoral immune response was monitored at day 42. As shown in Figure 6b, similar level of luciferase DNA expression into muscles was observed in both control and knock-down mice. Furthermore, the lack of Tmem176b expression did not affect the generation of humoral-mediated immune response. Altogether, these data demonstrate that endosomal internalization and DNA recognition pathways are not likely implicated in 704-mediated DNA vaccination.

However, the recognition of CpG motifs can also be carried out in the cytoplasm by DHX9 and DHX36, so we also evaluated if their overexpression could modulate the vaccine effect 704/DNA formulation. Using non-coding mRNA or mRNA

encoding DHX9 and DHX36, mixed with either CpGHigh or CpGLow plasmid, we observed that the overexpression of these two DNA sensors led to a significant increase of antibody titer triggered by plasmid bearing CpG motifs compared to control mRNA, while no effect was observed with plasmid without CpG motif (Figure 6c), and this for a similar production of the antigen of interest. Moreover, 704-mediated vaccination with the “regular” plasmid encoding βGalactosidase mixed with mRNA encoding DHX9 and DHX36 led to the same conclusion: these DNA sensors allowed for a better humoral immune generation whatever the DNA quantity, compared to a mix with non-coding mRNA (Figure 6d). Altogether, these data indicate that 704 is able to bring DNA into the cytosol by a direct delivery internalization pathway allowing for the stimulation of intracytoplasmic DNA sensors responsible for DNA immune stimulation.

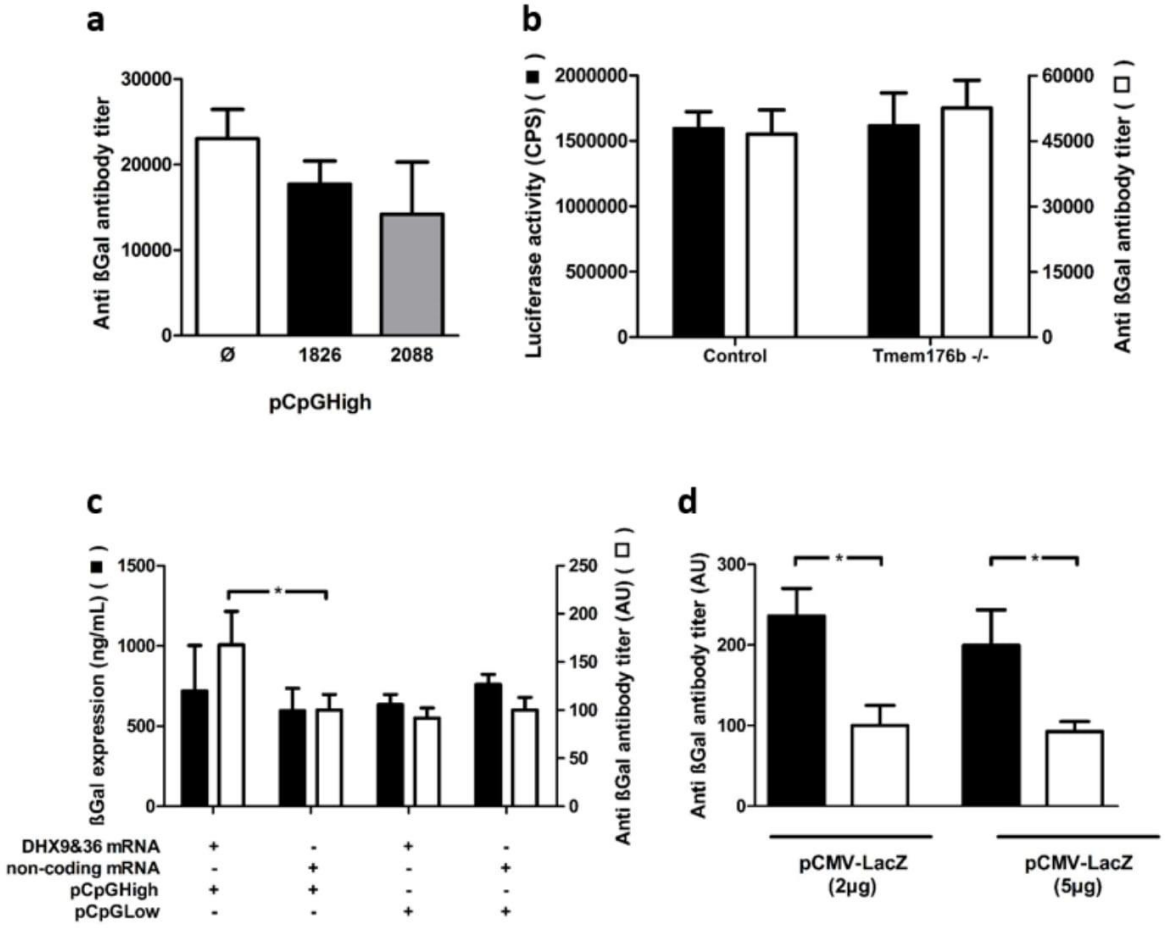


Figure 6 : 704-DNA vaccine bring DNA to the cytosol by a direct delivery mechanism. (a) Groups of mice (n=5) C57BL/6 were injected i.m with 5 µg of pCpGHigh alone (white) or either mixed with an ODN 1826 agonist of TLR9 (black) or an ODN 2088 antagonist of TLR9 (grey). Humoral immune response was determined at day 42. (b) Groups of mice (n=5) C57BL/6 (control) or C57Bl/6 Tmem176b-/- were injected i.m with 10 µg of pGWIZ-Luc or 10 µg of pCMV-LacZ formulated with 704. Luciferase activity (black) in *tibialis anterior* (n=10 muscles) was determined at day 7 and humoral immune response (n=5) (white) was determined at day 42. (c) Groups of mice (n=12) C57BL/6 were injected i.m at day 0 and 21 with 5 µg of pCpGHigh or pCpGLow mixed with 20 µg of mRNA encoding DHX9&36 or non-coding mRNA formulated with 704. Expression level of β-galactosidase (black) in *tibialis anterior* (n=6 muscles) was determined at day 7 and humoral immune response (n=9) (white) was determined at day 42. (d) Groups of mice (n=8) C57BL/6 were injected i.m at day 0 and 21 with 2 or 5 µg of pCMV-LacZ mixed with 20 µg of mRNA encoding DHX9&36 (black) or non-coding mRNA (white) formulated with 704. Humoral immune response was determined at day 42. Data are shown as mean ± SEM. Significant differences between groups are indicated. *P<0,05 **P<0.01 ***P<0.001 by Mann-Whitney test. Dose are given per *tibialis anterior.*

Discussion

In the present study, the main objectives were to validate the ability of 704-mediated DNA vaccine to induce the production of specific antibodies against gp120 HIV envelop proteins with nanograms of injected DNA and to determine the key immunological mechanisms responsible for the dramatic increase observed in DNA vaccination efficiency using this 704-based formulation.

Previous studies in our group have demonstrated that such vaccine formulations are capable of drastically improving the target protein production[12] while decreasing the quantity of necessary DNA from 50 to 1 µg.[13] In addition, block copolymer/DNA vaccines have already demonstrated a very good vaccination efficacy in a relevant mouse model of allergic asthma,[16,17] hepatocellular carcinoma,[15] mycobacterium abscessus,[35,36] and induce antibodies production against human neogenes.[37,38] Here, our results also clearly established that 704-mediated DNA vaccination in mice was able to trigger a high antibody production against gp120 HIV envelop proteins while reducing the plasmid dose required by 250 fold compared to unformulated plasmid.

The implication of resident cells at the site of injection appeared as an important factor for the generation of a protective humoral immune response. Indeed, it is commonly accepted that CPAs like dendritic cells play a crucial role by being locally transfected with plasmid DNA and presenting antigens via their MHC class I.[39] However, the involvement of muscle cells in such a process is still actively discussed.[40] In our case, the results of DNA vaccination with a plasmid bearing miRNA targeting sites clearly demonstrated that the expression in muscle cells is a key factor for antibodies production. Furthermore, we observed some contradictory results compared to data from the literature[41] that suggested that dendritic cells were

crucial to induce a protective adaptive immune response. Indeed, we showed that the lack of antigen expression into dendritic cells did not impair the induction of an effective DNA vaccination with 704.

This study provided key information about the crucial implication of nucleic acids adjuvant properties to obtain a robust innate and adaptive immune response by 704-mediated vaccination. Indeed, as the induction of an adaptive immune response proceeds through an effective innate immune stimulation,[42] a good nucleic acids based vaccine should effectively stimulate the pattern recognition receptors (PRRs) responsible for the immune induction in order to allow the secretion of numerous cytokines, interferons and the recruitment of immune cells. The FlowCytomix experiments into *tibialis anterior* after injections of DNA alone or formulated with 704 clearly indicated that the higher production of cytokines and interferons observed with the 704 is due to a better recognition of DNA by cellular DNA sensors, resulting in a stronger innate immune induction (704 block copolymer does not possess adjuvant properties[13] and is extensively described as improving DNA delivery in various organs including muscles,[15–17,43] heart[44–46] and lung[47]). This is in good agreement with data from the literature describing that many cellular receptors are able to recognize nucleic acids as a danger signal and in turn induce the establishment of an effective immune stimulation. [49]

Interestingly, we also highlighted that the nature of the delivered nucleic acid was of particular importance. Indeed, unmodified mRNAs were described as being able to be recognized by endosomal TLR7/8 RNA sensors. However, our experiments have shown that at the same amount and level of expression, RNA transfected with 704 failed to induce cytokines expression as well as specific antibodies production compared to DNA. This clearly demonstrates that the DNA

recognition is a crucial factor in the immunostimulation mechanism induced by 704 formulations and also strongly suggest that nucleic acids are delivered into the cytosol with 704.

Considering that MyD88- and STING-dependent pathways are responsible for the activation of signaling cascades involved in DNA recognition,[30,31] we first demonstrated that both pathways were of equal importance in 704 vaccination mechanism. Indeed, the lack of STING led to an impairment of specific antibodies production as well as a dramatic decrease in muscle immune stimulation which has attempted to be counterbalanced by the surexpression of MyD88-dependent DNA sensors responsible of CpG Recognition DHX9 and 36.[32] This is in line with results obtained in mice knockdown for MyD88 where we also observed a decrease in the humoral immune response. Moreover, the results of CpG experiments clearly confirmed MyD88 implication as plasmids bearing CpG motifs in their backbone both increase TH2 and pro-inflammatory cytokines secretion, which was correlated with a higher specific antibodies production.

Finally, our results also confirmed the direct delivery mechanism of DNA by 704 observed in previous studies.[14] Indeed, we first demonstrated that neither endosomal TLR9 DNA sensor agonist ODN 1826 nor antagonist ODN 2088 impact the efficacy of 704/DNA vaccine. Then, the results in Tmem176b -/- mice impaired for endocytosis clearly showed that this internalization pathway is not involved in 704-mediated mechanism. Moreover, we demonstrated the implication of DHX9 and DHX36 intracytoplasmic DNA sensors as their overexpression led to a huge increase of the humoral immune response, both with classical or CpG-enriched plasmids. As STING is also an adaptive molecule for cytosolic DNA sensors, we could conclude from this set of experiments that 704 allows for a direct delivery of DNA into cells

cytoplasm and that this property is crucial for the efficient stimulation of various intracytoplasmic DNA sensors responsible for the vaccination efficiency of 704 formulations.

In conclusion, the present work has shown that the 704-mediated DNA vaccine is able to trigger an effective production of specific antibodies against HIV envelop proteins while drastically reducing the amount of necessary DNA. The mechanism of action involves a direct delivery of DNA into muscles cells that efficiently stimulates intracytoplasmic DNA sensors while allowing a strong antigen expression. Therefore, 704 can easily be seen as an ideal synthetic vector for the future development of DNA vaccine and is currently under regulatory development for the treatment of human hepatocellular carcinoma.

ACKNOWLEDGEMENTS

The authors are very grateful to Benoit Barteau, Mustapha Si-Tahar and Michel Chignard for conducting experiments on MyD88-/-, TLR3-/- and MAVS-/- mice, and to Cédric Louvet and Maria-Cristina Cuturi for generously providing the murine model tmem176b-/-. We also thank Emilie Goudeau and Bérangère Evrard for excellent technical assistance for animal experiments and ELISA. This work was supported by special grants from BPI France financement (Paris, France) for Emerit and Hepavac. Thibault Colombani is supported by funds from IHU-CESTI (French government financial support managed by the National Research Agency “Investment Into The Future” program ANR-10-IBHU-005, co-supported by Région Pays de la Loire and Nantes Métropole).

References

(1) Fynan, E. F.; Webster, R. G.; Fuller, D. H.; Haynes, J. R.; Santoro, J. C.; Robinson, H. L. *Proc. Natl. Acad. Sci. U. S. A.* **1993**, *90* (24), 11478–11482.
(2) Saade, F.; Petrovsky, N. *Expert Rev. Vaccines* **2012**, *11* (2), 189–209.
(3) Fu, T. M.; Guan, L.; Friedman, A.; Schofield, T. L.; Ulmer, J. B.; Liu, M. A.; Donnelly, J. J. *J. Immunol. Baltim. Md 1950* **1999**, *162* (7), 4163–4170.
(4) Aihara, H.; Miyazaki, J. *Nat. Biotechnol.* **1998**, *16* (9), 867–870.
(5) Mir, L. M.; Bureau, M. F.; Gehl, J.; Rangara, R.; Rouy, D.; Caillaud, J.-M.; Delaere, P.; Branellec, D.; Schwartz, B.; Scherman, D. *Proc. Natl. Acad. Sci. U. S. A.* **1999**, *96* (8), 4262–4267.
(6) Mathiesen, I. *Gene Ther.* **1999**, *6* (4), 508–514.
(7) Widera, G.; Austin, M.; Rabussay, D.; Goldbeck, C.; Barnett, S. W.; Chen, M.; Leung, L.; Otten, G. R.; Thudium, K.; Selby, M. J.; Ulmer, J. B. *J. Immunol. Baltim. Md 1950* **2000**, *164* (9), 4635–4640.
(8) M, B.; F, B.; M, B.; Y, G.-C.; P, W.; D, S.; C, M. *Vaccine* **2001**, *19* (13–14), 1688–1693.
(9) Feltquate, D. M.; Heaney, S.; Webster, R. G.; Robinson, H. L. *J. Immunol. Baltim. Md 1950* **1997**, *158* (5), 2278–2284.
(10) Weiss, R.; Scheiblhofer, S.; Freund, J.; Ferreira, F.; Livey, I.; Thalhamer, J. *Vaccine* **2002**, *20* (25–26), 3148–3154.
(11) Coban, C.; Kobiyama, K.; Jounai, N.; Tozuka, M.; Ishii, K. J. *Hum. Vaccines Immunother.* **2013**, *9* (10), 2216–2221.
(12) Pitard, B.; Bello-Roufaï, M.; Lambert, O.; Richard, P.; Desigaux, L.; Fernandes, S.; Lanctin, C.; Pollard, H.; Zeghal, M.; Rescan, P.-Y.; Escande, D. *Nucleic Acids Res.* **2004**, *32* (20), e159–e159.
(13) McIlroy, D.; Barteau, B.; Cany, J.; Richard, P.; Gourden, C.; Conchon, S.; Pitard, B. *Mol. Ther. J. Am. Soc. Gene Ther.* **2009**, *17* (8), 1473–1481.
(14) Chèvre, R.; Le Bihan, O.; Beilvert, F.; Chatin, B.; Barteau, B.; Mével, M.; Lambert, O.; Pitard, B. *Nucleic Acids Res.* **2011**, *39* (4), 1610–1622.
(15) Cany, J.; Barteau, B.; Tran, L.; Gauttier, V.; Archambeaud, I.; Couty, J.-P.; Turlin, B.; Pitard, B.; Vassaux, G.; Ferry, N.; Conchon, S. *J. Hepatol.* **2011**, *54* (1), 115–121.
(16) Beilvert, F.; Tissot, A.; Langelot, M.; Mével, M.; Chatin, B.; Lair, D.; Magnan, A.; Pitard, B. *Hum. Gene Ther.* **2012**, *23* (6), 597–608.
(17) Rolland-Debord, C.; Lair, D.; Roussey-Bihouée, T.; Hassoun, D.; Evrard, J.; Cheminant, M.-A.; Chesné, J.; Braza, F.; Mahay, G.; Portero, V.; Sagan, C.; Pitard, B.; Magnan, A. *PloS One* **2014**, *9* (1), e85976.
(18) Dey, B.; Del Castillo, C. S.; Berger, E. A. *J. Virol.* **2003**, *77* (5), 2859–2865.
(19) Cicala, C.; Nawaz, F.; Jelicic, K.; Arthos, J.; Fauci, A. S. *Curr. Drug Targets* **2016**, *17* (1), 122–135.
(20) Dempsey, A.; Bowie, A. G. *Virology* **2015**, *479–480*, 146–152.
(21) Kobiyama, K.; Jounai, N.; Aoshi, T.; Tozuka, M.; Takeshita, F.; Coban, C.; Ishii, K. J. *Vaccines* **2013**, *1* (3), 278–292.
(22) Cho, J. H.; Youn, J. W.; Sung, Y. C. *J. Immunol. Baltim. Md 1950* **2001**, *167* (10), 5549–5557.
(23) Kutzler, M. A.; Weiner, D. B. *J. Clin. Invest.* **2004**, *114* (9), 1241–1244.
(24) Chen, J.-F.; Mandel, E. M.; Thomson, J. M.; Wu, Q.; Callis, T. E.; Hammond, S. M.; Conlon, F. L.; Wang, D.-Z. *Nat. Genet.* **2006**, *38* (2), 228–233.
(25) Brown, B. D.; Naldini, L. *Nat. Rev. Genet.* **2009**, *10* (8), 578–585.

(26) Ishii, K. J.; Akira, S. *Trends Immunol.* **2006**, *27* (11), 525–532.
(27) Heil, F.; Hemmi, H.; Hochrein, H.; Ampenberger, F.; Kirschning, C.; Akira, S.; Lipford, G.; Wagner, H.; Bauer, S. *Science* **2004**, *303* (5663), 1526–1529.
(28) Hornung, V.; Ellegast, J.; Kim, S.; Brzózka, K.; Jung, A.; Kato, H.; Poeck, H.; Akira, S.; Conzelmann, K.-K.; Schlee, M.; Endres, S.; Hartmann, G. *Science* **2006**, *314* (5801), 994–997.
(29) Alexopoulou, L.; Holt, A. C.; Medzhitov, R.; Flavell, R. A. *Nature* **2001**, *413* (6857), 732–738.
(30) Ishikawa, H.; Ma, Z.; Barber, G. N. *Nature* **2009**, *461* (7265), 788–792.
(31) Atianand, M. K.; Fitzgerald, K. A. *J. Immunol. Baltim. Md 1950* **2013**, *190* (5), 1911–1918.
(32) Kim, T.; Pazhoor, S.; Bao, M.; Zhang, Z.; Hanabuchi, S.; Facchinetti, V.; Bover, L.; Plumas, J.; Chaperot, L.; Qin, J.; Liu, Y.-J. *Proc. Natl. Acad. Sci. U. S. A.* **2010**, *107* (34), 15181–15186.
(33) Paludan, S. R.; Bowie, A. G. *Immunity* **2013**, *38* (5), 870–880.
(34) Segovia, M.; Louvet, C.; Charnet, P.; Savina, A.; Tilly, G.; Gautreau, L.; Carretero-Iglesia, L.; Beriou, G.; Cebrian, I.; Cens, T.; Hepburn, L.; Chiffoleau, E.; Floto, R. A.; Anegon, I.; Amigorena, S.; Hill, M.; Cuturi, M. C. *Am. J. Transplant. Off. J. Am. Soc. Transplant. Am. Soc. Transpl. Surg.* **2014**, *14* (5), 1021–1031.
(35) Le Moigne, V.; Rottman, M.; Goulard, C.; Barteau, B.; Poncin, I.; Soismier, N.; Canaan, S.; Pitard, B.; Gaillard, J.-L.; Herrmann, J.-L. *Vaccine* **2015**, *33* (18), 2118–2124.
(36) Le Moigne, V.; Belon, C.; Goulard, C.; Accard, G.; Bernut, A.; Pitard, B.; Gaillard, J.-L.; Kremer, L.; Herrmann, J.-L.; Blanc-Potard, A.-B. *Infect. Immun.* **2016**, *84* (10), 2895–2903.
(37) Arnaoty, A.; Pitard, B.; Bateau, B.; Bigot, Y.; Lecomte, T. *Methods Mol. Biol. Clifton NJ* **2012**, *859*, 293–305.
(38) Arnaoty, A.; Gouilleux-Gruart, V.; Casteret, S.; Pitard, B.; Bigot, Y.; Lecomte, T. *Mol. Genet. Genomics MGG* **2013**, *288* (7–8), 347–363.
(39) Kutzler, M. A.; Weiner, D. B. *Nat. Rev. Genet.* **2008**, *9* (10), 776–788.
(40) Shirota, H.; Petrenko, L.; Hong, C.; Klinman, D. M. *J. Immunol.* **2007**, *179* (1), 329–336.
(41) Akbari, O.; Panjwani, N.; Garcia, S.; Tascon, R.; Lowrie, D.; Stockinger, B. *J. Exp. Med.* **1999**, *189* (1), 169–178.
(42) Chaplin, D. D. *J. Allergy Clin. Immunol.* **2010**, *125* (2), S3–S23.
(43) Ezzine, S.; Vassaux, G.; Pitard, B.; Barteau, B.; Malinge, J.-M.; Midoux, P.; Pichon, C.; Baril, P. *Nucleic Acids Res.* **2013**, *41* (20), e192.
(44) Jespersen, T.; Membrez, M.; Nicolas, C. S.; Pitard, B.; Staub, O.; Olesen, S.-P.; Baró, I.; Abriel, H. *Cardiovasc. Res.* **2007**, *74* (1), 64–74.
(45) Piron, J.; Quang, K. L.; Briec, F.; Amirault, J.-C.; Leoni, A.-L.; Desigaux, L.; Escande, D.; Pitard, B.; Charpentier, F. *Mol. Ther. J. Am. Soc. Gene Ther.* **2008**, *16* (12), 1937–1943.
(46) Biliczki, P.; Girmatsion, Z.; Brandes, R. P.; Harenkamp, S.; Pitard, B.; Charpentier, F.; Hébert, T. E.; Hohnloser, S. H.; Baró, I.; Nattel, S.; Ehrlich, J. R. *Heart Rhythm* **2009**, *6* (12), 1792–1801.
(47) Richard-Fiardo, P.; Hervouet, C.; Marsault, R.; Franken, P. R.; Cambien, B.; Guglielmi, J.; Warnez-Soulie, J.; Darcourt, J.; Pourcher, T.; Colombani, T.; Haudebourg, T.; Peuziat, P.; Pitard, B.; Vassaux, G. *Biomaterials* **2015**, *45*, 10–17.

(48) Richard-Fiardo, P.; Hervouet, C.; Marsault, R.; Franken, P. R.; Cambien, B.; Guglielmi, J.; Warnez-Soulie, J.; Darcourt, J.; Pourcher, T.; Colombani, T.; Haudebourg, T.; Peuziat, P.; Pitard, B.; Vassaux, G. *Biomaterials* **2015**, *45*, 10–17.
(49) Junt, T.; Barchet, W. *Nat. Rev. Immunol.* **2015**, *15* (9), 529–544.
(50) Schlake, T.; Thess, A.; Fotin-Mleczek, M.; Kallen, K.-J. *RNA Biol.* **2012**, *9* (11), 1319–1330.

Article 2 : Développement de nouveaux adjuvants lipidiques pour l'immunothérapie anticancéreuse.

Les vaccins traditionnels basés sur l'utilisation de pathogènes vivants ou atténués induisent généralement une forte réponse immunitaire protectrice. En revanche, même si les nouvelles générations de vaccins à base de protéines ou d'ADN sont très attractifs (de par leur sécurité d'utilisation, leur bonne tolérance, et leur faible coût de production), leur faible immunogénicité nécessite l'ajout d'adjuvants afin d'induire une réponse immunitaire protectrice et durable dans le temps (Lee and Nguyen, 2015). Ces adjuvants ciblent souvent le système immunitaire inné en activant de nombreux récepteurs cellulaires (PRRs), afin de permettre l'expression de nombreuses molécules pro-inflammatoires et de co-stimulation nécessaire à la mise en place de réponses immunitaires inné et adaptative efficaces. Cela permet en outre, de diminuer la quantité d'antigènes nécessaire au sein d'une formulation vaccinale afin d'induire une réponse protectrice.

Les premiers adjuvants décrits comme pouvant améliorer les formulations vaccinales sont les sels d'aluminiums, reposant sur un mécanisme de dépôt permettant un contact prolongé entre le système immunitaire et l'antigène d'intérêt. Néanmoins, afin de se montrer optimaux, les adjuvants doivent aussi posséder la capacité de stimuler directement le système immunitaire. Ainsi, la molécule idéale se doit de posséder à la fois des propriétés immunostimulatrices tout en permettant la bonne délivrance de l'antigène. Les nanoparticules se sont avérées être des candidates prometteuses en tant qu'adjuvants pour l'immunothérapie, que ce soit par leurs propriétés à protéger et à permettre une délivrance prolongée de macromolécules, mais également de par les propriétés intrinsèques à impacter de nombreux mécanismes biologiques de manière dépendante de leur composition chimique, de leur taille, de leur charge ainsi que de leur nature (Watson et al., 2012; Smith et al., 2013). Dès lors, l'intérêt pour les liposomes a grandement augmenté ces dernières années. En effet, leur composition peu facilement être modifié afin de leur conférer les propriétés souhaitées, en faisant des molécules douées d'une grande versatilité et plasticité (Schwendener, 2014).

Initialement décrits comme des vecteurs pour la délivrance de molécules intracellulaires, les lipides cationiques se sont avérés ne pas être des molécules totalement inertes pour les cellules en activant notamment de nombreuses cascades cellulaires impliquées dans la réponse immunitaire (Lonez et al., 2012). Ces dérivés lipidiques ce sont par ailleurs avérés être des adjuvants prometteurs dans le cadre de protocoles d'immunothérapie (Vasievich et al., 2011; Wilmar et al., 2012; Meraz et al., 2014), aboutissant à l'étude de deux composés au sein d'essais précliniques (Christensen et al., 2011).

Ainsi les lipoaminoglycosides, des lipides cationiques dérivés d'aminoglycosides développés par notre équipe, apparaissent comme des molécules prometteuses en tant qu'adjuvants. En effet, en plus d'être capables de délivrer efficacement de nombreuses molécules au sein de cellules (acides nucléiques et protéines) (Chatin et al., 2015; Desigaux et al., 2007; Habrant et al., 2016; Mével et al., 2012, 2015), ils sont composés d'une tête polaire aminoglycoside ainsi que de chaînes d'acides gras précédemment décrites comme pouvant efficacement induire la stimulation de réponse immunitaire innée (Ward et al., 2002; Vangasseri et al., 2006). Dès lors, déterminer si cette nouvelle classe de molécule possède des propriétés

immunostimulatrices, l'influence de leur structure sur leur effet adjuvant, ainsi que les mécanismes et voies de signalisation associées, est d'une importance toute particulière. Cela permettra dans le futur d'optimiser ces dérivés lipidiques d'aminoglycosides en fonction des applications souhaitées : Avec un fort effet immunostimulateur pour leur utilisation en tant qu'adjuvants au sein de protocoles d'immunothérapie, ou bien avec un effet neutre sur le système immunitaire pour la thérapie génique. L'ensemble des données obtenues au cours de cette étude ont fait l'objet de la publication suivante en cours de révision dans la revue *Journal of the American Chemical Society.*

Article 2 : Aminoglycoside lipidic derivatives induce innate immunity and suppress tumor growth through phosphatidylinositol phospholipase C pathway and caveolae-dependent endocytosis

Aminoglycoside lipidic derivatives induce innate immunity and suppress tumor growth through phosphatidylinositol phospholipase C pathway and caveolae-dependent endocytosis.

Thibault Colombani[1], Thomas Haudebourg[1], Damien Habrant[2] and Bruno Pitard[1,2]

[1] CRCINA, INSERM, Université d'Angers, Université de Nantes, Nantes, France.

[2] In-Cell-Art, Nantes, France.

Correspondance: Bruno Pitard, InCellArt 21 rue La Noue-Bras-de-Fer 44200 Nantes – France. E-mail: bruno.pitard@univ-nantes.fr

Abstract

Broad innate immune stimulation by simple and fully characterized molecules is an active area of research in immunotherapy. To date, lipidic derivatives of bacterial monophosphoryl A or cationic lipids used to deliver nucleic acids are the only compounds able to stimulate innate immunity and mainly through interactions with Toll like receptors 2 and 4. Although these lipids lead to the production of cytokines through the NFκB cascade stimulation, there is a clear need for more efficient molecules to stimulate both Interferon and NFκB pathways. In these study, we measured the impact of structural variations on a series of ionizable lipids derived from naturally occurring aminoglycoside on the upregulation of key genes involved in the innate immunity. The ideal structure of this new generation of lipidic immunostimulator was characterized by a short succinyl linker between the two oleyl chains and the polar headgroup consisting of either Tobramycin (DOST) or Kanamycin (DOSK) belonging to 4,6-disubstituted 2-deoxystreptamine. They led to the upregulation of mRNA and protein levels of both cytokines and interferon in a dose and time depend manner in a large variety of cell populations. TLR2 and TLR4 located at the cell surface were not involved in the immune stimulation by them, whereas inhibitors of the caveloa internalization pathway and of phosphatydinositol phospholipase C decreased dramatically their immune stimulation activity. These results show that DOST and DOSK are two powerful synthetic immunostimulators allowing efficient broad innate immune stimulation by a breakthrough mechanism leading to efficient antitumor activity in mouse breast cancer model.

Introduction

Vaccination is one of the most important applications of immunology, improving the development of solutions against many human and animal health challenges like infectious diseases, cancers and allergies. Over the last few years, protein- and DNA-based vaccines have become very attractive due to their safety and low production cost. However, these classes of vaccines are usually not sufficiently immunogenic to induce a robust immunity and therefore require the additional use of adjuvants to trigger strong and long-lasting protective immune responses.[1]

Thanks to their versatility, the development of liposome-based adjuvants recently gained interest, as their composition (such as lipid composition, charge or size) may easily be modified to confer the desired properties.[2] Monophosphoryl lipid A (MPL) is a typical example. It is a Toll-like receptor (TLR) 4 agonist, which is a chemically detoxified derivative of the parent bacterial lipopolysaccharides (LPS).[3] MPL liposomes increase the production of pro-inflammatory cytokines and chemokines[4] through the activation of the NFκB pathway and are already used as adjuvant in licensed vaccines, in formulation with antigens or aluminum salts.[5,6]

Another class of synthetic lipidic molecules known as cationic lipids have also recently emerged as potential adjuvants. Indeed, several studies have demonstrated that cationic lipids were not totally inert for cells, as they induce the stimulation of many signaling pathways involved in immune response.[7–9] Cationic lipids are classically composed of 3 distinct parts, (i) a cationic polar headgroup (usually with protonated amino functions) to interact with negatively-charged phosphate moieties of nucleic acids, (ii) a lipophilic hydrophobic segment (usually made from alkyl chains or cholesterol) to improve interactions with cell membrane and (iii) a spacer linking

the hydrophilic and hydrophobic segments together and ensuring the amphiphilic character of the molecule. Moreover, like any synthetic compound, these molecules can easily be tuned to obtain the desired properties.[10] For example, RPR206252 and DiC14-amidine were described to be recognized respectively by TLR2[11] or TLR4[12], resulting in the activation of the NFkB pathway and also the NLRP3 inflammasome pathway. Furthermore, the use of cationic lipids as adjuvant *in vivo* is known to enhance immune responses induced by DNA vaccine against HIV-1,[13] to improve aluminum-based vaccine formulation[14] or to boost the adjuvant effect of MPL to suppress murine mammary tumor growth.[15]

However, improving the activation of the immune response is still an active and challenging area of research. The study of live-attenuated vaccines allowed to highlight the fact that activating multiple signaling pathways of innate immunity may be more effective than the activation of a single signaling pathway.[16] Thus, discovering a lipidic molecule able to stimulate NFkB pathway through TLRs but also another NFkB-independent signaling pathway by interacting with others receptors could potentially be of great interest to maximize the innate immune stimulation.

It is known in the literature that aminoglycosides, a family of amino-modified sugars produced by fungi, are capable of stimulating acute renal cells signaling[17] by allosterically activating the phosphatidylinositol phospholipase C (PLC),[18] resulting in the increase of intracellular calcium level and the activation of the extracellular signal-regulated kinases (ERK) pathway in a dose- and time- dependent manner.[19] In this context, we focused our attention on lipidic derivatives of the naturally occurring aminoglycosides, in order to determine if these molecules would be able to activate both dependent- and independent-NFkB pathway, paving the way for breakthrough improved mechanisms of innate stimulation.

Our objective was to conduct a structure-activity relationship (SAR) study in order to evaluate the influence of the structure of aminoglycoside lipidic derivatives on cell immunity, based on compounds that were previously prepared during structural optimization programs intended for the transfection of nucleic acids and recombinant proteins including antibodies.[20–24] Fourteen different lipo-aminoglycosides at different concentrations were assessed in this study, bearing different aminoglycoside polar headgroups (paromomycin, neomycin B, kanamycin A, tobramycin), spacers (succinyl, adipyl, serinyl, dithioglycolyl), or hydrophobic segments (dioleyl, distearyl, dipalmityl, dimiristyl, cholesterol). We first examined their ability to stimulate cell immunity *in-vitro* in order to determine the structural elements necessary to display adjuvant properties. This has allowed to identify 2 synthetic molecules (named DOST and DOSK) that were able to strongly stimulate the immune response in a large variety of cell types. In a second step, we explored the different signaling pathways and endocytosis mechanisms responsible for the cell stimulation triggered by these molecules, and investigated *in-vivo* their adjuvant properties through an immune competent 4T1 mouse model of breast cancer.

Material and Methods

Cationic Lipids preparation

Lipoaminoglycosides cationic lipids were kindly supplied by In-Cell-Art (Nantes, France), synthetized as previously described [20–24] and stored as powder at -20°C. Prior to the assays, they were diluted in endo-free water at a stock concentration of 2mg/mL (for *in-vitro* studies) or 40mg/mL (for *in-vivo* studies) then sonicated for 10-15min at room temperature. Stock solutions were stored up to 1 month at 4°C.

Cell and Culture conditions

Mouse skeletal muscle cell line (C2C12; CRL1772, ATCC, RockvilleMD, USA) were cultured in DMEM supplemented with 10% heat-inactivated Fetal Calf Serum (FCS, Eurobio, Courtaboeuf, France), 100U/mL penicillin (Life technologies, Villebon sur Yvette, France), 10µg/mL streptomycin (Life technologies) and 2mM L-glutamine (Life technologies).

Mouse Embryonic Fibroblast cell line (MEF; CRL-2907, ATCC) were maintained in IMDM supplemented with 10% heat-inactivated FCS, 100U/mL penicillin, 100 µg/mL streptomycin and 1x Non-essential amino acids (Life technologies).

Immature dendritic cell (JAWSII; CRL-11904, ATCC) were grown in RPMI1640 supplemented with 10% heat-inactivated FCS, 100U/mL penicillin, 10µg/mL streptomycin and 5ng/mL murine GM-CSF.

Peritoneal cavity cells were obtained as described by Avijit et al [25] and were cultured in RPMI 1640 supplemented with 10% FCS, 100U/mL penicillin, 100 µg/mL streptomycin and 2mM L-glutamine.

Bown Marrow-derived dendritic cell (BMDC) were extracted from femur bone morrow as described by Lutz et al,[26] cultured during 10 days in 60mm-dish in order to

reduced granulocytes contamination in RPMI 1640 supplemented with 10% FCS, 100U/mL penicillin, 100µg/mL streptomycin, 2mM L-glutamine, 50µM 2-mercaptoethanol and 30-200U/mL murine GM-CSF.

All cells were routinely maintained at 37°C in a humidified 5% CO2 /95% air containing atmosphere. The day prior treatment, cells were seeded in 24-well plates in order to achieve a confluence of 70-80%.

***In-vitro* stimulation**

The day after seeding, cells supernatants were replaced by fresh growth medium. Then, cells were treated during 2, 6 or 24 hours with Lipoaminoglycosides (3-10µg/mL), ultrapure LPS (100ng/mL) or Pam3CSK4 (100ng/mL) (Invivogen, Toulouse, France) diluted in Opti-MEM. When inhibitors of endocytosis or PLC were used, C2C12 cells were incubated for 1 hour with 5-(N-Ethyl-N-isopropyl)amiloride (150nM), Chlorpromazine hydrochloride (9µM), Genistein (90µM), or U73122 (1µM, Sigma-Aldrich) prior to the additions of activators (Sigma-Aldrich, Darmstadt, Germany).

Cell Viability

Twenty-four hours after treatment, cytotoxicity was measured using the Cell Titer 96 Non-Radioactive Cell Proliferation Assay in accordance with the manufacturer's instructions (Promega, Lyon, France). After solubilization of the formazan crystals, optical density was measured at 560 nm using a Victor X-3 multilabel plate reader (Perkinelmer, Villebon sur Yvette, France). Cell survival in the treated samples was calculated using a regression curve established from the untreated standard serial dilutions of the cell suspension.

Measurement of immune response

After stimulation, cell culture supernatant were collected and assayed for mouse CXCL10 secretion by using DuoSet Mouse CXCL10/IP-10/CRG-2 ELISA kit (R&D Systems, Minneapolis, USA) according to manufacturer's instruction and using a Victor X3 (Perkinelmer) microplate reader.

IFNβ1, IL-6, CXCL10, DAI and IFI204/16 expressions were determined by RT-qPCR. Total RNA from cells were extracted using Nucleospin RNA/protein kit (Macherey-Nagel, Hoerdt, France), according to the manufacturer protocol. RT-qPCR were then realized in 2 phase : first, reverse transcriptions of RNA in cDNA were conducted using High Capacity cDNA Reverse Transcription Kits (Life technologies) on GeneAmp® PCR System 9700 Thermal Cycler (Life technologies). Then, Real-time PCR were effectuated using Taqman® Gene expression assays on StepOnePlus™ Real-Time PCR System (Life technologies).

Probes used to amplify specific gene products from murine cDNA (Life technologies) were : for IL-1β : Mm00434228_m1 ; for IL-6 : Mm00446190_m1 ; for CXCL10 : Mm00445235_m1 ; for DAI : Mm00457979_m1 ; for IFI204 : Mm00492602_m1 ; for HPRT (Housekeeping gene) : Mm00446966_m1. Probes used to amplify specific gene products from human cDNA (Life technologies) were : for IL-1β : Hs01077958_s1 ; for IL-6 : Hs00985639_m1 ; for CXCL10 : Hs01124251_g1 ; for DAI : Hs01090106_m1 ; for IFI16 : Hs00194261 ; for HPRT (Housekeeping gene) : Hs99999909_m1.

DAI and IFI204 production was also confirmed by Western Blotting assay. Whole cell proteins were extracted also with Nucleospin RNA/Protein kit (Macherey-Nagel), fractionated by SDS-PAGE on mini-protean® TX gel 4-20%, and transferred to a 0.2µm nitrocellulose trans-blot turbo membrane (Bio-Rad, Marnes-la-Coquette, France) according to manufacturer's instructions. The membranes were blocked with 5% non-fat milk in Tris-Buffered Saline for 1h and then incubated overnight with primary antibody at 4°C. After washing membranes 3 times with Tris-buffered Saline, they were incubated with horseradish peroxidase conjugated secondary antibody for 1h at room temperature. The peroxidase activity associated with protein bands was detected by enhanced chemiluminescence using Clarity™ Western ECL Blotting Substrate (Bio-Rad) and measured with a ChemiDoc™ MP System (Bio-Rad). Antibodies used to detect murine protein bands were : For DAI : sc-271483 (Santa Cruz Biotechnology, Dallas, USA) ; for IFI204 : ab104409 (Abcam, Paris, France) ; for anti-rabbit-HRP : sc-2054 (Santa Cruz Biotechnology) ; for anti-mouse-HRP : sc-2055 (Santa Cruz Biotechnology).

Animals

BALB/c mice or Swiss mice 8 weeks old (Elevage Janvier, Le Genest, France) were housed in conventional conditions according to INSERM (Institut National de la Santé et de la Recherche Médicale) guidelines. All animal experiments were performed in accordance with the recommendations of French Ministry of Higher Education and Research, and approved by an ethics committee in animal experimentation under reference APAFIS#7897 and 4118.

***In-vivo* study**

For blood formulation and hematocrit level measurement, Swiss mice were injected intravenously with 100µg of DOSP or DOSK. Blood sample were collected from 1 day before to 3 days after injection, and analysis with Hemavet 950FS (Drew scientific, Dallas, USA).

Breast cancer tumors were established in BALB/c mice by intramammary injection of $1x10^5$ 4T1-luciferase cells. Ten days after cells injection (median tumor size = 100-200 mm^3), mice were treated with 2 weekly intratumoral injections as follows: Saline solution (control), DOSP (1mg) and DOSK (1mg). Then, at day 19 after initiation of tumor growth, mice were sacrificed and tumors were excised for weight and size analysis.

Statistical analysis

Statistical analyses were performed using GraphPad Prism software (La Jolla, CA, USA). Values are expressed as the mean ± SEM. Significant differences between groups are indicated * $P<0.05$ ** $p<0.01$ *** $p<0.01$ by Mann-Whitney test.

Results

Dose- and time-reponse of cell immune stimulation by DOSP

In order to assess the adjuvant properties of the aminoglycoside lipidic derivatives, we first evaluated their ability to trigger the expression of innate immune genes in C2C12 mouse cells having an intact interferon response system.[27] The first molecule we assessed is named DOSP and is composed of a dioleyl hydrophobic backbone, a succinyl spacer and a paromomycin headgroup with 4 protonable amino groups (Figure 1a). DOSP has demonstrated in previous studies to be an efficient transfection agent for DNA, siRNA and mRNA.[20,21]

After a treatment during 24 hours with increasing amounts of DOSP (from 0 to 10 µg/mL), we observed that C2C12 expressed key genes involved in innate immune response including interferon β1 (IFNβ1), chemokine (C-X-C Motif) Ligand 10 (CXCL10), DNA-Dependent Activator Of Interferon Regulatory Factors (DAI) and Interferon-Gamma Induced Protein 204 (IFI204) genes, in a dose-dependent manner compared to untreated cells (Figure 1b). However after incubation with DOSP, no stimulation of interleukin-6 (IL-6) was observed.

In order to refine the analysis, we have measured the kinetics of immune gene expression after a treatment with 10 µg/mL of DOSP. Results show that 6 hours after DOSP treatment, IFNβ1 and CXCL10 were already overexpressed compared to untreated cells (Figure 1c). Regarding DAI and IFI204, statistically significant increase compared to non-treated cells was observed mainly 24 h after DOSP treatment.

These results allowed us to determine the optimal experimental conditions that were used in the rest of the study (concentration of 10 µg/mL of lipo-aminoglycoside and readout after 24 hours).

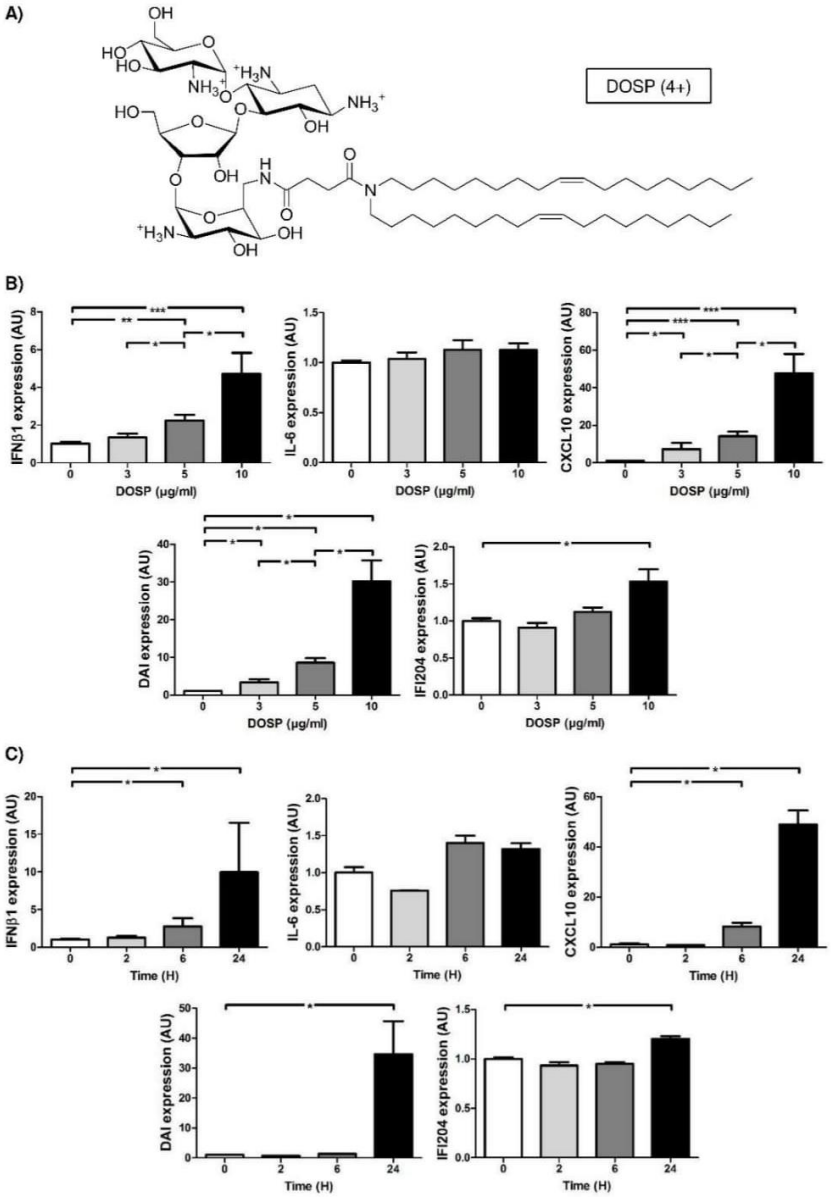


Figure 1: Effect of DOSP on cell immune response. (A) Structure of Di-Oleyl-Succinyl-Paromomycin (DOSP). (B-C) Effect of DOSP on the expression of innate immune genes as a function of (B) the concentration or (C) the duration of treatment. (B) Mouse myoblast cells (n=6) were incubated during 24 hours with DOSP at a concentration of 0 to 10 µg/mL. (C) Mouse myoblast cells (n=4) were not incubated or incubated 2, 6 or 24 hours with DOSP at a concentration of 10 µg/mL. Cytokines (IFNβ1 and IL-6), chemokine (CXCL10) and DNA sensors (DAI and IFI204) expression levels into cells were determined by RT-qPCR analysis, normalized against the expression levels of HPRT (housekeeping gene) and compared to non-treated cells (AU=1). Data are expressed as the $2^{-\Delta\Delta}$CT formula and are shown as mean ± SEM. Significant differences between groups are indicated. *P<0,05 **P<0.01 ***P<0.001 by Mann-Whitney test.

Relationships between lipo-aminoglycoside structure and innate immune stimulation

Then we assessed the influence of the aminoglycoside polar headgroup on innate immune stimulation. To this end, we have selected four molecules carrying the same hydrophobic segment (dioleyl chains) and spacer (succinyl) but with different cationic headgroups: DOSP, DOSN (neomycin B headgroup, 6 protonable amines), DOST (tobramycin headgroup, 4 protonable amines) and DOSK (kanamycin A headgroup, 3 protonable amines). The structures of the different molecules are depicted on Figure 2a. These 4 compounds can be divided into 2 subclasses, as paromomycin and neomycin are characterized by a 4,5-disubstituted 2-deoxystreptamine (4,5-DDS) ring, while tobramycin and kanamycin are characterized by a 4,6-disubstituted 2-deoxystreptamine (4,6-DDS) ring. As shown in Figure 2b, treating C2C12 cells with DOSP or DOSN only led to very low IFNβ1, IL-6, CXCL10, DAI and IFI204 overexpression compared to untreated cells. By contrast, treatment with DOST and DOSK at the same dose enhanced by 50 to 500 fold the expression of immune genes IFNβ1, CXCL10 and DAI and most importantly induced significantly pro-inflammatory cytokine IL-6 and IFI204 expression, compared to untreated cells.

As shown in Figure 2c, we have also confirmed by ELISA assay that the overexpression of CXCL10 induced by DOST and DOSK generated the chemokine protein production and secretion in the supernatant of cells, unlike what was observed for the other compounds DOSP and DOSN. We also followed DAI protein production by western blotting assay (Figure 2d). In a similar manner, DOST and DOSK led to a higher level of DAI compared to that observed with DOSP and DOSN.

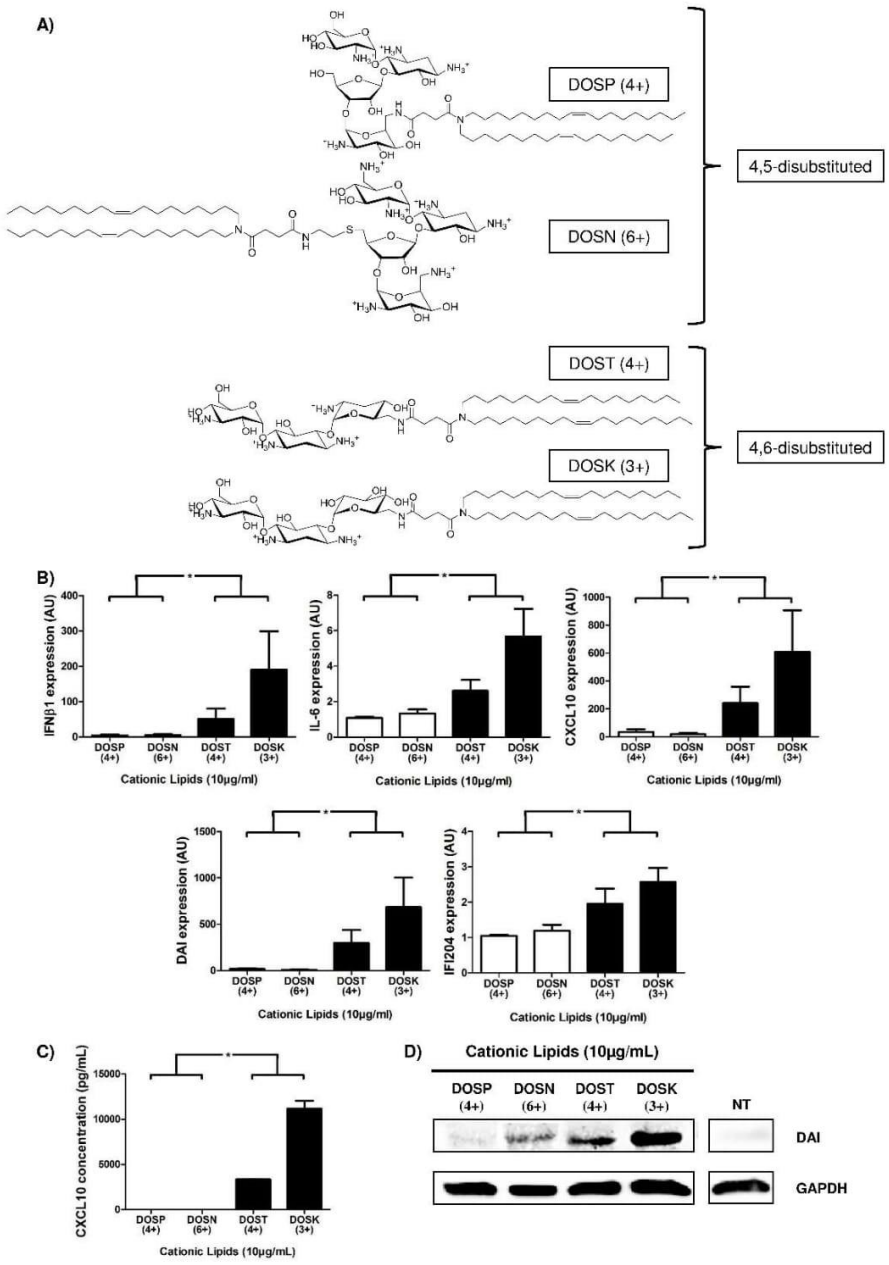


Figure 2: 4,6-disubstitued polar heads group Kanamycin and Tobramycin allow the best immune stimulation. (A) Structure of Di-Oleyl-Succinyl derived cationic lipids : DOST (Di-Oleyl-Succinyl-Tobramycin), DOSK (Di-Oleyl-Succinyl-Kanamycin A), DOSP (Di-Oleyl-Succinyl-Paromomycin) and DOSN (Di-Oleyl-Succinyl-Neomycin B). (B-D) Stimulation of innate immune response by Di-Oleyl-Succinyl derived cationic lipids in C2C12 cells. Mouse myoblast cells (n=4) were incubated 24 hours with 10µg/mL of DOSP, DOSN, DOST or DOSK, belonging to the 4,5-disubstituted 2-deoxystreptamine ring subclass (white) or 4,6-disubstituted 2-deoxystreptamine ring subclass (black) respectively. (B) Cytokines (IFNβ1 and IL-6), chemokine (CXCL10) and DNA sensors (DAI and IFI204) expression levels into cells were determined by RT-qPCR analysis, normalized against the expression levels of HPRT (housekeeping gene) and compared to non-treated cells (AU=1). Data are expressed as the $2^{-\Delta\Delta}$CT formula. (C) Chemokine CXCL10 level into supernatant were determined by ELISA analysis. (D) DAI DNA sensor proteins contained into cells were determined by Western Blot analysis and the level of GAPDH was used as a protein loading control. Data are shown as mean ± SEM. Significant differences between groups are indicated. *P<0,05 by Mann-Whitney test.

In the same experimental conditions, C2C12 cells were then treated with the 4 aminoglycoside cholesterol derivatives (CHOLP, CHOLN, CHOLT, CHOLK) bearing the same polar headgroup but a different hydrophobic moiety (Figure 3a). Figure 3b shows that the analyzed immune genes were not affected in their expression by the presence of the aminoglycoside cholesterol derivatives compared to untreated cells. Analysis of DAI protein production by western blot assay confirmed the absence of immune stimulation by the 4 cholesterol-based aminoglycosides (Figure 3c).

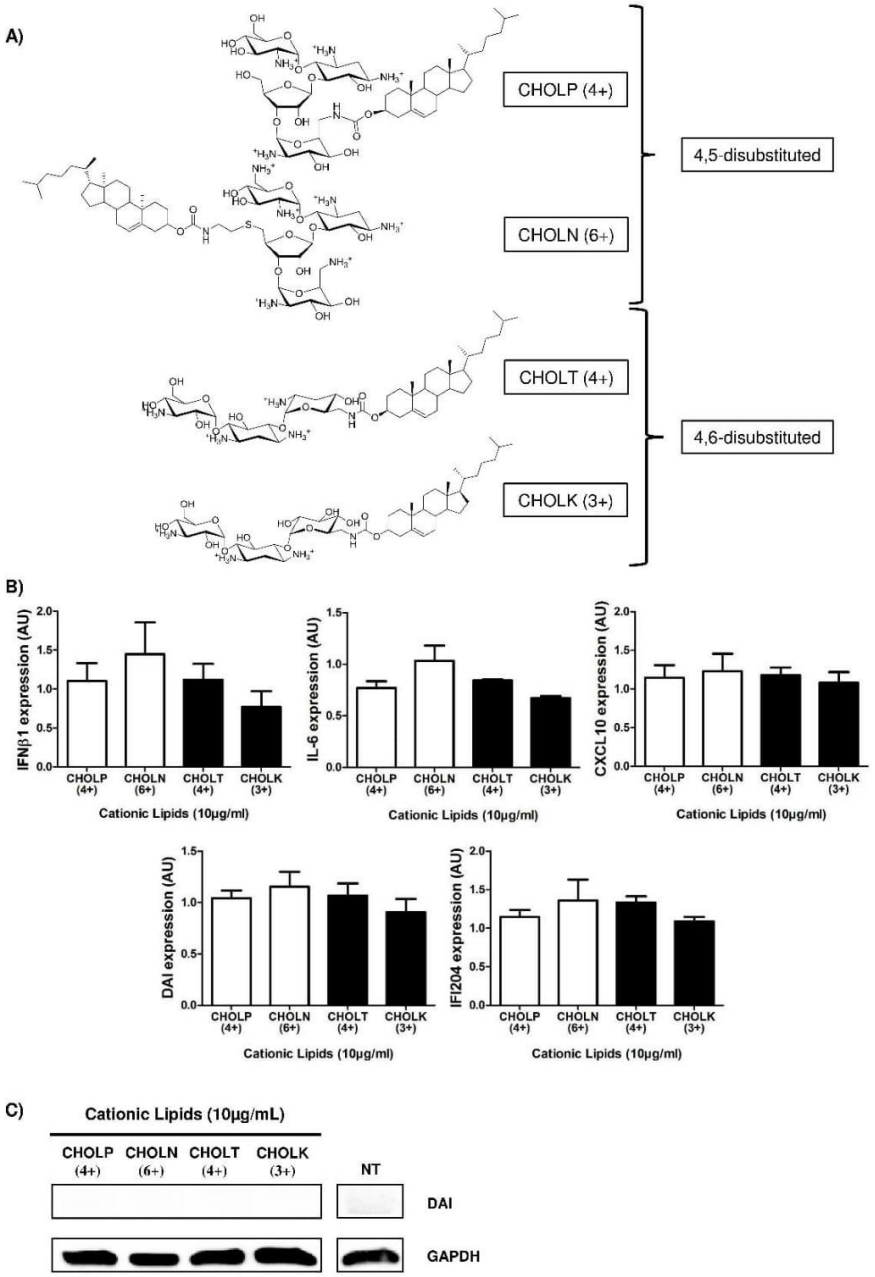


Figure 3: Cholesterol-derived cationic lipids failed to induce cell stimulation. (A) Structure of Cholesterol derived cationic lipids: CHOLT (Cholesterol-Tobramycin), CHOLK (Cholesterol-Kanamycin A), CHOLP (Cholesterol-Paromomycin) and CHOLN (Cholesterol-Neomycin B). (B-C) Stimulation of innate immune response by Cholesterol derived cationic lipids in C2C12 cells. Mouse myoblast cells (n=4) were incubated 24 hours with 10µg/mL of CHOLP, CHOLN, CHOLT or CHOLK, belonging to the 4,5-disubstituted 2-deoxystreptamine ring subclass (white) or 4,6-disubstituted 2-deoxystreptamine ring subclass (black) respectively. (B) Cytokines (IFNβ1 and IL-6), chemokine (CXCL10) and DNA sensors (DAI and IFI204) expression levels into cells were determined by RT-qPCR analysis, normalized against the expression levels of HPRT (housekeeping gene) and compared to non-treated cells (AU=1). Data are expressed as the $2^{-\Delta\Delta}$CT formula. (C) DAI DNA sensor proteins contained into cells were determined by Western Blot analysis and the level of GAPDH was used as a protein loading control. Data are shown as mean ± SEM. Significant differences between groups are indicated. *P<0,05 by Mann-Whitney test.

In parallel, we also investigated whether the polar headgroup consisting of aminoglycosides alone (i.e. not linked to any hydrophobic moiety) were responsible for the stimulation of the cell immunity. To this end, C2C12 cells were treated in the same conditions than in the previous experiments with 10 µg/mL of paromomycin, neomycin B, tobramycin or kanamycin A during 24 h (Figure 4). The results showed that aminoglycosides alone were not able to stimulate cytokines, chemokine, or DAI and IFI204 sensors expressions regardless of their subclass. These results strongly suggest that the amphiphilic character of the aminoglycoside lipidic derivatives with a diacyl moiety is necessary to generate a stimulation of the immune response.

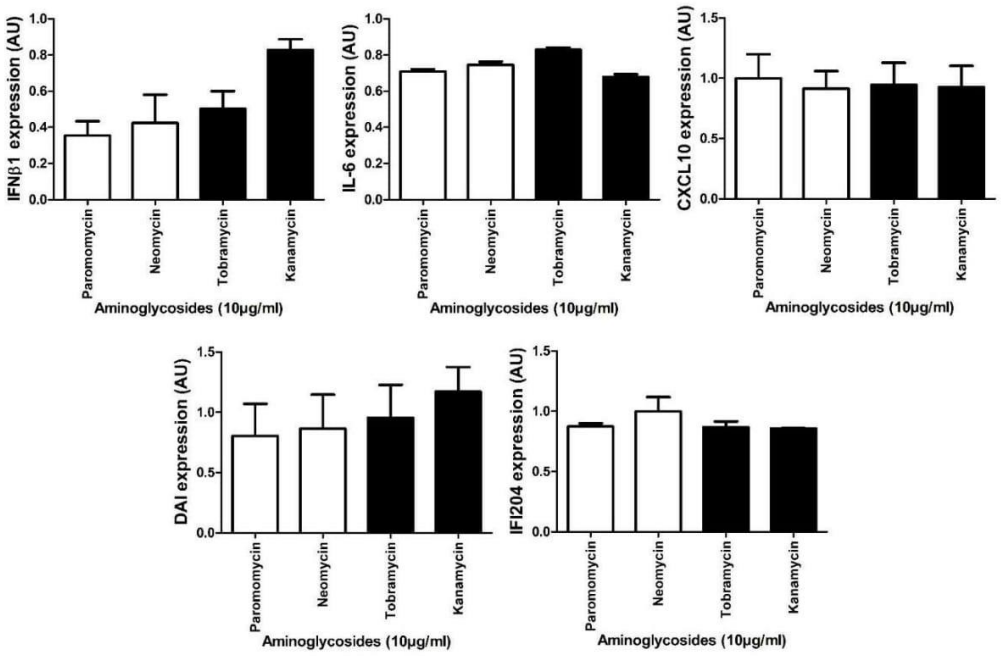


Figure 4: Aminoglycosides alone don't trigger cell immunity. Induction of innate immune gene expression by aminoglycosides in C2C12 cells. Mouse myoblast cells (n=4) were incubated 24 hours with 10µg/mL of paromomycin, neomycin B, tobramycin or kanamycin A belonging to the 4,5-disubstituted 2-deoxystreptamine ring subclass (white) or 4,6-disubstituted 2-deoxystreptamine ring subclass (black) respectively. Cytokines (IFNβ1 and IL-6), chemokine (CXCL10) and DNA sensors (DAI and IFI204) expression levels into cells were determined by RT-qPCR analysis, normalized against the expression levels of HPRT (housekeeping gene) and compared to non-treated cells (AU=1). Data are expressed as the $2^{-\Delta\Delta}$CT formula.

As polar headgroups alone and cholesterol derivatives did not lead to immune stimulation in C2C12 cells, we investigated the influence of the diacyl hydrophobic segment of lipo-aminoglycosides on C2C12 cells stimulation. To this end, we used as a starting point the molecule DOST that carries a hydrophobic portion consisting of a dioleyl chain (oleyl: 18 carbons with 1 insaturation, C18:1) with a tobramycin headgroup and a succinyl spacer. We assessed in this experiment 3 new molecules bearing different hydrophobic tails: i) DSST with a distearyl chain (stearyl: saturated 18 carbons, C18:0), ii) DPST with a dipalmityl chain (palmityl: saturated 16 carbons, C16:0) and iii) DMST with a dimyristyl chain (myristyl: saturated 14 carbons, C14:0) (Figure 5a). By comparing the stimulation observed after DOST and DSST treatment, we observed that removal of the unsaturation led to a strong decrease in C2C12 immune genes expression by 2 to 4 folds (Figure 5b). In a similar manner, compounds with shorter saturated alkyl chains DMST and DPST also induced a much lower expression of IFNβ1, IL-6 and CXCL-10 and failed to induce significantly DAI and IFI204 expressions. Western blot analysis of DAI and IFI204 production in treated C2C12 confirmed the expression results, where DOST and DSST induced DAI and IFI204 protein production, contrarily to what was observed with DMST and DPST (Figure 5c). These data indicate that not only the nature of the aminoglycoside itself plays an important role to trigger cell immunity, but also that the hydrophobic segment and both size and unsaturation of the alkyl chains influence the immuno-stimulatory properties to aminoglycoside lipidic derivatives.

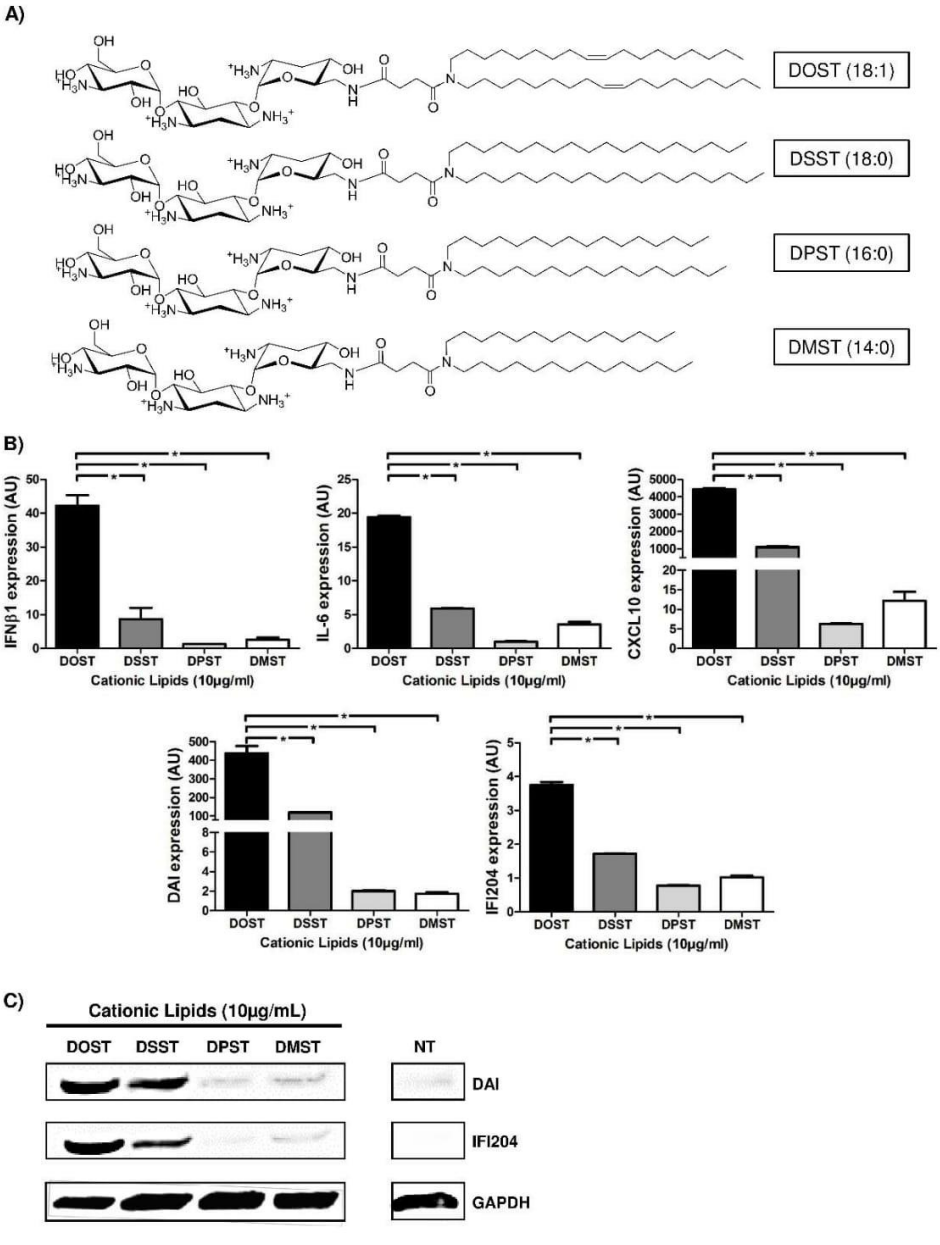


Figure 5: Implication of hydrophobic segment on C2C12 immune stimulation. (A) Structure of tobramycin derived cationic lipids. DOST (Di-Oleyl-Succinyl-Tobramycin), DSST (Di-Stearyl-Succinyl-Tobramycin), DPST (Di-Palmityl-Succinyl-Tobramycin), DMST (Di-Myristyl-Succinyl-Tobramycin) and CHOLT (Cholesterol-Tobramycin)**.** (B-C) Stimulation of innate immune response by tobramycin derived cationic lipids in C2C12 cells. Mouse myoblast cells (n=4) were incubated 24 hours with 10µg/mL of DOST, DSST, DPST, DMST or CHOLT. (B) Cytokines (IFNβ1 and IL-6) and chemokine (CXCL10) and DNA sensors (DAI and IFI204) expression levels into cells were determined by RT-qPCR analysis, normalized against the expression levels of HPRT (housekeeping gene) and compared to non-treated cells (AU=1). Data are expressed as the $2^{-\Delta\Delta}$CT formula. (C) DNA sensors (DAI and IFI204) proteins contained into cells were determined by Western Blot analysis and the level of GAPDH was used as a protein loading control. Data are shown as mean ± SEM. Significant differences between groups are indicated. *P<0,05 **P<0.01 by Mann-Whitney test.

Lastly, we investigated the influence of the spacer which links the cationic headgroup with the hydrophobic moiety on the innate immune stimulation. To this end, DOST was used as reference molecule with a 'succinic' spacer and modification at the linker level was investigated by (i) adding 2 methylene units forming an 'adipic' spacer (molecule named DOAT), (ii) introducing a diester function (molecule DOSST), or (iii) inserting a disulfide bridge (molecule DODT) (Figure 6a). As shown in Figure 6b, C2C12 treated with DOAT and DOSST had a lower expression of DAI, IFI204 (2 fold decrease compared to DOST treatment), IL-6 (3 fold), IFNβ1 (up to 4 fold) and CXCL10 (up to 4 fold). Interestingly, the compound DODT with the disulfide bridge was unable to induce any cell stimulation.

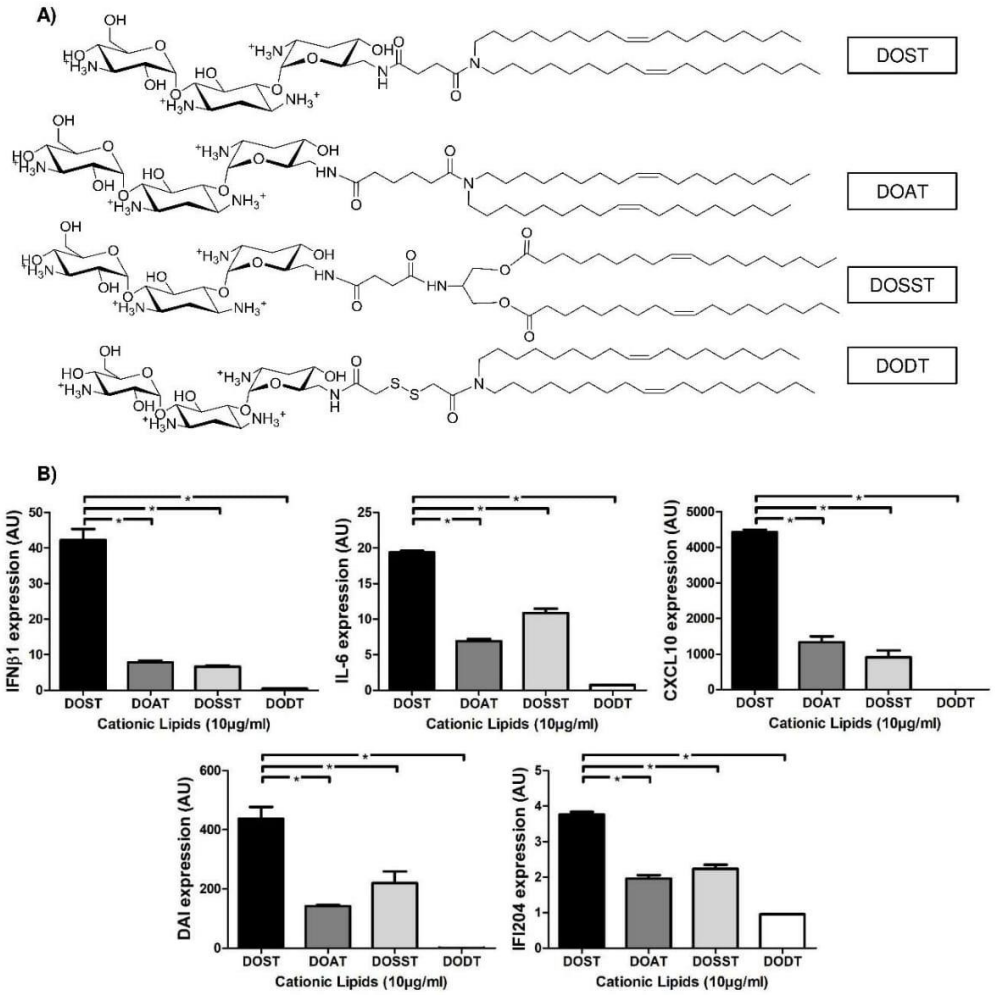


Figure 6: Importance of linker composition on C2C12 immune stimulation. (A) Structure of Di-Oleyl-tobramycin derived cationic lipids DOST (Di-Oleyl-succinyl-tobramycin), DOAT (Di-Oleyl-Adipyl-Tobramycin), DOSST (Di-Oleyl-Succinyl-Serinyl-Tobramycin) and DODT (Di-Oleyl-Dithioglycolyl-Tobramycin). (B-C) Stimulation of innate immune response by Di-Oleyl-tobramycin derived cationic lipids in C2C12 cells. Mouse myoblast cells (n=4) were incubated 24 hours with 10µg/mL of DOST, DOAT, DOSST or DODT. (B) Cytokines (IFNβ1 and IL-6), chemokine (CXCL10) and DNA sensors (DAI and IFI204) expression levels into cells were determined by RT-qPCR analysis, normalized against the expression levels of HPRT (housekeeping gene) and compared to non-treated cells (AU=1). Data are expressed as the $2^{-\Delta\Delta}$CT formula. Data are shown as mean ± SEM. Significant differences between groups are indicated. *P<0,05 **P<0.01 ***P<0.001 by Mann-Whitney test.

These results strongly suggest that the spacer constitutes an important structural element to consider for designing cationic lipids with potent adjuvant properties.

Based on this data, we have selected the top-two molecules DOST and DOSK for further evaluation and assessed their adjuvant properties on a panel of different cell populations (Figure 7). Using mouse embryonic fibroblasts (MEFs), murine immature dendritic cells (JAWSII), primary peritoneal cavity cells or bone-marrow-derived dendritic cells (BMDCs), we observed that both DOSK and DOST were able to efficiently stimulate immune genes expression. The best results for IFNβ1 and CXCL10 were obtained on peritoneal cavity cells, while a better expression of IL-6 on JAWSII and a stronger expression of DAI and IFI204 on BMDCs were observed. Of note, peritoneal cavity cells were unable to express DAI in all tested conditions. Altogether, these results confirm what was previously observed with C2C12 cells and highlight the efficacy of DOST and DOSK to stimulate innate immune genes in various cell types.

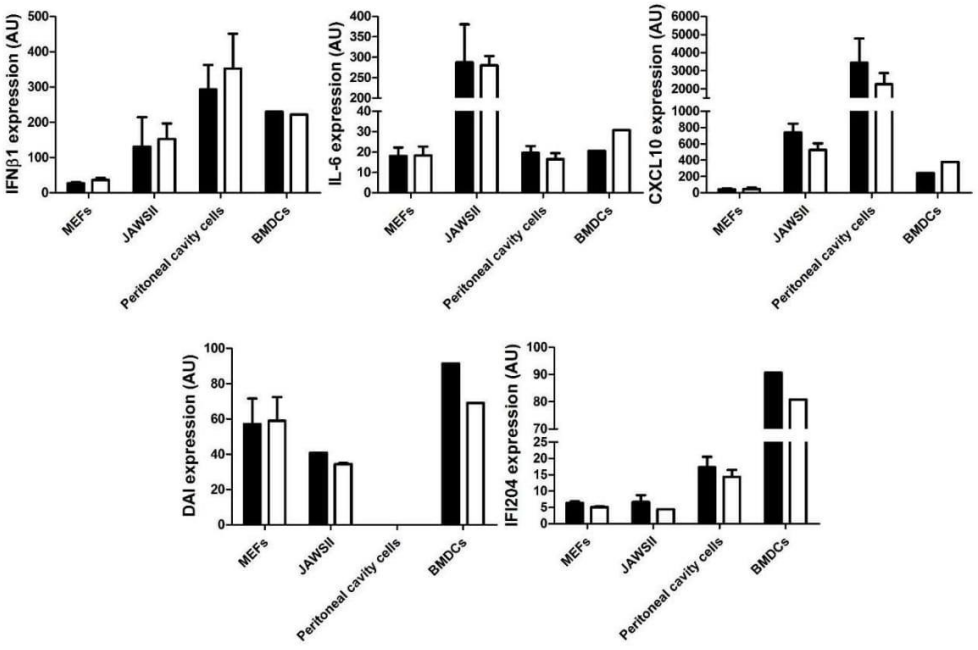


Figure 7: DOST and DOSK activate innate immune response on a wide panel of cells. MEFs, JAWSII, peritoneal cavity cells and BMDCs (n=4) were incubated 24 hours with DOST (black) and DOSK (white) at a concentration of 10 µg/mL. Cytokines (IFNβ1 and IL-6), chemokine (CXCL10) and DNA sensors (DAI and IFI204) expression levels into cells were determined by RT-qPCR analysis, normalized against the expression levels of HPRT (housekeeping gene) and compared to Non-treated cells (AU=1).Data are expressed as the $2^{-\Delta\Delta}$CT formula and are shown as mean ± SEM.

Induction of innate immune stimulation by DOST and DOSK is dependent of caveolae endocytosis

Endocytosis and endocytosis-like mechanisms are considered as the main pathways of internalization of lipids into cells. In the case of cationic lipids used as vectors for the delivery of nucleic acids (via lipoplex formation), it is commonly accepted in the literature that the internalization proceeds through clathrin- and caveolae-mediated endocytosis or macropinocytosis.[28–30]

Therefore, we investigated the importance of endocytosis on the ability of aminoglycoside lipidic derivatives to trigger an innate immune response. The objective of the experiment was to determine which mechanism(s) was (were) involved in the endocytosis of the class of compounds studied. For this study, the most active molecules DOSK and DOST were used. C2C12 cells were treated during 24h with 10 µg/mL of DOSK in the presence of endocytosis inhibitors in concentration conditions where cell growth was not affected (data not shown): Amiloride (a macropinocytosis inhibitor), Chlorpromazine (a clathrin-mediated endocytosis inhibitor) or Genistein (a caveolae-mediated endocytosis inhibitor). As shown in Figure 8a, Amiloride and Chlorpromazine induced a diminution in a 30-50% range of IFNβ1, IL-6 and CXCL10 compared to non-treated cells, but the expression of DAI and IFI204 was not affected. The situation was strongly different with Genistein, since inhibiting the caveolae-mediated endocytosis not only led to a dramatic decrease in IFNβ1, Il-6, CXCL10 expression (70-95% reduction compared to non-treated cells), but the DAI and IFI204 expression was also drastically reduced. Moreover, measuring by ELISA the CXCL10 level in C2C12 supernatant led to the same conclusions, that amiloride and chlorpromazine did not induce any reduction of the chemokine secretion, while the presence of genistein significantly reduced

CXCL10 concentration compared to non-treated cells (Figure 8b). These results strongly suggest that endocytosis is needed to induce innate immune stimulation but that the caveolae-mediated endocytosis is the dominant pathway for DOSK mediated stimulation. Same results were obtained with DOST (data not shown)

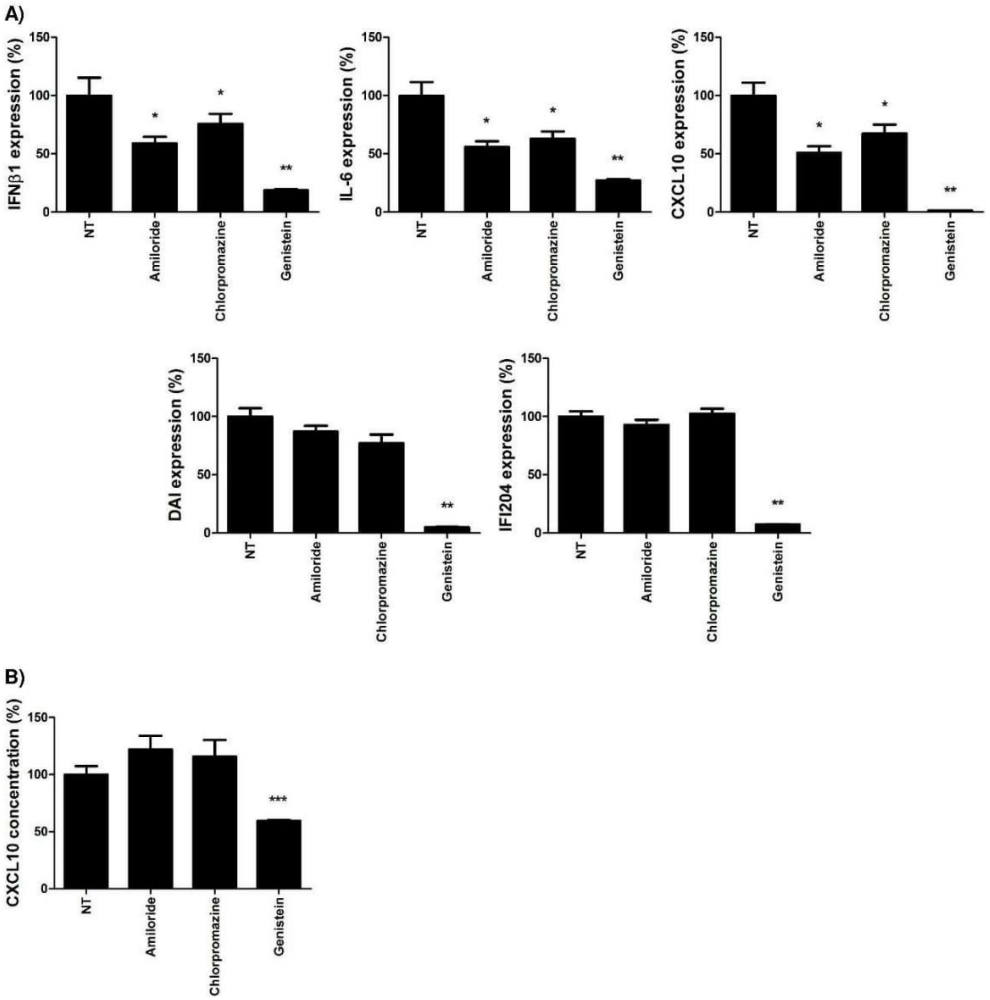


Figure 8: Role of endocytosis in C2C12 immune genes expression induced by DOSK. (A-B) Mouse myoblast cells (n=6) were incubated 24 hours with DOSK at a concentration of 10 µg/mL in the presence or absence of 150nM of amiloride or 9µM of chlorpromazine or 90µM of Genistein. (A) Cytokines (IFNβ1 and IL-6), chemokine (CXCL10) and DNA sensors (DAI and IFI204) expression levels into cells were determined by RT-qPCR analysis, normalized against the expression levels of HPRT (housekeeping gene) and compared to cells treated without inhibitors (expression=100%). Data are expressed as the $2^{-\Delta\Delta}$CT formula. (B) Chemokine CXCL10 level into supernatant were determined by ELISA analysis and compared to cells treated without inhibitors (concentration=100%). Data are shown as mean ± SEM. Significant differences between groups are indicated. *P<0,05 **P<0.01 by Mann-Whitney test.

Immunostimulatory properties of DOST and DOSK is TLR2, TLR4 independent and PLC-dependent

In order to identify which receptor(s) was (were) involved in the immune-stimulatory properties of DOSK, we first investigated the Toll-Like Receptor (TLR) 2 or 4 pathways, as TLR2 and TLR4 were described to be also involved in cationic lipids hydrophobic segments recognition.[11,12,14] It is known that C2C12 myoblast cells lack TLR2,[31] and we also did not observe any cell immune stimulation when C2C12 were treated with the known TLR4 agonist LPS (up to 10 µg/mL, data not shown). This data suggests that the adjuvant properties observed for DOSK and other lipo-aminoglycosides were independent of TLR2 and TLR4 pathways.

Then, we investigated whether or not the PLC pathway was involved in the case of DOSK. We treated C2C12 cells during 24 h with 10 µg/mL of DOSK in the presence of 1µM of a known PLC inhibitor (U73122) after confirming that it had no influence on cell survival (Figure 9a). As shown in Figure 9b, the inhibition of PLC led to a highly significant reduction of IFNβ1, IL-6, CXCL10 and DAI expression. This was confirmed by measuring the secretion of CXCL10 in the supernatant of C2C12 cells, as a strong diminution of CXCL10 concentration was measured in the presence of U73122 (Figure 9c).

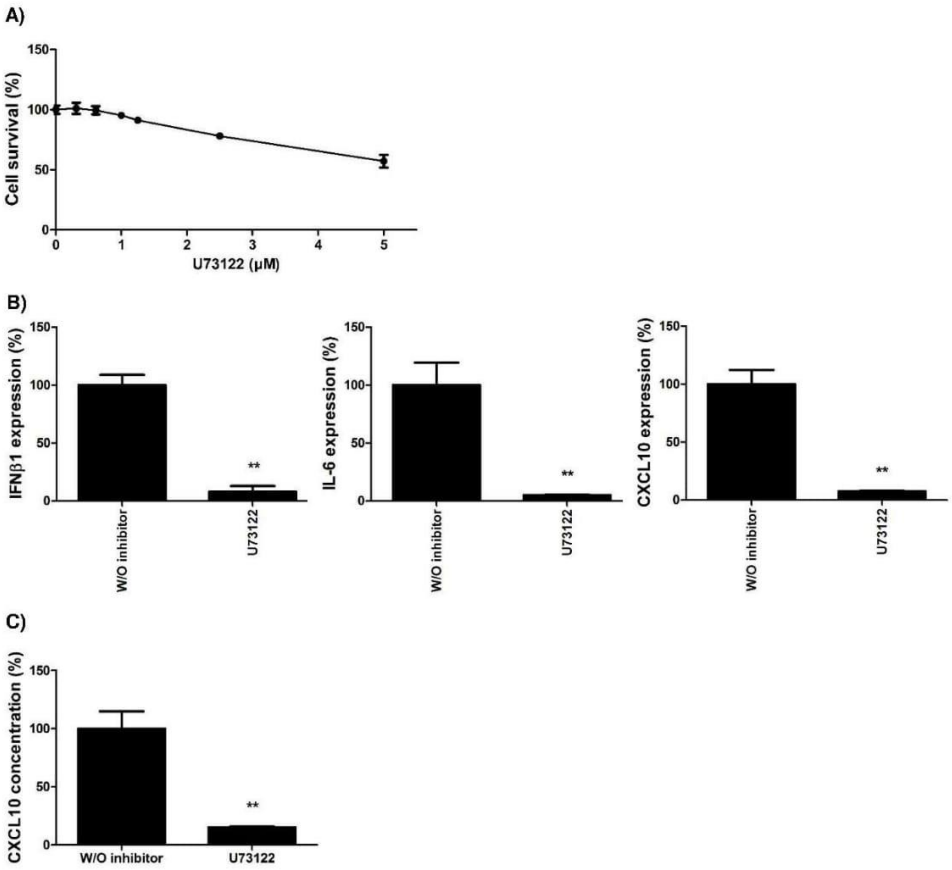


Figure 9: DOSK activates cell immunity through PLC dependent-pathway. (A) Percentage of cell survival on C2C12 cells. Mouse myoblast cells (n=3) were treated with U73122 at a concentration of 0 to 5µM during 24 hours. Cell viability was evaluated using the Cell Titer 96 Non-Radioactive Cell Proliferation Assay. (B-C) Mouse myoblast cells (n=6) were incubated 24 hours with DOSK at a concentration of 10 µg/mL in presence or absence of 1µM of U73122. (B) Cytokines (IFNβ1 and IL-6) and chemokine (CXCL10) expression levels into cells were determined by RT-qPCR analysis, normalized against the expression levels of HPRT (housekeeping gene) and compared to cells treated without inhibitors (expression=100%). (C) Chemokine CXCL10 level into supernatant were determined by ELISA analysis and compared to cells treated without inhibitors (concentration=100%). Data are shown as mean ± SEM. Significant differences between groups are indicated. *P<0,05 **P<0.01 by Mann-Whitney test.

In-vivo validation of adjuvant efficacy of lipo-aminoglycosides

In the perspective of demonstrating adjuvant properties of aminoglycoside lipidic derivatives *in vivo,* we first investigated the effect of these molecules in mice after intravenous injection. To this end, swiss mice were injected intravenously with DOSP or DOSK, and their blood formulations as well as their hematocrit levels were monitored one day before treatment and up to 3 days after injection (Figure 10a). Results show that, neither DOSP nor DOSK induced a variation in the concentration of white blood cells, lymphocytes, neutrophils, eosinophils and basophils compared to that observed on pre-treatment day. The same observation was made for the hematocrit levels. However, results show that DOSK induced a 4-fold increase in monocytes concentration.

Then we examined DOSP and DOSK impact on tumor growth through a well-established BALB/c 4T1 orthotopic breast tumor model.[15] Starting 10 days after intramammary injection of tumor cells (tumors volume = 200 mm^3), mice were treated with two weekly intratumoral injections of either saline solution (control), 1 mg of DOSP or 1mg of DOSK. At day 19, tumor were excised, weighed and photographed. As expected, tumors treated by DOSK had their growth decreased by 25% resulting in a strong homogeneous weight reduction (Figure 10b) and size reduction (Figure 10c) compared to control treatment. However, DOSP treatment led to a very heterogeneous tumor weight and size, without effect on their reduction.

Altogether, these results strongly suggest that the injection of DOSK was able to enhance the immune response at the site of injection, resulting in an important decrease in 4T1 mammary tumor growth.

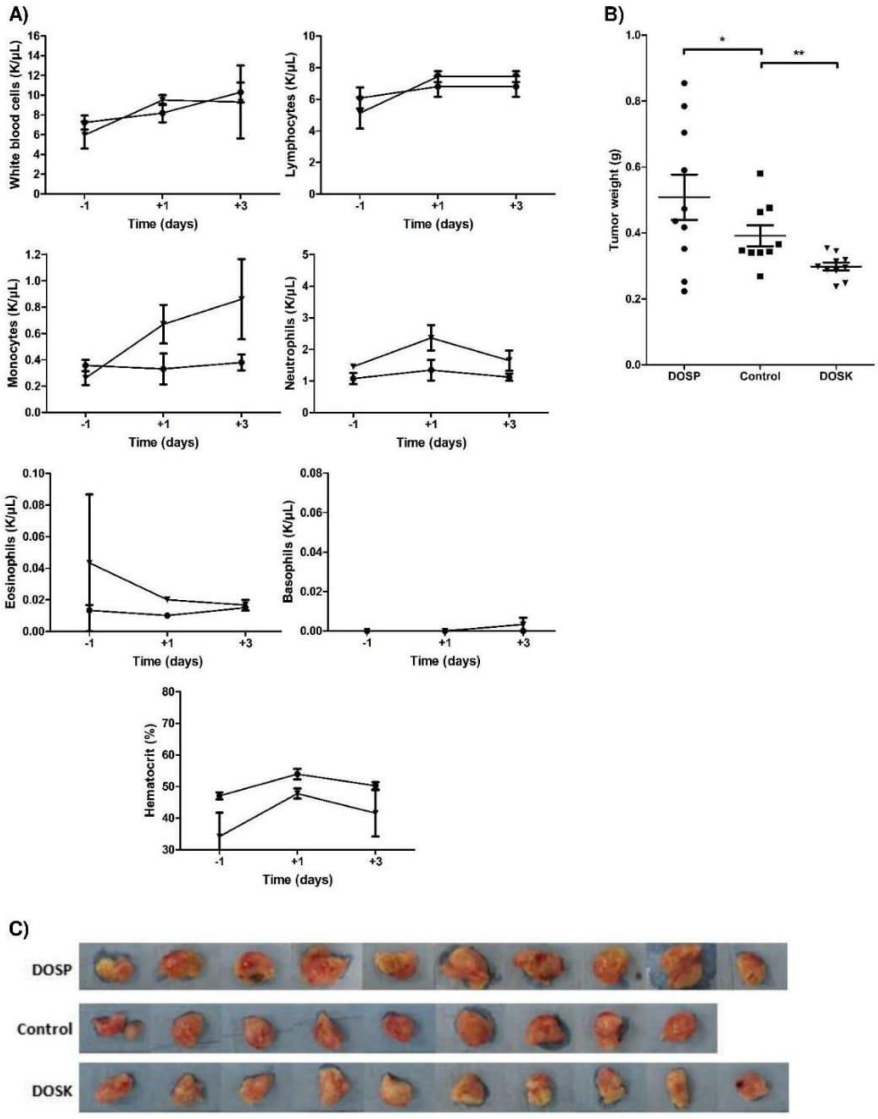


Figure 10: *In vivo* toxicity of lipo-aminoglycosides and impact on tumor growth. (A) *In vivo* toxicity. Swiss mice (n=3) were injected intravenously at day 0 with 100 µg of DOSP (●) or DOSK (▼). Blood formulation and hematocrit level of each mice were monitored from 1 day before and 3 days after injection. (B-C) BALB/c mice bearing orthotopic 4T1 tumors were treated with two weekly intratumoral injections of control vehicle (■), DOSP (●) or DOSK (▼) beginning on day 10 after intramammary injection of tumor cells (n = 9 or 10 / group). At day 19 after intramammary injections, tumors were excised and (B) weighed, then (C) photographed. Data are shown as mean ± SEM. Significant differences between groups are indicated (* $p<0.05$, ** $p<0.01$ compared to control by Mann-Whitney test).

Discussion

In the present study, the objective was to synthetize lipidic derivatives of natural compounds that are able to maximize immune stimulation with broad recognition of innate immune pathways and to report on the mechanisms leading to cell immune stimulation. To this end, we used a set of 14 different aminoglycoside-based cationic lipids with key structural modifications in order to perform a comprehensive study on the relationships between the chemical structure of the potential immune stimulator and the key proteins expression involved in innate immunity. The results of RT-qPCR, western blot and ELISAs showed that some of the tested molecules significantly up-regulated the genes involved in innate immune responses (IFNβ1, IL-6, CXCL10, DAI and IFI204), in a dose- and time-dependent manner. Moreover, this study provided key information about the structural properties necessary to obtain cell stimulation with aminoglycoside-based cationic lipids, since modifications of the polar headgroup, the hydrophobic segment or the spacer drastically modulated the adjuvant properties of these molecules.

For the cationic headgroup, some studies had previously suggested that the ability of cationic lipids to stimulate cell immune response was due to 'strong' (or 'dense') positive charges[7] that can be recognized as a danger signal at the cell surface and contribute to activate signaling cascades classically triggered by endogenous cationic compounds like pro-apoptotic or pro-inflammatory reactions.[32–36] All molecules assessed in the present study are based on an aminoglycoside polar headgroup and even if we have observed that the nature of the aminoglycoside (paromomycin, neomycin, kanamycin, or tobramycin) had a great impact on adjuvant properties, we did not notice any direct correlation between the number of positive charges and the stimulation of the immune response, as it was previously postulated.

Indeed, DOSN (with 6 positive charges) was not able to trigger any stimulation while DOSK (with only 3 positive charges) appeared as the best adjuvant in our experiments. In addition, DOSP and DOST (both with 4 positive charges) clearly displayed different adjuvant properties. On the other hand, we demonstrated that the structure of the cationic headgroup greatly influenced immune stimulation since aminoglycoside cationic derivatives belonging to the 4,6-DDS ring subclass (DOST and DOSK) were able to trigger a strong up-regulation of cell immune response compared to molecules from the 4,5-DDS ring subclass (DOSP and DOSN). This indicated that the recognition of aminoglycoside lipidic derivatives by the immune system probably proceeds through the specific recognition of the headgroup, rather than its global positive charge.

Interestingly, aminoglycosides alone without being linked to hydrophobic moiety, independently of their nature, were not able to stimulate cell immunity. This tends to indicate that the amphiphilic properties of the aminoglycoside lipidic derivatives, as well as their integrity, are prerequisite to confer adjuvant properties. This was confirmed by modifying the structure of the spacer, as this part of the molecule is crucial to determine the hydrophilic/hydrophobic balance of cationic lipids. Indeed, increasing the length of the spacer in the DOAT molecule (by adding two methylene units compared to the 'succinyl' spacer in DOST) dramatically reduced the stimulation of the immune response, indicating that the spacer should be as short as possible to trigger the best stimulation. Moreover, it is known that the structure of the spacer can also influence the stability of the cationic lipids, as biodegradable functions that will dictate the integrity of the molecules in intracellular or extracellular compartments can easily be introduced.[37–39] Here we clearly demonstrated that adding a diester function (DOSST) also decreased the ability of

aminoglycoside lipidic derivatives to induce a cellular response. As previously suggested,[24] we believe that this function favors a better mixing with lipids within the inner bilayer of the endosomes (due to a higher homology between DOSST and natural phospholipid), thus resulting in the formation of a mixture of DOSST and endogenous lipids leading to a reduction of the number of lipoaminoglycoside "monomers" available to interact with the immune system. Furthermore, the introduction of a disulfide bridge in the spacer of the cationic lipid (DODT) also completely suppressed the immunological properties of the cationic lipid. This function had already been reported as being degraded in intracellular compartments,[37,40] resulting in the separation of the polar headgroup and the hydrophobic segment, leading to the loss of the amphiphilic nature and disrupting the integrity of the molecule.

Regarding the hydrophobic segment, we first demonstrated that alkyl chains are necessary to provide adjuvant properties to cationic lipids. Indeed, all aminoglycosides derived from a cholesterol hydrophobic segment (CHOLP, CHOLN, CHOLK, CHOLT) did not induce any significant cell stimulation. These observations are quite consistent with data from the literature since it was described that cationic lipids derived from cholesterol hydrophobic domain are less inflammatory than those derived from fatty acids domains.[41] Regarding the composition of the alkyl chains, we demonstrated on our scaffolds that cationic lipids with 2 oleyl chains (DOST, C18:1) better stimulated the cell immunity compared to their saturated counterpart, either with the same length or with shorter chains (DSST, C18:0; DPST, C16:0 and DMST, C14:0).[7] Again, this suggests that the fluidity of the lipids is an important parameter. The results obtained with DMST appeared to be contradictory to previous data from

the literature that suggested that C14:0 alkyl chains were among the most effective hydrophobic domain to induce cell stimulation.[11] .

The differences observed in C2C12 cells stimulation with the set of molecules tested allowed us to identify two cationic lipids with strong adjuvant properties: DOST and DOSK. These 2 molecules display common structural features: i) the presence of an aminoglycoside polar headgroup belonging to the 4,6-DDS subclass (tobramycin or kanamycin), ii) a short 'succinyl' spacer and iii) an unsaturated dioleyl hydrophobic segment (C18:1). Furthermore, we clearly demonstrated that these 2 cationic lipids were extremely effective for triggering a cell immune response since they were able to stimulate various cell populations (MEFs, JAWSII, BMDCs and peritoneal cavity cells).

Internalization of lipids appeared as an important step in order to stimulate immune response since aminoglycosides alone did not lead to any cell stimulation. It is commonly accepted that the internalization mechanism proceeds through 3 endocytosis pathways: clathrin- and caveolae—mediated endocytosis and micropinocytosis.[28–30] In our case, the results of endocytosis inhibition experiments clearly showed that the caveolin-dependent endocytosis is the main pathway responsible for the internalization of DOSK, and as a consequence its ability to stimulate the immune response. However, we cannot exclude a slight involvement of the clathrin-mediated endocytosis and the macropinocytosis since their inhibition also down-regulated cytokines and chemokines production but to a lower extent compared to caveolin inhibition. These data seem to indicate that the recognition of aminoglycoside lipidic derivatives by immune system probably occurs via an intra-endosomal or intra-cytoplasmic receptor.

It is known that TLR2 and TLR4 can be involved in cationic lipids hydrophobic segments recognition.[11,12,14] In particular, RPR206252 and diC14-amidine were described to induce activation of TLR2 and TLR4 respectively. From a structural point of view, the best TLR2 ligands usually carry a hydrophobic domain in C14:0 or C16:0, while for TLR4 the best ligands are C12:0 and C14:0. The authors of this study concluded that C14 saturated chains were then most adapted to activate TLR signaling pathway. In our experiments, the molecule DMST carrying the dimyristyl hydrophobic segment (C14:0) provided negative results. Moreover, the cationic lipids DOST and DOSK, both carrying a dioleyl chains as hydrophobic segment (C18:1), induced a significant stimulation of the cell immune response despite the absence of TLR2 and TLR4.

Taken together, the results obtained with DOST and DOSK on innate immune stimulation strongly suggest that a specific receptor for these structures is probably involved. This receptor seems to be of particular importance, since we observed the activation of both innate immune pathways (NFkB and Interferon Regulatory Factors). This is in contrast to what was previously described in the literature, with the sole activation of either TLR2 or TLR4 receptors.

Indeed, in this study the tested cationic lipids were based on specific aminoglycoside headgroups, and it was previously described that aminoglycosides were able to trigger an allosteric activation of phosphatydinositol phospholipase C enzyme which is specific to this class of compounds (and not the results of their polycationic nature).[18] The inhibition of PLC by U73122 led to a dramatic decrease of cell immune stimulation by DOSK. This clearly demonstrated the implication of this enzyme as well as the predominance of PLC pathway on innate immune stimulation with aminoglycoside lipidic derivatives.

Comparing the structure of the natural ligand of PLC, phosphatidylinositol, with the best molecules of the series DOST and DOSK provided some information. Indeed, key similarities and differences are present that could explain the role of such cationic lipids on innate immune stimulation. The structure of phosphatidylinositol consists in a simple “sugar alcohol” polar head linked through a phosphate function to a hydrophobic domain made from two different C18 chains, derived respectively from stearic and arachidonic acids. Phosphatidylinositol is negatively charged at physiological pH and its cleavage by PLC also leads to a negatively charged polar moiety. It is unlikely that DOSK or DOST could also be substrates of the PLC enzyme, since there is no phosphate group in the structure of DOSK or DOST. Moreover, within the series of the 14 molecules tested, the one that appears to be closest in structure to phosphatidylinositol is DOSST carrying a diester function to link the oleyl chains. But DOSST was far less immunogenic than DOST with a simple ‘succinyl’ spacer. On the contrary, we hypothesized that aminoglycoside lipidic derivatives like DOST and DOSK could act as allosteric activator of the PLC enzyme. DOST and DOSK could bind to a specific site of the enzyme, changing its conformation and leading to an improved activation of the innate immune response. Based on our results, we could conclude that this interaction is based on very specific interactions, since modifications of the polar head, the linker and the hydrophobic chains lead to drastic changes in immune response. It appears that the molecules which induce the weakest steric effect are the most appropriate (tobramycin and kanamycin better than paromomycin and neomycin, succinyl linker better than adipic and longer spacer, dioleyl chain better than cholesterol). This information may help us designing in the future molecules with an improved efficacy.

Finally, we also demonstrated by our results the opportunity to consider the use of aminoglycoside lipidic derivatives as promising adjuvants for anti-cancerous immunotherapies. First, these molecules can be injected safely to mice without inducing any toxicity, since neither blood formulation nor hematocrit level was negatively influenced following intravenous injection of DOSP and DOSK. In addition, we have observed that DOSK tends to increase the number of circulating monocytes which are cells capable of migrating rapidly on inflamed site in order to differentiate into macrophages or dendritic cells and trigger an efficient immune response ([42–44]). Furthermore, we demonstrated that DOSK intratumoral injections were able to significantly reduce the tumor growth, weight, and size in a murine 4T1 breast tumor model. Knowing that we have already reported that lipo-aminoglycosides used in this study only induced a low *in vitro* toxicity[20–24] as well as no *in vivo* toxicity after intravenous injections, we strongly believe that DOSK antitumor effect is related to its intrinsic ability to stimulate immune signaling pathways. Thus, this suggests that this class of cationic lipids can be used for immunotherapy in a different way that through their ability to protect antigens and to deliver them efficiently into antigen presenting cells.

In conclusion, our work has shown that the entire structure of cationic lipids is to be considered for tailored molecules with optimal adjuvant properties. Indeed, we have determined that the use of a cationic lipid made of a polar aminoglycoside headgroup belonging to the 4,6-DDS ring subclass, a short spacer (succinyl), and a long unsaturated hydrophobic segment (Dioleyl), allows a strong stimulation of the innate immune response via a caveolae-mediated endocytosis and a PLC-dependent pathway. We discovered that the molecule DOSK was able to trigger NFκB independent and dependent cell immune stimulation in various cell types via a new

mechanism of activation and to generate a significant reduction of the tumor growth, in the mice model assessed. In addition, we know from previous studies that lipidic aminoglycosides also have the ability to transfect efficiently DNA, RNA, siRNA or proteins, and these properties can also be used for anti-tumoral or anti-viral immunotherapies in order to deliver antigens or to block specific signals that allow infection or tumorigenesis.

Acknowledgments

The authors are very grateful to Séverine Marionneau-Lambot and Thibauld Oullier from Cancéropôle Grand-Ouest for their technical assistance for murine 4T1 breast cancer model experiments. We are also indebted to P.Lehn and J.-M. Lehn for their pioneer works related to the synthesis of cationic lipids used in this study and for their stimulating discussions and constant interest in this work.

This work was supported by special grants from BPI France financement (Paris, France) for EMERIT project. T.C is supported by funds from IHU-CESTI (French government financial support managed by the National Research Agency “Investment Into The Future” program ANR-10-IBHU-005, co-supported by Région Pays de la Loire and Nantes Métropole).

References

(1) Lee, S.; Nguyen, M. T. *Immune Netw.* **2015**, *15* (2), 51.
(2) Schwendener, R. A. *Ther. Adv. Vaccines* **2014**, *2* (6), 159.
(3) Qureshi, N.; Takayama, K.; Ribi, E. *J. Biol. Chem.* **1982**, *257* (19), 11808.
(4) Didierlaurent, A. M.; Morel, S.; Lockman, L.; Giannini, S. L.; Bisteau, M.; Carlsen, H.; Kielland, A.; Vosters, O.; Vanderheyde, N.; Schiavetti, F.; Larocque, D.; Van Mechelen, M.; Garçon, N. *J. Immunol. Baltim. Md 1950* **2009**, *183* (10), 6186.
(5) Descamps, D.; Hardt, K.; Spiessens, B.; Izurieta, P.; Verstraeten, T.; Breuer, T.; Dubin, G. *Hum. Vaccin.* **2009**, *5* (5), 332.
(6) Beran, J. *Expert Opin. Biol. Ther.* **2008**, *8* (2), 235.
(7) Vangasseri, D. P.; Cui, Z.; Chen, W.; Hokey, D. A.; Falo, L. D.; Huang, L. *Mol. Membr. Biol.* **2006**, *23* (5), 385.
(8) Yan, W.; Chen, W.; Huang, L. *Mol. Immunol.* **2007**, *44* (15), 3672.
(9) Lonez, C.; Vandenbranden, M.; Ruysschaert, J.-M. *Adv. Drug Deliv. Rev.* **2012**, *64* (15), 1749.
(10) Altin, J. G.; Parish, C. R. *Methods San Diego Calif* **2006**, *40* (1), 39.
(11) Lonez, C.; Bessodes, M.; Scherman, D.; Vandenbranden, M.; Escriou, V.; Ruysschaert, J.-M. *Nanomedicine Nanotechnol. Biol. Med.*
(12) Tanaka, T.; Legat, A.; Adam, E.; Steuve, J.; Gatot, J.-S.; Vandenbranden, M.; Ulianov, L.; Lonez, C.; Ruysschaert, J.-M.; Muraille, E.; Tuynder, M.; Goldman, M.; Jacquet, A. *Eur. J. Immunol.* **2008**, *38* (5), 1351.
(13) Sasaki, S.; Fukushima, J.; Arai, H.; Kusakabe, K. I.; Hamajima, K.; Ishii, N.; Hirahara, F.; Okuda, K.; Kawamoto, S.; Ruysschaert, J. M.; Vandenbranden, M.; Wahren, B.; Okuda, K. *Eur. J. Immunol.* **1997**, *27* (12), 3121.
(14) Wilmar, A.; Lonez, C.; Vermeersch, M.; Andrianne, M.; Pérez-Morga, D.; Ruysschaert, J.-M.; Vandenbranden, M.; Leo, O.; Temmerman, S. T. *Vaccine* **2012**, *30* (2), 414.
(15) Meraz, I. M.; Savage, D. J.; Segura-Ibarra, V.; Li, J.; Rhudy, J.; Gu, J.; Serda, R. E. *Mol. Pharm.* **2014**, *11* (10), 3484.
(16) Querec, T.; Bennouna, S.; Alkan, S.; Laouar, Y.; Gorden, K.; Flavell, R.; Akira, S.; Ahmed, R.; Pulendran, B. *J. Exp. Med.* **2006**, *203* (2), 413.
(17) Ward, D. T.; Maldonado-Pérez, D.; Hollins, L.; Riccardi, D. *J. Am. Soc. Nephrol. JASN* **2005**, *16* (5), 1236.
(18) Morris, J. C.; Ping-Sheng, L.; Zhai, H. X.; Shen, T. Y.; Mensa-Wilmot, K. *J. Biol. Chem.* **1996**, *271* (26), 15468.
(19) Ward, D. T.; McLarnon, S. J.; Riccardi, D. *J. Am. Soc. Nephrol. JASN* **2002**, *13* (6), 1481.
(20) Desigaux, L.; Sainlos, M.; Lambert, O.; Chevre, R.; Letrou-Bonneval, E.; Vigneron, J.-P.; Lehn, P.; Lehn, J.-M.; Pitard, B. *Proc. Natl. Acad. Sci. U. S. A.* **2007**, *104* (42), 16534.
(21) Mével, M.; Sainlos, M.; Chatin, B.; Oudrhiri, N.; Hauchecorne, M.; Lambert, O.; Vigneron, J.-P.; Lehn, P.; Pitard, B.; Lehn, J.-M. *J. Control. Release Off. J. Control. Release Soc.* **2012**, *158* (3), 461.
(22) Mével, M.; Haudebourg, T.; Colombani, T.; Peuziat, P.; Dallet, L.; Chatin, B.; Lambert, O.; Berchel, M.; Montier, T.; Jaffrès, P.-A.; Lehn, P.; Pitard, B. *J. Gene Med.* **2015**.
(23) Chatin, B.; Mével, M.; Devallière, J.; Dallet, L.; Haudebourg, T.; Peuziat, P.; Colombani, T.; Berchel, M.; Lambert, O.; Edelman, A.; Pitard, B. *Mol. Ther. Nucleic Acids* **2015**, *4*, e244.
(24) Habrant, D.; Peuziat, P.; Colombani, T.; Dallet, L.; Gehin, J.; Goudeau, E.; Evrard, B.; Lambert, O.; Haudebourg, T.; Pitard, B. *J. Med. Chem.* **2016**.
(25) Ray, A.; Dittel, B. N. *J. Vis. Exp. JoVE* **2010**, No. 35.
(26) Lutz, M. B.; Kukutsch, N.; Ogilvie, A. L.; Rössner, S.; Koch, F.; Romani, N.; Schuler, G. *J. Immunol. Methods* **1999**, *223* (1), 77.

(27) Ljungberg, K.; Whitmore, A. C.; Fluet, M. E.; Moran, T. P.; Shabman, R. S.; Collier, M. L.; Kraus, A. A.; Thompson, J. M.; Montefiori, D. C.; Beard, C.; Johnston, R. E. *J. Virol.* **2007**, *81* (24), 13412.
(28) Zuhorn, I. S.; Kalicharan, R.; Hoekstra, D. *J. Biol. Chem.* **2002**, *277* (20), 18021.
(29) Khalil, I. A.; Kogure, K.; Akita, H.; Harashima, H. *Pharmacol. Rev.* **2006**, *58* (1), 32.
(30) Elouahabi, A.; Ruysschaert, J.-M. *Mol. Ther. J. Am. Soc. Gene Ther.* **2005**, *11* (3), 336.
(31) Boyd, J. H.; Divangahi, M.; Yahiaoui, L.; Gvozdic, D.; Qureshi, S.; Petrof, B. J. *Infect. Immun.* **2006**, *74* (12), 6829.
(32) Loscalzo, J. *J. Nutr.* **2004**, *134* (10 Suppl), 2798S.
(33) von Deutsch, A. W.; Mitchell, C. D.; Williams, C. E.; Dutt, K.; Silvestrov, N. A.; Klement, B. J.; Abukhalaf, I. K.; von Deutsch, D. A. *Gravitational Space Biol. Bull. Publ. Am. Soc. Gravitational Space Biol.* **2005**, *18* (2), 109.
(34) Coburn, R. F. *J. Cell. Physiol.* **2009**, *221* (3), 544.
(35) Verzola, D.; Famà, A.; Villaggio, B.; Rocco, M. D.; Simonato, A.; D'Amato, E.; Gianiorio, F.; Garibotto, G. *J. Inherit. Metab. Dis.* **2012**, *35* (6), 1011.
(36) Ray, R. M.; Li, C.; Bhattacharya, S.; Naren, A. P.; Johnson, L. R. *Cell. Signal.* **2012**, *24* (4), 931.
(37) Tang, F.; Hughes, J. A. *Biochem. Biophys. Res. Commun.* **1998**, *242* (1), 141.
(38) Wetzer, B.; Byk, G.; Frederic, M.; Airiau, M.; Blanche, F.; Pitard, B.; Scherman, D. *Biochem. J.* **2001**, *356* (Pt 3), 747.
(39) Martin, B.; Sainlos, M.; Aissaoui, A.; Oudrhiri, N.; Hauchecorne, M.; Vigneron, J.-P.; Lehn, J.-M.; Lehn, P. *Curr. Pharm. Des.* **2005**, *11* (3), 375.
(40) Shirazi, R. S.; Ewert, K. K.; Leal, C.; Majzoub, R. N.; Bouxsein, N. F.; Safinya, C. R. *Biochim. Biophys. Acta* **2011**, *1808* (9), 2156.
(41) Lv, H.; Zhang, S.; Wang, B.; Cui, S.; Yan, J. *J. Controlled Release* **2006**, *114* (1), 100.
(42) Parihar, A.; Eubank, T. D.; Doseff, A. I. *J. Innate Immun.* **2010**, *2* (3), 204.
(43) Kuhn, S.; Hyde, E. J.; Yang, J.; Rich, F. J.; Harper, J. L.; Kirman, J. R.; Ronchese, F. *J. Immunol.* **2013**, *191* (4), 1984.
(44) Jensen, S. S.; Parhamifar, L.; Henriksen, J.; Andresen, T. L. *Immunother. Open Access* **2016**.

Article 3 : Influence de l'assemblage supramoléculaire des liposomes sur l'efficacité de transfection.

Depuis les travaux pionniers de Felgner en 1987, de nombreux lipides cationiques ont été développés afin de délivrer un grand nombre de particules hydrophobes (comme les acides nucléiques, des peptides ou bien des protéines) en faisant une des catégories de vecteurs synthétiques les plus prometteuses pour la délivrance de molécules au sein de cellules (Mishra et al., 2013; Cortesi et al., 2014). Depuis, de très nombreuses études ont été effectuées afin d'améliorer l'efficacité de ces vecteurs (Draghici and Ilies, 2015) en se reposant classiquement sur la modification chimique de leurs structures que ce soit au niveau de la tête polaire ou bien du segment hydrophobe (Zhi et al., 2010, 2013). Néanmoins encore aujourd'hui, aucun vecteur unique et universel capable de délivrer différentes classes d'acides nucléiques (ADN, ARN, siRNA) de manière efficace au sein de différents types cellulaires n'a encore pu être identifié. Cela est notamment dû au fait que de très nombreux facteurs interdépendants régissent l'efficacité de transfection, comme l'internalisation des lipoplexes, l'échappement endosomal, la libération des acides nucléiques et l'entrée dans le noyau pour l'ADN.

Suite aux travaux prometteurs de l'équipe de J.M. Lehn sur le développement de lipides cationiques dérivés de la kanamycine capables de délivrer des acides nucléiques aussi bien *in vitro* que *in vivo* chez la souris (Belmont et al., 2002; Sainlos et al., 2005), notre équipe a développé de nouvelles molécules dérivés des aminoglycosides (comme la paromomycine, la néomycine, la kanamycine et la tobramycine) très efficaces pour la vectorisation d'ADN, d'ARNm et de siRNA (Desigaux et al., 2007; Mével et al., 2012; Habrant et al., 2016). La plupart des formulations à base de lipides cationiques contiennent également des co-lipides neutres afin d'augmenter la délivrance des acides nucléiques. Dès lors, par une approche originale basée sur la modulation de l'assemblage des phases lamellaires lipidiques, notre équipe a également étudié l'influence de l'assemblage supramoléculaire des lipoplexes sur l'efficacité de transfection, montrant que des liposomes hybrides (composé d'un lipide cationique possédant un espaceur amide et d'un co-lipide avec un espaceur phosphoramide) induisait une meilleure stabilité et transfection de l'ADN par rapport à des liposomes homogènes (avec des espaceurs amides) (Mével et al., 2015).

Néanmoins afin de valider ce nouveau concept, une étude physico-chimique plus approfondie est nécessaire, notamment afin d'observer l'impact de nouveaux liposomes hybrides « inverses » (avec un lipide cationique possédant un espaceur phosphoramide et un co-lipide avec un espaceur amide) et homogènes (avec des espaceurs phosphoaramides) sur la stabilité et l'efficacité de transfection de différentes classes d'acides nucléiques (ADN, ARNm et siRNA) au sein de différentes populations cellulaires. L'ensemble des données obtenues au cours de cette étude ont fait l'objet d'une publication dans la revue *Journal of Controlled Release.*

Article 3 : Self-assembling complexes between binary mixtures of lipids with different linkers and nucleic acids promote universal mRNA, DNA and siRNA delivery

Journal of Controlled Release 249 (2017) 131–142

Contents lists available at ScienceDirect

Journal of Controlled Release

journal homepage: www.elsevier.com/locate/jconrel

Self-assembling complexes between binary mixtures of lipids with different linkers and nucleic acids promote universal mRNA, DNA and siRNA delivery

Thibault Colombani [a,1], Pauline Peuziat [a,1], Laurence Dallet [b], Thomas Haudebourg [a], Mathieu Mével [a], Mathieu Berchel [c], Olivier Lambert [b], Damien Habrant [d], Bruno Pitard [a,d,*]

[a] CRCINA, INSERM, Université d'Angers, Université de Nantes, Nantes, France
[b] CBMN UMR-CNRS 5248, Université de Bordeaux IPB, Pessac, France
[c] UMR CNRS 6521, IFR 148 ScInBioS, Université de Bretagne Occidentale, Université Européenne de Bretagne, Brest, France
[d] In-Cell-Art, Nantes, France

ARTICLE INFO

Article history:
Received 21 September 2016
Accepted 28 January 2017
Available online 01 February 2017

Keywords:
Non-viral nucleic acids transfer
Cationic lipids
Helper lipids
Liposomes
In vitro transfection
Physico-chemical properties

ABSTRACT

Protein expression and RNA interference require efficient delivery of DNA or mRNA and small double stranded RNA into cells, respectively. Although cationic lipids are the most commonly used synthetic delivery vectors, a clear need still exists for a better delivery of various types of nucleic acids molecules to improve their biological activity. To optimize the transfection efficiency, a molecular approach consisting in modifying the chemical structure of a given cationic lipid is usually performed, but an alternative strategy could rely on modulating the supramolecular assembly of lipidic lamellar phases sandwiching the nucleic acids molecules. To validate this new concept, we synthesized on one hand two paromomycin-based cationic lipids, with either an amide or a phosphoramide linker, and on the other hand two imidazole-based neutral lipids, having as well either an amide or a phosphoramide function as linker. Combinations of cationic and helper lipids containing the same amide or phosphoramide linkers led to the formation of homogeneous lamellar phases, while hybrid lamellar phases were obtained when the linkers on the cationic and helper lipids were different. Cryo-transmission electron microscopy and fluorescence experiments showed that liposomes/nucleic acids complexes resulting from the association of nucleic acids with hybrid lamellar phases led to complexes that were more stable in the extracellular compartment compared to those obtained with homogeneous systems. In addition, we observed that the most active supramolecular assemblies for the delivery of DNA, mRNA and siRNA were obtained when the cationic and helper lipids possess linkers of different natures. The results clearly show that this supramolecular strategy modulating the property of the lipidic lamellar phase constitutes a new approach for increasing the delivery of various types of nucleic acid molecules.

© 2017 Elsevier B.V. All rights reserved.

1. Introduction

Synthetic delivery systems represent today an attractive and well-documented approach for the intracellular delivery of recombinant informative macromolecular drugs including proteins and nucleic acids [1,2]. Among synthetic vectors used to deliver nucleic acids inside the cells, cationic lipids are recognized as a classical and versatile family of nanocarriers [3].

The usual approach applied until now to optimize the transfection efficiency consisted in chemical modifications on the cationic lipid structure only [4,5]. Indeed, performing structure-activity relationship (SAR) is the strategy of choice in the field of medicinal chemistry for the "hit-to-lead" approach and has proven its efficacy in various applications such as enzyme inhibition, taking advantage of the fact that the drug of interest interacts directly with its target [6,7]. Regarding the design of cationic lipids used as delivery systems, a ceiling effect may have been reached with this SAR strategy. Indeed, almost 30 years after the pioneer work on the synthesis of the first cationic lipids [8] and even if great improvements have been achieved compared to the original molecules, the ultimate goal of identifying a unique and universal

Abbreviations: C2C12, mouse myoblast cell line; CR, charge ratios; CLN, cationic lipid with N-based linker; CLP, cationic lipid with P-based linker; Cryo-TEM, cryogenic transmission electron microscopy; DMEM, Dulbecco's Modified Eagle's Medium; DNA, deoxyribonucleic acid; EtBr, ethidium bromide; eGFP, enhanced green fluorescent protein; HeLa, human cervical cancer cells; HLN, helper lipid with N-based linker; HLP, helper lipid with P-based linker; HPRT, hypoxanthine-guanine phosphoribosyltransferase; FACS, fluorescence activated cell sorting; Luc, luciferase; MEF, mouse embryonic fibroblasts; MEM, minimum essential medium; mRNA, messenger Ribonucleic acid; qRT-PCR, quantitative Real-Time PCR; RNAi, RNA interference; siRNA, small interfering RNA.

* Corresponding author at: UMR 1232/CNRS ERL, IRS2, 22 bl Benoni Goullin 44200 Nantes, France.
E-mail address: bruno.pitard@univ-nantes.fr (B. Pitard).

[1] These authors equally contributed to this work.

http://dx.doi.org/10.1016/j.jconrel.2017.01.041
0168-3659/© 2017 Elsevier B.V. All rights reserved.

delivery system able to efficiently transfect different classes of nucleic acids (DNA, mRNA, siRNA) into different cell lines or primary cells has not been reached yet. This situation probably results from the fact that cationic lipids do no act by themselves as "medical drugs" but represent only one piece of a complex process involving numerous steps that all need to be overcome to reach good levels of transfection.

The mechanism of gene delivery is known to proceed via i) formation of the lipoplex (complex nucleic acid + cationic lipid), ii) cellular uptake by endocytosis, iii) endosomal escape, iv) release of the nucleic acid from the complex and v) protein expression in the case of mRNA, protein inhibition in the case of siRNA in the cytosol, or nuclear uptake then protein expression in the case of DNA [9–14]. In addition, another difficulty for the discovery of an "universal" vector probably relies on identifying molecular features adapted to different structures of nucleic acids such as single or double stranded RNA and double stranded DNA that moreover possess different molecular weights.

The structure of cationic lipids used in the field of nucleic acid delivery is typically divided into three distinct parts i) a positively charged headgroup, able to electrostatically interact with nucleic acids, ii) an hydrophobic tail, to allow interactions with the cell membranes and iii) a linker (spacer) that links the head and the tail moieties together. Our team has developed a specific class of cationic lipids, using aminoglycoside-based headgroup. Aminoglycosides represent a family of natural products with a precise 3D-organization carrying several positively charged primary amines and having the property of naturally binding to nucleic acids [15–20]. We assessed different aminoglycosides (including paromomycin, neomycin, kanamycin and tobramycin) in previous studies and prepared various combinations of aminoglycoside/linker/hydrophobic part conjugates. The resulting amphiphilic molecules proved to be efficient vectors for the delivery of DNA, siRNA and more recently mRNA [21–24].

A well-known strategy to enhance transfection efficiency of a given cationic lipid relies in the incorporation of a neutral helper lipid in the nucleic acid formulation, forming cationic liposomes with binary mixtures of lipids in the liposomal membrane [25]. The helper lipids are known to facilitate the endosomal escape and display structural features comparable to cationic lipids (headgroup/linker/hydrophobic domain), except that the headgroup does not carry any positive charge. In the present study, we used helper lipids with an imidazole headgroup, based on encouraging results from the literature [26].

We hypothesized that the various steps of the transfection mechanism could be affected by the self-assembling properties of the complexes formed between cationic lipids (or liposomes) and nucleic acids, rather than the structure of the cationic lipids (or liposomes) themselves [9]. In these supramolecular assemblies, the nucleic acid molecules are sandwiched between lipid bilayers forming a lamellar organization of various periodicities [27–29]. The transfection pathway is governed by "membrane interactions", as the membranes of the lipoplexes first interact with the cytoplasmic membranes for internalization, and then with the endosomal membrane to trigger the release of the transported molecules [10,12]. We believe that the gene delivery process could thus be optimized by taking advantage of a new strategy consisting in finely modulating the lamellar phases of the lipoplex membrane, in order to confer enhanced nucleic acids complexation and decomplexation properties, outside and inside the cells, respectively.

In a previous study on DNA transfection, we compared two different formulation systems made with the same cationic lipid whose structure consisted of a paromomycin headgroup, a dioleyl hydrophobic backbone and a nitrogen-based linker (amide bond) [30]. Two imidazole-based helper lipids with either a nitrogen or a phosphorous-based linker were used to prepare liposomes. We discovered that better stability and higher DNA transfection were obtained when the hybrid liposomes (meaning with N-based linker on the cationic lipid and P-based linker on the helper lipid) were used compared to homogeneous liposomes (with N-based linkers both on the cationic and helper lipids).

These interesting preliminary observations prompted us to further investigate on these types of supramolecular assemblies. In the present study we assessed the systems formed by the combination of two paromomycin-based cationic lipids and two neutral imidazole-based helper lipids with three types of nucleic acids, DNA, mRNA and siRNA. It is known that binary mixtures of lipids with different hydrophobic backbone (nature, chain length and/or insaturations) can give rise to spatial separation of phase domains in the membranes; we therefore decided to maintain the same hydrophobic moiety for the cationic and the helper lipids and selected a dioleyl backbone for this study. Regarding the linker, two bio-inspired functions consisting of either an amide (nitrogen-based) or a phosphoramide (phosphorous-based) bond were used to link the polar and the lipophilic parts together.

The combinations polar headgroup/linker/hydrophobic tail provided four molecules that were evaluated; two cationic lipids: **CLN** (cationic lipid with nitrogen-based linker) and **CLP** (cationic lipid with phosphorous-based linker), and two helper lipids: **HLN** (helper lipid with nitrogen-based linker) and **HLP** (helper lipid with phosphorous-based linker). With these four molecules, supramolecular assemblies consisting of associations of the two cationic lipids with the two neutral lipids led to either homogeneous lamellar phases (when the two lipids have the same linker, **CLN**:**HLN** and **CLP**:**HLP**) or hybrid ones (when the linkers on the two lipids are different, **CLN**:**HLP** and **CLP**:**HLN**).

The major objective of the work was to understand how the physicochemical properties of the lipoplexes can affect the stability and the transfection efficiency of nucleic acids and to decipher the potential "universal" transfection properties of these types of liposomal formulations.

2. Materials and methods

pGWIZ-Luc (Genlantis, San Diego, CA) is a plasmid encoding the luciferase reporter gene under the control of the human cytomegalovirus immediate-early gene promoter. pGWIZ-eGFP (Clontech, Mountain View, CA) is a plasmid encoding green fluorescent protein reporter gene, under the control of the human cytomegalovirus immediate-early gene promoter. Plasmids were purified from recombinant *Escherichia coli* by means of Endofree plasmid purification columns (Qiagen, Venlo, Netherlands).

mRNA encoding the luciferase and the green fluorescent protein were purchased from Trilink Biotechnologies (San Diego, CA).

Human anti-laminA/C siRNA (sc-35,776) was purchased in Santa Cruz Biotechnology (Dallas, Texas) and murine anti-laminA/C siRNA (sense sequence: GGA-CCU-CGA-GGC-UCU-UCU-C) was obtained from Eurogentec (Seraing, Belgium).

3. Lipids synthesis

All reagents were purchased from Acros Organics or Sigma-Aldrich and were used without further purification. Reactions requiring anhydrous conditions were performed under nitrogen. NMR experiments were recorded on a Bruker Advance 400 MHz spectrometer (400 MHz for ^{1}H, 100 MHz for ^{13}C and 162 MHz for [31] P). Spectra were acquired at 300 K, using deuterated methanol (MeOD) as solvent. Chemical shifts are reported in parts per million (ppm); coupling constant are reported in units of Hertz [Hz]. The following abbreviations were used: s = singlet, d = doublet, t = triplet, m = multiplet. High-resolution mass spectra (HRMS) were recorded with a qTOF Synaptg2 HDMS (Waters Corporation) apparatus; electrospray in positive mode was used. All the products were purified by flash chromatography (GRACE REVELERIS Flash Chromatography System) equipped with UV and DLS detectors. The purity of **CLP** was controlled by HPLC using UPLC H-Class from Waters using a gradient of H_2O + 0.1% Formic acid and CH_3CN.

3.1. Teoc-protected CLP (5)

4 (100 mg, 0.17 mmol) and **2** (205 mg, 0.17 mmol) were dissolved in dry CH_2Cl_2, then triethylamine (24 μL, 0.17 mmol) and $CBrCl_3$ (18.6 μL, 0.19 mmol) were added at 0 °C under nitrogen atmosphere. The reaction was stirred 30 min at 0 °C and overnight at 20 °C. After washing with water (2 × 50 mL) and with brine (50 mL), the organic phase was dried over Na_2SO_4, filtered, evaporated and purified by flash chromatography on silica column (CH_2Cl_2/MeOH 100/0 to 80/20) to give the desired compound as white solid (226 mg, 75% yield). ^{1}H NMR (CD_3OD): δ = 5.39–5.28 (m, 4H), 5.17–4.96 (m, 2H), 4.6 (m, 2H), 4.20–4.05 (m, 10H), 4.03–3.94 (m, 5H), 3.91–3.75 (m, 5H), 3.70–3.35 (m; 13H), 3.21–3.07 (m, 2H), 2.04–1.98 (m, 8H), 1.72–1.66 (m, 4H), 1.46–1.22 (m, 44H), 1.06–0.97 (m, 8H), 0.91 (t, J = 5.6 Hz, 6H), 0.07–0.05 (m, 36H). ^{31}P NMR (CD_3OD): 9.04 ppm. HRMS for $C_{83}H_{162}N_5O_{25}Si_4PNa$ $[M + Na]^+$, calculated 1795.0096; found 1795.0271.

3.2. CLP

Compound **5** (150 mg, 0.085 mmol) was dissolved in DCM (3 mL). TFA (2 mL) was added at 0 °C under nitrogen atmosphere. The reaction was stirred 30 min at 0 °C and 1 h at 20 °C. After concentration, purification by reverse-phase flash chromatography (H_2O + 0.1%TFA/MeOH 100/0 to 0/100) and lyophilization, the desired compound was obtained as white powder (133 mg, 95% yield). ^{1}H NMR (CD_3OD): δ = 5.54 (d, J = 3.6 Hz, 1H), 5.39–5.34 (m, 4H), 5.2 (m, 1H), 4.45 (t_{app}, J = 5.6 Hz, 1H), 4.33–4.31 (m, 1H), 4.19–4.14 (m, 2H), 4.02–3.96 (m, 5H), 3.92–3.89 (m, 2H), 3.83–3.78 (m, 4H), 3.67–3.60 (m, 3H), 3.51–3.46 (m, 1H), 3.36 (m, 1H), 3.26–3.10 (m, 5H), 2.48–2.40 (m, 1H), 2.09–1.95 (m, 7H), 1.87–1.79 (m, 1H), 1.71–1.67 (m, 4H), 1.42–1.30 (m, 44H), 0.90 (t, J = 6.6 Hz, 6H); ^{13}C NMR (75 MHz, CD_3OD, 25 °C): δ = 130.9, 130.8, 111.3, 98.6, 97.2, 85.5, 83.4, 81.2, 76.9, 76.1, 76.0, 75.5, 74.1, 17.8, 70.8, 69.3, 68.1, 62.4, 60.9, 55.7, 53.2, 51.3, 30.7, 42.2, 33.6, 33.0, 31.5, 31.4, 30.9, 30.8, 30.6, 30.4, 30.3, 30.2, 28.2, 28.1, 26.8, 23.7, 14.4 ppm; ^{31}P NMR (CD_3OD): 9.03 ppm; HRMS for $C_{59}H_{115}N_5O_{17}P$ $[M + H]^+$, calculated 1196.8053; found 1196.8026.

4. Cationic liposomes formulations

Liposomes formulations were made as previously described with a cationic lipid (**CLN** or **CLP**) and a helper lipid (**HLN** or **HLP**) at a molar ratio of 1:1 [23]. Briefly, liposomes were prepared by the lipid film hydration technique. Both lipids and helper lipids were placed in a round bottom flask and a dry lipid film was made by a slow rotary evaporation of the solvent. The dry lipid film was then hydrated with H_2O overnight at 4 °C. The final lipid solution was sonicated for 15 min to ensure a uniform and appropriate particle size (around 180 nm).

5. Preparation of lipoplexes

Nucleic acids-liposomes complexes were formed by vigorously mixing equal volumes of the nucleic acids solution with the liposomes solution, at the suitable concentration leading to different charge ratios (±). Lipoplexes were prepared in NaCl 150 mM. For transfection experiments, 0.5 μg of DNA or mRNA and 0.15 μg of siRNA were used.

6. Cryogenic transmission electron microscopy

CryoTEM imaging of cationic lipid/DNA complexes were performed as previously described. Complexes are formulated in 150 mM NaCl or DMEM and a 5 μL sample drop was applied to a holey carbon coated copper grid, the excess was blotted with a filter paper, and the grid was plunged into a liquid ethane bath cooled with liquid nitrogen (Leica EM CPC). Specimens were observed at a temperature of ~ −170 °C, using a cryo holder, with a FEI Tecnai F20 electron microscope operating at 200 kV. Images were recorded with a 2 k × 2 k USC1000 CCD camera (Gatan) at a nominal magnification of 50,000× under low-dose conditions.

7. DNA release

In order to follow the progress of DNA release, we used residual ethidium bromide (EtBr) fluorescence measurements carried out on a Jobin-Yvon spex Fluoromax-4 spectrofluorometer (Horiba Jobin Yvon, Kyoto, Japan). Residual fluorescence displayed upon intercalation between non-complexed DNA base pairs was monitored (excitation, 260 nm; emission, 560 nm). DNA-lipids complexes (1 mL at 1 μg/mL of DNA) were formed in NaCl 150 mM final concentration, or 10 mM Hepes (pH 7.2). The kinetics of increase in EtBr fluorescence was monitored after the rapid addition of 10 μL of a solution containing polyphosphates (Sodium hexametaphosphate) (Sigma-Aldrich, Saint-Louis, MO), at a concentration of 4 mg/mL A magnetic stirrer at the bottom of the quartz cell ensured the homogenization of the solution.

8. Cell culture

The transfection activity of the various vectors was evaluated in transient transfection experiments on human cervical cancer cell line (HeLa), murine myoblast cell line (C2C12), and mouse embryonic fibroblast cell line (MEF) as well as in primary cells as in rat aorta smooth muscle cells and human fibroblasts. Cells were grown at 37 °C in a humidified 5% CO_2/95% air incubator.

The medium used for HeLa, C2C12 and rat aorta smooth muscle cells was Dulbecco's Modified Eagle's Medium (DMEM) (Life Technologies, Carlsbad, CA), with a glucose concentration of 4.5 g/L for the HeLa and C2C12 or 1 g/L for the rat aorta smooth muscle cells, supplemented with Fetal Calf Serum 10% (v/v), 2 mM L-glutamine 1% (v/v) and antibiotics (penicillin/streptomycin) 1% (v/v). MEF cells were cultivated in Iscove's Modified Dulbecco's Medium (IMEM) (Life Technologies, Carlsbad, CA) supplemented with Fetal Calf Serum 10% (v/v), MEM (minimum essential medium) Non-Essential Amino Acids (Life Technologies, Carlsbad, CA) 1% (v/v) and antibiotics (penicillin/streptomycin) 1% (v/v). The medium used for human fibroblasts was DMEM with a glucose concentration of 4.5 g/L, with Glutamax™, supplemented with HyClone™ Fetal Bovine Serum (Life Technologies, Carlsbad, CA) 10% (v/v), MEM Non-Essential Amino Acids 1% (v/v) and Sodium Pyruvate 1% (v/v).

9. In vitro cell transfection

The day before transfection, cellular suspensions of 1 mL were seeded into 24-well culture plates to reach a final concentration resulting in approximately 70% confluence after 24 h. Thirty minutes before transfection, medium was removed and replaced by 450 μL of fresh complete medium. Then, lipoplexes solution (50 μL) prepared 15 min before, containing 0.5 μg of plasmid DNA or mRNA, or 0.15 μg siRNA was added to each well.

Cells were cultured for an additional 24 h before gene expression or inhibition was determined.

Luciferase activity was measured using the Luciferase Assay System kit (Promega, Madison, WI) according to manufacturer's recommendations. Briefly, the cells layers were rinsed with 500 μL of PBS and lysed with 300 μL of Reporer Lysis Buffer 1× (Promega, Madison, WI) supplemented with complete Mini Protease Inhibitor Cocktail (Roche Applied Sciences, Penzberg, Germany). To ensure cell lysis, cells were subjected to a freezing cycle overnight. Then cell lysates were centrifuged at 10,000rpm for 5 min, and 20 μL of supernatant were assayed for luciferase activity using Promega luciferase substrate. Luminescence was recorded on a victor X-3 multilabel plate reader (Perkin Elmer, Waltham, MA). All measurements were performed in duplicate.

For flow cytometry experiments, cells were rinsed, collected and resuspended in phosphate buffer saline (PBS) with 1% (w/v) bovine serum albumin (BSA). The resulting cell suspension was assayed for GFP expression by flow cytometer analysis using a LRS II flow cytometer (Becton Dickinson, Franklin Lakes, NJ). The percentage of GFP positive cells and the mean fluorescence intensity were determined using the flow cytometer program.

For gene silencing experiment, cells were washed after 24 h of incubation, lysed using the NucleoSpin® RNA/Protein assay (Macherey Nagel, Düren, Germany) to purify RNA and quantified with NanoDrop 1000 Spectrophotometer (ThermoFisher Scientific, Waltham, MA). RT-qPCR were then realized in 2 phases. First, reverse transcriptions of RNA in cDNA were conducted using High Capacity cDNA Reverse Transcription Kits (Life technologies) on GeneAmp® PCR System 9700 Thermal Cycler (Life technologies). Then, the expression of laminA/C and HPRT was quantified by Real-time PCR using Taqman® Gene expression assays on StepOnePlus™ Real-Time PCR System (Life technologies). Results were normalized against the expression levels of endogenous HPRT and expressed according to the 2-ΔΔCT formula. Probes used to amplify specific gene products from human or murine cDNA (Life technologies) were Hs00153462_m1 for human laminA/C, Hs99999909_m1 for human HPRT, Mm00497783_m1 for murine laminA/C and Mm00446966_m1 for murine HPRT.

10. In vitro cytotoxicity

For in vitro cytotoxicity experiments, cells were transfected as described above, with lipoplexes containing 0.5 μg of DNA. After 24 h of incubation, the amount of viable cells was assed using Annexin V staining protocol (eBioscience, San Diego, CA). Cells were treated as recommended by the manufacturer and the results were analyzed using a BD™ LRS II flow cytometer (Becton Dickinson).

11. In vivo transfection in animal model

Swiss mice (Elevage Janvier, Le Genest, France) were housed in conventional conditions according to INSERM guidelines. Mice aged 8 weeks were used for experiments. For intramuscular (i.m.) luciferase reporter gene transfection, mice were anesthetized by isoflurane inhalation, then different DNA-hybrid and homogeneous liposomes formulations were injected into both *tibialis anterior* muscles using an Insumed Pic Indolore 30G syringe (Artsana, Grandate, Italy). Two sites were injected per animal, 10 μg DNA doses are given per *tibialis anterior*. After seven days *tibialis anterior* muscles were dissected, and immediately frozen in liquid nitrogen. Luciferase expression was then quantified in muscle extracts using the Luciferase Assay System kit (Promega, Madison, WI), according to the manufacturer's protocol.

12. Statistical analysis

Data were recorded as mean ± standard deviation, which were calculated with the Prism program (GraphPad Software, La Jolla, CA). The significance of differences between groups was assessed using a Mann Whitney test when two groups were compared. A p value less than 0.05 indicated a statistically significant difference.

13. Results

13.1. Synthesis

As stated previously, we used two different cationic lipids with a paromomycin headgroup, a dioleyl hydrophobic backbone and either a N-based or a P-based linker (**CLN** and **CLP**), and two different helper lipids with an imidazole headgroup, a dioleyl hydrophobic backbone and either an N-based or a P-based linker (**HLN** and **HLP**).

CLN (also known as DOSP) [22], **HLN**[30] and **HLP** (also known as MM-27) [31] were prepared using described procedures. The synthetic route for the preparation **CLP** is depicted in Fig. 1. The hydrophobic part *O,O*-dioleylphosphite **2** was prepared by a transesterification-like reaction between *O,O*-diphenylphosphite **1** and oleyl alcohol [32]. For the polar headgroup, the synthesis started with paromomycin sulfate **3**, and after a 3-step sequence previously described involving protecting group manipulations, the adduct **4** was obtained [22]. **2** and **4** then reacted under Atherton-Todd conditions [33] to provide the conjugate **5** with a phosphorous linker between the aminoglycoside and the hydrophobic moieties. Finally, the Teoc protecting groups were removed by treatment of **5** with trifluoroacetic acid to afford **CLP** as its TFA salt.

With these four molecules in hands, we next examined the behavior of the supramolecular assemblies formed by complexing nucleic acids with each of the four different combinations of liposomes: **CLN**:**HLN** (homogeneous "NN" liposomes), **CLP**:**HLP** (homogeneous "PP" liposomes), **CLN**:**HLP** (hybrid "NP" liposomes) and **CLP**:**HLN** (hybrid "PN" liposomes). The various liposome structures are depicted in Fig. 2, where neutral lipids are intercalated between cationic lipids and dioleyl chains interact with each other to form the lipidic membrane, leaving the positive charges of paromomycin at the surface of the liposomes.

13.2. Physicochemical characterization by cryoTEM

Lipoplexes were generated by mixing plasmid DNA with the four liposome combinations and were observed by cryoTEM in NaCl 150 mM media (Fig. 3A–D). With both **CLN**:**HLP** and **CLP**:**HLN** hybrid liposomes, lipoplexes showed heterogeneous assemblies (Fig. 3A and D). These structures appeared as stacks of several lipid layers separated by electron-dense layers likely corresponding to DNA molecules. In these complexes, the DNA appeared to be strongly bound to the lipid membranes. The observations were different with **CLN**:**HLN** and **CLP**:**HLP** homogeneous liposomes, as lipoplexes in these cases appeared as smaller aggregates of short grapes displaying polymorphic structures (Fig. 3B and C). No stacks of layers of lipid and DNA were visible, suggesting that DNA was not fully entrapped between lipidic bilayers. This was confirmed by the observation of few empty liposomes and some free DNA fragments at the vicinity of the liposomes (Fig. 3B, black arrow).

These observations in the regular complexation media NaCl prompted us to further investigate the structure of the liposomes in a more complex media mimicking the extracellular conditions. We anticipated that the differences observed between homogeneous and hybrid liposomes could be amplified in a cell culture medium like DMEM (Dulbecco's Modified Eagle Medium) that is composed of high contents of amino acids and vitamins. We therefore repeated the previous experiment replacing NaCl by DMEM media and observed by cryoTEM the structures of the DNA/liposomes complexes (Figs. 3E-H). Lipoplexes prepared from homogeneous liposomes **CLN**:**HLN** and **CLP**:**HLP** presented a significant difference compared to NaCl and a well-defined onion-like organization with concentric layers of lipids was observed (no DNA was intercalated, Fig. 3F and G). Observation of the external layer revealed that the DNA fragments were located at the surface (black arrows). With hybrid liposomes **CLN**:**HLP** and **CLP**:**HLN** (Fig. 3E and H), the complexes were less affected by the media replacement and complexes with various morphologies were observed, with DNA molecules strongly entrapped inside the lipoplexes.

14. DNA release

Then, we investigated whether the four types of supramolecular assemblies could have different DNA decomplexation properties. After adding small anionic polyphosphates (consisting of 6 phosphate units) to the complexes formed between DNA and the different liposomes, we could determine the decomplexation properties of the different supramolecular assemblies by measuring the ethidium bromide fluorescence.

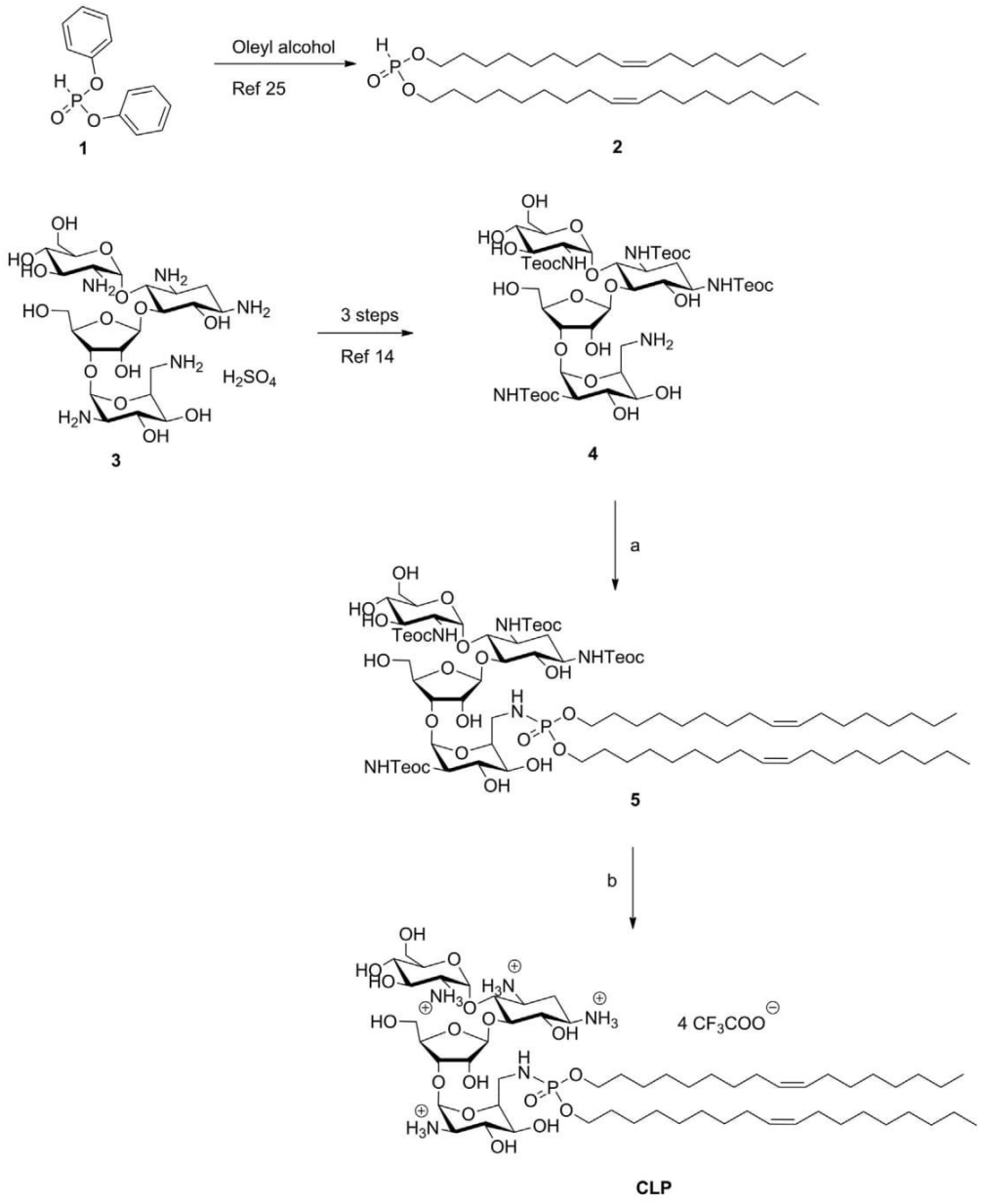


Fig. 1. Synthesis of CLP via the Atherton-Todd reaction. Reagents and conditions: a) 2, DCM, Et_3N, $CBrCl_3$, 75%, b) TFA, DCM, 95%.

The initial state (t = 0 s) showed some differences between homogeneous and hybrid liposomes. Indeed for the hybrid liposomes (**CLN**:**HLP** and **CLP**:**HLN**), the fluorescence was close to 0, indicating that the DNA was fully complexed and not accessible by EtBr, while some fluorescence was already detected for the homogeneous liposomes (**CLP**:**HLP** and **CLN**:**HLN**). This is in good agreement with what was observed in the electron microscopy experiment, as for homogeneous liposomes some DNA fragments were observed as non-complexed and therefore were suitable for EtBr intercalation.

Measuring the kinetics of decomplexation upon polyphosphate addition at a pH 7.1 indicated that depending on the supramolecular assemblies, the decomplexation behaviors were also different. Indeed, in these conditions the two homogenous liposomes **CLN**:**HLN** and **CLP**:**HLP** display the same rapid decomplexation properties and a quick increase in the fluorescence was monitored few seconds after the polyphosphates addition (at t = 45 s, Fig. 4). This indicates that DNA complexes were not robust, since ethidium bromide was able to be intercalated in the base pairs of DNA that were liberated from the complexes after the addition of polyphosphates. By contrast, for DNA complexes with the two hybrid liposomes **CLN**:**HLP** and **CLP**:**HLN**, the fluorescent signal remained stable at a low level even after addition of the polyphosphates, showing that the DNA binding in these supramolecular assemblies was strong enough to resist to these decomplexing conditions.

14.1. In vitro nucleic acids transfection

The transfection efficiency of the different liposomes was then evaluated on three cell lines and in more challenging to transfect primary cells. In order to be able to draw general conclusions on nucleic acid delivery rather than focusing on a specific format, we decided to

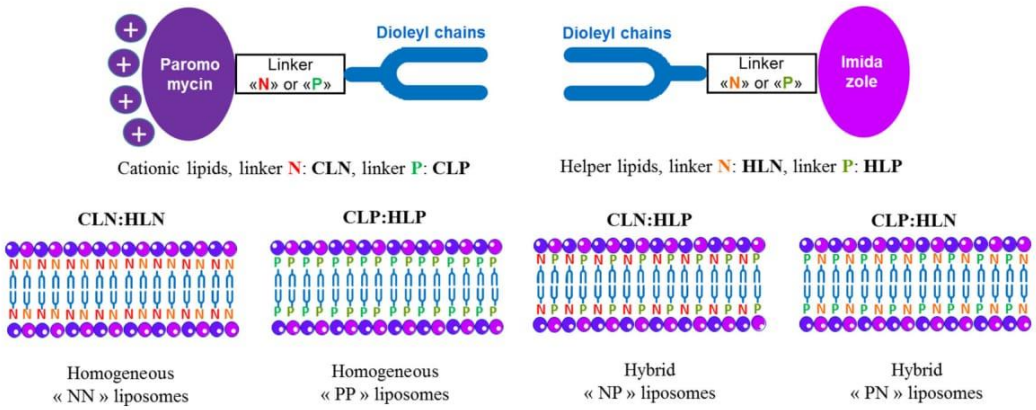


Fig. 2. Schematic representation of the different lipidic supramolecular assemblies.

investigate the delivery potential of the four liposomes with 3 different types of nucleic acids: DNA, mRNA and siRNA.

14.1.1. In vitro delivery of plasmid DNA in different cell types

We first evaluated the transfection potency of the four liposomes formulating a plasmid DNA encoding firefly luciferase in different cell types: HeLa (Fig. 5A), C2C12 (Fig. 5B), mouse embryonic fibroblast (MEF, Fig. 5C), rat aorta muscle cells (Fig. 5D) and human fibroblasts (Fig. 5E). In all tested conditions, cells transfected with hybrid liposomes **CLN**:**HLP** (black bars, left) or **CLP**:**HLN** (black bars, right) showed higher luciferase activity than those transfected with homogenous liposomes **CLN**:**HLN** (grey bars, left) and **CLP**:**HLP** (grey bars, right). These results clearly indicate that the nature of the linker in the helper lipid has a huge impact on the transfection efficiency, since independently of the cationic lipids structure (either **CLN** or **CLP**), statistically significant differences in luciferase expression levels were observed between homogeneous and hybrid liposomes. Taken together, both hybrid liposomes appeared to be efficient transfection systems and displayed comparable transfection potency.

In order to further validate those observations on DNA transfection efficacy, we measured by cell cytometry the percentage of transfected cells using GFP encoding plasmid formulated with the different liposomes, in HeLa (Fig. 6A), C2C12 (Fig. 6B), MEF (Fig. 6C) and rat aorta muscle cells (Fig. 6D). Fig. 6A reveals that HeLa cells showed about 40% of GFP positive cells transfected with the two hybrid liposomes **CLN**:**HLP** and **CLP**:**HLN** compared to approximately 20% GFP expressing cells transfected with the homogeneous liposomes **CLN**:**HLN** and **CLP**:**HLP**. Trends were comparable with the other cell types and the best results for each cell type were always obtained with the hybrid liposomes, with approximately 25% of GFP positive C2C12 and MEF cells and 15% of rat aorta smooth muscle cells expressing GFP with the best conditions. In this set of experiments, no noticeable difference was detected between the two hybrid liposomes.

It should be noted here that these transfection results were obtained in non-optimized conditions, as the objectives of the study rely on understanding the differences between hybrid and homogeneous liposomes, rather than improving the transfection potency of one specific delivery system.

The obtained results in these DNA transfection experiments confirmed our preliminary results [30], indicating that the best combination in a liposomal formulation is seen when the linkers on the cationic and helper lipids are of different natures. In order to go deeper in the analyses of these formulation systems, we decided to investigate if this behavior was specific to DNA or would be applicable also to other types of nucleic acids.

14.1.2. In vitro delivery of mRNA in different cell lines

We then evaluated the transfection efficiency of another class of nucleic acids as we assessed the formulation of the cationic liposomes with mRNA encoding luciferase (Fig. 7). The mRNA transfection was

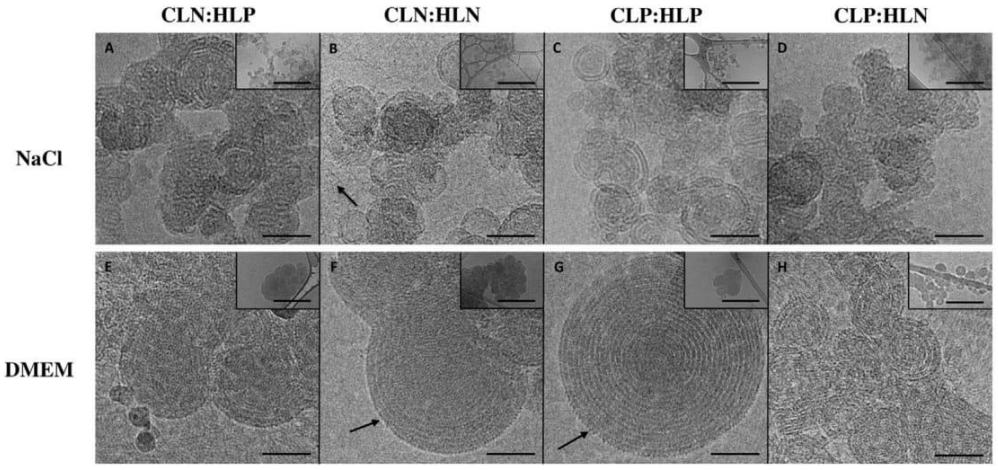


Fig. 3. Cryo-TEM images of cationic liposomes/DNA complexes in NaCl 150 mM (A–D) and in DMEM (E–H). DNA was complexed with liposomes of CLN:HLP (A and E), CLN:HLN (B and F), CLP:HLP (C and G) or CLP:HLN (D and H). Black arrow denote free DNA fragment. Insets: a large field of view of each condition. Scale bars 50 nm (inset 0.5 μm).

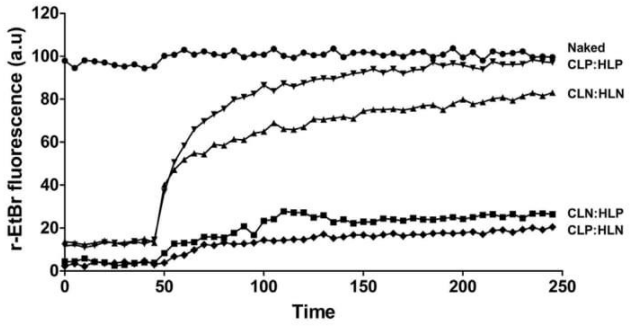


Fig. 4. Modelisation of the DNA release by the liposomes at extracellular pH. The compaction of DNA by cationic lipids was monitored by the exclusion of ethidium bromide (EtBr) molecules from the complexes. 4 μg of EtBr were added to DNA-lipids complexes (2 mL). The residual EtBr fluorescence was assayed using a Jobin-Yvon spex Fluoromax-4 spectrofluorimeter. Complexes CLN:HLN (triangle), CLP:HLP (inversed triangle), CLN:HLP (square) and CLP:HLN (diamond) were obtained by mixing cationic liposomes with 10 μg of plasmid DNA, at pH = 7.1. Naked DNA was used as a control (circle). Solutions were buffered with HEPES buffer 10 mM, NaCl 150 mM (pH 7.1). At t = 45 s, release of DNA from cationic lipids was induced by adding 10 μL of a polyphosphate solution at 4 mg/mL to the complexes.

assessed on different cell lines: HeLa (Fig. 7A), C2C12 (Fig. 7B), MEF (Fig. 7C), rat aorta smooth muscle cells (Fig. 7D) and human fibroblasts (Fig. 7E). The results confirmed the previous observations made for DNA, as for a given cationic lipid **CLN** or **CLP** and independently of the cell types, the best transfections were in all cases obtained for the hybrid liposomes when comparing to the homogenous versions (**CLN**:**HLP** vs **CLN**:**HLN** and **CLP**:**HLN** vs **CLP**:**HLP** respectively). Comparing the relative efficacy of the two hybrid systems, we could observe for the five cell types that the highest luciferase expression was obtained with the **CLP**:**HLN** system.

To better assess the efficacy of the hybrid liposomes for mRNA transfection, we transfected cells with mRNA encoding GFP and observed live cells after 24 h by microscopy (Fig. 8). The results confirmed what was obtained with luciferase mRNA, as the highest transfection was obtained with the hybrid liposome **CLP**:**HLN**. Both hybrid liposomes displayed much higher transfection compared to homogeneous liposomes (compare **CLN**:**HLP** with **CLN**:**HLN** and **CLP**:**HLN** with **CLP**:**HLP**, respectively).

14.1.3. Gene silencing experiments

In order to complete the picture for the compatibility of these delivery systems with different types of nucleic acids, we next performed

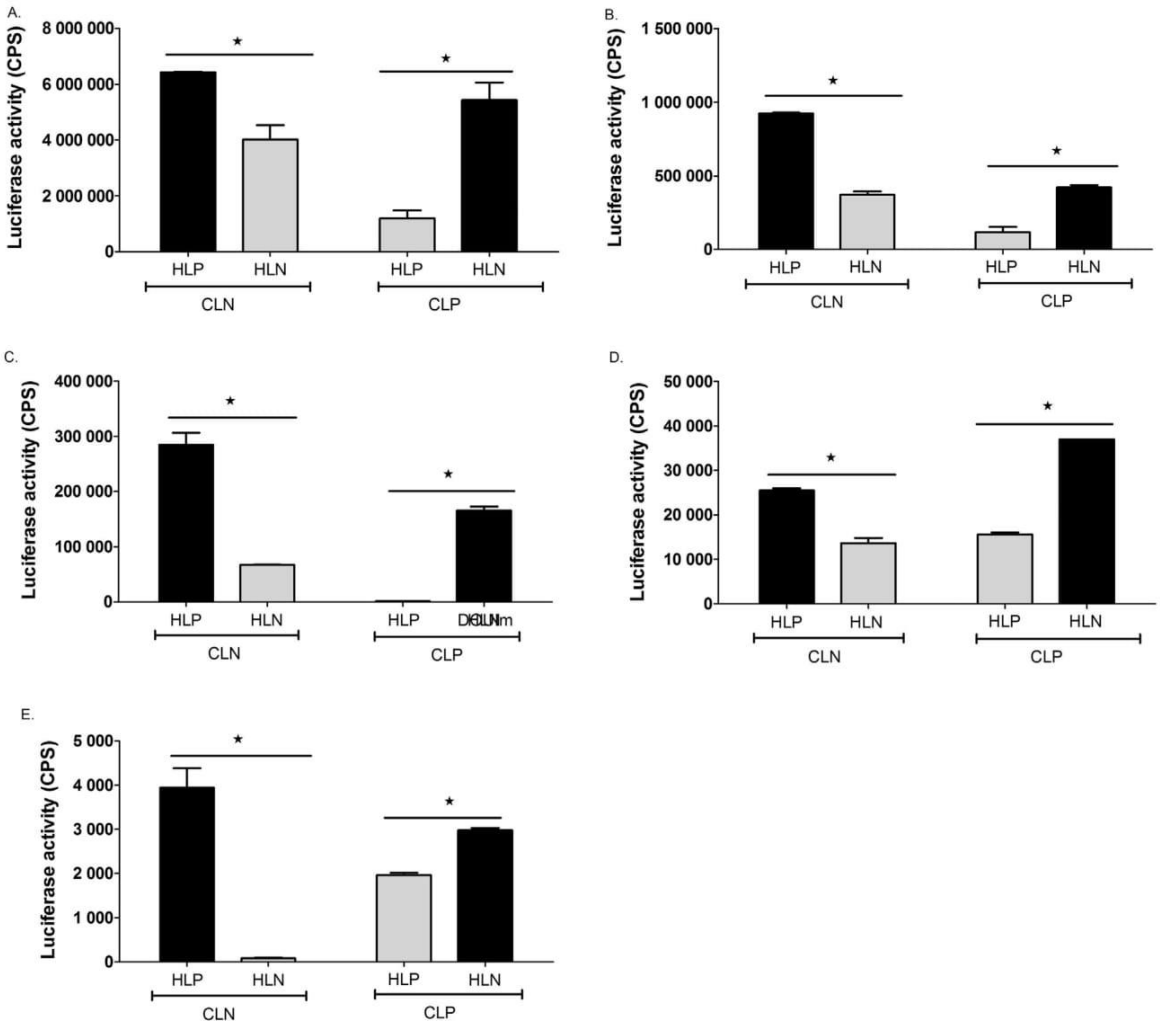


Fig. 5. Plasmid DNA encoding luciferase transfection, in various cell types, in NaCl 150 mM. HeLa cells (A), C2C12 cells (B), MEF cells (C), or rat aorta smooth muscle cells (D), and human fibroblasts (E) were transfected with 0.5 μg of plasmid DNA, encoding luciferase, complexed in NaCl 150 mM with a cationic lipid (CLN or CLP) associated with a helper lipid (HLN or HLP). Plates were incubated 24 h before cells lysis and luciferase activity measurement.

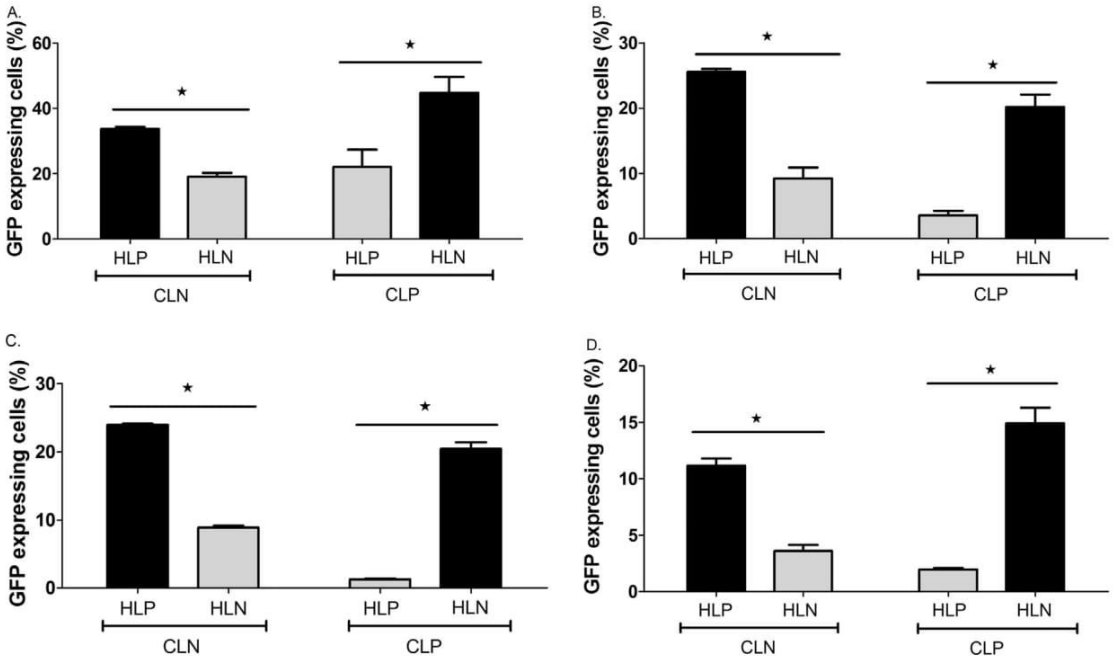


Fig. 6. Percentage of GFP expressing cells after a plasmid DNA transfection, in NaCl 150 mM. HeLa cells (A), C2C12 cells (B), MEF cells (C), or rat aorta smooth muscle cells (D) were transfected with 0.5 μg of plasmid DNA, encoding GFP, complexed in NaCl 150 mM with a cationic lipid (CLN or CLP) associated with a helper lipid (HLN or HLP). Plates were incubated 24 h before FACS analysis.

experiments to determine which liposomal formulation was the most adapted for RNAi experiments. Results in Fig. 9 indicated that after formulation of siRNA with the different liposomes, the best inhibition was in turn obtained with the hybrid versions, with consistently around 50% inhibition for both **CLN**:**HLP** and **CLP**:**HLN** on HeLa and C2C12 cells. For the homogeneous liposomes **CLN**:**HLN** and **CLP**:**HLP**, the inhibition ranged between 20 and 40% for both cell types. Again, the inhibitions observed here were obtained in non-optimized conditions in order to reveal more easily the differences between hybrid and homogeneous liposomes.

14.1.4. Cell viability

The four liposomes were next tested for their toxicity into HeLa cells with the Annexin V staining protocol (Fig. 10). Results showed that the toxicity was very low for the four studied liposomes - homogenous and hybrid - with a cell viability superior to 90% in all conditions.

14.1.5. In vivo transfection efficiency in animal model

In order to strength the results obtained in vitro with different nucleic acids, we performed in vivo experiments in an animal model. Wild type mice were injected intramuscularly with DNA encoding luciferase with hybrid liposomes **CLN**:**HLP** (black bars, left) or **CLP**:**HLN** (black bars) and homogenous liposomes **CLN**:**HLN** (grey bars, left) and **CLP**:**HLP** (grey bars, right). After 7 days, luciferase expression in injected muscles (Fig. 11) was higher with hybrid liposomes compared to homogeneous ones. This result clearly shows that hybrid liposomes have also enhanced transfection capabilities not only in vitro but also in vivo.

15. Discussion

In the present study, the objective was to optimize the nucleic acids synthetic delivery systems and demonstrate the essential role of the liposomal membrane to ensure an efficient transfection process. Our approach relied on supramolecular tuning of the liposomes formed by association of a cationic lipid with a helper lipid. In this purpose, we have synthesized two cationic lipids with a paromomycin headgroup, a dioleyl hydrophobic moiety and either an N-based or a P-based linker (**CLN** and **CLP**, respectively) and two neutral lipids with an imidazole headgroup, a dioleyl hydrophobic moiety and either an N-based or a P-based linker (**HLN** and **HLP**, respectively). Association of the cationic and helper lipids led to two homogeneous (**CLN**:**HLN** and **CLP**:**HLP**) or two hybrid (**CLN**:**HLP** and **CLP**:**HLN**) liposomes.

The results of the cryoTEM experiments and the decomplexation studies provided interesting data on the structural differences between homogeneous and hybrid assemblies. We observed that coordinating or not the nature of the linkers in the cationic and helper lipids had a great impact on the structure of the lipoplexes and on the DNA binding. For complexes where weak bonds between the cationic liposomes and the DNA were observed (homogenous liposomes), we demonstrated that the complexation media has a huge influence on the structure. The liposomes assembled themselves in concentric layers in DMEM media, as they will probably do in the absence of DNA. This indicated that the architecture of the complexes was dictated by the external environment. The situation was very different with hybrid liposomes: as the DNA was strongly bound to the complexes, the complexation media only had a limited impact. In this case, the driving force of the complex architecture was directly related to the binding force between cationic liposomes and DNA molecules.

Regarding the relative stability of the DNA molecules inside the complexes, the observations made were somewhat surprising. Indeed, the DNA binding was stronger in the case of hybrid liposomes compared to homogeneous systems. This somewhat contradicts the dogma that well organized architectures are preferred to induce higher stability of DNA complexes. These results can however be rationalized. Indeed, the main property that confers DNA stability relies on electrostatic interactions between the positively charged headgroup of the cationic lipid and the negatively charged phosphate moieties of the DNA molecules. When the cationic lipids are part of highly organized membranes (NN or PP liposomes), their polar headgroup is “frozen” in the structure and therefore possess a reduced degree of mobility to interact with DNA. On the other hand, membranes of NP or PN liposomes present

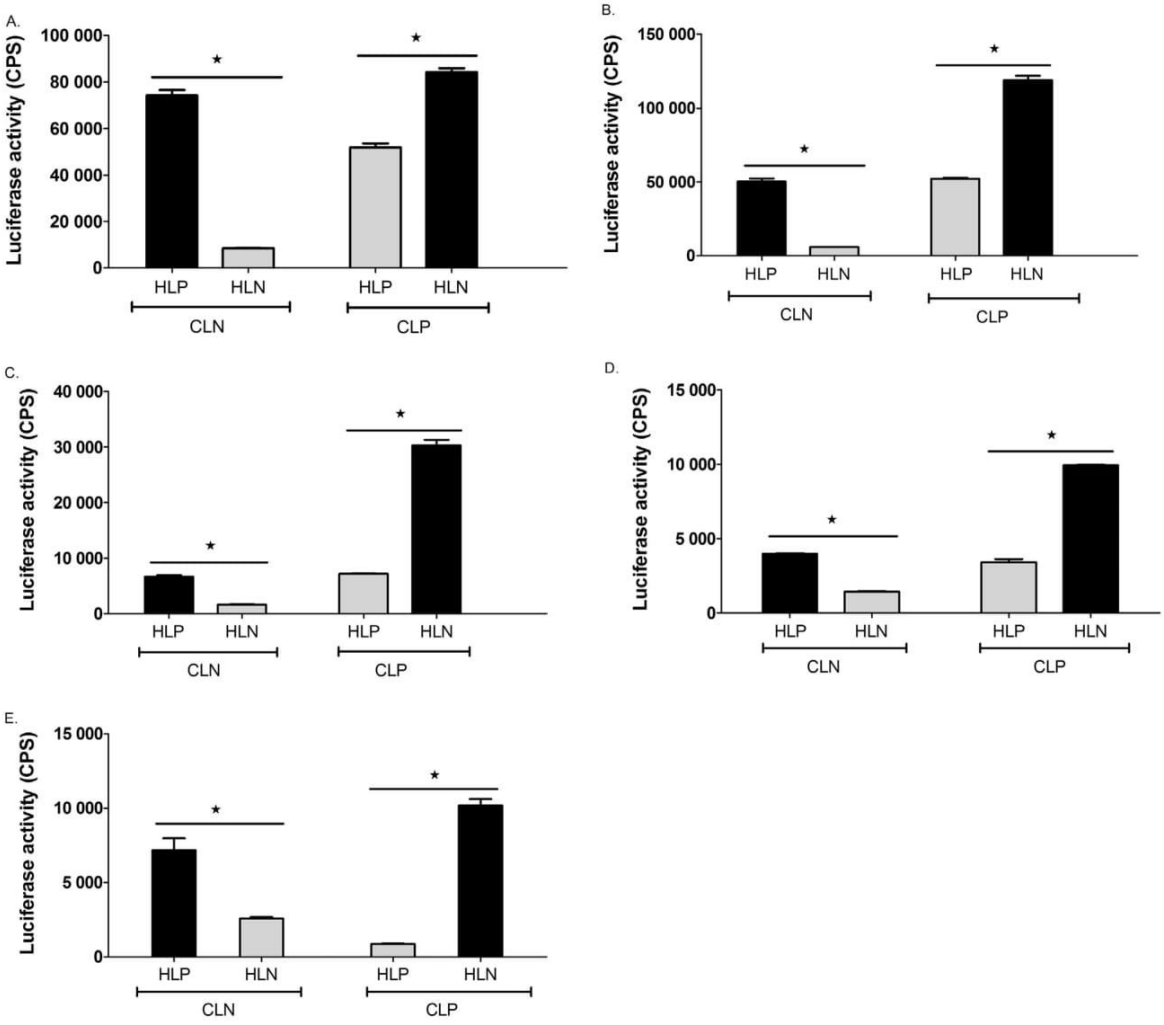


Fig. 7. mRNA transfection on HeLa, C2C12, MEF, or primary cells in NaCl 150 mM. HeLa cells (A), C2C12 cells (B), MEF cells (C), or rat aorta smooth muscle cells (D), and human fibroblasts (E), were transfected with 0,5 μg of mRNA, encoding luciferase, complexed in NaCl 150 mM with a lipid (CLN or CLP) associated with a helper lipid (HLN or HLP). Plates were incubated 24 h before cells lysis and luciferase activity measurement.

defects at the membrane level that allow for an improved flexibility of the cationic headgroups that in turn can lead to a better charge matching with DNA. The differences in DNA interactions are probably at the origin of the observations made in the cryoTEM and polyphosphates experiments, as the hybrid complexes **CLN**:**HLP** and **CLP**:**HLN** clearly appeared more adapted for improved DNA binding than homogeneous complexes **CLN**:**HLN** and **CLP**:**HLP**.

The structural differences between homogeneous and hybrid lipoplexes observed by cryoTEM in DMEM media indicated a crucial difference at the lipoplex surface. Indeed, the onion-like organization obtained with **CLN**:**HLN** and **CLP**:**HLP** homogeneous liposomes clearly showed an external corona with negatively charged DNA molecules. This is most likely detrimental for good interactions with cellular membranes that are composed of negatively charged molecules like proteins or proteoglycans. The structure itself of these assemblies thus appeared to be non-optimal for an efficient cellular entry. In addition, the DNA located in the external coating of the homogeneous assemblies is in direct contact with the surrounding environment and is therefore prone to degradation. As a result, a reduced number of DNA molecules may still be effective to enter the cells.

Opposite observations were made with hybrid systems, as all the DNA molecules were strongly bound to cationic liposomes and entrapped inside the complexes. The external membrane layer of these complexes was therefore composed of cationic and helper lipids, which represent molecules well adapted to interact with the membrane components. It was therefore anticipated that the structure of hybrid liposomes was more suitable for cell internalization.

These observations were directly translated in the in vitro transfection experiments, as in all tested conditions hybrid liposomes provided significantly higher transfection than the homogeneous versions, independently of the nucleic acid type (DNA, mRNA and siRNA), the cell type (HeLa, C2C12, MEF, rat aorta muscle cells and human fibroblasts) or the encoded protein (luciferase and GFP).

In the case of DNA, on average both hybrid liposomes **CLN**:**HLP** and **CLP**:**HLN** displayed comparable transfection. For mRNA, the trend was in favor of **CLP**:**HLN** for a better transfection, indicating that this liposome may provide a spatial orientation more favorable for single stranded mRNA than **CLN**:**HLP**.

It is known that the structure of the cationic lipids or liposomes can have an impact in the different steps of the transfection process. In particular, our team previously demonstrated that the endosomal escape was highly dependent on the nature of the cationic lipids [14]. The mechanism of lipid-mixing relies on the interactions between the positively charged headgroups of the cationic lipids and the anionic

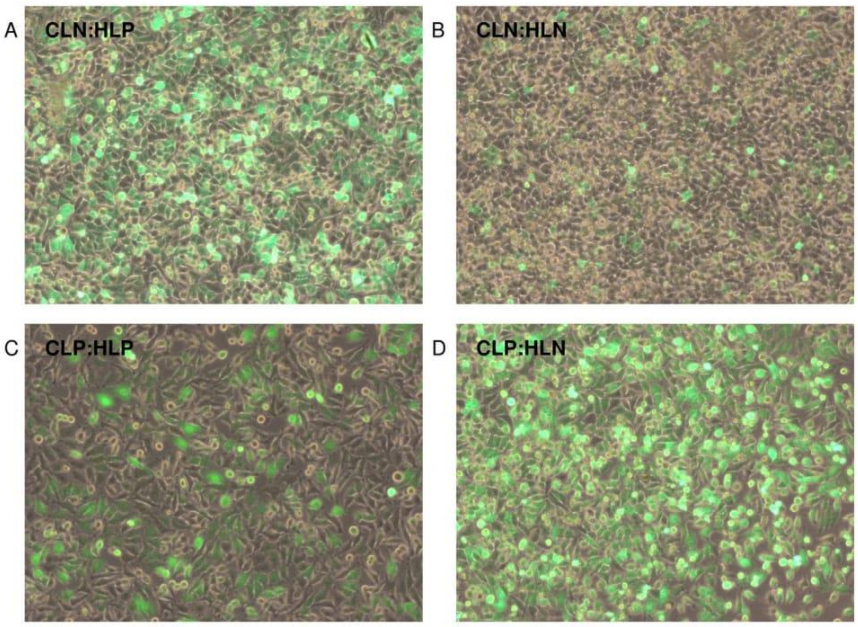


Fig. 8. eGFP mRNA transfection on HeLa cells. HeLa cells were transfected with 0.5 μg of mRNA, encoding eGFP, complexed in NaCl 150 mM with a liposomes CLN:HLP (A), CLN:HLN (B), CLP:HLP (C) or CLP:HLN (D). Plates were incubated 24 h before cells observation.

phospholipids of the endosomal membrane [13,34]. Indeed these interactions lead to the formation of new neutral multilamellar lipidic structures causing the disruption of the endosomal membrane and the release of the nucleic acids in the cytosol. In our case, the different combinations **CLN**:**HLN**, **CLP**:**HLP**, **CLN**:**HLP** and **CLP**:**HLN** were all prepared from the same aminoglycoside paromomycin and therefore most likely induced a similar endosomal escape mechanism. Moreover, we have clearly demonstrated that the superiority of hybrid systems was observed for different types of nucleic acids having different "final destination" (cytosol for mRNA and siRNA, nucleus for DNA). The differences of transfection observed between homogenous and hybrid systems therefore probably do not arise from different behaviors in the intracellular compartment. Moreover, the cytotoxicity assay performed demonstrated similar cell viability for the 4 combinations tested, attesting that the improved transfection ability of hybrid liposomes was not related to a difference in toxicity.

We strongly believe that the cationic liposomes/nucleic acids interactions in the extracellular environment are the key aspects to consider. As it was demonstrated in the cryoTEM and the polyphosphates experiments, the hybrid supramolecular assemblies appeared to be well-suited for protecting the nucleic acid molecules through a strong binding to the cationic liposomes. The morphology of the hybrid liposomal membranes themselves allows for improved electrostatic interactions with DNA - and probably with mRNA and siRNA as well - that induces better internalization and thus better transfection. This was confirmed by GFP experiments, as we observed that the percentage of transfected cells is reduced with homogeneous liposomes compared to hybrid liposomes.

The well-known and widely used first generation Lipofectamine™ relies on such a hybrid system with a cationic lipid DOSPA (containing a N-based linker) and a helper lipid DOPE (P-based linker) [35]. Moreover, the efficacy of hybrid liposomes has recently reached an unprecedented point as lipoplexes consisting of DOTMA:DOPE formulated mRNA were recently assessed in a phase I clinical trial for the treatment of melanoma [36]. Intravenous administration of formulated mRNA was able to activate dendritic cells in various lymphoid tissues and therefore this strategy was seen as a potential technological platform for the treatment of various types of cancers. These two hybrid supramolecular

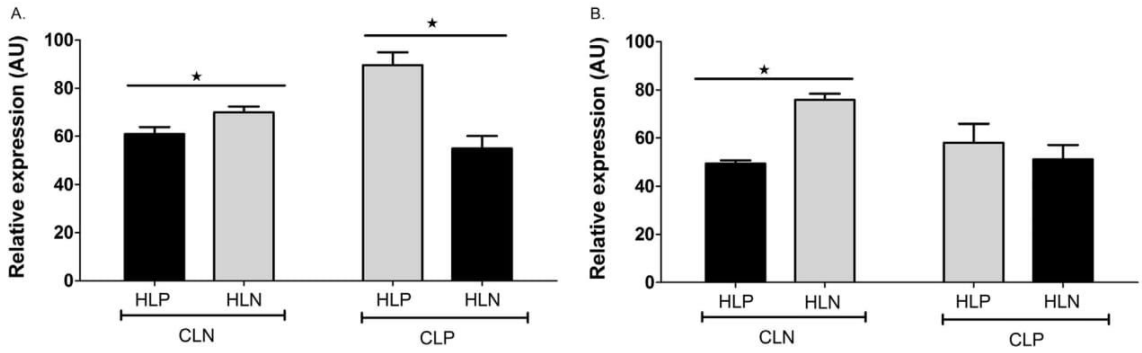


Fig. 9. Inhibition of LaminA/C expression. HeLa cells (A) or C2C12 cells (B) were transfected with 150 ng of LaminA/C iRNA, complexed with each liposomes in NaCl 150 mM. The gene expression levels of LaminA/C were measured by qPCR analysis, normalized against the expression levels of HPRT (housekeeping gene). The results are expressed as the 2-ΔΔCT formula. Bars represent mean values ± SEM for two independent experiments in duplicate.

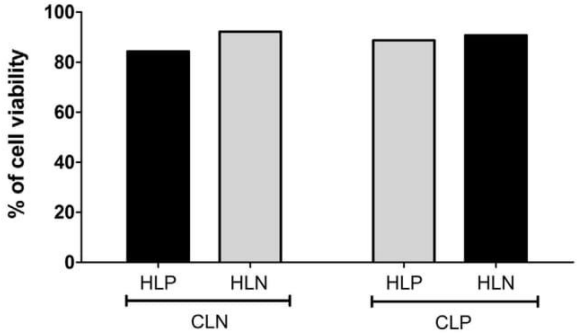


Fig. 10. Percentage of HeLa cells survival. HeLa cells were transfected with 0.5 μg of plasmid DNA, complexed with a cationic lipid (CLN or CLP) associated with a helper lipid (HLN or HLP). Plates were incubated 24 h before cytotoxicity measurement. Percentage of cells survival was determined using eBioscience® Annexin V staining protocol.

assemblies have been used for many years, but mismatching the linkers of the two molecules constituting the liposomes was probably not seen as a key point.

To conclude, our results suggest that the organization of the lipidic bilayer in the lipoplexes is crucial to provide efficient delivery of nucleic acids in vitro and in vivo, by influencing the binding strength between the nucleic acids and the delivery system. Here we shed the light on a new parameter of the lipidic bilayer at a supramolecular level, which is a criterion that now needs to be taken into consideration to obtain good interactions between the delivery vehicle and the nucleic acid to be transported in extracellular conditions, leading to improved transfection efficiency.

Aknowledgements

The authors are very grateful to Delphine Béziau, Virgine Forest, Stéphanie Lemarchand-Mindé and Martine Le Cunff for her technical assistance. This work was supported by special grants from the "Association Française contre les Myopathies" (Evry, France) and from BPIFrance financement (Paris, France) for Emerit and Hepavac. We are also indebted to P. Lehn and J.-M. Lehn for their pioneer works related to the synthesis of cationic lipids used in this study and for their stimulating discussions and constant interest in this work.

This work was realized in the context of the IHU-Cesti project which received French government financial support managed by the National Research Agency via the "Investment Into The Future" program ANR-10-IBHU-005. The IHU-Cesti project is also supported by Nantes Metropole and the Pays de la Loire Region. Laurence Dallet and Thibault Colombani are supported by funds from IHU-Cesti (Investissement d'Avenir ANR-10-IBHU-005, region Pays de la Loire et Nantes Métropole).

The author report that no competing financial interests or conflicts of interest exist.

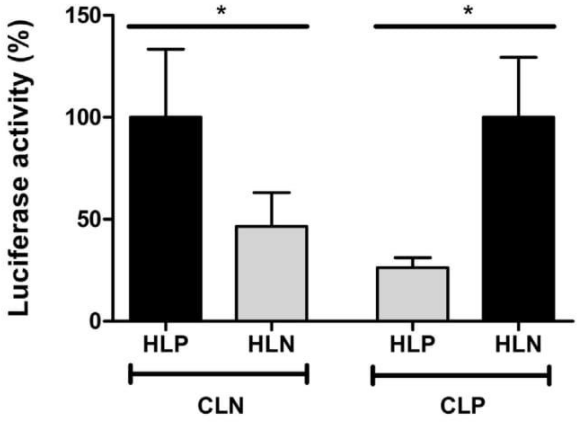


Fig. 11. In vivo transfection efficiency. Swiss mice were injected intramuscularly with 10 μg of plasmid DNA, encoding luciferase, complexed with liposomes consisting of cationic lipids (CLN or CLP) combined with helper lipids (HLN or HLP). Luciferase expression was determined in crushed muscle 7 days after injection. Bars represent the mean of at least 6 individual muscles and the error bar the SEM.

References

[1] M.A. Mintzer, E.E. Simanek, Nonviral vectors for gene delivery, Chem. Rev. 109 (2) (2009) 259–302.
[2] H. Yin, R.L. Kanasty, A.A. Eltoukhy, A.J. Vegas, J.R. Dorkin, D.G. Anderson, Non-viral vectors for gene-based therapy, Nat. Rev. Genet. 15 (8) (2014) 541–555.
[3] B. Draghici, M.A. Ilies, Synthetic nucleic acid delivery systems: present and perspectives, J. Med. Chem. 58 (10) (2015) 4091–4130.
[4] D. Zhi, S. Zhang, S. Cui, Y. Zhao, Y. Wang, D. Zhao, The headgroup evolution of cationic lipids for Gene delivery, Bioconjug. Chem. 24 (4) (2013) 487–519.
[5] D. Zhi, S. Zhang, B. Wang, Y. Zhao, B. Yang, S. Yu, Transfection efficiency of cationic lipids with different hydrophobic domains in gene delivery, Bioconjug. Chem. 21 (4) (2010) 563–577.
[6] K.H. Bleicher, H.-J. Böhm, K. Müller, A.I. Alanine, Hit and lead generation: beyond high-throughput screening, Nat. Rev. Drug Discov. 2 (5) (2003) 369–378.
[7] G.M. Keseru, G.M. Makara, Hit discovery and hit-to-lead approaches, Drug Discov. Today 11 (15–16) (2006) 741–748.
[8] P.L. Felgner, T.R. Gadek, M. Holm, R. Roman, H.W. Chan, M. Wenz, J.P. Northrop, G.M. Ringold, M. Danielsen, Lipofection: a highly efficient, lipid-mediated DNA-transfection procedure, Proc. Natl. Acad. Sci. U. S. A. 84 (21) (1987) 7413–7417.
[9] N. Dan, D. Danino, Structure and kinetics of lipid-nucleic acid complexes, Adv. Colloid Interf. Sci. 205 (2014) 230–239.
[10] I.A. Khalil, K. Kogure, H. Akita, H. Harashima, Uptake pathways and subsequent intracellular trafficking in nonviral gene delivery, Pharmacol. Rev. 58 (1) (2006) 32–45.
[11] J. Rejman, M. Conese, D. Hoekstra, Gene transfer by means of lipo- and polyplexes: role of clathrin and caveolae-mediated endocytosis, J. Liposome Res. 16 (3) (2006) 237–247.
[12] A.K. Varkouhi, M. Scholte, G. Storm, H.J. Haisma, Endosomal escape pathways for delivery of biologicals, J. Control. Release Off. J. Control. Release Soc. 151 (3) (2011) 220–228.
[13] Y. Xu, F.C. Szoka, Mechanism of DNA release from cationic liposome/DNA complexes used in cell transfection, Biochemistry (Mosc) 35 (18) (1996) 5616–5623.
[14] O. Le Bihan, R. Chèvre, S. Mornet, B. Garnier, B. Pitard, O. Lambert, Probing the in vitro mechanism of action of cationic lipid/DNA lipoplexes at a nanometric scale, Nucleic Acids Res. 39 (4) (2011) 1595–1609.
[15] T. Constantinou-Kokotou, G. Karikas, G. Kokotos, Study of aminoglycoside-nucleic acid interactions by an HPLC method, Bioorg. Med. Chem. Lett. 11 (8) (2001) 1015–1018.
[16] D.P. Arya, R.L. Coffee, B. Willis, A.I. Abramovitch, Aminoglycoside-nucleic acid interactions: remarkable stabilization of DNA and RNA triple helices by neomycin, J. Am. Chem. Soc. 123 (23) (2001) 5385–5395.
[17] K. Rege, S. Hu, J.A. Moore, J.S. Dordick, S.M. Cramer, Chemoenzymatic synthesis and high-throughput screening of an aminoglycoside-polyamine library: identification of high-affinity displacers and DNA-binding ligands, J. Am. Chem. Soc. 126 (39) (2004) 12306–12315.
[18] K. Rege, A. Ladiwala, S. Hu, C.M. Breneman, J.S. Dordick, S.M. Cramer, Investigation of DNA-binding properties of an aminoglycoside-polyamine library using quantitative structure-activity relationship (QSAR) models, J. Chem. Inf. Model. 45 (6) (2005) 1854–1863.
[19] M. Hendrix, E.S. Priestley, G.F. Joyce, C.H. Wong, Direct observation of aminoglycoside-RNA interactions by surface plasmon resonance, J. Am. Chem. Soc. 119 (16) (1997) 3641–3648.
[20] L. Frolov, A. Dix, Y. Tor, A.B. Tesler, Y. Chaikin, A. Vaskevich, I. Rubinstein, Direct observation of aminoglycoside-RNA binding by localized surface plasmon resonance spectroscopy, Anal. Chem. 85 (4) (2013) 2200–2207.
[21] M. Sainlos, M. Hauchecorne, N. Oudrhiri, S. Zertal-Zidani, A. Aissaoui, J.-P. Vigneron, J.-M. Lehn, P. Lehn, Kanamycin A-derived cationic lipids as vectors for gene transfection, Chembiochem Eur. J. Chem. Biol. 6 (6) (2005) 1023–1033.
[22] M. Mével, M. Sainlos, B. Chatin, N. Oudrhiri, M. Hauchecorne, O. Lambert, J.-P. Vigneron, P. Lehn, B. Pitard, J.-M. Lehn, Paromomycin and neomycin B derived cationic lipids: synthesis and transfection studies, J. Control. Release Off. J. Control. Release Soc. 158 (3) (2012) 461–469.
[23] L. Desigaux, M. Sainlos, O. Lambert, R. Chevre, E. Letrou-Bonneval, J.-P. Vigneron, P. Lehn, J.-M. Lehn, B. Pitard, Self-assembled lamellar complexes of siRNA with lipidic aminoglycoside derivatives promote efficient siRNA delivery and interference, Proc. Natl. Acad. Sci. U. S. A. 104 (42) (2007) 16534–16539.
[24] D. Habrant, P. Peuziat, T. Colombani, L. Dallet, J. Gehin, E. Goudeau, B. Evrard, O. Lambert, T. Haudebourg, B. Pitard, Design of ionizable lipids to overcome the limiting step of endosomal escape: application in the intracellular delivery of mRNA, DNA, and siRNA, J. Med. Chem. 59 (7) (2016) 3046–3062.
[25] H. Farhood, N. Serbina, L. Huang, The role of dioleoyl phosphatidylethanolamine in cationic liposome mediated gene transfer, Biochim. Biophys. Acta 1235 (2) (1995) 289–295.

[26] P. Midoux, C. Pichon, J.-J. Yaouanc, P.-A. Jaffrès, Chemical vectors for gene delivery: a current review on polymers, peptides and lipids containing histidine or imidazole as nucleic acids carriers, Br. J. Pharmacol. 157 (2) (2009) 166–178.
[27] B. Pitard, Supramolecular assemblies of DNA delivery systems, Somat. Cell Mol. Genet. 27 (1–6) (2002) 5–15.
[28] B. Pitard, O. Aguerre, M. Airiau, A.M. Lachagès, T. Boukhnikachvili, G. Byk, C. Dubertret, C. Herviou, D. Scherman, J.F. Mayaux, et al., Virus-sized self-assembling lamellar complexes between plasmid DNA and cationic micelles promote gene transfer, Proc. Natl. Acad. Sci. U. S. A. 94 (26) (1997) 14412–14417.
[29] B. Pitard, N. Oudrhiri, J.P. Vigneron, M. Hauchecorne, O. Aguerre, R. Toury, M. Airiau, R. Ramasawmy, D. Scherman, J. Crouzet, et al., Structural characteristics of supramolecular assemblies formed by guanidinium-cholesterol reagents for gene transfection, Proc. Natl. Acad. Sci. U. S. A. 96 (6) (1999) 2621–2626.
[30] M. Mével, T. Haudebourg, T. Colombani, P. Peuziat, L. Dallet, B. Chatin, O. Lambert, M. Berchel, T. Montier, P.-A. Jaffrès, et al., Important role of phosphoramido linkage in imidazole-based dioleyl helper lipids for liposome stability and primary cell transfection, J. Gene Med. 18 (1–3) (2016) 3–15.
[31] M. Mével, C. Neveu, C. Gonçalves, J.-J. Yaouanc, C. Pichon, P.-A. Jaffrès, P. Midoux, Novel neutral imidazole-lipophosphoramides for transfection assays, Chem. Commun. (Camb) 27 (2008) 3124–3126.
[32] M. Mével, T. Montier, F. Lamarche, P. Delépine, T. Le Gall, J.-J. Yaouanc, P.-A. Jaffrès, D. Cartier, P. Lehn, J.-C. Clément, Dicationic lipophosphoramidates as DNA carriers, Bioconjug. Chem. 18 (5) (2007) 1604–1611.
[33] S.S. Le Corre, M. Berchel, H. Couthon-Gourvès, J.-P. Haelters, P.-A. Jaffrès, Atherton-Todd reaction: mechanism, scope and applications, Beilstein J. Org. Chem. 10 (2014) 1166–1196.
[34] I.M. Hafez, N. Maurer, P.R. Cullis, On the mechanism whereby cationic lipids promote intracellular delivery of polynucleic acids, Gene Ther. 8 (15) (2001) 1188–1196.
[35] B. Dalby, S. Cates, A. Harris, E.C. Ohki, M.L. Tilkins, P.J. Price, V.C. Ciccarone, Advanced transfection with lipofectamine 2000 reagent: primary neurons, siRNA, and high-throughput applications, Methods 33 (2) (2004) 95–103.
[36] L.M. Kranz, M. Diken, H. Haas, S. Kreiter, C. Loquai, K.C. Reuter, M. Meng, D. Fritz, F. Vascotto, H. Hefesha, et al., Systemic RNA delivery to dendritic cells exploits antiviral defence for cancer immunotherapy, Nature 534 (7607) (2016) 396–401.

CONCLUSION ET PERSPECIVES

Conclusion et Perspectives

Que ce soit dans le cadre de la thérapie génique ou bien de l'immunothérapie, la compréhension des propriétés immunostimulatrices des vecteurs et des molécules qu'ils transportent revêt un intérêt crucial afin (i) de ne pas engendrer d'effets indésirables, ainsi que (ii) pour le développement de molécules adaptées à chaque application. De plus, l'amélioration de la délivrance des acides nucléiques représente également un facteur clé dans l'optimisation de ces différentes biothérapies.

Au cours de ce travail de thèse, nous avons orienté nos travaux sur l'étude de 2 catégories de vecteurs synthétiques : les copolymères à blocs amphiphiles et les lipides cationiques, afin de déterminer les mécanismes leur permettant de stimuler efficacement la réponse immunitaire. De plus, nous nous sommes intéressés à l'optimisation de l'assemblage supramoléculaire des lipoplexes dans l'optique de développer un vecteur universel pour les différentes classes d'acides nucléiques au sein de différentes populations cellulaires.

Compréhension des mécanismes immunologiques du 704 en vue d'un développement préclinique chez l'homme.

Déjà validé au cours d'un protocole immunothérapie dans un modèle d'hépatocarcinome murin (actuellement en développement préclinique), nous avons pu confirmer l'efficacité de la vaccination à ADN médiée par le 704 dans le contexte du VIH, notamment en permettant la production spécifique d'anticorps dirigés contre des protéines d'enveloppe (gp120). De plus et de manière cohérente, ce travail a mis en évidence que la formulation d'ADN au 704 permettait d'induire la sécrétion de nombreuses cytokines pro-inflammatoires de type TH2, favorable à l'induction d'une forte réponse immunitaire à médiation humorale.

Au cours de cette étude, nous avons également pu démontrer l'importance cruciale de l'expression de l'antigène d'intérêt dans les fibres musculaires striées squelettiques afin d'engendrer une forte production d'anticorps spécifiques, tout en écartant une quelconque implication de l'expression du plasmide par les cellules dendritiques. Cela suggère fortement l'implication d'autres cellules et/ou mécanismes immunitaires dans l'induction d'une réponse protectrice par le 704. Ainsi, des expériences complémentaires sont nécessaires afin de déterminer les cellules immunitaires impliquées dans la mise en place de la réponse immunitaire suite à l'injection d'une formulation vaccinale à base de 704, en observant les différentes cellules recrutées au niveau du site d'injection, mais également en déterminant si le 704 ne permet pas de transfecter d'autres cellules notamment au niveau des ganglions lymphatiques.

Plusieurs expériences ont par ailleurs permis de mettre en évidence l'implication de différents PRRs sur l'induction de la réponse immunitaire innée puis adaptative par les vaccins à acides nucléiques médiés par le 704. Tout d'abord, l'utilisation d'ARN à la place d'ADN a échoué tant sur la production d'une réponse à médiation humorale efficace que sur l'induction de la sécrétion de cytokines pro-inflammatoires, suggérant dès lors le rôle clé des senseurs à ADN dans la stimulation de la réponse immunitaire. Ces résultats ont par ailleurs été confirmés par l'ajout d'un ADN non-codant à la

formulation vaccinale, réduisant d'un facteur 10 la quantité d'ADN codant nécessaire à l'induction de la même production d'anticorps spécifiques. Puis, par l'intermédiaire de souris déficientes pour les protéines adaptatrices MyD88 et STING, nous avons pu mettre en évidence l'implication à parts égales des cascades de signalisation induites par la reconnaissance de motifs CpG ou d'ADNdb intracytoplasmique dans la réponse immunitaire générée par les vaccins à ADN médiés par le 704. Nous avons pu confirmer ces résultats en observant l'effet bénéfique de l'ajout de motifs CpG sur les plasmides délivrés par le 704, tant sur la production de cytokines pro-inflammatoires que sur l'induction d'une forte réponse immunitaire à médiation humorale. Enfin, nous avons également pu mettre en évidence l'importance du mécanisme de délivrance direct de l'ADN dans le cytoplasme par le 704, en démontrant que l'ajout d'agonistes des TLR9 (des senseurs à ADN intra-endosomaux) n'induit aucun bénéfice sur l'effet vaccinal, que l'absence d'endocytose chez les souris Tmem176b-/- n'impactait ni l'expression de l'antigène ni l'induction d'une réponse immunitaire à médiation humorale efficace, et enfin que la surexpression de DHX9 et 36 (des senseurs à ADN intracytoplasmiques) permet d'améliorer l'efficacité de la réponse immunitaire.

Dès lors, il apparaît que le mécanisme essentiel impliqué dans l'efficacité des vaccins à ADN formulés avec le 704 repose sur la stimulation efficace des différents senseurs à ADN intracytoplasmiques. Néanmoins, même si nous avons identifié l'intérêt de cibler DHX9 et 36, il nous faut encore identifier les récepteurs impliqués dans la cascade de stimulation dépendante de la protéine adaptatrice STING. Cela pourra nous permettre dans le futur d'optimiser davantage les propriétés adjuvantes des plasmides, mais également de nous ouvrir de nouveaux champs des possibles dans l'amélioration des formulations vaccinales notamment en y ajoutant des d'acides nucléiques codant pour différents senseurs à ADN afin d'améliorer la reconnaissance de l'ADN une fois présent dans le cytoplasme et ainsi induire une réponse immunitaire plus efficace.

Stimulation de la réponse immuntaire par les lipides cationiques dérivés d'aminoglycosides

Initialement développés au cours de programmes d'optimisations structurales destinés à l'amélioration de la transfection d'acides nucléiques et de protéines recombinantes au sein de différentes populations cellulaires, les lipoaminoglycosides se sont avérés être des molécules douées de propriétés immunostimulatrices capables d'induire l'expression de protéines clefs dans la réponse immunitaire innée, de manière dépendante de leur concentration et de la durée de leur utilisation.

Par le biais d'une étude structure-activité, nous avons déterminé des critères structuraux nécessaires à la stimulation de la réponse immunitaire par ces dérivés lipidiques d'aminoglycosides. Cela a permis de mettre en évidence l'importance de l'intégralité de leur structure sur leurs propriétés adjuvantes, ainsi que de proposer une structure type des lipoaminoglycosides immunostimulants : une tête polaire aminoglycoside appartenant à la famille des anneaux 4,6-disubstituées 2-deoxystreptamine, (ii) un espaceur court de type succinyl, et (iii) un long segment hydrophobe insaturé de type dioleyl. Néanmoins, de nombreuses autres modifications structurales sont encore envisageables, et poursuivre une étude structure-activité complémentaire afin d'étudier l'influence d'autres têtes polaires aminoglycosides de

familles différentes (comme la ribostamycine) ou bien l'impact de segments hydrophobes plus long ou comportant davantage d'insaturations, pourrait permettre à l'avenir d'améliorer encore les propriétés adjuvantes de ces molécules. De même, étudier l'effet de l'ajout de co-lipides aux lipoaminoglycosides pourrait s'avérer prometteur pour améliorer leur effet immunostimulateur. Cela a notamment déjà été décrit avec l'ajout de DOPE à certains liposomes cationiques. Contrairement à ce qui a été précédemment proposé dans la littérature, nous n'avons ni pu mettre en évidence une influence du nombre de charges positives sur la stimulation de la réponse immunitaire, ni pu confirmer l'effet immunostimulateur des chaines alkyles C14 saturées (suggérées comme étant parmi les segments hydrophobes les plus immunostimulateurs). Dès lors, cela laisse supposer que la reconnaissance des lipoaminoglycosides se fait par l'intermédiaire de récepteurs spécifiques, pouvant reconnaître les têtes polaires et/ou les segments hydrophobes de ces molécules.

Par la suite, plusieurs résultats nous ont permis de déterminer les différents mécanismes et voies de signalisation mise en jeux lors de la stimulation de la réponse immunitaire par les lipoaminoglycosides. Premièrement, l'internalisation de ces dérivés lipidiques est apparue comme une étape importante au vu de l'absence de stimulation cellulaire engendrée par les têtes polaires seules. De plus, cette internalisation c'est avérée être majoritairement dépendante de l'endocytose cavéole-dépendante, même si nous n'avons pas pu exclure l'implication mineure des autres mécanismes de la pinocytose. Deuxièmement, nous avons également souligné l'absence d'implication du TLR2 et TLR4 (récepteurs classiquement impliqués dans la reconnaissance de dérivés lipidiques) dans la stimulation cellulaire engendrée par les lipoaminoglycosides. En revanche nous avons pu mettre en évidence le rôle central de la PLC, probablement par l'intermédiaire d'une interaction directe avec ces lipides cationiques. Cela est d'ailleurs cohérent avec les études précédentes décrivant les aminoglycosides comme des activateurs allostériques de cette enzyme. Néanmoins, il pourrait être intéressant d'investiguer dans une prochaine étude si les intégrines ou le CD14 peuvent également être impliqués dans la reconnaissance des lipoaminoglycosides, ou bien d'autres récepteurs spécifiques des glycoprotéines comme le CD1d, afin d'approfondir nos connaissances sur la détection de ces dérivés lipidiques dans le but d'optimiser encore leurs structures et propriétés adjuvantes.

Enfin, nous avons pu également clairement démontrer au cours de cette étude que les lipoaminoglycosides sont à prendre en considération en tant qu'adjuvants prometteurs pour des protocoles d'immunothérapies anticancéreuses. En effet, en plus de pouvoir être injectés de manière sûre chez la souris sans induire de toxicité, ces molécules sont capables d'induire une réduction significative de la croissance tumorale (dans un modèle de tumeurs mammaires murines). Les lipoaminoglycosides étant avant tout des molécules capables de transfecter efficacement l'ADN, l'ARNm, les siRNA et les protéines, une des perspectives de développement de ce travail peut par ailleurs être leur utilisation en tant que vecteurs au sein de protocoles d'immunothérapies antivirales ou anticancéreuses, afin de permettre (i) la délivrance d'un antigène d'intérêt ou bien (ii) le blocage d'un signal favorable à la tumorogénèse ou l'infection afin de réorienter le système immunitaire. De plus, la vectorisation d'ADN ou d'ARNm peut être intéressante sur un autre point : pouvant eux même être reconnus par de multiples récepteurs et donc agir en tant qu'adjuvants, leur délivrance pourra permettre l'activation de multiples voies de signalisation impliquées dans la réponse immunitaire innée en synergie avec la stimulation engendrée par les lipoaminoglycosides,

aboutissant à la mise en place d'une réponse bien plus efficace (comme l'a souligné l'étude des vaccins vivants atténués).

Développement d'une approche originale basée sur l'assemblage supramoléculaire des lipoplexes pour le développement de vecteurs de transfections universels

Les travaux récents menés au sein de notre équipe par Mével et al ont contribué au développement d'une approche originale basée sur l'influence de l'assemblage supramoléculaire des lipoplexes, afin d'améliorer la stabilité de l'ADN au sein de ces complexes ainsi que l'efficacité de leur délivrance au sein des cellules. Cette étude avait permis de montrer l'intérêt de former des liposomes hybrides plutôt qu'homogènes pour la transfection, néanmoins de nombreuses questions restaient en suspens, telles que l'application à d'autres combinaisons de lipides cationiques/co-lipides ou à d'autres acides nucléiques de ces observations.

Ainsi, afin de valider ce nouveau paramètre à prendre en considération au niveau de l'assemblage supramoléculaire de la bicouche lipidique, nous avons synthétisé 2 lipides cationiques composés (i) d'une tête polaire paromomycine, (ii) d'un segment hydrophobe dioleyl, et (iii) d'un espaceur amide ou phosphoramide formant respectivement le CLN ou le CLP. De même, nous avons également produit 2 co-lipides composés (i) d'une tête polaire imidazole, (ii) un segment hydrophobe dioleyl, et (iii) d'un espaceur amide ou phosphoramide formant respectivement le HLN ou le HLP. Ainsi, l'association de ces lipides cationiques et de ces co-lipides a permis la formation de liposomes dits homogènes (CLN:HLN, CLP:HLP) ou hybrides (CLN:HLP, CLP:HLN).

Au cours de l'étude de ces liposomes, nous avons dans un premier temps pu démontrer le grand intérêt de la formulation de liposomes hybrides, permettant d'induire une forte fixation et stabilité de l'ADN au sein des lipoplexes comparés aux liposomes homogènes. Cela va notamment avoir une forte répercussion à la surface des lipoplexes. En effet bien que la structure « en oignon » soit conservée, nous avons clairement pu établir que les liposomes homogènes présentaient de l'ADN à leur surface, ce qui a un impact négatif tant pour l'interaction avec les membranes cellulaires que pour la protection de l'ADN qui va être susceptible à la dégradation. Pour ce qui est des liposomes hybrides, nous avons pu démontrer que l'ADN est profondément intégré au sein des lipoplexes, étant dès lors bien protégé et laissant toutes interactions possibles. Néanmoins, des expériences complémentaires seraient intéressantes à mener, afin de confirmer ce comportement avec d'autres acides nucléiques tels que les ARNm ou les siRNA, afin de renforcer l'intérêt de la formulation de ces liposomes hybrides.

De plus, nous avons pu confirmer ces observations par des expériences de transfection de différentes lignées cellulaires ou cellules primaires. En effet, peu importe la classe d'acide nucléique, nous avons pu montrer que les liposomes hybrides permettent une meilleure efficacité de transfection comparée aux liposomes homogènes. Dès lors, il serait intéressant d'investiguer à l'avenir si ces liposomes hybrides sont doués de la capacité à délivrer simultanément et efficacement une combinaison d'acides nucléiques différents, ce qui en ferait ainsi des vecteurs

universels pour la transfection d'acides nucléiques avec des applications prometteuses dans le domaine de l'édition génétique (notamment médiée par les Crispr/Cas9).

Conclusion générale

Les résultats obtenus au cours de cette thèse montrent le rôle crucial de l'optimisation de la délivrance de macromolécules au sein de cellules, ainsi que l'importance de la compréhension de l'interaction entre le système immunitaire, les vecteurs, et les acides nucléiques, afin de développer des formulations spécifiques à chaque application biothérapeutique.

En effet dans le contexte de l'immunothérapie ou de la vaccination, formuler un ADN contenant des motifs CpG au copolymère à bloc 704 est une stratégie prometteuse ayant fait ses preuves dans de nombreux protocoles thérapeutiques, et qui est actuellement en cours de développement préclinique pour une future application chez l'homme. De même, l'optimisation de la structure chimique d'autres vecteurs synthétiques de la famille des lipoaminoglycosides a permis le développement de composés possédant des propriétés immunostimulatrices, en faisant de potentiels adjuvants pour l'immunothérapie anticancéreuse et ouvrant la voie à leur utilisation en tant que « vecteurs-adjuvants ».

En parallèle, cette étude a également permis d'obtenir de précieuses informations dans le cadre de la thérapie génique. Ainsi pour le transfert de gènes, l'utilisation d'acides nucléiques et de vecteurs immunologiquement neutres et permettant une bonne délivrance cellulaire est à privilégier. Dès lors, on choisira l'utilisation du 704 qui est un vecteur inerte pour le système immunitaire, en combinaison avec de l'ARN ou des plasmides CpG Free. De même, nous avons pu mettre en avant que certains lipoaminoglycosides (possédant une tête pôlaire 4,5-disubstituées 2-deoxystreptamine, et/ou un espaceur long succinyl-serinyl, et/ou un segment hydrophobe dipalmityl/cholesterol) n'induisent pas de réponse immunitaire, et peuvent voir leur efficacité de transfection améliorer en les formulant avec un co-lipide neutre dans l'optique de former des liposomes hybrides.

ANNEXES

Annexes

Article 4

Habrant, D., Peuziat, P., **Colombani, T**., Dallet, L., Gehin, J., Goudeau, E., Evrard, B., Lambert, O., Haudebourg, T., and Pitard, B. (2016). Design of ionizable lipids to overcome the limiting step of endosomal escape - Application in the intracellular delivery of mRNA, DNA and siRNA. J. Med. Chem.

Article 5

Mével, M., Haudebourg, T., **Colombani, T.**, Peuziat, P., Dallet, L., Chatin, B., Lambert, O., Berchel, M., Montier, T., Jaffrès, P.-A., et al. (2015). Important role of phosphoramido linkage in imidazole-based dioleyl helper lipids for liposome stability and primary cell transfection. J. Gene Med.

Article 6

Chatin, B., Mével, M., Devallière, J., Dallet, L., Haudebourg, T., Peuziat, P**., Colombani, T.**, Berchel, M., Lambert, O., Edelman, A., et al. (2015). Liposome-based Formulation for Intracellular Delivery of Functional Proteins. Mol. Ther. Nucleic Acids *4*, e244.

Article 7

Richard-Fiardo, P., Hervouet, C., Marsault, R., Franken, P.R., Cambien, B., Guglielmi, J., Warnez-Soulie, J., Darcourt, J., Pourcher, T., **Colombani, T.**, et al. (2015). Evaluation of tetrafunctional block copolymers as synthetic vectors for lung gene transfer. Biomaterials *45*, 10–17.

Article 4 : Design of ionizable lipids to overcome the limiting step of endosomal escape - Application in the intracellular delivery of mRNA, DNA and siRNA.

Journal of Medicinal Chemistry

Article

pubs.acs.org/jmc

Design of Ionizable Lipids To Overcome the Limiting Step of Endosomal Escape: Application in the Intracellular Delivery of mRNA, DNA, and siRNA

Damien Habrant,[†,⊥] Pauline Peuziat,[‡,§,⊥] Thibault Colombani,[‡,§] Laurence Dallet,[∥] Johan Gehin,[†] Emilie Goudeau,[†] Bérangère Evrard,[†] Olivier Lambert,[∥] Thomas Haudebourg,[‡,§] and Bruno Pitard*[,†,‡,§]

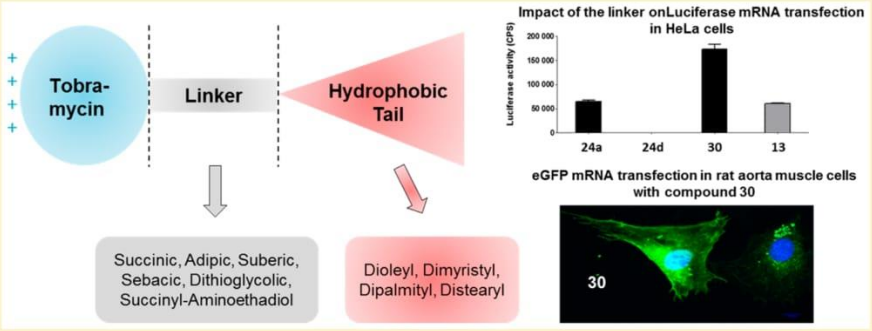
[†]In-Cell-Art, 21 rue de la Noue Bras de Fer, 44200 Nantes, France

[‡]Unité INSERM UMR1087, CNRS UMR 6291, 8 quai Moncousu, 44007 Nantes, France

[§]Université de Nantes, L'institut du Thorax, 8 quai Moncousu, 44007 Nantes, France

[∥]CBMN UMR-CNRS 5248 IECB, Université de Bordeaux 1-IPB, Allée Geoffroy Saint Hilaire, Pessac F-33600, France

Supporting Information



ABSTRACT: The intracellular delivery of nucleic acid molecules is a complex process involving several distinct steps; among these the endosomal escape appeared to be of particular importance for an efficient protein production (or inhibition) into host cells. In the present study, a new series of ionizable vectors, derived from naturally occurring aminoglycoside tobramycin, was prepared using improved synthetic procedures that allow structural variations on the linker and hydrophobic domain levels. Complexes formed between the new ionizable lipids and mRNA, DNA, or siRNA were characterized by cryo-TEM experiments and their transfection potency was evaluated using different cell types. We demonstrated that lead molecule **30**, bearing a biodegradable diester linker, formed small complexes with nucleic acids and provided very high transfection efficiency with all nucleic acids and cell types tested. The obtained results suggested that the improved and "universal" delivery properties of **30** resulted from an optimized endosomal escape, through the lipid-mixing mechanism.

INTRODUCTION

Messenger RNA (mRNA)-based drugs have recently emerged as a new promising therapeutic class to deliver genetic information.[1,2] Indeed, mRNA offers several advantages compared to long-studied plasmid DNA. Unlike DNA, mRNA has the characteristic of being translated directly in the cytoplasm and being fully metabolized. Moreover, there is no risk of genome integration for mRNA, which represents one of the main drawbacks of DNA-based therapeutics. For these reasons, there is currently a growing interest in mRNA and its potential applications for humans. Therapeutic approaches involving RNA interference (RNAi) are also actively investigated.[3,4] RNAi is a post-transcriptional process triggered by the introduction of small-interfering RNA (siRNA), which leads to gene silencing in a sequence-specific manner.

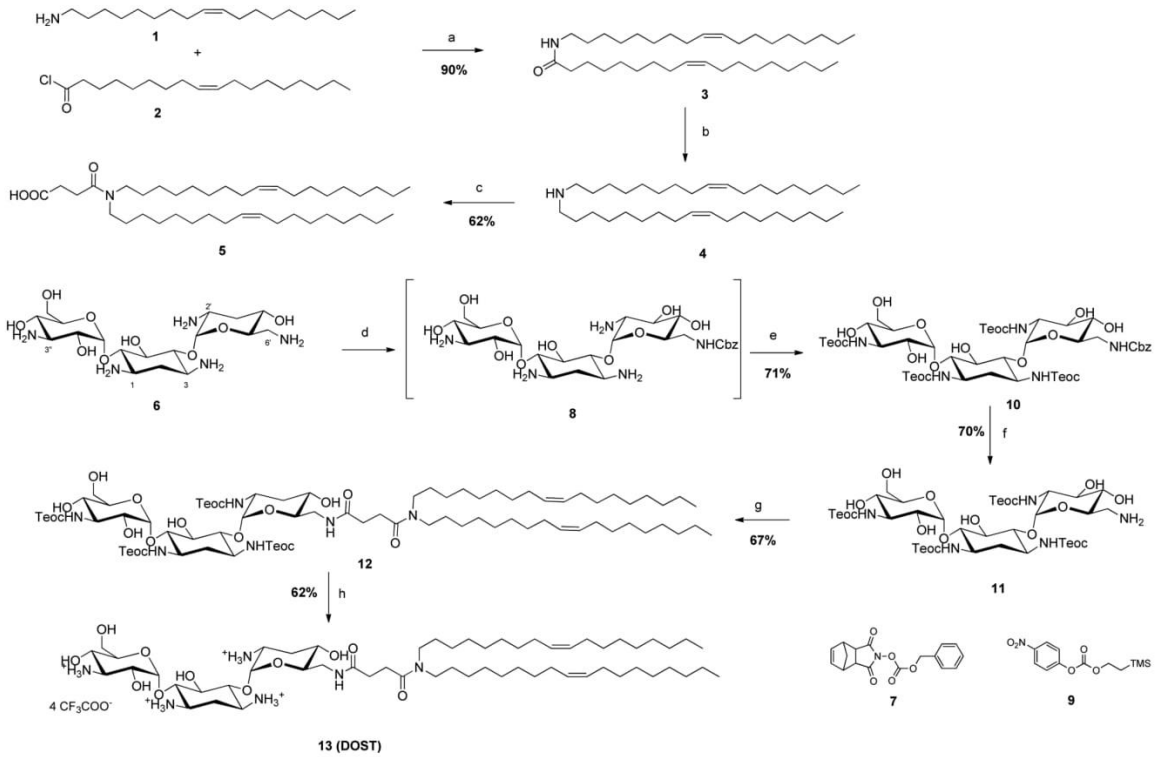
As unformulated nucleic acids do not promote sufficient levels of gene expression (or inhibition in the case of siRNA), a critical issue for the efficient application of gene therapy to human diseases are the vectors used to improve the delivery of nucleic acids into host cells.[5−7] Viral vectors have proven their high efficiency in DNA transfer; however, they can lead to undesired immunological responses and are still limited for the delivery of more specific nucleic acids such as mRNA or siRNA.[8−11] These observations have led to the development of nonviral synthetic vectors. Within the difference classes of nonviral vectors, several structure−activity relationships (SARs) have been performed in order to improve the ability of cationic amphiphilic molecules to formulate and deliver nucleic acids.[12−19] However, due to the complex process of delivery, no universal structural feature has been clearly identified, and the majority of ionizable lipids described in the literature require the presence of a helper

Received: October 28, 2015
Published: March 4, 2016

ACS Publications © 2016 American Chemical Society

DOI: 10.1021/acs.jmedchem.5b01679
J. Med. Chem. 2016, 59, 3046−3062

Scheme 1. Synthesis of Di-oleyl-succinyl-tobramycin (13)[a]



[a]Reagents and conditions: (a) Et_3N, DCM, 20 h, rt; (b) $LiAlH_4$, THF, 12 h, 55 °C; (c) succinic anhydride, Et_3N, DCM, 12 h, rt; (d) **7**, Et_3N, DMF, H_2O, 24 h, rt; (e) **8**, Et_3N, DMF, 48 h, 55 °C; (f) H_2, 10% Pd/C, MeOH, H_2O, 12 h, rt; (g) **5**, HBTU, DMAP, DMF, 12 h, rt; (h) TFA, DCM, 2 h, rt.

fusogenic lipid to achieve efficient transfection efficiency via liposomal formulations.

The accepted mechanism for the intracellular delivery of nucleic acids mediated by ionizable lipids consists in several distinct steps: formation of the lipoplex, binding to the cell membrane, endocytosis, destabilization of the endosomal membrane, and release of the nucleic acid. The endosomal escape pathway for improved delivery of genetic information has been recently investigated, but only few reports mention ionizable lipids.[20−23] The recent study from Zerial and co-workers concluded that the endosomal escape "provides the major opportunity to improve the delivery system".[22]

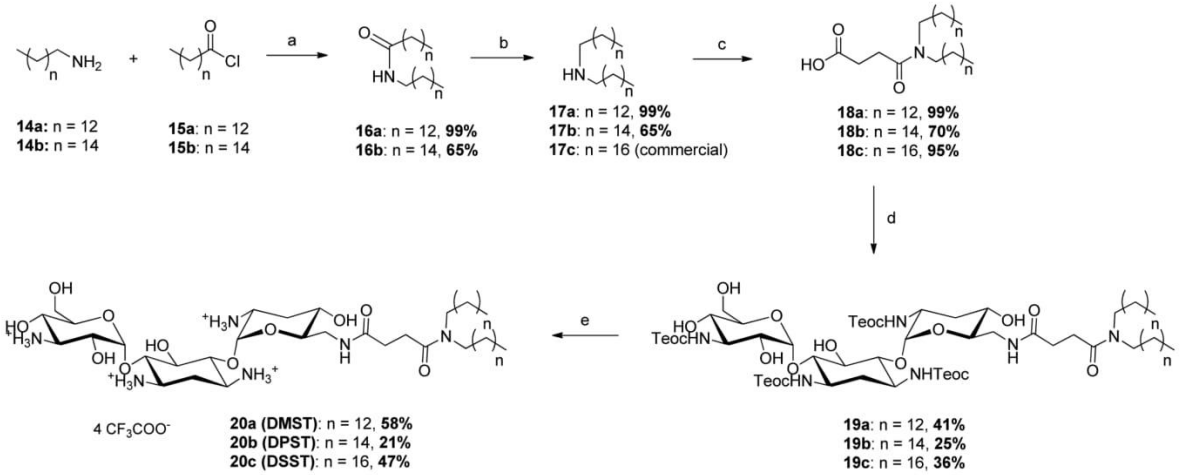
The endosomal escape step has been described to be mediated by the ionizable lipids used as delivery vehicles.[24,25] Indeed, when lipoplexes composed of ionizable lipids and nucleic acids interact with the endosomal membranes, the anionic phospholipids (usually located on the cytoplasmic-facing monolayer of the membrane) flip toward the inside of the endosome, causing the destabilization of the membrane. Neutral ion pairs between the positively charged lipids used as delivery vehicle and the negatively charged phospholipids of the membrane are then formed. This "lipid mixing" mechanism leads to the formation of new multilamellar lipid structures and thus to the disruption of the integrity of the endosomal membrane. Cryo-TEM experiments have demonstrated that the structures of the newly formed lipidic assemblies are highly dependent on the nature of the ionizable lipids.[26] After this step, nucleic acid molecules are present in the cytosol without being surrounded by a closed endosomal membrane and are able to diffuse. The interactions between the ionizable lipids and the anionic phospholipids are therefore of crucial importance to drive the efficient release of the nucleic acids.

If different in their mechanism of action, the different classes of nucleic acids mRNA, DNA, and siRNA share some common features concerning their delivery mechanism. Thus, identifying and overcoming common limiting step(s) may help for the design of universal delivery vehicles. In this purpose, we decided to prepare various ionizable lipids based on the aminoglycoside tobramycin, which was used as a model of a 4,6-disubstitued 2-deoxystreptamine derivatives. Aminoglycosides are natural products able to provide a versatile polycationic framework because several amino groups are present in their structure (together with numerous hydroxyl functions). The family of aminoglycoside derivatives already showed promising results for the delivery of plasmid DNA and siRNA.[27−31] Interestingly aminoglycosides are also known to be natural binders to three-dimensional RNA structures, which make them of particular interest for the development of mRNA therapeutics.[32,33]

Despite of being promising candidates for nucleic acids delivery, this family still lacks a SAR study to elucidate the key structural features required to provide improved transfection efficiency through facilitated endosomal escape. Using a rational approach, our objective was to discover simple and versatile ionizable lipids, able to reach high levels of transfection without the need of a helper lipid. We herein report on the synthesis and the characterization of a new series of lipidic aminoglycoside derivatives and their corresponding transfection efficiency in

DOI: 10.1021/acs.jmedchem.5b01679
J. Med. Chem. 2016, 59, 3046−3062

Scheme 2. Synthesis of Di-myristyl-succinyl-tobramycin (20a), Di-palmityl-succinyl-tobramycin (20b), and Di-stearyl-succinyl-tobramycin (20c)[a]



[a]Reagents and conditions: (a) Et_3N, THF, 20 h, rt; (b) $LiAlH_4$, THF, 12 h, 55 °C; (c) succinic anhydride, Et_3N, DCM, 12 h, rt; (d) **11**, HBTU, DMAP, DMF, 12 h, rt; (e) TFA, DCM, 2 h, rt.

different cell types using three distinct types of nucleic acids: mRNA, DNA, and siRNA.

RESULTS

Synthesis of Aminoglycoside-Derived Ionizable Lipids.

Ionizable lipids are amphiphilic molecules, commonly composed of three distinct parts: an ionizable headgroup, a linker (also called spacer), and a lipophilic moiety. They interact with nucleic acids, forming condensed aggregates named lipoplexes.[34] In the present study, we aimed at assessing different parameters that may be involved in the lipid mixing mechanism and therefore in the nucleic acid delivery: (1) the optimal configuration of the hydrophobic domain (length, insaturation), (2) the importance of the distance between the ionizable headgroup and the lipophilic domain (by changing the length of the linker), and (3) the behavior of environment-sensitive linkers, supposed to be perturbed after reaching the intracellular compartment (reduced pH, presence of enzymes, and reducing agents). The last category is of particular interest because the presence of biodegradable functions in the linker was described to be associated with higher transfection efficiency and with decreased toxicity compared to "classical" linkers.[35−39]

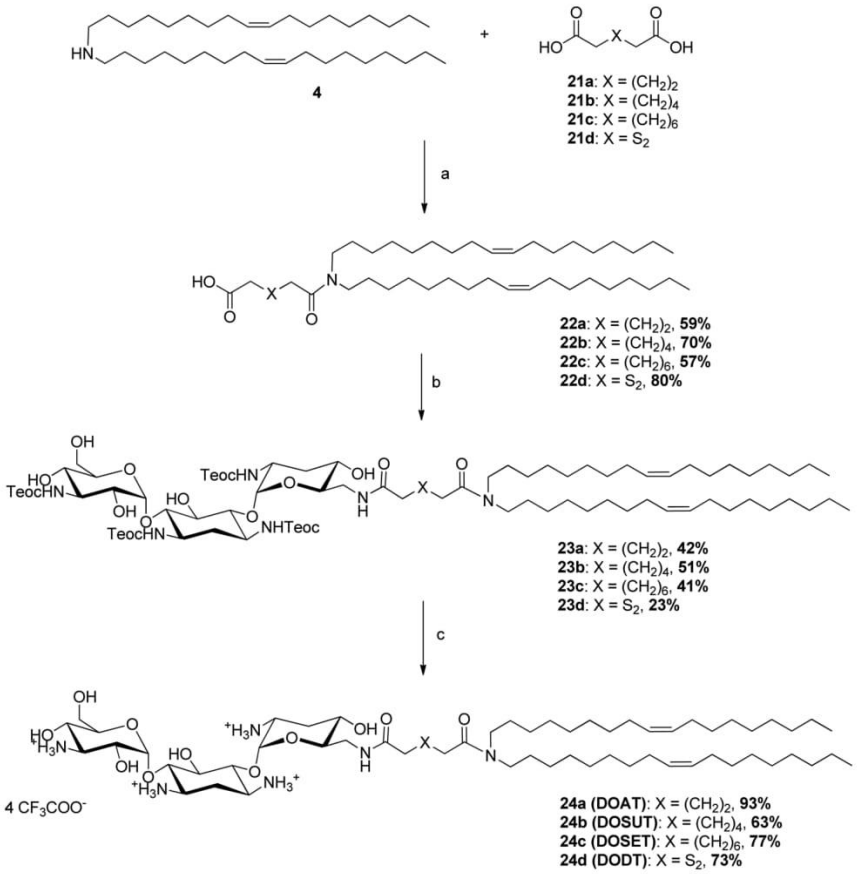
The starting point of our SAR was the molecule **13** (DOST for di-oleyl-succinyl-tobramycin), which is composed of a succinyl linker and two oleyl chains as hydrophobic moiety.[31] The general strategy for the preparation of **13** followed the synthetic route already described for this type of compound (Scheme 1).[27−31] The linker-hydrophobic tail was prepared in three simple steps. First, oleylamine **1** and oleoyl chloride **2** were coupled to form amide **3**, which was then reduced by $LiAlH_4$ to dioleylamine **4**. Then, addition of succinic anhydride furnished the "DOS" moiety **5** in good yield. Concerning the aminoglycoside part, the described strategy employing orthogonal protecting groups was applied. Starting with tobramycin, selective Cbz-protection of the primary amine on the 6′-position was achieved using bulky acylating agent *N*-benzyloxycarbonyloxy-5-norbornene-2,3-dicarboximide (Nor-Cbz **7**).[40] The four remaining secondary amines of **8** (positions 1, 3, 2′, and 3″) were then protected with a Teoc group by 2-(trimethylsilyl)ethyl *p*-nitrophenylcarbonate (Teoc-ONp **9**). As an improvement to the described procedure, we were able to perform these consecutive protection steps in a single pot: tobramycin was first dissolved in H_2O/Et_3N mixture before addition of Nor-Cbz in DMF. After 24 h, a solution of Teoc-ONp in DMF was added, and the mixture stirred for 48 h at 55 °C. This sequential addition of protecting groups allowed for the preparation of fully protected tobramycin derivative **10** in a single step and with a good 71% yield. Catalytic hydrogenation of **10** allowed for the deprotection of the Cbz group and the liberation of the primary amine to give **11**. Then, peptide-like coupling between carboxylic acid **5** and amine **11** was performed using HBTU and DMAP in DMF to produce the protected compound **12**. Finally, **12** was treated by TFA in DCM, which allowed for the isolation of the final compound **13** as a TFA salt.

A series of new analogues derived from **13** was then synthesized. For their preparation, these molecules used the common intermediate **11**, but the linker-hydrophobic tail conjugate was different. As described in the introduction, the first parameters we wanted to assess were the influence of the double bond in the lipophilic chains and the length of the chains themselves. In this context, we prepared different symmetrical dialkyl amines, inspired by the synthesis of scaffold **5** (Scheme 2). Myristylamine **14a** and palmitylamine **14b**, respectively, reacted with myristoyl chloride **15a** and palmitoyl chloride **15b** to give amides **16a** and **16b**, respectively, which were then reduced with $LiAlH_4$ to the corresponding symmetrical amines **17a** and **17b**. The linker part was introduced by reaction of these amines, as well as commercially available distearylamine **17c**, with succinic anhydride to give the conjugates **18a−c** in overall good yields. As previously described, these carboxylic acids were coupled with the tobramycin amino derivative **11**, before removal of the Teoc groups by TFA. This sequence allowed for the preparation of three new molecules: **20a** (DMST for di-myristyl-succinyl-tobramycin), **20b** (DPST for di-palmityl-succinyl-tobramycin), and **20c** (DSST for di-stearyl-succinyl-tobramycin).

Next, we wanted to assess the influence of the linker on the transfection efficiency. In this purpose, two types of linkers were considered: the first type was a linker that was simply elongated,

DOI: 10.1021/acs.jmedchem.5b01679
J. Med. Chem. 2016, 59, 3046−3062

Scheme 3. Synthesis of Di-oleyl-adipyl-tobramycin (24a), Di-oleyl-suberyl-tobramycin (24b), Di-oleyl-sebacyl-tobramycin (24c), and Di-oleyl-dithioglycolyl-tobramycin (24d)[a]



[a]Reagents and conditions: (a) EDC, DMAP, THF, 12 h, rt; (b) **11**, HBTU, DMAP, DMF, 12 h, rt; (c) TFA, DCM, 2 h, rt.

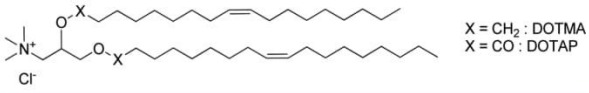
by introducing supplementary methylene units compared to the original succinyl linker, and for the second type, the linker was modified to contain biodegradable functions (disulfide bridge or diester).

In this context, dioleylamine **4** reacted with different dicarboxylic acids (adipic **21a**, suberic **21b**, sebacic **21c**, and dithioglycolic **21d** acids), in the presence of EDC/DMAP to give the corresponding conjugates **22a–d**, in moderate yields (Scheme 3). Similarly, these conjugates were coupled with amine **11**, and after, Teoc-removal gave four new analogues: **24a** (DOAT for di-oleyl-adipyl-tobramycin), **24b** (DOSUT for di-oleyl-suberyl-tobramycin), **24c** (DOSET for di-oleyl-sebacyl-tobramycin), and **24d** (DODT for di-oleyl-dithioglycolyl-tobramycin).

The two most hydrophobic ionizable lipids **24b** and **24c** could not be assessed in the transfection experiments, due to solubility issues in water (unlike the other molecules, we observed for these two compounds a visible precipitate when water was added). Despite being bad news for our structure–activity relationship study, this indicates that too lipophilic compounds cannot be used as efficient nanocarriers for nucleic acids in our tested conditions.

Lastly, the compound **30** (DOSST for di-oleyl-succinyl-serinyl-tobramycin) bearing a diester function was prepared (Scheme 4). This molecule was inspired by the structure of

Scheme 4. Structures of DOTMA and DOTAP



DOTAP, a well-studied commercial cationic lipid, known as the diester equivalent of DOTMA.[41,42]

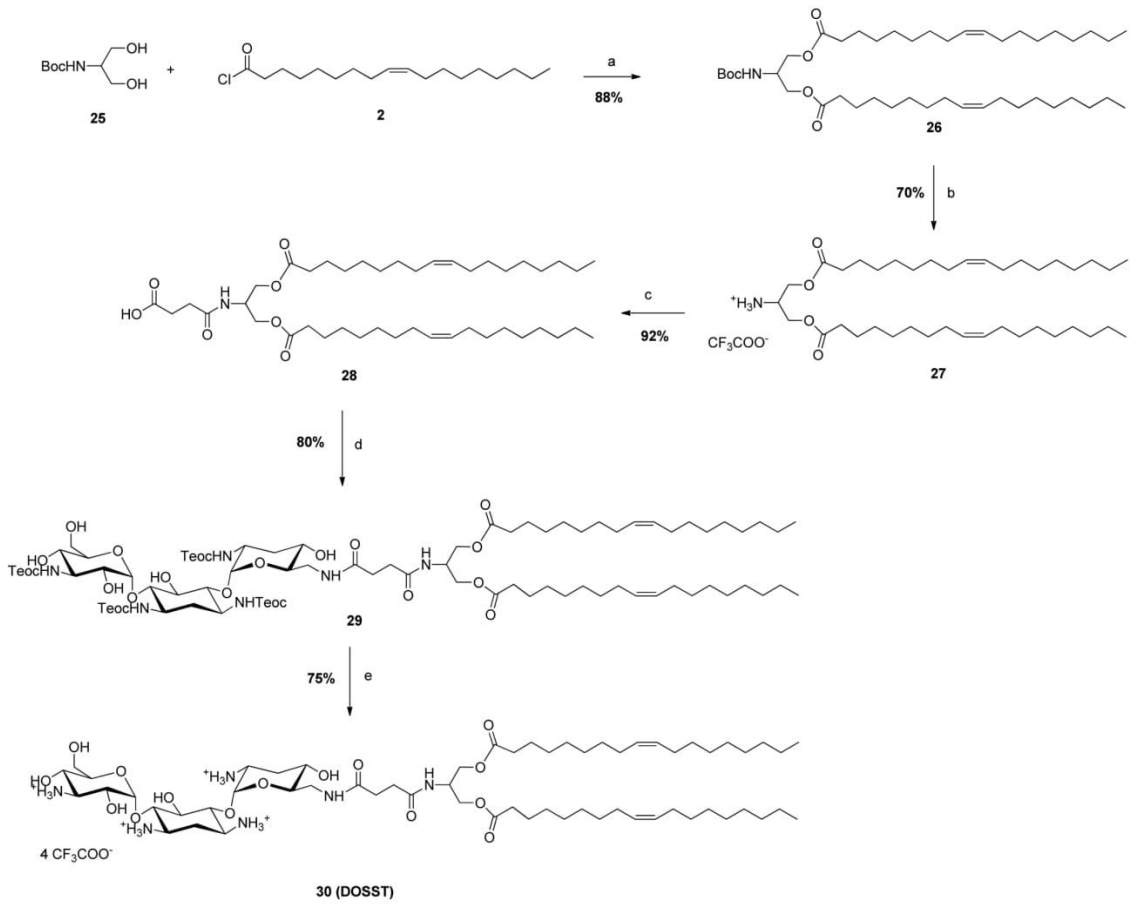
The synthesis started with *N*-Boc serinol **25**, which was diacylated with oleoyl chloride to give **26**. After TFA treatment and reaction with succinic anhydride, the conjugate **28** was obtained. Similarly, the carboxylic acid function of **28** reacted with the amino group of **11** and gave access to the final compound **30** after removal of the protecting groups.

With these molecules in hand, experiments were carried out to study whether the chemical structure of the linker and/or the hydrophobic tail had an impact on the transfection efficiency of different classes of nucleic acids.

Transfection Efficiency Evaluation. Many transfection reagents have been described to lead to effective gene transfer in cell lines, but their transfection potencies are still limited in mammalian primary cells. Yet, transfecting primary cells is a major concern as these cells are biologically more relevant and mimic *in vivo* situation with better accuracy. In this context, we decided to evaluate the transfection efficiency not only on HeLa

DOI: 10.1021/acs.jmedchem.5b01679
J. Med. Chem. 2016, 59, 3046–3062

Scheme 5. Synthesis of Di-oleyl-succinyl-serinyl-tobramycin (30)[a]



[a]Reagents and conditions: (a) pyridine, $CHCl_3$, 12 h, rt; (b) TFA, DCM, 2 h, rt; (c) succinic anhydride, Et_3N, DCM, 12 h, rt; (d) **11**, HBTU, DMAP, DMF, 12 h, rt; (e) TFA, DCM, 2 h, rt.

cell lines but also on two types of primary cells: rat aorta muscle and human fibroblasts cells.

First, we evaluated the efficiency of the tobramycin lipidic derivatives for the mRNA transfection (Figure 1). In this first set of experiments, we observed that all cell types displayed a similar trend where three compounds provided better transfection efficiency compared to the reference compound **13**. Results indeed showed that the formulation with **30** containing a diester linker led to a much higher level of luciferase expression (2- to 3-fold) compared to **13**. Complexes of **24a**/mRNA (adipic linker) and **20b**/mRNA (palmityl derivative) also led to a slightly higher luciferase expression compared to **13**, on the three cell types. On the other hand, cells transfected with myristyl and stearyl compounds, **20a** and **20c**, showed lower expression than cells transfected with **13**, while compound **24d** with a disulfide bridge produced almost no luciferase signal in the tested conditions. These observations for **24d** were similar for the other nucleic acids. This suggests that the disulfide bridge in the structure of **24d** is detrimental for the transfection efficiency; the peculiar behavior of this compound will be discussed in a following section.

In addition, we formulated mRNA encoding eGFP with the reference lipid **13** and the best candidate for mRNA **30** to observe transfected cells by microscopy (Figure 2). HeLa cells (Figure 2A,D) and human fibroblasts cells (Figure 2B,E) transfected with **13** or **30** showed approximately the same percentage of eGFP expressing cells (about 80% for HeLa and 30% for fibroblasts) and the same viability (about 90% in both cases). Thus, both **13** and **30** confirmed their high transfection efficiency, with a low toxicity. Interestingly, the observation at a higher magnification of rat aorta smooth muscle cells transfected with **30**/mRNA complexes showed higher expression of eGFP protein than cells transfected with **13**/mRNA complexes (Figure 2C,F). Compared to reference molecule **13**, compound **30** seems to have the capacity to bring more copies of mRNA inside the cells, which leads to higher expression levels.

After these results with mRNA, we performed experiments with two other types of nucleic acids, DNA and siRNA, to evaluate the versatile character of these new compounds. In this context, the transfection activities of lipoplexes formed by the formulation of plasmid DNA with either compound **13** or one of its derivatives were measured by a luciferase assay on different cell lines (Figure 3). For the cell line HeLa (Figure 3A,B), no significant difference was observed, as all molecules displayed high luciferase expression, with the exception of disulfide compound **24d**, where no luciferase was produced. However, the more-difficult-to-transfect aorta muscle cells and the human fibroblasts cells showed some differences between the molecules,

DOI: 10.1021/acs.jmedchem.5b01679
J. Med. Chem. 2016, 59, 3046−3062

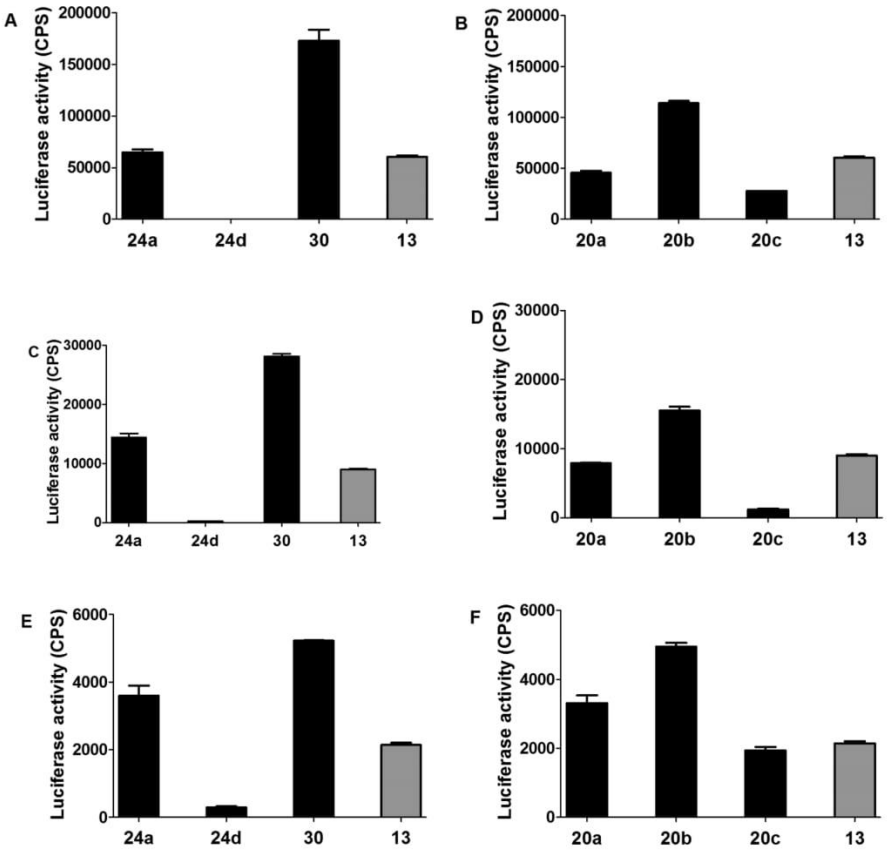


Figure 1. *In vitro* transfection of mRNA encoding luciferase in different cells. HeLa cells (A,B), rat aorta smooth muscle cells (C,D), and human fibroblasts cells (E,F) were transfected with 0.5 μg of mRNA formulated with each ionizable lipid at a charge ratio of 5. Data represent mean ± SEM luciferase activity in counts per second (CPS) 24 h post-transfection for each nanocarrier compared to **13** (gray).

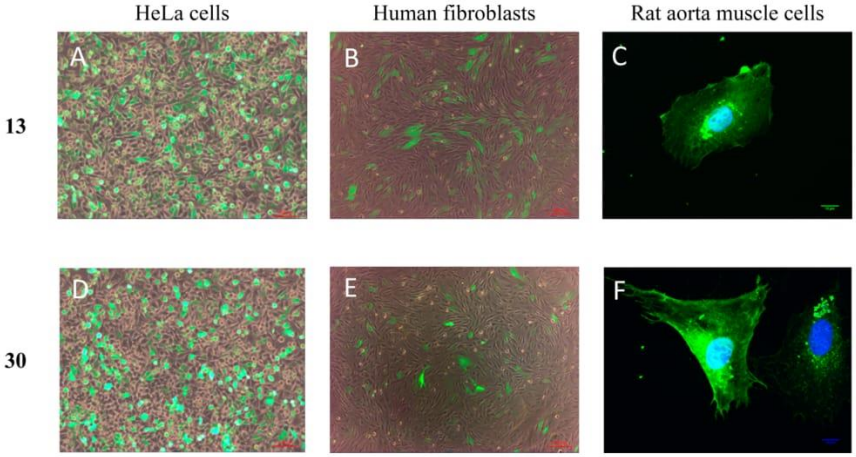


Figure 2. *In vitro* transfection of eGFP mRNA formulated with **13** in HeLa (A), human fibroblasts (B), and rat aorta muscle cells (C), or with **30** in HeLa (D), human fibroblasts (E), and rat aorta muscle cells (F). Cells were transfected with 0.5 μg of mRNA formulated with **13** or **30** at a charge ratio of 5. Plates were incubated 24 h before microscopy observation.

and both cell types displayed similar trends (Figure 3C–F). Indeed, in both cases, the best transfection efficiency was again obtained with diester **30**, which led to higher expression values than the reference molecule **13**. Concerning the molecule with an adipic linker **24a**, the expression was comparable to the results obtained with **13**. However, we could clearly see that changing the hydrophobic tail had a negative impact on the transfection of these two types of cells. Indeed, myristyl **20a**, palmityl **20b**, and stearyl **20c** derivatives all displayed lower expression compared to **13**.

DOI: 10.1021/acs.jmedchem.5b01679
J. Med. Chem. 2016, 59, 3046–3062

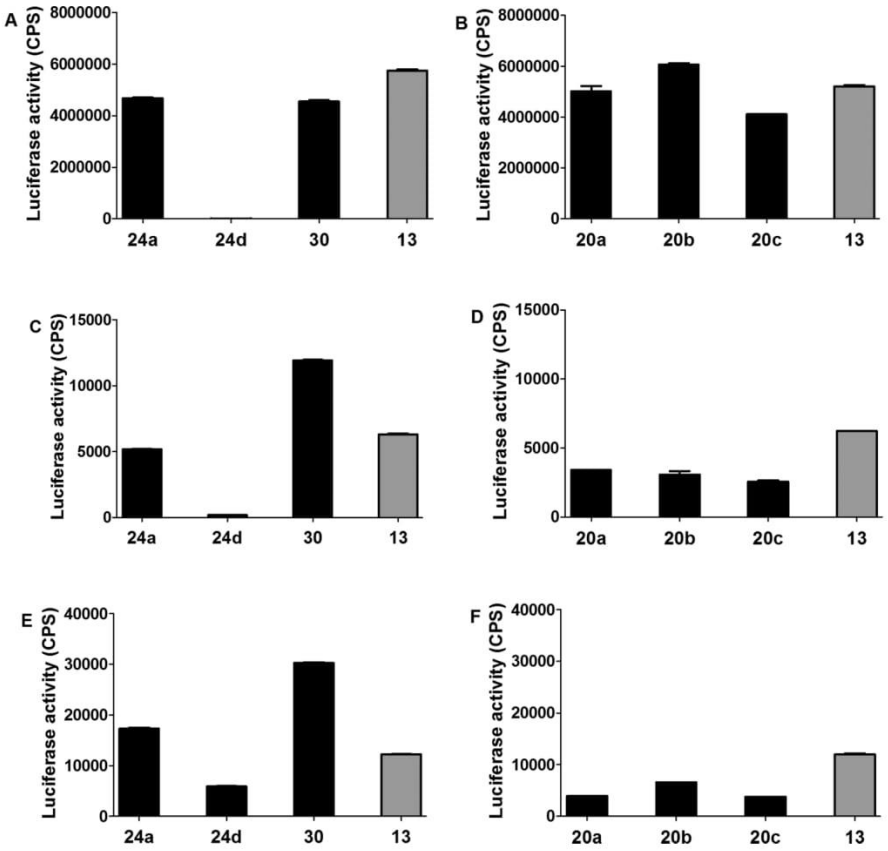


Figure 3. *In vitro* transfection of plasmid DNA encoding luciferase in different cells. HeLa cells (A,B), rat aorta smooth muscle cells (C,D), and human fibroblasts cells (E,F) were transfected with 0.5 μg of DNA formulated with each ionizable lipid at a charge ratio of 5. Data represent mean ± SEM luciferase activity in counts per second (CPS) 24 h post-transfection for each nanocarrier compared to **13** (gray).

These experiments led us to the conclusion that both the linker and the hydrophobic tail had an impact on the DNA transfection efficiency in primary cells, with the dioleyl chains showing the best results compared to smaller and/or nonsaturated chains. The linker as well proved to be an important part, as either lower transfection (disulfide **24d**) or better transfection (diester **30**) compared to the reference molecule **13** was obtained.

In addition, we evaluated the transfection efficiency by measuring the percentage of transfected HeLa cells by flow cytometry. For this purpose, DNA plasmids encoding eGFP were formulated with the lipid **13** or one of its analogues. The results confirmed the trends observed in the DNA luciferase assay and in the eGFP mRNA experiment. Indeed, **24a** (adipic linker) and **30** (diester linker) both displayed similar or slightly higher expression levels (75−80% of transfected cells) compared to **13** (70% of transfected cells), while myristyl, palmityl, and stearyl derivatives were less efficient than **13** (with approximately 50% of transfected cells for **20a**, **20b**, and **20c**). As in previous experiments, low transfection was observed with disulfide-containing lipid **24d**.

We next assessed the gene silencing potential after transfection with the various ionizable lipids. We performed RNAi experiments with siRNA targeting the endogenous lamin A/C expression in murine or human cells (Figure 4). Here, RT-qPCR results indicated that cells transfected with **13**/siRNA, **24a**/siRNA, and **30**/siRNA complexes had very little residual lamin A/C expression, with less than 15% in HeLa and human fibroblasts cells and around 20−25% in C2C12 cells, compared to cells transfected with nonformulated siRNA (which resulted in more than 95% of expression, data not shown). These results clearly demonstrate that these complexes allow for the efficient knockdown of the expression of an endogenous gene in different cell types. However, modifying the hydrophobic tail to myristyl, palmityl, or stearyl chains had a negative impact on the transfection, as **20a**, **20b**, and **20c** all displayed less efficient gene silencing properties with higher residual lamin A/C expression measured compared to **13**. Finally, as observed for mRNA and DNA, compound **24d** with a disulfide linker did not lead to any inhibition of expression compared to negative control (unformulated siRNA).

The versatile potency of **30** and **13** was evaluated in head-to-head comparison experiments with commercially available Lipofectamine 3000 (Thermo Fisher Scientific). In the tested conditions, **30** appeared to be more potent than Lipofectamine 3000 for the *in vitro* transfection of mRNA and DNA, when siRNA experiments provided similar activities for both compounds (see Supporting Information, Figures S19−21). In addition, the cell survival was much higher with **30** (with close to 100% survival) compared to Lipofectamine 3000 (around 20% survival) in our experiments (see Supporting Information, Figure S22).

Characterization of the Lipoplexes by CryoTEM. Morphologies of complexes made with selected candidates **13**, **24a** (adipic linker), and **30** (diester linker) and nucleic acids,

DOI: 10.1021/acs.jmedchem.5b01679
J. Med. Chem. 2016, 59, 3046−3062

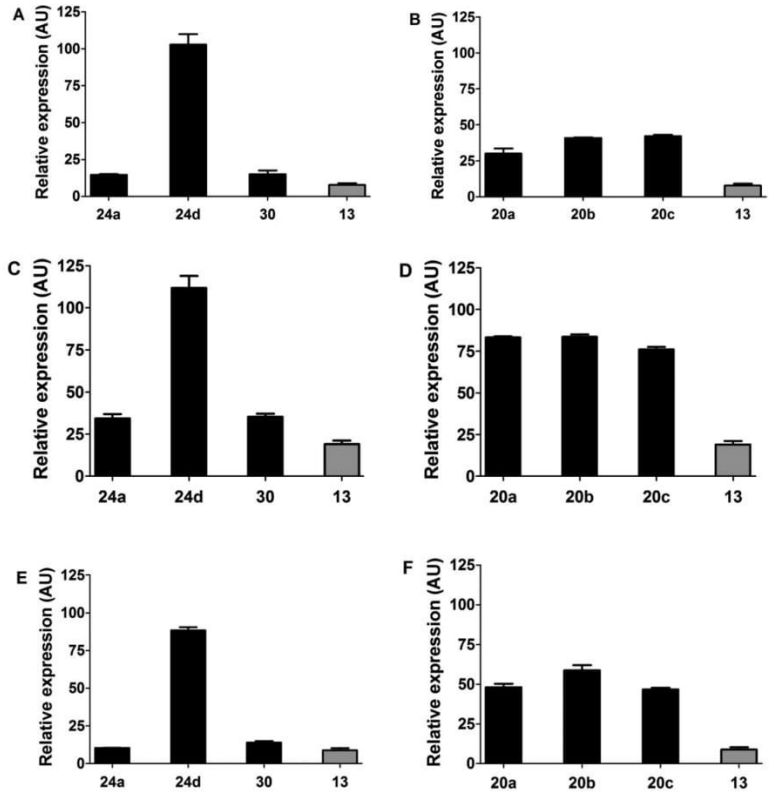


Figure 4. Inhibition of lamin A/C expression. HeLa cells (A,B), C2C12 cells (C,D), or human fibroblast cells (E,F) were transfected with 150 ng (A,B) or 300 ng (C−F) of siRNA, formulated with each ionizable lipid at a charge ratio of 5 and compared to **13** (gray). The gene expression levels of lamin A/C were measured by qPCR analysis, normalized against the expression levels of HPRT (housekeeping gene). The results are expressed as the 2-ΔΔCT formula. Bars represent mean values ± SEM.

either mRNA (Figure 5A−C), plasmid DNA (Figure 5D−F), or siRNA (Figure 5G−I) were then observed by cryoTEM.

In the case of mRNA, the complexes exhibited various sizes, depending on the molecule. Complexes made with **13** exhibited sizes in a range of 200−500 nm while those formed with **24a** appeared of about 200−300 nm (Figure 5A,B). Interestingly, very small complexes (about 70 nm in diameter) were observed with **30**, in addition to larger complexes (200 to 500 nm) (Figure 5C). The morphology of these ARN complexes contained small globular features with sizes ranging about 20 nm in diameter.

Plasmid DNA mixed with **24a** formed very large complexes, larger than 1 μm (Figure 5E). In contrast, the sizes of DNA complexes formed with **13** and **30** were in the range of 200 and 500 nm (Figure 5D,F). As in the case of mRNA, small globular features (about 40 nm) comprising lipid and DNA appeared to assemble together leading to larger structures.

Finally, complexes formed with siRNA are similar to those formed with mRNA and DNA. Complexes made with **13** and **24a** had a size in the range of 80 to 150 nm (Figure 5G,H), while those formed with **30** were of about 100 nm (Figure 5I). Like mRNA complexes, the structures of these siRNA complexes contained small globular features about 20 nm in diameter.

Complexation Study of Disulfide Compound 24d. Regardless of what type of nucleic acid we have used, the previous experiments showed that molecule **24d**, containing a disulfide bridge in the linker, was a very poor transfection agent. In order to better understand the mechanism and the reasons for such poor performance, we analyzed the formulations obtained with DNA and **24d** by monitoring the size of the lipoplexes and the DNA complexation.

The size of the lipoplex, which is linked to the colloidal stability, is a key parameter for nucleic acid delivery. To assess the mean diameter of the system, dynamic light scattering was used. Figure 6A illustrates the evolution of the mean diameter as a function of the charge ratio; we could observe that **24d** follows the classical three-zone colloidal stability observed for many ionizable lipids.[43] Zone A (CR 0.2 to 1) comprised colloidally stable complexes with a negative charge ratio and uncondensed DNA surrounding the lipoplexes. Zone B complexes were essentially neutrally charged (CR 1.5 to 2) with condensed DNA contained within colloidally unstable aggregates. Lipoplexes from zone B exhibited a visible precipitate. Thus, an arbitrary value of 700 nm was attributed to those complexes since the diameter of the precipitated lipoplexes could not be measured by dynamic light scattering. Finally, zone C (CR > 2.5) lipoplexes were composed of colloidally stable particles with condensed DNA and positive charges, thus strongly repelling each other.

Agarose gel electrophoresis experiments on a 0.8% agarose gel stained with ethidium bromide were used to follow DNA complexation, by assessing the relative amounts of DNA that were free or incorporated into the lipoplex. Figure 6B shows that the amount of free DNA decreased as the charge ratio (±) increased. For charge ratios between 0 and 1, free DNA molecules were present and migrated out of the well. For charge ratios above 1,

DOI: 10.1021/acs.jmedchem.5b01679
J. Med. Chem. 2016, 59, 3046−3062

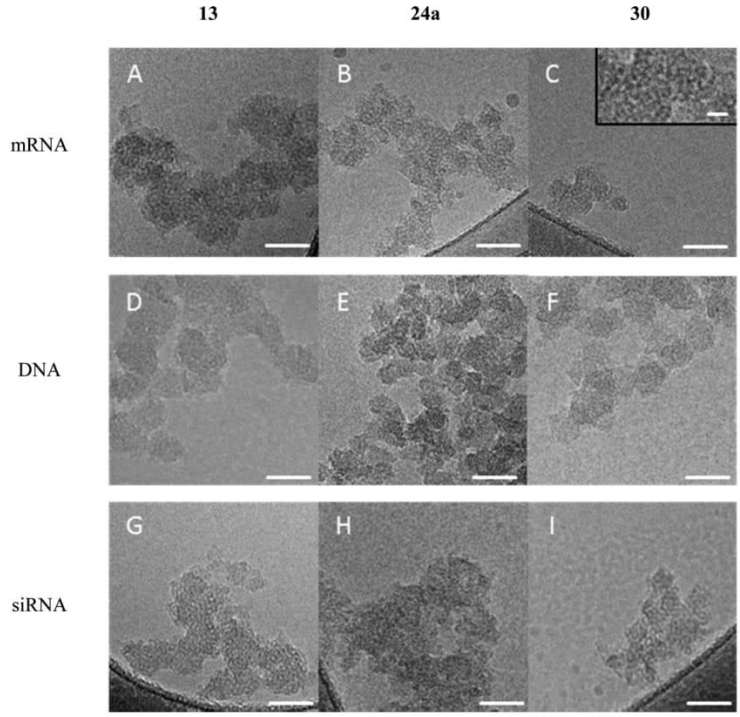


Figure 5. CryoTEM images of complexes made of mRNA mixed with **13** (A), **24a** (B), or **30** (C), plasmid DNA mixed with **13** (D), **24a** (E), or **30** (F), and siRNA mixed with **13** (G), **24a** (H), or **30** (I). Scale bars are 50 nm (A–I) and 10 nm (inset). Complexes were prepared by mixing 0.5 μg of nucleic acids with the corresponding lipid at charge ration (±) of 5.

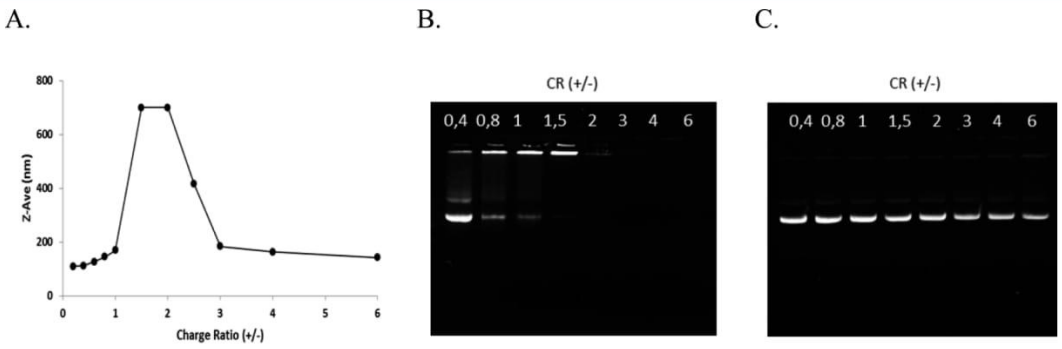


Figure 6. Physico-chemical characterization of **24d**/DNA lipids complexes. (A) Colloidal stability of lipoplexes, as a function of the charge ratio and determined by dynamic light scattering. The analysis was done after 10 min of complexation at room temperature. Lipoplexes from zones A and C were stable; whereas those from zone B exhibited a visible precipitate (thus, an arbitrary value of 700 nm was attributed). (B,C) Agarose gel electrophoresis of lipoplexes of DNA formulated with **24d** in the absence (B) or in the presence (C) of 10 mM DTT.

no free DNA was observed and aggregates were formed, which did not migrate out of the well. Again, this behavior is classical for ionizable lipids used as transfection reagents.

The same electrophoresis experiment was repeated after 30 min of incubation of the **24d**/DNA lipoplexes in the presence of reducing agent DTT (Figure 6C). What was observed is a quantitative release of the DNA after incubation with DTT, independently of the charge ratio (±). This suggests that the DTT treatment of the **24d**/DNA complexes led to the cleavage of the S–S bond, the perturbation of the lipoplexes, and that the DNA molecules that were entrapped in the lipoplexes became free and migrated out of the well. This was in good agreement with what was expected and confirmed the ability of DTT to reduce cleavable functions as the disulfide bridge.

These two experiments illustrated that **24d** is able to complex DNA in the same way as other ionizable lipids in nonreducing environment (the other molecules prepared previously were also tested for comparison and showed similar behaviors, data not shown). The experimental observations were different in the presence of reducing agent DTT, as **24d** entirely lost his ability to form lipoplex. For the other molecules of the series, the DTT treatment had no impact on the lipoplexes (data not shown).

Liposomal Formulations. Next, we decided to investigate the behavior of disulfide **24d** and diester **30** (our best candidate) lipids used as liposomal form, where a different delivery mechanism takes place. In this context, liposomes were prepared by mixing **24d** or **30** with neutral colipid DOPE, in a 1:1 molar ratio, as previously described.[31] The liposome preparations were then

DOI: 10.1021/acs.jmedchem.5b01679
J. Med. Chem. 2016, 59, 3046–3062

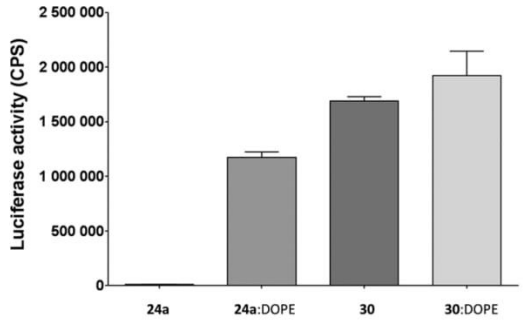


Figure 7. *In vitro* transfection of plasmid DNA encoding luciferase in different cells comparing micellar (**24a**, **30**) and liposomal (**24a**:DOPE, **30**:DOPE) formulations. HeLa cells were transfected with 0.5 μg of DNA formulated with each formulation at a charge ratio of 5. Data represent mean ± SEM luciferase activity in count per second (CPS) 24 h post-transfection for each nanocarrier.

formulated with DNA, at a charge ratio of 5, and the transfection efficiency compared to micellar formulations (Figure 7). The results obtained showed that, as seen in Figure 3, micellar preparations of **24d** were not able to transfect DNA molecules. The results were different when the liposomal formulation was used, as high transfection efficiency was observed with **24d**:DOPE liposomes, that reached almost the same level as the diester **30** under the micellar form. However, results showed that for molecule **30**, formulations as micellar or liposomal form provided approximately the same transfection efficiency.

■ DISCUSSION

These sets of results coming from the study of the transfection efficiency with three different types of nucleic acids gave us some useful information about the properties of the aminoglycoside lipidic derivatives and their mechanism of action.

It was observed that "parent" molecule **13** is a good and versatile transfecting agent. Indeed, it provided good transfection potency in the case of mRNA and DNA and was also among the best molecules tested for gene silencing using siRNA. This strengthens the data available in the literature about **13** and related aminoglycoside family members as efficient vectors for nucleic acid delivery.[27−31]

In addition, the new tobramycin lipidic derivatives described in this study allowed us to draw some conclusions on the key structural features of this type of molecule.

Concerning the hydrophobic domain, we could observe that all modifications (with the exception of palmityl derivative **20b** in the mRNA experiments, Figure 1) led to detrimental effects compared to the dioleyl chain present in the reference molecule **13**. It can therefore be concluded that saturated and/or shorter than C18 chains are less effective for nucleic acid delivery. This observation is rather in good agreement with what was previously described in the literature about other families of ionizable lipids and could be attributed to less favorable conditions for the endosomal escape.[18]

The linker and hydrophobic portions of compound **30** were designed using encouraging results from the literature with ionizable lipid DOTAP. Indeed, DOTAP, which contains ester functions in the linker and two oleyl chains as hydrophobic part, showed higher transfection efficiency and reduced toxicity compared to DOTMA, its analogue bearing ether functions.[41,42] In our experiments, the introduction of such ester functions on the linker (with similar hydrophobic domain than in the case of **13**) also led to improved transfection efficiency. This was especially true in the case of mRNA, where **30** appeared to be 2- to 3-fold more efficient than reference molecule **13**, on the three cell types tested, leading to very high transfection.

The fluorescence experiments using eGFP mRNA and DNA as reporter genes provided some insights on the mechanism of this improved delivery. Indeed, the percentage of transfected cells obtained with HeLa and fibroblasts cells for **13** and **30** were very similar. The pictures in Figure 2 clearly show that **13** was as efficient as **30** in terms of numbers of transfected cells (with approximately 80% of transfected HeLa cells and 30% of human fibroblasts) and that both compounds display very low cytotoxicity, with around 90% of viable cells. The improved efficacy of **30** is therefore not related to a lower toxicity (as we could expect with results comparing DOTMA and DOTAP). More surprisingly, it does not seem to be correlated to a better biodegradability either. Indeed, we performed stability studies where **13** and **30** were mixed with porcine liver esterases, and we followed by HPLC the degradation of the molecules. We were expecting that **30** would degrade faster than **13**, due to the presence of the ester bonds that should be cleaved by these enzymes and that the improved features of **30** could be explained by a better biodegradability. Unfortunately, no difference could be detected in terms of stability toward these esterases (data not shown).

The better efficiency of **30** could be explained by the fluorescence experiment on rat aorta muscle cells. The observations of single transfected cells clearly showed that the transfection with **30** led to a higher expression of eGFP protein compared to **13** (Figure 2C,F). This seems to demonstrate that, for the same number of transfected cells, **30** is able to deliver more copies of mRNA encoding eGFP inside the cell cytoplasm. We believe that this could result from an improved release mechanism of nucleic acids in the cytosol. Indeed, the fact that **30** was the best molecule of the series both for mRNA and DNA transfection, and one of the best for siRNA, tends to indicate that the improved feature of **30** influences the same step of the delivery mechanism, independently of the nucleic acid transported.

As stated in the introduction, the mechanism for the intracellular delivery of nucleic acids mediated by ionizable lipids is composed of several distinct steps, and the key endosomal escape step is influenced by the ionizable lipids used as delivery vehicles.[24,25] In our case, the presence of ester bonds in the linker portion of **30**, which makes it endogenous to natural lipids, may be responsible for better hydrophobic interactions with the natural anionic phospholipids, when compared to the other molecules of the series. The better transfection potency of **30** may be a consequence of these improved interactions, favoring the formation of new bilayer structures obtained from the association of the anionic lipids from the membrane and the cationic lipids from the lipoplex. Results tend to suggest that these interactions are able to promote a more efficient release of mRNA, DNA, or siRNA from the lipoplex and from the endosome.

Molecule **24d**, with a disulfide function in the linker structure, provided negative results in all types of nucleic acids under micellar form but still allowed us to drive some conclusions. Previous reports have demonstrated that the introduction of a disulfide bridge in the structure of a given ionizable lipid can lead to the reduction of the lipid in the intracellular compartment, causing the destabilization of the complex and the release of the DNA into the cytosol. However, this improved release compared to nonreducible molecules was not necessarily

DOI: 10.1021/acs.jmedchem.5b01679
J. Med. Chem. 2016, 59, 3046−3062

associated with improved transfection efficacy in micellar complexes, and the effect was more pronounced in liposomal formulations.[35−39] We have shown in our study that **24d** was able to complex nucleic acids in a similar way than the other molecules of the series. However, in the presence of reducing agent DTT, **24d** showed a quantitative release of the DNA molecules in the gel retardation assay (Figure 6). It can therefore be envisioned that such reduction of the disulfide bridge may also occur in the endosomal compartment, leading to the separation of the tobramycin headgroup and the lipophilic tail. This seems to be detrimental for the lipid mixing mechanism because both electrostatic and hydrophobic interactions are necessary to trigger the disruption of the endosomal membrane. With the lipid **24d**, the nucleic acids entrapped in the endosome are therefore not released in the cytoplasm and are degraded by fusion with lysosomes. To confirm the prevalence of the lipid mixing mechanism in the previous tests, we performed additional experiments where **24d** was used as a liposomal form, in an equimolar formulation with the neutral fusogenic colipid DOPE, which induces another endosomal escape mechanism. In this experiment, the **24d**:DOPE formulation proved to be effective for the intracellular delivery of plasmid DNA, while the **24d** micellar version did not transfect at all (Figure 7). The mechanism that takes place in the presence of the colipid is different since DOPE is known to lead to a fusion and destabilization of the membrane at reduced pH.[44]

These results demonstrated that the endosomal escape is a key step for the effective delivery of nucleic acids when using a micellar formulation. In the case of low-transfecting agents like **24d**, the ineffectiveness of the lipid mixing mechanism can be counterbalanced by the addition of a neutral colipid able to induce an alternative fusion mechanism for the disruption of the endosomal membrane.

Formulating a given ionizable synthetic delivery system with a neutral colipid (in our case, DOPE) usually led to higher transfection potency compared to the micellar form, but increases the complexity of the formulation. In our case, the results demonstrated that the micellar form of **30** was able to reach the same transfection as the **30**:DOPE liposomes (Figure 7). These results suggest that the two mechanisms (lipid-mixing with micelles and fusion with liposomes) are well-distinct since no synergistic effect was observed with **30**.

Rational design of **30** allowed us to reach the same transfection efficiency in the presence or in the absence of the helper lipid DOPE. We assumed that the usually observed lower efficacy of the micellar form was compensated by the improved lipid mixing mechanism with **30**. This property is of particular interest for the development of a simple, single-component delivery system.

In addition, cryoTEM analysis of mRNA, DNA, and siRNA formulations with **30** led to complexes with small globular features (20−40 nm, Figure 5). In general, complexes formed with **30** were found to be rather small, especially in the case of mRNA where 70 nm complexes were observed. The improved properties observed with **30** for the delivery of mRNA could also be associated with these small complexes, as reports indicate that the endocytosis pathway is dependent on the size of the particles.[45−47] In particular, Hoekstra et al. described that for complexes with sizes below 200 nm, the clathrin-mediated pathway of entry was involved, while internalization with caveolae was present for larger particles.[48] We hypothesized that **30**/mRNA complexes could induce a clathrin-mediated endocytosis, while the larger lipoplexes were internalized via caveolae, but further studies will be necessary to clearly understand the influence of the ionizable lipids on the size of the complexes and therefore on the mechanisms of endocytosis.

In conclusion, we assessed the ability of tobramycin lipidic derivatives to efficiently deliver genetic information with various types of nucleic acids. This structure−activity relationship led to the identification of the tobramycin-derived lipid **30**, which provided excellent transfection efficiency on different cell types with mRNA, DNA, and siRNA. We assumed that these improved properties were related to the presence of endogenous ester functions that favor the lipid mixing mechanism and trigger a more efficient endosomal escape of the nucleic acids. From the generated data, **30** appears to be an efficient, monocomponent and versatile delivery system, forming small particles when formulated with nucleic acids, and therefore, it represents a very promising candidate for further development, especially in the innovative field of mRNA-based therapeutics.

■ EXPERIMENTAL SECTION

General Methods for Synthesis. All commercially available materials were purchased from Sigma-Aldrich, with the exception of tobramycin, which was purchased from Carbosynth, and were used without further purification. NMR experiments were recorded on a Bruker Advance 400 MHz spectrometer (400 MHz for ^{1}H and 100 MHz for ^{13}C). Spectra were acquired at 300 K, using deuterated chloroform ($CDCl_3$) or deuterated methanol (MeOD) as the solvent. Chemical shifts for ^{1}H and ^{13}C spectra were recorded in parts per million using the residual nondeuterated solvent as the internal standard (for $CDCl_3$, 7.26 ppm, ^{1}H, 77.16 ppm, ^{13}C; for MeOD, 3.31 ppm, ^{1}H, 49.00 ppm, ^{13}C). TFA signals were not described in the ^{13}C spectra. Flash chromatographies were performed on a Grace Reveleris system, equipped with either Reveleris Silica cartridges, using a gradient of MeOH in DCM as mobile phase or Reveleris C18 reversed-phase cartridges, using a gradient of MeOH in H_2O (+ 0.05% TFA) as mobile phase. The detection was performed with an evaporative light-scattering detector (ELSD). High-resolution mass spectrometry experiments were performed on a qTOF Synaptg2 HDMS (Waters Corporation) apparatus; electrospray in positive mode was used (ion trap). UHPLC analyses were run on a Waters ACQUITY H-Class system equipped with an ELSD detector. Analyses were performed on an ACQUITY UPLC HSS T3 column (2.1 × 50 mm, particle size 1.8 μm). The mobile phase consisted of ACN/H_2O (50/50) + 0.1% TFA (A) and ACN + 0.1% TFA (B). All final compounds showed purity higher than 95%.

*Dioleamide (**3**).* To a solution of oleylamine **1** (6 mL, 18.23 mmol) in DCM (75 mL) were successively slowly added oleoyl chloride **2** (6.03 mL, 18.23 mmol) and Et_3N (2.53 mL, 18.23 mmol) at 0 °C. The mixture was stirred 1 h at 0 °C and then 20 h at rt. The mixture was then washed with H_2O and brine, and the organic phase was dried over $MgSO_4$ and concentrated. The residue was purified by flash chromatography (DCM/MeOH) to give the expected amide **3** as a white sticky solid (8.73 g, 90%). ^{1}H NMR ($CDCl_3$, 25 °C) δ 0.89 (t, J = 7.2 Hz, 6H), 1.25−1.31 (m, 42H), 1.48−1.51 (m, 2H), 1.63−1.65 (m, 2H), 1.89−2.06 (m, 8H), 2.16 (t, J = 7.6 Hz, 2H), 3.25 (t, J = 6.8 Hz, 2H), 5.31−5.45 (m, 4H).

*Dioleylamine (**4**).* To a suspension of $LiAlH_4$ (1.56 g, 41.03 mmol, 2.5 equiv) in THF (80 mL) was slowly added a solution of dioleamide **3** (8.73 g, 16.41 mmol, 1 equiv) in THF (20 mL) at 0 °C. The mixture was then heated overnight at 55 °C. Once the mixture cooled down to rt, H_2O (1.5 mL), NaOH 15% (1.5 mL), and H_2O (4.5 mL) were successively and slowly added. The resulting mixture was filtered and the precipitate washed with DCM. The filtrate was dried over $MgSO_4$ and concentrated *in vacuo*. The residue was used in the next step without any further purification. ^{1}H NMR ($CDCl_3$, 25 °C) δ 0.88 (t, J = 6.4 Hz, 6H), 1.25−1.29 (m, 44H), 1.45−1.49 (m, 4H), 1.98−2.03 (m, 8H), 2.60 (t, J = 7.2 Hz, 4H), 5.33−5.38 (m, 4H).

*4-(Dioleylamino)-4-oxobutanoic Acid (**5**).* To a solution of crude **4** (16.41 mmol) in DCM (300 mL) were successively added succinic anhydride (3.28 g, 32.82 mmol, 2 equiv) and Et_3N (4.5 mL, 32.82 mmol,

DOI: 10.1021/acs.jmedchem.5b01679
J. Med. Chem. 2016, 59, 3046−3062

2 equiv). The mixture was stirred at rt overnight, then quenched by addition of 1 M HCl. After extraction, the organic layer was further washed with 1 M HCl and water (3 times), dried over $MgSO_4$, and concentrated *in vacuo*. The residue was purified by flash chromatography (DCM/MeOH) to afford the desired acid **5** (6.35 g, 62% over 2 steps). ^{1}H NMR ($CDCl_3$, 25 °C) δ 0.88 (t, J = 7.2 Hz, 6H), 1.26−1.30 (m, 44H), 1.52−1.56 (m, 4H), 1.97−2.04 (m, 8H), 2.68 (s, 4H), 3.22 (t, J = 7.5 Hz, 2H), 3.32 (t, J = 7.5 Hz, 2H), 5.30−5.38 (m, 4H), 11.90 (bs, 1H).

*6′-Benzyloxycarbonyl-1,2′,3,3″-tetra((trimethylsilyl)-ethylcarbamate)-tobramycin (**10**).* Tobramycin **6** (1 g, 2.14 mmol, 1 equiv) was dissolved in H_2O (10 mL). Et_3N (0.3 mL, 2.14 mmol, 1 equiv) and a solution of *N*-benzyloxycarbonyloxy-5-norbornene-2, 3-dicarboximide **7** (0.67 g, 2.14 mmol, 1 equiv) in DMF (10 mL) were successively added and the mixture stirred at rt for 24 h. A solution of 2-(trimethylsilyl)ethyl-4-nitrophenylcarbonate **9** (2.65 g, 11.12 mmol, 5.2 equiv) in DMF (20 mL) and Et_3N (1.55 mL, 11.12 mmol, 5.2 equiv) were then added, and the yellow solution was stirred at 55 °C. After 48 h, the mixture was concentrated and the residue taken up with EtOAc, before washing with 1 M NaOH (3 times), water, and brine. The organic fraction was dried over $MgSO_4$ and concentrated *in vacuo*. The residue was purified by flash chromatography (DCM/MeOH) to afford the expected product **10** (1.8 g, 71%). ^{1}H NMR (MeOD, 25 °C) δ 0.04−0.06 (m, 36H), 0.99−1.03 (m, 8H), 1.48−1.51 (m, 1H), 1.64−1.70 (m, 1H), 1.99−2.10 (m, 2H), 3.40−3.76 (m, 15H), 3.89−3.91 (m, 1H), 4.08−4.16 (m, 8H), 5.06−5.13 (m, 4H), 7.35−7.37 (m, 5H). ^{13}C NMR (MeOD, 25 °C) δ −1.4, 18.6, 18.7, 34.3, 35.7, 42.4, 51.3, 51.6, 57.6, 62.1, 64.0, 66.6, 69.4, 71.8, 73.5, 74.8, 76.7, 83.0, 84.2, 99.3, 99.8, 128.9, 129.0, 129.5, 138.4, 158.5, 158.7, 159.8, 160.1.

*1,2′,3,3″-Tetra((trimethylsilyl)ethylcarbamate)-tobramycin (**11**).* To a solution of **10** (1.8 g, 1.52 mmol, 1 equiv) in degassed wet MeOH (containing 10% of H_2O, 50 mL) was added 10% Pd/C (0.21 g, 0.1 equiv). Three cycles of vacuum/N_2 were applied, followed by three cycles of vacuum/H_2. The mixture was stirred overnight, then filtered over a pad of Celite, and washed with MeOH. The filtrate was concentrated *in vacuo* and the residue purified by flash chromatography (DCM/MeOH) to afford the expected free amine **11** (1.09 g, 70%). ^{1}H NMR (MeOD, 25 °C) δ 0.00−0.02 (m, 36H), 0.94−0.98 (m, 8H), 1.45−1.49 (m, 1H), 1.57−1.65 (m, 1H), 1.91−2.05 (m, 2H), 2.59−2.64 (m, 1H), 2.94−2.97 (m, 1H), 3.33−3.55 (m, 6H), 3.55−3.74 (m, 7H), 3.86−3.88 (m, 1H), 4.03−4.17 (m, 8H), 5.02 (s, 1H), 5.20 (s, 1H). ^{13}C NMR (MeOD, 25 °C) δ −1.4, 18.5, 18.6, 18.7, 30.7, 34.6, 43.3, 51.2, 51.3, 51.6, 62.2, 63.9, 64.0, 64.2, 67.5, 69.3, 71.8, 73.5, 73.9, 74.7, 76.7, 76.9, 81.9, 84.1, 98.2, 99.3, 99.8, 158.5, 158.7, 158.9, 160.0.

*N,N-Dioleyl-succinamide-1,2′,3,3″-tetra((trimethylsilyl)-ethylcarbamate)-tobramycin (**12**).* To a solution of **11** (1 g, 0.95 mmol, 1 equiv) in DMF (15 mL) was added a solution of **5** (0.713 g, 1.045 mmol, 1.1 equiv) in DMF (50 mL). HBTU (432 mg, 1.14 mmol, 1.2 equiv) and DMAP (350 mg, 2.85 mmol, 3 equiv) were successively added, and the mixture was stirred at rt overnight. After concentration, the residue was taken up with EtOAc before washing with NH_4Cl_{sat}, H_2O, and brine. The organic layer was dried over $MgSO_4$ and concentrated *in vacuo*. The residue was purified by flash chromatography (DCM/MeOH) to afford the expected compound **12** (1.05 g, 67%). ^{1}H NMR (MeOD, 25 °C) δ 0.05−0.06 (m, 36H), 0.90 (t, J = 6.7 Hz, 6H), 0.99−1.03 (m, 8H), 1.30−1.35 (m, 52H), 1.53−1.63 (m, 6H), 2.02−2.05 (m, 9H), 2.53−2.68 (m, 4H), 3.33−3.76 (m, 13H), 3.90−3.94 (m, 1H), 4.06−4.16 (m, 8H), 5.07 (s, 1H), 5.33−5.38 (m, 4H). ^{13}C NMR (MeOD, 25 °C) δ −1.3, 14.5, 18.6, 18.7, 18.8, 23.8, 27.9, 28.2, 28.8, 29.5, 29.9, 30.3, 30.4, 30.5, 30.6, 30.8, 30.9, 31.8, 33.1, 33.6, 34.2, 41.3, 47.6, 51.3, 51.7, 57.6, 62.2, 64.0, 64.2, 66.9, 67.4, 69.5, 71.8, 73.5, 74.8, 77.0, 82.0, 84.1, 98.6, 99.7, 130.8, 130.9, 158.5, 158.7, 158.8, 160.1, 173.4, 175.6.

*Dioleyl-succinyl-tobramycin (**13**).* To a suspension of **12** (1 g, 0.61 mmol) in DCM (5 mL) was slowly added TFA (10 mL) at 0 °C. The solution was stirred at rt for 2 h, then concentrated. After three consecutive additions of MeOH and subsequent evaporations, the residue was purified by flash chromatography (reverse phase, C18-Silica, H_2O (+0.05%TFA)/MeOH) and lyophilized to give **13** (0.575 g, 62%). ^{1}H NMR (MeOD, 25 °C) δ 0.90 (t, J = 6.7 Hz, 6H), 1.29−1.31 (m, 52H), 1.44−1.63 (m, 4H), 1.98−2.03 (m, 8H), 2.19−2.22 (m, 1H), 2.51−2.53 (m, 3H), 2.69−2.72 (m, 2H), 3.39−3.92 (m, 14H), 5.09 (s, 1H), 5.33−5.42 (m, 4H), 5.43 (s, 1H). ^{13}C NMR (MeOD, 25 °C) δ 14.5, 23.7, 27.9, 28.7, 29.1, 29.3, 30.2, 30.3, 30.4, 30.5, 30.6, 30.8, 31.0, 31.6, 33.0, 33.6, 40.7, 47.5, 50.0, 50.9, 56.7, 62.0, 65.7, 67.6, 69.9, 75.4, 76.1, 80.9, 85.5, 96.7, 101.8, 130.8, 130.9, 173.7, 175.6. HRMS: calculated for $C_{58}H_{111}N_6O_{11}$ $[M + H]^+$ = 1067.8311, found 1067.8340.

*Dimyristamide (**16a**).* To a solution of myristylamine **14a** (1 g, 4.68 mmol) in THF (40 mL) were successively slowly added myristoyl chloride **15a** (1.27 mL, 4.68 mmol) and Et_3N (0.65 mL, 4.68 mmol) at 0 °C. A precipitate immediately formed after Et_3N addition. After 20 h at rt, the solid was filtered, washed with H_2O, and dried to give the expected amide **16a** as a white sticky solid (1.94 g, 99%). ^{1}H NMR ($CDCl_3$, 25 °C) δ 0.87 (t, J = 6.8 Hz, 6H), 1.24−1.27 (m, 44H), 1.45−1.47 (m, 2H), 2.14 (t, J = 8.0 Hz, 2H), 3.22 (q, J = 6.8 Hz, 2H), 5.37 (bs, 1H).

*Dipalmitamide (**16b**).* To a solution of palmitylamine **14a** (1 g, 4.14 mmol) in THF (35 mL) and DMF (30 mL) were successively slowly added palmitoyl chloride **15b** (1.26 mL, 4.14 mmol) and Et_3N (0.58 mL, 4.14 mmol) at 0 °C. The mixture was stirred 1 h at 0 °C and then 20 h at rt. After addition of EtOAc, the mixture was washed with H_2O and brine; the organic phase was dried over $MgSO_4$ and concentrated. The residue was purified by flash chromatography (DCM/MeOH) to give the expected amide **16b** as a white solid (1.44 g, 65%). ^{1}H NMR ($CDCl_3$, 25 °C) δ 0.88 (t, J = 6.8 Hz, 6H), 1.25−1.28 (m, 50H), 1.46−1.50 (m, 2H), 1.46−1.50 (m, 2H), 2.14 (t, J = 7.6 Hz, 2H), 3.23 (q, J = 6.8 Hz, 2H), 5.35 (bs, 1H).

*Dimyristylamine (**17a**).* Following the procedure described for compound **4**, reduction of **16a** (1 g, 2.36 mmol) by $LiAlH_4$ (0.23 g, 5.89 mmol) in THF (55 mL) provided amine **17a**, which was used in the next step without any further purification. ^{1}H NMR ($CDCl_3$, 25 °C) δ 0.88 (t, J = 6.8 Hz, 6H), 1.24−1.28 (m, 50H), 2.59 (t, J = 7.2 Hz, 2H).

*Dipalmitylamine (**17b**).* Following the procedure described for compound **4**, reduction of **16b** (1 g, 2.08 mmol) by $LiAlH_4$ (0.20 g, 5.21 mmol) in THF (55 mL) provided amine **17b**, which was used in the next step without any further purification. ^{1}H NMR ($CDCl_3$, 25 °C) δ 0.87 (t, J = 6.8 Hz, 6H), 1.25−1.29 (m, 58H), 2.58 (t, J = 7.2 Hz, 2H).

*4-(Dimyristylamino)-4-oxobutanoic Acid (**18a**).* Following the procedure described for compound **5**, addition of succinic anhydride (0.37 g, 3.68 mmol) on **17a** (0.96 g, 1.84 mmol) in DCM (50 mL), in the presence of Et_3N (0.50 mL, 3.68 mmol), provided the desired acid **18a** (0.94 g, 99%). ^{1}H NMR ($CDCl_3$, 25 °C) δ 0.88 (t, J = 6.8 Hz, 6H), 1.23−1.28 (m, 44H), 1.48−1.60 (m, 4H), 2.69 (s, 4H), 3.20−3.24 (m, 2H), 3.30−3.34 (m, 2H).

*4-(Dipalmytoylamino)-4-oxobutanoic Acid (**18b**).* Following the procedure described for compound **5**, addition of succinic anhydride (0.27 g, 2.70 mmol) on **17b** (0.63 g, 1.35 mmol) in DCM (50 mL), in the presence of Et_3N (0.38 mL, 3.70 mmol), provided the desired acid **18b** (0.47 g, 71%). ^{1}H NMR ($CDCl_3$, 25 °C) δ 0.88 (t, J = 6.8 Hz, 6H), 1.23−1.28 (m, 52H), 1.43−1.55 (m, 4H), 2.69 (s, 4H), 3.20−3.24 (m, 2H), 3.30−3.34 (m, 2H).

*4-(Distearylamino)-4-oxobutanoic Acid (**18c**).* Following the procedure described for compound **5**, addition of succinic anhydride (0.38 g, 3.83 mmol) on distearylamine **17c** (1 g, 1.92 mmol) in DCM (50 mL), in the presence of Et_3N (0.53 mL, 3.83 mmol), provided the desired acid **18c** (1.14 g, 95%). ^{1}H NMR ($CDCl_3$, 25 °C) δ 0.88 (t, J = 6.8 Hz, 6H), 1.23−1.28 (m, 60H), 1.48−1.60 (m, 4H), 2.69 (s, 4H), 3.20−3.24 (m, 2H), 3.30−3.34 (m, 2H).

*N,N-Dimyristyl-succinamide-1,2′,3,3″-tetra((trimethylsilyl)-ethylcarbamate)-tobramycin (**19a**).* Following the procedure described for compound **12**, reaction of amine **11** (200 mg, 0.18 mmol) with acid **18a** (102 mg, 0.20 mmol), in the presence of HBTU (83 mg, 0.22 mmol) and DMAP (66 mg, 0.54 mmol) in DMF (10 mL), provided the expected compound **19a** (117 mg, 41%). ^{1}H NMR (MeOD, 25 °C) δ 0.05 (m, 36H), 0.90 (t, J = 6.8 Hz, 6H), 0.99−1.04 (m, 8H), 1.28−1.41 (m, 45H), 1.51−1.55 (m, 2H), 1.63−1.67 (m, 3H), 1.98−2.16 (m, 2H), 2.54−2.71 (m, 4H), 3.30−3.77 (m, 18H), 3.91−3.93 (m, 1H), 4.09−4.18 (m, 9H), 5.08−5.12 (m, 1H), 5.26 (s, 1H). ^{13}C NMR (MeOD, 25 °C) δ −1.3, 14.5, 18.6, 18.7, 18.8, 23.8, 27.9, 28.2, 28.8, 30.5, 30.7, 30.8, 30.9, 31.9, 33.1, 41.4, 47.5, 51.3, 51.6, 57.7, 62.2, 64.0, 64.2, 64.6,

DOI: 10.1021/acs.jmedchem.5b01679
J. Med. Chem. 2016, 59, 3046−3062

66.7, 69.4, 71.9, 73.6, 74.8, 76.8, 77.0, 99.3, 99.8, 158.5, 158.7, 158.9, 160.1, 173.4, 175.6.

*N,N-Dipalmytoyl-succinamide-1,2′,3,3″-tetra((trimethylsilyl)-ethylcarbamate)-tobramycin (**19b**).* Following the procedure described for compound **12**, reaction of amine **11** (200 mg, 0.18 mmol) with acid **18b** (113 mg, 0.20 mmol), in the presence of HBTU (83 mg, 0.22 mmol) and DMAP (66 mg, 0.54 mmol) in DMF (10 mL), provided the expected compound **19b** (74 mg, 25%). ^{1}H NMR (MeOD, 25 °C) δ 0.05 (m, 36H), 0.90 (t, J = 6.8 Hz, 6H), 0.99−1.03 (m, 8H), 1.26−1.38 (m, 53H), 1.51−1.54 (m, 2H), 1.63−1.66 (m, 3H), 1.98−2.12 (m, 2H), 2.54−2.75 (m, 4H), 3.30−3.76 (m, 18H), 3.91−3.93 (m, 1H), 4.08−4.18 (m, 9H), 5.07−5.11 (m, 1H), 5.24 (s, 1H). ^{13}C NMR (MeOD, 25 °C) δ −1.3, 14.5, 18.6, 18.7, 18.8, 23.8, 27.9, 28.1, 28.8, 30.4, 30.5, 30.6, 30.7, 30.8, 31.9, 33.1, 41.4, 47.5, 51.3, 51.7, 57.7, 62.2, 64.0, 64.2, 64.6, 66.7, 69.4, 71.9, 73.5, 74.8, 76.8, 77.1, 99.3, 99.8, 158.5, 158.7, 158.9, 160.1, 173.4, 175.6.

*N,N-Distearyl-succinamide-1,2′,3,3″-tetra((trimethylsilyl)-ethylcarbamate)-tobramycin (**19c**).* Following the procedure described for compound **12**, reaction of amine **11** (200 mg, 0.18 mmol) with acid **18c** (124 mg, 0.20 mmol), in the presence of HBTU (83 mg, 0.22 mmol) and DMAP (66 mg, 0.54 mmol) in DMF (10 mL), provided the expected compound **19c** (110 mg, 36%). ^{1}H NMR (MeOD, 25 °C) δ 0.07 (m, 36H), 0.92 (t, J = 6.8 Hz, 6H), 1.00−1.05 (m, 8H), 1.28−1.41 (m, 61H), 1.51−1.54 (m, 2H), 1.55−1.71 (m, 3H), 1.96−2.14 (m, 2H), 2.53−2.74 (m, 4H), 3.30−3.84 (m, 18H), 3.91−3.93 (m, 1H), 4.10−4.26 (m, 9H), 5.09−5.12 (m, 1H), 5.26 (s, 1H). ^{13}C NMR (MeOD, 25 °C) δ −1.4, 14.7, 18.6, 18.7, 18.8, 23.9, 27.9, 28.0, 28.8, 29.9, 30.3, 30.4, 30.5, 30.6, 30.7, 30.8, 31.2, 32.0, 33.3, 41.6, 47.6, 51.2, 51.8, 57.5, 62.2, 64.0, 64.1, 64.5, 66.6, 69.4, 72.0, 73.4, 74.9, 76.8, 77.1, 99.2, 99.9, 158.5, 158.7, 158.9, 160.2, 173.5, 175.6.

*Dimyristyl-succinyl-tobramycin (**20a**).* Following the procedure described for **13**, treatment of **19a** (97 mg, 0.060 mmol) by TFA (2 mL) in DCM (1 mL) provided **20a** (49 mg, 58%). ^{1}H NMR (MeOD, 25 °C) δ 0.91 (t, J = 7.2 Hz, 6H), 1.22−1.32 (m, 45H), 1.44−1.54 (m, 2H), 1.57−1.64 (m, 2H), 1.95−2.03 (m, 2H), 2.19−2.23 (m, 1H), 2.51−2.54 (m, 2H), 2.70−2.73 (m, 2H), 3.32−3.40 (m, 4H), 3.42−3.60 (m, 7H), 3.65−3.68 (m, 2H), 3.71−3.91 (m, 7H), 5.09 (d, J = 3.6 Hz, 1H), 5.44 (d, J = 3.2 Hz, 1H). ^{13}C NMR (MeOD, 25 °C) δ 14.4, 23.7, 27.9, 28.1, 28.7, 29.1, 29.7, 30.4, 30.5, 30.6, 30.7, 30.8, 31.0, 31.7, 33.1, 40.7, 47.5, 50.1, 51.0, 56.7, 62.0, 65.8, 67.6, 70.0, 75.4, 75.5, 76.2, 81.2, 85.6, 96.8, 101.8, 173.8, 175.6. HRMS: calculated for $C_{50}H_{98}N_6O_{11}$ $[M + H]^+$ = 959.7372, found 959.7354.

*Dipalmityl-succinyl-tobramycin (**20b**).* Following the procedure described for **13**, treatment of **19b** (74 mg, 0.046 mmol) by TFA (2 mL) in DCM (1 mL) provided **20b** (14 mg, 21%). ^{1}H NMR (MeOD, 25 °C) δ 0.90 (t, J = 7.2 Hz, 6H), 1.11−1.29 (m, 53H), 1.42−1.54 (m, 2H), 1.57−1.65 (m, 2H), 1.94−2.02 (m, 2H), 2.19−2.21 (m, 1H), 2.51−2.55 (m, 2H), 2.62−2.71 (m, 2H), 3.31−3.39 (m, 4H), 3.40−3.53 (m, 7H), 3.64−3.69 (m, 2H), 3.75−3.90 (m, 7H), 5.09 (d, J = 3.2 Hz, 1H), 5.43 (d, J = 2.8 Hz, 1H); ^{13}C NMR (MeOD, 25 °C) δ 14.4, 23.7, 27.9, 28.1, 28.7, 29.1, 29.4, 29.7, 30.4, 30.5, 30.6, 30.7, 30.8, 31.0, 31.7, 33.1, 40.7, 47.5, 50.1, 50.9, 56.7, 62.0, 65.7, 67.6, 70.0, 75.5, 76.3, 81.0, 85.5, 96.8, 101.8, 173.8, 175.6. HRMS: calculated for $C_{54}H_{106}N_6O_{11}$ $[M + H]^+$ = 1015.7998, found 1015.7961.

*Distearyl-succinyl-tobramycin (**20c**).* Following the procedure described for **13**, treatment of **19c** (60 mg, 0.036 mmol) by TFA (2 mL) in DCM (1 mL) provided **20c** (26 mg, 47%). ^{1}H NMR (MeOD, 25 °C) δ 0.90 (t, J = 6.8 Hz, 6H), 1.23−1.40 (m, 61H), 1.48−1.58 (m, 2H), 1.59−1.68 (m, 2H), 1.93−2.05 (m, 2H), 2.16−2.24 (m, 1H), 2.49−2.59 (m, 2H), 2.60−2.72 (m, 2H), 3.31−3.40 (m, 4H), 3.40−3.59 (m, 7H), 3.62−3.70 (m, 2H), 3.73−3.95 (m, 7H), 5.09 (d, J = 3.6 Hz, 1H), 5.44 (d, J = 3.2 Hz, 1H). ^{13}C NMR (MeOD, 25 °C) δ 14.4, 23.7, 27.9, 28.1, 28.7, 29.1, 29.7, 30.4, 30.5, 30.7, 30.8, 31.7, 33.1, 40.7, 47.5, 50.1, 50.9, 56.8, 62.1, 65.9, 67.7, 70.0, 75.6, 76.4, 81.0, 85.6, 89.2, 96.8, 101.9, 173.8, 175.6. HRMS: calculated for $C_{58}H_{114}N_6O_{11}$ $[M + H]^+$ = 1071.8624, found 1071.8660.

*6-(Dioleylamino)-6-oxohexanoic Acid (**22a**).* Dioleylamine **4** (250 mg, 0.52 mmol, 1 equiv) and adipic acid **21a** (152 mg, 1.04 mmol, 2 equiv) were dissolved in THF (60 mL). EDC (120 mg, 0.62 mmol, 1.2 equiv) and DMAP (31 mg, 0.26 mmol, 0.5 equiv) were added, and the mixture stirred at rt overnight. After concentration, the residue was taken up with EtOAc before washing with NH_4Cl_{sat}, H_2O, and brine. The organic layer was dried over $MgSO_4$ and concentrated *in vacuo*. The residue was purified by flash chromatography (DCM/MeOH) to afford the expected compound **22a** (200 mg, 59%). ^{1}H NMR ($CDCl_3$, 25 °C) δ 0.87 (t, J = 6.8 Hz, 6H), 1.26−1.29 (m, 44H), 1.42−1.56 (m, 4H), 1.58−1.74 (m, 4H), 1.99−2.01 (m, 8H), 2.30−2.36 (m, 2H), 2.80 (t, J = 7.6 Hz, 2H), 3.18 (t, J = 7.6 Hz, 2H), 3.27 (t, J = 7.6 Hz, 2H), 5.31−5.42 (m, 4H). ^{13}C NMR ($CDCl_3$, 25 °C) δ 14.2, 23.9, 24.9, 25.8, 27.1, 27.2, 27.9, 29.0, 29.1, 29.2, 29.3, 29.4, 29.5, 29.6, 29.7, 29.8, 29.9, 30.5, 31.7, 32.0, 32.8, 34.1, 46.3, 48.2, 129.8, 130.0, 172.5, 178.3.

*8-(Dioleylamino)-8-oxooctanoic Acid (**22b**).* Following the procedure described for **22a**, dioleylamine **4** (500 mg, 0.96 mmol) reacted with suberic acid **21b** (340 mg, 1.93 mmol) in THF (40 mL), in the presence of EDC (220 mg, 1.16 mmol) and DMAP (59 mg, 0.48 mmol, 0.5 equiv) to give compound **22b** (452 mg, 70%). ^{1}H NMR ($CDCl_3$, 25 °C) δ 0.88 (t, J = 6.7 Hz, 6H), 1.26−1.29 (m, 48H), 1.49−1.52 (m, 4H), 1.63−1.67 (m, 4H), 2.00−2.04 (m, 8H), 2.28 (t, J = 7.6 Hz, 2H), 2.35 (t, J = 7.6 Hz, 2H), 3.18 (t, J = 7.6 Hz, 2H), 3.27 (d, J = 7.6 Hz, 2H), 5.34−5.38 (m, 4H). ^{13}C NMR ($CDCl_3$, 25 °C) δ 14.1, 23.5, 24.5, 25.4, 25.5, 25.6, 26.8, 26.9, 27.0, 27.2, 27.8, 28.6, 28.9, 29.1, 29.2, 29.3, 29.4, 29.5, 29.6, 29.7, 29.8, 31.5, 31.8, 31.9, 32.6, 32.9, 33.9, 46.1, 48.1, 129.7, 129.8, 129.9, 173.0, 178.4.

*10-(Dioleylamino)-10-oxodecanoic Acid (**22c**).* Following the procedure described for **22a**, dioleylamine **4** (500 mg, 0.96 mmol) reacted with sebacic acid **21c** (390 mg, 1.93 mmol) in THF (40 mL), in the presence of EDC (220 mg, 1.16 mmol) and DMAP (59 mg, 0.48 mmol, 0.5 equiv) to give compound **22c** (382 mg, 52%). δ ^{1}H NMR ($CDCl_3$, 25 °C) δ 0.88 (t, J = 6.7 Hz, 6H), 1.26−1.30 (m, 52H), 1.49−1.53 (m, 4H), 1.62−1.64 (m, 4H), 2.00−2.05 (m, 8H), 2.27 (t, J = 7.6 Hz, 2H), 2.34 (t, J = 7.6 Hz, 2H), 3.19 (t, J = 7.6 Hz, 2H), 3.27 (d, J = 7.6 Hz, 2H), 5.30−5.36 (m, 4H). ^{13}C NMR ($CDCl_3$, 25 °C) δ 14.1, 22.7, 24.7, 25.5, 25.6, 26.9, 27.0, 27.2, 27.8, 28.9, 29.0, 29.2, 29.3, 29.4, 29.5, 29.6, 29.7, 29.8, 31.8, 31.9, 32.6, 33.0, 34.0, 46.1, 48.1, 129.7, 129.8, 130.0, 173.1, 178.7.

*2-(Dioleylamino)-2-dithioglycolic Acid (**22d**).* Following the procedure described for **22a**, dioleylamine **4** (250 mg, 0.52 mmol) reacted with dithioglycolic acid **21d** (190 mg, 1.93 mmol) in DMF (60 mL), in the presence of EDC (110 mg, 0.62 mmol) and DMAP (30 mg, 0.25 mmol, 0.5 equiv) to give compound **22d** (283 mg, 80%). ^{1}H NMR ($CDCl_3$, 25 °C) δ 0.87 (t, J = 6.8 Hz, 6H), 1.24−1, 28 (m, 44H), 1.53−1.57 (m, 4H), 1.97−2.20 (m, 8H), 3.22 (t, J = 7.6 Hz, 2H), 3.34 (t, J = 7.6 Hz, 2H), 3.56 (s, 2H), 3.71 (s, 2H), 5.31−5.40 (m, 4H). ^{13}C NMR ($CDCl_3$, 25 °C) δ 14.2, 22.8, 25.8, 26.0, 27.0, 27.1, 27.2, 27.3, 29.1, 29.2, 29.3, 29.4, 29.5, 29.6, 29.8, 29.9, 31.6, 31.9, 32.0, 32.7, 41.1, 41.8, 47.1, 49.0, 129.8, 130.1, 169.1, 171.3.

*N,N-Dioleyl-adipamide-1,2′,3,3″-tetra((trimethylsilyl)-ethylcarbamate)-tobramycin (**23a**).* Following the procedure described for compound **12**, reaction of amine **11** (283 mg, 0.27 mmol) with acid **22a** (220 mg, 0.30 mmol), in the presence of HBTU (121 mg, 0.32 mmol) and DMAP (99 mg, 0.81 mmol) in DMF (30 mL), provided the expected compound **23a** (189 mg, 42%). ^{1}H NMR (MeOD, 25 °C) δ 0.05 (s, 36H), 0.90 (t, J = 7.2 Hz, 6H), 0.98−1.03 (m, 8H), 1.23−1.41 (m, 45H), 1.53−1.66 (m, 10H), 1.90−2.10 (m, 8H), 2.28−2.32 (m, 2H), 2.38−2.41 (m, 2H), 3.32−3.76 (m, 16H), 3.90−3.93 (m, 1H), 4.01−4.16 (m, 8H), 5.07 (s, 1H), 5.13 (s, 1H), 5.33−5.41 (m, 4H). ^{13}C NMR ($CDCl_3$, 25 °C) δ −1.3, 14.5, 18.6, 18.7, 18.8, 23.8, 26.3, 26.8, 27.9, 28.1, 28.2, 28.8, 30.1, 30.2, 30.3, 30.4, 30.5, 30.6, 30.9, 33.1, 33.7, 36.7, 41.1, 47.3, 51.4, 51.8, 57.6, 62.2, 64.0, 64.1, 69.4, 71.8, 73.5, 74.8, 76.7, 82.9, 84.0, 99.2, 99.7, 130.8, 130.9, 158.5, 158.7, 158.9, 160.1, 174.8, 176.8.

*N,N-Dioleyl-suberamide-1,2′,3,3″-tetra((trimethylsilyl)-ethylcarbamate)-tobramycin (**23b**).* Following the procedure described for compound **12**, reaction of amine **11** (117 mg, 0.11 mmol) with acid **22b** (84 mg, 0.12 mmol), in the presence of HBTU (51 mg, 0.13 mmol) and DMAP (42 mg, 0.34 mmol) in DMF (10 mL), provided the expected compound **23b** (98 mg, 51%). ^{1}H NMR (MeOD, 25 °C) δ 0.06 (s, 36H), 0.90 (t, J = 7.2 Hz, 6H), 1.00−1.03 (m, 8H), 1.29−1.39 (m, 49H), 1.51−1.64 (m, 10H), 1.98−2.04 (m, 8H), 2.25−2.30 (m, 2H), 2.33−2.37 (m, 2H), 3.35−3.76 (m, 16H), 3.88−3.93 (m, 1H),

DOI: 10.1021/acs.jmedchem.5b01679
J. Med. Chem. 2016, 59, 3046−3062

4.08−4.17 (m, 8H), 5.07 (s, 1H), 5.13 (s, 1H), 5.33−5.39 (m, 4H). ^{13}C NMR ($CDCl_3$, 25 °C) δ −1.3, 14.5, 18.6, 18.7, 23.8, 26.6, 27.0, 27.8, 28.0, 28.2, 28.8, 30.2, 30.3, 30.4, 30.5, 30.6, 30.8, 30.9, 33.1, 34.0, 36.8, 41.1, 47.2, 51.4, 57.6, 62.2, 64.0, 66.5, 69.4, 71.8, 73.5, 74.8, 76.6, 83.0, 99.3, 99.8, 130.8, 130.9, 158.5, 158.6, 158.8, 160.1, 175.1, 177.1.

*N,N-Dioleyl-sebacamide-1,2′,3,3″-tetra((trimethylsilyl)-ethylcarbamate)-tobramycin (**23c**).* Following the procedure described for compound **12**, reaction of amine **11** (105 mg, 0.10 mmol) with acid **22c** (79 mg, 0.11 mmol), in the presence of HBTU (47 mg, 0.12 mmol) and DMAP (37 mg, 0.30 mmol) in DMF (10 mL), provided the expected compound **23c** (73 mg, 41%). ^{1}H NMR (MeOD, 25 °C) δ 0.07 (s, 36H), 0.86 (t, J = 7.2 Hz, 6H), 0.94−0.98 (m, 8H), 1.25−1.36 (m, 53H), 1.48−1.56 (m, 10H), 1.97−2.10 (m, 8H), 2.20−2.24 (m, 2H), 2.27−2.31 (m, 2H), 3.35−3.76 (m, 16H), 3.88−3.92 (m, 1H), 4.01−4.13 (m, 8H), 5.02 (s, 1H), 5.06 (s, 1H), 5.28−5.35 (m, 4H). ^{13}C NMR ($CDCl_3$, 25 °C) −1.3, 14.5, 18.6, 18.7, 18.8, 23.8, 26.8, 27.1, 27.8, 28.0, 28.2, 28.8, 30.2, 30.3, 30.4, 30.5, 30.7, 30.8, 30.9, 33.1, 33.7, 34.1, 36.9, 41.1, 47.2, 51.4, 57.7, 62.2, 64.0, 66.6, 69.5, 71.8, 73.6, 74.8, 76.6, 83.1, 99.4, 99.9, 130.8, 130.9, 131.0, 158.5, 158.7, 158.9, 160.1, 175.2, 177.3.

*N,N-Dioleyl-dithioglycolamide-1,2′,3,3″-tetra((trimethylsilyl)-ethylcarbamate)-tobramycin (**23d**).* Following the procedure described for compound **12**, reaction of amine **11** (320 mg, 0.31 mmol) with acid **22d** (230 mg, 0.34 mmol), in the presence of HBTU (137 mg, 0.36 mmol) and DMAP (110 mg, 0.90 mmol) in DMF (40 mL), provided the expected compound **23d** (122 mg, 23%). ^{1}H NMR (MeOD, 25 °C) δ 0.01 (s, 36H), 0.85 (t, J = 7.2 Hz, 6H), 0.94−0.98 (m, 8H), 1.25−1.39 (m, 45H), 1.51−1.64 (m, 6H), 1.90−2.04 (m, 8H), 3.35−3.70 (m, 20H), 3.83−3.90 (m, 1H), 4.07−4.11 (m, 8H), 5.02 (s, 1H), 5.11 (s, 1H), 5.28−5.33 (m, 4H). ^{13}C NMR (MeOD, 25 °C) −1.3, 14.5, 18.6, 18.7, 18.8, 23.8, 27.8, 28.0, 28.2, 28.7, 30.2, 30.3, 30.4, 30.5, 30.6, 30.8, 30.9, 33.1, 33.6, 42.9, 47.7, 51.4, 57.7, 62.2, 64.0, 66.6, 69.5, 71.8, 73.2, 74.8, 76.8, 84.0, 99.2, 99.9, 130.8, 130.9, 158.5, 158.7, 158.9, 160.1, 170.4, 172.3.

*Dioleyl-adipyl-tobramycin (**24a**).* Following the procedure described for **13**, treatment of **23a** (150 mg, 0.09 mmol) by TFA (6 mL) in DCM (3 mL) provided **24a** (131 mg, 93%). ^{1}H NMR (MeOD, 25 °C) δ 0.92 (t, J = 6.7 Hz, 6H), 1.21−1.39 (m, 45H), 1.48−1.70 (m, 10H), 1.94−2.08 (m, 8H), 2.17−2.23 (m, 1H), 2.25−2.30 (m, 2H), 2.38−2.41 (m, 2H), 2.51−2.57 (m, 1H), 3.31−3.38 (m, 4H), 3.42−3.49 (m, 7H), 3.63−3.70 (m, 1H), 3.71−3.93 (m, 7H), 5.10 (d, J = 3.2 Hz, 1H), 5.32−5.38 (m, 4H), 5.45 (d, J = 3.7 Hz, 1H). ^{13}C NMR (MeOD, 25 °C) δ 14.4, 23.7, 26.2, 26.5, 27.8, 28.1, 28.8, 30.1, 30.2, 30.3, 30.4, 30.5, 30.6, 30.8, 31.1, 33.1, 33.8, 36.6, 40.8, 47.4, 49.8, 50.0, 50.9, 56.7, 58.7, 66.0, 67.6, 69.9, 75.5, 75.9, 81.1, 85.5, 97.0, 101.7, 130.8, 130.9, 174.8, 176.7. HRMS: calculated for $C_{60}H_{114}N_6O_{11}$ $[M + H]^+$ = 1095.8624, found 1095.8629.

*Dioleyl-suberyl-tobramycin (**24b**).* Following the procedure described for **13**, treatment of **23b** (98 mg, 0.06 mmol) by TFA (4 mL) in DCM (3 mL) provided **24b** (57 mg, 63%). ^{1}H NMR (MeOD, 25 °C) δ 0.90 (t, J = 7.2 Hz, 6H), 1.29−1.36 (m, 49H), 1.51−1.53 (m, 1H), 1.54−1.72 (m, 9H), 1.95−2.04 (m, 8H), 2.17−2.23 (m, 3H), 2.33−2.37 (m, 2H), 2.48−2.52 (m, 1H), 3.31−3.42 (m, 11H), 3.61−3.92 (m, 8H), 5.08 (d, J = 3.6 Hz, 1H), 5.32−5.38 (m, 4H), 5.45 (d, J = 3.2 Hz, 1H). ^{13}C NMR (MeOD, 25 °C) δ 14.5, 23.7, 26.6, 26.8, 27.8, 28.0, 28.1, 28.7, 29.7, 30.1, 30.2, 30.3, 30.5, 30.6, 30.8, 31.1, 33.1, 34.0, 36.9, 40.8, 47.3, 49.8, 50.0, 50.9, 56.7, 62.0, 65.9, 67.6, 69.9, 75.4, 75.5, 75.6, 81.3, 85.6, 97.1, 101.7, 130.8, 130.9, 175.1, 177.1. HRMS: calculated for $C_{62}H_{119}N_6O_{11}$ $[M + H]^+$ = 1123.8937, found 1123.8940.

*Dioleyl-sebacyl-tobramycin (**24c**).* Following the procedure described for **13**, treatment of **23c** (73 mg, 0.04 mmol) by TFA (4 mL) in DCM (3 mL) provided **24c** (52 mg, 77%). ^{1}H NMR (MeOD, 25 °C) δ 0.92 (t, J = 6.8 Hz, 6H), 1.29−1.36 (m, 53H), 1.54−1.69 (m, 10H), 1.97−2.06 (m, 8H), 2.15−2.28 (m, 3H), 2.31−2.38 (m, 2H), 2.47−2.55 (m, 1H), 3.31−3.56 (m, 10H), 3.67−3.94 (m, 9H), 5.09 (d, J = 3.6 Hz, 1H), 5.35−5.37 (m, 4H), 5.47 (d, J = 3.2 Hz, 1H). ^{13}C NMR (MeOD, 25 °C) δ 14.5, 23.8, 26.8, 26.9, 27.8, 28.0, 28.1, 28.7, 30.1, 30.2, 30.3, 30.4, 30.6, 30.8, 31.1, 33.1, 34.1, 36.9, 40.8, 49.8, 50.0, 50.9, 56.7, 62.0, 65.9, 67.6, 69.9, 75.4, 75.5, 75.7, 81.3, 85.6, 97.1, 101.7, 130.8, 130.9, 175.2, 177.2. HRMS: calculated for $C_{64}H_{123}N_6O_{11}$ $[M + H]^+$ = 1151.9250, found 1151.9252.

*Dioleyl-dithioglycolyl-tobramycin (**24d**).* Following the procedure described for **13**, treatment of **23d** (116 mg, 0.07 mmol) by TFA (6 mL) in DCM (3 mL) provided **24d** (78 mg, 73%). ^{1}H NMR (MeOD, 25 °C) δ 0.90 (t, J = 7.2 Hz, 6H), 1.23−1.34 (m, 45H), 1.52−1.69 (m, 6H), 1.95−2.03 (m, 8H), 2.20−2.23 (m, 1H), 2.47−2.54 (m, 1H), 3.31−3.37 (m, 6H), 3.46−3.68 (m, 7H), 3.73−3.93 (m, 10H), 5.08 (d, J = 3.6 Hz, 1H), 5.35−5.38 (m, 4H), 5.46 (d, J = 3.2 Hz, 1H). ^{13}C NMR (MeOD, 25 °C) δ 14.5, 23.8, 26.1, 27.8, 28.0, 28.1, 28.6, 30.1, 30.3, 30.4, 30.5, 30.6, 30.8, 31.3, 33.1, 33.6, 34.7, 41.4, 42.0, 42.8, 47.7, 51.0, 56.7, 62.0, 66.1, 67.6, 69.9, 75.5, 75.6, 85.7, 97.0, 101.7, 130.8, 130.9, 170.4, 172.1. HRMS: calculated for $C_{58}H_{110}N_6O_{11}S_2$ $[M + H]^+$ = 1131.7786, found 1131.779.

*2-((tert-Butoxycarbonyl)amino)propane-1,3-diyl Dioleate (**26**).* *N*-Boc-serinol **25** (500 mg, 2.61 mmol, 1 equiv) was dissolved in $CHCl_3$ (30 mL). Pyridine (0.63 mL, 7.84 mmol, 3 equiv) and oleoyl chloride (1.73 mL, 5.23 mmol, 2 equiv) were successively added and the mixture stirred at rt overnight. The mixture was then washed with NH_4Cl_{sat}, H_2O, and brine. The organic fraction was dried over $MgSO_4$ before purification by flash chromatography (DCM/MeOH), providing **26** (1.55 g, 88%). ^{1}H NMR ($CDCl_3$, 25 °C) δ 0.88 (t, J = 7.2 Hz, 6H), 1.19−1.34 (m, 40H), 1.45 (s, 9H), 1.56−1.63 (m, 4H), 1.98−2.05 (m, 8H), 2.31 (t, J = 7.6 Hz, 4H), 4.05−4.20 (m, 5H), 4.76−4.78 (bs, 1H), 5.30−5.37 (m, 4H). ^{13}C NMR ($CDCl_3$, 25 °C) δ 14.0, 23.7, 26.0, 28.1, 28.8, 30.2, 30.3, 30.4, 30.5, 30.6, 30.8, 30.9, 33.1, 34.9, 50.1, 64.1, 80.5, 130.8, 130.9, 157.9, 175.0.

*2-Aminopropane-1,3-diyldioleate Trifluoroacetate Salt (**27**).* To a solution of **26** (1.55 g, 2.15 mmol) in DCM (20 mL) was added TFA (2 mL) at 0 °C. The reaction mixture was stirred for 1 h at 0 °C and 2 h at rt, then concentrated. After three coevaporations with MeOH, the residue was purified by flash chromatography (DCM/MeOH) to provide **27** (1.11 g, 70%). ^{1}H NMR ($CDCl_3$, 25 °C) δ 0.88 (t, J = 6.8 Hz, 6H), 1.18−1.37 (m, 40H), 1.57−1.60 (m, 4H), 1.97−2.02 (m, 8H), 2.34 (t, J = 7.2 Hz), 3.73 (bs, 1H), 4.25−4.32 (m, 2H), 4.35−4.42 (m, 2H), 5.32−5.45 (m, 4H). ^{13}C NMR ($CDCl_3$, 25 °C) δ 14.1, 23.7, 25.8, 28.1, 30.2, 30.3, 30.4, 30.5, 30.6, 30.8, 33.1, 34.5, 50.7, 62.2, 130.8, 130.9, 174.4.

*4-((1,3-Bis(oleoyloxy)propan-2-yl)amino)-4-oxobutanoic Acid (**28**).* To a solution of **27** (1.11 g, 1.51 mmol, 1 equiv) in DCM (50 mL) were successively added succinic anhydride (0.358 g, 3.58 mmol, 2 equiv) and Et_3N (1 mL, 7.16 mmol, 4 equiv). The mixture was stirred at rt overnight, then quenched by addition of HCl 1M. After extraction, the organic layer was further washed with 1 M HCl and water (three times), dried over $MgSO_4$, and concentrated *in vacuo*. The residue was purified by flash chromatography (DCM/MeOH) to afford the desired acid **28** (1.01 g, 92%). ^{1}H NMR (MeOD, 25 °C) δ 0.90 (t, J = 7.2 Hz, 6H), 1.24−1.38 (m, 40H), 1.58−1.62 (m, 4H), 2.00−2.03 (m, 8H), 2.34 (t, J = 7.2 Hz, 4H), 2.48 (t, J = 7.6 Hz, 2H), 2.57 (t, J = 7.6 Hz, 2H), 4.06−4.17 (m, 4H), 4.33−4.36 (m, 1H), 5.28−5.38 (m, 4H). ^{13}C NMR ($CDCl_3$, 25 °C) δ 14.5, 23.8, 26.0, 28.2, 29.9, 30.2, 30.3, 30.4, 30.5, 30.6, 30.8, 31.6, 32.7, 33.1, 34.9, 52.2, 63.7, 130.8, 130.9, 147.6, 175.0, 176.2.

*2-(4-(1′,2″,3′,3‴-Tetra((trimethylsilyl)ethylcarbamate)-tobramycin-amino)-4-oxobutanamido)propane-1,3-diyldioleate (**29**).* Following the procedure described for compound **12**, reaction of amine **11** (141 mg, 0.13 mmol) with acid **28** (107 mg, 0.15 mmol), in the presence of HBTU (61 mg, 0.16 mmol) and DMAP (49 mg, 0.40 mmol) in DMF (40 mL), provided the expected compound **29** (182 mg, 80%). ^{1}H NMR (MeOD, 25 °C) δ 0.04−0.05 (m, 36H), 0.90 (t, J = 6.8 Hz, 6H), 0.99−1.03 (m, 8H), 1.26−1.38 (m, 41H), 1.55−1.69 (m, 6H), 1.93−2.12 (m, 9H), 2.33 (t, J = 7.2 Hz, 4H), 2.54 (s, 4H), 3.32−3.80 (m, 15H), 3.90−3.93 (m, 1H), 4.03−4.25 (m, 12H), 4.37−4.40 (m, 1H), 5.07 (s, 1H), 5.18 (s, 1H), 5.32−5.39 (m, 4H). ^{13}C NMR (MeOD, 25 °C) δ −1.4, 14.5, 18.6, 18.7, 18.8, 23.7, 26.0, 28.1, 30.2, 30.3, 30.4, 30.6, 30.8, 31.9, 33.1, 34.2, 34.9, 41.4, 47.9, 51.3, 51.6, 57.7, 62.2, 63.6, 64.0, 64.2, 66.9, 69.4, 71.8, 73.5, 74.8, 76.9, 82.4, 98.8, 99.8, 130.8, 130.9, 158.5, 158.8, 160.1, 174.6, 175.0, 175.2.

*Dioleyl-succinyl-serinyl-tobramycin (**30**).* Following the procedure described for **13**, treatment of **29** (180 mg, 0.10 mmol) by TFA (6 mL) in DCM (3 mL) provided **30** (125 mg, 75%). ^{1}H NMR (MeOD, 25 °C)

DOI: 10.1021/acs.jmedchem.5b01679
J. Med. Chem. 2016, 59, 3046−3062

δ 0.85 (t, J = 7.2 Hz, 6H), 1.19−1.32 (m, 41H), 1.51−1.60 (m, 4H), 1.88−2.03 (m, 9H), 2.09−2.18 (m, 1H), 2.31 (t, J = 7.2 Hz, 4H), 2.45−2.53 (m, 4H), 3.32−3.52 (m, 7H), 3.58−3.65 (m, 2H), 3.67−3.89 (m, 8H), 4.09 (m, 4H), 4.24−4.30 (m, 1H), 5.04 (d, J = 3.6 Hz, 1H), 5.28−5.31 (m, 4H), 5.37 (d, J = 3.2 Hz, 1H). ^{13}C NMR (MeOD, 25 °C) δ 14.5, 23.7, 26.0, 28.2, 30.2, 30.3, 30.4, 30.5, 30.6, 30.8, 31.1, 31.4, 31.7, 33.1, 34.9, 41.0, 49.8, 50.3, 51.0, 51.5, 56.7, 62.0, 63.5, 66.0, 67.6, 70.0, 75.5, 76.1, 96.9, 101.7, 130.8, 130.9, 175.0, 175.2. HRMS: calculated for $C_{61}H_{113}N_6O_{15}$ $[M + H]^+$ = 1169.8264, found 1169.8269.

Preparation of Complexes Solution. Formulations of nucleic acids with lipids were prepared as previously described.[31] Briefly, equal volume of nucleic acids (0.5 μg for DNA and mRNA and 0.15 μg or 0.3 μg for siRNA) was mixed with lipids, at a charge ratio (±) of 5 for *in vitro* transfection or at a charge ratio ranging from 0.1 to 6 for physicochemical characterization.

Physico-Chemical Characterization. The size distribution as a function of the charge ratio of lipoplexes was measured by dynamic light scattering using a Zeta-Sizer Nano Series Nano ZS-90 (Malvern). Complexes (100 μL) were made by mixing 1 μg of DNA and ionizable lipids, in NaCl 150 mM final concentration at different charge ratios ranged from 0.1 to 6. The particles with a size over 700 nm were considered as colloidally unstable. Ethidium bromide fluorescence measurements and retardation assays were performed as described.[31]

Nucleic Acids. pGWIZ-Luc (Genlantis) is a plasmid encoding the luciferase reporter gene under the control of the human cytomegalovirus immediate-early gene promoter. pGWIZ-eGFP (Clontech) is a plasmid encoding green fluorescent protein reporter gene, under the control of the human cytomegalovirus immediate-early gene promoter. Plasmids were purified from recombinant *Escherichia coli* by means of Endofree plasmid purification columns (Qiagen). mRNA encoding the luciferase and the green fluorescent protein was purchased from Trilink.

Human anti-lamin A/C siRNA (sc-35776) was purchased from Santa Cruz Biotechnology, and murine anti-lamin A/C siRNA (sense sequence: GGA-CCU-CGA-GGC-UCU-UCU-C) was obtained from Eurogentec.

Cell and Culture Conditions. The transfection activity of the various vectors was evaluated in transient transfection experiments with three different cell types. HeLa and C2C12 cells were grown in Dulbecco's modified Eagle's medium (DMEM) with a glucose concentration of 4.5 g/L, supplemented with 10% fetal calf serum, 1% of L-glutamine, and 1% of antibiotics (penicillin/streptomycin).

Primary cells as in rat aorta smooth muscle cells were provided by Nathalie Vaillant from the Institut du Thorax, in Nantes. Rat aorta smooth muscle cells were grown in Dulbecco's modified Eagle's medium (DMEM) with a glucose concentration of 1 g/L, supplemented with 10% fetal calf serum, 1% of L-glutamine, and 1% of antibiotics (penicillin/streptomycin). Human fibroblasts were provided by Caroline Chariau and Laurent David from the Nantes iPSC core facility. The medium used was Dulbecco's modified Eagle's medium (DMEM) with a glucose concentration of 4.5 g/L, with Glutamax, supplemented with HyClone Fetal Bovine Serum 10%, MEM Non-Essential Amino Acids 1%, and Sodium Pyruvate 1%.

All cells were routinely maintained at 37 °C in a humidified 5% CO_2/95% air containing atmosphere.

***In Vitro* Cell Transfection Assay.** Twenty-four hours prior to transfection cells were seeded in 24-well culture plates at a density of 55 000 cells per well for HeLa and for rat aorta smooth muscle cells and 31 000 cells per well for Human fibroblasts, in 1 mL of complete medium and incubated at 37 °C in a humidified 5% CO_2/95% air containing atmosphere.

Thirty minutes before transfection, medium was removed and replaced by 400 μL of fresh complete medium. One hundred microliters of lipoplexes was prepared by mixing two equal solutions containing the nucleic acids (0.5 μg for DNA and mRNA and 0.15 μg or 0.3 μg for siRNA) and the ionizable lipid at a charge ratios (±) of 5.

Luciferase Assay. After 24 h of incubation at 37 °C, 5% humidified CO_2, cells were washed with PBS and lysed in Reporter Lysis Buffer 1× (Promega) supplemented with 1 tablet per 50 mL of complete Mini Protease Inhibitor Cocktail (Roche Applied Sciences) according to manufacturer's recommendations. After overnight freezing cycle, cell lysates were centrifuged at 10 000 rpm during 5 min. Luciferase activity was measured on an aliquot of supernatant using the Luciferase Assay System kit (Promega) according to manufacturer's recommendations. Luminescence was recorded on a Victor X-3 multilabel plate reader (PerkinElmer). All measurements were performed in duplicate.

Microscopy. For fluorescence observation, rat aorta muscle cells were washed with PBS and fixed with 4% paraformaldehyde for 15 min at room temperature. Then, slides were mounted with Prolong Gold Antifading Reagent with DAPI (Life Technologies) and incubated for 24 h at room temperature before observation under a Zeiss Axiovert 200 microscope with an apotome unit and using appropriate filters. Images were treated using ImageJ 1.42q software.

Gene Silencing Experiments. For gene silencing experiment, cells were washed after 24 h of incubation, lysed using the NucleoSpin RNA/Protein assay (Macherey Nagel) to purify RNA, and quantified with NanoDrop 1000 Spectrophotometer (ThermoFisher Scientific). RT-qPCR were then realized in two phases. First, reverse transcriptions of RNA in cDNA were conducted using High Capacity cDNA Reverse Transcription Kits (Life Technologies) on GeneAmp PCR System 9700 Thermal Cycler (Life Technologies). Then, the expression of lamin A/C and HPRT was quantified by Real-Time PCR using Taqman Gene expression assays on StepOnePlus Real-Time PCR System (Life Technologies). Results were normalized against the expression levels of endogenous HPRT and expressed according to the 2-ΔΔCT formula. Probes used to amplify specific gene products from human or murine cDNA (Life technologies) were Hs00153462_m1 for human lamin A/C, Hs99999909_m1 for human HPRT, Mm00497783_m1 for murine lamin A/C, and Mm00446966_m1 for murine HPRT.

■ ASSOCIATED CONTENT

Supporting Information

The Supporting Information is available free of charge on the ACS Publications website at DOI: 10.1021/acs.jmedchem.5b01679.

^{1}H and ^{13}C NMR spectra of final compounds and head-to-head data with commercial Lipofectamine 3000 (PDF)

SMILES data (XLSX)

■ AUTHOR INFORMATION

Corresponding Author

*E-mail: bruno.pitard@incellart.com. Phone: (+33) 2 40 71 67 17.

Author Contributions

⊥These authors contributed equally to this work.

Notes

The authors declare no competing financial interest.

■ ACKNOWLEDGMENTS

The authors are very grateful to Caroline Chariau and Laurent David from Nantes iPSC core facility for their technical assistance for human fibroblast experiments and to Nathalie Vaillant for providing rat aorta smooth muscle cells. We are also indebted to P. Lehn and J.-M. Lehn for their pioneer works related to the synthesis of cationic lipids used in this study and for their stimulating discussions and constant interest in this work. We also thank S. Fukuyama for fruitful discussions throughout this study. The authors thank Marion Decossas for assistance with cryoTEM. This work was supported by special grants from BPI France Financement (Paris, France) for EMERIT project and from Région Pays de la Loire for HEPAVAC project. T.C. and L.D. are supported by funds from IHU-Cesti (French government financial support managed by the National Research Agency "Investment Into The Future" program ANR-10-IBHU-005, cosupported by Région Pays de la Loire and Nantes Métropole).

DOI: 10.1021/acs.jmedchem.5b01679
J. Med. Chem. 2016, 59, 3046−3062

■ ABBREVIATIONS USED

C2C12, mouse myoblast cell line; DMAP, 4-(dimethylamino)-pyridine; DMEM, Dulbecco's modified Eagle's medium; DMST, di-myristyl-succinyl-tobramycin; DOAT, di-oleyl-adipyl-tobramycin; DODT, di-oleyl-dithioglycolyl-tobramycin; DOSET, di-oleyl-sebacyl-tobramycin; DOSUT, di-oleyl-suberyl-tobramycin; DOSST, di-oleyl-succinyl-serinyl-tobramycin; DOST, di-oleyl-succinyl tobramycin; DPST, di-palmityl-succinyl-tobramycin; DSST, di-stearyl-succinyl-tobramycin; EDC, *N*-(3-(dimethylamino)-propyl)-*N*′-ethylcarbodiimide hydrochloride; eGFP, enhanced green fluorescent protein; HBTU, *N*,*N*,*N*′,*N*′-tetramethyl-*O*-(1*H*-benzotriazol-1-yl)uronium hexafluorophosphate; HeLa, human cervical cancer derived cells; HEPES, 4-(2-hydroxyethyl)-piperazine-1-ethanesulfonic acid; HPRT, hypoxanthine-guanine phosphoribosyltransferase; MEM, minimum essential medium; qRT-PCR, quantitative real-time PCR; RNAi, RNA interference; siRNA, small interfering RNA; SEM, standard error of mean

■ REFERENCES

(1) Sahin, U.; Kariko, K.; Türeci, O. mRNA based therapeutics: developing a new class of drugs. *Nat. Rev. Drug Discovery* **2014**, *13*, 759−780.

(2) Geall, A. J.; Mandl, C. W.; Ulmer, J. B. RNA: the new revolution in nucleic acid vaccines. *Semin. Immunol.* **2013**, *25*, 152−159.

(3) Whitehead, K. A.; Langer, R.; Anderson, D. A. Knocking down barriers: advances in siRNA delivery. *Nat. Rev. Drug Discovery* **2009**, *8*, 129−138.

(4) Resnier, P.; Montier, T.; Mathieu, V.; Benoit, J. P.; Passirani, C. A review of the current status of siRNA nanomedicines in the treatment of cancer. *Biomaterials* **2013**, *34*, 6429−6443.

(5) Mulligan, R. C. The basic science of gene therapy. *Science* **1993**, *260*, 926−932.

(6) Anderson, W. F. Human gene therapy. *Nature* **1998**, *392*, 25−30.

(7) Ibraheem, D.; Elaissari, A.; Fessi, H. Gene therapy and DNA delivery systems. *Int. J. Pharm.* **2014**, *459*, 70−83.

(8) Walther, W.; Stein, U. Viral vectors for gene transfer: a review of their use in the treatment of human diseases. *Drugs* **2000**, *60*, 249−271.

(9) Waehler, R.; Russell, S. J.; Curiel, D. T. Engineering targeted viral vectors for gene therapy. *Nat. Rev. Genet.* **2007**, *8*, 573−587.

(10) Warnock, J. N.; Daigre, C.; Al-Rubeai, M. Introduction to viral vectors. *Methods Mol. Biol.* **2011**, *737*, 1−25.

(11) Vannucci, L.; Lai, M.; Chiuppesi, F.; Ceccherini-Nelli, L.; Pistello, M. Viral vectors: a look back and ahead on gene transfer technology. *New Microbiol.* **2013**, *36*, 1−22.

(12) Mintzer, M. A.; Simanek, E. E. Nonviral vectors for gene delivery. *Chem. Rev.* **2009**, *109*, 259−302.

(13) Guo, X.; Huang, L. Recent Advances in Non-viral Vectors for Gene Delivery. *Acc. Chem. Res.* **2012**, *45*, 971−979.

(14) Junquera, E.; Aicart, E. Cationic lipids as transfecting agents of DNA in gene therapy. *Curr. Top. Med. Chem.* **2014**, *14*, 649−663.

(15) Junquera, E.; Aicart, E. Recent progress in gene therapy to deliver nucleic acids with multivalent cationic vectors. *Adv. Colloid Interface Sci.* **2015**, DOI: 10.1016/j.cis.2015.07.003.

(16) Yin, H.; Kanasty, R. L.; Eltoukhy, A. A.; Vegas, A. J.; Dorkin, J. R.; Anderson, D. G. Non-viral vectors for gene-based therapy. *Nat. Rev. Genet.* **2014**, *15*, 541−555.

(17) Zhi, D.; Zhang, S.; Cui, S.; Zhao, Y.; Wang, Y.; Zhao, D. The headgroup evolution of cationic lipids for gene delivery. *Bioconjugate Chem.* **2013**, *24*, 487−519.

(18) Zhi, D.; Zhang, S.; Wang, B.; Zhao, Y.; Yang, B.; Yu, S. Transfection efficiency of cationic lipids with different hydrophobic domains in gene delivery. *Bioconjugate Chem.* **2010**, *21*, 563−577.

(19) Draghici, B.; Ilies, M. A. Synthetic nucleic acid delivery systems: present and perspectives. *J. Med. Chem.* **2015**, *58*, 4091−4130.

(20) Wan, Y.; Moyle, P. M.; Toth, I. Endosome escape strategies for improving the efficacy of oligonucleotide delivery systems. *Curr. Med. Chem.* **2015**, *22*, 3326−3346.

(21) Varkouhi, A. K.; Scholte, M.; Storm, G.; Haisma, H. J. Endosomal escape pathways for delivery of biologicals. *J. Controlled Release* **2011**, *151*, 220−228.

(22) Gilleron, J.; Querbes, W.; Zeigerer, A.; Borodovsky, A.; Marsico, G.; Schubert, U.; Manygoats, K.; Seifert, S.; Andree, C.; Stöter, M.; Epstein-Barash, H.; Zhang, L.; Koteliansky, V.; Fitzgerald, K.; Fava, E.; Bickle, M.; Kalaidzidis, Y.; Akinc, A.; Maier, M.; Zerial, M. Image-based analysis of lipid nanoparticle-mediated siRNA delivery, intracellular trafficking and endosomal escape. *Nat. Biotechnol.* **2013**, *31*, 638−650.

(23) Gujrati, M.; Malamas, A.; Shin, T.; Jin, E.; Sun, Y.; Lu, Z. R. Multifunctional cationic lipid-based nanoparticles facilitate endosomal escape and reduction-triggered cytosolic siRNA release. *Mol. Pharmaceutics* **2014**, *11*, 2734−2744.

(24) Hafez, I. M.; Maurer, N.; Cullis, P. R. On the mechanism whereby cationic lipids promote intracellular delivery of polynucleic acids. *Gene Ther.* **2001**, *8*, 1188−1196.

(25) Xu, Y.; Czoka, F. C. Mechanism of DNA release from cationic liposome/DNA complexes used in cell transfection. *Biochemistry* **1996**, *35*, 5616−5623.

(26) Le Bihan, O.; Chèvre, R.; Mornet, S.; Garnier, B.; Pitard, B.; Lambert, O. Probing the in vitro mechanism of action of cationic lipid/DNA lipoplexes at a nanometric scale. *Nucleic Acids Res.* **2011**, *39*, 1595−1609.

(27) Belmont, P.; Aissaoui, A.; Hauchecorne, M.; Oudrhiri, N.; Petit, L.; Vigneron, J. P.; Lehn, J. M.; Lehn, P. Aminoglycoside-derived cationic lipids as efficient vectors for gene transfection *in vitro* and *in vivo*. *J. Gene Med.* **2002**, *4*, 517−526.

(28) Sainlos, M.; Belmont, P.; Vigneron, J. P.; Lehn, P.; Lehn, J. M. Aminoglycoside-derived cationic lipids for gene transfection: Synthesis of kanamycin A derivatives. *Eur. J. Org. Chem.* **2003**, *15*, 2764−2774.

(29) Sainlos, M.; Hauchecorne, M.; Oudrhiri, N.; Zertal-Zidani, S.; Aissaoui, A.; Vigneron, J. P.; Lehn, J. M.; Lehn, P. Kanamycin A-derived cationic lipids as vectors for gene transfection. *ChemBioChem* **2005**, *6*, 1023−1033.

(30) Mevel, M.; Sainlos, M.; Chatin, B.; Oudrhiri, N.; Hauchecorne, M.; Lambert, O.; Vigneron, J. P.; Lehn, P.; Pitard, B.; Lehn, J. M. Paromomycin and neomycin B derived cationic lipids: synthesis and transfection studies. *J. Controlled Release* **2012**, *158*, 461−469.

(31) Desigaux, L.; Sainlos, M.; Lambert, O.; Chevre, R.; Letrou-Bonneval, E.; Vigneron, J. P.; Lehn, P.; Lehn, J. M.; Pitard, B. Self-assembled lamellar complexes of siRNA with lipidic aminoglycoside derivatives promote efficient siRNA delivery and interference. *Proc. Natl. Acad. Sci. U. S. A.* **2007**, *104*, 16534−16539.

(32) Hendrix, M.; Priestley, E. S.; Joyce, G. F.; Wong, C. H. Direct observation of aminoglycoside-RNA interactions by surface plasmon resonance. *J. Am. Chem. Soc.* **1997**, *119*, 3641−3648.

(33) Thomas, J. R.; Hergenrother, P. J. Targeting RNA with small molecules. *Chem. Rev.* **2008**, *108*, 1171−1224.

(34) Elouahabi, E.; Ruysschaert, J. M. Formation and intracellular trafficking of lipoplexes and polyplexes. *Mol. Ther.* **2005**, *11*, 336−347.

(35) Martin, B.; Sainlos, M.; Aissaoui, A.; Oudrhiri, N.; Hauchecorne, N.; Vigneron, J. P.; Lehn, J. M.; Lehn, P. The design of cationic lipids for gene delivery. *Curr. Pharm. Des.* **2005**, *11*, 375−394.

(36) Wetzer, B.; Byk, G.; Frederic, M.; Airiau, M.; Blanche, F.; Pitard, P.; Scherman, D. Reducible cationic lipids for gene transfer. *Biochem. J.* **2001**, *356*, 747.

(37) Lv, H.; Zhang, S. B.; Wang, B.; Cui, S. H.; Yan, J. Toxicity of cationic lipids and cationic polymers in gene delivery. *J. Controlled Release* **2006**, *114*, 100−109.

(38) Tang, F.; Hughes, J. A. Introduction of a disulfide bond into a cationic lipid enhances transgene expression of plasmid DNA. *Biochem. Biophys. Res. Commun.* **1998**, *242*, 141−145.

(39) Shirazi, R. S.; Ewert, K. K.; Leal, C.; Majzoub, R. N.; Bouxsein, N. F.; Safinya, C. R. Synthesis and characterization of degradable multivalent cationic lipids with disulfide bond spacer for gene delivery. *Biochim. Biophys. Acta, Biomembr.* **2011**, *1808*, 2156−2166.

(40) Streicher, W.; Loibner, H.; Hildebrandt, J.; Turnowsky, F. Synthesis and structure/activity relationships of new guanidino

DOI: 10.1021/acs.jmedchem.5b01679
J. Med. Chem. 2016, 59, 3046−3062

derivatives of aminoglycoside antibiotics. *Drugs Exp. Clin. Res.* **1983**, *9*, 591−598.
(41) Leventis, R.; Silvius, J. R. Interactions of mammalian cells with lipid dispersions containing novel metabolizable cationic amphiphiles. *Biochim. Biophys. Acta, Biomembr.* **1990**, *1023*, 124−132.
(42) Behr, J. P. Gene transfer with synthetic cationic amphiphiles: prospects for gene therapy. *Bioconjugate Chem.* **1994**, *5*, 382−389.
(43) Barteau, B.; Chèvre, R.; Letrou-Bonneval, E.; Labas, R.; Lambert, O.; Pitard, B. Physicochemical parameters of non-viral vectors that govern transfection efficiency. *Curr. Gene Ther.* **2008**, *8*, 313−323.
(44) Khalil, I. A.; Kogure, K.; Akita, H.; Harashima, H. Uptake pathways and subsequent intracellular trafficking in nonviral gene delivery. *Pharmacol. Rev.* **2006**, *58*, 32−45.
(45) Baichao, M.; Shubiao, Z.; Huiming, J.; Budiao, Z.; Hongtao, L. Lipoplex morphologies and their influences on transfection efficiency in gene delivery. *J. Controlled Release* **2007**, *123*, 184−194.
(46) Wasungu, L.; Hoekstra, D. Cationic lipids, lipoplexes and intracellular delivery of genes. *J. Controlled Release* **2006**, *116*, 255−264.
(47) Billiet, L.; Gomez, J. P.; Berchel, M.; Jaffrès, P. A.; Le Gall, T.; Montier, T.; Bertrand, E.; Cheradame, H.; Guégan, P.; Mével, M.; Pitard, B.; Benvegnu, T.; Lehn, P.; Pichon, C.; Midoux, P. Gene transfer by chemical vectors, and endocytosis routes of polyplexes, lipoplexes and lipopolyplexes in a myoblast cell line. *Biomaterials* **2012**, *33*, 2980−2990.
(48) Rejman, J.; Oberle, V.; Zuhorn, I. S.; Hoekstra, D. Size-dependent internalization of particles via the pathways of clathrin and caveolae-mediated endocytosis. *Biochem. J.* **2004**, *377*, 159−169.

DOI: 10.1021/acs.jmedchem.5b01679
J. Med. Chem. 2016, 59, 3046−3062

Article 5 : Important role of phosphoramido linkage in imidazole-based dioleyl helper lipids for liposome stability and primary cell transfection.

THE JOURNAL OF GENE MEDICINE
J Gene Med 2016; **15**: 3–15.
Published online in Wiley Online Library (wileyonlinelibrary.com) **DOI:** 10.1002/jgm.2869

RESEARCH ARTICLE

Important role of phosphoramido linkage in imidazole-based dioleyl helper lipids for liposome stability and primary cell transfection

Mathieu Mével[1,2†]
Thomas Haudebourg[1,2†]
Thibault Colombani[1,2]
Pauline Peuziat[1,2]
Laurence Dallet[1,2,3]
Benoît Chatin[1,2]
Olivier Lambert[3]
Mathieu Berchel[4]
Tristan Montier[5,6]
Paul-Alain Jaffrès[4]
Pierre Lehn[5]
Bruno Pitard[1,2*]

[1]*Unité INSERM UMR 1087, CNRS UMR 6291, Nantes, France*

[2]*Université de Nantes, l'institut du thorax, Nantes, France*

[3]*CBMN UMR-CNRS 5248 IECB, Université de Bordeaux 1-IPB, Pessac, France*

[4]*UMR CNRS 6521, IFR 148 ScInBioS, Université de Bretagne Occidentale, Université Européenne de Bretagne, Brest, France*

[5]*Unité INSERM 1078, IFR 148 ScInBioS, Université de Bretagne Occidentale, Université Européenne de Bretagne, Brest Cedex, France*

[6]*Service de Génétique Moléculaire et d'histocompatibilité, CHUR, Brest, France*

*Correspondence to: B. Pitard, INCELL-ART, 21 rue La Noue Bras de Fer, 44200 Nantes, France.
E-mail: bruno.pitard@incellart.com
†These authors contributed equally to this work.

Received: 4 September 2015
Revised: 28 October 2015
Accepted: 29 October 2015

Copyright © 2015 John Wiley & Sons, Ltd.

Abstract

Background To optimize synthetic gene delivery systems, there is a need to develop more efficient lipid formulations. Most cationic lipid formulations contain 'helper' neutral lipids because of their ability to increase DNA delivery, in particular by improving endosomal escape of DNA molecules via the pH-buffering effect of protonatable groups and/or fusion with the lipid bilayer of endosomes.

Methods We evaluated the influence of the linker structure between the two oleyl chains in the helper lipid on transfection efficiency in cell lines, as well as in primary cells (hepatocytes/cardiomyocytes). We reported the synthesis of two new pH-buffering imidazole helper lipids characterized by a polar headgroup containing one (compound **6**) or two (compound **5**) imidazole groups and two oleyl chains linked by an amide group. We studied their association with the aminoglycoside lipidic derivative dioleylsuccinylparomomycin (DOSP), which contains two oleyl chains linked to the aminoglycoside polar headgroup via an amide function. We compared the morphology and transfection properties of such binary liposomes of DOSP/**5** and DOSP/**6** with those of liposomes combining DOSP with another imidazole-based dioleyl helper lipid (MM27) in which a phosphoramido group acts as a linker between the two oleyl chains and imidazole function.

Results The phosphoramido linker in the helper lipid induces a major difference in terms of morphology and resistance to decomplexation at physical pH for DOSP/helper lipid complexes.

Conclusions This hybrid dioleyl linker composition of DOSP/MM27 led to higher transfection efficiency in cell lines and in primary cells compared to complexes with homogeneous dioleyl linker. Copyright © 2015 John Wiley & Sons, Ltd.

Keywords helper lipid; liposome; non viral vector; primary cell; transfection

Introduction

Developing new, highly efficient and nontoxic gene delivery systems remains an important challenge for both basic and clinical research. Indeed, cationic lipids and polymers have been used routinely ever since Felgner *et al*. [1]

and Wu *et al.* [2] demonstrated their capacities to deliver nucleic acid in vitro. Most cationic liposome systems for nucleic acid delivery are based on the formulation of a cationic lipid with a neutral helper lipid such as dioleylphosphatidyl-choline (DOPC) [3], dioleoyl-L-α-phosphatidylethanolamine (DOPE) [4] or cholesterol [5]. The formation of lipoplexes that results from the association of preformed cationic liposomes and DNA molecules is mainly driven by electrostatic interactions between the positive charges of the cationic lipid headgroups and the negative phosphate groups along the DNA molecules. This interaction determines both the characteristics and the transfection potential of lipoplexes. The structure of lipoplexes formed from various cationic lipids and DNA were extensively analysed by cryo-transmission electron microscopy (cryo-TEM) and showed ordered multilamellar particles characterized by an even spacing [6,7].

Lipoplexes are internalized within cells via endocytosis and thus trapped in the endosomes without access to the cytosol and subsequently to the nucleus. Therefore, escape of lipoplexes from endosomes is essential for efficient gene transfection [8] and needs to occur rapidly to avoid the subsequent degradation of DNA by specific enzymes in lysosomes. To allow endosomal escape, the use of a helper lipid in the cationic lipid formulation remains the preferred and most investigated strategy.

The neutral helper lipid DOPE, a natural fusogenic lipid, has been extensively used in cationic liposome formulations [9]. It has been proposed that DOPE may promote fusion with the endosomal membrane allowing thereby release of the DNA into the cytoplasm, and improvement of its intracellular trafficking [10]. However, DOPE has limited utility *in vivo* because its high fusogenic nature, which helps to promote transfection *in vitro*, renders lipoplexes too unstable with respect to aggregation in the more complex *in vivo* environment[11].

The suggested proton-sponge effect has been used recently to design two lipophosphoramidate helper lipids, MM27 and MM37, which are derivatives from histamine or histidine, respectively [12–15]. It was shown that the use of these helper lipids enhances transfection levels by up to 100-fold compared to formulation with DOPE.

Such an effect can be explained by two factors: (i) these helper lipids have strong proton absorbing capabilities as a result of their imidazole rings (pK_a of approximately 6). Indeed, because of their low pKa value, imidazole rings should be unprotonated at pH 7 prior to lipoplex entry into cells and become protonated post-endocytosis when the endosomal compartments are acidified to pH 5.5. This phenomenon leads to chloride accumulation, organelle swelling and eventual endosomolysis by an osmotic shock type mechanism, finally allowing the release of DNA. (ii) MM27-based formulations were more fusogenic at pH 6 than at pH 7.4. This property contributes to destabilize the endosomal membrane. The development of fusogenic lipids or helper lipids constitutes a strategy that was reported previously [16–18].

Over recent years, we have directed our research efforts towards the development of a novel family of cationic lipids characterized by cationic headgroups consisting of aminoglycosides [19–22]. We reasoned that aminoglycosides should constitute cationic moieties of great interest because of their natural affinity for nucleic acids, as well as their structural variety and multifunctionality [23–25]. Our previous studies clearly demonstrated the feasibility of using an aminoglycoside as headgroup of a cationic lipid and validated our approach. The lipidic aminoglycoside derivative of paromomycin, termed DOSP and bearing an aminoglycoside as polar headgroup and a dioleylamino hydrophobic backbone, was indeed found to be efficient for gene transfection of various cell lines *in vitro*.

The MM27 imidazole-based helper lipid has been associated in different studies with monocationic lipophosphoramidates, displaying different polar heads but sharing the same phosphoramido linker between the two hydrophobic oleyl chains, leading to liposomes with a homogeneous dioleyl linker [12,26,27]. In all of these studies, the results showed that using MM27 enhanced transfection levels were obtained in most cases. Nevertheless, the efficiency of MM27 with a polycationic lipid having a different linker between the two oleyl chains and the polar head remains to be demonstrated for DNA transfection in particular on primary cells.

Therefore, we investigated whether associating the cationic lipid DOSP with an imidazole-based helper lipid displaying (i) a similar amido linker between the oleyl chains, leading to liposomes with a homogeneous dioleyl linker, or (ii) a phosphoramido linker as in MM27, leading to liposomes with a hybrid dioleyl linker, would be preferable for the stability of complexes with DNA and for the enhancement of gene transfection efficiency.

In the present study, we describe the synthesis and use of such imidazole-based helper lipids having an amido or phosphoramido linker. Furthermore, we also characterized the DNA complexation and transfection properties of the polycationic lipid DOSP when formulated with these helper lipids using not only cell lines, but also primary cells.

Materials and methods

All reagents were purchased from Acros Organics (Thermo Fisher Scientific, Waltham, MA, USA) or Sigma-Aldrich (St Louis, MO, USA) and were used without further purification. Reactions requiring anhydrous conditions were performed under nitrogen. Column chromatographies

Copyright © 2015 John Wiley & Sons, Ltd.

were conducted on silica gel Kieselgel SI60 (40–63 μm) obtained from Merck (Darmstadt, Germany). Dichloromethane was distilled from calcium hydride under argon prior to use. Triethylamine was dried and distilled over KOH. Nuclear magnetic resonance (NMR) spectra were recorded at room temperature with a Bruker AC 300 spectrometer at 300 MHz (^{1}H), 75 MHz (^{13}C) or with an AVANCE 400 MHz at 400 MHz (^{1}H) and 100 MHz (^{13}C) (Bruker Instruments, Inc., Billerica, MA, USA). Chemical shifts are reported in parts per million (p.p.m.); coupling constants are reported in units of Hertz (Hz) (s, singlet; d, doublet; t, triplet; q, quartet; quin, quintet; br, broad singlet). When needed, ^{13}C heteronuclear heteronuclear multiple-quantum correlation (HMQC) and heteronuclear multiple-bond correlation (HMBC) were used to unambiguously establish structures. High-resolution mass spectra (HRMS) were recorded with a hybrid LTQ-orbitrap spectrometer (ESI$^+$) (Thermo Fisher Scientific, Waltham, MA, USA) and with a Autoflex III SmartBeam spectrometer (Bruker Daltonik GmbH, Bremen, Germany) (MALDI). Lipofectamine was obtained from Thermo Fisher Scientific (Grand Island, NY, USA).

The synthesis of dioleylamine (**1**) has been reported previously [21].

Synthesis

General procedure for the synthesis of the amino ampliphiles
Dioleylamine (200 mg, 0.39 mmol) was dissolved in dry CH_2Cl_2, then triphosgene (115 mg, 0.39 mmol) was added at 0°C under a nitrogen atmosphere followed by the addition of dry NEt_3 (270 µl, 1.95 mmol). The reaction was stirred 30 min at 0°C and 90 min at 20°C. The formation of the carbamoylchloride was confirmed by ^{1}H NMR. After evaporation under reduced pressure, 20 ml of dry CH_2Cl_2 was added to the crude product. The solution was then added drop by drop, under a nitrogen atmosphere, to a solution of TREN (1.16 ml, 7.8 mmol) in 30 ml of dry CH_2Cl_2 or to a solution of ethylenediamine (521 µl, 7.8 mmol) in 30 ml of dry CH_2Cl_2. The solution was stirred overnight at 20°C. After washing with water (2 × 50 ml) and with brine (50 ml), the organic phase was dried over Na_2SO_4, filtered and evaporated to give the desired compound as yellow oil. (yield: **3** = 91%; **4** = 94%).

3-(2-(bis(2-aminoethyl)amino)ethyl)-1,1-di((Z)-octadec-9-enyl)urea (3). ^{1}H NMR ($CDCl_3$): 0.85 (t, 6H, CH_3, $^3J_{H\text{-}H}$ = 6.3 Hz); 1.24 (m, 44H, CH_2); 1.48 (m, 4H, CH_2 β-N); 1.64 (4H, 2 NH_2); 1.98 (m, 8H, CH_2 α-CH=CH); 2.50 (m, 4H $(CH_2)_2N$); 2.56 (m, 2H, CH_2N); 2.73 (m, 4H, 2 CH_2NH_2); 3.16 (t, 4H, CH_2 α-N, $^3J_{H\text{-}H}$ = 7.5 Hz); 3.27 (m, 2H, CH_2NH); 5.15 (m, 1H, NH); 5.29 (m, 4H, CH=CH); ^{13}C NMR ($CDCl_3$): 14,0 (s, 2 CH_3), 22.6–32.5 (s, 28 CH_2 fatty chains), 38.6 (s, $CONHCH_2$), 39.9 (2 CH_2NH_2), 47.3 (s, 2 CH_2 α-N), 54.0 (s, CH_2N), 57.1 (s, 2 CH_2N), 129.7 (s, 2 CH=CH), 129.9 (s, 2 CH=CH), 157.7 (CO); HRMS for $C_{43}H_{87}N_5ONa$ $[M+Na]^+$, calcd 712.6803 found 712.6792.

3-(2-aminoethyl)-1,1-di((Z)-octadec-9-enyl)urea (4). ^{1}H NMR ($CDCl_3$): 0.87 (t, 6H, CH_3, $^3J_{H\text{-}H}$ = 6.8 Hz); 1.26 (m, 44H, CH_2); 1.53 (m, 4H, CH_2 β-N); 1.54 (m, 2H, NH_2); 2.00 (m, 8H, CH_2 α-CH=CH); 2.82 (t, 2H, CH_2NH_2, $^3J_{H\text{-}H}$ = 5.6 Hz); 3.16 (t, 4H, CH_2 α-N, $^3J_{H\text{-}H}$ = 7.6Hz); 3.28 (m, 2H, CH_2NH); 4.81 (m, 1H, NH); 5.34 (m, 4H, CH=CH); ^{13}C NMR ($CDCl_3$): 14.1 (s, 2 CH_3), 22.6–32.0 (s, 28 CH_2 fatty chains), 41.9 (s, CH_2NH_2), 43.0 (s, $CONHCH_2$), 47.4 (s, 2 CH_2 α-N), 129.8 (s, 2 CH=CH); 130.0 (s, 2 CH=CH); 157.9 (CO); HRMS for $C_{39}H_{77}N_3ONa$ $[M+H]^+$, calcd 604.6139 found 604.6131.

General procedure for the synthesis of the imidazolo amphiphiles
Compounds **3** (300 mg, 0.43 mmol) and **4** (262 mg, 0.43 mmol) were dissolved in absolute ethanol, then imidazole carboxaldehyde (87 mg, 0.9 mmol or 45.5 mg, 0.47 mmol) and an excess of Na_2SO_4 was added under a nitrogen atmosphere. The reaction was heated at reflux for 4 h. The formation of the imine was confirmed by ^{1}H NMR. After filtration and evaporation under reduce pressure, 20 ml of a solution of MeOH and CH_2Cl_2 (50/50) was added to the crude product. Then $NaBH_4$ (97.6 mg, 2.58 mmol or 48.8 mg, 1.29 mmol) was added under a nitrogen atmosphere at 0°C. The reaction was stirred 1 h at 0°C and overnight at 20°C. After evaporation the residue was dissolved in CH_2Cl_2 (50 ml), washed, respectively, with a solution of 10% Na_2CO_3 in water, water and brine, dried over Na_2SO_4, filtered and evaporated. After purification by silica column chromatography (CH_2Cl_2/MeOH 100/0–80/20), these compounds were obtained as orange oils. (yield: **5** = 95%; **6** = 85%).

3-(2-(bis(2-((1H-imidazol-2-yl)methylamino)ethyl)amino) ethyl)-1,1-di((Z)-octadec-9 enyl)urea (5). ^{1}H NMR ($CDCl_3$): 0.86 (t, 6H, CH_3, $^3J_{H\text{-}H}$ = 6.4 Hz); 1.24 (m, 44H, CH_2); 1.45 (m, 4H, CH_2 β-N); 1.97 (m, 8H, CH_2 α-CH=CH); 2.50 (m, 6H $(CH_2)_3N$); 2.61 (m, 4H, 2 CH_2NH); 3.09 (t, 4H, CH_2 α-N, $^3J_{H\text{-}H}$ = 7.6 Hz); 3.27 (m, 2H, CH_2NH); 3.90 (m, 4H, CH_2-Imidazole); 5.23 (m, 1H, NH); 5.33 (m, 4H, CH=CH); 6,92 (s, 4H, CH from Imidazole); ^{13}C NMR ($CDCl_3$): 14 (s, 2 CH_3), 22.5–32.5 (s, 28 CH_2 fatty chains), 39.6 (s, $CONHCH_2$), 45.7 (s, 2 CH_2NH), 46.0 (s, 2 CH_2-Im), 47.4 (s, 2 CH_2 α-N), 53.2 (s, 2 CH_2N), 53.4 (s, CH_2N), 121.8 (s, 4 CH from Imidazole), 129.7 (s, 2 CH=CH), 129.9 (s, 2 CH=CH), 147.0 (s, 2 C from Imidazole), 158.3 (CO); HRMS for $C_{51}H_{95}N_9ONa$ $[M+Na]^+$, calcd 872.7552 found 872.7552.

3-(2-((1H-imidazol-2-yl)methylamino)ethyl)-1,1-di((Z)-octadec-9-enyl)urea (6). ^{1}H NMR ($CDCl_3$): 0.87 (t, 6H,

Copyright © 2015 John Wiley & Sons, Ltd.

CH_3, $^3J_{H\text{-}H}$ = 7.2 Hz); 1.26 (m, 44H, CH_2); 1.51 (m, 4H, CH_2 β-N); 2.01 (m, 8H, CH_2 α-CH=CH); 2.80 (m, 2H, CH_2NH); 3.16 (t, 4H, CH_2 α-N, $^3J_{H\text{-}H}$ = 7.2 Hz); 3.36 (m, 2H, CH_2NH); 3.94 (m, 2H, CH_2-Imidazole); 5.01 (m, 1H, NH); 5.34 (m, 4H, CH=CH); 6,96 (s, 2H, CH from Imidazole); ^{13}C NMR ($CDCl_3$): 14.1 (s, 2 CH_3), 22.6–32.0 (s, 28 CH_2 fatty chains), 39.8 (s, $CONHCH_2$), 45.6 (s, CH_2-Im), 47.5 (s, 2 CH_2 α-N), 49.0 (s, CH_2NH), 122.0 (s, 2 CH from Imidazole), 129.7 (s, 2 CH=CH), 130.0 (s, 2 CH=CH), 146.1 (s, C from Imidazole), 158.3 (CO); HRMS for $C_{43}H_{81}N_5ONa$ $[M+Na]^+$, calcd 706.6333 found 706.6339.

Plasmids

pCMV-Luc (Genlantis, San Diego, CA, USA) is a plasmid encoding the luciferase reporter gene under the control of the human cytomegalovirus immediate-early gene promoter. pCMV-GFP (Clontech, Palo Alto, CA, USA) is a plasmid encoding green fluorescent protein reporter gene, under the control of the human cytomegalovirus immediate–early gene promoter. Plasmids were purified from recombinant Escherichia coli by means of Endofree plasmid purification columns (Qiagen, Hilden, Germany).

Preparation of cationic lipids formulations for *in vitro* use

All lipids were stored as stock solutions in anhydrous organic solvents ($CHCl_3$, MeOH or a mixture of both), at −20°C. Formulations were made with a cationic lipid DOSP with or without helper lipids (MM27, **5** and **6**) at a standard molar ratio of 1:1 (mol/mol) to give a cationic liposome suspension with a fixed total positive charge concentration of 10 mM in water for *in vitro* assays, considering DOSP bears four positive charges per molecule. Appropriate volumes of each lipid stock were placed in a round-bottom flask (typically 5 ml). The solvent was slowly removed *in vacuo* to ensure production of an even lipid film. The film was rehydrated overnight at 4°C with water at a defined volume. The resulting solution was sonicated for 10–15 min at room temperature to form liposomes of appropriate size.

Preparation of DNA lipoplexes

Formulation of DNA with DOSP liposomes were prepared as previously described [28]. Briefly, an equal volume of DNA (10 μg for physico-chemical characterization or 0.5 μg for *in vitro* cells transfection) was mixed with DOSP liposomes associated or not with a helper lipid (MM27, **5** and **6**), at a charge ratio (+/−) of 4.

Cryo-TEM microscopy

Formulation complexes were prepared at 10 μg DNA/ml at a charge ratio (+/−) of 4, in NaCl at a final concentration of 150 mM. Five-microliter samples were deposited onto a holey carbon coated copper grid; the excess was blotted with a filter paper, and this grid was plunged into a liquid ethane bath cooled with nitrogen (Leica EM CPC; Leica Microsystems, Wetzlar, Germany). Specimens were maintained at a temperature of approximatively −170°C, using a cryo holder (Gatan Inc., Pleasanton, CA, USA), and were observed with a FEI Tecnai F20 electron microscope operating at 200 kV and at a nominal magnification (×50 000) under low-dose conditions. Images were recorded with a 2K × 2K Gatan slow scan CCD camera.

Entrapment efficiency

Ethidium bromide (EtBr) fluorescence measurements were performed to determine the compaction of DNA by liposomes and were carried out on a Jobin-Yvon spex Fluoromax-4 spectrofluorimeter (Horiba Instruments, Irvine, CA, USA). Residual fluorescence displayed upon intercalation between noncomplexed DNA base pairs was monitored (excitation, 260 nm; emission, 560 nm) after adding EtBr (4 μg). DNA–lipid complexes (2 ml) were formed at a charge ratio of 4, ensuring complete complexation, and a kinetic analysis was used to monitor the increase of EtBr fluorescence after rapidly adding 10 μl of a solution containing sodium hexametaphosphate, at a concentration of 4 mg/ml. These small and highly diffusible polyphosphates can competitively form complexes with cationic lipids as a result of the negative charges borne by the phosphates. A magnetic stirrer at the bottom of the quartz cell ensured the homogenization of the solution.

The influence of the pH on DNA release was studied by forming the complexes in 10 mM HEPES buffer at pH 7 or 7.16 to mimic extracellular conditions and 10 mM MES buffer at pH 5.26, 6.36 or 6.5, modelling endosomal conditions.

Cell and culture conditions

The transfection activity of the various vectors was evaluated in transient transfection experiments with four different cell lines. The cells lines tested were the HEK293 cell line, which is adenovirus-transformed human embryo kidney cells, and the C2C12, which is derived from mouse myoblast. All cells were grown in Dulbecco's modified

Copyright © 2015 John Wiley & Sons, Ltd.

Eagle's medium (DMEM) supplemented with 10% fetal calf serum (FCS), 1% of L-glutamine and 1% of antibiotics (Pen/Strep) and routinely maintained at 37°C in a humidified 5% CO_2/95% air containing atmosphere.

For cardiomyocytes, briefly, newborn rat ventricles were dissected and dissociated in 9 ml of ADS buffer (NaCl 6.8 g/l, HEPES 4.76 g/l, NaH_2PO_4 120 mg/l, KCl 400 mg/l, glucose 1 g/l, $MgSO_4$ 100 mg/l, pH 7.4) containing 430 mg/ml of collagenase and 500 mg/ml of pancreatin at 37°C with gentle shaking. After 20 min of incubation, 1 ml of FCS was added and supernatant was centrifuged to collect cells. Then, total heart cells were separated by centrifugation on a 46–65% Percoll gradient. Cardiomyocytes were collected, seeded onto gelatine-coated plates and cultured during 24 h before transfection in a medium containing DMEM, 17% of medium 199, 10% of heat inactivated horse serum, 5% FCS and 1% of antibiotics (Pen/Strep).

24-well culture plates of fresh hepatocytes were obtained from Biopredic (Saint Gregoire, France).

Twenty-four hours prior to transfection, HEK, C2C12 and rat neonatal cardiomyocyte cells were seeded in 24-well culture plates at a density of 100 000 cells per well for HEK, 40 000 cells per well for C2C12 and 100 000 cells per well for rat neonatal cardiomyocytes, in 1 ml of complete medium and incubated at 37°C in a humidified 5% CO_2/95% air containing atmosphere.

Transfection

Twenty-four hours prior to transfection, cells were seeded as described above. Lipoplexes were prepared by mixing two equal solutions containing 0.5 μg of plasmid DNA and the lipidic vector at a charge ratio (+/−) of 4. Lipofectamine® (Thermo Fisher Scientific) was used in accordance with the manufacturer's instructions. Before transfection, medium was removed and replaced by 400 μl of fresh complete medium and 100 μl of lipoplex.

Luciferase assay

After 24 h of incubation at 37°C, 5% humidified CO_2, cells were washed and lysed in Reporter Lysis Buffer 1X (Promega, Madison, WI, USA) supplemented with complete Mini Protease Inhibitor Cocktail (Roche Applied Sciences, Penzberg, Germany) in accordance with the manufacturer's instructions. Cell lysates were centrifuged at 9000 ***g*** for 5 min at 4°C. Luciferase activity was measured on an aliquot of supernatant using the Luciferase Assay System kit (Promega) in accordance with the manufacturer's instructions. Luminescence was recorded on a Victor X-3 multilabel plate reader (Perkin Elmer, Waltham, MA, USA). All measurements were performed in triplicate.

Cell viability

Twenty-four hours prior to transfection, cells were seeded as described above. Before transfection, medium was removed and replaced by 400 μl of fresh complete medium. Each well received 0.5 μg of pCMV-Luc plasmid complexed to lipidic vectors in OptiMEM® at the same charge ratios used for transfection. As a control, Lipofectamine® was used in accordance with the manufacturer's instructions. Cells on the standard plate received only vehicle (OptiMEM®). After 24 h of incubation at 37°C, 5% humidified CO_2, cytotoxicity was measured using the Cell Titer 96 Non Radioactive Cell Proliferation Assay in accordance with the manufacturer's instructions (Promega). After solubilization of the formazan crystals, optical density was read at 560 nm using a Victor X-3 multilabel plate reader. Cell survival in the treated samples was calculated using a regression curve established from the untreated standard serial dilutions of the cell suspension. All measurements were performed in triplicate.

Flow cytometry experiments

Twenty-four hours after transfection, samples of cells (10^5 to 10^6) were collected and re-suspended in phosphate-buffer saline (PBS). The resulting cell suspension was assayed for the expression of GFP by flow cytometer analysis using a FACScalibur flow cytometer (Becton-Dickinson Biosciences, Franklin Lakes, NJ, USA). The percentage of GFP-positive cells was determined using the flow cytometer program. All measurements were performed in triplicate.

Fluorescence microscopy

GFP expression in cardiomyocytes was visualized 24 h following lipid transfection. Cells were washed with PBS and fixed with 3.7% paraformaldehyde solution for 10 min at room temperature. Glass coverslips were mounted with ProLong antifade DAPI reagent (Thermo Fisher Scientific) and visualized with an Axiovert epifluorescence microscope (Carl Zeiss, Oberkochen, Germany). Images were treated using ImageJ, version 1.42q (NIMH, Bethesda, MD, USA).

Statistical analysis

Statistical analysis was performed using Prism (GraphPad Software Inc., San Diego, CA, USA). Values are expressed

Copyright © 2015 John Wiley & Sons, Ltd.

as the mean ± SEM. Significant differences between groups are indicated ($*p < 0.05$ and $**p < 0.01$) by the Mann–Whitney *U*-test.

Results and Discussion

Synthesis of the imidazolo lipidic derivatives

To highlight the importance of the linker between the two acyl chains present in the structure of imidazole-based helper lipids, we compared the transfection efficiency of two types of liposomes. The first liposome tested forms a hybrid lipidic membrane resulting from the association of the cationic lipid DOSP, with the imidazole-based helper lipid MM27, containing, respectively, an amido and phosphoramido linker between the two oleyl chains and the polar head (Figure 1). The other two formulations constitute homogeneous binary liposomes resulting from the association of DOSP with imidazole-based helper lipids also bearing a dioleylamido hydrophobic backbone.

To synthesize imidazole-based helper lipids with a dioleylamido backbone, we attempted the coupling of carbamoylchloride of DOLA (**1**) to histamine in one step, as carried out for MM27. Unfortunately, the solubility of histamine was very low in organic solvents, except in methanol. Because the high reactivity of (**1**) with the methanol led to the formation of the methyl carbamate derivative, the introduction of the imidazole ring on the helper lipid was achieved by another chemical method.

The synthetic routes for the derivatives **5** and **6** reported in the present study are illustrated in Figure 2. We first generated the carbamoyl chloride of DOLA (**1**) *in situ*, by reaction of **1** [21] with triphosgene [29,30]. This compound was not isolated, although its formation was confirmed by ^{1}H NMR. Indeed, the signal of the methylene protons in α of the nitrogen in DOLA at 2.60 p.p.m. disappeared after 2 h and new signals at

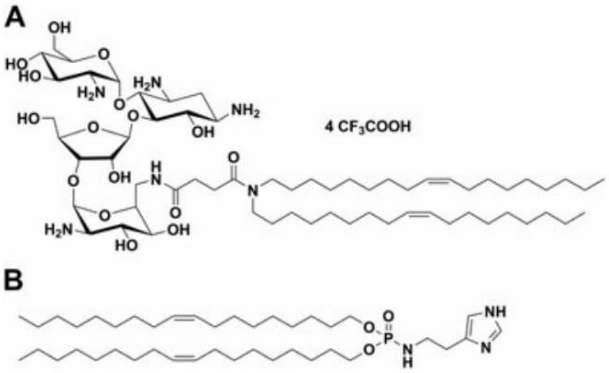


Figure 1. Structure of DOSP (A) and MM27 (B)

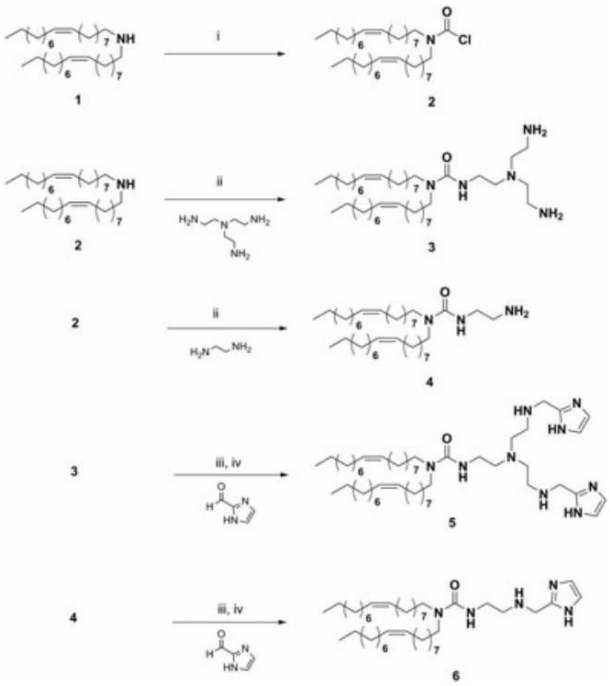


Figure 2. Synthesis of the imidazolo amphiphile ureas. (i) Triphosgene, NEt_3, CH_2Cl_2, 0°C for 30 min, 20°C for 90 min (ii) Excess TREN or ethylenediamine, CH_2Cl_2, room temperature, overnight (3: 91%, 4: 94%) (iii) Imidazole carboxhaldehyde, Na_2SO_4, EtOH, 4 h, reflux (iv) $NaBH_4$, CH_2Cl_2/MeOH (50/50), room temperature, overnight (5: 95%, 6: 85%).

3.30 p.p.m. were observed. This deshielding confirmed the formation of the N-COCl group. Then, the coupling between the amines (TREN and ethylenediamine) and this intermediate **2** afforded the amphiphiles ureas **3** and **4** in yields of 91% and 94%, respectively. To avoid the formation of the di- or tri-substituted compounds, a large excess of amines was used as reported previously [26]. The reductive amination ensuing [31] afforded compounds **5** and **6** in two steps, in a yield of 95%. The formation of the imines, in the first step of the reductive amination, was confirmed by ^{1}H NMR via apparition of a characteristic signal at 8.2 p.p.m.

These two steps sequence allowed us to obtain these new compounds **5** and **6** with an overall yield of approximately 80%.

Morphology and structure of complexes formed with DNA

Next, we studied the morphology of liposomes made of DOSP with helper lipid MM27 or **6** and their organization when complexed with plasmid DNA. We investigated whether supramolecular particles resulting from the

Copyright © 2015 John Wiley & Sons, Ltd.

association of DNA with cationic liposomes that include helper lipids possessing either an amido or phophoramido linker, could have different morphologies inducing different properties.

We observed, by cryo-TEM (Figure 3), that both lipid mixtures formed unilamellar liposomes (Figures 3A and 3B), with DOSP/MM27 being much larger than DOSP/**6**, which produced very small liposomes; this observation was also confirmed by dynamic light scattering-based methods (data not shown). In the presence of plasmid DNA (similar lipid to DNA ratio), large assemblies were formed with DOSP/MM27 (Figure 3C). These structures revealed stacks of lipid layers separated by DNA strands, showing that DNA molecules were tightly bound to lipid membrane as previously described for lipoplexes [7] (Figure 3E). By contrast, assemblies formed with DOSP/**6** were smaller (Figure 3D). Moreover, the plasmid DNA did not appear to be densely packed. Stacks of layers of lipid and DNA were scarcely visible and intact liposomes were present, suggesting that DNA molecules were loosely bound to liposome. Note that DNA strands were visible at the vicinity of the assemblies (Figure 3F, inset). This strongly indicates that the linker between the two acyl chains present in the structure of imidazole-based helper lipid plays a critical role in the morphology and structure of DNA complexes. Unexpectedly, hybrid lipidic membrane led to a tighter DNA complexation than that observed with homogeneous lipidic membrane.

Decomplexation of hybrid and homogeneous complexes

Next, we investigated whether the supramolecular assemblies illustrated in Figure 3, resulting from the association of DNA with cationic liposomes that include helper lipids possessing either an amido or phophoramido linker, could have different decomplexation behaviour. Accordingly, we

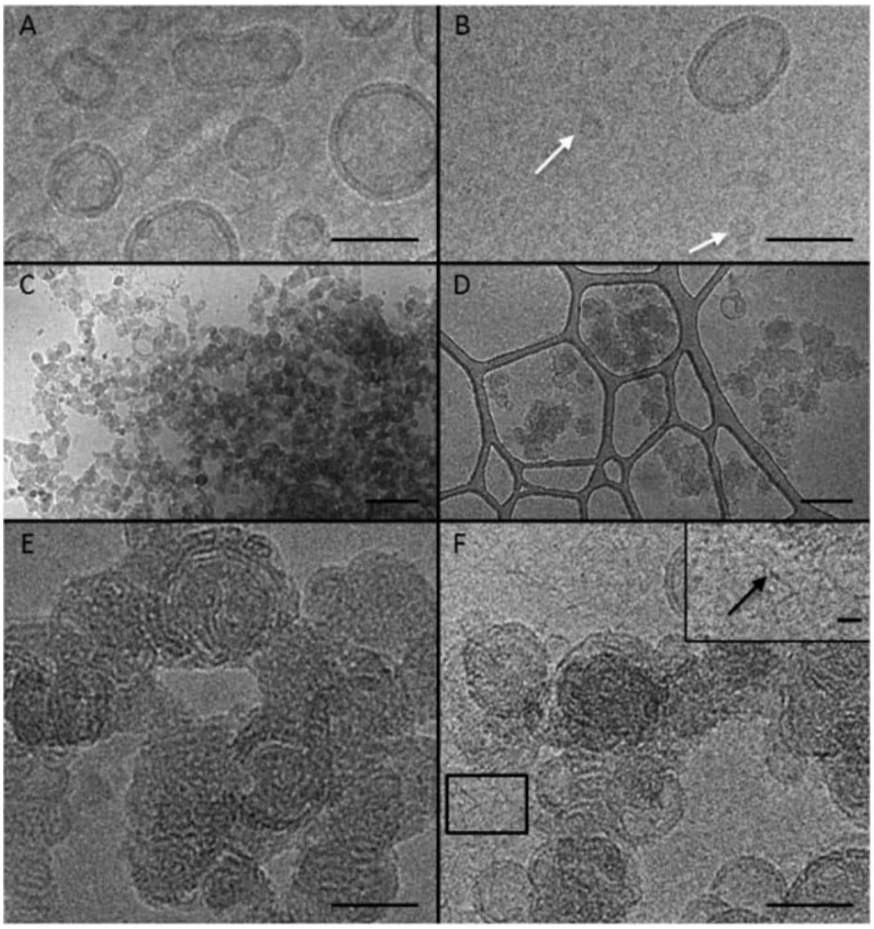


Figure 3. CryoTEM images of liposomes made of DOSP with colipid MM27 or 6 and complexed with DNA. (A) DOSP/MM27 liposome (C, E) DOSP/MM27 with DNA (B) DOSP/6 liposome. Note the presence of very small liposomes (white arrows) (D, F) DOSP/6 with DNA. Inset: note DNA strands are visible (black arrow). Scale bars = 0.5 μm (A, B, E, F), 50 nm (C, D) and 10 nm (inset).

Copyright © 2015 John Wiley & Sons, Ltd.

submitted DOSP/MM27-DNA and DOSP/**6**-DNA complexes to small anionic polyphosphates of six phosphate units and measured the decomplexation of DNA by the increase of EtBr fluorescence as a result of the intercalation of the fluorescent probe between the base pairs of decomplexed DNA molecules. Figure 4A shows that, at acidic pH 5.26, the kinetics of the fluorescence increase upon the addition of polyphosphates was similar between the two types of assemblies and reached 80% after a few seconds. These results indicate that, in an acid environment mimicking the endosomal pH, DNA decomplexation was very fast and was not influenced by whether the imidazole ring is linked via a dioleylphosphoramido or dioleylamido lipidic backbone. Measuring the kinetics of decomplexation at different pH, ranging from 5.26–7.1, showed that the fluorescent signal for DOSP/**6**-DNA complexes was 80% for every pH condition of the medium (Figure 4B), indicating that DNA complexes were not stable. By contrast, with DOSP/MM27-DNA complexes, the fluorescent signal depended on the pH of the medium and, for pH 7.1, which is the same as in extracellular conditions, the fluorescent signal was almost the same in the presence or in the absence of polyphosphates, indicating that DNA complexes were stable. Therefore, the addition of polyphosphates on the two different types of assemblies led either to the same DNA decomplexation irrespective of the pH for DOSP/**6** complexes or to a much lower decomplexation with DOSP/MM27 when the pH increase and reached neutrality. To rule out any effect of the electrostatic forces between the positively-charged complexes and the polyphosphate that might be different between the two liposomes, we measured the zeta potential of the two types of complexes at the different pH values. As shown in Figure 4C, the zeta potential was the same for DOSP/MM27 and DOSP/**6**-DNA complexes, irrespective of pH. Altogether, this strongly suggests that DOSP/MM27-DNA complexes were more resistant than DOSP/**6**-DNA complexes at pH 7.2 mimicking the

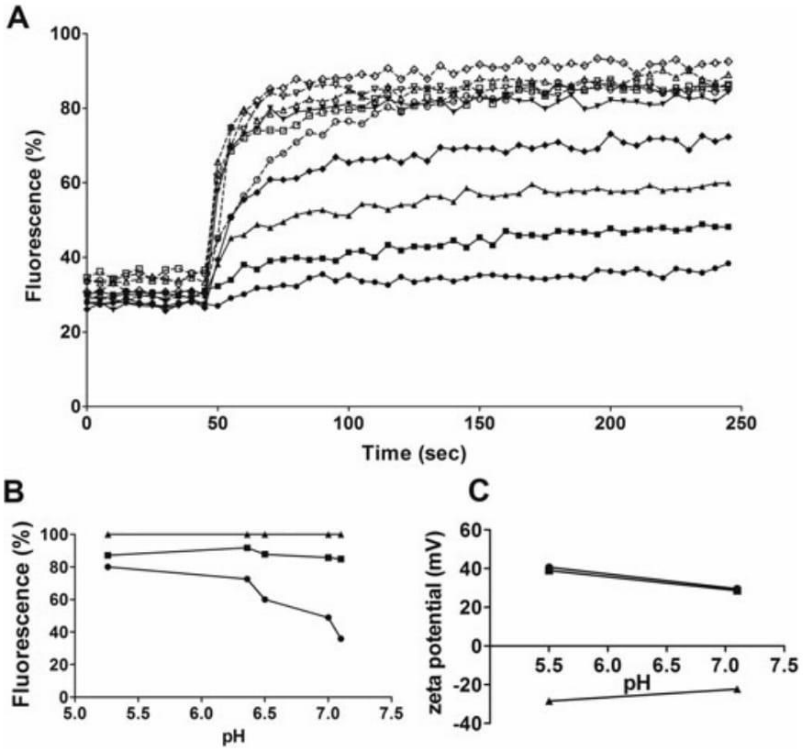


Figure 4. Influence of the lipidic structure of the helper lipid on the decomplexation of DOSP/MM27 and DOSP/6-DNA lipoplexes. The compaction of DNA by cationic liposomes was monitored by EtBr fluorescence (A, B). The residual fluorescence was assayed using a Jobin-Yvon spex Fluoromax-4 spectrofluorimeter. (A) Complexes DOSP/MM 27 (full pattern) or DOSP/6 (empty pattern) were obtained by mixing cationic liposomes with 10 µg of plasmid DNA, at a charge ratio (+/−) of 4 in 150 mM NaCl and 10 mM MES or HEPES to generate the different pH: pH 5.26 (inversed triangle), pH 6.36 (diamond), pH 6.5 (triangle), pH 7 (square) and pH 7.1 (circle). Fifty seconds after fluorescence measurement corresponding to DOSP/MM27 and DOSP/6-DNA lipoplexes, 10 µl of a polyphosphate solution at 4 mg/ml was added to the complexes. The fluorescence signal was then measured for 250 s. (B) representation of the fluorescence signal obtained with DOSP/MM27 (circles) and DOSP/6-DNA (squares) complexes, 250 s after addition of the polyphosphate solution. A control was conducted in the same experimental conditions with naked DNA (triangles). (C) Zeta potential measurement of DOSP/MM 27 (circle) or DOSP/6-DNA (square) complexes prepared at charge ratio of 4 (+/−) in 150 mM NaCl and 10 mM of MES or HEPES to give pH of 5.5 and 7.2. Naked DNA was used as a control in the same experimental conditions (triangle).

Copyright © 2015 John Wiley & Sons, Ltd.

extracellular pH because they were not affected by the decomplexating agent. These results suggest that the lipid membrane with hybrid dioleyl linker that led to DNA strands being tightly bound to liposomes results in lipoplexes with more resistance to DNA complexation at extracellular physiological pH.

Cell viability

The cytotoxicity of the DOSP used alone or formulated with the helper lipids MM27, **5** or **6**, was tested on the HEK cell line. Figure 5 shows that the cell viability varied between 80% and 100% when using DOSP, DOSP/MM27, DOSP/**5** and DOSP/**6** compared to the 70% obtained with Lipofectamine®. It is interesting to note that no cytotoxicity was observed with DOSP/MM27 on the HEK cell line, which is in agreement with results in the C2C12 cell line reported by Billiet *et al.* [27].

Altogether, we established that the dioleylphosphoramido backbone helper lipid MM27 formulated with DOSP induced lower cytotoxicity compared to dioleylamido lipid formulations **5** and **6**.

In vitro transfection efficiency on adherent cell lines

Next, the formulations of DOSP or DOSP/imidazole-based helper lipids (MM27, **5** and **6**) were tested for their efficiency in transfecting a plasmid DNA encoding for the luciferase or the GFP, in two different cell lines: a kidney cell line HEK and a muscular cell line C2C12.

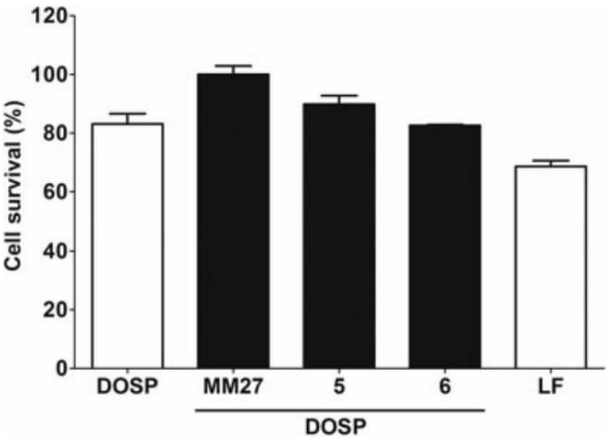


Figure 5. Percentage of cell survival on HEK cell line. Cells were transfected with 0.5 µg of pCMV-Luc plasmid complexed with DOSP (white bars), DOSP/MM27, DOSP/5 and DOSP/6 (black bars) or Lipofectamine® (LF) (white bars). Lipofectamine® was used in accordance with the manufacturer's instructions. Cytotoxicity was evaluated using the Cell Titer 96 Non Radioactive Cell Proliferation Assay.

Figure 6 shows the luciferase expression level obtained after plasmid transfection of HEK (Figure 6A) or C2C12 (Figure 6B) using the DOSP alone or formulated with the helper lipid MM27, **5** or **6**. Transfection efficiencies were compared with the commercial transfection agent Lipofectamine®. The results showed that the DOSP/MM27 led to a higher level of luciferase expression compared to the DOSP alone or Lipofectamine®. The presence of the helper lipids **5** or **6** did not increase the transfection efficiency compared to MM27, suggesting that mixture of cationic lipid and helper lipid with similar dioleylamido hydrophobic backbone is not favorable for transfection. These results highlight the importance of the linker within the backbone structure of the colipid, which directly impacted upon transfection activity.

Next, we assessed the percentage of transfected cells using the formulations DOSP, DOSP/MM27, DOSP/**5** and DOSP/**6**

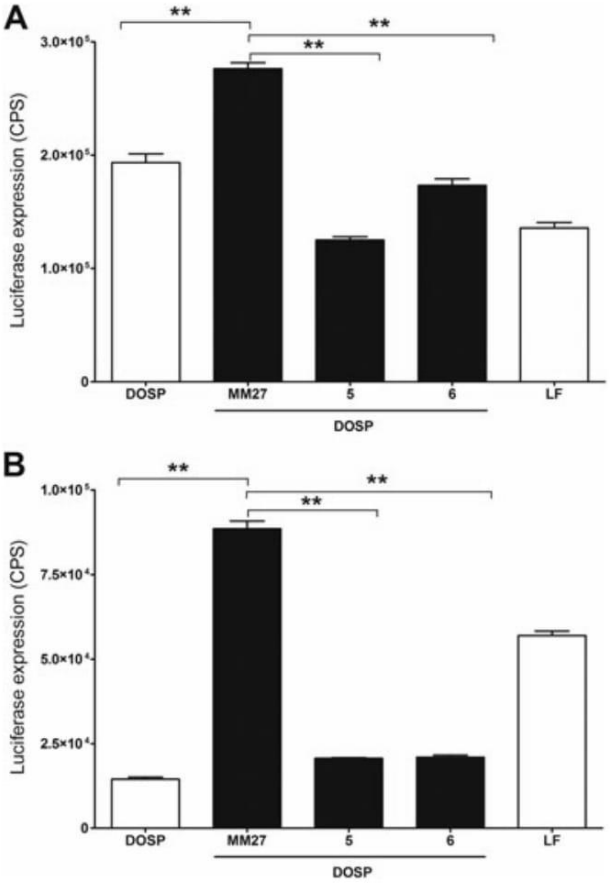


Figure 6. Effect of helper lipids on luciferase transfection activity. Plasmid DNA transfection was performed on HEK (A) and C2C12 cells (B). Cells were transfected with 0.5 µg of plasmid DNA, encoding luciferase, complexed with DOSP (white bars), DOSP/helper lipids (black bars) or Lipofectamine® (white bars). Lipofectamine® mediated transfections were performed in accordance with the manufacturer's instructions. Plates were incubated 24 h before cell lysis and luciferase activity measurement.

Copyright © 2015 John Wiley & Sons, Ltd.

combined with a plasmid encoding the GFP. The percentage of cells expressing the GFP transgene was assessed by fluorescence-activated cell sorting (FACS) on both cell lines. Figure 7 shows that the percentage of transfected HEK cells (Figure 7A) and C2C12 cells (Figure 7B) was optimal in the presence of the dioleylphosphoramido hydrophobic backbone helper lipid MM27. This result suggests that the use of hybrid liposomes with respect to the dioleyl linker enhances the number of transfected cells, probably as a result of their increased stability.

Taken together, we confirmed that adding a helper lipid to the lipoplex formulation can enhance the efficiency of gene delivery. Furthermore, we demonstrated that the structure of the dioleyl linker is an essential parameter for transfection efficacy. The use of the dioleylphosphoramido hydrophobic backbone of the helper lipid MM27 associated with the cationic lipid DOSP, leading to liposomes with hybrid dioleyl linker, is demonstrated as the optimal combination to use for the efficient *in vitro* DNA transfection of adherent cell lines. Moreover, the use of two different plasmids, namely luciferase and GFP, attests that the formulation behaviours were not influenced by the DNA sequence or the nature of the transgene. These results also suggest the importance of having a phospholipid, acting as biomimetic agent, in cationic liposomes formulations. Indeed, the biomimetic vector obtained with hybrid liposomes offered the possibility of enhancing transfection efficiency by facilitating the transfer of lipoplexes through phospholipid-rich cellular membranes.

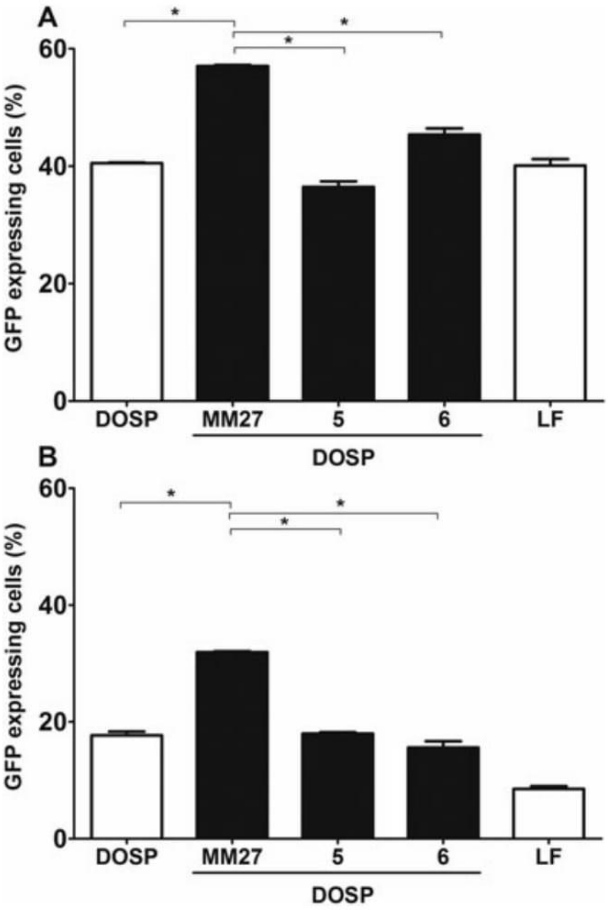


Figure 7. Effect of helper lipids on GFP transfection activity. Plasmid DNA transfection was performed on HEK (A) and C2C12 cells (B). Cells were transfected with 0.5 μg of plasmid DNA, encoding GFP, complexed with DOSP (white bars), DOSP/helper lipids (black bars) or Lipofectamine® (white bars). Lipofectamine® mediated transfections were performed in accordance with the manufacturer's instructions. Plates were incubated 24 h before flow cytometry experiment.

In vitro transfection efficiency on primary cells

Several reagents have been identified for efficiently transfecting cell lines, although effective gene transfer in primary mammalian cells, including cardiomyocytes and hepatocytes, is still limited. Primary cells are often preferred over transformed or immortalized cell lines because they are biologically more relevant and mimic the *in vivo* situation much closely. Thus, new products need to be developed to overcome these limitations. Based on the transfection activity obtained on HEK and C2C12, the DOSP/MM27 formulation was selected to assess DNA transfection of rat neonatal cardiomyocytes and mice hepatocytes. The results illustrated in Figures 8 and 9 show the optimal luciferase values and the percentages of transfected cells obtained with DOSP, DOSP/MM27 and Lipofectamine® in cardiomyocytes and hepatocytes, respectively.

Figures 8A and 9A show that the imidazole-based helper lipid MM27, leading to liposomes with hybrid lipidic membranes, was required for efficient luciferase reporter gene expression. Indeed, DOSP formulated with MM27 increased luciferase expression compared to DOSP alone or Lipofectamine®.

To characterize more precisely the transfection efficiency of the DOSP/MM27 compounds, we investigated the transfection of a plasmid DNA encoding the GFP protein, aiming to determine the number of cardiomyocytes successfully transfected. Figure 8 shows that the number of positive cells expressing the GFP protein was increased with the DOSP/MM27 formulation (Figures 8D and 8E) compared to Lipofectamine® (Figures 8B and 8C).

We also evaluated the transfection efficiency of DOSP, DOSP/MM27 and Lipofectamine® by FACS analysis on hepatocytes. Figure 9B shows that the number of positive cells expressing the GFP protein was increased with the DOSP/MM27 formulation compared to DOSP alone or Lipofectamine®.

In vitro experiments on cell lines or primary cells demonstrated clearly that the use of liposomes with hybrid dioelyl

Copyright © 2015 John Wiley & Sons, Ltd.

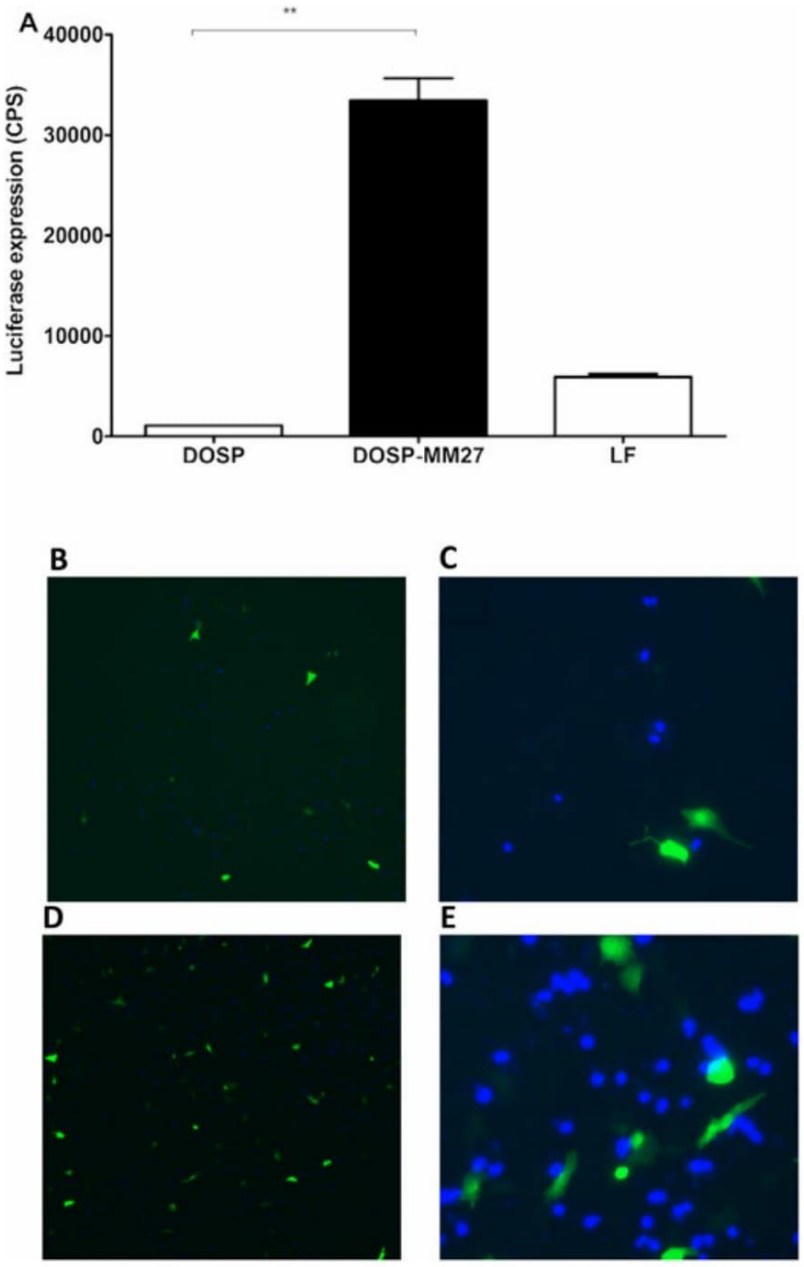


Figure 8. Transfection activity in newborn rat cardiomyocytes. (A) Cells were transfected with 0.5 μg of pCMV-Luc plasmid complexed with DOSP (white bars), DOSP/MM27 (black bars) or Lipofectamine® (white bars). Cells were also transfected with 0.5 μg of plasmid DNA, encoding eGFP, complexed with DOSP/MM27 (D, E) or Lipofectamine® (B, C). Lipofectamine® mediated transfections were performed in accordance with the manufacturer's instructions. Plates were incubated 24 h before cells lysis and luciferase activity measurement or fluorescence microscopy analysis.

linker formed from amido-based cationic lipid and phosphoramido helper lipid (association of DOSP with MM27) is a key factor for *in vitro* transfection efficiency. Knowing that the morphology and structure of complexes were strongly affected by the presence of hybrid or homogenous linkers between the two oleyl chains, and also that complexes made with hybrid linker were not decomplexed at neutral pH in the presence of decomplexating agent, the mechanism by which transfection efficiency was increased would be more related to a better resistance and internalization of complexes in more cells, rather than a facilitated intracellular trafficking of DNA.

Copyright © 2015 John Wiley & Sons, Ltd.

J Gene Med 2016; **15**: 3–15.
DOI: 10.1002/jgm

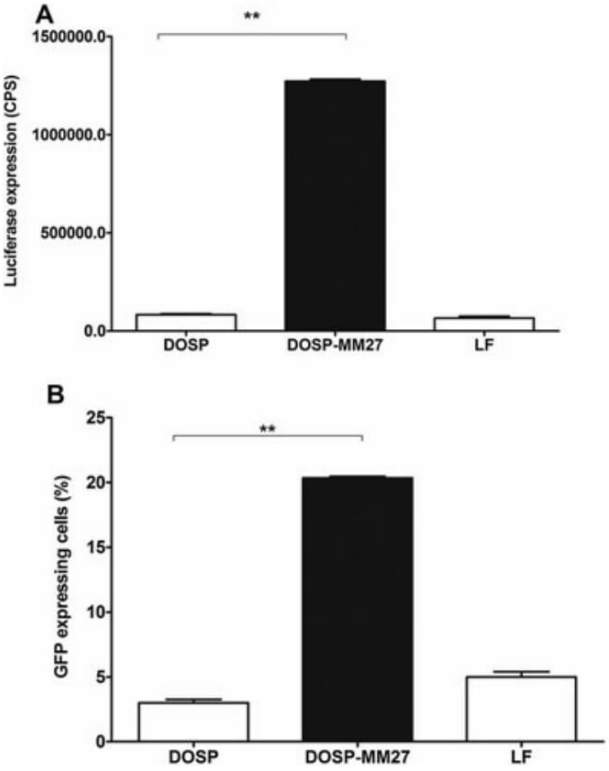


Figure 9. Transfection activity in primary mice hepatocytes. (A) Cells were transfected with 0.5 µg of pCMV-Luc plasmid complexed with DOSP (white bars), DOSP/MM27 (black bars) or Lipofectamine® (white bars). (B) Cells were also transfected with 0.5 µg of plasmid DNA, encoding eGFP, complexed with DOSP (white bars), DOSP/MM27 (black bars) or Lipofectamine® (white bars). Lipofectamine® mediated transfections were performed in accordance with the manufacturer's instructions. Plates were incubated 24 h before cells lysis and luciferase activity measurement or FACS analysis.

Conclusions

Taken together, the findings of the present study demonstrate the importance of the linker between the two acyl chains within the hydrophobic backbone structure on the helper lipid for promoting efficient gene transfer *in vitro*. Liposomes with hybrid dioleyl linker consisting of the dioleylphosphoramido backbone helper lipid MM27 formulated with DOSP led to high transgene expression, and a high percentage of transfected cells with very low cytotoxicity *in vitro*, compared to formulations of DOSP with the homogeneous dioleylamido hydrophobic backbone helper lipids **5** and **6**. The mechanism of action of those hybrid lipid membrane DNA complexes is probably related to the structure of complexes where DNA is densely packed and resistant to decomplexation in extracellular conditions and labile in endosomal conditions. Therefore, defects at the lipid membrane level, probably induced by the different dioleyl linkers in the cationic and imidazole-based lipids, led to a more favourable situation with respect to the DNA complexation rather than homogeneous lipid membranes.

Further work is in progress aiming to clarify whether the best association for generating hybrid membranes is the cationic polar headgroup linked to the dioleylamido backbone and the imidazole ring on the dioleyphosphoramido backbone or the inverse situation.

Acknowledgements

We thank Delphine Béziau, Virgine Forest, Stéphanie Lemarchand-Mindé and Martine Le Cunff for technical assistance. This work was supported by special grants received from the 'Association Française contre les Myopathies' (Evry, France) and from BPIFrance financement (Paris, France) for Emerit and Hepavac. This work was realized in the context of the IHU-Cesti project, which received French government financial support managed by the National Research Agency via the 'Investment Into The Future' program ANR-10-IBHU-005. The IHU-Cesti project is also supported by Nantes Metropole and the Pays de la Loire Region. Laurence Dallet and Thibault Colombani are supported by funds received from IHU-Cesti (Investissement d'Avenir ANR-10-IBHU-005, région Pays de la Loire et Nantes Métropole). The authors report that no competing financial interests or conflicts of interest exist.

References

1. Felgner PL, Gadek TR, Holm M, *et al.* Lipofection: a highly efficient, lipid-mediated DNA-transfection procedure. *Proc Natl Acad Sci USA* 1987; **84**: 7413–7417.
2. Wu GY, Wu CH. Receptor-mediated in vitro gene transformation by a soluble DNA carrier system. *J Biol Chem* 1987; **262**: 4429–4432.
3. Hefesha H, Loew S, Liu X, *et al.* Transfer mechanism of temoporfin between liposomal membranes. *J Control Release* 2011; **150**: 279–286.
4. Hattori Y, Suzuki S, Kawakami S, *et al.* The role of dioleoylphosphatidylethanolamine (DOPE) in targeted gene delivery with mannosylated cationic liposomes via intravenous route. *J Control Release* 2005; **108**: 484–495.
5. Mukherjee K, Bhattacharyya J, Sen J, *et al.* Covalent grafting of common trihydroxymethylaminomethane in the headgroup region imparts high serum compatibility and mouse lung transfection property to cationic amphiphile. *J Med Chem* 2008; **51**: 1967–71.
6. Pitard B, Aguerre O, Airiau M, *et al.* Virus-sized self-assembling lamellar complexes between plasmid DNA and cationic micelles promote gene transfer. *Proc Natl Acad Sci USA* 1997; **94**: 14412–14417.
7. Pitard B, Oudrhiri N, Vigneron JP, *et al.* Structural characteristics of supramolecular assemblies formed by guanidinium-cholesterol reagents for gene transfection. *Proc Natl Acad Sci USA* 1999; **96**: 2621–2626.
8. Khalil IA, Kogure K, Akita H, Harashima H. Uptake pathways and subsequent

Copyright © 2015 John Wiley & Sons, Ltd.

intracellular trafficking in nonviral gene delivery. *Pharmacol Rev* 2006; **58**: 32–45.
9. Gao X, Huang L. Cationic liposome-mediated gene transfer. *Gene Ther* 1995; **2**: 710–722.
10. Safinya CR. Structures of lipid-DNA complexes: supramolecular assembly and gene delivery. *Curr Opin Struct Biol* 2001; **11**: 440–448.
11. Li S, Rizzo MA, Bhattacharya S, Huang L. Characterization of cationic lipid-protamine-DNA (LPD) complexes for intravenous gene delivery. *Gene Ther* 1998; **5**: 930–937.
12. Mével M, Neveu C, Gonçalves C, *et al.* Novel neutral imidazole-lipophosphoramides for transfection assays. *Chem Commun* 2008; **27**: 3124–3126.
13. Maury B, Gonçalves C, Tresset G, *et al.* Influence of pDNA availability on transfection efficiency of polyplexes in non-proliferative cells. *Biomaterials* 2014; **35**: 5977–5985.
14. Leng Q, Chou S-T, Scaria PV, *et al.* Increased tumor distribution and expression of histidine-rich plasmid polyplexes. *J Gene Med* 2014; **16**: 317–328.
15. Kos P, Lächelt U, Herrmann A, *et al.* Histidine-rich stabilized polyplexes for cMet-directed tumor-targeted gene transfer. *Nanoscale* 2015; **7**: 5350–5362.
16. Budker V, Gurevich V, Hagstrom JE, *et al.* pH-sensitive, cationic liposomes: a new synthetic virus-like vector. *Nat Biotechnol* 1996; **14**: 760–764.
17. Kostarelos K, Miller AD. Synthetic, self-assembly ABCD nanoparticles; a structural paradigm for viable synthetic non-viral vectors. *Chem Soc Rev* 2005; **34**: 970–994.
18. Midoux P, Pichon C, Yaouanc J-J, Jaffrès P-A. Chemical vectors for gene delivery: a current review on polymers, peptides and lipids containing histidine or imidazole as nucleic acids carriers. *BrJ Pharmacol* 2009; **157**: 166–178.
19. Belmont P, Aissaoui A, Hauchecorne M, *et al.* Aminoglycoside-derived cationic lipids as efficient vectors for gene transfection in vitro and *in vivo*. *J Gene Med* 2002; **4**: 517–526.
20. Sainlos M, Belmont P, Vigneron J-P, *et al.* Aminoglycoside-derived cationic lipids for gene transfection: synthesis of kanamycin A derivatives. *Eur J Org Chem* 2003; **15**: 2764–2774.
21. Sainlos M, Hauchecorne M, Oudrhiri N, *et al.* Kanamycin A-derived cationic lipids as vectors for gene transfection. *Chembiochem* 2005; **6**: 1023–1033.
22. Mével M, Sainlos M, Chatin B, *et al.* Paromomycin and neomycin B derived cationic lipids: synthesis and transfection studies. *J Control Release* 2012; **158**: 461–469.
23. Arya DP, Coffee RL, Willis B, Abramovitch AI. Aminoglycoside-nucleic acid interactions: remarkable stabilization of DNA and RNA triple helices by neomycin. *J Am Chem Soc* 2001; **123**: 5385–5395.
24. Rege K, Hu S, Moore JA, *et al.* Chemoenzymatic synthesis and high-throughput screening of an aminoglycoside-polyamine library: identification of high-affinity displacers and DNA-binding ligands. *J Am Chem Soc* 2004; **126**: 12306–12315.
25. Rege K, Ladiwala A, Hu S, *et al.* Investigation of DNA-binding properties of an aminoglycoside-polyamine library using quantitative structure-activity relationship (QSAR) models. *J Chem Inf Model* 2005; **45**: 1854–1863.
26. Mével M, Breuzard G, Yaouanc J-J, *et al.* Synthesis and transfection activity of new cationic phosphoramidate lipids: high efficiency of an imidazolium derivative. *Chembiochem* 2008; **9**: 1462–1471.
27. Billiet L, Gomez J-P, Berchel M, *et al.* Gene transfer by chemical vectors, and endocytosis routes of polyplexes, lipoplexes and lipopolyplexes in a myoblast cell line. *Biomaterials* 2012; **33**: 2980–2990.
28. Chèvre R, Le Bihan O, Beilvert F, *et al.* Amphiphilic block copolymers enhance the cellular uptake of DNA molecules through a facilitated plasma membrane transport. *Nucleic Acids Res* 2011; **39**: 1610–1622.
29. Igarashi Y, Yanagisawa E, Ohshima T, *et al.* Synthesis and evaluation of carbamate prodrugs of a phenolic compound. *Chem Pharm Bull (Tokyo)* 2007; **55**: 328–333.
30. Jitsuoka M, Tsukahara D, Ito S, *et al.* Synthesis and evaluation of a spiro-isobenzofuranone class of histamine H3 receptor inverse agonists. *Bioorg Med Chem Lett* 2008; **18**: 5101–5106.
31. Kaur N, Delcros J-G, Archer J, *et al.* Designing the polyamine pharmacophore: influence of N-substituents on the transport behavior of polyamine conjugates. *J Med Chem* 2008; **51**: 2551–2560.

Copyright © 2015 John Wiley & Sons, Ltd.

View publication stats

Article 6 : Liposome-based Formulation for Intracellular Delivery of Functional Proteins

Citation: Molecular Therapy—Nucleic Acids (2015) 4, e244; doi:10.1038/mtna.2015.17
© 2015 The American Society of Gene & Cell Therapy All rights reserved 2162-2531/15
www.nature.com/mtna

Liposome-based Formulation for Intracellular Delivery of Functional Proteins

Benoît Chatin[1,2], Mathieu Mével[1,2], Julie Devallière[1,2], Laurence Dallet[3], Thomas Haudebourg[1,2], Pauline Peuziat[1,2], Thibault Colombani[1,2], Mathieu Berchel[4], Olivier Lambert[3], Aleksander Edelman[5] and Bruno Pitard[1,2,6]

The intracellular delivery of biologically active protein represents an important emerging strategy for both fundamental and therapeutic applications. Here, we optimized *in vitro* delivery of two functional proteins, the β-galactosidase (β-gal) enzyme and the anti-cytokeratin8 (K8) antibody, using liposome-based formulation. The guanidinium-cholesterol cationic lipid bis (guanidinium)-tren-cholesterol (BGTC) (bis (guanidinium)-tren-cholesterol) combined to the colipid dioleoyl phosphatidylethanolamine (DOPE) (dioleoyl phosphatidylethanolamine) was shown to efficiently deliver the β-gal intracellularly without compromising its activity. The lipid/protein molar ratio, protein amount, and culture medium were demonstrated to be key parameters affecting delivery efficiency. The protein itself is an essential factor requiring selection of the appropriate cationic lipid as illustrated by low K8 binding activity of the anti-K8 antibody using guanidinium-based liposome. Optimization of various lipids led to the identification of the aminoglycoside lipid dioleyl succinyl paromomycin (DOSP) associated with the imidazole-based helper lipid MM27 as a potent delivery system for K8 antibody, achieving delivery in 67% of HeLa cells. Cryo-transmission electron microscopy showed that the structure of supramolecular assemblies BGTC:DOPE/β-gal and DOSP:MM27/K8 were different depending on liposome types and lipid/protein molar ratio. Finally, we observed that K8 treatment with DOSP:MM27/K8 rescues the cyclic adenosine monophosphate (cAMP)-dependent chloride efflux in F508del-CFTR expressing cells, providing a new tool for the study of channelopathies.
Molecular Therapy—Nucleic Acids (2015) **4**, e244; doi:10.1038/mtna.2015.17; published online 23 June 2015
Subject Category: Mechanisms of gene and nucleic acid transfer/transfection Vector trafficking and biodistribution

Introduction

Protein-based therapeutics represents a major breakthrough in medicine with more than 100 proteins approved for clinical use. One recent development has been the use of recombinant proteins, including hormones like the insulin-like growth factor,[1] enzymes[2] and antibodies such as rituximab.[3] All these molecules have extracellular targets which emphasize one of the major current limitations of this therapy namely the lack of an efficient way to deliver functional polypeptides into the cell. Numerous proteins need to be transported intracellularly to exert their therapeutic action but do not spontaneously cross plasma membranes due to their important size and biochemical properties. New methods to deliver functionally active proteins into the cells would extend use of therapeutic proteins to attractive intracellular targets and would be a powerful tool for laboratory investigation. Furthermore, protein delivery could overcome some drawbacks of gene therapy, in particular the difficulty of controlling expression levels and the oncogenic risk associated with transgene integration into the host cell genome. For treatments of cancers, infectious diseases or generation of induced pluripotent stem cell, that require only a transient expression of the transgene, delivery of protein represents a promising and safe approach.

In this context, various strategies are currently available for intracellular delivery. Microinjection allows the efficient transduction of a controlled amount of protein directly into the cell cytoplasm, but can only be applied to a small number of cells. Electroporation also allows the transport of therapeutic molecules. Electric pulse delivery created permeabilized areas in the cell membrane but has associated undesirable characteristics like damaging effects to the membrane affecting viability and poor cell targeting. Recently, new methods involving engineering of the protein to be delivered have been developed. However, this technology requires its fusion with a particular class of peptides named protein transduction domains (PTDs) or cell penetrating peptides (CPPs)[4,5] which can interfere with protein folding, leading to a loss of biological function. Another attractive nonviral gene transfer approach is based on lipid encapsulation. Cationic lipids have shown to be efficient vehicle for transmembrane delivery of nucleic acids such as DNA or siRNAs and have more recently been used to transfer proteins.[6–8] Lipid-based delivery system does not require protein engineering step, the procedure is simplified and the amount of protein required reduced. Over the past few decades, liposomes have evolved from being inert drug carriers to highly responsive delivery system, with active targeting, increased stealth, and controlled drug-release properties.[9] These amphiphilic compounds spontaneously associate with oligonucleotides forming supramolecular assemblies taken up by cells. The mechanism of action is well established, having been studied extensively for gene transfer process.[10] The positively charged macromolecule/lipid complex interacts with the negatively charged cell plasma membrane, leading to its internalization through endocytosis. Once in the

[1]Unité INSERM UMR 1087, CNRS UMR 6291, Nantes, France; [2]Université de Nantes, L'institut du Thorax, Nantes, France; [3]CBMN UMR-CNRS 5248, Université de Bordeaux IPB, Pessac, France; [4]UMR CNRS 6521, IFR 148 ScInBioS, Université de Bretagne Occidentale, Université Européenne de Bretagne, Brest, France; [5]Faculté de médecine Paris-Descartes, INSERM U845, Paris, France; [6]Present address: InCellArt, Nantes, France. Correspondence: Bruno Pitard, InCellArt 21 rue La Noue-Bras-de-Fer 44200 Nantes – France. E-mail: bruno.pitard@univ-nantes.fr
Keywords: antibody delivery; ionizable lipids; intracellular delivery; supramolecular assembly
Received 13 November 2014; accepted 17 April 2015; published online 23 June 2015. doi:10.1038/mtna.2015.17

endocytic pathway, the cargo molecule avoids lysosomal degradation and reaches cytosol by destabilization of the endosomal membrane structure.[11] The ability of liposomes to cross plasma membranes and deliver their cargoes into the cytoplasm greatly depends on their physico-chemical properties. Although the properties of lipoplexes are well known,[12] protein-based complexes are still ill defined. Thus, there is a need to develop and characterize efficient and safe synthetic intracellular protein delivery systems.

In the present study, we have identified cationic lipid formulations able to deliver into cells two types of proteins, enzyme and antibody. The guanidinium-cholesterol cationic lipid bis (guanidinium)-tren-cholesterol (BGTC) was combined to the colipid dioleoyl phosphatidylethanolamine (DOPE) to efficiently transport the β-galactosidase (β-gal) enzyme intracellularly. Transfection parameters (lipid/protein molar ratio, cytotoxicity, and culture medium) were optimized and β-gal activity quantified confirming that protein structure and function were not modified as a result of complexation. The aminoglycoside lipid dioleyl succinyl paromomycin (DOSP) associated with the imidazole-based helper lipid MM27 was shown to achieve intracellular delivery of biologically active anti-cytokeratin 8 (K8) antibody. The relationship between the physicochemical properties of these two supramolecular assemblies and their transfection efficiency were investigated by cryo-transmission electron microscopy (cryo-TEM). Finally, we evaluated the liposome DOSP:MM27 as a potential delivery system of the K8 therapeutic antibody for cystic fibrosis (CF). CF is a frequent and lethal disease, caused by mutation in the gene encoding the chloride channel cystic fibrosis transmembrane conductance regulator (CFTR). More than 1,900 mutations of the *CFTR* gene have been described, although the deletion of the phenylalanine residue at position 508 (F508del) is the most abundant in CF patients, with an occurrence of approximately 70%. F508del causes retention of the mutated-CFTR in the endoplasmic reticulum preventing the correct localization of CFTR channels at the plasma membrane.[13,14] It was shown that K8 protein interacts with F508del-CFTR and is implicated in its retention in endoplasmic reticulum.[15] Thus, we tested whether delivering K8 antibody to F508del-CFTR expressing HeLa cells would destabilize F508del-CFTR and K8 interaction leading to the functional plasma membrane expression of F508del-CFTR.

Results

Optimization of the lipid/protein formulation for β-galactosidase delivery

Based on the screening of a cationic lipid library, we identified two compounds able to deliver β-galactosidase (β-gal) in cultured HeLa cells. **Figure 1a** shows that the fatty acid derivative DOSP, and the cholesterol derivative BGTC, complexed with β-gal at various cationic lipid/protein molecular ratios (MR),

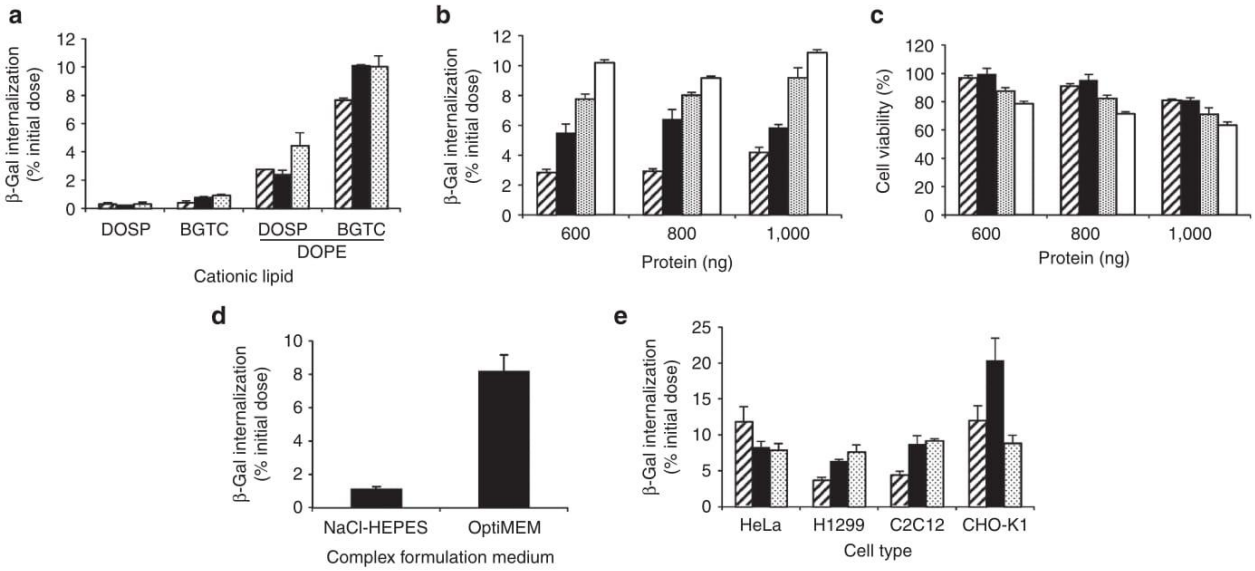


Figure 1 Intracellular delivery of the reporter protein β-gal complexed with various lipid formulations. (**a**) Internalization of β-gal complexed with micelles composed of bis (guanidinium)-tren-cholesterol (BGTC) or DOSP and liposomes formed of BGTC:DOPE or DOSP:DOPE in HeLa cells. β-gal protein (800 ng) was formulated with cationic lipids in OptiMEM at various lipid/protein molar ratio (MR): 1000 (dashed bars), 1,500 (black bars), or 2,000 (dotted bars). Complexes were added on cells for 8 hours before cells lysis and β-gal activity measurement. Results are expressed as percentage of the initial dose of protein used to form complexes. (**b,c**) Effect of protein amount and MR on internalization efficiency and cytoxicity in HeLa cells. β-gal protein (600, 800, 1,000 ng) was formulated with BGTC:DOPE in OptiMEM at various MR: 1,000 (dashed bars), 1,500 (black bars), 2,000 (dotted bars), or 2,500 (white bars). Percentage of internalization and cell viability were assessed by β-gal activity measurement and MTT assay respectively. (**d**) Effect of the formulation medium on transfection efficiencies. Percentage of β-gal internalization was evaluated by delivering 800 ng of protein formulated with BGTC:DOPE at a MR of 2,000 in NaCl-HEPES or OptiMEM medium. (**e**) Internalization of β-gal complexed with BGTC:DOPE in various cell types. β-gal protein (800 ng) was formulated with liposomes in OptiMEM at various lipid/protein molar ratio (MR): 1,000 (dashed bars), 1,500 (black bars), or 2,000 (dotted bars) and incubated with HeLa, H1299, C2C12, or CHO-K1 cells. Results are expressed as the mean percentage of three representative experiments ± SD.

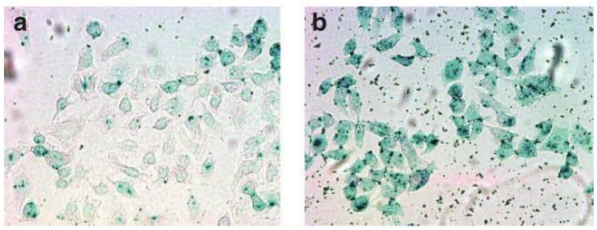


Figure 2 β-gal internalization over time in HeLa cells. β-gal protein (800 ng) was complexed with bis (guanidinium)-tren-cholesterol (BGTC):DOPE at a MR of 1,500. Complexes were added onto cells in serum-free DMEM for 15 minutes (**a**) or 4 hours (**b**). Cells were subsequently washed, fixed and stained with X-gal.

led to β-gal internalization into cells. These cationic lipids used alone as micelles showed a limited efficacy, but combined with the neutral lipid DOPE to form liposomes, dramatically increased the internalization efficiency (0.3 ± 0.1% for DOSP versus 4.44 ± 0.8% for DOSP:DOPE and 0.94 ± 0.05% for BGTC versus 10.1 ± 0.6% for BGTC:DOPE of β-gal intracellular delivery, MR 2,000). Spontaneous internalization of β-gal was not seen in these conditions. We further optimized the efficiency of the delivery by exploring the properties of the BGTC:DOPE formulation. The effect of increased amount of protein on internalization efficiency was assessed in parallel with cytotoxic effect. **Figure 1b** shows that the percentage of protein internalized into cells increased with the lipid/protein MR reaching ~10% of the protein initial dose, whereas no significant increase was achieved using growing amount of β-gal (600–1,000 ng) at a fixed MR. We observed that the optimal protein delivery was achieved with 1,000 ng of β-gal complexed with BGTC:DOPE using a MR of 2,500, which led to a 40% reduction in cell viability (**Figure 1c**). To avoid extensive cell death, we chose to work with 800 ng of protein complexed with BGTC:DOPE at a MR of 1,500 leading to the delivery of 6% of the protein into the cells without compromising their viability. We next investigated the impact of the formulation medium of BGTC:DOPE/β-gal complexes on protein delivery process. The amount of internalized β-gal showed a sevenfold increase in uptake of complexes formulated in OptiMEM compared to NaCl-HEPES buffer (8.2 ± 1.2% for OptiMEM versus 1.14 ± 0.2% for NaCl-HEPES of β-gal internalization, **Figure 1d**). Finally, the ability of BGTC:DOPE to deliver proteins into various cell lines was assessed. **Figure 1e** shows that BGTC:DOPE triggered β-gal internalization in lung carcinoma cells (H1299) myoblasts (C2C12) and ovary cells (CHO-K1), with similar effectiveness than in HeLa cells.

To investigate the localization of β-gal after intracellular internalization and validate that internalized protein is functional, HeLa cells were incubated with BGTC:DOPE/β-gal complexes and an X-gal staining was performed on cells after 15 minutes or 4 hours. Results showed that for short incubation time (15 minutes), the β-gal activity was low as illustrated by the faint blue color in cell cytosol (**Figure 2a**). In contrast, after 4 hours, the cells exhibited a dense blue color within the cytoplasm highlighting an enhanced β-gal activity corresponding to an increase of functional enzyme within the cytoplasm after probably its release from endosome (**Figure 2b**)

Optimization of the lipid/protein formulation for K8 antibody delivery

In recent years, therapeutic antibodies have been shown to be of great importance for clinical use. Expanding their application to intracellular targets is an emerging concept that would have many applications mainly by modulating intracellular protein-protein interactions. With this aim, we tested the ability of cationic lipids to deliver an antibody in its native conformation, thus capable of recognizing its antigenic intracellular target. An fluorescein isothiocyanate (FITC)-tagged monoclonal immunoglobulin directed against human cytokeratin 8 (FITC-K8) was delivered into HeLa cells using BGTC and DOSP associated or not with the colipid DOPE (**Figure 3a**,**b**,**d**,**e**). After 4 hours of incubation, only few cells displayed cytoplasmic fluorescence and K8 antibody was mostly detected in complexes surrounding the cells. This prompted us to test whether a different neutral colipid could improve the antibodies delivery. The formulation of BGTC as liposomes with the imidazole-based helper lipid named MM27, did not lead to a significant change in the percentage of positive cells (**Figure 3c**). However, the use of the DOSP:MM27 formulation dramatically increased the number of FITC-labeled cells (**Figure 3f**,**g**,**h**). The percentage of K8-labeled cells was quantified and revealed that 67% of the total population was transfected using the DOSP:MM27 formulation compared to 14 and 8% with DOSP:DOPE and BGTC:MM27 respectively (**Figure 3i**).

DOSP:MM27-mediated anti-K8 antibody delivery led to an intense labeling of the cell cytoskeleton, visible after 4 and 24 hours (**Figure 4a**,**b**) of incubation with the complexes, demonstrating the ability of DOSP:MM27 liposomes to deliver the antibody over an extended period of time. Although fixation can produce artifacts, the cytoskeletal staining pattern observed in PFA-fixed HeLa cells treated with DOSP:MM27/FITC-K8 liposomes (**Figure 4c**) was comparable with the staining seen in living cells after transfection (**Figure 4a**,**b**). In order to confirm the capacity of the liposome to achieve intracellular delivery of biologically active FITC-K8 antibody, cells transfected with DOSP:MM27/FITC-K8 were fixed, permeabilized, and then incubated with a rabbit polyclonal anti-K8 antibody, followed by immunostaining with a secondary anti-rabbit AlexaFluor 546. FITC-K8 and K8 antibodies recognize different epitopes on the same K8 target, respectively the C-terminus and the N-terminus around the serine at position 73. Confocal microscopy observation (**Figure 4d**) revealed that FITC-K8 delivered by liposome localized mainly on fiber structures characteristic of cytoskeletal staining pattern. In addition, FITC-K8 appeared to colocalize with the AlexaFluor 546 signal resulting from K8 immunostaining providing evidence of the functionality of the delivered antibody (**Figure 4e**,**f**).

Physicochemical characterization of BGTC:DOPE/β-gal and DOSP:MM27/K8 complexes

Next, we investigated the physicochemical properties of the complexes obtained by mixing β-gal or K8 antibody with BGTC:DOPE or DOSP:MM27 liposomes respectively. Migration of BGTC:DOPE/β-gal assemblies was performed on a native polyacrylamide gel electrophoresis to precisely quantify protein complexation by the cationic molecules.

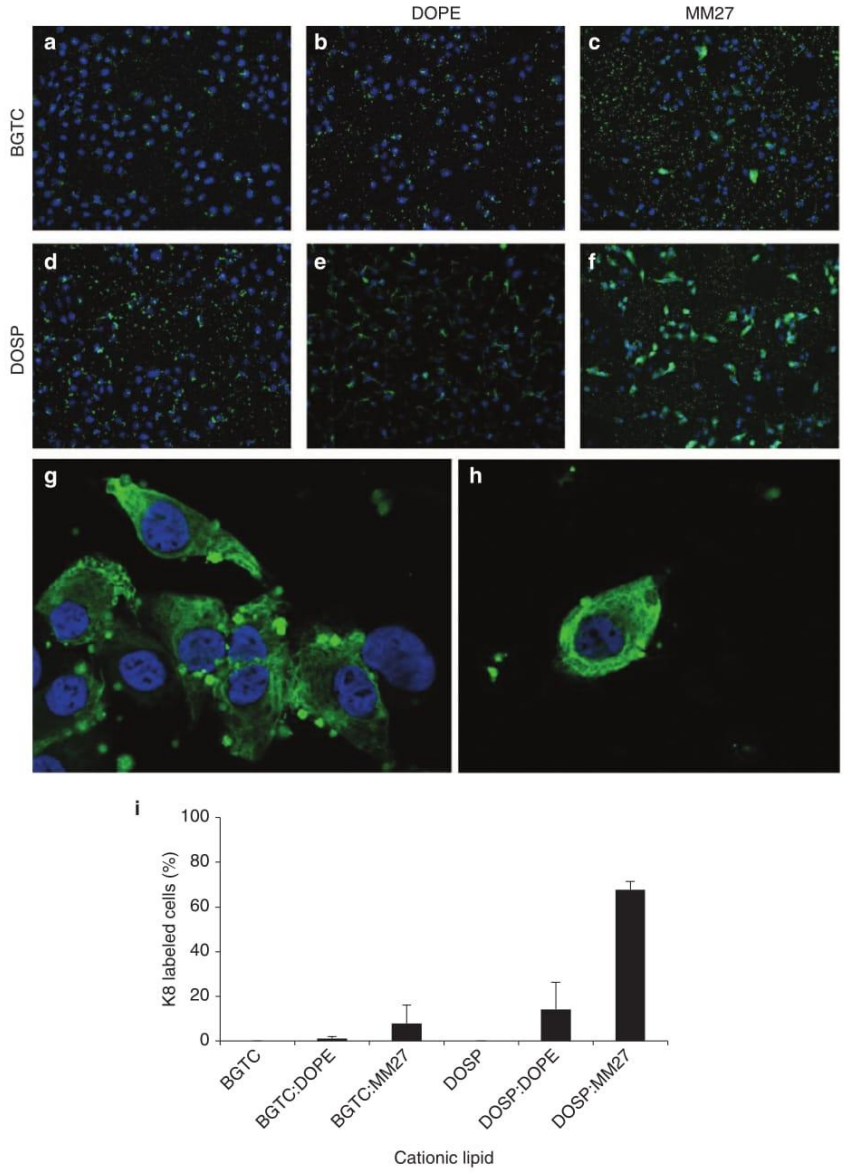


Figure 3 Intracellular delivery of the FITC-K8 antibody complexed with various lipid formulations. Hela cells were treated with FITC-K8 (800 ng) formulated with bis (guanidinium)-tren-cholesterol (BGTC) (**a**), BGTC:DOPE (**b**), BGTC:MM27 (**c**), DOSP (**d**), DOSP:DOPE (**e**), or DOSP:MM27 (**f**) (**g**) and (**h**), at a molar ratio of 1,500. In each condition, cells were incubated for 4 hours with the lipid/FITC-K8 complexes before fixation and mounting with ProLong antifade DAPI reagent. (**i**) Quantification of K8-positive cells after transfection with BGTC, BGTC:DOPE, BGTC:MM27, DOSP, DOSP:DOPE, and DOSP:MM27. Results are expressed as the mean percentage of three representative experiments ± SD.

Figure 5a shows that the amount of uncomplexed β-gal, free protein migrating through the gel, decreased rapidly as the MR raised with a consequent amount of β-gal complexed with BGTC:DOPE at a molar ratio of 100. Lipid/protein MR above 200 resulted in aggregates that did not migrate out of the well showing that BGTC:DOPE liposome allowed the efficient complexation of the protein and its compaction into stable complexes at high MR. Protein complexation was also evaluated for FITC-K8 antibody and DOSP:MM27. Fluorescent analysis was used to determine the amount of residual free antibody present in supernatant after DOSP:MM27/FITC-K8 formulation depending on lipid/protein MR. Figure 5b shows that around 40% of FITC-K8 was associated with DOSP:MM27 at a MR of 100. Elevating the MR increased the percentage of FITC-K8 complexation with 100% FITC-K8 associated with DOSP:MM27 from a MR of 400.

To further elucidate the mechanism of action of liposomes, various lipid mixture conditions were analyzed by cryoTEM. Figure 6 shows the morphology and assembly of the supramolecular complexes of BGTC:DOPE/β-gal using different MR. At high MR of 1,500, liposomes were generally spherical unilamellar vesicles forming large aggregates (Figure 6a–c).

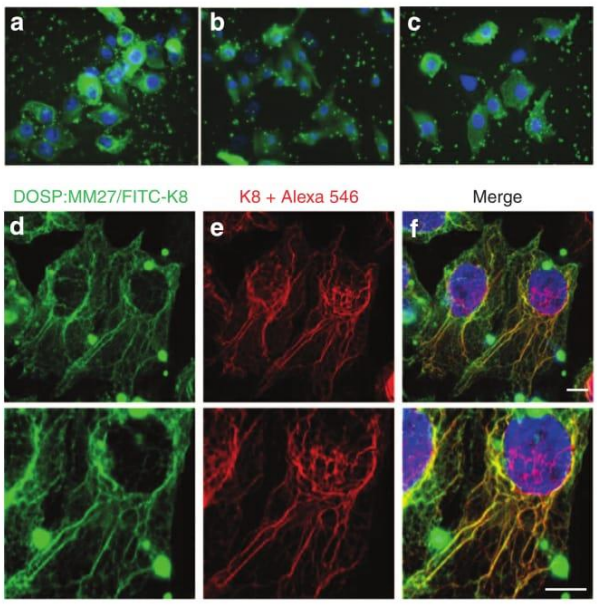


Figure 4 Intracellular localization of FITC-K8 antibody delivered by DOSP:MM27 liposome. Hela cells were plated on 24-well plate and incubated with DOSP:MM27/FITC-K8 complexes for 4 hours (**a**) or 24 hours (**b**) and observed under microscope without further treatment. Hela cells were plated on 24-well plate, incubated with DOSP:MM27/FITC-K8 complexes for 4 hours and fixed with PFA before microscope observation (**c**). Hela cells were plated on glass coverslips, incubated with DOSP:MM27/FITC-K8 complexes for 4 hours, fixed and immunostained with a rabbit anti-K8 and a secondary anti-rabbit AlexaFluor® 546 (red). Nuclei stained using DAPI (blue), FITC-K8 (green) (**d**) and K8 staining (red) (**e**) are visualized under confocal fluorescence microscope as superimposition of images (merge) (**f**). Lower panel shows higher magnification. Scale bar = 10 µm.

The β-gal protein appeared to be entrapped within aggregates, occasionally forming protein layers/junctions between two lipid membranes (black arrows). At a MR of 750 (**Figure 6d–f**), protein junctions were more frequently encountered suggesting a higher amount of protein bound to liposome surfaces. The particles displayed more polymorphic structures: spherical vesicles coexist with vesicles of irregular shape as well as multiwalled and fused vesicles. At a MR of 375 (**Figure 6g–i**), liposomes formed larger isolated multilamellar objects decorated with proteins on their external surfaces (white arrows).

In order to explain the significant difference in the K8 delivery efficiency between formulations, we next investigated by cryoTEM the structure of complexes formed with K8 and various liposome preparations. BGTC:DOPE and BGTC:MM27 lipid mixtures formed unilamellar liposomes. In the presence of K8 antibody, both mixtures formed micron-size aggregates due to protein–lipid interaction (**Figure 7a,b**). For BGTC:DOPE, protein densities were visible at liposome surface as well as between lipid membranes without forming regular organization (white arrows, **Figure 7a**). DOSP:DOPE mixture produced liposomes, heterogeneous in size and lamellar organization. In contact with anti-K8, liposome aggregation was observed, indicative of a strong protein–lipid interaction (**Figure 7c**). However, it remained difficult to provide structural details on lipid/protein interaction due to liposome heterogeneity. Unlike others,

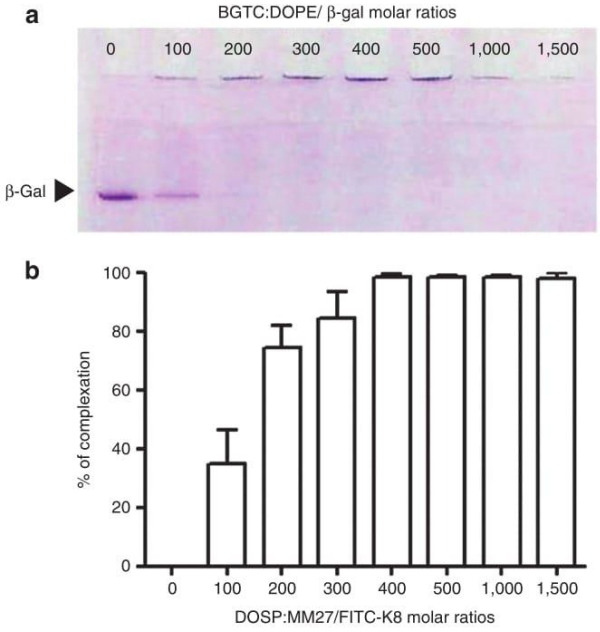


Figure 5 Complexation of the β-gal anti-FITC-K8 protein with the BGTC:DOPE or DOSP:MM27 lipids depending on molar ratios. Lipid-proteins complexes were formed in OptiMEM at various molar ratios (100–1,500) and nonassociated proteins were visualized on a native-PAGE gel for the β-gal (**a**) or measured by fluorospectrometer for the FITC-K8 (**b**).

DOSP:MM27 mixture was not organized in liposome but in 20 nm domains showing no evidence of internal structure. When mixed with anti-K8 antibody, DOSP:MM27 formed 1–2 µm lipoplexes consisting of aggregated spherical elements (**Figure 7d**). At higher magnification, these spherical arrangements were seen as "onion-like" concentric multilamellar structures of 100–200 nm diameter exposing protein densities at their surfaces (white arrows **Figure 7d**) but internally devoid of proteins.

Functional impact of anti-K8 antibody delivery on F580del-CFTR trafficking

We finally tested the ability of the DOSP:MM27/K8 complexes to restore the F508del-CFTR trafficking in mutated HeLa cells. It was demonstrated that K8 was bound directly to the F508del *in vivo* causing retention of the mutated F508del-CFTR channel in the endoplasmic reticulum and its absence in the plasma membrane.[16] Furthermore, it was shown that inhibition of K8 expression by pharmacological molecules or siRNA in F508del-expressing HeLa cells led to the recovery of CFTR-dependent iodide efflux.[15,16] On the basis of this recent discovery, we hypothesized that delivering K8 antibody to F508del-CFTR expressing HeLa cells would disrupt F508del-CFTR and K8 interaction leading to the correction of the F508del-CFTR trafficking defect. It is known that the interaction between F508del-CFTR and K8 occurs through the N-terminal of the K8 protein. In order to ensure that the observed effect is specific, we used an antiK8 recognizing the C-terminus of the K8 target as an irrelevant antibody control.

The recovery of F508del-CFTR processing was monitored by measuring the cAMP-dependent anionic conductance

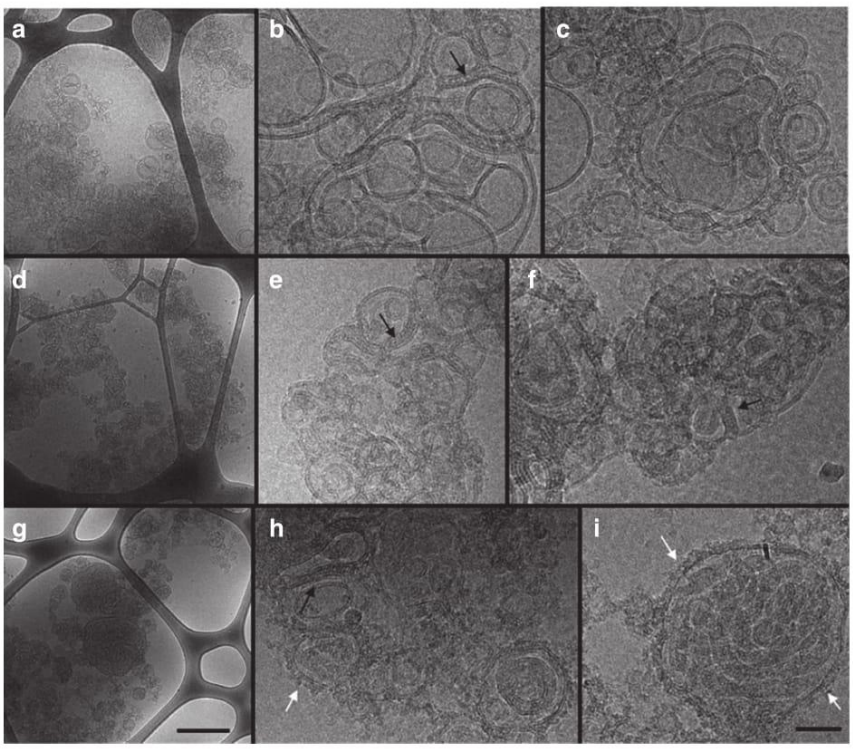


Figure 6 CryoTEM images of β-gal complexed with BGTC:DOPE liposomes formulated at various cationic lipid/protein ratios. (**a–c**) MR = 1,500; (**d–f**) MR = 750; (**g–i**) MR = 375. Black arrows denote β-gal protein accumulation forming junctions between lipid membranes. White arrows denote protein densities coated at the surface of liposomes. Scale bars, 0.5 µm (**a,d,g**) and 50 nm (**b,c,e,f,h,i**).

through the plasma membrane of F508del-CFTR expressing cells using halide-sensitive probe, 6-methoxy-N-ethylquinolinium iodide (MEQ) (Figure 8). Upon addition of cAMP to initiate channel opening and exchange of extracellular I^- for nitrate $NO3^-$, MEQ fluorescence increased in WT-CFTR expressing cells (triangles) as CFTR-mediated anion transport results in replacement of intracellular I^- with nonquenching NO_3^-. Under iodide perfusion, fluorescence of intracellular MEQ was rapidly quenched by entry and collision with iodide ions. WT-CFTR expressing cells treated or not with DOSP:MM27/K8 displayed a similar behavior but a reduced fluorescence amplitude was detected in nontreated cells. In contrast, F508del-CFTR expressing cells, untreated (cross) or treated with DOSP:MM27/antiK8 C-ter (circle), showed a weak response with a low anionic conductance illustrated by the attenuated fluorescence changes. Finally, F508del-CFTR expressing cells transfected with DOSP:MM27/antiK8 N-ter (diamonds) displayed a robust and prompt increase in MEQ fluorescence under cAMP stimulation, followed by a rapid quenching after iodide perfusion. Altogether, these results indicate that delivering K8 antibody into F508del-CFTR expressing cells using liposomes rescues cAMP-dependent anionic conductance, suggesting a partial restoration of F508del-CFTR channel trafficking towards the plasma membrane.

Discussion

In this study, we demonstrate rapid and efficient delivery of catalytic protein and antibodies into the cytosol of cultures cells using liposome-based formulation. Intracellular delivery of functional proteins provides a potential tool to replace missing, dysfunctional and poorly expressed proteins or antagonize key intracellular pathways. Protein-based therapeutics is a promising approach for several biomedical applications including stem cell engineering, imaging, and signaling studies.

Delivery of β-gal was chosen as a test of the efficacy of lipid formulations since this multimeric enzyme is susceptible to inactivation during the delivery process. The availability of a highly sensitive detection test, and the possibility to observe its presence in the cell cytoplasm by X-gal staining, allowed us to perform a screening of cationic lipids library. Furthermore, as detection is based on enzymatic activity, this is a stringent way to ascertain that analyzed compounds deliver proteins that retain, at least partially, their active conformation. Although most of the cationic lipids tested proved to be inefficient to deliver the enzyme into cultured HeLa cells, two molecules, DOSP and BGTC, were able to transport a low but detectable amount of the initial protein dose into the cells when used as micellar solutions. BGTC is a cholesterol-based lipid bearing two guanidinium polar head-groups[17] and DOSP is a fatty-acid-based molecule bearing a paromomycin head-group.[18,19] These two compounds are commonly used for their high DNA and siRNA transfection potentials and their lack of toxicity. In order to enhance their protein delivery activities, we formulated them as liposomal suspensions combined with the neutral lipid, DOPE. We observed a dramatic increase in the activity for DOSP:DOPE and BGTC:DOPE without noticeable toxicity. DOPE is commonly

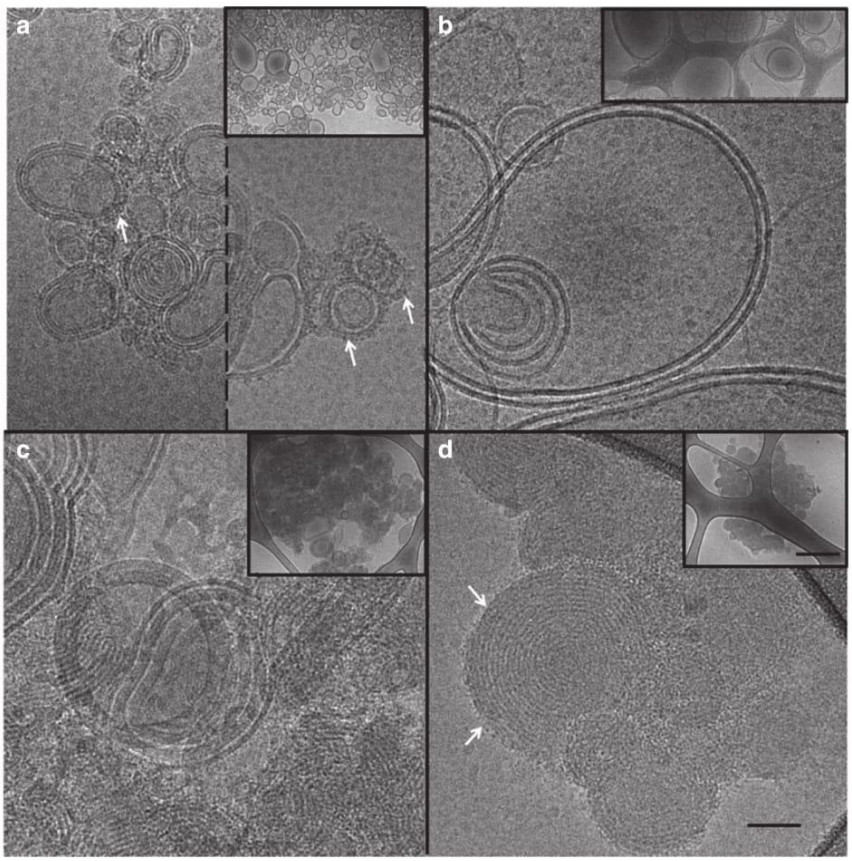


Figure 7 CryoTEM images of cationic lipid/K8 antibody complexes. (**a**) BGTC:DOPE, (**b**) BGTC:MM27, (**c**) DOSP:DOPE, (**d**) DOSP:MM27. White arrows denote protein densities visible at liposome surfaces and between lipid membranes. Insets correspond to a larger view of each condition. Scale bars 50 nm (inset 500 nm).

used in nucleic acid transfection reagents to promote endosomal membrane disruption.[12,20] It is likely that cationic lipids used alone led to the cellular internalization of the protein, followed by lysosomal degradation. Adding DOPE to the formulation would promote the delivery of the enzyme to the cytosol before fusion of endosomes with lysosomes. It is to be noted that cells were lyzed with reporter lysis buffer directly into culture plates following transfection. We assume that the amount of internalized β-gal may be slightly overestimated by quantifying external liposomes that bind cell membrane. Nevertheless, extensive phosphate-buffered saline (PBS) washing removed most of the complexes and microscopy analysis confirmed the delivery of the β-gal into the cytosol. X-gal staining of cells treated with BGTC:DOPE/β-gal lipoplexes showed detectable staining throughout the cytosol of all treated cells, confirming catalytic activity of the enzyme. Interestingly, β-gal activity was still detectable after 24 hours of incubation, indicating a prolonged release of the enzyme into the cells and/or a prolonged protein half-life in the cytosol.

We then investigated whether liposomes could deliver not only enzymes but proteins with binding activities such functional antibodies into HeLa cells. An FITC-tagged antibody directed against human cytokeratin 8 was formulated with BGTC and DOSP, in the presence or absence of DOPE. None of the conditions tested by varying the protein dose and the molar ratio, enabled entry of the antibody into the cells. Microscopy observation showed confined FITC fluorescence staining area suggesting that lipoplexes were trapped in the endosomal system. Lack of efficiency for cationic lipid-mediated antibody delivery has already been observed in previous studies. It was described that antibodies delivered by Saint-2:DOPE were localized in the cell but formed confined staining area, independent of their targets, probably indicating endosomal sequestration of Saint2:DOPE/antibodies.[8] Addressing this issue, we chose to enhance the endosomal escape step by using MM27, an imidazole-bearing neutral lipid. It has been reported previously that this compound is 100-fold more efficient than DOPE in promoting DNA transfection.[21,22] It was shown that the amines of the imidazole head-group, neutral at physiological pH, undergo protonation in acidic organelles, leading to endosomal membrane disruption by a proton-sponge mechanism.[23] We demonstrated that FITC-K8 delivered by DOSP:MM27 localized mainly on fiber cytokeratin network for at least 24 hours, confirming the functionality of the antibody. Moreover, we observed that 70% of treated cells were labeled after 4 hours, showing a dramatic improvement compared with DOSP and DOSP:DOPE-mediated delivery. Altogether, these findings indicate that the efficiency of the delivery system varies greatly depending on the protein type, and that vectors have to be adapted and optimized according to the cargo. This

contrasts with DNA or RNA delivery which takes advantage of the universal structure of nucleic acids. Indeed, nucleic acids, independently of the nucleotide sequence, present the same structure and electrical charge, unlike peptides and proteins, whose physicochemical parameters vary greatly.

We used cryo-TEM to better understand the supramolecular organization of cationic lipid/protein complexes. We observed that the mixing of BGTC:DOPE liposomes with β-gal at the optimal MR of 1,500 promoted aggregation, resulting in large, globally spherical complexes. Protein molecules were present within the aggregates and occasionally formed protein layers between two lipid membranes, so-called protein junctions. As β-gal molecule is a tetramer, it exposed several binding sites for liposome, promoting contacts between two lipid membranes and causing liposomal aggregation. Whereas liposomes were mostly free of protein at their surface at a MR of 1,500, lower MR complexes formed larger isolated objects decorated with proteins on their external surfaces. We hypothesized that protein coating on liposome surface observed at suboptimal MR, prevented liposome aggregation as well as interaction and fusion of liposome with the endosomal membrane. A tight contact between the lipoplex surface and the endosomal membrane is essential to promote mixing of lipids by "flip-flop" between the two bilayers, resulting in endosomal membrane destabilization and disruption.[10,20,24] As a result, the delivered protein is susceptible to degradation in the lysosome and is unable to access cytosol. Based on these observations, we suggest that the optimal ratio of 1,500 corresponds to a balance between two unfavorable situations. For lower ratios, the protein densities, exposed at the liposome surface, prevent the fusion between endosomal membranes and cationic lipids, while toxicity is induced at higher ratios reducing the delivery efficiency.

The study of the liposome structures formed by cationic lipids with the anti-K8 antibody highlights a different mechanism of delivery. DOSP:MM27/K8 showed a unique organization forming clusters of onion-like structures bearing antibodies on their surfaces but devoid of proteins. Such remodeling of cationic lipid-based assemblies to multilamellar concentric structures has already been described with cationic lipid/nucleic acid complexes.[25] This arrangement suggests that liposomes escape endosome through membrane disruption by a proton-sponge mechanism, while the large amount of MM27 per lipoplex offers a high buffering capacity. During endocytic trafficking, endolysosomes are acidified by the action of an ATPase enzyme that transports protons from the cytosol into the vesicle. It is proposed that MM27 prevents acidification of endocytic vesicles, causing the ATPase to transport more protons to reach acidic pH. The accumulation of protons in the vesicle is balanced by an influx of counter ions which ultimately causes osmotic swelling and rupture of the endosome membrane.[26] Through this mechanism, liposomes can be released into the cytosol without requiring a tight contact between the endosomal membrane and the lipoplexes.

Finally, we took advantage of the DOSP:MM27 delivery system to investigate the ability of anti-cytokeratin 8 antibodies to disrupt the interaction between cytokeratin 8 and F508del-CFTR. This interaction has previously been shown to impair the trafficking of this mutated channel toward the plasma membrane where it is partially functional, leading to cystic fibrosis.[15,16,27] The evaluation of transmembrane anionic efflux by MEQ fluorescence measurement showed that the delivery of antibodies against cytokeratin 8 led to the restoration of a cAMP-dependent anionic conductance at the surface of F508del-CFTR-expressing cells. These preliminary results have to be confirmed but strongly suggest that antibody-mediated disruption of the interaction between cytokeratin 8 and F508del-CFTR can restore the trafficking of this mutated channel towards the plasma membrane. This approach would provide a tool for the study of channelopathies and development of future therapeutic strategies.

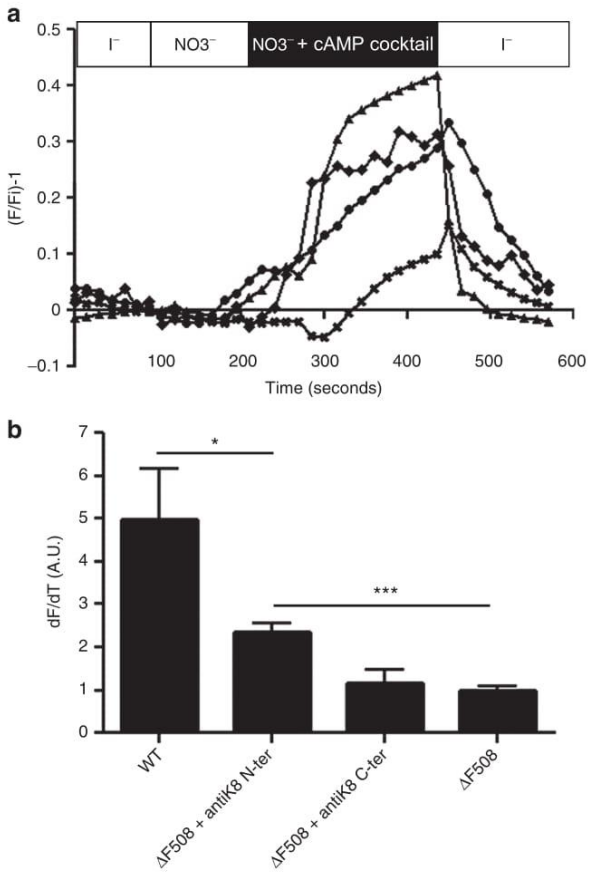


Figure 8 Rescue of F508del-CFTR activity by K8 antibody delivery. (**a**) MEQ fluorescence assay was performed on WT-CFTR cells treated with DOSP:MM27/K8 (triangles), on F508del-CFTR cells treated with DOSP:MM27/antiK8 N-ter (diamonds) or DOSP:MM27/antiK8 C-ter (circle) and untreated F508del-CFTR cells (cross). The fluorescence ratio is calculated as (F/F_i) - 1, F = Fluorescence intensity at indicated time points and F_i = Initial fluorescence intensity under iodide perfusion. (**b**) Quenching slopes of MEQ fluorescence registered for 30 seconds upon addition of cAMP and exchange of extracellular nitrate ($NO3^-$) for iodide ions (I^-).

Materials and methods

Preparation of liposomes and micelles. The lipids BGTC, DOSP, and MM27 were synthesized respectively as previously described.[18,21] The neutral lipid DOPE (dioleoylphosphatidyl-ethanolamine) was purchased from Avanti Polar Lipids (Alabaster, AL). Liposome formulations were prepared

by dissolving a cationic lipid (BGTC or DOSP) alone or with a neutral lipid (MM27 or DOPE) in chloroform at a molar ratio of 1. The solvent was removed using a rotary evaporator under vacuum at room temperature and the lipidic film rehydrated with ultrapure water for 24 hours at 4 °C at a final concentration of 10 mmol/l. The resulting suspension was sonicated for 15 minutes to obtain liposomes of 100–200 nm diameter.

Formulation of lipid/protein complexes. β-galactosidase (β-gal) (Roche Applied Science, Penzberg, Germany), rabbit anti-cytokeratin 8 antibody (K8) (ab51152, Abcam, Cambridge, UK) or mouse fluorescein conjugated anti-cytokeratin 8 antibody (FITC-K8) (ab87010, Abcam) were diluted with pH 7.4 buffer solution (120 mmol/l NaCl, 20 mmol/l 4-(2-hydroxyethyl)-1-piperazineethanesulfonic acid (HEPES)) or OptiMEM (Life Technologies, Carlsbad, CA) medium to the indicated final concentration. Lipids were diluted in water or OptiMEM at lipid/protein molar ratios (MR) from 100 to 2,500 and added to protein solution (v/v). The resulting solution was mixed gently and incubated for 15 minutes at room temperature before incubation with cells.

Polyacrylamide gel electrophoresis of lipid/protein complexes. BGTC:DOPE/β-gal complexes were prepared with 10 µg β-gal at various lipid/protein MR in pH 7.4 buffer solution (120 mmol/l NaCl, 20 mmol/l HEPES). After 15 minutes incubation at room temperature, 5 µl of the preparation were mixed with 5 µl Blue-Orange loading buffer (Promega, Madison, WI). Migration was performed on a nondenaturing polyacrylamide gel (5% stacking, 7% resolving) for 2 hours and the β-gal protein revealed by Coomassie blue staining.

Spectrofluorometer analysis. DOSP:MM27/anti-K8-FITC antibody complexes were formed in OptiMEM at various molar ratios (100–1,500) and incubated at room temperature for 15 minutes. Samples were centrifuged for 5 minutes at 13,000 g and supernatants were removed for determination of anti-K8-FITC content using a Fluoromax-4 (Horiba scientific, Kyoto, Japan). A standard curve correlating fluorescence and anti-K8-FITC antibody concentration was used to determine the amount of residual free antibody presents in supernatant after complexation.

Cell culture. HeLa (human cervical adenocarcinoma), H1299 (human non-small cell lung carcinoma), and C2C12 (murine myoblasts cells) were cultured in Dulbecco's Modified Eagle's medium (DMEM) (Life Technologies). HeLa cells expressing WT-CFTR or F508del-CFTR were cultured in DMEM supplemented with 450 µg/ml Zeocin (Invivogen, San Diego, CA). CHO-K1 from hamster ovary was cultured in F12-K medium (Life Technologies). All media were supplemented with 2 mmol/l L-glutamine, 10 µg/ml streptomycin, 100 U/ml penicillin, and 10% fetal calf serum obtained from Life Technologies. Cells were cultured at 37 °C in a 5% CO_2 humidified atmosphere.

Protein transfection. The day before transfection, cells were seeded at a density of ~7.0×10^4 cells per well of a 24-well plate in 0.5 ml of the appropriate complete growth medium to obtain 70–80% confluence the day of transfection. For each well, media was replaced 30 minutes before transfection with 0.4 ml of serum-free medium. Lipid/protein complexes prepared in 0.1 ml volume were added to cells. After 4 hours incubation, fetal calf serum was added at a final concentration of 10% and transfection was stopped at indicated time.

β-galactosidase activity assays

β-gal expression quantification. Cells were washed three times with PBS 1× and lysed with 0.3 ml of Reporter Lysis Buffer (Promega) supplemented with a protease inhibitor cocktail (Roche Applied Science). One freeze-thaw cycle was performed to ensure complete lysis. β-gal expression was quantified using the β-Glo Assay system from Promega according to manufacturer instructions. The amount of β-gal originally used for complexation (600, 800, or 1,000 ng) was used as control and arbitrarily fixed at 100%. Luminescence was read using the Victor-X3 multilabel plate reader (Perkin-Elmer, Waltham, MA).

Staining of β-gal-containing cells. HeLa cells were grown on glass coverslips. After treatment, cultures were washed three times with PBS 1×, fixed with 3.7% paraformaldehyde at room temperature and incubated in staining solution (400 µg/ml X-gal, 2 mmol/l $MgCl_2$, 4 mmol/l $K_3[Fe(CN)_6]$, 4 mmol/l $K_4[Fe(CN)_6]$). Slides were mounted with PBS in the presence of glycerol (50% v/v) and observed under an optical microscope.

MTT assay. After treatments, cells were washed, medium was replaced by 100 µl 3-(4,5-dimethylthiazol-2-yl) 2,5-diphenyltetrazodium (MTT) per well (1 mg/ml) diluted in complete medium, and cells were incubated at 37 °C for 4 hours. Then MTT solution was replaced by dimethyl sulfoxide (DMSO) (100 µl/well) and optical density was recorded at 550 nm. All assays were performed in triplicate.

Fluorescence microscopy. The internalization and intracellular fate of the FITC-K8 antibody was visualized 4 and 24 hours following lipid transfection. Cells were washed with PBS and fixed with 3.7% paraformaldehyde solution for 10 minutes at room temperature. Glass coverslips were mounted with ProLong antifade DAPI reagent (Life Technologies) and visualized with a Zeiss (Oberkochen, Germany) Axiovert epifluorescence microscope.

In order to confirm the association of the FITC-K8 antibody with its K8 target, cells were first transfected with the mouse FITC-K8 using DOSP:MM27 liposome, fixed and subsequently stained with the rabbit anti-K8 and a secondary anti-rabbit AlexaFluor 546. In brief, cells were fixed in PBS containing 3.7% paraformaldehyde and permeabilized with PBS containing 4% bovine serum albumin (BSA) (Sigma) and 0.1% saponin (Sigma, Saint-Louis, MO) for 20 minutes. Cells were washed with PBS, blocked with 10% goat serum diluted in PBS-4% BSA-0.1% saponin for 1 hour. Coverslips were then incubated with anti-K8 (1:200 dilution) antibodies overnight at 4 °C. Cells were rewashed and incubated for 1 hour with goat anti-rabbit AlexaFluor 546 (1:2,000 dilution) (Life Technologies) and mounted with ProLong antifade DAPI reagent. Colocalization was visualized using a laser-scanning confocal microscope (Carl Zeiss). Images were treated using ImageJ 1.42q software.

Cryo-TEM. Cryo-TEM imaging of cationic lipid/protein complexes were performed as previously described.[28] Complexes were formulated in 120 mmol/l NaCl and 20 mmol/l HEPES,

pH 7.4, and a 5 µl sample drop was applied to a holey carbon coated copper grid, the excess was blotted with a filter paper, and the grid was plunged into a liquid ethane bath cooled with liquid nitrogen (Leica EM CPC). Specimens were observed at a temperature of ~−170 °C, using a cryo holder, with a FEI Tecnai F20 electron microscope operating at 200 kV. Images were recorded with a 2k × 2k SlowScan CCD camera (Gatan) at a nominal magnification of 50,000× under low-dose conditions.

MEQ fluorescence assay. HeLa cells stably expressing WT-CFTR or F508del-CFTR were grown on glass coverslips for 24 hours and K8 antibody was delivered using DOSP:MM27 in serum-free medium (RM1500, 1.5 µg antibody). Four hours after antibody treatment, MEQ probe was loaded into cells by hypotonic shock permeabilization. Cells were washed with an iodide-containing isotonic solution (138 mmol/l NaI, 2.4 mmol/l K_2HPO_4, 0.8 mmol/l KH_2PO_4, 10 mmol/l HEPES, 1 mmol/l $CaSO_4$, 10 mmol/l D-glucose, pH 7.4) and incubated for 2 minutes in a hypotonic solution containing the halide-sensitive probe, MEQ (Life Technologies) (10 mmol/l MEQ, 110 mmol/l NaI, 1.92 mmol/l K_2HPO_4, 0.64 mmol/l KH_2PO_4, 8 mmol/l HEPES, 0.8 mmol/l $CaSO_4$, 8 mmol/l D-Glucose, pH 7.4). Hypotonic solution was removed and cells incubated with the isotonic solution for 15 minutes recovery. Coverslips were mounted in perfusion chamber continuously supplied with the isotonic solution at 37 °C, and basal fluorescence level observed under a Leica DMI6000B epifluorescence microscope equipped with environmental control. Cells were subsequently perfused with a nitrate-containing solution (138 mmol/l $NaNO_3$, 2.4 mmol/l K_2HPO_4, 0.8 mmol/l KH_2PO_4, 10 mmol/l HEPES, 1 mmol/l $CaSO_4$, 10 mmol/l D-Glucose, pH 7.4) and a cAMP stimulatory cocktail (500 µmol/l cptAMPc, 25 µmol/l forskolin, 100 µmol/l IBMX) was added to initiate channel opening. After 180 seconds, nitrate-containing solution was finally replaced by iodide isotonic solution to quench MEQ fluorescence. Intracellular fluorescence was monitored over time using MetaFluor software (Molecular Devices, Sunnyvale, CA). Results are expressed as relative fluorescence (F/F_i) - 1, F is the fluorescence intensity at time points indicated on the x-axis after background subtraction and compensation of MEQ photobleaching, and F_i the basal MEQ fluorescence obtained under iodide perfusion.

Acknowledgments. The authors are very grateful to the Cellular and Tissular Imaging Core Facility of Nantes University (MicroPICell) for excellent technical expertise in cell imaging. They are also indebted to Pierre and Jean-Marie Lehn for their pioneer works related to the synthesis of cationic lipids used in this study and also to Paul-Alain Jaffres for his work on imidazole based-lipids. This work was supported by special grants from the "Association Française contre les Myopathies" (Evry, France), from "Agence Nationale de la Recherche" (Paris, France) for IHU-CESTI, and from BPIFrance financement (Paris, France) for Emerit and Hepavac.

1. Fintini, D, Brufani, C and Cappa, M (2009). Profile of mecasermin for the long-term treatment of growth failure in children and adolescents with severe primary IGF-1 deficiency. *Ther Clin Risk Manag* **5**: 553–559.
2. Aviezer, D, Brill-Almon, E, Shaaltiel, Y, Hashmueli, S, Bartfeld, D, Mizrachi, S *et al.* (2009). A plant-derived recombinant human glucocerebrosidase enzyme–a preclinical and phase I investigation. *PLoS One* **4**: e4792.
3. Maloney, DG (2012). Anti-CD20 antibody therapy for B-cell lymphomas. *N Engl J Med* **366**: 2008–2016.
4. Ho, A, Schwarze, SR, Mermelstein, SJ, Waksman, G and Dowdy, SF (2001). Synthetic protein transduction domains: enhanced transduction potential *in vitro* and in vivo. *Cancer Res* **61**: 474–477.
5. Järver, P and Langel, U (2006). Cell-penetrating peptides–a brief introduction. *Biochim Biophys Acta* **1758**: 260–263.
6. Zelphati, O, Wang, Y, Kitada, S, Reed, JC, Felgner, PL and Corbeil, J (2001). Intracellular delivery of proteins with a new lipid-mediated delivery system. *J Biol Chem* **276**: 35103–35110.
7. Dalkara, D, Zuber, G and Behr, JP (2004). Intracytoplasmic delivery of anionic proteins. *Mol Ther* **9**: 964–969.
8. van der Gun, BT, Monami, A, Laarmann, S, Raskó, T, Slaska-Kiss, K, Weinhold, E *et al.* (2007). Serum insensitive, intranuclear protein delivery by the multipurpose cationic lipid SAINT-2. *J Control Release* **123**: 228–238.
9. Noble, GT, Stefanick, JF, Ashley, JD, Kiziltepe, T and Bilgicer, B (2014). Ligand-targeted liposome design: challenges and fundamental considerations. *Trends Biotechnol* **32**: 32–45.
10. Le Bihan, O, Chèvre, R, Mornet, S, Garnier, B, Pitard, B and Lambert, O (2011). Probing the *in vitro* mechanism of action of cationic lipid/DNA lipoplexes at a nanometric scale. *Nucleic Acids Res* **39**: 1595–1609.
11. Wasungu, L and Hoekstra, D (2006). Cationic lipids, lipoplexes and intracellular delivery of genes. *J Control Release* **116**: 255–264.
12. Barteau, B, Chèvre, R, Letrou-Bonneval, E, Labas, R, Lambert, O and Pitard, B (2008). Physicochemical parameters of non-viral vectors that govern transfection efficiency. *Curr Gene Ther* **8**: 313–323.
13. White, MB, Amos, J, Hsu, JM, Gerrard, B, Finn, P and Dean, M (1990). A frame-shift mutation in the cystic fibrosis gene. *Nature* **344**: 665–667.
14. Denning, GM, Anderson, MP, Amara, JF, Marshall, J, Smith, AE and Welsh, MJ (1992). Processing of mutant cystic fibrosis transmembrane conductance regulator is temperature-sensitive. *Nature* **358**: 761–764.
15. Colas, J, Faure, G, Saussereau, E, Trudel, S, Rabeh, WM, Bitam, S *et al.* (2012). Disruption of cytokeratin-8 interaction with F508del-CFTR corrects its functional defect. *Hum Mol Genet* **21**: 623–634.
16. Lipecka, J, Norez, C, Bensalem, N, Baudouin-Legros, M, Planelles, G, Becq, F *et al.* (2006). Rescue of DeltaF508-CFTR (cystic fibrosis transmembrane conductance regulator) by curcumin: involvement of the keratin 18 network. *J Pharmacol Exp Ther* **317**: 500–505.
17. Vigneron, JP, Oudrhiri, N, Fauquet, M, Vergely, L, Bradley, JC, Basseville, M *et al.* (1996). Guanidinium-cholesterol cationic lipids: efficient vectors for the transfection of eukaryotic cells. *Proc Natl Acad Sci USA* **93**: 9682–9686.
18. Mével, M, Sainlos, M, Chatin, B, Oudrhiri, N, Hauchecorne, M, Lambert, O *et al.* (2012). Paromomycin and neomycin B derived cationic lipids: synthesis and transfection studies. *J Control Release* **158**: 461–469.
19. Desigaux, L, Sainlos, M, Lambert, O, Chevre, R, Letrou-Bonneval, E, Vigneron, JP *et al.* (2007). Self-assembled lamellar complexes of siRNA with lipidic aminoglycoside derivatives promote efficient siRNA delivery and interference. *Proc Natl Acad Sci USA* **104**: 16534–16539.
20. Zuhorn, IS and Hoekstra, D (2002). On the mechanism of cationic amphiphile-mediated transfection. To fuse or not to fuse: is that the question? *J Membr Biol* **189**: 167–179.
21. Mével, M, Neveu, C, Gonçalves, C, Yaouanc, J-J, Pichon, C, Jaffrès, P-A, *et al.* (2008). Novel neutral imidazole-lipophosphoramides for transfection assays. *Chem Commun Camb Engl* **27**: 3124–3126.
22. Billiet, L, Gomez, J-P, Berchel, M, Jaffrès, P-A, Le Gall, T, Montier, T *et al.* (2012). Gene transfer by chemical vectors, and endocytosis routes of polyplexes, lipoplexes and lipopolyplexes in a myoblast cell line. *Biomaterials* **33**: 2980–2990.
23. Midoux, P, Pichon, C, Yaouanc, J-J and Jaffrès, P-A (2009). Chemical vectors for gene delivery: a current review on polymers, peptides and lipids containing histidine or imidazole as nucleic acids carriers. *Br. J. Pharmacol.* **157**: 166–178.
24. Xu, Y and Szoka, FC (1996). Mechanism of DNA release from cationic liposome/DNA complexes used in cell transfection *Biochemistry (Mosc.)* **35**: 5616–5623.
25. Pitard, B, Oudrhiri, N, Vigneron, JP, Hauchecorne, M, Aguerre, O, Toury, R *et al.* (1999). Structural characteristics of supramolecular assemblies formed by guanidinium-cholesterol reagents for gene transfection. *Proc Natl Acad Sci USA* **96**: 2621–2626.
26. Pack, DW, Hoffman, AS, Pun, S and Stayton, PS (2005). Design and development of polymers for gene delivery. *Nat Rev Drug Discov* **4**: 581–593.
27. Davezac, N, Tondelier, D, Lipecka, J, Fanen, P, Demaugre, F, Debski, J *et al.* (2004). Global proteomic approach unmasks involvement of keratins 8 and 18 in the delivery of cystic fibrosis transmembrane conductance regulator (CFTR)/deltaF508-CFTR to the plasma membrane. *Proteomics* **4**: 3833–3844.
28. Pitard, B, Bello-Roufaï, M, Lambert, O, Richard, P, Desigaux, L, Fernandes, S *et al.* (2004). Negatively charged self-assembling DNA/poloxamine nanospheres for *in vivo* gene transfer. *Nucleic Acids Res* **32**: e159.

This work is licensed under a Creative Commons Attribution-NonCommercial-NoDerivs 4.0 International License. The images or other third party material in this article are included in the article's Creative Commons license, unless indicated otherwise in the credit line; if the material is not included under the Creative Commons license, users will need to obtain permission from the license holder to reproduce the material. To view a copy of this license, visit http://creativecommons.org/licenses/by-nc-nd/4.0/

Article 7 : Evaluation of tetrafunctional block copolymers as synthetic vectors for lung gene transfer.

Biomaterials 45 (2015) 10–17

Contents lists available at ScienceDirect

Biomaterials

journal homepage: www.elsevier.com/locate/biomaterials

Evaluation of tetrafunctional block copolymers as synthetic vectors for lung gene transfer

Peggy Richard-Fiardo [a, b, 1], Catherine Hervouet [a, b, 1], Robert Marsault [a, b], Philippe R. Franken [a, b], Béatrice Cambien [a, b], Julien Guglielmi [a, b], Julie Warnez-Soulie [a, b], Jacques Darcourt [a, b], Thierry Pourcher [a, b], Thibault Colombani [c, d], Thomas Haudebourg [c, d], Pauline Peuziat [c, d], Bruno Pitard [c, d], Georges Vassaux [a, b, *]

[a] Laboratoire TIRO, UMRE 4320, iBEB, DSV, CEA, Nice, France
[b] Université de Nice-Sophia Antipolis, Nice, France
[c] INSERM UMR1087, CNRS UMR 6291, Nantes, France
[d] Université de Nantes, l'institut du thorax, Nantes, France

ARTICLE INFO

Article history:
Received 12 September 2014
Accepted 20 December 2014
Available online 13 January 2015

Keywords:
Tetrafunctional block copolymers
Lungs
Gene therapy
Nonviral vector
Molecular imaging

ABSTRACT

In the present study, we evaluated, in mice, the efficacy of the tetrafunctional block copolymer 704 as a nonviral gene delivery vector to the lungs. SPECT/CT molecular imaging of gene expression, biochemical assays, and immunohistochemistry were used. Our dataset shows that the formulation 704 resulted in higher levels of reporter gene expression than the GL67A formulation currently being used in a clinical trial in cystic fibrosis patients. The inflammatory response associated with this gene transfer was lower than that induced by the GL67A formulation, and the 704 formulation was amenable to repeated administrations. The cell types transfected by the 704 formulation were type I and type II pneumocytes, and transgene expression could not be detected in macrophages. These results emphasize the relevance of the 704 formulation as a nonviral gene delivery vector for lung gene therapy. Further studies will be required to validate this vector in larger animals, in which the lungs are more similar to human lungs.
© 2014 Elsevier Ltd. All rights reserved.

1. Introduction

Gene transfer to the lungs has many potential applications in inherited and acquired diseases. Historically, the pathology at the forefront of the development of lung gene therapy strategies has been cystic fibrosis (CF). To date, more than 400 CF patients have been included in various phase I and phase I/II clinical trials, using different types of viral and nonviral gene delivery vectors [1]. Another inherited disease, alpha-1 antitrypsin deficiency, has been the focus of intense gene therapy research, both at the preclinical and clinical levels (for a review, see Ref. [2]). Gene therapy has also been considered for more common pathologies with mixed genetic and environmental causes, such as asthma and chronic obstructive pulmonary disease [2], in addition to which serious acquired diseases for which available treatments are inefficient and unsatisfactory – such as cancer (primary lung cancer or metastasis) and acute lung injury/acute respiratory distress syndrome – may also benefit from advances in lung gene transfer [2].

At the heart of a successful gene therapy approach lies a gene delivery vector that is relevant to the pathology and compatible with the therapeutic schedule. Viral vectors are usually very efficient at promoting gene transfer to the lungs, but they are also immunogenic/proinflammatory [3]. This property makes them inappropriate for applications in pathologies in which the lungs are severely inflamed and/or that require repeated administrations. A notable exception is the recent development of integrating lentiviruses pseudotyped with Sendai virus envelope proteins that can promote long-lasting transgene expression in rodent models [4,5]. Nonviral gene delivery vectors represent another class of vectors, which are entirely synthetic and are, usually, less likely to induce a strong inflammatory response. As a result, they may be relevant in pathologies that require transient gene expression and/or repeated administrations. In this context, the "gold standard" in the field is the cationic lipid, GL67A (Genzyme corporation), complexed with

* Corresponding author. Laboratoire TIRO, UMRE4320, Faculté de Médecine, 28 avenue Valombrose, 06107 Nice Cedex 2, France.
E-mail address: vassaux@unice.fr (G. Vassaux).
[1] Equal contributors.

http://dx.doi.org/10.1016/j.biomaterials.2014.12.051
0142-9612/© 2014 Elsevier Ltd. All rights reserved.

plasmid DNA. This formulation has been tested extensively in various preclinical models [6–9] and has been administered to healthy volunteers and CF patients [10,11]. Based on the promising results of these studies, a randomized, double-blind, placebo-controlled phase IIB clinical trial of repeated application of this formulation in patients with CF is currently underway [12]. Although GL67A was the best available nonviral gene transfer reagent when tested by the UK Cystic Fibrosis Gene Therapy Consortium [7], room for improvement exists, particularly in terms of inflammatory effects [13].

Block copolymers represent an attractive class of new nonviral gene delivery vectors. The administration of DNA formulated with a nonionic, amphiphilic block copolymer has been shown to promote significant gene transfer to skeletal and cardiac muscles [14,15]. Intratracheal delivery of this formulation to the lungs was also shown to promote gene transfer to a level equivalent to that obtained with a polyethylenimine (PEI)-based formulation, but with reduced inflammation [16]. Tetrafunctional block copolymers, which have a tetrafunctional structure consisting of four poly(-ethylene oxide)/poly(propylene oxide) blocks centered on an ethylenediamine moiety, form small complexes with DNA, as observed using electron microscopy [17]. This type of formulation has also been shown convincingly to promote muscle gene transfer for various applications [17–19] and evidence exists that these formulations may be relevant as lung gene transfer reagents [20].

In the present study, we have assessed the lung gene transfer promoted by tetrafunctional block copolymers, and compared it with that obtained using GL67A. In this set of experiments, the block copolymer 704 was taken as a prototype. A first series of experiments was performed using SPECT/CT imaging of the expression of the Na/I symporter (NIS) as a reporter gene [21]. This imaging method detects the accumulation of radioactive iodide or $^{99m}TcO_4^-$ in the organs and tumors in which NIS is expressed endogenously or ectopically [22–25]. In a second phase, the study was expanded using more classical biochemical assays and immunohistochemistry.

2. Materials and methods

2.1. Animals

Animal housing and procedures were conducted according to the French Agriculture Ministry guidelines and were approved by the local ethics committee. Eight-week-old female BALB/c mice were obtained from Janvier (Le Genest Saint Isle, France).

2.2. Plasmids

The plasmids, pCDNA3mNIS (pNIS) [26] and pCIK-CAT (pCAT) [16], encoding the murine Na/I symporter (NIS) and the chloramphenicol acetyl transferase (CAT) (generous gift of D. Gill, Oxford UK) reporter genes, respectively, were purified from recombinant *E. coli* using the EndoFree plasmid purification kit (Qiagen, Chatsworth, CA).

2.3. Gene transfer agents

Clinical-grade GL67A was a gift from the UK Cystic Fibrosis Gene Therapy Consortium. This cationic lipid was formulated with DNA as previously described [6]. The physicochemical properties of the complex have been reported previously [27]. Poloxamer (Lutrol®) and tetrafunctional block copolymers (304, 704, 904) were provided by InCellArt (Nantes, France). Stock solutions (20% w/v) were prepared in water and stored at 4 °C. Formulations of DNA with copolymers were prepared by mixing equal volumes of poloxamer or tetrafunctional block copolymer stock solution in water with plasmid DNA solution at the desired concentration in buffered solution [28]. The physicochemical properties of the DNA/tetrafunctional block copolymer (304, 704, 904) complexes used for *in vivo* experiments are presented in Table 1.

2.4. Intratracheal gene delivery

BALB/c mice were anesthetized with ketamine (70 mg/kg) and xylazine (15 mg/kg), injected intraperitoneally. After anesthesia, plasmid DNA, formulated with the different nonviral gene transfer agents (GL67 or polymers), or 5×10^8 PFU recombinant adenovirus, AdCMV-NIS, encoding the Na/I symporter [24], was instilled intratracheally as a bolus (volume, 100 μl for GL67 and 50 μl for polymers and adenovirus) through a 22-gauge catheter. All complexes administered contained 80 μg plasmid DNA.

Table 1
Physicochemical properties of nanocomplexes used in this study.

Nanocomplexes	Diameter size (nm)	Zeta-potential (mV)
DNA/304	167 ± 30	−10 ± 0.7
DNA/704	251 ± 30	−18 ± 6.8
DNA/904	337 ± 40	−19 ± 1.0

2.5. MicroSPECT/CT studies

Mice were injected intraperitoneally with 100 MBq ^{99m}Tc pertechnetate ($^{99m}TcO_4^-$) obtained from a freshly eluted $^{99}Mo/^{99m}Tc$ generator. Precisely 20 min later, mice were imaged under isoflurane anesthesia (Baxter, Aerane). SPECT/CT scans were performed on a microSPECT/CT scanner (eXplore speCZT CT120, General Electric), using a previously published protocol [25,29]. Image analyses and quantitative determinations were performed using the "AMIDE" software [30,31]. For quantitative analysis of SPECT signals, the activities in the five brightest spots in the lungs were determined for each of the experimental animals. From the microCT images, the lung radiodensities of mice (expressed in Hounsfield units) were calculated and averaged from six three-dimensional regions of interest (2 mm diameter) outlined on each left and right lung.

2.6. CAT reporter gene assay

Mice were culled by cervical dislocation. The lungs were dissected and quantified for CAT expression as previously described [16]. Bronchoalveolar lavage fluid (BALF) was collected after washing the lungs three times with 500 μl sterile phosphate-buffered saline buffer containing a protease inhibitor cocktail (Roche Diagnostics, Meyland, France). BALF fluid was centrifuged (10,000 g, 5 min, 4 °C), and the supernatant and the pellet (containing the cells of the BALF) were used for protein analysis.

2.7. Histochemistry and histopathology

Immediately after euthanasia of the mice, the lungs were dissected, paraffin embedded, and cut into 4-μm-thick sections. Immunostaining of CAT was performed as previously described [20]. The sections were counterstained with Harris hematoxylin (Sigma, France).

2.8. Interleukin-6 assay

IL-6 levels were measured in the different lung compartments (lung lysates, BALF, and cells from BALF) of mice intratracheally injected with nonviral gene transfer agents. The assay was performed by ELISA (Quantikine, mouse IL-6), according to the manufacturer's instructions (R&D Systems, Minneapolis, USA). The IL-6 level was determined in 100 μl supernatant following the supplier's instructions. A standard curve was included for each microplate using the recombinant IL-6 protein (R&D Systems, Minneapolis, USA). Each lung extract was analyzed in triplicate. Protein content was measured with a bicinchoninic acid (BCA) protein assay kit.

2.9. CD45 flow cytometry assay

After euthanasia of mice intratracheally injected with nonviral gene transfer agents, the lungs were perfused with cold PBS. Lung tissues were digested with type IV collagenase and DNAse I (Roche) for 30 min at 37 °C, then incubated with mouse Fc-blocking antibody (CD16CD32, BD). The recovered cells (1×10^6 cells) were stained with APC-conjugated anti-CD45 antibody (BD), after lysis of red blood cells with ACK (Ammonium-Chloride-Potassium) lysis buffer (Invitrogen). As a negative control, APC-conjugated, irrelevant mouse isotype IgG (BD) was used instead of anti-CD45 antibody. After washing, the stained cells were examined by flow cytometry using the FACSCanto II (BD). BD FACSDiva™ software was used for subsequent data analysis.

2.10. Statistical analysis

Statistical analysis was performed using Prism (GraphPad software). Dual comparisons were made using the Student's t-test and comparisons between multiple conditions were analyzed using ANOVA. Statistical significance was set at $P = 0.05$.

3. Results

3.1. Evaluation of gene transfer to the lungs by SPECT/CT imaging

Examples of SPECT/CT images of NIS gene transfer obtained 48 h after intratracheal administration of formulations of tetrafunctional

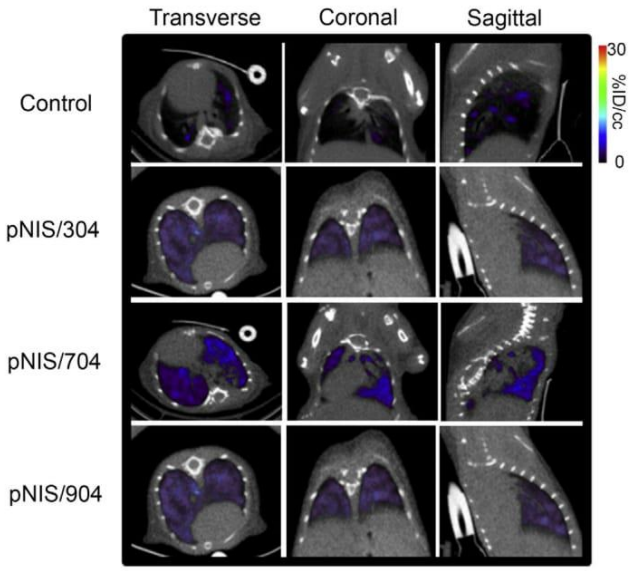


Fig. 1. *In vivo* imaging of NIS expression by microSPECT/CT. Representative SPECT/CT transverse, coronal, and sagittal sections of three-dimensional images in the thoraxes of noninjected (control) BALB/c mice, or mice administered with various nonviral gene delivery vectors. NIS-encoding plasmid (80 μg) (pNIS) was complexed with 304, 704, or 904. The complexes (pNIS/304, pNIS/704, pNIS/904) were administered though lung instillation (n = 3 animals per condition). Forty-eight hours later, mice received an intraperitoneal injection of 100 MBq $^{99m}TcO_4^-$ and were imaged with a microSPECT/CT camera (eXplore speCZT, General Electric). %ID/cc: percentage of dose injected per cubic centimeter.

block copolymers 304, 704 or 904 complexed with an expression plasmid encoding NIS are presented in Fig. 1. In all cases, discrete spots of signals are present in the lungs of mice administered with either pNIS/304, pNIS/704 or pNIS/904. Quantitative analysis of the data was performed by drawing regions of interest around the five brightest spots in the lungs, and the radiotracer content in these regions was calculated. Using this method of quantification, the formulation pNIS/704 provided the highest accumulation of the radiotracer amongst the different nonviral vectors tested (control: 4 ± 1 %ID/cc; pNIS/304: 8.1 ± 0.5 %ID/cc; pNIS/704: 12 ± 1.8 %ID/cc; pNIS/904: 9.2 ± 0.5 %ID/cc. p value <0.05 for pNIS/704 versus pNIS/304 or pNIS/904 and $p < 0.01$ for pNIS/704 versus control). In the following experiments, the block copolymer 704 was chosen because of its efficiency. In addition, this vector is prepared at a large scale and is currently under development for a gene therapy clinical trial.

We next used SPECT/CT imaging to compare gene transfer induced by intratracheal administration of a recombinant adenovirus encoding NIS (AdCMV-NIS) and formulations in which an expression plasmid encoding NIS was complexed with either the cationic lipid, GL67A (pNIS/GL67A), or the block copolymer, 704 (pNIS/704) (Fig. 2). Intratracheal administration of 5×10^8 PFU AdCMV-NIS led, 48 h later, to a strong signal in the lung (35 ± 8 %ID/cc), corresponding to radiotracer accumulation in the cells transduced by the vector (Fig. 2B). When the same experiment was repeated using a formulation in which an expression plasmid encoding NIS was complexed with cationic lipid GL67A (pNIS/GL67A), a much lower, NIS-specific signal was observed in the lungs of the transfected mice (7.4 ± 1 %ID/cc) (Fig. 2C), illustrating the superiority of adenovirus lung transduction compared to nonviral transfection. SPECT/CT imaging of gene transfer induced by the

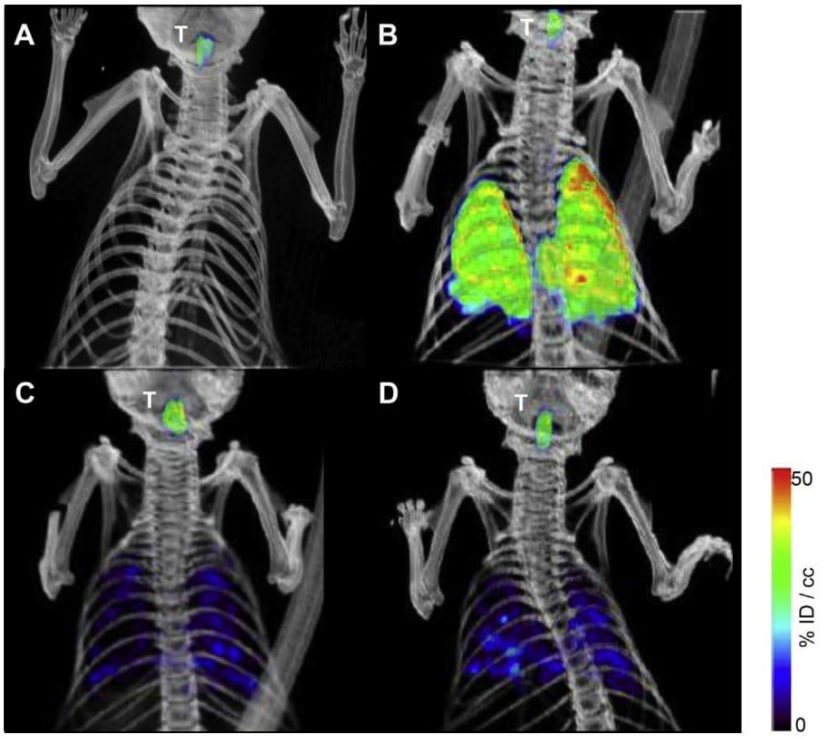


Fig. 2. Volume-rendered, fused SPECT/CT images of the thoracic regions of mice administered intratracheally with gene delivery vectors. SPECT images of BALB/c mice administered intratracheally with (A) saline, (B) 5×10^8 PFU AdCMV-NIS, (C) pNIS/GL67A (80 μg plasmid), or (D) pNIS/704 (80 μg plasmid). Forty-eight hours after administration of the various formulations, mice received an intraperitoneal injection of 100 MBq $^{99m}TcO_4^-$ and were imaged with a microSPECT/CT camera (eXplore speCZT, General Electric). %ID/cc: percentage of dose injected per cubic centimeter.

tetrafunctional block copolymer 704 led to a slightly brighter signal in the lungs (Fig. 2D). Quantitative analysis of the data revealed that the pNIS/704 formulation provided a higher accumulation of radiotracer than pNIS/GL67A (12 ± 1.8 %ID/cc versus 7.4 ± 1 %ID/cc; $p < 0.05$, $n = 3$ animals per condition).

3.2. Biochemical evaluation of gene transfer to the lungs

To confirm these observations, we next compared the extent of gene transfer induced by either GL67A or 704, using CAT as a reporter gene. In these experiments, intratracheal administrations of pCAT/GL67A or pCAT/704 were performed and transgene expression was measured two days (Fig. 3) or seven days (Fig. 4) later. Individual experiments (Fig. 3B–E) showed heterogeneity in gene transfer between experiments (Fig. 3B versus 3D, for example) and within a group, between individual mice (Fig. 3B for pCAT/GL67A and Fig. 3D for pCAT/704). Statistical analysis of the whole dataset (Fig. 3A) showed a highly significant difference in CAT expression induced by pCAT/704 versus pCAT/GL67A. Transgene expression with pCAT/704 was nearly three times higher than that with pCAT/GL67A. This superior efficacy of pCAT/704 was also observed seven days after intratracheal administration of the formulation, in the lung lysates, bronchoalveolar lavage fluids (BALF) and cells present in the BALF (Fig. 4).

3.3. Inflammatory responses

Fig. 5A shows representative microCT images of lungs treated with various formulations known to promote gene transfer to the lungs. As expected, adenovirus administration resulted in an important opacification of the lungs, suggesting significant inflammation. The radiodensity of the lungs is less important when nonviral gene delivery vectors are administered (Fig. 5A). Quantitative analysis (Fig. 5B) confirmed that, amongst the different gene delivery vectors tested, adenovirus induced the greatest opacity, followed by pCAT/lutrol, pCAT/304, pCAT/904, pCAT/GL67A and pCAT/704. The difference in density in the lungs of mice treated with the 704 formulation was significantly lower than that of mice treated with the GL67A formulation ($p < 0.05$). Analysis of the densities in separate lungs revealed an equal opacity in both lungs

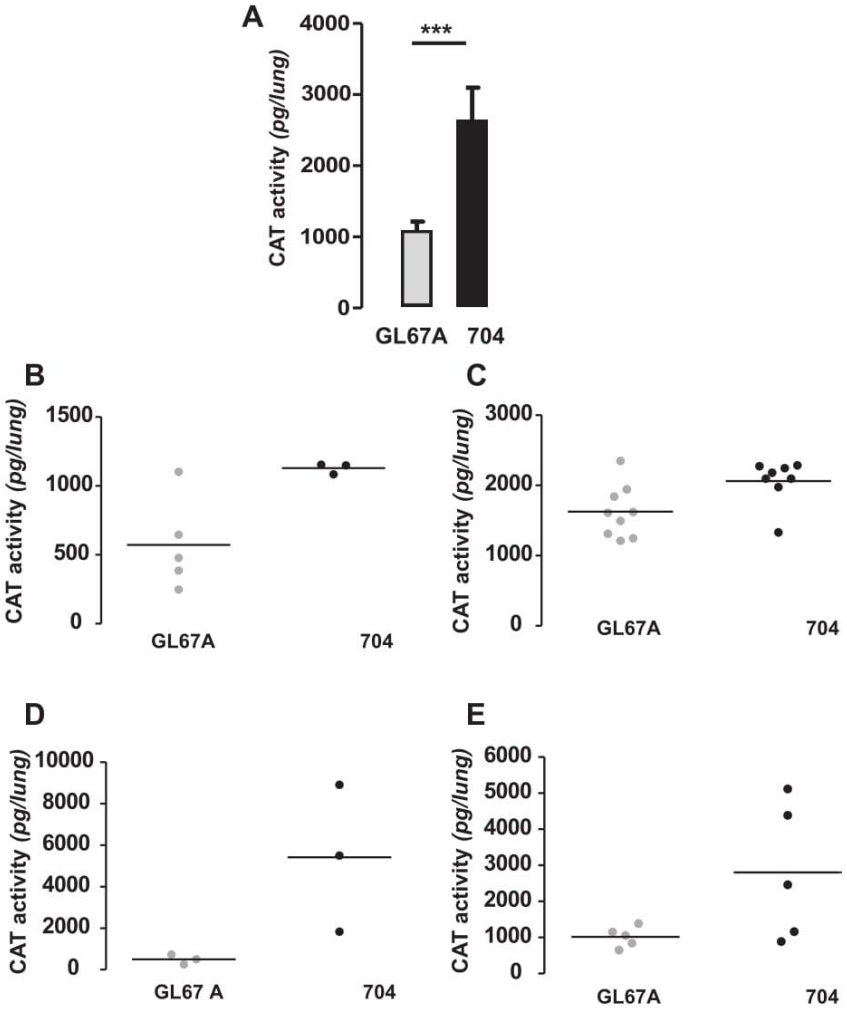


Fig. 3. Comparison of *in vivo* lung transfection efficacies using a biochemical assay. (A) CAT reporter plasmid (pCAT, 80 μg) was formulated with either GL67 or 704. The formulations were administered intratracheally. Two days later, the efficiency of gene transfer was evaluated by measuring CAT activity in the lung. Each column represents the mean ± *s.e.m.* of the CAT activity measured in 25 experimental animals in each group. *** = $p < 0.001$. (B–E) Some individual experiments in which the gene transfer efficacies of pCAT/GL67A and pCAT/704 were directly compared are also plotted. Each symbol represents an individual animal and the horizontal bar indicates group means.

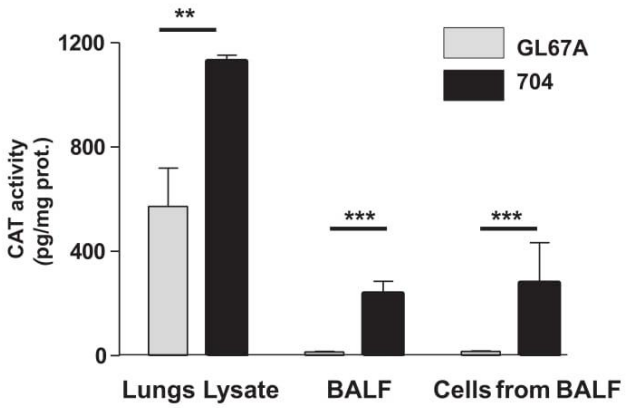


Fig. 4. CAT transgene expression in the lungs of mice seven days after nonviral gene transfer. CAT activity was measured in the lung homogenate, bronchoalveolar lavage fluid (BALF) or cells from the BALF, seven days after intratracheal instillation of pCAT/GL67A (80 μg plasmid) (gray bars) or pCAT/704 (80 μg plasmid) (black bars). Each column represents the mean ± *s.e.m.* of eight individual experiments. ** = $p < 0.01$, *** = $p < 0.001$.

in pCAT/704-treated mice, while a significant difference was observed in the lungs of pCAT/GL67A-treated animals, in which the right lobe was consistently more opaque than the left lobe (Fig. 5C).

The inflammatory response was then measured directly through the analysis of IL-6 production, as a cytokine marker of inflammation, in the lungs of pCAT/GL67A- or pCAT/704-treated mice. Fig. 6A shows that, at all times observed, the production of IL-6 was significantly greater in the lungs of pCAT/GL67A-treated mice than in those of pCAT/704-treated mice. To confirm these observations, the numeration of leukocytes (CD45-positive cells) in the lungs of mice instilled with either saline (control), pCAT/GL67A, or pCAT/704, was determined. The data presented in Fig. 6B show an important increase in the number of these cells in pCAT/GL67A-treated lungs, while this number is in the same range in pCAT/704-treated and control lungs.

3.4. Immunohistological determination of the types of cells transfected

To determine the types of cells transfected, lung sections of mice administered either saline buffer (Fig. 7A) or pCAT/704 (Fig. 7B, C) were stained with a CAT-specific antibody. Fig. 7B and C shows that both type I and type II pneumocytes were transfected, while CAT-specific staining was consistently absent in macrophages.

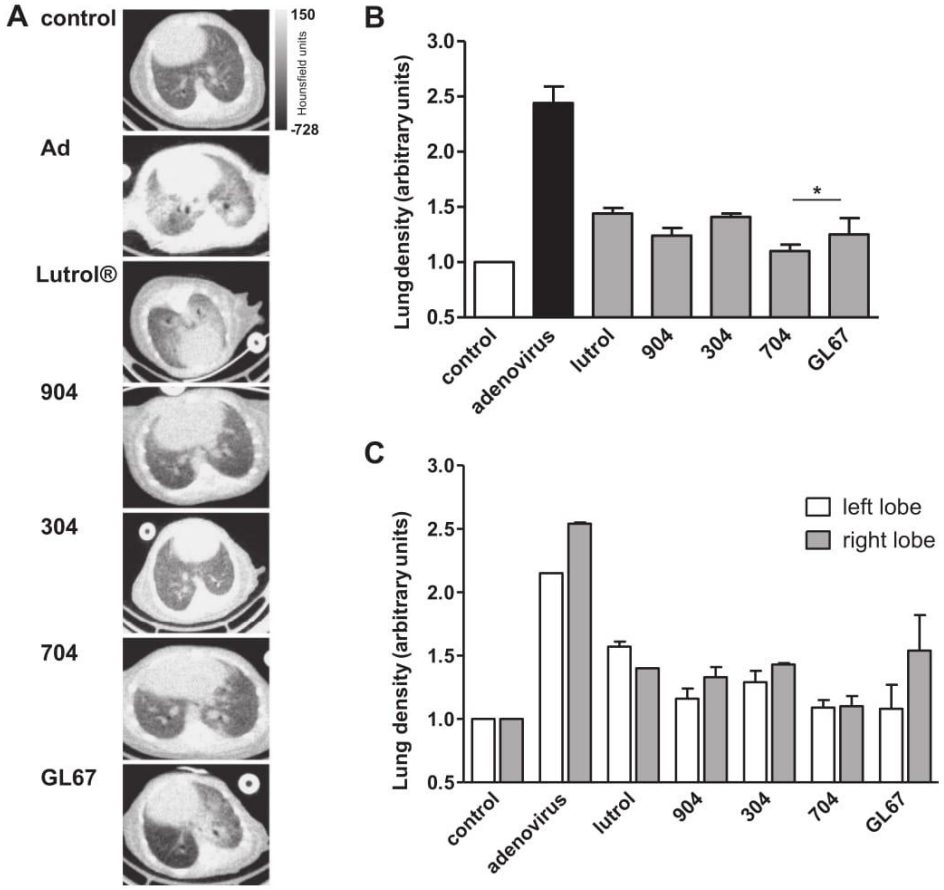


Fig. 5. Effect of gene transfer on lung radiodensity. (A) Representative transverse slices from CT images of BALB/c mice injected intratracheally with (from top to bottom) saline buffer, 5×10^8 PFU adenoviral vector, or a NIS-encoding plasmid (80 μg) formulated either with 3% Lutrol, 0.25% 904, 5% 304, 0.25% 704 vector, or GL67A. Forty-eight hours after the lung instillation, mice were imaged with a microSPECT/CT camera (eXplore speCZT, General Electric). ROIs were drawn in the left and right lung lobes and the average lung density (expressed in Hounsfield units) was normalized to the control (saline-administered) group. (B) Average values in the whole lungs, (C) values in the right and left lobes. Each column represents the mean ± *s.e.m.* of at least six individual experiments. * = $p < 0.05$.

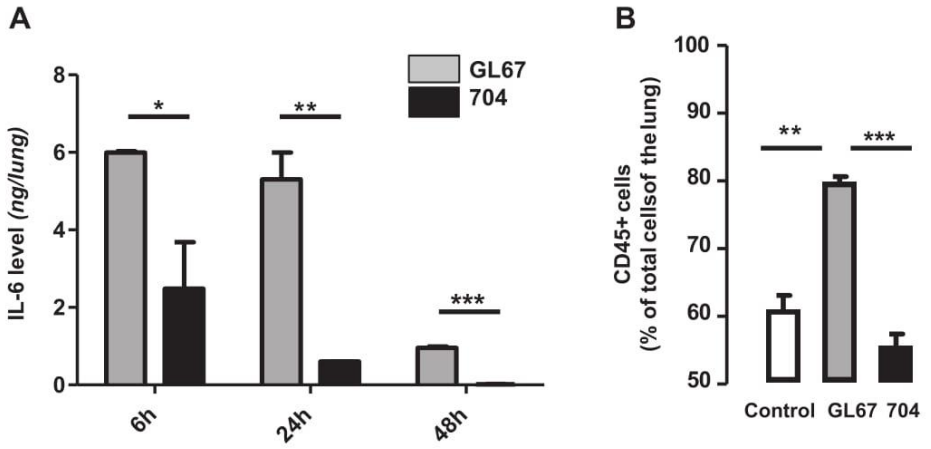


Fig. 6. Inflammatory response following intratracheal instillation of GL67 or 704 formulations complexed with pCAT. (A) Lung IL-6 contents were determined by enzyme-linked immunosorbent assay at the indicated time points after intratracheal instillation of pCAT/GL67A or pCAT/704 (80 μg plasmid). (B) Flow cytometric analysis of CD45-positive cells in lungs after GL67-or 704-mediated gene transfer. Lung-infiltrating inflammatory $CD45^+$ cells were counted by flow cytometry 24 h after intratrachial instillation of BALB/c mice with a saline PBS buffer (control mice), or with pCAT/GL67A or pCAT/704 (80 μg plasmid). The absolute number of total and $CD45^+$ cells in the lungs was determined in four separate experiments with two or three mice per group in each experiment. The results presented are pooled data from all of these experiments (mean ± *s.e.m.*). The percentage of CD45-positive cells relative to total lung cells is presented. * = $p < 0.05$; ** = $p < 0.01$; *** = $p < 0.001$.

3.5. Re-administration of pNIS/704

In a separate experiment, we evaluated whether a second administration of pCAT/704 was efficacious and could further increase the level of gene transfer. In these experiments, intratracheal administration was performed in mice (n = 29) at day zero. CAT activity in the lung lysates was measured two days (n = 7) or seven days (n = 14) later, whilst the eight remaining animals were given another intratracheal administration of pCAT/704. Two days after this second administration, CAT activity in the lungs was measured. Fig. 8 shows that the level of CAT expression in the lungs at day 2 had decreased slightly by day 7. Re-administration of an equivalent dose of pCAT/704 resulted in a very significant increase in the CAT activity, to reach more than twice the level at day 7. These results demonstrate that re-administration of the 704 formulation is possible within a week, resulting in an increase in gene transfer.

4. Discussion

Tetrafunctional block copolymers are branched block copolymers consisting of poly(ethylene oxide) and poly(propylene oxide) blocks fixed to an aliphatic diamine [17]. At physiological pH, they bear one positive charge per molecule [32], and complexation of DNA by this class of agent leads to the formation of negatively charged nanospheres [17]. These complexes form colloids that are stable for several weeks at room temperature. Three tetrafunctional block copolymers have been well described for their ability to complex DNA and to promote gene transfer, namely 304, 704 and 904 [17], and one of the main goals of the present study was to compare the lung transfection capabilities of these three copolymers with those of other well-known gene transfer agents. Molecular imaging of gene transfer by SPECT/CT, using the NIS gene as a reporter gene, revealed that this class of nonviral gene delivery vector was capable of transfecting the lungs, but at a level well below that achieved with a recombinant, nonreplicating adenovirus.

Adenovirus-mediated gene transfer to the lung has already been visualized by scintigraphy and PET [33]. The present dataset expands this observation and demonstrates that monitoring nonviral gene transfer in the lungs using SPECT/CT imaging of NIS expression is also feasible. Bioluminescence imaging of gene transfer to the lung has also been proposed [9,34], but this technology does not at this stage provide the three-dimensional images allowed by SPECT/CT.

For a quantitative analysis of the images, the number of "bright spots" in the lungs was determined and regions of interest were drawn around these brightest spots. Radiotracer content in these regions was calculated. Using this method of quantification, the formulation pNIS/704 provided the highest accumulation of radiotracer amongst the nonviral vectors.

Biochemical analysis was used to confirm the imaging data. Evaluation of the expression of the CAT protein two days after intratracheal administration of a plasmid encoding CAT, with either the GL67A or 704 formulation, showed that pCAT/704 was three times more efficient than pCAT/GL67A ($p < 0.001$). This highly statistically significant observation was obtained on a total of 25 animals in each group. However, there was a great interindividual variability, as illustrated in Fig. 3B–E. This wide variability has already been documented for GL67A in sets of experiments performed in other laboratories, and its causes are unclear [9]. One week after administration, transgene expression mediated by both formulations remained detectable and a statistically significant difference in transgene expression remained, despite the transient nature of lung transfection mediated by nonviral delivery vectors.

The inflammatory response was first assessed by analyzing microCT images of lungs treated with various formulations known to promote gene transfer to this organ. In this analysis, the assumption is that the opacity of the lungs is related to the inflammatory status of the organ. In the panel tested, pNIS/704 appeared to be one of the least proinflammatory formulations, and the lungs administered with pNIS/704 were significantly less opaque than those administered pNIS/GL67A, suggesting a lower level of inflammation triggered by the 704 formulation. Surprisingly, although the opacity of both lobes was equivalent in the lungs of pNIS/704-administered animals, the right lobe was consistently more opaque than the left lobe in the lungs of pNIS/GL67A-treated animals (Fig. 5C). This observation suggests a preferential deposit of pNIS/GL67A in the right lobe, which may be due to the viscosity of the formulation and the position of the animal during the intratracheal administration. In any case, this asymmetric opacity was only observed with pNIS/GL67A. The superior inflammatory response induced by intratracheal administration of pCAT/GL67A

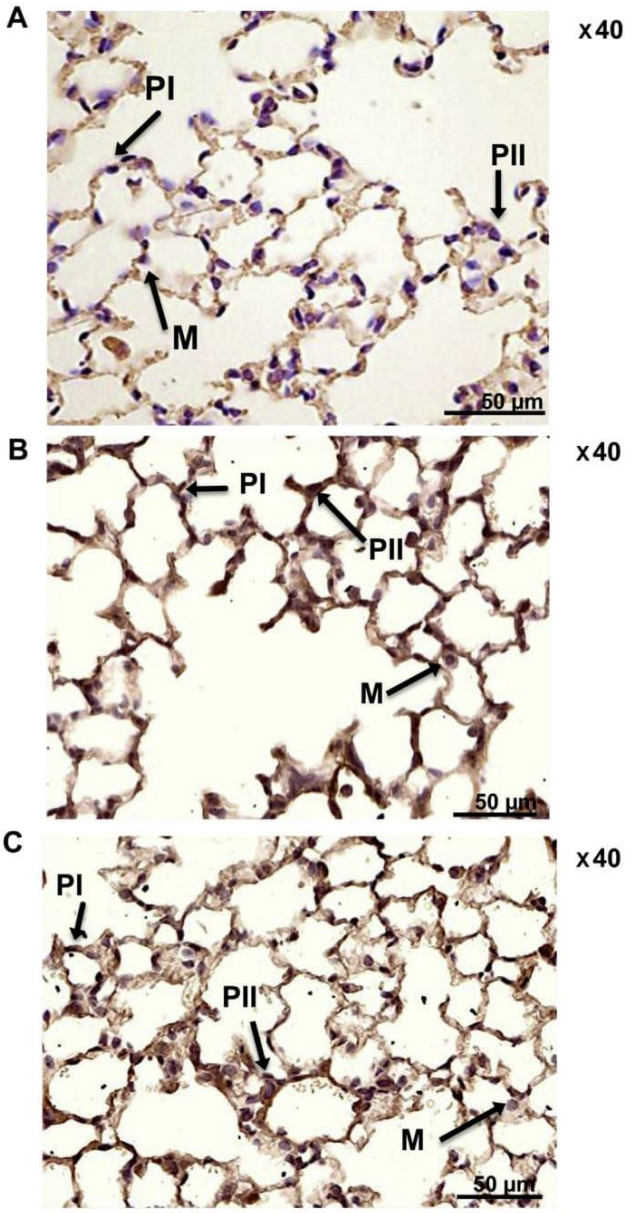


Fig. 7. Immunohistochemical localization of the CAT protein following pCAT/704 lung transfection. Representative sections are shown from animals intratracheally administered with PBS (A) or with pCAT/704 (80 µg plasmid). On day 2 post instillation, CAT expression was assessed in the lungs of mice, by immunohistochemistry. Fours animals were analyzed per group and staining was consistent between animals in each group. B and C show immunohistochemical sections obtained from two different animals. PI, type I pneumocyte; PII, type II pneumocyte; M, macrophage.

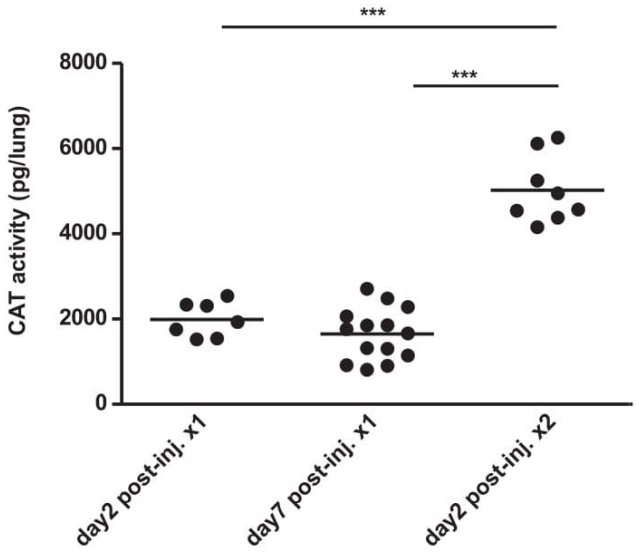


Fig. 8. Lung transfection efficacy of the DNA/704 formulation after a single- or double-dose regime. CAT activity in whole-lung lysates was assessed two and seven days after the first instillation, and two days after a second instillation of pCAT/704 (80 µg plasmid). Each symbol represents an individual animal and the horizontal bars indicate group means. *** = $p < 0.001$.

was confirmed by the measurement of IL-6 secretion in the lungs and the numeration of CD45-positive leukocyte infiltration in this organ. In line with the low inflammatory effect of this formulation, re-administration of pCAT/704 one week after an initial instillation resulted in a further increase in transgene expression, suggesting a possible utilization of this vector in the context of repeated dosing. In addition, macroscopic observations and histological analysis of the heart, liver, spleen and kidney of mice administered intratracheally with the 704 formulation failed to show any noticeable changes in these organs (not shown).

In terms of cell types transfected by the 704 formulation, immunohistochemical analysis demonstrated an absence of transgene-specific staining in macrophages and a strong transgene expression in pneumocytes (types I and II). The most likely explanation may be that the nanoparticles are taken up by the three types of cells, but gene transfer only occurs in pneumocytes. In macrophages, the DNA/704 complexes are likely to be phagocytosed and destroyed in the lysosome. *In vivo* uptake of lipoplexes and polyplexes by macrophages or Kupfer cells, without significant gene transfer, has been widely reported [35]. A similar observation was published with polypropylenimine dendrimer/DNA (PPIG3/DNA) nanoparticles. These PPIG3 nanoparticles were capable of transfecting, *in vivo*, epidermoid, ovarian and tongue cell squamous carcinomas, and they were also taken up by macrophages but without transgene expression [23]. In this context, the tetrafunctional block copolymer 704 complexed with DNA is very likely to be taken up by resident alveolar macrophages in the lungs, without detectable gene transfer in these cells.

In another series of experiments, we used SPECT/CT imaging of NIS gene expression to determine the pattern of transgene expression allowed by systemic injection of the 704 formulation. In these experiments, pNIS/704 (with up to 150 µg DNA) was injected into the tail vein of mice. No obvious toxicity was observed, and analysis of whole-body images revealed a lack of transgene expression in any tissues forty eight hours after administration (not shown), suggesting that the DNA/704 formulation is ineffective when a systemic route of injection is applied. Upon systemic administration, DNA/704 nanocomplexes travel into the circulation and, in the absence of active, specific transport, have to pass through the pores/fenestrations of normal vessels passively in order to reach the various organs and tissues. Measuring the sizes of these fenestrations and pores precisely represents a technical challenge, but functional studies as well as scanning electron microscopic analysis of the liver fenestrations in different species has indicated diameters ranging from 80 to 180 nm [36]. Considering that the diameter of the DNA/704 complex used in this study is greater than 200 nm (Table 1), an element of explanation for the

lack of gene transfer mediated by the 704 formulation may reside in the fact that the particles are simply too big to pass through the fenestrations. In any case, altogether, our studies demonstrate that DNA/704 complexes are to be used in loco-regional applications such as intramuscular [17,18], intracardiac [17] or intratracheal administrations (this study).

5. Conclusion

Overall, our study demonstrates that tetrafunctional block copolymers, and in particular formulation 704, are nonviral gene delivery vectors that are relevant for utilization in lung gene therapy. The low inflammatory stimulation is an additional beneficial factor when repeated administrations are envisaged. However, further studies will be required to fully validate this vector. In particular, the applicability of this promising formulation will have to be tested in larger animal models, in which the lungs are more similar to human lungs [7,37]. In addition, glycosylation has been suggested as a strategy to improve gene transfer to lung cells [38,39]. Considering that poloxamine block copolymers are easily amenable to chemical modifications, including glycosylation, this class of compounds can at this stage be considered as promising lead compounds with great potential.

Acknowledgments

This work was supported by “Vaincre la Mucoviscidose”, INSERM, and the French National Research Agency (ANR). The authors would like to thank the UK Cystic Fibrosis Gene Therapy Consortium for providing clinical-grade GL67A and Dr. U. Griesenbach (Imperial College London, UK) for helpful discussions. We thank the IRCAN Genomics Core Facility, the IRCAN Animal Core Facility and the Cytomed Platform (Nice) for providing access to their equipment.

References

[1] Davies JC, Alton EW. Gene therapy for cystic fibrosis. Proc Am Thorac Soc 2010;7:408–14.
[2] Griesenbach U, Alton EW. Expert opinion in biological therapy: update on developments in lung gene transfer. Expert Opin Biol Ther 2013;13:345–60.
[3] Griesenbach U, Alton EW. Gene transfer to the lung: lessons learned from more than 2 decades of CF gene therapy. Adv Drug Deliv Rev 2009;61:128–39.
[4] Griesenbach U, Inoue M, Meng C, Farley R, Chan M, Newman NK, et al. Assessment of F/HN-pseudotyped lentivirus as a clinically relevant vector for lung gene therapy. Am J Respir Crit Care Med 2012;186:846–56.
[5] Mitomo K, Griesenbach U, Inoue M, Somerton L, Meng C, Akiba E, et al. Toward gene therapy for cystic fibrosis using a lentivirus pseudotyped with Sendai virus envelopes. Mol Ther 2010;18:1173–82.
[6] Griesenbach U, Meng C, Farley R, Wasowicz MY, Munkonge FM, Chan M, et al. The use of carboxymethylcellulose gel to increase non-viral gene transfer in mouse airways. Biomaterials 2010;31:2665–72.
[7] McLachlan G, Davidson H, Holder E, Davies LA, Pringle IA, Sumner-Jones SG, et al. Pre-clinical evaluation of three non-viral gene transfer agents for cystic fibrosis after aerosol delivery to the ovine lung. Gene Ther 2011;18:996–1005.
[8] Griesenbach U, Vicente CC, Roberts MJ, Meng C, Soussi S, Xenariou S, et al. Secreted Gaussia luciferase as a sensitive reporter gene for in vivo and ex vivo studies of airway gene transfer. Biomaterials 2011;32:2614–24.
[9] Griesenbach U, Meng C, Farley R, Cheng SH, Scheule RK, Davies MH, et al. In vivo imaging of gene transfer to the respiratory tract. Biomaterials 2008;29:1533–40.
[10] Sorscher EJ, Logan JJ, Frizzell RA, Lyrene RK, Bebok Z, Dong JY, et al. Gene therapy for cystic fibrosis using cationic liposome mediated gene transfer: a phase I trial of safety and efficacy in the nasal airway. Hum Gene Ther 1994;5:1259–77.
[11] Alton EW, Stern M, Farley R, Jaffe A, Chadwick SL, Phillips J, et al. Cationic lipid-mediated CFTR gene transfer to the lungs and nose of patients with cystic fibrosis: a double-blind placebo-controlled trial. Lancet 1999;353:947–54.
[12] Alton EW, Boyd AC, Cheng SH, Cunningham S, Davies JC, Gill DR, et al. A randomised, double-blind, placebo-controlled phase IIB clinical trial of repeated application of gene therapy in patients with cystic fibrosis. Thorax 2013.
[13] Tagalakis AD, McAnulty RJ, Devaney J, Bottoms SE, Wong JB, Elbs M, et al. A receptor-targeted nanocomplex vector system optimized for respiratory gene transfer. Mol Ther 2008;16:907–15.
[14] Lemieux P, Guerin N, Paradis G, Proulx R, Chistyakova L, Kabanov A, et al. A combination of poloxamers increases gene expression of plasmid DNA in skeletal muscle. Gene Ther 2000;7:986–91.
[15] Pitard B, Pollard H, Agbulut O, Lambert O, Vilquin JT, Cherel Y, et al. A nonionic amphiphile agent promotes gene delivery in vivo to skeletal and cardiac muscles. Hum Gene Ther 2002;13:1767–75.
[16] Desigaux L, Gourden C, Bello-Roufai M, Richard P, Oudrhiri N, Lehn P, et al. Nonionic amphiphilic block copolymers promote gene transfer to the lung. Hum Gene Ther 2005;16:821–9.
[17] Pitard B, Bello-Roufai M, Lambert O, Richard P, Desigaux L, Fernandes S, et al. Negatively charged self-assembling DNA/poloxamine nanospheres for in vivo gene transfer. Nucleic Acids Res 2004;32:e159.
[18] McIlroy D, Barteau B, Cany J, Richard P, Gourden C, Conchon S, et al. DNA/amphiphilic block copolymer nanospheres promote low-dose DNA vaccination. Mol Ther 2009;17:1473–81.
[19] Beilvert F, Tissot A, Langelot M, Mevel M, Chatin B, Lair D, et al. DNA/amphiphilic block copolymer nanospheres reduce asthmatic response in a mouse model of allergic asthma. Hum Gene Ther 2012;23:597–608.
[20] Richard-Fiardo P, Cambien B, Pradelli E, Beilvert F, Pitard B, Schmid-Antomarchi H, et al. Effect of fractalkine-Fc delivery in experimental lung metastasis using DNA/704 nanospheres. Cancer Gene Ther 2011;18:761–72.
[21] Richard-Fiardo P, Franken PR, Lamit A, Marsault R, Guglielmi J, Cambien B, et al. Normalisation to blood activity is required for the accurate quantification of Na/I symporter ectopic expression by SPECT/CT in individual subjects. PLoS One 2012;7:e34086.
[22] Peerlinck I, Merron A, Baril P, Conchon S, Martin-Duque P, Hindorf C, et al. Targeted radionuclide therapy using a Wnt-targeted replicating adenovirus encoding the Na/I symporter. Clin Cancer Res 2009;15:6595–601.
[23] Chisholm EJ, Vassaux G, Martin-Duque P, Chevre R, Lambert O, Pitard B, et al. Cancer-specific transgene expression mediated by systemic injection of nanoparticles. Cancer Res 2009;69:2655–62.
[24] Tran L, Ouisse LH, Richard-Fiardo P, Franken PR, Darcourt J, Cornilleau G, et al. Adrenal gland infection by serotype 5 adenovirus requires coagulation factors. PLoS One 2013;8:e62191.
[25] Cambien B, Franken PR, Lamit A, Mauxion T, Richard-Fiardo P, Guglielmi J, et al. 99mTcO4–, Auger-mediated thyroid stunning: dosimetric requirements and associated molecular events. PLoS One 2014;9:e92729.
[26] Dayem M, Basquin C, Navarro V, Carrier P, Marsault R, Chang P, et al. Comparison of expressed human and mouse sodium/iodide symporters reveals differences in transport properties and subcellular localization. J Endocrinol 2008;197:95–109.
[27] Sanders NN, De Smedt SC, Demeester J. Mobility and stability of gene complexes in biogels. J Control Release 2003;87:117–29.
[28] Bello-Roufai M, Lambert O, Pitard B. Relationships between the physicochemical properties of an amphiphilic triblock copolymers/DNA complexes and their intramuscular transfection efficiency. Nucleic Acids Res 2007;35:728–39.
[29] Merron A, Baril P, Martin-Duque P, de la Vieja A, Tran L, Briat A, et al. Assessment of the Na/I symporter as a reporter gene to visualize oncolytic adenovirus propagation in peritoneal tumours. Eur J Nucl Med Mol Imaging 2010;37:1377–85.
[30] Loening AM, Gambhir SS. AMIDE: a free software tool for multimodality medical image analysis. Mol Imaging 2003;2:131–7.
[31] Breuilly M, Malandain G, Guglielmi J, Marsault R, Pourcher T, Franken PR, et al. Amplitude-based data selection for optimal retrospective reconstruction in micro-SPECT. Phys Med Biol 2013;58:2657–74.
[32] Armstrong JK, Chowdhry BZ, Snowden MJ, Dong J, Leharne SA. The effect of pH and concentration upon aggregation transitions in aqueous solutions of poloxamine T701. Int J Pharm 2001;229:57–66.
[33] Niu G, Krager KJ, Graham MM, Hichwa RD, Domann FE. Noninvasive radiological imaging of pulmonary gene transfer and expression using the human sodium iodide symporter. Eur J Nucl Med Mol Imaging 2005;32:534–40.
[34] Richard JC, Factor P, Ferkol T, Ponde DE, Zhou Z, Schuster DP. Repetitive imaging of reporter gene expression in the lung. Mol Imaging 2003;2:342–9.
[35] Nishikawa M, Takakura Y, Hashida M. Pharmacokinetics of plasmid DNA-based non-viral gene medicine. Adv Genet 2005;53:47–68.
[36] Jacobs F, Wisse E, De Geest B. The role of liver sinusoidal cells in hepatocyte-directed gene transfer. Am J Pathol 2010;176:14–21.
[37] Manunta MD, McAnulty RJ, McDowell A, Jin J, Ridout D, Fleming J, et al. Airway deposition of nebulized gene delivery nanocomplexes monitored by radioimaging agents. Am J Respir Cell Mol Biol 2013;49:471–80.
[38] Grosse S, Aron Y, Honore I, Thevenot G, Danel C, Roche AC, et al. Lactosylated polyethylenimine for gene transfer into airway epithelial cells: role of the sugar moiety in cell delivery and intracellular trafficking of the complexes. J Gene Med 2004;6:345–56.
[39] Roche AC, Fajac I, Grosse S, Frison N, Rondanino C, Mayer R, et al. Glycofection: facilitated gene transfer by cationic glycopolymers. Cell Mol Life Sci 2003;60:288–97.

BIBLIOGRAPHIE

Bibliographie

Abe, T., and Barber, G.N. (2014). Cytosolic-DNA-mediated, STING-dependent proinflammatory gene induction necessitates canonical NF-κB activation through TBK1. J. Virol. *88*, 5328–5341.

Ablasser, A., Bauernfeind, F., Hartmann, G., Latz, E., Fitzgerald, K.A., and Hornung, V. (2009). RIG-I-dependent sensing of poly(dA:dT) through the induction of an RNA polymerase III-transcribed RNA intermediate. Nat. Immunol. *10*, 1065–1072.

Ahmad-Nejad, P., Häcker, H., Rutz, M., Bauer, S., Vabulas, R.M., and Wagner, H. (2002). Bacterial CpG-DNA and lipopolysaccharides activate Toll-like receptors at distinct cellular compartments. Eur. J. Immunol. *32*, 1958–1968.

Akira, S., and Takeda, K. (2004). Toll-like receptor signalling. Nat. Rev. Immunol. *4*, 499–511.

Akira, S., Uematsu, S., and Takeuchi, O. (2006). Pathogen Recognition and Innate Immunity. Cell *124*, 783–801.

Albiger, B., Dahlberg, S., Henriques-Normark, B., and Normark, S. (2007). Role of the innate immune system in host defence against bacterial infections: focus on the Toll-like receptors. J. Intern. Med. *261*, 511–528.

Alexopoulou, L., Holt, A.C., Medzhitov, R., and Flavell, R.A. (2001). Recognition of double-stranded RNA and activation of NF-kappaB by Toll-like receptor 3. Nature *413*, 732–738.

Almofti, M.R., Harashima, H., Shinohara, Y., Almofti, A., Baba, Y., and Kiwada, H. (2003). Cationic liposome-mediated gene delivery: biophysical study and mechanism of internalization. Arch. Biochem. Biophys. *410*, 246–253.

Ammi, R., De Waele, J., Willemen, Y., Van Brussel, I., Schrijvers, D.M., Lion, E., and Smits, E.L.J. (2015). Poly(I:C) as cancer vaccine adjuvant: knocking on the door of medical breakthroughs. Pharmacol. Ther. *146*, 120–131.

Aramaki, Y., Takano, S., and Tsuchiya, S. (1999). Induction of apoptosis in macrophages by cationic liposomes. FEBS Lett. *460*, 472–476.

Aramaki, Y., Takano, S., Arima, H., and Tsuchiya, S. (2000). Induction of apoptosis in WEHI 231 cells by cationic liposomes. Pharm. Res. *17*, 515–520.

Arisaka, M., Nakamura, T., Yamada, A., Negishi, Y., and Aramaki, Y. (2010). Involvement of protein kinase Cdelta in induction of apoptosis by cationic liposomes in macrophage-like RAW264.7 cells. FEBS Lett. *584*, 1016–1020.

Asai, Y., Makimura, Y., Kawabata, A., and Ogawa, T. (2007). Soluble CD14 discriminates slight structural differences between lipid as that lead to distinct host cell activation. J. Immunol. Baltim. Md 1950 *179*, 7674–7683.

Barteau, B., Chèvre, R., Letrou-Bonneval, E., Labas, R., Lambert, O., and Pitard, B. (2008). Physicochemical parameters of non-viral vectors that govern transfection efficiency. Curr. Gene Ther. *8*, 313–323.

Behr, J.P., Demeneix, B., Loeffler, J.P., and Perez-Mutul, J. (1989). Efficient gene transfer into mammalian primary endocrine cells with lipopolyamine-coated DNA. Proc. Natl. Acad. Sci. U. S. A. *86*, 6982–6986.

Beilvert, F., Tissot, A., Langelot, M., Mével, M., Chatin, B., Lair, D., Magnan, A., and Pitard, B. (2012). DNA/amphiphilic block copolymer nanospheres reduce asthmatic response in a mouse model of allergic asthma. Hum. Gene Ther. *23*, 597–608.

Belmont, P., Aissaoui, A., Hauchecorne, M., Oudrhiri, N., Petit, L., Vigneron, J.-P., Lehn, J.-M., and Lehn, P. (2002). Aminoglycoside-derived cationic lipids as efficient vectors for gene transfection in vitro and in vivo. J. Gene Med. *4*, 517–526.

Bergsbaken, T., Fink, S.L., and Cookson, B.T. (2009). Pyroptosis: host cell death and inflammation. Nat. Rev. Microbiol. *7*, 99–109.

Billiet, L., Gomez, J.-P., Berchel, M., Jaffrès, P.-A., Le Gall, T., Montier, T., Bertrand, E., Cheradame, H., Guégan, P., Mével, M., et al. (2012). Gene transfer by chemical vectors, and endocytosis routes of polyplexes, lipoplexes and lipopolyplexes in a myoblast cell line. Biomaterials *33*, 2980–2990.

Boehme, K.W., and Compton, T. (2004). Innate Sensing of Viruses by Toll-Like Receptors. J. Virol. *78*, 7867–7873.

van den Boorn, J.G., Barchet, W., and Hartmann, G. (2012). Nucleic acid adjuvants: toward an educated vaccine. Adv. Immunol. *114*, 1–32.

Brisson, M., and Huang, L. (1999). Liposomes: conquering the nuclear barrier. Curr. Opin. Mol. Ther. *1*, 140–146.

Brubaker, S.W., Bonham, K.S., Zanoni, I., and Kagan, J.C. (2015). Innate Immune Pattern Recognition: A Cell Biological Perspective. Annu. Rev. Immunol. *33*, 257–290.

Burdette, D.L., Monroe, K.M., Sotelo-Troha, K., Iwig, J.S., Eckert, B., Hyodo, M., Hayakawa, Y., and Vance, R.E. (2011). STING is a direct innate immune sensor of cyclic di-GMP. Nature *478*, 515–518.

Cai, X., Chiu, Y.-H., and Chen, Z.J. (2014). The cGAS-cGAMP-STING Pathway of Cytosolic DNA Sensing and Signaling. Mol. Cell *54*, 289–296.

Calder, P.C. (2006). n-3 polyunsaturated fatty acids, inflammation, and inflammatory diseases. Am. J. Clin. Nutr. *83*, 1505S–1519S.

Cany, J., Barteau, B., Tran, L., Gauttier, V., Archambeaud, I., Couty, J.-P., Turlin, B., Pitard, B., Vassaux, G., Ferry, N., et al. (2011). AFP-specific immunotherapy impairs growth of autochthonous hepatocellular carcinoma in mice. J. Hepatol. *54*, 115–121.

Carmona-Ribeiro, A.M. (2000). Interactions between cationic liposomes and drugs or biomolecules. An. Acad. Bras. Ciênc. *72*, 39–44.

Carmona-Ribeiro, A.M., Ortis, F., Schumacher, R.I., and Armelin, M.C.S. (1997). Interactions between Cationic Vesicles and Cultured Mammalian Cells. Langmuir *13*, 2215–2218.

Cerboni, S., Gentili, M., and Manel, N. (2013). Diversity of pathogen sensors in dendritic cells. Adv. Immunol. *120*, 211–237.

Chatin, B., Mével, M., Devallière, J., Dallet, L., Haudebourg, T., Peuziat, P., Colombani, T., Berchel, M., Lambert, O., Edelman, A., et al. (2015). Liposome-based Formulation for Intracellular Delivery of Functional Proteins. Mol. Ther. Nucleic Acids *4*, e244.

Chen, W., Yan, W., and Huang, L. (2007). A simple but effective cancer vaccine consisting of an antigen and a cationic lipid. Cancer Immunol. Immunother. *57*, 517–530.

Chèvre, R., Le Bihan, O., Beilvert, F., Chatin, B., Barteau, B., Mével, M., Lambert, O., and Pitard, B. (2011). Amphiphilic block copolymers enhance the cellular uptake of DNA molecules through a facilitated plasma membrane transport. Nucleic Acids Res. *39*, 1610–1622.

Chiu, Y.-H., Macmillan, J.B., and Chen, Z.J. (2009). RNA polymerase III detects cytosolic DNA and induces type I interferons through the RIG-I pathway. Cell *138*, 576–591.

Christensen, D., Korsholm, K.S., Andersen, P., and Agger, E.M. (2011). Cationic liposomes as vaccine adjuvants. Expert Rev. Vaccines *10*, 513–521.

Cohen, R.N., van der Aa, M.A.E.M., Macaraeg, N., Lee, A.P., and Szoka, F.C. (2009). Quantification of plasmid DNA copies in the nucleus after lipoplex and polyplex transfection. J. Control. Release Off. J. Control. Release Soc. *135*, 166–174.

Collins, M., and Thrasher, A. (2015). Gene therapy: progress and predictions. Proc R Soc B *282*, 20143003.

Conner, S.D., and Schmid, S.L. (2003). Regulated portals of entry into the cell. Nature *422*, 37–44.

Cortesi, R., Campioni, M., Ravani, L., Drechsler, M., Pinotti, M., and Esposito, E. (2014). Cationic lipid nanosystems as carriers for nucleic acids. New Biotechnol. *31*, 44–54.

Cullis, P.R., Hope, M.J., and Tilcock, C.P. (1986). Lipid polymorphism and the roles of lipids in membranes. Chem. Phys. Lipids *40*, 127–144.

Dauty, E., and Verkman, A.S. (2005). Actin cytoskeleton as the principal determinant of size-dependent DNA mobility in cytoplasm: a new barrier for non-viral gene delivery. J. Biol. Chem. *280*, 7823–7828.

Dean, D.A. (1997). Import of plasmid DNA into the nucleus is sequence specific. Exp. Cell Res. *230*, 293–302.

Dean, D.A., Dean, B.S., Muller, S., and Smith, L.C. (1999). Sequence requirements for plasmid nuclear import. Exp. Cell Res. *253*, 713–722.

Dean, D.A., Strong, D.D., and Zimmer, W.E. (2005). Nuclear entry of nonviral vectors. Gene Ther. *12*, 881–890.

Debierre-Grockiego, F. (2010). Glycolipids are potential targets for protozoan parasite diseases. Trends Parasitol. *26*, 404–411.

Desigaux, L., Sainlos, M., Lambert, O., Chevre, R., Letrou-Bonneval, E., Vigneron, J.-P., Lehn, P., Lehn, J.-M., and Pitard, B. (2007). Self-assembled lamellar complexes of siRNA with lipidic aminoglycoside derivatives promote efficient siRNA delivery and interference. Proc. Natl. Acad. Sci. U. S. A. *104*, 16534–16539.

Draghici, B., and Ilies, M.A. (2015). Synthetic Nucleic Acid Delivery Systems: Present and Perspectives. J. Med. Chem. *58*, 4091–4130.

Dymond, M.K., and Attard, G.S. (2008). Cationic type I amphiphiles as modulators of membrane curvature elastic stress in vivo. Langmuir ACS J. Surf. Colloids *24*, 11743–11751.

Elouahabi, A., and Ruysschaert, J.-M. (2005). Formation and intracellular trafficking of lipoplexes and polyplexes. Mol. Ther. J. Am. Soc. Gene Ther. *11*, 336–347.

Erridge, C., Kennedy, S., Spickett, C.M., and Webb, D.J. (2008). Oxidized phospholipid inhibition of toll-like receptor (TLR) signaling is restricted to TLR2 and TLR4: roles for CD14, LPS-binding protein, and MD2 as targets for specificity of inhibition. J. Biol. Chem. *283*, 24748–24759.

Farhood, H., Bottega, R., Epand, R.M., and Huang, L. (1992). Effect of cationic cholesterol derivatives on gene transfer and protein kinase C activity. Biochim. Biophys. Acta *1111*, 239–246.

Felgner, P.L., Gadek, T.R., Holm, M., Roman, R., Chan, H.W., Wenz, M., Northrop, J.P., Ringold, G.M., and Danielsen, M. (1987). Lipofection: a highly efficient, lipid-mediated DNA-transfection procedure. Proc. Natl. Acad. Sci. U. S. A. *84*, 7413–7417.

Felgner, P.L., Tsai, Y.J., Sukhu, L., Wheeler, C.J., Manthorpe, M., Marshall, J., and Cheng, S.H. (1995). Improved cationic lipid formulations for in vivo gene therapy. Ann. N. Y. Acad. Sci. *772*, 126–139.

Feng, Q., Hato, S.V., Langereis, M.A., Zoll, J., Virgen-Slane, R., Peisley, A., Hur, S., Semler, B.L., van Rij, R.P., and van Kuppeveld, F.J.M. (2012). MDA5 detects the double-stranded RNA replicative form in picornavirus-infected cells. Cell Rep. *2*, 1187–1196.

Field, A.K., Tytell, A.A., Lampson, G.P., and Hilleman, M.R. (1967). Inducers of interferon and host resistance. II. Multistranded synthetic polynucleotide complexes. Proc. Natl. Acad. Sci. U. S. A. *58*, 1004–1010.

Filion, M.C., and Phillips, N.C. (1997). Toxicity and immunomodulatory activity of liposomal vectors formulated with cationic lipids toward immune effector cells. Biochim. Biophys. Acta *1329*, 345–356.

Fu, T.M., Guan, L., Friedman, A., Schofield, T.L., Ulmer, J.B., Liu, M.A., and Donnelly, J.J. (1999). Dose dependence of CTL precursor frequency induced by a DNA vaccine and correlation with protective immunity against influenza virus challenge. J. Immunol. Baltim. Md 1950 *162*, 4163–4170.

Funami, K., Sasai, M., Ohba, Y., Oshiumi, H., Seya, T., and Matsumoto, M. (2007). Spatiotemporal Mobilization of Toll/IL-1 Receptor Domain-Containing Adaptor Molecule-1 in Response to dsRNA. J. Immunol. *179*, 6867–6872.

Gantner, B.N., Simmons, R.M., Canavera, S.J., Akira, S., and Underhill, D.M. (2003). Collaborative Induction of Inflammatory Responses by Dectin-1 and Toll-like Receptor 2. J. Exp. Med. *197*, 1107–1117.

Geiger, R.C., Taylor, W., Glucksberg, M.R., and Dean, D.A. (2006). Cyclic stretch-induced reorganization of the cytoskeleton and its role in enhanced gene transfer. Gene Ther. *13*, 725–731.

Gilleron, J., Querbes, W., Zeigerer, A., Borodovsky, A., Marsico, G., Schubert, U., Manygoats, K., Seifert, S., Andree, C., Stöter, M., et al. (2013). Image-based analysis of lipid nanoparticle-mediated siRNA delivery, intracellular trafficking and endosomal escape. Nat. Biotechnol. *31*, 638–646.

Ginhoux, F., and Jung, S. (2014). Monocytes and macrophages: developmental pathways and tissue homeostasis. Nat. Rev. Immunol. *14*, 392–404.

Gitlin, L., Barchet, W., Gilfillan, S., Cella, M., Beutler, B., Flavell, R.A., Diamond, M.S., and Colonna, M. (2006). Essential role of mda-5 in type I IFN responses to polyriboinosinic:polyribocytidylic acid and encephalomyocarditis picornavirus. Proc. Natl. Acad. Sci. U. S. A. *103*, 8459–8464.

Gonçalves, C., Berchel, M., Gosselin, M.-P., Malard, V., Cheradame, H., Jaffrès, P.-A., Guégan, P., Pichon, C., and Midoux, P. (2014). Lipopolyplexes comprising imidazole/imidazolium lipophosphoramidate, histidinylated polyethyleneimine and siRNA as efficient formulation for siRNA transfection. Int. J. Pharm. *460*, 264–272.

Goodridge, H.S., Simmons, R.M., and Underhill, D.M. (2007). Dectin-1 stimulation by Candida albicans yeast or zymosan triggers NFAT activation in macrophages and dendritic cells. J. Immunol. Baltim. Md 1950 *178*, 3107–3115.

Goubau, D., Rehwinkel, J., and Reis e Sousa, C. (2010). PYHIN proteins: center stage in DNA sensing. Nat. Immunol. *11*, 984–986.

Graessmann, M., Menne, J., Liebler, M., Graeber, I., and Graessmann, A. (1989). Helper activity for gene expression, a novel function of the SV40 enhancer. Nucleic Acids Res. *17*, 6603.

Gringhuis, S.I., den Dunnen, J., Litjens, M., van der Vlist, M., Wevers, B., Bruijns, S.C.M., and Geijtenbeek, T.B.H. (2009). Dectin-1 directs T helper cell differentiation

by controlling noncanonical NF-kappaB activation through Raf-1 and Syk. Nat. Immunol. *10*, 203–213.

Gross, O., Thomas, C.J., Guarda, G., and Tschopp, J. (2011). The inflammasome: an integrated view. Immunol. Rev. *243*, 136–151.

Gupta, S.K., Bajwa, P., Deb, R., Chellappa, M.M., and Dey, S. (2014). Flagellin A Toll-Like Receptor 5 Agonist as an Adjuvant in Chicken Vaccines. Clin. Vaccine Immunol. CVI *21*, 261–270.

Ha, T.T.N., Huy, N.T., Murao, L.A., Lan, N.T.P., Thuy, T.T., Tuan, H.M., Nga, C.T.P., Tuong, V.V., Dat, T.V., Kikuchi, M., et al. (2011). Elevated Levels of Cell-Free Circulating DNA in Patients with Acute Dengue Virus Infection. PLOS ONE *6*, e25969.

Habrant, D., Peuziat, P., Colombani, T., Dallet, L., Gehin, J., Goudeau, E., Evrard, B., Lambert, O., Haudebourg, T., and Pitard, B. (2016). Design of ionizable lipids to overcome the limiting step of endosomal escape - Application in the intracellular delivery of mRNA, DNA and siRNA. J. Med. Chem.

Hafez, I.M., and Cullis, P.R. (2001). Roles of lipid polymorphism in intracellular delivery. Adv. Drug Deliv. Rev. *47*, 139–148.

Heil, F., Hemmi, H., Hochrein, H., Ampenberger, F., Kirschning, C., Akira, S., Lipford, G., Wagner, H., and Bauer, S. (2004). Species-specific recognition of single-stranded RNA via toll-like receptor 7 and 8. Science *303*, 1526–1529.

Hemmi, H., Takeuchi, O., Kawai, T., Kaisho, T., Sato, S., Sanjo, H., Matsumoto, M., Hoshino, K., Wagner, H., Takeda, K., et al. (2000). A Toll-like receptor recognizes bacterial DNA. Nature *408*, 740–745.

Hemmi, H., Kaisho, T., Takeuchi, O., Sato, S., Sanjo, H., Hoshino, K., Horiuchi, T., Tomizawa, H., Takeda, K., and Akira, S. (2002). Small anti-viral compounds activate immune cells via the TLR7 MyD88-dependent signaling pathway. Nat. Immunol. *3*, 196–200.

Hornung, V., Rothenfusser, S., Britsch, S., Krug, A., Jahrsdörfer, B., Giese, T., Endres, S., and Hartmann, G. (2002). Quantitative Expression of Toll-Like Receptor 1–10 mRNA in Cellular Subsets of Human Peripheral Blood Mononuclear Cells and Sensitivity to CpG Oligodeoxynucleotides. J. Immunol. *168*, 4531–4537.

Hornung, V., Guenthner-Biller, M., Bourquin, C., Ablasser, A., Schlee, M., Uematsu, S., Noronha, A., Manoharan, M., Akira, S., de Fougerolles, A., et al. (2005). Sequence-specific potent induction of IFN-alpha by short interfering RNA in plasmacytoid dendritic cells through TLR7. Nat. Med. *11*, 263–270.

Hornung, V., Ellegast, J., Kim, S., Brzózka, K., Jung, A., Kato, H., Poeck, H., Akira, S., Conzelmann, K.-K., Schlee, M., et al. (2006). 5'-Triphosphate RNA is the ligand for RIG-I. Science *314*, 994–997.

Hoving, J.C., Wilson, G.J., and Brown, G.D. (2014). Signalling C-Type lectin receptors, microbial recognition and immunity. Cell. Microbiol. *16*, 185–194.

Huen, A.O., and Rook, A.H. (2014). Toll receptor agonist therapy of skin cancer and cutaneous T-cell lymphoma. Curr. Opin. Oncol. *26*, 237–244.

Ilyinskii, P.O., Roy, C.J., O'Neil, C.P., Browning, E.A., Pittet, L.A., Altreuter, D.H., Alexis, F., Tonti, E., Shi, J., Basto, P.A., et al. (2014). Adjuvant-carrying synthetic vaccine particles augment the immune response to encapsulated antigen and exhibit strong local immune activation without inducing systemic cytokine release. Vaccine *32*, 2882–2895.

Ishikawa, H., and Barber, G.N. (2008). STING is an endoplasmic reticulum adaptor that facilitates innate immune signalling. Nature *455*, 674–678.

Itoh, K., Watanabe, A., Funami, K., Seya, T., and Matsumoto, M. (2008). The Clathrin-Mediated Endocytic Pathway Participates in dsRNA-Induced IFN-β Production. J. Immunol. *181*, 5522–5529.

Iwaoka, S., Nakamura, T., Takano, S., Tsuchiya, S., and Aramaki, Y. (2006). Cationic liposomes induce apoptosis through p38 MAP kinase-caspase-8-Bid pathway in macrophage-like RAW264.7 cells. J. Leukoc. Biol. *79*, 184–191.

Janeway, C.A., Jr (1989). Approaching the asymptote? Evolution and revolution in immunology. Cold Spring Harb. Symp. Quant. Biol. *54 Pt 1*, 1–13.

Jiao, S., Williams, P., Berg, R.K., Hodgeman, B.A., Liu, L., Repetto, G., and Wolff, J.A. (1992). Direct Gene Transfer into Nonhuman Primate Myofibers In Vivo. Hum. Gene Ther. *3*, 21–33.

Jones, J.W., Kayagaki, N., Broz, P., Henry, T., Newton, K., O'Rourke, K., Chan, S., Dong, J., Qu, Y., Roose-Girma, M., et al. (2010). Absent in melanoma 2 is required for innate immune recognition of Francisella tularensis. Proc. Natl. Acad. Sci. U. S. A. *107*, 9771–9776.

Junt, T., and Barchet, W. (2015). Translating nucleic acid-sensing pathways into therapies. Nat. Rev. Immunol. *15*, 529–544.

Kaiser, W.J., and Offermann, M.K. (2005). Apoptosis induced by the toll-like receptor adaptor TRIF is dependent on its receptor interacting protein homotypic interaction motif. J. Immunol. Baltim. Md 1950 *174*, 4942–4952.

Kamiya, H., Fujimura, Y., Matsuoka, I., and Harashima, H. (2002). Visualization of intracellular trafficking of exogenous DNA delivered by cationic liposomes. Biochem. Biophys. Res. Commun. *298*, 591–597.

Kastenmüller, K., Wille-Reece, U., Lindsay, R.W.B., Trager, L.R., Darrah, P.A., Flynn, B.J., Becker, M.R., Udey, M.C., Clausen, B.E., Igyarto, B.Z., et al. (2011). Protective T cell immunity in mice following protein-TLR7/8 agonist-conjugate immunization requires aggregation, type I IFN, and multiple DC subsets. J. Clin. Invest. *121*, 1782–1796.

Kato, H., Takeuchi, O., Mikamo-Satoh, E., Hirai, R., Kawai, T., Matsushita, K., Hiiragi, A., Dermody, T.S., Fujita, T., and Akira, S. (2008). Length-dependent recognition of

double-stranded ribonucleic acids by retinoic acid-inducible gene-I and melanoma differentiation-associated gene 5. J. Exp. Med. *205*, 1601–1610.

Kawai, T., and Akira, S. (2007). Signaling to NF-kappaB by Toll-like receptors. Trends Mol. Med. *13*, 460–469.

Kawai, T., and Akira, S. (2010). The role of pattern-recognition receptors in innate immunity: update on Toll-like receptors. Nat. Immunol. *11*, 373–384.

Kawai, T., Takahashi, K., Sato, S., Coban, C., Kumar, H., Kato, H., Ishii, K.J., Takeuchi, O., and Akira, S. (2005). IPS-1, an adaptor triggering RIG-I- and Mda5-mediated type I interferon induction. Nat. Immunol. *6*, 981–988.

Kay, M.A. (2011). State-of-the-art gene-based therapies: the road ahead. Nat. Rev. Genet. *12*, 316–328.

Kedmi, R., Ben-Arie, N., and Peer, D. (2010). The systemic toxicity of positively charged lipid nanoparticles and the role of Toll-like receptor 4 in immune activation. Biomaterials *31*, 6867–6875.

Khalil, I.A., Kogure, K., Akita, H., and Harashima, H. (2006). Uptake pathways and subsequent intracellular trafficking in nonviral gene delivery. Pharmacol. Rev. *58*, 32–45.

Kim, J.-I., Lee, C.J., Jin, M.S., Lee, C.-H., Paik, S.-G., Lee, H., and Lee, J.-O. (2005). Crystal structure of CD14 and its implications for lipopolysaccharide signaling. J. Biol. Chem. *280*, 11347–11351.

Kim, T., Pazhoor, S., Bao, M., Zhang, Z., Hanabuchi, S., Facchinetti, V., Bover, L., Plumas, J., Chaperot, L., Qin, J., et al. (2010). Aspartate-glutamate-alanine-histidine box motif (DEAH)/RNA helicase A helicases sense microbial DNA in human plasmacytoid dendritic cells. Proc. Natl. Acad. Sci. U. S. A. *107*, 15181–15186.

Kim, Y.-M., Brinkmann, M.M., Paquet, M.-E., and Ploegh, H.L. (2008). UNC93B1 delivers nucleotide-sensing toll-like receptors to endolysosomes. Nature *452*, 234–238.

van der Kleij, D., and Yazdanbakhsh, M. (2003). Control of inflammatory diseases by pathogens: lipids and the immune system. Eur. J. Immunol. *33*, 2953–2963.

Koltover, I., Salditt, T., Rädler, J.O., and Safinya, C.R. (1998). An inverted hexagonal phase of cationic liposome-DNA complexes related to DNA release and delivery. Science *281*, 78–81.

Korsholm, K.S., Andersen, P.L., and Christensen, D. (2012). Cationic liposomal vaccine adjuvants in animal challenge models: overview and current clinical status. Expert Rev. Vaccines *11*, 561–577.

Kreiss, P., Cameron, B., Rangara, R., Mailhe, P., Aguerre-Charriol, O., Airiau, M., Scherman, D., Crouzet, J., and Pitard, B. (1999). Plasmid DNA size does not affect the physicochemical properties of lipoplexes but modulates gene transfer efficiency. Nucleic Acids Res. *27*, 3792–3798.

Kreiter, S., Diken, M., Pascolo, S., Nair, S.K., Thielemans, K.M., and Geall, A. (2016). RNA Vaccination Therapy: Advances in an Emerging Field. J. Immunol. Res. *2016*.

Krieg, A.M., Yi, A.K., Matson, S., Waldschmidt, T.J., Bishop, G.A., Teasdale, R., Koretzky, G.A., and Klinman, D.M. (1995). CpG motifs in bacterial DNA trigger direct B-cell activation. Nature *374*, 546–549.

Kumar, V.V., Pichon, C., Refregiers, M., Guerin, B., Midoux, P., and Chaudhuri, A. (2003). Single histidine residue in head-group region is sufficient to impart remarkable gene transfection properties to cationic lipids: evidence for histidine-mediated membrane fusion at acidic pH. Gene Ther. *10*, 1206–1215.

Kusumoto, K., and Ishikawa, T. (2010). Didodecyldimethylammonium bromide (DDAB) induces caspase-mediated apoptosis in human leukemia HL-60 cells. J. Control. Release Off. J. Control. Release Soc. *147*, 246–252.

Labat-Moleur, F., Steffan, A.M., Brisson, C., Perron, H., Feugeas, O., Furstenberger, P., Oberling, F., Brambilla, E., and Behr, J.P. (1996). An electron microscopy study into the mechanism of gene transfer with lipopolyamines. Gene Ther. *3*, 1010–1017.

Landolfo, S., Gariglio, M., Gribaudo, G., and Lembo, D. (1998). The Ifi 200 genes: An emerging family of IFN-inducible genes. Biochimie *80*, 721–728.

Latz, E., Schoenemeyer, A., Visintin, A., Fitzgerald, K.A., Monks, B.G., Knetter, C.F., Lien, E., Nilsen, N.J., Espevik, T., and Golenbock, D.T. (2004). TLR9 signals after translocating from the ER to CpG DNA in the lysosome. Nat. Immunol. *5*, 190–198.

Lebeer, S., Vanderleyden, J., and De Keersmaecker, S.C.J. (2010). Host interactions of probiotic bacterial surface molecules: comparison with commensals and pathogens. Nat. Rev. Microbiol. *8*, 171–184.

Lee, S., and Nguyen, M.T. (2015). Recent Advances of Vaccine Adjuvants for Infectious Diseases. Immune Netw. *15*, 51–57.

Lee, H.K., Lund, J.M., Ramanathan, B., Mizushima, N., and Iwasaki, A. (2007). Autophagy-Dependent Viral Recognition by Plasmacytoid Dendritic Cells. Science *315*, 1398–1401.

Leon-Ponte, M., Kirchhof, M.G., Sun, T., Stephens, T., Singh, B., Sandhu, S., and Madrenas, J. (2005). Polycationic lipids inhibit the pro-inflammatory response to LPS. Immunol. Lett. *96*, 73–83.

Levy, M.Y., Barron, L.G., Meyer, K.B., and Szoka, F.C. (1996). Characterization of plasmid DNA transfer into mouse skeletal muscle: evaluation of uptake mechanism, expression and secretion of gene products into blood. Gene Ther. *3*, 201–211.

Liu, M.A. (2011). DNA vaccines: an historical perspective and view to the future. Immunol. Rev. *239*, 62–84.

Liu, L., Botos, I., Wang, Y., Leonard, J.N., Shiloach, J., Segal, D.M., and Davies, D.R. (2008). Structural Basis of Toll-Like Receptor 3 Signaling with Double-Stranded RNA. Science *320*, 379–381.

Liu, S., Chen, J., Cai, X., Wu, J., Chen, X., Wu, Y.-T., Sun, L., and Chen, Z.J. (2013). MAVS recruits multiple ubiquitin E3 ligases to activate antiviral signaling cascades. eLife *2*, e00785.

Lonez, C., Vandenbranden, M., and Ruysschaert, J.-M. (2012). Cationic lipids activate intracellular signaling pathways. Adv. Drug Deliv. Rev. *64*, 1749–1758.

Lonez, C., Bessodes, M., Scherman, D., Vandenbranden, M., Escriou, V., and Ruysschaert, J.-M. (2014). Cationic lipid nanocarriers activate Toll-like receptor 2 and NLRP3 inflammasome pathways. Nanomedicine Nanotechnol. Biol. Med. *10*, 775–782.

Lu, Y., and Swartz, J.R. (2016). Functional properties of flagellin as a stimulator of innate immunity. Sci. Rep. *6*, 18379.

Lu, Y.-C., Yeh, W.-C., and Ohashi, P.S. (2008). LPS/TLR4 signal transduction pathway. Cytokine *42*, 145–151.

Luby-Phelps, K. (2000). Cytoarchitecture and physical properties of cytoplasm: volume, viscosity, diffusion, intracellular surface area. Int. Rev. Cytol. *192*, 189–221.

Ma, Y., and He, B. (2014). Recognition of herpes simplex viruses: toll-like receptors and beyond. J. Mol. Biol. *426*, 1133–1147.

Marriott, I. (2012). Viral CNS infections: role of glial pattern recognition receptors in neuroinflammation. Microb. Immunol. *3*, 201.

Martin, B., Sainlos, M., Aissaoui, A., Oudrhiri, N., Hauchecorne, M., Vigneron, J.-P., Lehn, J.-M., and Lehn, P. (2005). The design of cationic lipids for gene delivery. Curr. Pharm. Des. *11*, 375–394.

Mata-Haro, V., Cekic, C., Martin, M., Chilton, P.M., Casella, C.R., and Mitchell, T.C. (2007). The vaccine adjuvant monophosphoryl lipid A as a TRIF-biased agonist of TLR4. Science *316*, 1628–1632.

McIlroy, D., Barteau, B., Cany, J., Richard, P., Gourden, C., Conchon, S., and Pitard, B. (2009). DNA/amphiphilic block copolymer nanospheres promote low-dose DNA vaccination. Mol. Ther. J. Am. Soc. Gene Ther. *17*, 1473–1481.

Melchior, F., and Gerace, L. (1995). Mechanisms of nuclear protein import. Curr. Opin. Cell Biol. *7*, 310–318.

Meraz, I.M., Savage, D.J., Segura-Ibarra, V., Li, J., Rhudy, J., Gu, J., and Serda, R.E. (2014). Adjuvant cationic liposomes presenting MPL and IL-12 induce cell death, suppress tumor growth, and alter the cellular phenotype of tumors in a murine model of breast cancer. Mol. Pharm. *11*, 3484–3491.

Mesika, A., Kiss, V., Brumfeld, V., Ghosh, G., and Reich, Z. (2005). Enhanced intracellular mobility and nuclear accumulation of DNA plasmids associated with a karyophilic protein. Hum. Gene Ther. *16*, 200–208.

Mével, M., Neveu, C., Gonçalves, C., Yaouanc, J.-J., Pichon, C., Jaffrès, P.-A., and Midoux, P. (2008). Novel neutral imidazole-lipophosphoramides for transfection assays. Chem. Commun. 3124–3126.

Mével, M., Sainlos, M., Chatin, B., Oudrhiri, N., Hauchecorne, M., Lambert, O., Vigneron, J.-P., Lehn, P., Pitard, B., and Lehn, J.-M. (2012). Paromomycin and neomycin B derived cationic lipids: synthesis and transfection studies. J. Control. Release Off. J. Control. Release Soc. *158*, 461–469.

Mével, M., Haudebourg, T., Colombani, T., Peuziat, P., Dallet, L., Chatin, B., Lambert, O., Berchel, M., Montier, T., Jaffrès, P.-A., et al. (2015). Important role of phosphoramido linkage in imidazole-based dioleyl helper lipids for liposome stability and primary cell transfection. J. Gene Med.

Meylan, E., Burns, K., Hofmann, K., Blancheteau, V., Martinon, F., Kelliher, M., and Tschopp, J. (2004). RIP1 is an essential mediator of Toll-like receptor 3–induced NF-κB activation. Nat. Immunol. *5*, 503–507.

Midoux, P., LeCam, E., Coulaud, D., Delain, E., and Pichon, C. (2002). Histidine containing peptides and polypeptides as nucleic acid vectors. Somat. Cell Mol. Genet. *27*, 27–47.

Midoux, P., Pichon, C., Yaouanc, J.-J., and Jaffrès, P.-A. (2009). Chemical vectors for gene delivery: a current review on polymers, peptides and lipids containing histidine or imidazole as nucleic acids carriers. Br. J. Pharmacol. *157*, 166–178.

Mishra, D., Hubenak, J.R., and Mathur, A.B. (2013). Nanoparticle systems as tools to improve drug delivery and therapeutic efficacy. J. Biomed. Mater. Res. A *101*, 3646–3660.

Mogensen, T.H. (2009). Pathogen Recognition and Inflammatory Signaling in Innate Immune Defenses. Clin. Microbiol. Rev. *22*, 240–273.

Montier, T., Benvegnu, T., Jaffrès, P.-A., Yaouanc, J.-J., and Lehn, P. (2008). Progress in cationic lipid-mediated gene transfection: a series of bio-inspired lipids as an example. Curr. Gene Ther. *8*, 296–312.

Motta, V., Soares, F., Sun, T., and Philpott, D.J. (2015). NOD-Like Receptors: Versatile Cytosolic Sentinels. Physiol. Rev. *95*, 149–178.

Muruve, D.A., Pétrilli, V., Zaiss, A.K., White, L.R., Clark, S.A., Ross, P.J., Parks, R.J., and Tschopp, J. (2008). The inflammasome recognizes cytosolic microbial and host DNA and triggers an innate immune response. Nature *452*, 103–107.

Neuhaus, F.C., and Baddiley, J. (2003). A continuum of anionic charge: structures and functions of D-alanyl-teichoic acids in gram-positive bacteria. Microbiol. Mol. Biol. Rev. MMBR *67*, 686–723.

O'Donnell, V.B., and Murphy, R.C. (2012). New families of bioactive oxidized phospholipids generated by immune cells: identification and signaling actions. Blood *120*, 1985–1992.

Ostuni, R., Zanoni, I., and Granucci, F. (2010). Deciphering the complexity of Toll-like receptor signaling. Cell. Mol. Life Sci. CMLS *67*, 4109–4134.

Pack, D.W., Hoffman, A.S., Pun, S., and Stayton, P.S. (2005). Design and development of polymers for gene delivery. Nat. Rev. Drug Discov. *4*, 581–593.

Paludan, S.R. (2015). Activation and Regulation of DNA-Driven Immune Responses. Microbiol. Mol. Biol. Rev. *79*, 225–241.

Paludan, S.R., Bowie, A.G., Horan, K.A., and Fitzgerald, K.A. (2011). Recognition of herpesviruses by the innate immune system. Nat. Rev. Immunol. *11*, 143–154.

Pashine, A., Valiante, N.M., and Ulmer, J.B. (2005). Targeting the innate immune response with improved vaccine adjuvants. Nat. Med. *11*, S63–S68.

Pétrilli, V., Dostert, C., Muruve, D.A., and Tschopp, J. (2007). The inflammasome: a danger sensing complex triggering innate immunity. Curr. Opin. Immunol. *19*, 615–622.

Pezzoli, D., Kajaste-Rudnitski, A., Chiesa, R., and Candiani, G. (2013). Lipid-Based Nanoparticles as Nonviral Gene Delivery Vectors. In Nanomaterial Interfaces in Biology, P. Bergese, and K. Hamad-Schifferli, eds. (Humana Press), pp. 269–279.

Piazza, M., Yu, L., Teghanemt, A., Gioannini, T., Weiss, J., and Peri, F. (2009). Evidence of a specific interaction between new synthetic antisepsis agents and CD14. Biochemistry (Mosc.) *48*, 12337–12344.

Piazza, M., Calabrese, V., Baruffa, C., Gioannini, T., Weiss, J., and Peri, F. (2010). The cationic amphiphile 3,4-bis(tetradecyloxy)benzylamine inhibits LPS signaling by competing with endotoxin for CD14 binding. Biochem. Pharmacol. *80*, 2050–2056.

Pichlmair, A., Schulz, O., Tan, C.P., Näslund, T.I., Liljeström, P., Weber, F., and Reis e Sousa, C. (2006). RIG-I-mediated antiviral responses to single-stranded RNA bearing 5’-phosphates. Science *314*, 997–1001.

Pitard, B. (2002). Supramolecular assemblies of DNA delivery systems. Somat. Cell Mol. Genet. *27*, 5–15.

Pitard, B., Aguerre, O., Airiau, M., Lachagès, A.M., Boukhnikachvili, T., Byk, G., Dubertret, C., Herviou, C., Scherman, D., Mayaux, J.F., et al. (1997). Virus-sized self-assembling lamellar complexes between plasmid DNA and cationic micelles promote gene transfer. Proc. Natl. Acad. Sci. U. S. A. *94*, 14412–14417.

Pitard, B., Oudrhiri, N., Vigneron, J.P., Hauchecorne, M., Aguerre, O., Toury, R., Airiau, M., Ramasawmy, R., Scherman, D., Crouzet, J., et al. (1999). Structural characteristics of supramolecular assemblies formed by guanidinium-cholesterol reagents for gene transfection. Proc. Natl. Acad. Sci. U. S. A. *96*, 2621–2626.

Pollard, H., Remy, J.S., Loussouarn, G., Demolombe, S., Behr, J.P., and Escande, D. (1998). Polyethylenimine but not cationic lipids promotes transgene delivery to the nucleus in mammalian cells. J. Biol. Chem. *273*, 7507–7511.

Ray, R.M., Li, C., Bhattacharya, S., Naren, A.P., and Johnson, L.R. (2012). Spermine, a molecular switch regulating EGFR, integrin β3, Src, and FAK scaffolding. Cell. Signal. *24*, 931–942.

Regen, T., van Rossum, D., Scheffel, J., Kastriti, M.-E., Revelo, N.H., Prinz, M., Brück, W., and Hanisch, U.-K. (2011). CD14 and TRIF govern distinct responsiveness and responses in mouse microglial TLR4 challenges by structural variants of LPS. Brain. Behav. Immun. *25*, 957–970.

Rejman, J., Oberle, V., Zuhorn, I.S., and Hoekstra, D. (2004). Size-dependent internalization of particles via the pathways of clathrin- and caveolae-mediated endocytosis. Biochem. J. *377*, 159–169.

Richard, J.P., Melikov, K., Brooks, H., Prevot, P., Lebleu, B., and Chernomordik, L.V. (2005). Cellular uptake of unconjugated TAT peptide involves clathrin-dependent endocytosis and heparan sulfate receptors. J. Biol. Chem. *280*, 15300–15306.

Ropert, C., and Gazzinelli, R.T. (2000). Signaling of immune system cells by glycosylphosphatidylinositol (GPI) anchor and related structures derived from parasitic protozoa. Curr. Opin. Microbiol. *3*, 395–403.

Ruysschaert, J.M., el Ouahabi, A., Willeaume, V., Huez, G., Fuks, R., Vandenbranden, M., and Di Stefano, P. (1994a). A novel cationic amphiphile for transfection of mammalian cells. Biochem. Biophys. Res. Commun. *203*, 1622–1628.

Ruysschaert, J.M., el Ouahabi, A., Willeaume, V., Huez, G., Fuks, R., Vandenbranden, M., and Di Stefano, P. (1994b). A novel cationic amphiphile for transfection of mammalian cells. Biochem. Biophys. Res. Commun. *203*, 1622–1628.

Sacramento, C.B., Moraes, J.Z., Denapolis, P.M.A., and Han, S.W. (2010). Gene expression promoted by the SV40 DNA targeting sequence and the hypoxia-responsive element under normoxia and hypoxia. Braz. J. Med. Biol. Res. *43*, 722–727.

Sainlos, M., Hauchecorne, M., Oudrhiri, N., Zertal-Zidani, S., Aissaoui, A., Vigneron, J.-P., Lehn, J.-M., and Lehn, P. (2005). Kanamycin A-derived cationic lipids as vectors for gene transfection. Chembiochem Eur. J. Chem. Biol. *6*, 1023–1033.

Saito, T., Hirai, R., Loo, Y.-M., Owen, D., Johnson, C.L., Sinha, S.C., Akira, S., Fujita, T., and Gale, M. (2007). Regulation of innate antiviral defenses through a shared repressor domain in RIG-I and LGP2. Proc. Natl. Acad. Sci. *104*, 582–587.

Sasai, M., Tatematsu, M., Oshiumi, H., Funami, K., Matsumoto, M., Hatakeyama, S., and Seya, T. (2010a). Direct binding of TRAF2 and TRAF6 to TICAM-1/TRIF adaptor participates in activation of the Toll-like receptor 3/4 pathway. Mol. Immunol. *47*, 1283–1291.

Sasai, M., Linehan, M.M., and Iwasaki, A. (2010b). Bifurcation of Toll-like receptor 9 signaling by adaptor protein 3. Science *329*, 1530–1534.

Sato, S., Sugiyama, M., Yamamoto, M., Watanabe, Y., Kawai, T., Takeda, K., and Akira, S. (2003). Toll/IL-1 Receptor Domain-Containing Adaptor Inducing IFN-β (TRIF)

Associates with TNF Receptor-Associated Factor 6 and TANK-Binding Kinase 1, and Activates Two Distinct Transcription Factors, NF-κB and IFN-Regulatory Factor-3, in the Toll-Like Receptor Signaling. J. Immunol. *171*, 4304–4310.

Saxena, M., and Yeretssian, G. (2014). NOD-Like Receptors: Master Regulators of Inflammation and Cancer. Front. Immunol. *5*, 327.

Scheiermann, J., and Klinman, D.M. (2014). Clinical evaluation of CpG oligonucleotides as adjuvants for vaccines targeting infectious diseases and cancer. Vaccine *32*, 6377–6389.

Scherman, D., Bessodes, M., Cameron, B., Herscovici, J., Hofland, H., Pitard, B., Soubrier, F., Wils, P., and Crouzet, J. (1998). Application of lipids and plasmid design for gene delivery to mammalian cells. Curr. Opin. Biotechnol. *9*, 480–485.

Schroder, K., and Tschopp, J. (2010). The inflammasomes. Cell *140*, 821–832.

Schwendener, R.A. (2014). Liposomes as vaccine delivery systems: a review of the recent advances. Ther. Adv. Vaccines *2*, 159–182.

Serrato, R.V. (2014). Lipopolysaccharides in diazotrophic bacteria. Front. Cell. Infect. Microbiol. *4*, 119.

Sharma, S., and Fitzgerald, K.A. (2011). Innate Immune Sensing of DNA. PLoS Pathog *7*, e1001310.

Smith, D.M., Simon, J.K., and Baker, J.R. (2013). Applications of nanotechnology for immunology. Nat. Rev. Immunol. *13*, 592–605.

Sonawane, N.D., Szoka, F.C., and Verkman, A.S. (2003). Chloride accumulation and swelling in endosomes enhances DNA transfer by polyamine-DNA polyplexes. J. Biol. Chem. *278*, 44826–44831.

Stamatatos, L., Leventis, R., Zuckermann, M.J., and Silvius, J.R. (1988). Interactions of cationic lipid vesicles with negatively charged phospholipid vesicles and biological membranes. Biochemistry (Mosc.) *27*, 3917–3925.

Strober, W., Murray, P.J., Kitani, A., and Watanabe, T. (2006). Signalling pathways and molecular interactions of NOD1 and NOD2. Nat. Rev. Immunol. *6*, 9–20.

Tada, R., Hidaka, A., Iwase, N., Takahashi, S., Yamakita, Y., Iwata, T., Muto, S., Sato, E., Takayama, N., Honjo, E., et al. (2015). Intranasal Immunization with DOTAP Cationic Liposomes Combined with DC-Cholesterol Induces Potent Antigen-Specific Mucosal and Systemic Immune Responses in Mice. PloS One *10*, e0139785.

Takano, S., Aramaki, Y., and Tsuchiya, S. (2003). Physicochemical properties of liposomes affecting apoptosis induced by cationic liposomes in macrophages. Pharm. Res. *20*, 962–968.

Takaoka, A., Wang, Z., Choi, M.K., Yanai, H., Negishi, H., Ban, T., Lu, Y., Miyagishi, M., Kodama, T., Honda, K., et al. (2007). DAI (DLM-1/ZBP1) is a cytosolic DNA sensor and an activator of innate immune response. Nature *448*, 501–505.

Tanaka, T., Legat, A., Adam, E., Steuve, J., Gatot, J.-S., Vandenbranden, M., Ulianov, L., Lonez, C., Ruysschaert, J.-M., Muraille, E., et al. (2008). DiC14-amidine cationic liposomes stimulate myeloid dendritic cells through Toll-like receptor 4. Eur. J. Immunol. *38*, 1351–1357.

Tatematsu, M., Ishii, A., Oshiumi, H., Horiuchi, M., Inagaki, F., Seya, T., and Matsumoto, M. (2010). A Molecular Mechanism for Toll-IL-1 Receptor Domain-containing Adaptor Molecule-1-mediated IRF-3 Activation. J. Biol. Chem. *285*, 20128–20136.

Tyagi, M., Rusnati, M., Presta, M., and Giacca, M. (2001). Internalization of HIV-1 tat requires cell surface heparan sulfate proteoglycans. J. Biol. Chem. *276*, 3254–3261.

Ulmer, J.B., Donnelly, J.J., Parker, S.E., Rhodes, G.H., Felgner, P.L., Dwarki, V.J., Gromkowski, S.H., Deck, R.R., DeWitt, C.M., and Friedman, A. (1993). Heterologous protection against influenza by injection of DNA encoding a viral protein. Science *259*, 1745–1749.

Unterholzner, L., Keating, S.E., Baran, M., Horan, K.A., Jensen, S.B., Sharma, S., Sirois, C.M., Jin, T., Xiao, T., Fitzgerald, K.A., et al. (2010). IFI16 is an innate immune sensor for intracellular DNA. Nat. Immunol. *11*, 997–1004.

Vanaja, S.K., Rathinam, V.A.K., and Fitzgerald, K.A. (2015). Mechanisms of inflammasome activation: recent advances and novel insights. Trends Cell Biol. *25*, 308–315.

Vangasseri, D.P., Cui, Z., Chen, W., Hokey, D.A., Falo, L.D., and Huang, L. (2006). Immunostimulation of dendritic cells by cationic liposomes. Mol. Membr. Biol. *23*, 385–395.

Varkouhi, A.K., Scholte, M., Storm, G., and Haisma, H.J. (2011). Endosomal escape pathways for delivery of biologicals. J. Control. Release Off. J. Control. Release Soc. *151*, 220–228.

Vasievich, E.A., Chen, W., and Huang, L. (2011). Enantiospecific adjuvant activity of cationic lipid DOTAP in cancer vaccine. Cancer Immunol. Immunother. *60*, 629–638.

Vaughan, E.E., DeGiulio, J.V., and Dean, D.A. (2006). Intracellular trafficking of plasmids for gene therapy: mechanisms of cytoplasmic movement and nuclear import. Curr. Gene Ther. *6*, 671–681.

Veeranki, S., and Choubey, D. (2012). Interferon-inducible p200-family protein IFI16, an innate immune sensor for cytosolic and nuclear double-stranded DNA: Regulation of subcellular localization. Mol. Immunol. *49*, 567–571.

Verzola, D., Famà, A., Villaggio, B., Rocco, M.D., Simonato, A., D'Amato, E., Gianiorio, F., and Garibotto, G. (2012). Lysine triggers apoptosis through a NADPH oxidase-dependent mechanism in human renal tubular cells. J. Inherit. Metab. Dis. *35*, 1011–1019.

Wang, X., Quinn, P.J., and Yan, A. (2015). Kdo2 -lipid A: structural diversity and impact on immunopharmacology. Biol. Rev. Camb. Philos. Soc. *90*, 408–427.

Ward, D.T., McLarnon, S.J., and Riccardi, D. (2002). Aminoglycosides increase intracellular calcium levels and ERK activity in proximal tubular OK cells expressing the extracellular calcium-sensing receptor. J. Am. Soc. Nephrol. JASN *13*, 1481–1489.

Wasungu, L., and Hoekstra, D. (2006). Cationic lipids, lipoplexes and intracellular delivery of genes. J. Control. Release Off. J. Control. Release Soc. *116*, 255–264.

Watson, D.S., Endsley, A.N., and Huang, L. (2012). Design considerations for liposomal vaccines: Influence of formulation parameters on antibody and cell-mediated immune responses to liposome associated antigens. Vaccine *30*, 2256–2272.

Wells, J.M. (2011). Immunomodulatory mechanisms of lactobacilli. Microb. Cell Factories *10*, S17.

Wilmar, A., Lonez, C., Vermeersch, M., Andrianne, M., Pérez-Morga, D., Ruysschaert, J.-M., Vandenbranden, M., Leo, O., and Temmerman, S.T. (2012). The cationic lipid, diC14 amidine, extends the adjuvant properties of aluminum salts through a TLR-4- and caspase-1-independent mechanism. Vaccine *30*, 414–424.

Wolff, J.A., and Budker, V. (2005). The mechanism of naked DNA uptake and expression. Adv. Genet. *54*, 3–20.

Wolff, J.A., Malone, R.W., Williams, P., Chong, W., Acsadi, G., Jani, A., and Felgner, P.L. (1990). Direct gene transfer into mouse muscle in vivo. Science *247*, 1465–1468.

Wrobel, I., and Collins, D. (1995). Fusion of cationic liposomes with mammalian cells occurs after endocytosis. Biochim. Biophys. Acta *1235*, 296–304.

Wu, J., and Chen, Z.J. (2014). Innate Immune Sensing and Signaling of Cytosolic Nucleic Acids. Annu. Rev. Immunol. *32*, 461–488.

Wu, J., Sun, L., Chen, X., Du, F., Shi, H., Chen, C., and Chen, Z.J. (2013). Cyclic-GMP-AMP Is An Endogenous Second Messenger in Innate Immune Signaling by Cytosolic DNA. Science *339*.

Xie, P. (2013). TRAF molecules in cell signaling and in human diseases. J. Mol. Signal. *8*, 7.

Xiong, F., Mi, Z., and Gu, N. (2011). Cationic liposomes as gene delivery system: transfection efficiency and new application. Pharm. *66*, 158–164.

Xu, Y., and Szoka, F.C. (1996). Mechanism of DNA release from cationic liposome/DNA complexes used in cell transfection. Biochemistry (Mosc.) *35*, 5616–5623.

Yan, W., Chen, W., and Huang, L. (2007). Mechanism of adjuvant activity of cationic liposome: phosphorylation of a MAP kinase, ERK and induction of chemokines. Mol. Immunol. *44*, 3672–3681.

Yan, W., Chen, W., and Huang, L. (2008). Reactive oxygen species play a central role in the activity of cationic liposome based cancer vaccine. J. Control. Release Off. J. Control. Release Soc. *130*, 22–28.

Yang, P., An, H., Liu, X., Wen, M., Zheng, Y., Rui, Y., and Cao, X. (2010). The cytosolic nucleic acid sensor LRRFIP1 mediates the production of type I interferon via a β-catenin-dependent pathway. Nat. Immunol. *11*, 487–494.

Zabner, J., Fasbender, A.J., Moninger, T., Poellinger, K.A., and Welsh, M.J. (1995). Cellular and Molecular Barriers to Gene Transfer by a Cationic Lipid. J. Biol. Chem. *270*, 18997–19007.

Zanoni, I., Ostuni, R., Capuano, G., Collini, M., Caccia, M., Ronchi, A.E., Rocchetti, M., Mingozzi, F., Foti, M., Chirico, G., et al. (2009). CD14 regulates the dendritic cell life cycle after LPS exposure through NFAT activation. Nature *460*, 264–268.

Zanoni, I., Ostuni, R., Marek, L.R., Barresi, S., Barbalat, R., Barton, G.M., Granucci, F., and Kagan, J.C. (2011). CD14 controls the LPS-induced endocytosis of Toll-like receptor 4. Cell *147*, 868–880.

Zelensky, A.N., and Gready, J.E. (2005). The C-type lectin-like domain superfamily. FEBS J. *272*, 6179–6217.

Zhang, X., Brann, T.W., Zhou, M., Yang, J., Oguariri, R.M., Lidie, K.B., Imamichi, H., Huang, D.-W., Lempicki, R.A., Baseler, M.W., et al. (2011a). Ku70 Is a Novel Cytosolic DNA Sensor that Induces Type-III Rather than Type-I IFN. J. Immunol. Baltim. Md 1950 *186*, 4541–4545.

Zhang, X.-X., McIntosh, T.J., and Grinstaff, M.W. (2012). Functional lipids and lipoplexes for improved gene delivery. Biochimie *94*, 42–58.

Zhang, Z., Yuan, B., Lu, N., Facchinetti, V., and Liu, Y.-J. (2011b). DHX9 Pairs with IPS-1 To Sense Double-Stranded RNA in Myeloid Dendritic Cells. J. Immunol. *187*, 4501–4508.

Zhi, D., Zhang, S., Wang, B., Zhao, Y., Yang, B., and Yu, S. (2010). Transfection efficiency of cationic lipids with different hydrophobic domains in gene delivery. Bioconjug. Chem. *21*, 563–577.

Zhi, D., Zhang, S., Cui, S., Zhao, Y., Wang, Y., and Zhao, D. (2013). The headgroup evolution of cationic lipids for gene delivery. Bioconjug. Chem. *24*, 487–519.

Zhong, B., Yang, Y., Li, S., Wang, Y.-Y., Li, Y., Diao, F., Lei, C., He, X., Zhang, L., Tien, P., et al. (2008). The adaptor protein MITA links virus-sensing receptors to IRF3 transcription factor activation. Immunity *29*, 538–550.

Zuhorn, I.S., Kalicharan, R., and Hoekstra, D. (2002). Lipoplex-mediated transfection of mammalian cells occurs through the cholesterol-dependent clathrin-mediated pathway of endocytosis. J. Biol. Chem. *277*, 18021–18028.

UNIVERSITE BRETAGNE LOIRE

UNIVERSITÉ DE NANTES

Thèse de Doctorat

Thibault COLOMBANI

Compréhension immunologique de la stimulation de la réponse immunitaire par des molécules synthétiques : Applications thérapeutiques

Immunological understanding of immune response stimulation by synthetic molecules: therapeutic applications

Résumé

Le développent des biothérapies a connu un essor sans précédent ces dernières années, permettant l'émergence de nombreuses solutions thérapeutiques répondant à de multiples défis en santé humaine et animale afin de lutter contre des maladies héréditaires ou acquises. Parmi ces stratégies, le transfert de gênes revêt un intérêt tout particulier, permettant à la fois de réparer des cellules défectueuses en leur apportant une copie saine du gène, ou bien d'activer efficacement le système immunitaire par l'expression d'un antigène d'intérêt thérapeutique. Néanmoins, malgré le développement de nombreux outils de thérapie génique ou d'immunothérapie, de nombreuses limitations persistent à ce jour.

Au cours de cette thèse, les résultats obtenus ont permis le développement et l'optimisation d'outils afin d'outrepasser ces limites. Tout d'abord, nous avons pu élucider les mécanismes d'actions du copolymère à blocs 704, une nouvelle classe de vecteurs qui permet d'induire une réponse vaccinale optimale en délivrant de manière directe des acides nucléiques au sein des cellules musculaires et en stimulant des récepteurs à ADN intracellulaires. De plus, ces travaux ont permis de démontrer qu'une nouvelle classe de molécules adjuvantes, les lipoaminoglycosides, permet de stimuler efficacement le système immunitaire en plus de conduire à la régression de la croissance de tumeurs mammaires murines. Enfin, ces résultats ont pu montrer l'importance de l'assemblage supramoléculaire des lipoplexes sur l'efficacité de transfection afin de développer un vecteur universel pour la délivrance de différentes classes d'acides nucléiques.

Dès lors, l'optimisation de la délivrance de macromolécules au sein de cellules et la compréhension de l'interaction entre le système immunitaire / le vecteur / les acides nucléiques nous ont permis d'établir des stratégies afin de développer des formulations spécifiques à chaque application biothérapeutique.

Mots clés :

Lipides cationiques, Système immunitaire, Adjuvant, Vaccination à ADN, Immunothérapie, vecteurs synthétiques, ADN

Abstract

The development of biotherapies experienced an unprecedented growth in recent years, allowing the emergence of many therapeutic solutions to many challenges in human and animal health in order to fight against hereditary or acquired diseases. Among these strategies, gene transfer is of particular interest, making it possible either to repair defective cells by providing them a healthy copy of the gene, or to effectively activate the immune system by expressing an antigen of therapeutic interest. Nevertheless, despite the development of numerous tools for gene therapy or immunotherapy, many limitations persist.

During this thesis, the results obtained allowed the development and optimization of tools in order to go beyond these limits. First, we have been able to elucidate the mechanism of action of the block copolymer 704, a new class of vectors which allows to induce an optimal vaccine response by directly delivering nucleic acids into muscle cells and by stimulating intracellular DNA sensors. Moreover, this work has demonstrated that a new class of adjuvant molecules, lipoaminoglycosides, can stimulate efficiently the immune system in addition to lead to the regression of murine mammary tumors growth. Finally, these results showed the importance of the supramolecular assembly of lipoplexes on the transfection efficiency in order to develop a universal vector for the delivery of different classes of nucleic acids.

Therefore, the optimization of macromolecules delivery within cells and the understanding of the interaction between the immune system / vector / nucleic acids allowed us to establish strategies in order to develop specific formulations for each biotherapeutic applications.

Key Words

Cationic Lipids, Immune system, Adjuvant, DNA vaccine, Immunotherapy, Synthetic vectors, DNA